

BIOCATALYTIC AND BIOMIMETIC STUDIES

OF

POLYPHENOL OXIDASE

THESIS

**Submitted in fulfilment of the
requirements for the Degree of
DOCTOR OF PHILOSOPHY
of Rhodes University**

by

STEPHANIE GAIL BURTON

**Department of Biochemistry and Microbiology
Rhodes University**

December 1993

ABSTRACT

Mushroom polyphenol oxidase (EC 1.14.18.1) was investigated to determine its potential for application as a biocatalyst in the synthesis of *o*-quinones, in organic medium. In order to determine the kinetic properties of the biocatalyst, a system was devised which comprised an immobilised polyphenol oxidase extract, functioning in chloroform. The system was hydrated by the addition of buffer. A simple method for the consistent measurement of reaction rates in this heterogenous system was designed and used to obtain detailed enzyme kinetic data relating to optimisation of reaction conditions and substrate specificity. The aqueous content of the system was optimised using *p*-cresol as a substrate.

A crude, immobilised extract of *Agaricus bisporus* was used to hydroxylate and oxidise a range of selected *p*-substituted phenolic substrates, yielding, as the sole products, *o*-quinones. These products were efficiently reduced to catechols by extracting the reaction mixtures with aqueous ascorbic acid solution. The biocatalytic system was also successfully utilised to produce *L*-DOPA, the drug used to treat Parkinson's disease, from *L*-acetyl tyrosine ethylester (ATEE). Michaelis-Menten kinetics were used to obtain apparent K_m and V values with respect to the selected phenolic substrates, and the kinetic parameters obtained were found to correlate well with the steric requirements of the substrates and with their hydrophobicity. In the course of the investigation, a novel ^1H NMR method was used to facilitate measurement of the UV molar absorption coefficients of the *o*-quinones in reaction mixtures, thus avoiding the necessity to isolate these unstable, water-sensitive products.

The biocatalytic system was extended to a continuous process, in which the immobilised enzyme was shown to function successfully in the chloroform medium for several hours, with high conversion rates. Modifications, involving partial purification and the addition of a surfactant, were investigated to determine their effect on the kinetic parameters. The results obtained using partially purified enzyme indicated that the removal of extraneous protein and/or melanoid material lead to a reduced capacity for conversion of sterically demanding substrates. The addition of the anionic detergent, sodium dodecyl sulphate (SDS), enhanced the ability of the biocatalyst to bind and oxidise sterically demanding substrates. These effects are attributed to changes in the polar state of groups within the protein binding pocket, which result in altered flexibility and hydrophobicity.

Computer modelling of several biomimetic dinuclear copper complexes also indicated the importance of flexibility for effective biocatalysis. Novel binuclear copper (I) complexes, containing a flexible biphenyl spacer and imidazole or benzimidazole donors, were prepared and analysed using NMR, UV, AA and cyclic voltammetric techniques. The complexes were also shown, in a detailed kinetic study, to mimic the catecholase activity of polyphenol oxidase by oxidising 3,5-di-*tert*-butylcatechol, and to catalyse the coupling of the phenolic substrate 2,4-di-*tert*-butylphenol. However, the complexes were apparently too flexible to react with smaller substrates. These biomimetic complexes provided valuable insights into the nature of the dinuclear copper binding site.

TABLE OF CONTENTS

CHAPTER 1	1
INTRODUCTION	1
1.1 POLYPHENOL OXIDASE	1
1.1.1 Background to the study of polyphenol oxidase	1
1.1.2 Early research on tyrosinase, and melanin biosynthesis	3
1.1.3 Polyphenol oxidases from various sources	4
1.1.3 (1) Plant polyphenol oxidases	5
1.1.3 (2) Mushroom polyphenol oxidase	7
1.1.3 (3) Other microbial polyphenol oxidases	8
1.1.3 (4) Invertebrate polyphenol oxidases	9
1.1.3 (5) Mammalian tyrosinases	10
1.1.4 The mechanism of polyphenol oxidase-catalysed reactions	10
1.1.5 The lag phase in phenolase activity	13
1.1.6 Reaction inactivation of polyphenol oxidase	14
1.1.7 Reactions of products subsequent to polyphenol oxidase-catalysed oxidation	15
1.1.8 Substrates for polyphenol oxidases	16
1.1.9 Inhibitors of polyphenol oxidases	21
1.2 THE ACTIVE SITE IN POLYPHENOL OXIDASE	23
1.2.1 The structure of the "Type III" active site	23
1.2.2 The Type III copper centres in tyrosinase and haemocyanin	24
1.2.3 Early results of haemocyanin studies	24
1.2.4 More recent studies on haemocyanins	26
1.2.5 Studies on <i>Neurospora crassa</i> tyrosinase	27
1.2.6 A possible mechanism for tyrosinase	28
1.2.7 A current model for the dinuclear copper binding site	30
1.3 BIOCATALYSIS WITH POLYPHENOL OXIDASE	32
1.3.1 Biocatalysis	32
1.3.2 Biocatalysis in organic media	33
1.3.3 The manipulation of non-aqueous biocatalytic systems	34
1.3.3 (1) The effect of the solvent on selectivity	34
1.3.3 (2) The effect of non-aqueous solvents on protein stability	34
1.3.3 (3) Immobilisation of enzymes	34

1.3.3 (4) Medium engineering	35
1.3.3 (5) Protein engineering	36
1.3.4 Biocatalysis involving polyphenol oxidase	36
1.3.5 Biocatalysis with polyphenol oxidase in organic medium	37
1.4 THE BIOMIMETIC APPROACH TO COPPER METALLOPROTEIN MODELS	40
1.4.1 Introductory remarks	40
1.4.2 The chemistry of copper complexes	41
1.4.2 (1) Copper-catalysed oxidation reactions	41
1.4.2 (2) Mechanisms of copper-catalysed oxidations of phenols	43
1.4.2 (3) Reactions with copper complexes and oxygen: coordination considerations	45
1.4.3 Choice of ligands for binuclear copper complexes	46
1.4.4 Complexes synthesised as biomimetic models for Haemocyanin and Tyrosinase	47
1.4.4 (1) Early complexes	48
1.4.4 (2) Dinuclear copper complexes synthesised to model the protein endogenous bridge	50
1.4.4 (3) The nature of the peroxide bridge in dioxygen-containing complexes	50
1.4.4 (4) Mononuclear and dimerising complexes	52
1.4.4 (5) Dinuclear complexes	55
1.4.4 (6) A model for the oxygen binding in oxyhaemocyanin and oxytyrosinase	59
1.4.5 Monooxygenase models	60
1.4.5 (1) Hydroxylation of the arene moiety in the ligand	60
1.4.5 (2) Oxidation of exogenous substrates	62
1.4.5 (3) A proposed mechanism for monooxygenase activity	64
1.5 OBJECTIVES	68
CHAPTER 2	69
A BIOCATALYTIC SYSTEM USING POLYPHENOL OXIDASE	69
2.1 INTRODUCTION	69
2.1.1 Use of polyphenol oxidase in organic medium	69
2.1.2 The effects of organic solvents on enzymes	70
2.1.3 The role of water in non-aqueous biocatalysis	71
2.1.4 Practical systems for non-aqueous biocatalysis	72
2.1.5 The biocatalytic system in the present study	73

2.2 RESULTS AND DISCUSSION	74
2.2.1 Isolation and purification of polyphenol oxidase from mushrooms	74
2.2.1 (1) Extract A: Crude polyphenol oxidase extract from mushrooms	74
2.2.1 (2) Extract B: Partial purification of crude polyphenol oxidase	75
2.2.1 (3) Extract C: Removal of endogenous phenolics from the crude extract	77
2.2.1 (4) Comparison of activities of extracts A, B and C	77
2.2.2 Comparison of extracts A, B, and C, using Polyacrylamide Gel Electrophoresis (PAGE)	78
2.2.2 (1) Detection of protein components by SDS-PAGE	78
2.2.2 (2) Determination of activity in extracts by non-denaturing PAGE	81
2.2.2 (3) Detection of laccase activity	82
2.2.2 (4) Detection of copper-containing proteins by PAGE	84
2.2.3 Immobilisation of polyphenol oxidase	84
2.2.4 Assay procedures	85
2.2.4 (1) Activity assay in aqueous medium: the "Dopachrome assay"	85
2.2.4 (2) Activity assay for the biocatalyst in organic medium	86
2.2.4 (3) Correlation of dopachrome and <i>p</i> -cresol assays	87
2.2.5 Optimisation of the water requirement in the biocatalytic system	88
2.2.6 Investigation of further purification procedures	90
2.2.6 (1) Chromatography using DEAE-Cellulose	90
2.2.6 (2) Chromatography by size exclusion	91
2.2.7 Application of the polyphenol oxidase biocatalytic system in chloroform	92
2.2.7 (1) Oxidation of <i>p</i> -cresol in chloroform, by the polyphenol oxidase biocatalyst	93
2.2.7 (2) Conversion of ATEE to <i>L</i> -DOPA	95
2.3 CONCLUSIONS	96
2.4 EXPERIMENTAL	97
2.4.1 Crude extract A	97
2.4.2 Partially purified extract B: Ammonium sulphate fractionation	98
2.4.3 PVPP-purified extract C	98
2.4.4 PAGE analysis of polyphenol oxidase extracts	99

2.4.5	SDS-PAGE comparison of extracts and commercial enzyme	99
2.4.6	Non-denaturing PAGE analysis of polyphenol oxidase extracts	100
2.4.7	Detection of copper in the polyphenol oxidase extracts by PAGE	101
2.4.8	Immobilisation of polyphenol oxidase extracts	101
2.4.9	Protein assays	102
2.4.10	"Dopachrome" assay for polyphenol oxidase activity	103
2.4.11	Enzyme activity assay in the organic system	104
2.4.12	Optimisation of water requirement in the biocatalytic system	104
2.4.13	Chromatography on DEAE-cellulose	106
2.4.14	Chromatography on Toyopearl HW-50S	107
2.4.15	Oxidation of <i>p</i> -cresol	109
2.4.16	Oxidation of ATEE and production of <i>L</i> -DOPA	111
2.4.17	Isolation of DOPA from oxidation of ATEE by polyphenol oxidase	112
CHAPTER 3		113
A KINETIC STUDY OF THE POLYPHENOL OXIDASE BIOCATALYST		113
3.1	INTRODUCTION	113
3.1.1	Substrate specificity	113
3.1.2	Principles involved in enzyme kinetic studies	114
3.1.3	Investigation of the kinetic properties of biocatalysts in non-aqueous media	116
3.1.4	Investigation of the polyphenol oxidase biocatalyst in chloroform	118
3.2	RESULTS AND DISCUSSION	119
3.2.1	Selection of substrates for a kinetic analysis	119
3.2.2	Determination of UV-visible absorption characteristics of <i>o</i> -quinone products	122
3.2.2 (1)	Measurement of wavelengths of maximum absorbance for <i>o</i> -quinones	122
3.2.2 (2)	Determination of molar absorption coefficients, ϵ	124
3.2.3	Determination of kinetic parameters for the biocatalyst in chloroform	126
3.2.4	Correlation of the calculated kinetic parameters with the properties of the substrates	129
3.2.5	Limitations on the size of substrates which can be oxidised by polyphenol oxidase in chloroform	132
3.3	CONCLUSIONS	134

3.4 EXPERIMENTAL	135
3.4.1 Screening of substrates using PAGE	135
3.4.2 Determination of wavelengths of maximum absorbance for <i>o</i> -quinones	135
3.4.3 Determination of molar absorption coefficients	137
3.4.4 Measurement of reaction rates for biocatalysis	140
CHAPTER 4	145
MODIFICATIONS TO THE POLYPHENOL OXIDASE BIOCATALYTIC SYSTEM	145
4.1 INTRODUCTION	145
4.1.1 Purification of polyphenol oxidase	145
4.1.2 Removal of melanins from the polyphenol oxidase catalyst	146
4.1.3 Activation of polyphenol oxidase	147
4.2 RESULTS AND DISCUSSION	148
4.2.1 The effects of partial purification on the kinetics of the biocatalyst	148
4.2.2 The effects of removing endogenous melanins from the biocatalytic system	152
4.2.3 Determination of the effects of varying concentrations of SDS on the rate of oxidation of <i>p</i> -cresol	155
4.2.4 The effects of addition of SDS on the kinetics of the biocatalytic system	156
4.2.5 Longer-term effects of SDS on the biocatalyst	160
4.3 CONCLUSIONS	161
4.4 EXPERIMENTAL	162
4.4.1 Measurement of kinetic parameters for biocatalyst prepared from the partially purified extract B	162
4.4.2 Measurement of kinetic parameters for oxidation of <i>p</i> -substituted phenols, catalysed by biocatalyst prepared from extract C	164
4.4.3 Preliminary experiment to show increased rates of reaction in the presence of SDS	166
4.4.4 Comparison of rates of oxidation of <i>p</i> -cresol catalysed by polyphenol oxidase biocatalyst hydrated with buffer or water	167
4.4.5 Measurement of rates of oxidation of <i>p</i> -cresol by the polyphenol oxidase biocatalyst in the presence of varying concentrations of SDS	167
4.4.6 Measurement of rates of oxidation of <i>p</i> -substituted phenols, catalysed by polyphenol oxidase biocatalyst in the presence of 2	

mM SDS	169
4.4.7 Determination of longer term effects of SDS on the biocatalyst	171
CHAPTER 5	173
APPLICATION OF POLYPHENOL OXIDASE IN A CONTINUOUS FLOW SYSTEM	173
5.1 INTRODUCTION	173
5.2 RESULTS AND DISCUSSION	173
5.2.1 Columns 1 - 4, using <i>p</i> -cresol as substrate and crude enzyme	175
5.2.2 Column 5, using partially purified enzyme	177
5.2.3 Column 6, using PVPP-treated enzyme	178
5.2.4 Column 7, using ATEE as substrate	178
5.2.5 Columns 8 and 9, using <i>p</i> -isopropylphenol as substrate	178
5.2.6 Water content in the continuous flow systems	179
5.2.7 Isolation of products and reduction of <i>o</i> -quinones to catechols	181
5.3 CONCLUSIONS	182
5.4 EXPERIMENTAL	183
5.4.1 Protein determinations	183
5.4.2 (2) Reduction of product from Column 1	185
5.4.3 Column 2, using 50mM <i>p</i> -cresol as substrate	185
5.4.4 Column 3, using 20mM <i>p</i> -cresol as substrate	187
5.4.5 (1) Column 4, using <i>p</i> -cresol in the presence of SDS	187
5.4.5 (2) Reduction of product from Column 4	188
5.4.6 (1) Column 5, using partially purified enzyme	189
5.4.6 (2) Reduction of product from Column 5	190
5.4.7 (1) Column 6, using PVPP-treated enzyme extract	190
5.4.7 (2) Reduction of product from Column 6	191
5.4.8 (1) Column 7, using ATEE as substrate	191
5.4.8 (2) Reduction of product from Column 7	192
5.4.9 Column 8, using <i>p</i> -isopropylphenol as substrate	192
5.4.10 (1) Column 9, using <i>p</i> -isopropylphenol as substrate, and SDS	193
5.4.10 (2) Reduction of product from Column 9	194
CHAPTER 6	195
BIOMIMETIC STUDIES OF TYROSINASE: MOLECULAR MODELLING	195
6.1 INTRODUCTION	195
6.1.1 Biomimetic chemistry	195
6.1.2 Molecular recognition considerations	195

6.1.3	Molecular mechanics	196
6.1.4	Molecular mechanics calculations for dinuclear copper complexes	197
6.1.5	Factors to be considered in modelling polyphenol oxidase	198
6.2	RESULTS AND DISCUSSION	199
6.2.1	Molecular Modelling using ALCHEMY II®	199
6.2.2	Modelling using HyperChem®	210
6.3	CONCLUSION	215
6.4	EXPERIMENTAL	215
6.4.1	Modelling with ALCHEMY®	215
6.4.2	Modelling using HyperChem®	216
CHAPTER 7		217
SYNTHESIS OF BIOMIMETIC COPPER COMPLEXES		217
7.1	INTRODUCTION	217
7.1.1	Synthesis of biomimetic dinuclear copper complexes	217
7.2	RESULTS AND DISCUSSION	220
7.2.1	Syntheses of the copper complexes	220
7.2.1 (1)	Synthesis of biphenyl-2,2'-dicarbaldehyde	220
7.2.1 (2)	Synthesis of tetrakis(acetonitrile)copper (I) hexafluorophosphate	221
7.2.1 (3)	Synthesis of complex I	221
7.2.2	Synthesis of complex II	226
7.2.2 (1)	Synthesis of Complexes IIA and IIB by template condensation	226
7.2.2 (2)	Synthesis of the ligand 92	230
7.2.2 (3)	Synthesis of complex IIC	233
7.2.3	Synthesis of complex III	233
7.2.3 (1)	Synthesis of the ligand 97	233
7.2.3 (2)	Synthesis of complex IIIA	238
7.2.3 (4)	Reactions of the starting materials 86 and 96 with [Cu(MeCN) ₄ (PF ₆) ₂]	242
7.2.4	Decomposition of complex I	245
7.3	CONCLUSIONS	246
7.4	EXPERIMENTAL	247
7.4.1	Synthesis of biphenyl-2,2'-dicarbaldehyde	247
7.4.2	Synthesis of tetrakis(acetonitrile)copper (I) hexafluorophosphate	247
7.4.3	Preparation of ligand system 89	247

7.4.4 Preparation of complex I	248
7.4.5 Preparation of histamine	249
7.4.6 Preparation of complex IIA	249
7.4.7 Preparation of complex IIB	249
7.4.8 Preparation of ligand system 92	250
7.4.9 Preparation of ligand system 94	250
7.4.10 Preparation of complex IIC	250
7.4.11 Preparation of 2-(2-aminoethyl)benzimidazole	251
7.4.12 Preparation of ligand system 97	251
7.4.13 Preparation of ligand system 98	252
7.4.14 Preparation of complex IIIA	252
7.4.15 Preparation of complex IIIB	252
7.4.16 Reaction of biphenyl-2,2'-dialdehyde 86 with $[\text{Cu}(\text{MeCN})_4][\text{PF}_6]$	253
7.4.17 Reaction of 2-(2-benzimidazolyl)ethylamine 96 with $[\text{Cu}(\text{MeCN})_4][\text{PF}_6]$	253
7.4.18 Decomposition of complex I	253
7.4.19 Isolation of oxygenated product from complex IIIA	255
CHAPTER 8	
ANALYSES OF THE COPPER COMPLEXES	259
8.1 INTRODUCTION	259
8.1.1 Atomic Absorption Spectrophotometry	259
8.1.2 UV-visible Spectrophotometry	260
8.1.3 Electrochemical characteristics of copper dinuclear complexes	262
8.2 RESULTS AND DISCUSSION	266
8.2.1 Atomic Absorption Spectrophotometric Analysis	266
8.2.2 UV-Visible Spectrophotometric Analysis	267
8.2.2 (1) Complex I	270
8.2.2 (2) Complex IIC	271
8.2.2 (3) Complex IIA	272
8.2.2 (4) Complex IIB	272
8.2.2 (5) Complex IIIA	273
8.2.2 (6) Complex IIIB	273
8.2.3 Electrochemical analysis	283
8.3 CONCLUSIONS	285
8.3.1 Atomic absorption analysis	285
8.3.2 UV-Visible spectroscopy	285

8.3.3 Electrochemical analysis	287
8.4 EXPERIMENTAL	287
8.4.1 Atomic Absorption Spectrophotometric analysis of copper complexes	287
8.4.2 Measurement of UV-Visible spectra	288
8.4.3 Isolation of oxygenated product IIIA' from complex IIIA	290
8.4.4 Electrochemical analysis	290
 CHAPTER 9	
THE CATALYTIC ACTIVITY OF THE COPPER COMPLEXES	292
9.1 INTRODUCTION	292
9.2 RESULTS AND DISCUSSION	294
9.2.1 Uncatalysed reaction of DTBP and DTBC with oxygen	294
9.2.2 Oxidation of DTBP catalysed by complex I	294
9.2.3 Oxidation of DTBP and DTBC, catalysed by other copper complexes	296
9.2.4 Identification of the products of the catalytic oxidations of DTBP and DTBC	296
9.2.5 Determination of the molar extinction coefficient for the coupled oxidation product 117	299
9.3 CONCLUSION	309
9.3.1 The catalytic activity of the copper complexes	309
9.3.2 The nature of the reaction products	309
9.3.3 The mechanism of the oxidation reactions	311
9.3.4 The kinetic analysis of the reactions catalysed by the copper complexes	312
9.4 EXPERIMENTAL	314
9.4.1 Oxidation of DTBP and DTBC , catalysed by complex I	314
9.4.2 Investigation of the products from oxidation of DTBP and DTBC, catalysed by copper complexes	315
9.4.3 Preparation of 3,5-di- <i>tert</i> -butyl- <i>o</i> -benzoquinone (DTBQ)	316
9.4.4 Determination of the UV molar absorption coefficient of 3,3',5,5'-tetra- <i>tert</i> -butyl-2,2'-dihydroxybiphenyl	316
9.4.5 Kinetic analysis of catalytic oxidation reactions	317
 CHAPTER 10	322
CONCLUSION	

ABBREVIATIONS

AA	atomic absorption
ATEE	<i>N</i> -acetyl- <i>L</i> -tyrosine ethyl ester
CV	cyclic voltammetry
CT	charge transfer
DOPA	2,4-dihydroxyphenylalanine
DTBC	3,5-di- <i>tert</i> -butylcatechol
DTBP	2,4-di- <i>tert</i> -butylphenol
EPR	electron paramagnetic resonance
EXAFS	extended X-ray absorption fine structure
GC	gas chromatography
HPLC	high performance liquid chromatography
IR	infra red
LMCT	ligand-to-metal charge transfer
MLCT	metal-to-ligand charge transfer
NMR	nuclear magnetic resonance
PVPP	polyvinylpyrrolidone
PAGE	polyacrylamide gel electrophoresis
SCF- $X\alpha$ -SW	self-consistent field $X\alpha$ -scattered wave
SDS	sodium dodecyl sulphate
SEM	standard error in the mean
UV	ultra violet

LIST OF TABLES

Table 1.1: Oxygen-activating metalloenzymes	2
Table 1.2: Properties of polyphenol oxidases from various sources	5
Table 1.3: Some plant polyphenol oxidases reported in the recent literature	7
Table 1.4: Examples of substrates and inhibitors of polyphenol oxidase	17
Table 1.5: Substrates of polyphenol oxidase in <i>Mucuna pruriens</i> cells	18
Table 1.6: Substrates of insect polyphenol oxidase	19
Table 1.7: Classification of copper proteins according to spectroscopic properties	23
Table 1.8: Derivatives of haemocyanin	25
Table 1.9: Derivatives prepared from tyrosinase	27
Table 1.10: Copper-catalysed oxidations of phenols	42
Table 1.11: Coordination geometry for Cu (I) and Cu (II)	45
Table 1.12: pK_b values for N-donor groups	46
Table 1.13: Examples of complexes with different bridging groups	51
Table 2.1: Application of polyphenol oxidase in organic solvents	70
Table 2.2: Results of ammonium sulphate fractionation of Extract A	76
Table 2.3: Extract A, B, and C: Protein concentrations and dopachrome activities	78
Table 2.4: Results of SDS-PAGE analysis of polyphenol oxidase extracts	80
Table 2.5: Correlation of activity with protein components in polyphenol oxidase extracts	82
Table 2.6: Water content of constituents of the biocatalytic system	89
Table 2.7: Effect of varying hydration on initial rates of reaction in the organic biocatalytic system	89
Table 2.8: Results of protein and activity assays of purified polyphenol oxidase	92
Table 2.9: Results of conversion of <i>p</i> -cresol to 4-methylcatechol, catalysed by polyphenol oxidase biocatalyst in chloroform	94
Table 2.10: Results from the oxidation of ATEE, catalysed by polyphenol oxidase biocatalyst, in chloroform	96
Table 2.11: Ammonium sulphate fractionation of extract A	98
Table 2.12: SDS-PAGE analysis of polyphenol oxidase extracts	100
Table 2.13: Determination of tyrosinase in extracts A, B and C by PAGE analysis	101
Table 2.14: Data from standard curve for protein determinations	102
Table 2.15: Protein assays for freeze-dried polyphenol oxidase extracts	103
Table 2.16: Dopachrome activities of biocatalysts containing extracts A, B, and C	104

Table 2.17: Results from organic assays to determine optimal hydration requirements in the biocatalytic system	105
Table 2.18: Data for protein standard curve using absorbance at 280 nm	106
Table 2.19: Results of activity and protein assays of fractions from DEAE-cellulose column	107
Table 2.20: Results of protein and activity assays of fractions from Toyopearl column	108
Table 2.21: Results of GC and UV analysis of samples from oxidation of <i>p</i> -cresol by tyrosinase	110
Table 2.22: Results of HPLC analysis of product from oxidation of <i>p</i> -cresol	110
Table 2.23: Results of GC analysis of oxidation of ATEE by polyphenol oxidase	111
Table 2.24: HPLC analysis of product from oxidation of ATEE	112
Table 2.25: Formation of DOPA: HPLC analysis of product	112
Table 3.1: Results of PAGE screening of substrates	121
Table 3.2: Phenols selected as substrates for the kinetic analysis using polyphenol oxidase	122
Table 3.3: Wavelengths of maximum absorbance for <i>o</i> -quinones	123
Table 3.4: Molar absorption coefficients determined using polyphenol oxidase	124
Table 3.5: Apparent kinetic parameters measured for the formation of <i>o</i> -quinones from a range of <i>p</i> -substituted phenols, by polyphenol oxidase in chloroform	127
Table 3.6: Correlation of kinetic parameters with steric, hydrophobic, and electronic properties of the substrates	130
Table 3.7: Dimensions of substrates from molecular modelling	132
Table 3.8: Results of PAGE screening of substrates	136
Table 3.9: Results of NMR determination of molar absorption coefficients	138
Table 3.10: 400 MHz ¹ H-NMR data for phenolic substrates and <i>o</i> -quinone products	139
Table 3.11: Data from measurement of initial rates of oxidation of <i>p</i> -alkylphenols	140
Table 3.12: Results of kinetic analysis of rate measurements	144
Table 4.1: Kinetic parameters determined for the oxidation of selected <i>p</i> -substituted phenols by biocatalysts prepared from extracts A and B	148
Table 4.2: Comparison of kinetic parameters determined for the oxidation of selected <i>p</i> -substituted phenols, using biocatalyst prepared from extracts A and C	153
Table 4.3: Rates of oxidation of <i>p</i> -cresol catalysed by the polyphenol oxidase biocatalyst in the presence of varying concentrations of SDS	156
Table 4.4: Comparison of kinetic parameters determined for the oxidation of selected <i>p</i> -substituted phenols by the polyphenol oxidase biocatalyst in the presence and absence of 2 mM SDS	158

Table 4.5: Comparison of the extent of denaturation occurring in the biocatalyst in the presence and absence of SDS	160
Table 4.6: Rates of oxidation of <i>p</i> -substituted phenols by polyphenol oxidase biocatalyst prepared from extract B	163
Table 4.7: Kinetic parameters for oxidation of <i>p</i> -substituted phenols, catalysed by biocatalyst prepared from extract B	164
Table 4.8: Rates of oxidation of <i>p</i> -substituted phenols by biocatalyst prepared from extract C	165
Table 4.9: Kinetic parameters calculated for the biocatalyst prepared from extract C	166
Table 4.10: Results of preliminary experiment to show the increase in reaction rates for the biocatalyst in the presence of SDS	167
Table 4.11: Comparison of rates of oxidation of <i>p</i> -cresol, catalysed by biocatalyst hydrated by buffer and water	167
Table 4.12: Rates of oxidation of <i>p</i> -cresol, catalysed by polyphenol oxidase biocatalyst in the presence of varying concentrations of SDS	168
Table 4.13: Rates of oxidation of <i>p</i> -substituted phenols, catalysed by the polyphenol oxidase biocatalyst in the presence of 2 mM SDS	169
Table 4.14: Kinetic parameters for the oxidation of <i>p</i> -substituted phenols catalysed by the polyphenol oxidase biocatalyst in the presence of SDS	171
Table 4.15: Dopachrome assays of activity in samples of biocatalyst exposed to SDS in chloroform for 18 h	172
Table 4.16: Rates of oxidation of <i>p</i> -cresol by biocatalyst after exposure to SDS for 18 h	172
Table 5.1: Data from continuous flow system; columns 1 - 9	174
Table 5.2: Water content in constituents of continuous flow system	179
Table 5.3: Protein concentrations in enzyme extracts	183
Table 5.4: Data from Column 1, converting <i>p</i> -cresol using crude enzyme	184
Table 5.5: Data from Column 2, using 50mM <i>p</i> -cresol as substrate	186
Table 5.6: Results from Column 3, using 20mM <i>p</i> -cresol as substrate	187
Table 5.7: Results obtained for Column 4, in the presence of SDS	188
Table 5.8: Data from Column 5, using partially purified enzyme	189
Table 5.9: Data from Column 6, using PVPP-treated enzyme	190
Table 5.10: Data from Column 7, using ATEE as substrate	191
Table 5.11: Data from Column 8, using <i>p</i> -isopropylphenol as substrate	192
Table 5.12: Data from Column 9, using <i>p</i> -isopropylphenol as substrate, in the presence of SDS	193

Table 6.1: Copper-copper separations in modelled complexes	203
Table 6.2: Conformational energy measurements for complexes I - XII	209
Table 6.3: Data obtained from modelling derivatives of complex III using HyperChem®	211
Table 7.1: Structures of complexes I - III, proposed for synthesis	218
Table 7.2: ¹ H NMR spectral data for Complexes IIB and 91	228
Table 7.3: Decomposition of complex I	245
Table 7.4: Data for decomposition of Complex I	254
Table 8.1: Examples of UV-visible d-d absorptions of copper (II) complexes	260
Table 8.2: MLCT absorptions of copper (I) complexes	261
Table 8.3 UV-visible spectral features of products from reactions of copper complexes with oxygen	262
Table 8.4: Analysis of the copper content in the copper complexes by atomic absorption spectrophotometry	266
Table 8.5: Results of UV-visible spectral analysis of copper complexes	268
Table 8.6: Results of cyclic voltammetric analysis of complexes	283
Table 8.7: Transitions observed in UV-visible spectra of copper complexes	285
Table 8.8: Copper (II) d-d transitions observed for oxygenated copper complexes	286
Table 8.9: Results of atomic absorption analysis	288
Table 8.10: Results of UV-Visible analysis of Copper complexes	289
Table 8.11: Conditions used to measure cyclic voltammograms of copper complexes	291
Table 9.1: Results of TLC analysis of reaction mixtures resulting from the oxidation of DTBP and DTBC, catalysed by copper complexes	297
Table 9.2: ¹ H NMR and IR spectral data for DTBC, DTBQ, and the product of the catalytic oxidation of DTBC	298
Table 9.3: Spectral data for the coupled product 11	299
Table 9.4: Extent of oxidative coupling of DTBP, catalysed by copper complexes	299
Table 9.5: Analysis of enzyme kinetic data obtained with DTBC as substrate	305
Table 9.6: Analysis of enzyme kinetic data obtained using DTBP as substrate	305
Table 9.7: Catalytic efficiencies of the copper complexes	306
Table 9.8: Photometric data for the oxidation of DTBP by complex I	314
Table 9.9: Ratio of product:substrate from integrals in ¹ H NMR spectrum of DTBP	316
Table 9.10: Rates of absorbance increase recorded for oxidations of DTBC, catalysed by copper complexes	318

Table 9.11: Rates of absorbance increase recorded for oxidations of DTBP catalysed by copper complexes	319
Table 9.12: Initial reaction rates measured for the oxidation of DTBC, catalysed by copper complexes	320
Table 9.13: Initial reaction rates measured for oxidation of DTBP catalysed by copper complexes	321

LIST OF SCHEMES

Scheme 1.1: The biosynthesis of melanins	4
Scheme 1.2: Formation of lignins <i>via</i> the phenylpropanoid pathway	6
Scheme 1.3: Quinone tanning in insect cuticle	9
Scheme 1.5: Mechanism of polyphenol oxidase proposed by Mason (1959)	11
Scheme 1.6: Mechanism for polyphenol oxidase proposed by Ochiai (1973)	11
Scheme 1.7: Mechanism for polyphenol oxidase proposed by Lerch (1981)	13
Scheme 1.8: Mechanism for polyphenol oxidase activity, and the phenolase lag phase (Garcia-Carmona <i>et al.</i> , 1987)	14
Scheme 1.9: Reaction sequence proposed to explain the reaction inactivation of polyphenol oxidase by catechol	14
Scheme 1.10: pH-Dependent formation of dopachrome	15
Scheme 1.11: The reaction pathway of dopachrome decarboxylation	16
Scheme 1.12: Hydroxylation of estradiol by tyrosinase	18
Scheme 1.13: Coupled products resulting from tyrosinase-catalysed reactions	19
Scheme 1.14: Inhibition of polyphenol oxidase by azide ions	21
Scheme 1.15: Proposed mechanism for reaction of copper (II)/amine systems	44
Scheme 1.16: Synthesis of complex 57	57
Scheme 1.17: Proposed mechanism for monooxygenase activity of macrocyclic complexes	64
Scheme 1.18: Mechanism proposed for a side-on bridged dicopper site	65
Scheme 1.19: Proposed mechanism for models of tyrosinase	66
Scheme 1.20: Proposed mechanism for tyrosinase monooxygenase activity	67
Scheme 6.1: Complexes to be modelled by molecular mechanics, prior to their proposed synthesis	198
Scheme 6.2: Complexes modelled using ALCHEMY II®	200
Scheme 6.3: Derivatives of complex III, including binding of dioxygen and DTBP, modelled using HyperChem®	210
Scheme 7.1: Preparation of biphenyl-2,2'-dicarbaldehyde 86	221
Scheme 7.2: Preparation of complex I	222
Scheme 7.3: Preparation of complexes IIA - IIC	226
Scheme 7.4: Preparation of complexes IIIA and IIIB	234
Scheme 9.1: Mechanism of oxidation of catechols by dinuclear copper complexes	311
Scheme 9.2: Mechanism of oxidative phenolic coupling	312

LIST OF FIGURES

Figure 1.1 A spectroscopically effective model for oxyhaemocyanin proposed by Solomon (1983)	25
Figure 1.2: Mechanism of phenolic binding to tyrosinase	29
Figure 1.3: Proposed mechanism for tyrosinase phenolase activity	31
Figure 1.4: Proposed mechanism for the oxidation of catechols, catalysed by CuCl/pyridine	43
Figure 1.5: Model of the dinuclear copper binding site	48
Figure 1.6: Possible modes of binding of oxygen in dinuclear copper binding site	54
Figure 1.7: Proposed model for bonding of oxygen in haemocyanin	59
Figure 2.1: Procedure for fractional ammonium sulphate precipitation of crude polyphenol oxidase	76
Figure 2.2: SDS-PAGE analysis of polyphenol oxidase extracts	79
Figure 2.3: Non-denaturing PAGE of polyphenol oxidase extracts	83
Figure 2.4: Graph of absorbance vs time for a typical dopachrome assay	86
Figure 2.5: Absorbance vs time graph for a typical biocatalytic assay in the organic system, using <i>p</i> -cresol as the substrate	87
Figure 2.6: Correlation of dopachrome and <i>p</i> -cresol assays for biocatalyst prepared from crude extract A	88
Figure 2.7: Elution profile of protein and polyphenol oxidase activity for DEAE-cellulose column	90
Figure 2.8: Elution profile for protein and polyphenol oxidase activity for size exclusion (Toyopearl HW-50S) column	91
Figure 2.9: Progress of the utilisation of <i>p</i> -cresol by polyphenol oxidase in the biocatalytic system	94
Figure 2.10: Graph of GC count vs time for the conversion of ATEE, catalysed by polyphenol oxidase	95
Figure 2.11: Graph of mobility vs log(Molecular mass) from SDS-PAGE results	99
Figure 2.12: Standard curve for protein determinations using Folin-Lowry method	102
Figure 2.13: Protein standard curve using absorbance at 280 nm	107
Figure 3.1: Graph of initial rate v against substrate concentration s for an enzyme-catalysed reaction which obeys the Michaelis-Menten equation	115
Figure 3.2: Hanes plot of s/v against s , used to determine kinetic parameters	116
Figure 3.3: Photographs showing PAGE gels stained to detect tyrosinase activity using a range of substrates: tyrosine (A), DOPA (B), and <i>p</i> -cresol (C)	120

Figure 3.4: UV-visible spectra showing the formation of 4-methyl- <i>o</i> -benzoquinone from <i>p</i> -cresol, catalysed by polyphenol oxidase in chloroform.	123
Figure 3.5: ¹ H NMR spectra of reaction mixtures used to determine molar absorption coefficients for <i>o</i> -quinones .	125
Figure 3.6: Graph of v vs s for the oxidation of <i>p</i> -cresol by polyphenol oxidase in chloroform	126
Figure 3.7: Hanes plots obtained from kinetic measurements using polyphenol oxidase to oxidise selected <i>p</i> -substituted phenols	128
Figure 3.8: Correlation of catalytic efficiency (A) and Michaelis constant (B) of the polyphenol oxidase biocatalyst with the steric nature of <i>p</i> -substituted phenols	129
Figure 3.9: Correlation of catalytic efficiencies for the oxidation of phenolic substrates, catalysed by polyphenol oxidase; substrates: <i>p</i> -alkylphenols (A), and <i>p</i> -halophenols and <i>p</i> -methoxyphenol (B)	131
Figure 3.10: Proposed "Box" model of the binding pocket in polyphenol oxidase in chloroform, with <i>t</i> -butylphenol molecule "fitted" into available space	133
Figure 4.1: Hanes plots for the oxidation of selected <i>p</i> -substituted phenols, catalysed by the biocatalyst prepared from partially purified polyphenol oxidase extract B (units of s/v are min.mg); substrates: (A) <i>p</i> -cresol (B) <i>p</i> -fluorophenol (C) <i>p</i> -isopropylphenol	149
Figure 4.2: Comparisons of the kinetic parameters determined for selected <i>p</i> -substituted phenols, catalysed by polyphenol oxidase biocatalyst prepared from extract B	150
Figure 4.3: Hanes plot for the oxidation of selected <i>p</i> -substituted phenols, catalysed by the biocatalyst prepared from extract C; substrates: (A) <i>p</i> -cresol (B) <i>p</i> -fluorophenol (C) <i>p</i> -isopropylphenol	152
Figure 4.4: Comparison of the kinetic parameters for the oxidation of selected <i>p</i> -substituted phenols, catalysed by biocatalysts prepared from the extracts A and C	154
Figure 4.5: Hanes plots for the oxidation of selected <i>p</i> -substituted phenols, catalysed by the polyphenol oxidase biocatalyst prepared from extract A, in the presence of 2 mM SDS; substrates: (A) <i>p</i> -cresol (B) <i>p</i> -isopropylphenol (C) <i>p</i> - <i>tert</i> -butylphenol (D) 2,4-di- <i>tert</i> -butylphenol (DTBP)	157
Figure 4.6: Comparison of kinetic parameters for the oxidation of selected <i>p</i> -substituted phenols, catalysed by the polyphenol oxidase biocatalyst prepared from extract A, in the presence of 2 mM SDS	159

Figure 5.1: Continuous flow system	175
Figure 5.2: Rates of reaction for Columns 2 and 3	176
Figure 5.3: Peaks from GC analysis for Column 5	177
Figure 5.4: Rates of reaction for Columns 5 (A), 7 (B), and 9 (C)	180
Figure 6.1: Rearrangement of the copper coordination upon binding of phenol	199
Figure 6.2: Conformations of spacers in copper complexes	202
Figure 6.3: Photographs showing the open conformations of biomimetic models of complexes III and IX, prior to addition of the dioxygen bridge	204
Figure 6.4: Photographs showing the conformations of biomimetic models with dioxygen bridges, modelled using Alchemy II®	205
Figure 6.5: Photographs showing models of derivatives of complex III	212
Figure 7.1: Relative rotation of the phenyl rings in the biphenyl spacer	218
Figure 7.2: ¹ H NMR spectrum of biphenyl-2,2'-dicarbaldehyde 86	223
Figure 7.3: IR spectrum of ligand 89, used to prepare complex I	224
Figure 7.4: 60 MHz ¹ H NMR spectrum of ligand 89	224
Figure 7.5: ¹ H NMR spectrum (A) and ¹³ C NMR spectrum (B) of complex I	225
Figure 7.6: IR spectra of complex IIA (A) and complex IIB (B)	228
Figure 7.7: ¹ H NMR spectrum of complex IIA	229
Figure 7.8: ¹ H NMR spectrum of complex IIB	229
Figure 7.9: ¹ H NMR spectrum of crude ligand 92	231
Figure 7.10: ¹ H NMR spectrum of ligand 92 after purification by flash chromatography	231
Figure 7.11: ¹ H NMR spectrum (A) and ¹³ C NMR spectrum of ligand 94	232
Figure 7.12: ¹ H NMR spectrum of complex IIC in CD ₃ COCD ₃	235
Figure 7.13: ¹ H NMR spectrum of complex IIC in CD ₃ CN	235
Figure 7.14: ¹ H NMR spectrum of 2-(2-aminoethyl)benzimidazole 96	236
Figure 7.15: ¹ H NMR spectrum of ligand 97	236
Figure 7.16: ¹ H NMR spectrum (A) and ¹³ C NMR spectrum (B) of ligand 98	237
Figure 7.17: ¹ H NMR spectrum (A) and ¹³ C NMR spectrum of complex IIIA in CD ₃ CN	239
Figure 7.18: ¹ H NMR spectrum of complex IIIA in CD ₃ OD in the absence (A) and the presence (B) of air	240
Figure 7.19: ¹ H NMR spectra of complex IIIA in CD ₂ Cl ₂ in the absence (A) and the presence (B) of air	241

Figure 7.20: ^1H NMR spectrum of complex IIIB in CD_3CN	243
Figure 7.21: ^1H NMR spectrum of the reaction mixture containing biphenyl-2,2'-dicarbaldehyde 86 and $[\text{Cu}(\text{MeCN})_4][\text{PF}_6]$	244
Figure 7.22: ^1H NMR spectrum of the reaction mixture containing 2-(2-aminoethyl)benzimidazole 96 and $[\text{Cu}(\text{MeCN})_4][\text{PF}_6]$	244
Figure 7.23: 2-D NMR (HETCOR) spectra of ligand 94	256
Figure 7.24: 2-D NMR [COSY (A) and HETCOR (B)] spectra of ligand 98	257
Figure 7.25: 2-D NMR (HETCOR) spectrum of complex IIIB	258
Figure 7.26: Graph of $\ln(A_\infty - A_0/A_t - A_0)$ vs time for the decomposition of complex I	255
Figure 8.1: A typical cyclic voltammogram, for the redox process $\text{X} \rightarrow \text{X}^+$	265
Figure 8.2: UV spectrum for complex I in MeCN (A) in the absence of air at 25°C ; (B) in the presence of air at 25°C ; (C) in the absence of air at -70°C ; (D) in the presence of air at -70°C	274
Figure 8.3: UV spectrum for complex I in MeOH (A) in the absence of air at 25°C ; (B) in the presence of air at 25°C	274
Figure 8.4: UV spectrum for complex I in CH_2Cl_2 (A) in the absence of air at 25°C ; (B,C) in the presence of air at 25°C ; (D) in the absence of air at -70°C ; (E) in the presence of air at -70°C	275
Figure 8.5: UV spectrum for complex IIC in MeCN (A) in the absence of air at 25°C ; (B) in the presence of air at 25°C ; (C) in the absence of air at -70°C ; (D) in the presence of air at -70°C	276
Figure 8.6: UV spectrum for complex IIC in MeOH (A) in the absence of air at 25°C ; (B,C) in the absence of air at -70°C ; (D) in the absence of air at -70°C ; (E) in the presence of air at -70°C	277
Figure 8.7: UV spectrum for complex IIC in CH_2Cl_2 (A) in the absence of air at 25°C ; (B) in the presence of air at 25°C	278
Figure 8.8: UV spectrum for complex IIA in MeCN (A) in the absence of air at 25°C ; (B) in the presence of air at 25°C ; (C) in the absence of air at -70°C ; (D) in the presence of air at -70°C	278
Figure 8.9: UV spectrum for complex IIA in MeOH (A) in the absence of air at 25°C ; (B) in the presence of air at 25°C ; (C) in the absence of air at -70°C ; (D) in the presence of air at -70°C	279
Figure 8.10: UV spectrum for complex IIA in CH_2Cl_2 (A) in the absence of air at 25°C ; (B) in the presence of air at 25°C	279
Figure 8.11: UV spectrum for complex IIB in CH_2Cl_2 (A) in the absence of air at 25°C ; (B) in the presence of air at 25°C	280

Figure 8.12: UV spectrum for complex IIIA in MeCN (A) in the absence of air at 25°C; (B) in the presence of air at 25°C	280
Figure 8.13: UV spectrum for complex IIIA in MeOH (A) in the absence of air at 25°C; (B,C) in the presence of air at 25°C	280
Figure 8.14: UV spectrum for complex IIIA in CH ₂ Cl ₂ (A) in the absence of air at 25°C; (B) in the presence of air at 25°C; (C) in the absence of air at -70°C; (D) in the presence of air at -70°C (E) oxidation product IIIA'	281
Figure 8.15: UV spectrum for complex IIIB in CH ₂ Cl ₂ (A) in the absence of air at 25°C; (B,C) in the presence of air at 25°C	282
Figure 8.16: Cyclic voltammograms obtained for dinuclear copper complexes: (A) complex I (B) complex IIA (C) complex IIB (D) complex IIC (E) complex IIIA (F) complex IIIB; numbers show potentials of redox reactions	284
Figure 8.17: Standard curve for AA analysis of copper	287
Figure 9.1: UV-visible spectra of DTBP (A) and DTBC (B), before and after oxygenation	294
Figure 9.2: UV-visible spectra of the products of oxidation of DTBP (A) and DTBC (B), catalysed by complex I	295
Figure 9.3: Rates of oxidation of DTBP, catalysed by complex I, in the presence (1) and (2), and the absence (3) and (4), of triethylamine	295
Figure 9.4: ¹ H NMR spectra of DTBP (A), DTBC (B) and DTBQ (C)	300
Figure 9.5: ¹ H NMR spectra of the reaction mixture obtained in the oxidation of DTBC, catalysed by the complex IIIA	301
Figure 9.6: ¹ H NMR spectra of DTBQ obtained by TLC after oxidation of DTBC, catalysed by complex IIB	301
Figure 9.7: ¹ H NMR spectra of the reaction mixtures obtained in the oxidation of DTBP, catalysed by the complexes I (A), IIB (B), IIIA (C) and IIIB (D)	302
Figure 9.8: ¹ H and ¹³ C NMR spectra of the product of oxidation of DTBP, catalysed by the complex IIIB	303
Figure 9.9: IR spectra of the oxidation products obtained in the oxidation of DTBC (A) and DTBP (B), catalysed by complex IIIB	304
Figure 9.10: Hanes plots for the oxidation of DTBC, catalysed by the copper complexes	307
Figure 9.11: Hanes plots for the oxidations of DTBP, catalysed by the copper complexes	308

ACKNOWLEDGEMENTS

I am indebted to many colleagues and friends who have assisted and encouraged me over the four years that this research has taken.

My supervisors, Professor John Duncan, Professor Perry Kaye and Professor Peter Rose, have given me a great deal of advice, support and encouragement, for which I thank them very sincerely. I am also very grateful to Professor John Duncan for facilitating my two trips overseas, to attend international conferences on biocatalysis which were invaluable in the development of this thesis.

I would also like thank AECL (pty) Ltd. for very generous financial support, and researchers in the Biotechnology and Chemistry divisions of AECL Research and Development for their interest. In particular, I am grateful to Mr. Colin Kenyon, Dr. Clive Moore, Dr. John Strachan and Dr. Jannie Pretorius for their assistance.

The polyphenol oxidase project at Rhodes University was initiated by Dr. Patsy Goetsch, and I am grateful to her for her help in getting started. Discussions with Dr. Tobela Nyokong, about some (to me) unfamiliar areas of physical and inorganic chemistry, have been most enlightening. She also assisted with the electrochemical investigation, and I wish to thank her for her time and interest.

Scientific research is not possible without the support of efficient technicians and I would like to thank Miss Moira Pogrand, Mr Aubrey Sonemann, Mr Andy Soper and Mr John Keulder for their willing and expert assistance. I am eternally grateful to Dr. Mike Davies-Coleman and Professor Lambe Parolis for help with the production of this thesis. I would also like to thank Dr. Dean Brady and Miss Cathy Logie for their efficient proof-reading of the thesis, and Mrs Joan Miles for her cooperation in the word-processing.

My family have made inestimable contributions towards this degree. My husband, Mike, has lived with me and learned with me, supported me and believed in me through some difficult times, and his devotion even extended to his undertaking the typing of the reference section of this thesis. My daughters, Justine and Leigh, have also been very helpful, patient and understanding. I would like them all to know that I have valued their support and friendship.

This thesis is dedicated to my family, in appreciation of their confidence in me.

CHAPTER 1

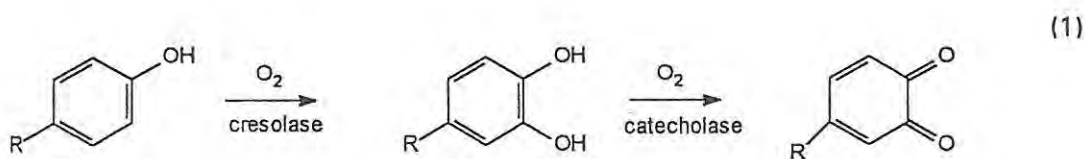
INTRODUCTION

The research fields of Biocatalysis and Biomimetics have the common aim of combining biological and chemical principles in endeavouring to exploit the potential of enzymic catalysis. This thesis reports a study on polyphenol oxidase from these two major perspectives. Firstly, the potential of the enzyme as a biocatalyst for application in organic syntheses was explored, and secondly, some theoretical and practical aspects of chemical models for the enzyme were investigated. This introduction gives a survey of the literature relating to the nature of polyphenol oxidase as well as to biocatalytic and biomimetic research on the enzyme. The objectives of the present study are defined at the end of this chapter.

1.1 POLYPHENOL OXIDASE

1.1.1 Background

Polyphenol oxidases (EC 1.14.18.1) are monooxygenases which catalyse two reactions, *viz.*, the *ortho*-hydroxylation of phenols and the oxidation of catechols (1,2-dihydroxybenzenes) to *ortho*-quinones utilising molecular oxygen [reaction (1)]. Phenols and catechols can be substrates for the enzymes, and the product of the reaction is generally found to be the *o*-quinone in both cases. The initial reaction (hydroxylation of the phenol) is often referred to as "cresolase" or "phenolase" activity, and the second reaction (oxidation of the catechol) is called "catecholase" activity (Kertesz and Zito, 1965). These terms are in common use, and they are used in this thesis to differentiate between the two reactions. The *o*-quinone products usually undergo subsequent chemical reactions to give characteristic dark coloured compounds known collectively as melanins.



In common with a number of other oxygen-activating enzymes (see Table 1.1), polyphenol oxidases are metalloenzymes, the metal in the active site being copper. The names "tyrosinase", "phenol oxidase" and "polyphenolase" are also commonly used for this enzyme, and "tyrosinase" is used interchangeably with "polyphenol oxidase" in this thesis.

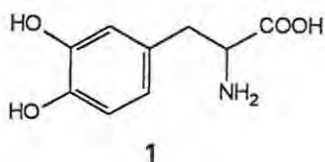
The first tyrosinase was discovered in 1895 when a black pigment was observed in the mushroom *Russula nigricans* (Bourquelot and Bertrand, 1895). The enzyme was named "tyrosinase" in reference to the substrate, tyrosine, which was found to be converted into the black pigment (Bertrand, 1896). Subsequently, polyphenol oxidases have been found to be widely distributed in both the plant and animal kingdoms, where their functions are mainly in pigment production for defensive purposes (Lerner and Fitzpatrick, 1950). In spite of the endeavours of numerous chemists and biologists in research spanning almost a century, and the accumulation of an enormous literature, the structures of most polyphenol oxidases are not yet fully elucidated. The properties of their binding sites and the mechanisms of their reactions remain the subject of wide-ranging current research.

Table 1.1: Oxygen-activating metalloenzymes (Karlín and Gultneh, 1985, and Vigato *et al.*, 1990)

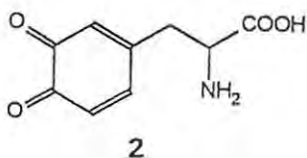
Enzyme	Example	Occurrence	Function
Blue oxidases	Laccase Ascorbate oxidase Ceruloplasmin	Fungi, plants Plants Serum	Oxidation Oxidation Oxidation, metal transport
Non-blue oxidases	Amine oxidase Galactose oxidase	Animals Moulds	Collagen formation Galactose oxidation
Oxygen carriers	Haemocyanin	Molluscs, arthropods	Oxygen transport
Copper mono-oxygenases	Polyphenol oxidase Dopamine β -hydroxylase	Plants, skin, insects, melanoma Adrenals	Aromatic hydroxylation and oxidation Noradrenalin formation
Enzymes containing other metals as well as or in place of copper	Superoxide dismutase Cytochrome c oxidase Methane monooxygenase	Red blood cells Mitochondria Bacteria	Peroxide detoxification Oxygen reduction Oxygen reduction, alkane oxidation

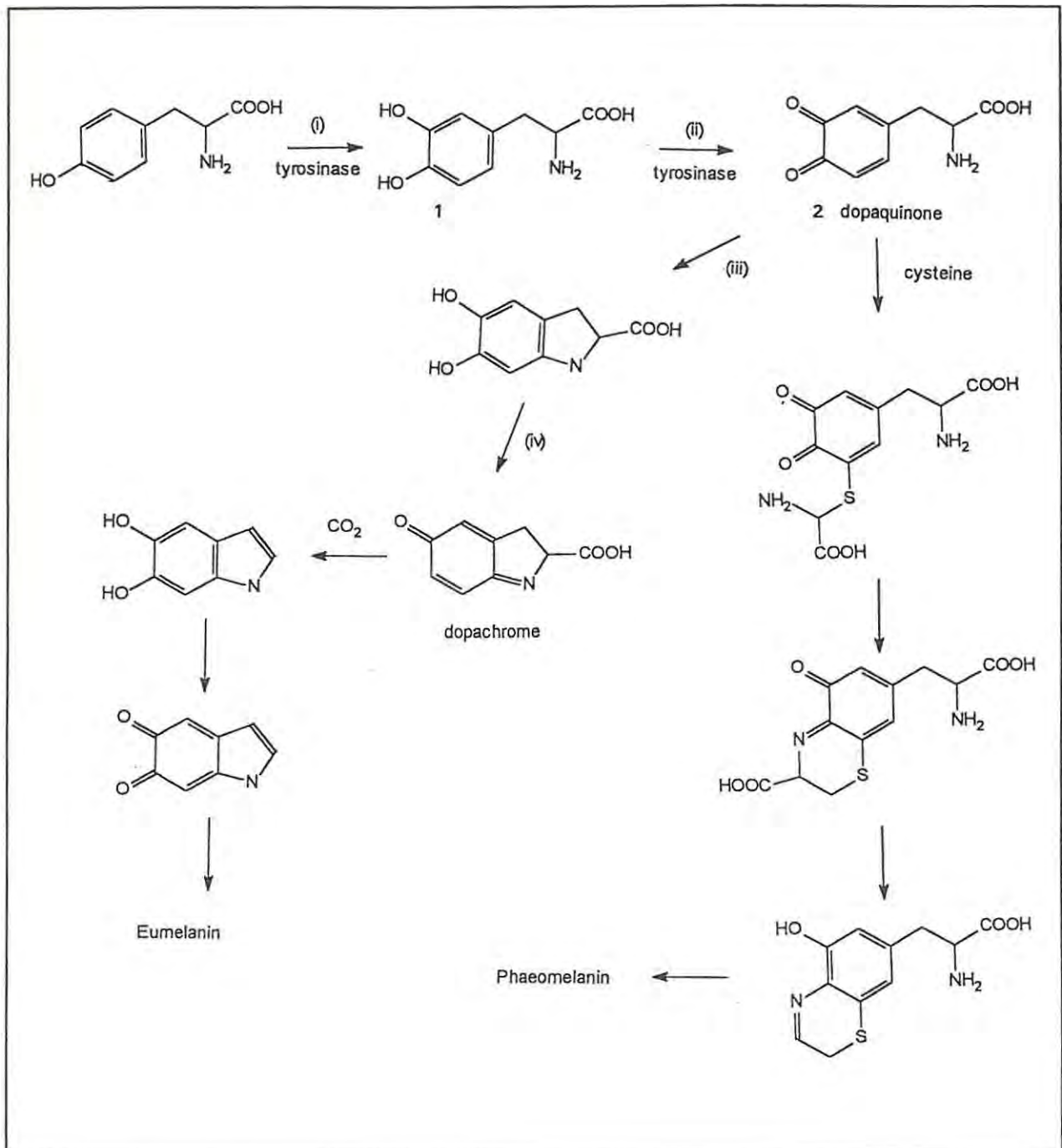
1.1.2 Early research on tyrosinase, and melanin biosynthesis

The *o*-quinones resulting from the oxidative activity of tyrosinase undergo a complex series of non-enzymic chemical changes which ultimately yield melanins. These are complex, high molecular weight polymeric pigments, found uncombined or conjugated with proteins, in pigmented tissues. The protective and cosmetic significance of their role in human pigmentation in particular, prompted much of the early research into the activity of mammalian tyrosinase. In addition, the presence of intense melanoid pigmentation in melanoma cells has stimulated interest in the link between tyrosinase activity and cancer. In initial studies involving human diseases, correlations were established between adrenal hypofunction and increased pigmentation in sufferers of Addison's disease, and between melanoma and the presence of catechol derivatives in the urine. When mammalian polyphenol oxidase was discovered in human cells, Block (1927, cited in Lerner and Fitzpatrick, 1950) proposed that it should be named "DOPA oxidase" in view of its specificity for the substrate 3,4-dihydroxyphenylalanine (DOPA), 1. Both cresolase and catecholase activities were later found in other mammalian cells, however, and the name was changed to tyrosinase (Lerner and Fitzpatrick, 1950).



The intermediacy of DOPA in the conversion of tyrosine to melanins, and the utilisation of molecular oxygen, were proved as early as 1928 (Raper, 1928). Mason (1947 and 1959) made much progress towards elucidating the reactions leading to the formation of melanins. Scheme 1.1 shows a general pathway for the formation of melanins (Hearing and Jimenez, 1987). Only the initial steps, (i) and (ii) are enzyme-catalysed, and the subsequent interconversions are spontaneous chemical reactions resulting from the reactivity of the *o*-quinones. Thus the black skin pigment, eumelanin, is formed as granules (melanosomes) in the melanocyte cells in animals. Phaeomelanins, the pigments responsible for the red and yellow colours in hair, feathers and fur, are formed by interaction of the intermediate, dopaquinone, (2, Scheme 1.1) with cysteine to produce sulphur-containing polymers (Prota, 1972).





Scheme 1.1: The biosynthesis of melanins (Hearing and Jimenez, 1987)

1.1.3 Polyphenol oxidases from various sources

Polyphenol oxidases have been found in groups as diverse as prokaryotes, fungi, higher plants, arthropods, amphibians and mammals. Potato polyphenol oxidase, for instance, was discovered in 1938 and was used to show the presence of copper in the polyphenol oxidase active site

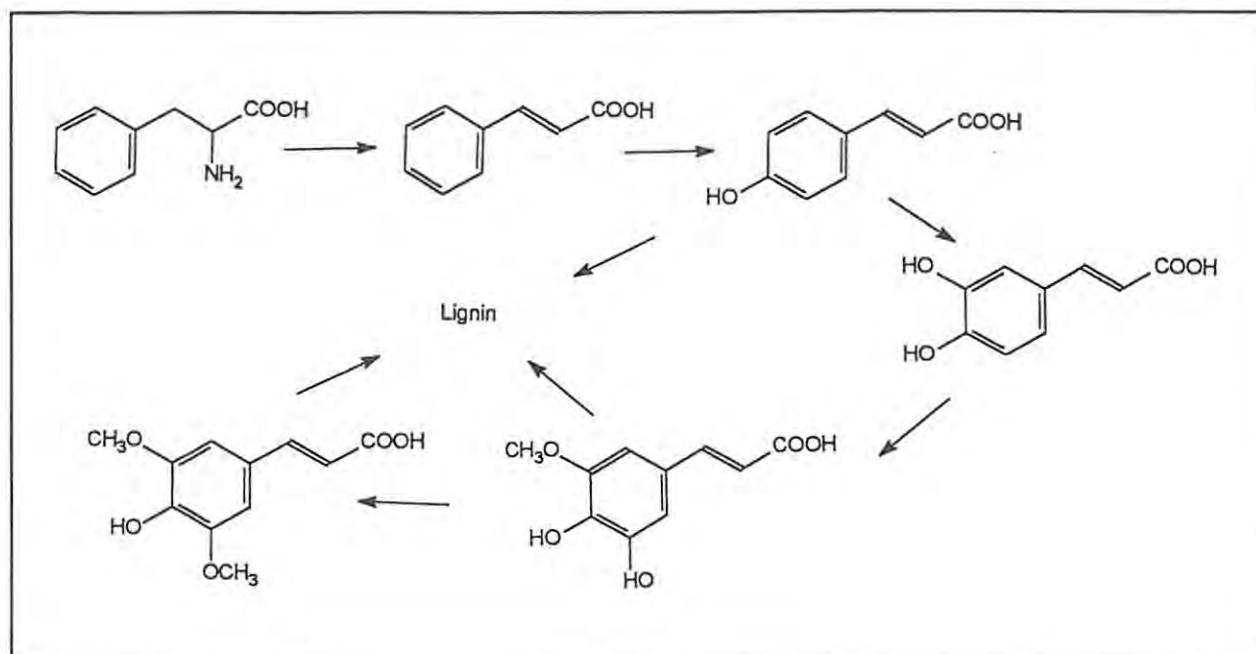
(Kubowitz, 1938). In all cases, the enzymes are found to occur in more than one active form, and many are polymeric (see Table 1.2). Mushroom tyrosinase is unusual in having non-identical subunits (see Section 1.1.3). The substrate specificity of the enzymes varies from plant sources (where a number of different phenolic and catecholic substrates are oxidised) to higher animals (where the specificity is quite narrow) and mammalian cells (which utilise only DOPA or closely related substrates) (Robb, 1984).

Table 1.2: Properties of polyphenol oxidases from various sources (Lerch, 1981)

Source	Molecular weight	Properties
<i>Streptomyces</i>	29000	2 copper atoms per molecule
<i>Neurospora</i>	46000	2 copper atoms per molecule 2 allelic forms
Mushroom	26000 - 120000	4 copper atoms per tetramer 4 isoenzymic forms
Potato	290000	4 copper atoms per molecule Various forms
Insect	80000	2 copper atoms per molecule 2 subunits
Human melanoma	66700	2 copper atoms per molecule Various forms

1.1.3 (1) Plant polyphenol oxidases

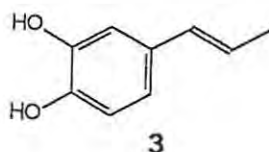
The role of plant polyphenol oxidases is usually protective; melanins are formed at injury sites, and act as a physical barrier as well as being bacteriostatic. It has also been suggested that polyphenol oxidases are involved in the formation of lignins, *via* the phenylpropanoid pathway (Scheme 1.2) (Robb, 1984).



Scheme 1.2: Formation of lignins *via* the phenylpropanoid pathway (Robb, 1984)

Many plant polyphenol oxidases are present in the plant in a latent or inactive form which is activated by solubilisation, activator binding, or proteolysis, *e.g.* broad bean polyphenol oxidase (Robb *et al.*, 1966 and 1984) and grape polyphenol oxidase (Lerner and Mayer, 1976). This aspect is discussed in more detail in Chapter 4.

Plant polyphenol oxidases are also of great importance in the food industry, where enzymic browning, *i.e.* the formation of melanins on cut surfaces of foods such as bananas and potatoes, may be undesirable. Fermentation of tea also involves tyrosinase activity however, where it results in desirable flavour and colour changes (Scott, 1975). Grape polyphenol oxidases have been extensively studied because of the importance of quinone reaction products such as caffeoyl tartrate **3**, in wine (Cheynier *et al.*, 1990; Sánchez-Ferrer and García-Carmona, 1992a).



The literature on plant polyphenol oxidases is extensive, and since it is not possible to provide an exhaustive citation, some representative examples are summarised in Table 1.3.

Table 1.3: Some plant polyphenol oxidases reported in the recent literature

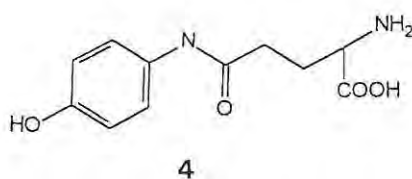
Source	Result	Reference
Apple	Substrate: chlorogenic acid; optimum pH 4.0	Murata <i>et al.</i> , 1992
<i>Arctium lappa</i>	Substrate: phloroglucinol, chlorogenic acid	Murao <i>et al.</i> , 1993
Spinach	Low activity in winter, inhibited by oxalate, activated by Cu ²⁺	Watanabe <i>et al.</i> , 1991
Avocado pear	Membrane bound, activated by trypsin	Medina <i>et al.</i> , 1991
Cucumber	Present only in skin	Miller <i>et al.</i> , 1990
Peach	Various substrates	Lee <i>et al.</i> , 1990
Pears	Enzyme purified by removal of endogenous phenolics	Smith and Montgomery, 1985
Grape	Most activity in mature and crushed grapes	Wisseman and Lee, 1980
Potato	Substrates: tyrosine, DOPA, chlorogenic acid; sequential mechanism	Matheis and Belitz, 1977

1.1.3 (2) Mushroom polyphenol oxidase

The tyrosinase found in the common mushroom, *Agaricus bisporus*, has been utilised in many studies, since it is readily obtainable in relatively large quantities. The existence of several isoenzymes, which are interconvertible to some extent (depending on factors such as pH, buffer ionic strength, and protein concentration) was demonstrated by Jolley and Mason (1965). These authors suggested that monomeric units could associate to form dimers and higher polymers such as a tetramer, and that the isoenzymes were a result of this multiplicity. The low molecular weight isoenzymes were found to be active, and therefore contained at least one active site. Before the pairing of the copper atoms in tyrosinase was known, a minimal molecular weight of 31800 per copper atom was regarded as applying to one subunit of the enzyme (Kertesz, 1965). The tetrameric form was suggested to be the major active form of mushroom tyrosinase (Jolley *et al.*, 1974) but the quaternary structure was only elucidated when the dissimilar nature of the subunits was discovered (Strothkamp *et al.*, 1976). The β -isoenzyme was isolated and found to have two types of subunit, called the "light" and "heavy" subunits. Their molecular weights were found to be 13400 and 43000 respectively. The tetrameric form was shown to be composed of two light and two heavy subunits, making up a molecular weight of 112800 which was close to the

observed value of 120000. The predominant smaller isoenzyme, observed to have a molecular weight of 69000, comprised one heavy and two light subunits. The subunits could be separated by treatment with detergents and heat, and re-aggregated in detergent-free solutions. Four isoenzymes are currently recognised, *viz.*, α , β , γ , and δ forms. They exhibit differences in their ratios of cresolase and catecholase activities (Lerch, 1981).

In addition to the role of formation of melanins for protection, a metabolic regulatory function has been proposed for the polyphenol oxidase in mushrooms. The oxidation of γ -L-glutaminy-4-hydroxybenzene 4 produces the corresponding quinone, and this product is thought to inhibit some sulphhydryl dependent enzymes, hence inducing dormancy (Boekelheide, 1980).



1.1.3 (3) Other microbial polyphenol oxidases

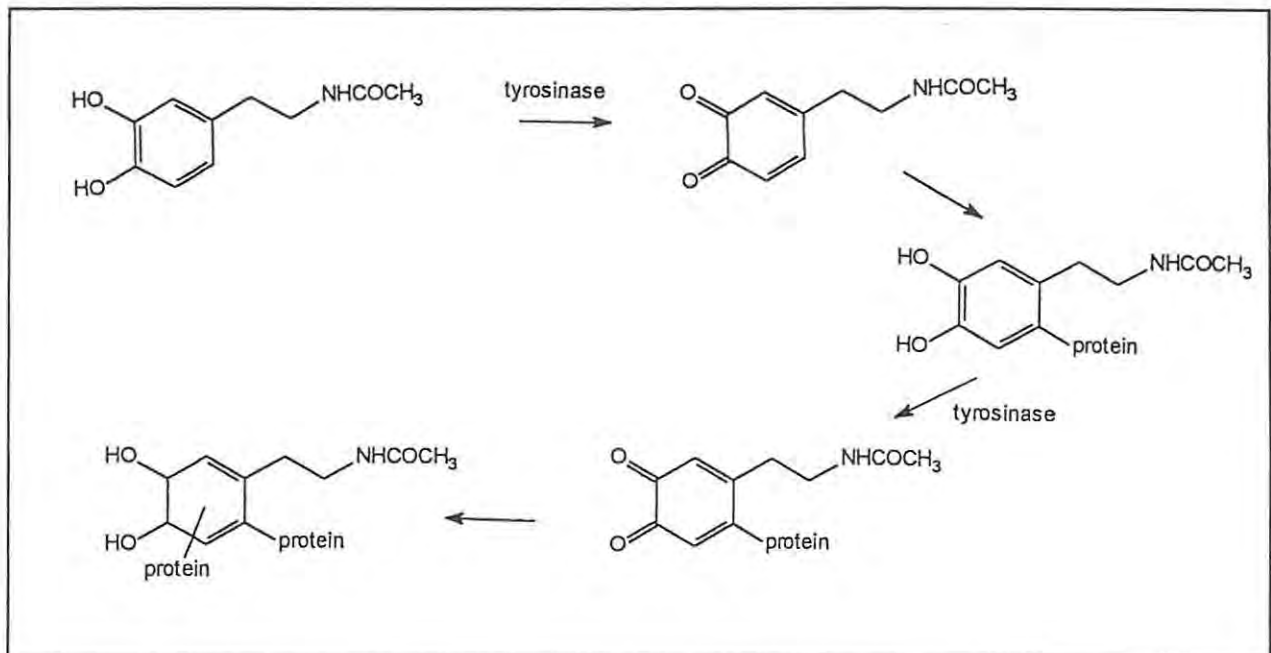
While a number of bacteria have been found to produce tyrosinase, the most studied sources are *Streptomyces glaucescens* and *Neurospora crassa*. The *Neurospora* enzyme was first purified for study in 1963 (Fling *et al.*, 1963) and four forms were reported, with a molecular weight of approximately 33000 for the monomeric unit, and differing in thermostability and electrophoretic properties. Since this enzyme could be produced and purified relatively easily, and because it was found to be simpler in structure than the mushroom enzyme, it has been studied extensively. Horowitz *et al.* (1970) reported an effective purification and assay procedure using DOPA as the substrate. Valuable information, much of which is now found to be relevant to all tyrosinase enzymes, has been reported by Lerch and co-workers. These authors have established the amino acid sequence, copper coordination sites, and kinetic properties of the *Neurospora* enzyme. (Lerch, 1976; Deinum *et al.*, 1976; Pfiffner and Lerch, 1981; Lerch 1982; Lerch, 1983; Lerch *et al.*, 1986; Huber and Lerch, 1987). The molecular weight was correctly established as 42000, and the copper atoms were found to occur in pairs, one pair per molecule, coordinated by histidine residues. The structure and mechanism of *Neurospora* tyrosinase are discussed in the relevant sections in this introduction.

The polyphenol oxidase obtained from *Streptomyces* shares 24% homology with the *Neurospora* enzyme, and has a molecular weight of approximately 30000 (Huber *et al.*, 1985). It exhibits slight differences from the latter enzyme, in activity, specificity, and the ligand environment of the copper

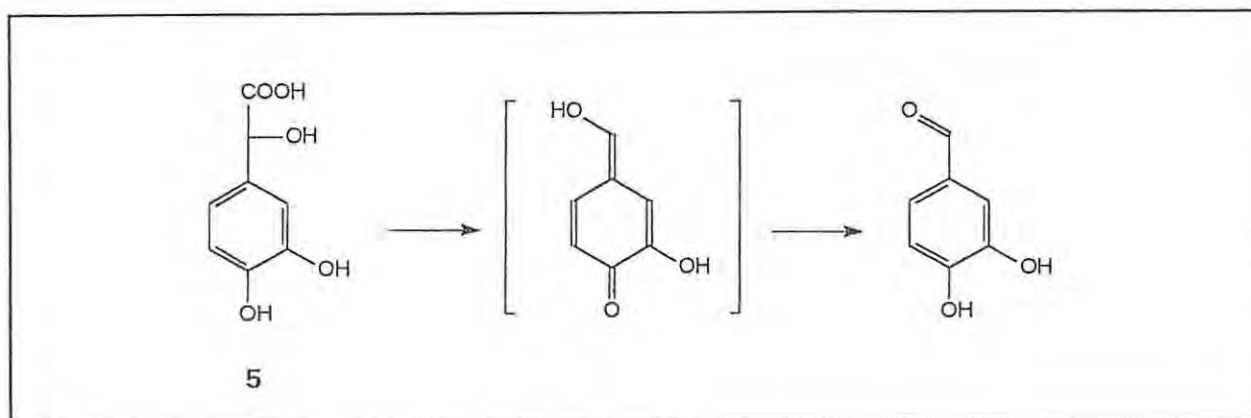
ions (Huber and Lerch, 1988). The gene for this enzyme has recently been identified and cloned into *E. coli*, and future molecular biological work is likely to provide useful insights into tyrosinase structure and function.

1.1.3 (4) Invertebrate polyphenol oxidases

In insects and helminthes, formation of the cuticle is followed by a tanning process in which *N*-acetyldopamine is oxidised by tyrosinase, and the quinoid product then reacts with proteins to form a tough, dark covering (Scheme 1.3) (Suguraman, 1986). The oxidation of the substrate 3,4-dihydroxymandelic acid (5 in Scheme 1.4), catalysed by insect polyphenol oxidases, has elicited much interest because of an unusual oxidative decarboxylation which occurs after the enzymic reaction (Suguraman, 1986; Cabanes *et al.*, 1988; Suguraman *et al.*, 1989; Bouheroum *et al.*, 1989). Insect polyphenol oxidase-catalysed reactions have been used to establish the mechanism of the rearrangement of dopachrome (see Section 1.1.7).



Scheme 1.3: Quinone tanning in insect cuticle (Suguraman, 1986)



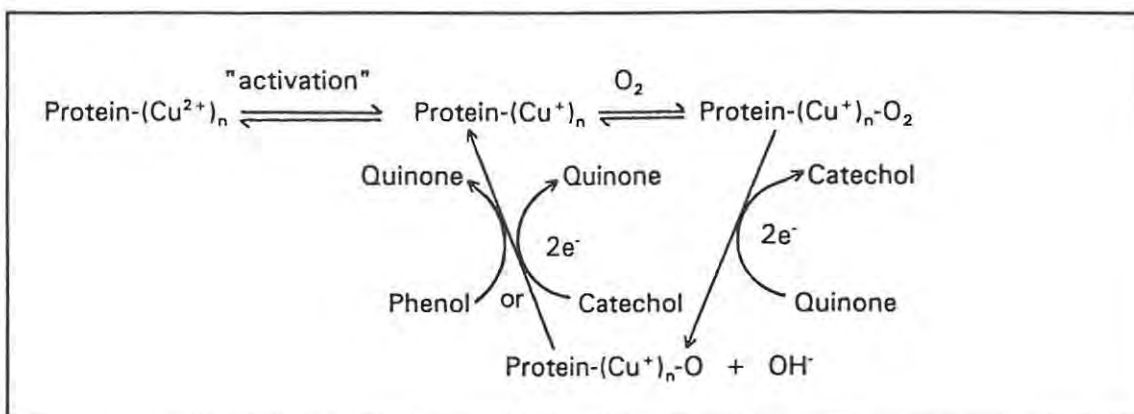
Scheme 1.4: Oxidative decarboxylation of 3,4-dihydroxymandelic acid (Cabanés *et al.*, 1988)

1.1.3 (5) Mammalian tyrosinases

Mammalian tyrosinase from sources such as mouse epidermis, hamster melanoma, and human melanoma have been used for various studies, and the results have been found to be similar to those obtained with mushroom tyrosinase, although the mammalian enzyme is more specific for DOPA (Hearing *et al.*, 1980; Pomerantz and Warner, 1967). Mammalian tyrosinase occurs membrane-bound, in melanocytes, in polymorphic forms which have molecular weights of approximately 55000 before post-translational glycosylation; no primary sequences are available because of the small amounts which have been obtained (Hearing and Jiminez, 1987). The catechol *L*-DOPA and its analogs are toxic to melanoma cells, which is thought to be due to the formation of reactive quinone products which inhibit DNA polymerase, or to the formation of free radical decomposition products of catechols (Picardo *et al.*, 1987 and Prezioso *et al.*, 1990).

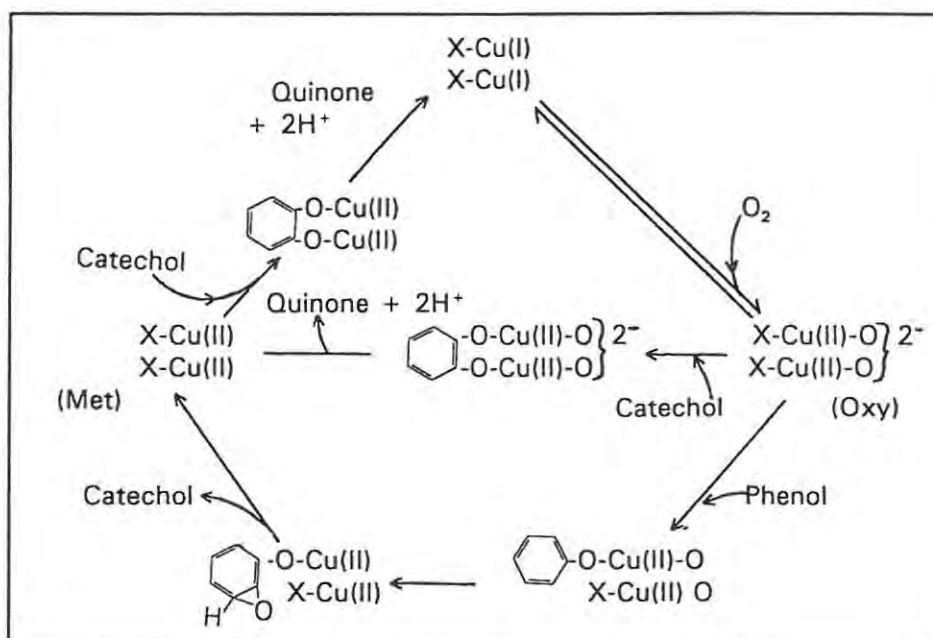
1.1.4 The mechanism of polyphenol oxidase-catalysed reactions

Polyphenol oxidases from various sources have been utilised in kinetic investigations, and the results are generally taken to apply to all members of the group. Polyphenol oxidase-catalysed reactions exhibit complex reaction kinetics, due to the sequential nature of the reactions and therefore, many investigations were carried out before the mechanism was explained. Mason (1959) proposed the mechanism shown in Scheme 1.5, in which the copper ions were shown to be reduced and then oxidised while bound to the protein:



Scheme 1.5: Mechanism of polyphenol oxidase proposed by Mason (1959)

A more complex mechanism, accommodating the observed conversion of two catechol molecules per turnover, was suggested by Ochiai (1973) (Scheme 1.6):

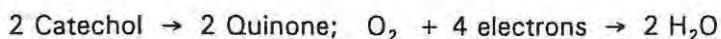


Scheme 1.6: Mechanism for polyphenol oxidase proposed by Ochiai (1973)

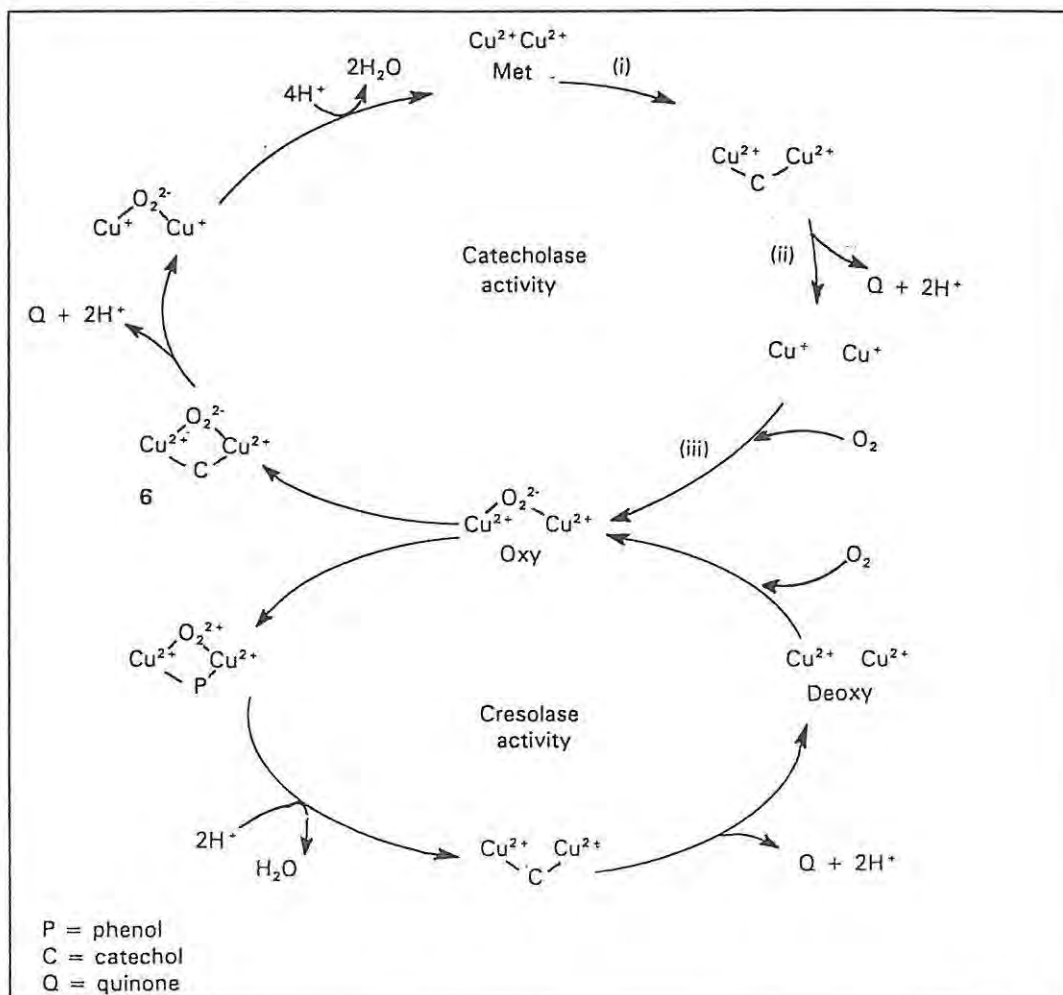
The combination of the enzyme with oxygen prior to substrate binding was established by Ingraham (1957), using a range of phenolic substrates, and this obligatory order of binding has subsequently been confirmed. However, the dependence of the Michaelis constant (with respect to oxygen) on the nature of catecholic substrates suggests that the order of binding is not necessarily sequential

in the case of catecholase activity (Duckworth and Coleman, 1970; Gutteridge and Robb, 1973; Lerch and Ettlinger, 1972). Conformational changes resulting from binding of oxygen or the substrate could affect K_m values (Mayer and Harel, 1979). In the case of high concentrations of DOPA, the reaction system apparently has a ping-pong mechanism (Vanni *et al.*, 1990).

A complete mechanism which would account for the observed stoichiometry *viz.*:



and the reversible reduction and oxidation of the two copper ions, as well as the cresolase activity, was proposed by Lerch (1981) (Scheme 1.7). In this mechanism, the phenolic substrate is only able to react with the oxygenated form of the enzyme, but a catechol can react with both the oxy and deoxy forms. (This is relevant to the explanation of the lag phase discussed in the next section.) The term "met" refers to the non-oxygenated form of the enzyme in which the copper ions are in the +2 oxidation state; this is inactive with respect to phenolase activity, but can be converted to the "oxy" form by reaction with the catechol (steps (i) to (iii) in Scheme 1.7).

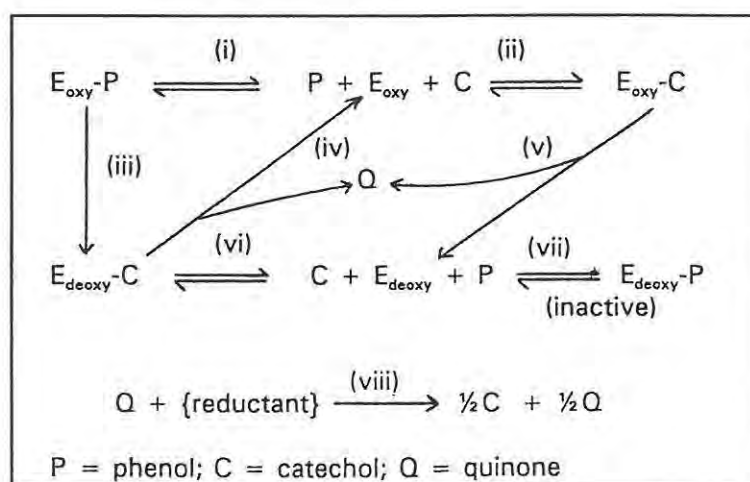


Scheme 1.7: Mechanism for polyphenol oxidase proposed by Lerch (1981)

1.1.5 The lag phase in phenolase activity

A significant feature of tyrosinase kinetics is an initial lag phase which is observed when phenolic substrates are used, but which is absent if the substrate is a catechol. This lag phase is abolished by the addition of small amounts of various reductants, *eg.* DOPA (García-Carmona *et al.*, 1987), other catechols (Osaki, 1963), melaniñ (Menter *et al.*, 1990), certain metal ions (Ros *et al.*, 1993), and serine (García-Carmona *et al.*, 1987). The lag phase is explained as being a result of competition between the phenolic and catecholic substrates, and a dynamic adjustment of the rates of enzyme-catalysed steps. A certain amount of time is required for a specific level of the catechol to accumulate, and once this has been achieved, the catechol is regenerated sufficiently rapidly by step (viii) (Scheme 1.8) to maintain an increasing proportion of the enzyme in the active copper (II) state. The copper (II) form can then react with oxygen and then the phenol, and thus the lag is gradually overcome. This is supported by the fact that the lag phase was not observed when the enzyme was stored under nitrogen, when a larger fraction of the enzyme would be preserved in a copper (I) state (Vanni *et al.*, 1990).

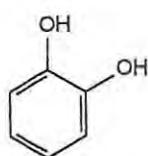
The mechanism proposed for metal ion-induced shortening of the lag time involves the formation of traces of DOPA (from tyrosine) which then reacts as explained above (Ros *et al.*, 1993). Any other reductant, such as serine, would act in a similar way. The deoxy enzyme-phenol complex $E_{\text{deoxy}}\cdot\text{P}$ (Scheme 1.8) constitutes a "dead-end" in that the deoxy form of the enzyme cannot react with the phenol although it can bind to it (García-Carmona *et al.*, 1987; Cabanes *et al.*, 1987). Also in connection with non-enzymic reactions, low concentrations of catechol (1,2-dihydroxyphenol, 7) and 4-methylcatechol were reported to have a synergistic effect on the oxidation of DOPA by mushroom tyrosinase. This was attributed to the ability of these catechols to oxidise DOPA non-enzymatically to dopaquinone (Schved and Kahn, 1992).



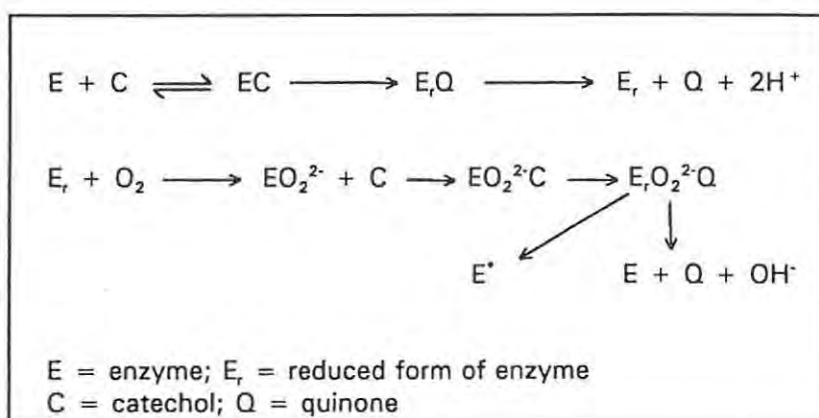
Scheme 1.8: Mechanism for polyphenol oxidase activity, and the phenolase lag phase (García-Carmona *et al.*, 1987)

1.1.6 Reaction inactivation of polyphenol oxidase

Early investigations, in which catechol, **7**, was used as the substrate, showed that rapid reaction inactivation occurred. The well known science writer, Isaac Asimov, studied this reaction and reported a detailed analysis of the kinetics in his doctoral dissertation (Asimov and Dawson, 1950). The inactivation was proposed to result from the *o*-quinone product reacting with a nucleophilic group in the protein (Wood and Ingraham, 1965). Tyrosinase was one of the first enzymes to have the term "suicide enzyme" applied to it, because this inactivation was regarded as the result of irreversible reaction between a product of the enzyme-catalysed reaction and the protein pocket containing the binding site of the enzyme. Since the reaction inactivation was observed to occur concurrently with oxidation of catechol to *o*-benzoquinone, the reaction sequence shown in Scheme 1.9 was suggested (Dietler and Lerch, 1979). Here, the inactivated enzyme, E^* , is formed from the complex of the oxygenated enzyme with the bound *o*-quinone product.



7



Scheme 1.9: Reaction sequence proposed to explain the reaction inactivation of polyphenol oxidase by catechol (Dietler and Lerch, 1979)

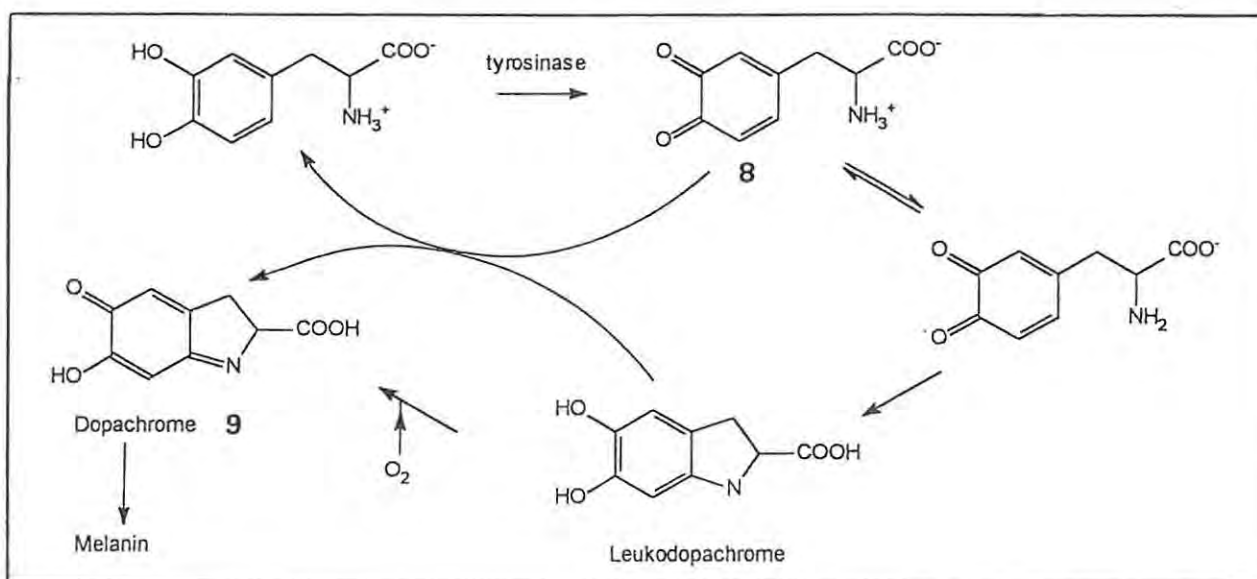
However, destruction of Histidine-306 of *Neurospora* tyrosinase was subsequently observed during reaction inactivation, with a corresponding loss of one copper atom per molecule. This was suggested to be the result of attack by hydroxyl radicals, formed during incomplete reduction of the peroxide-bridged enzyme intermediate **7** (Scheme 1.7, Section 1.1.4) (Lerch, 1981). This

Fenton-type reactivity is likely to be minimised in normal enzyme functioning, by tight binding of the peroxide ion to the dicopper unit (Wilcox *et al.*, 1985). In fact, only one tyrosine molecule is inactivated in approximately every 5000 turnovers (Lerch, 1981). This theory of inactivation (by free radical reactions) is supported by the results of investigations carried out under conditions which excluded the possibility of quinone accumulation, but permitted the phenolase activity of tyrosinase (Golan-Goldhirsch and Whittaker 1985).

Dye-sensitive photoinactivation of mushroom tyrosinase has also been attributed to interaction of the enzyme with active oxygen species such as O_2^- (Parkin and Lowum, 1990). Tyrosinase exhibits irreversible inactivation induced by UV radiation; this was also attributed to partial denaturation resulting from disruption of intramolecular interactions by free radicals (Kahn and Ali, 1986; Shah *et al.*, 1987).

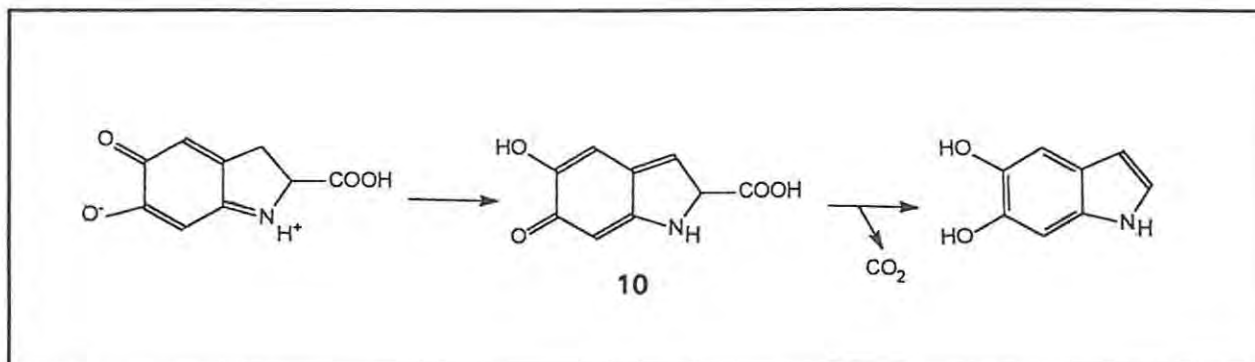
1.1.7 Reactions of products subsequent to polyphenol oxidase-catalysed oxidation

Recent investigations have shown that melanin formation is pH-dependent, and this is rationalised by taking into account the rearrangement of dopaquinone- H^+ **8** which is actually the product of the enzymic reaction, to dopachrome **9** (Scheme 1.10) (García-Cánovas *et al.*, 1982a and b). DOPA is formed, as the dopaquinone- H^+ is converted, and this gradually activates the met (copper (III), non-oxygenated) form of the enzyme, thus increasing the phenolase reaction rate and abolishing the lag phase (Cabanes *et al.*, 1987).



Scheme 1.10: pH-Dependent formation of dopachrome (García-Cánovas *et al.*, 1982a; Cabanes *et al.*, 1987)

In the formation of melanins, the decarboxylation step [step (v) in Scheme 1.1, Section 1.1.1] has also been re-examined recently. The revised mechanism, shown in Scheme 1.11, includes the quinone-methide intermediate **10**, which forms prior to the decarboxylation reaction (Costantini *et al.*, 1991). Direct observation of the quinone-methide was reported subsequently (Al-Kazwini *et al.*, 1992).



Scheme 1.11: The reaction pathway of dopachrome decarboxylation (Costantini *et al.*, 1991)

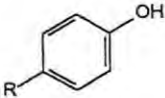
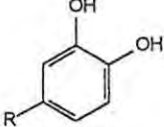
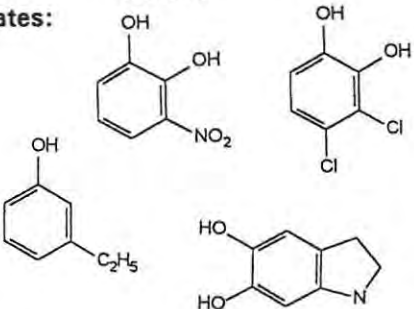
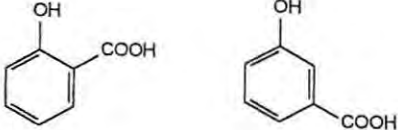
Transition metal ions, such as Cu²⁺, Co²⁺, Fe²⁺ and Zn²⁺ have been shown to alter the kinetics and the course of melanin formation. This has been attributed to their interaction with dopachrome which causes decreased decarboxylation, and results in melanins forming with additional carboxyl groups (Palumbo *et al.*, 1987; 1988; 1990).

1.1.8 Substrates for polyphenol oxidases

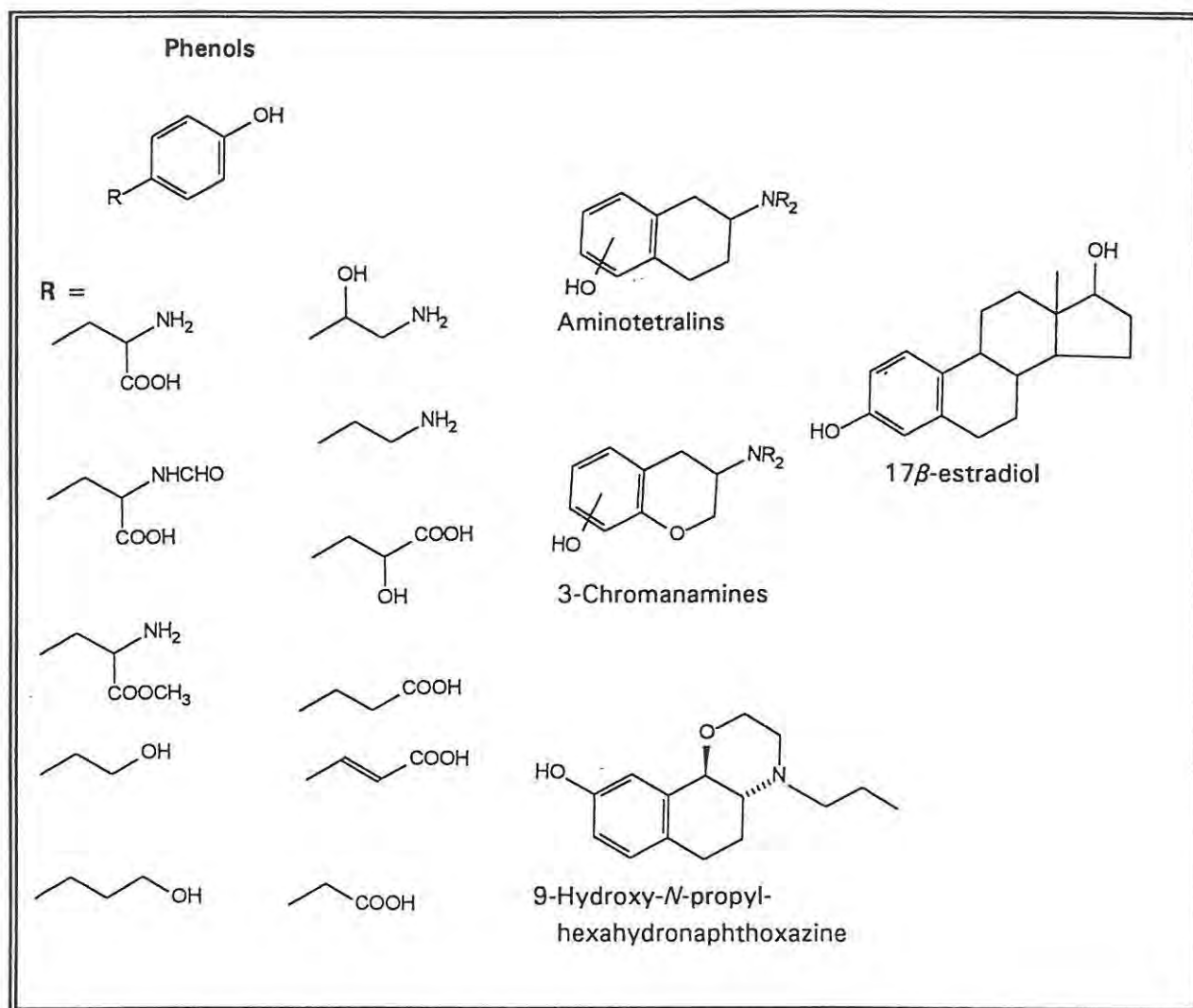
The range of substrates which can be transformed by polyphenol oxidases is generally very broad, particularly in the case of enzymes from plant sources. The natural substrates are normally regarded to be tyrosine and DOPA, at least for mammalian tyrosinase. (Mammalian tyrosinase is far more specific than other tyrosinases but it is seldom used because it is difficult to obtain). Numerous authors have reported a variety of substrates for polyphenol oxidase-catalysed aromatic hydroxylations and oxidations. Many of these reactions have found application in biocatalytic systems as discussed in Section 2.1; the objective of the present section is to give a general view of the range of substrates observed to be suitable for tyrosinase under conventional conditions.

Mushroom tyrosinase was found to catalyse the transformation of all the phenols shown in Table 1.4, to give *o*-quinones in aqueous systems (Passi and Nazzaro-Porro, 1981); the rates were found to be greatest if the phenol had a *para*-substituent which was electron-donating. If the *para*-substituent was an electron-acceptor, the phenol was observed to be a competitive inhibitor of the enzyme. Phenols with substituents *ortho* to the hydroxyl were reported not to be recognised.

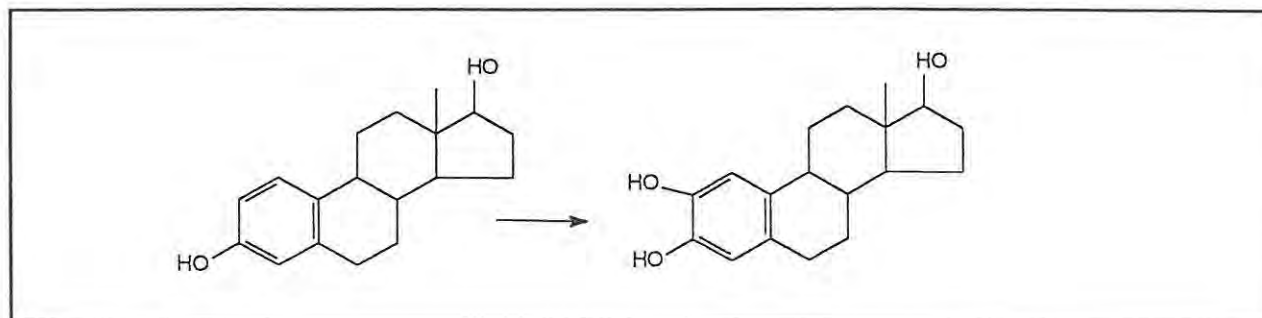
Table 1.4: Examples of substrates and inhibitors of polyphenol oxidase (Passi and Nazzaro-Porro, 1981; Yasunobu, 1959)

Phenol	Catechol	Others
		<p>Substrates:</p>  <p>Inhibitors:</p> 
<p>Substrate:</p> <p>R = OCH₃ OC₂H₅ CH₃ C(CH₃)₃ OCH₂C₆H₅ CH(CH₃)₂ CH₂CH₂NHCOCH₃</p> <p>Halogen</p> <p>Inhibitor:</p> <p>R = NO₂ COOH CHO COOCH₃ COOC₂H₅</p>	<p>Substrate:</p> <p>R = CH₃ OCH₃ OC₂H₅ C(CH₃)₃</p> <p>Inhibitor:</p> <p>R = NO₂ COOH COCH₂NCH₃ CHO</p>	

Pras and co-workers have shown the formation of many catechols using alginate-entrapped plant cells (*Mucuna pruriens*), in aqueous medium, in the presence of ascorbic acid (which reduced quinones to catechols). These are summarised in Table 1.5 (Pras *et al.*, 1988; Pras, 1988; Pras *et al.*, 1990; Woerdenberg *et al.*, 1990).

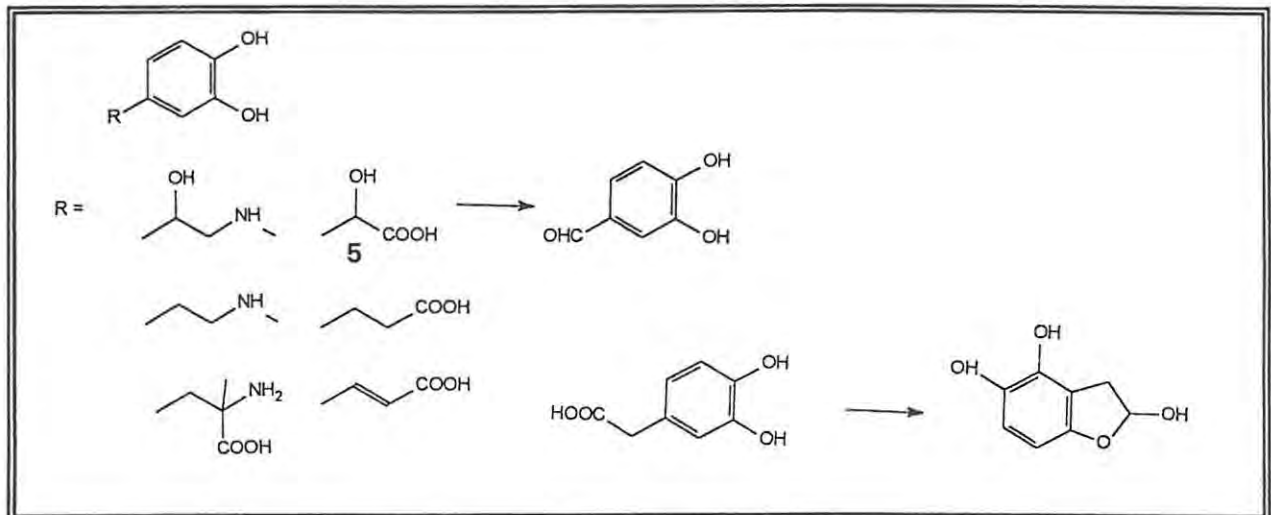
Table 1.5: Substrates of polyphenol oxidase in *Mucuna pruriens* cells

The preparation of 2-hydroxyestradiol from estradiol, and the incorporation of the product into melanin, were also reported by Jacobsohn and Jacobsohn (1984; 1992; Jacobsohn *et al.*, 1988) (Scheme 1.12)

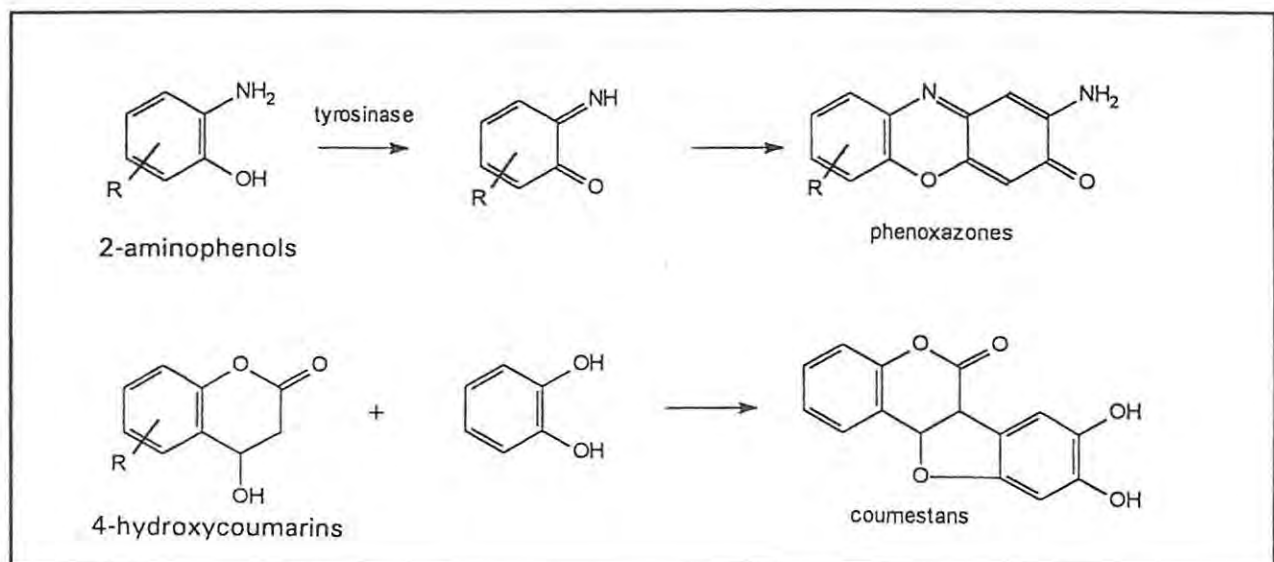
Scheme 1.12: Hydroxylation of estradiol by tyrosinase (Jacobsohn *et al.*, 1988)

In studies on the activity of polyphenol oxidase found in insect cuticle, Suguraman and co-workers have reported the transformation of dopamine and related catechols, and 3,4-dihydroxymandelic acid **5** (Table 1.6). In some cases, the reactions yielded coupled products resulting from reactions subsequent to the enzymic step (Suguraman, 1987; Suguraman *et al.*, 1987; Suguraman *et al.*, 1990).

Table 1.6: Substrates of insect polyphenol oxidase (Suguraman *et al.*, 1990)

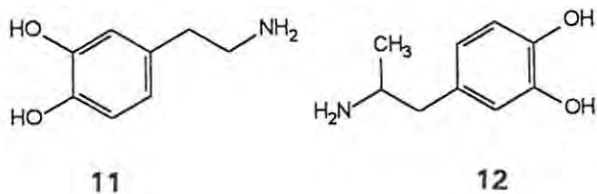


Coupled products from tyrosinase-catalysed reactions have also been reported in other cases; the oxidation products of 2-aminophenols were converted to phenoxazones (Toussaint and Lerch, 1987) and 4-hydroxycoumarins gave coumestans (Bhalerao *et al.*, 1989) (Scheme 1.13).

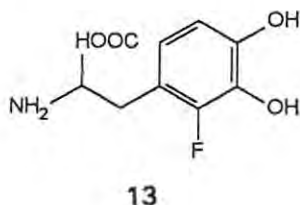


Scheme 1.13: Coupled products resulting from tyrosinase-catalysed reactions

Dopamine, **11** and its analogs, *eg.* α -methylnoradrenalin **12**, also serve as substrates for tyrosinase, and the transformation of dopamine has been proposed as a minor pathway for the oxidation of DOPA *in vivo* (Jiminez *et al.*, 1984; Jiminez *et al.*, 1985).

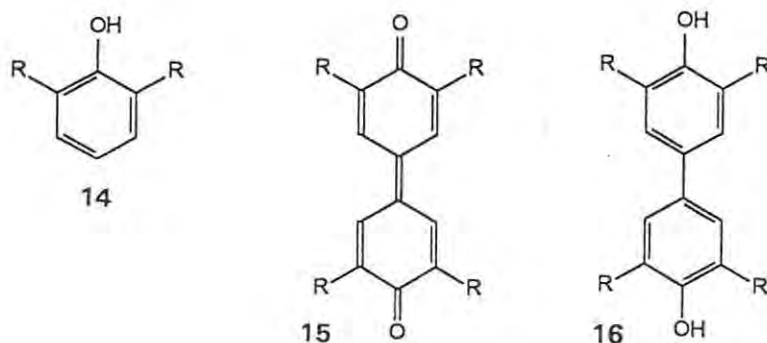


Fluorinated substrates such as compound **13** have been investigated because fluoride has been observed to be released as a result of tyrosinase activity. This fluoride is toxic to cancer cells, and thus there is potential for treatment of tyrosinase-rich melanoma with these substrates (Rice *et al.*, 1987; Phillips *et al.*, 1990).



Tyrosinase is also capable of hydroxylating and oxidising tyrosine residues in peptides (Yasunobu *et al.*, 1959) and proteins (Sizer, 1953). This is important in the production of moisture-resistant adhesives, as exemplified by mussel glue. Tyrosinase has been used in the production of synthetic glues which are similar in composition to these (Yamamoto *et al.*, 1992).

Of particular interest in the present study are the transformations of hindered phenols such as **14**, where the products are reported to be coupled biphenyls, such as **15** and **16** (Pandey *et al.*, 1990). Similar coupled products were reported by Andersen *et al.* (1992), in the conversion of 4-methylcatechol and *N*-acetyldopamine by insect cuticle tyrosinase.

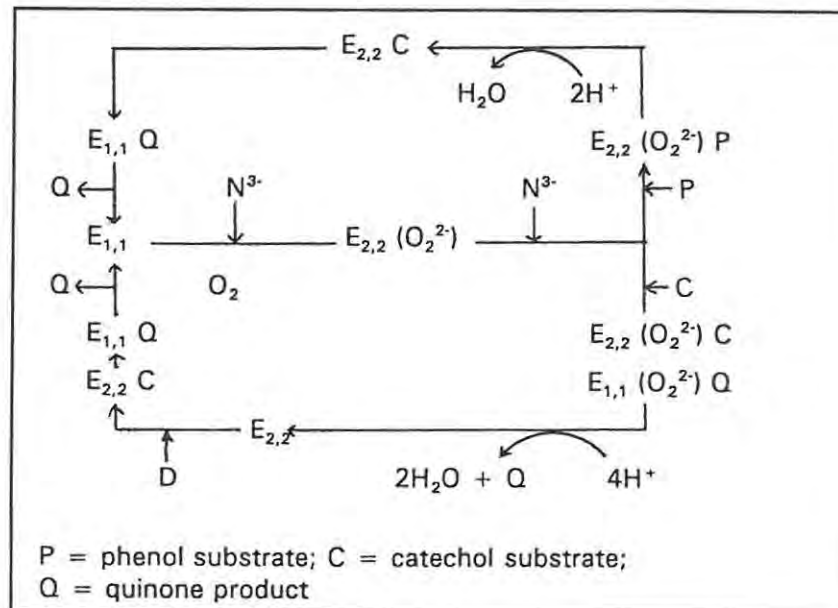


Thus, the range of substrates which can be transformed in aqueous medium includes some very bulky molecules. This aspect of tyrosinase activity will be discussed further in Chapter 3.

1.1.9 Inhibitors of polyphenol oxidases

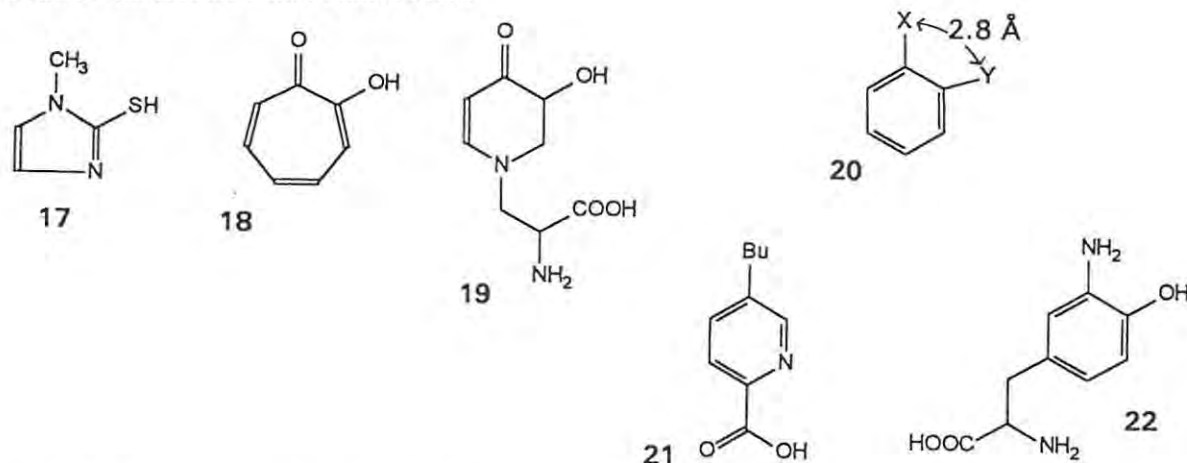
Inhibitors of polyphenol oxidase fall into three main groups: (i) small molecule or ions which bind to the copper centre in the active site, (ii) aromatic inhibitors which compete with phenolic substrates in binding to the active site, and (iii) compounds which reduce or oxidise the copper ions (Janovitz-Klapp *et al.*, 1990).

Ions such as azide and cyanide complex with the copper ions in the active site and may cause their loss from the protein (Beltramini *et al.*, 1984a and b). Removal of the inhibitor results in at least partial recovery of activity, since the copper can be recombined with the apoenzyme (Lerch, 1981). The binding of small molecules such as these have been useful in studying the nature of the dinuclear copper site in the copper protein haemocyanin as well as tyrosinase (see Section 1.2). Azide reacts with both copper (I) and (II) forms of tyrosinase, causing a mixed type inhibition; the steps in the reaction pathway where azide can interfere are shown in Scheme 1.14 (Healey and Strothkamp, 1981):

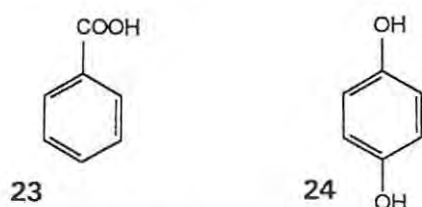


Scheme 1.14: Inhibition of polyphenol oxidase by azide ions (Healey and Strothkamp, 1981)

The anti-thyroid drug methimazole, **17**, also inhibits mushroom polyphenol oxidase, by chelating the copper ions (Hanlon and Shuman, 1975; Andrawis and Kahn, 1986). Tropolone, **18** and mimosine, **19** act in a similar way, by complexing with the copper ions and thus competing with the substrate by blocking the active site (Kahn and Andrawis, 1985). Treatment of thalassaemia (a disorder involving excess iron in the body) with 3-hydroxypridine-4-ones (of which mimosine is an example) has the undesirable side-effect of inhibiting normal tyrosinase function and thus causing a lack of normal pigmentation (Hider and Lerch, 1989). These inhibitors all share the general structure **20**, in which the dimensions allow the bridging of the dinuclear copper unit by the atoms X and Y (the nature of which depend on the inhibitor), making them very potent inhibitors. In the same way, fusaric acid, **21** and 3-aminotyrosine, **22** are effective inhibitors of tyrosinase (Maddaluno and Faull, 1988).



Benzoic acid, **23** and hydroquinone, **24** act as simple competitive inhibitors, which bind strongly to the enzyme (Chen and Chavin, 1972; Menon *et al.*, 1990).



Reducing agents such as sulphite ions and mercaptoethanol inhibit the enzyme by reducing the active site copper ions, and oxidising agents such as sodium nitroferricyanide do so by oxidising the copper ions (Aasa *et al.*, 1978; Chen and Chavin, 1972). In both cases the reversibility of the copper redox reaction, which is crucial in the mechanism (see Section 1.1.4), is precluded. Some controversy has existed over the effect of ascorbic acid on tyrosinase, which is relevant in the light of the frequent use of this acid to reduce quinones to catechols in the presence of the enzyme. However, Varoquaux and Sarris (1979) showed that it has neither activating nor inhibitory effects on mushroom tyrosinase.

1.2 THE ACTIVE SITE IN POLYPHENOL OXIDASE

No complete structure elucidations have been reported for polyphenol oxidases; the difficulties inherent in the purification of multi-subunit enzymes, and the multiplicity which polyphenol oxidases exhibit, contribute to the lack of progress in defining their protein structures. The amino acid composition and sequence for *Neurospora* tyrosinase was published by Lerch (1982, 1983). In the case of mushroom tyrosinase, the amino acid composition was determined by Jolley *et al.* (1969a). In the absence of crystals sufficiently pure for X-ray crystallographic analysis, the solid state structure of the proteins remains undefined. Far more attention has been devoted to intensive investigations of the dinuclear copper binding site which is present in the group of "Type III" copper proteins, of which tyrosinase is a member.

1.2.1 The structure of the "Type III" active site

Type III copper proteins are characterised by the presence of an anti-ferromagnetically coupled pair of copper atoms in their binding sites, and by the unique spectral features resulting from this (see Table 1.7). The group includes polyphenol oxidases, and the oxygen-carrying proteins, haemocyanins, which are found in crustaceans, arthropods, and molluscs. Haemocyanins are multi-subunit proteins of considerable complexity, and their primary function is to carry oxygen in the bloodstream of the animals in which it occurs. Some haemocyanins have been shown to have tyrosinase activity, but this is likely to be of lesser importance.

Table 1.7: Classification of copper proteins according to spectroscopic properties (Adman, 1991)

Type	Source	Characteristic
I	Azurin, plastocyanin	Blue, intense absorption near 600nm, EPR active Role in electron transfer
II	Galactose oxidase, Superoxide dismutase	Normal absorption features, strong EPR signals Catalyse chemical reactions
III	Haemocyanin, Tyrosinase	Magnetically coupled copper atoms, EPR-silent, Strong absorption near 330nm Catalyse oxidations

The striking similarity between haemocyanins and tyrosinases was first recognised in the light of two observations: firstly, haemocyanins, *eg.* in *Cancer* (crab) blood, were found to have catecholase activity (Bhagvat and Richter, 1938), and secondly, the unusual spectral and magnetic features (described below) were common to both groups. The UV-visible absorption spectra of the Type III proteins are characterised by strong bands which develop upon oxygenation of the proteins. Treatment of mushroom tyrosinase with hydrogen peroxide results in reversible oxygenation, and the oxygenated form exhibits strong absorbances at 345nm ($\epsilon = 9000 \text{ M}^{-1}\text{cm}^{-1}$) and 600nm ($\epsilon = 600 \text{ M}^{-1}\text{cm}^{-1}$) (Jolley *et al.*, 1974). Similarly, oxyhaemocyanin shows strong, multiple ligand-to-metal charge transfer absorptions at 345nm ($\epsilon = 20000 \text{ M}^{-1}\text{cm}^{-1}$) and 570nm ($\epsilon = 1000 \text{ M}^{-1}\text{cm}^{-1}$) (Karlin and Gultneh, 1985).

The rationalisation of the properties of Type III copper proteins has involved contributions from workers in wide-ranging fields; its development is described here in approximately chronological order.

1.2.2 The Type III copper centres in tyrosinase and haemocyanin

The presence of the copper atoms in mushroom tyrosinase was known very early, but their coupling was only demonstrated in 1973 (Schoot Uiterkamp and Mason, 1973), using EPR measurements. This confirmed the close relationship between haemocyanin and tyrosinase. The magnetic susceptibility of mushroom tyrosinase was also measured and was found to indicate diamagnetic character, which could only be explained if the copper atoms were situated close together in the protein (Makino *et al.*, 1974). The circular dichroism (CD) spectrum of mushroom tyrosinase showed three bands, again similar to haemocyanin (Schoot Uiterkamp *et al.*, 1976). The tyrosinase from *Neurospora* was also shown to contain two EPR-silent copper atoms; treatment of this protein with β -mercaptoethanol resulted in the detection of paramagnetic copper, indicating destruction of the coupling (Deinum *et al.*, 1976). γ -Radiation was used to destroy the coupling in *Cancer* haemocyanin, producing an uncoupled dicopper site where one copper ion was reduced to Cu^+ , but the other was not. This was suggested to indicate some dissimilarity between the environments of the two copper atoms (Symons and Petersen, 1978).

1.2.3 Early results of haemocyanin studies

Various forms of haemocyanin were generated with different active site arrangements, and their spectral features investigated (Eickman *et al.*, 1979). Table 1.8 shows the derivatives generated, their names and properties. Analysis of the charge transfer (CT) spectra and magnetic properties

of the derivatives indicated that oxygen was bound as an end-to-end peroxide (O_2) bridge across the two copper atoms. The oxygen bridge was proposed to be positioned in the equatorial plane between the two copper atoms.

An endogenous bridge between the copper atoms was proposed, to explain the observation that the copper atoms could still be coupled even in the absence of bound oxygen (Himmelwright *et al.*, 1980a; Solomon, 1983). The existence of this endogenous bridge, initially thought to be a protein side chain, water, or hydroxide, has been the subject of controversy for several years, and at present its existence and/or nature remain undecided. A "spectroscopically effective" model for oxyhaemocyanin was developed, which explained the spectral properties of the protein in the absence of a known chemical structure (Figure 1.1) (Solomon, 1987).

Table 1.8: Derivatives of haemocyanin (Eickman *et al.*, 1979)

Derivative	Name	Properties
Cu(II) .. Cu(II)	met	Coupled, EPR-silent
Cu(II). O_2 . Cu(II)	oxy	Coupled, absorbs at 330nm, 650nm
Cu(I) .. Cu(I)	deoxy	Coupled, colourless
Cu(II) .. Cu(I)	half-met	EPR-active
Cu(II) .. -	met-apo	Paramagnetic
Cu(II) Cu(II)	dimer	Not coupled, paramagnetic

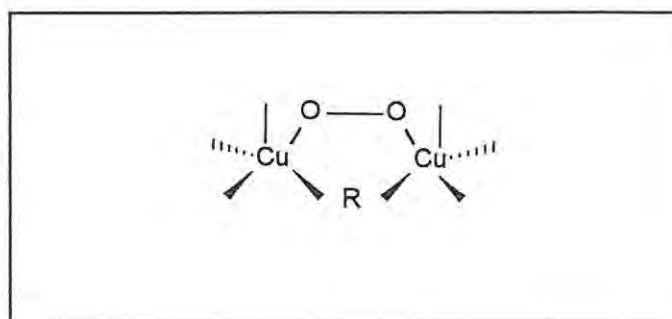


Figure 1.1 A spectroscopically effective model for oxyhaemocyanin proposed by Solomon (1983)

A series of studies were carried out on the ability of haemocyanin to bind oxygen and various other small molecule ligands such as azide ions and carbon monoxide. EPR studies on met-haemocyanins from various sources showed that exogenous ligands could alter the distance between the copper

atoms, and that the active site of arthropod haemocyanin could be disrupted by ligand binding (Wilcox *et al.*, 1984). The distance between the copper atoms in the azide derivative of haemocyanin was reported to be 3.6Å (Pate *et al.*, 1989).

The resonance Raman spectrum of oxyhaemocyanin indicated that the copper atoms were coordinated by imidazole groups, with two ligands in the tetragonal plane of each copper atom, and a third in an apical position. The spectra showed small variations indicating differences between mollusc and arthropod proteins (Larrabee and Spiro, 1980). Additional evidence for the ligation of the copper atoms by imidazole groups was provided by luminescence studies on haemocyanin derivatives with bound carbon monoxide (Sorrell and Borovik, 1986; Sorrell *et al.*, 1988).

Reaction with cyanide ions resulted in the removal of copper from haemocyanin. The change in conformation which apparently accompanied the loss of the first copper atom was an indication that there is some inequivalence in the sites of the two copper atoms. Thus, one copper atom seems to be more shielded from the exterior than the other (Beltramini *et al.*, 1984a and 1984b).

1.2.4 More recent studies on haemocyanins

The structures of several haemocyanins have been studied: in molluscs, the proteins have tubular structures with as many as 10 protomers, and in arthropods they are generally found to have multiples of hexamers. The haemocyanin in *Limulus polyphenus*, for instance, has 48 subunits (Adman, 1991). Major progress in determining the Type III binding site structure was made following the X-ray crystal structure determination for haemocyanin from the arthropod *Panulirus interruptus* (Gaykema *et al.*, 1984 and 1985; Volbeda and Hol, 1989a, b; Volbeda *et al.*, 1989). The protein was found to have six monomeric units arranged in a trimer of dimers, with the presence of flexible cavities accessible to oxygen, in which the copper atoms were bound (Adman, 1990). Each of the two copper atoms were shown to be coordinated to three histidine imidazolyl groups, two in equatorial positions and one further away, in an axial coordination position. The distance between the copper atoms was found to be 3.6Å. No evidence was found for an endogenous bridge originating in the protein, but the presence of water or hydroxyl could not be ruled out. This protein was crystallised in the deoxy form and, therefore, could give no indication of the oxygen bridging mode. However, the haemocyanin from *Limulus* was crystallised in the oxy form, revealing a peroxide bridge with a $\eta^2:\eta^2$ conformation, bridging copper ions situated 3.4 ± 0.2 Å apart. No evidence for an endogenous or exogenous bridge was found, and the nearest water or hydroxyl group was 4 - 5 Å away from the copper ions.

Research on haemocyanins is still proceeding (for example, Makino and Ohnaka, 1993; Beltramini *et al.*, 1992), and molecular biological studies are becoming increasingly important in elucidating these structures as well as the mechanisms of their oxygen binding (Lang and van Holde, 1991).

1.2.5 Studies on *Neurospora crassa* tyrosinase

Similar studies on *Neurospora crassa* tyrosinase indicated that tyrosinase also binds oxygen as a peroxide bridge, and that oxytyrosinase exhibits a UV-visible spectrum very similar to that of oxyhaemocyanin (see Table 1.9). Resonance Raman Spectroscopy was used to determine the unusually low (755 cm^{-1}) stretching frequency of the peroxide (Himmelwright *et al.*, 1980b).

Table 1.9: Derivatives prepared from tyrosinase (Lerch, 1987)

Derivative	Name	Properties
Cu(II) .. Cu(II)	met	Green, EPR-silent
Cu(II). O ₂ .Cu(II)	oxy	Blue, EPR-silent
Cu(I) .. Cu(I)	deoxy	Colourless, EPR silent
Cu(II) Cu(II)	dimer	EPR-active
Cu(II) .. Cu(I)	half-met	EPR-active

Analysis of the tyrosinase derivatives formed by binding azide, nitrite, bromide, etc., showed that the exogenous ligands could bridge the copper atoms. The UV-visible absorption and CD spectra of the azide derivative indicated that the two N³-Cu bonds, and therefore the two copper sites, were not equivalent (Pate *et al.*, 1989). Binding of a second azide to the copper site resulted in disruption of the active site, which was thought to be consistent with disruption of an endogenous bridge (Himmelwright *et al.*, 1980b). Cyanide ions were observed to displace the peroxide in oxytyrosinase, and then to remove the copper ions (Beltramini *et al.*, 1990a). The luminescence properties of the carbon monoxide derivative were found to be very similar to those of the equivalent haemocyanin derivative, which supported the evidence for the two proteins having similar binding sites (Kuiper *et al.*, 1980).

Replacement of the copper (II) with cobalt (II) ions was found to lead to the loss of enzymic activity. Addition of potassium cyanide to the cobalt-substituted enzyme resulted in removal of only one cobalt ion from the active site, indicating some asymmetry in the site (Ruegg and Lerch, 1981).

The copper ions in the enzyme were shown to be important in stabilising the structure by linking different parts of the protein, since the apoenzyme was observed to be less stable than the holoenzyme (Ruegg *et al.*, 1982).

The determination of the primary structure of *N. crassa* tyrosinase and, subsequently, its higher structure (Lerch, 1982 and 1983) showed it to have a simpler structure than haemocyanin or mushroom tyrosinase; it has a single chain of 407 amino acids, an *N*-acetyl-blocked N-terminus, a chemically modified cysteine residue at position 94, and exists in three allelic forms. Comparison of the tyrosinases from *Neurospora* and *Streptomyces*, and the haemocyanins from one mollusc and two arthropods, showed a high degree of homology between the proteins, particularly in a region near the C-terminal end. Three invariant histidine residues were identified as the ligands to one copper atom (Copper B), in each case. The coordination of the second copper atom in each case was found to be more variable, which was suggested to be due to independent evolution after the development of the site for Copper B (Lerch *et al.*, 1986; Lerch and Germann, 1988). The destruction of the histidine residues coordinating Copper B (His-188, -193, and -289) resulted in loss of this copper, and the loss of activity. Similarly, destruction of His-306 caused loss of activity; this residue was thus likely to coordinate to Copper A (Lerch, 1987). Differences in CD spectra have shown that the tyrosinases from *Neurospora* and *Streptomyces* have some differences in their copper ligand environments (Huber and Lerch, 1988).

1.2.6 A possible mechanism for tyrosinase

The major difference between tyrosinase and haemocyanin lies in the much greater accessibility of the tyrosinase binding site. Thus, ligands were found to be more easily displaced from tyrosinase, and exogenous phenolic substrates can react at the active site (Solomon *et al.*, 1987; Beltramini *et al.*, 1990b). In an extended X-ray absorption fine structure (EXAFS) study, Woolery *et al.* (1984) showed that the dinuclear binding site of oxytyrosinase was less rigid than that of oxyhaemocyanin, and that the former could more easily accommodate the molecular motions involved in catalysis.

Addition of the competitive inhibitor mimosine (19, Section 1.1.9) to *N. crassa* tyrosinase, which resulted in the loss of the absorption due to peroxide-to-copper (II) CT and formation of a phenolate-to-copper (II) CT absorption, gave an early indication that the inhibitor binds at the same site as oxygen (Winkler *et al.*, 1981). Gray and Solomon (1981) proposed that the copper-copper distance in tyrosinase was suitable for axial coordination of catechol, *via* its two hydroxyl groups, to the two copper ions. A phenolic substrate was suggested to coordinate initially in an axial

manner, but then to undergo a rearrangement to trigonal bipyramidal geometry (see Figure 1.2). This was thought to result in labilisation of the peroxide bridge because it would become polarised as a result of the rearrangement (Solomon, 1988a, b).

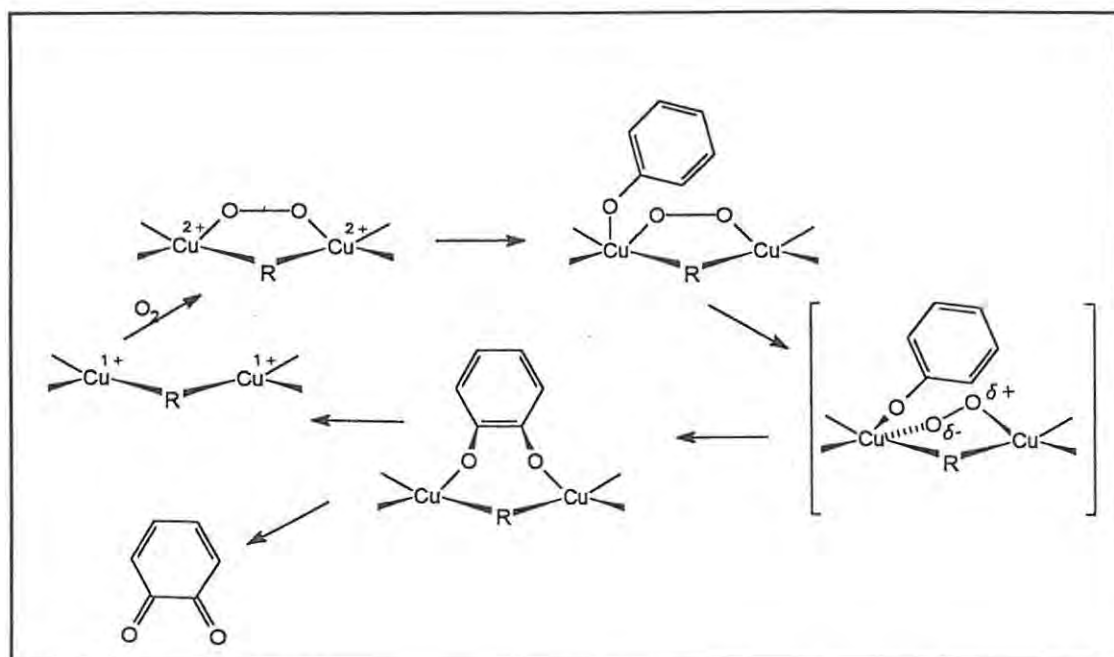


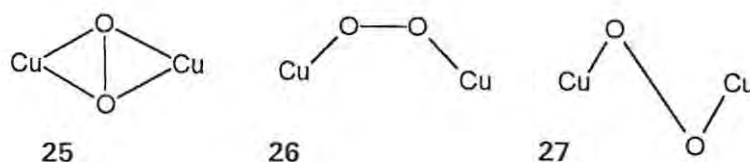
Figure 1.2: Mechanism of phenolic binding to tyrosinase (Winkler *et al.*, 1981)

Further studies on the displacement of oxygen from oxytyrosinase, with carboxylate inhibitors, supported the concept of a rearrangement as suggested in Figure 1.2, and showed that this rearrangement was more difficult when the substrate was sterically bulky *eg.* *tert*-butylphenol. In addition, the protein pocket was suggested to play an important role in stabilising the substrate analog binding, by π -interactions with the aromatic ring of the substrate analog. Higher binding affinities were reported for substrate analogs where the carboxylate group was conjugated with the aromatic ring (Wilcox *et al.*, 1985).

The binding and subsequent reaction of catechols is subject to fewer steric and geometric requirements than in the case of phenols; the rearrangement is not required and, therefore, there is more effective turnover of catechols (Solomon, 1988a, b).

1.2.7 A current model for the dinuclear copper binding site

Recent results, obtained using modern techniques and reported in the last three years, have led to the formulation of a coherent model of the binding sites in haemocyanin and tyrosinase. Ross and Solomon (1990) used molecular orbital considerations to explain the observed stretching frequency of the oxygen-oxygen bond, and broken symmetry, spin-unrestricted SCF- $X\alpha$ -scattered wave calculations to show that the binding modes 25 and 26 were possible for the peroxide in oxyhaemocyanin. Kitajima *et al* (1988) had previously proposed mode 25 for model complexes which closely resembled oxyhaemocyanin [see Section 1.4.4 (4)]. Either of these modes, or the *trans* mode 27, would be capable of mediating the superexchange between the copper atoms which is necessary for their anti-ferromagnetic nature (Maddaluno and Geissner-Prettre, 1991). Subsequently, Ross and Solomon (1991) showed that the side-on mode, 25, was the most likely, from theoretical calculations. Their calculations were correlated with spectral observations by Paul *et al.* (1991).



Molecular orbital considerations show that the peroxide in mode 25 can act as a π -acceptor ligand, causing the Cu-O_2^{2-} bond to be stronger because there is more ligand-metal overlap. This also weakens the oxygen-oxygen bond, making it more reactive as well as less negative (Solomon *et al.*, 1992).

A proposed mechanism for the activity of tyrosinase, based on these considerations, is shown below (Figure 1.3) (Solomon *et al.*, 1992; Solomon and Lowery, 1993). The phenolic substrate is suggested to coordinate initially from the axial position, and electron density is donated from the substrate into the lowest unoccupied molecular orbital (LUMO) of the oxy-dicopper unit, which is anti-bonding with respect to the oxygen-oxygen and copper-oxygen bonds. This initiates oxygen transfer to the *ortho* position of the phenyl ring, resulting in the formation of bound catechol. Electron transfer from the catechol to the copper atoms generates the deoxy site and releases the *o*-quinone.

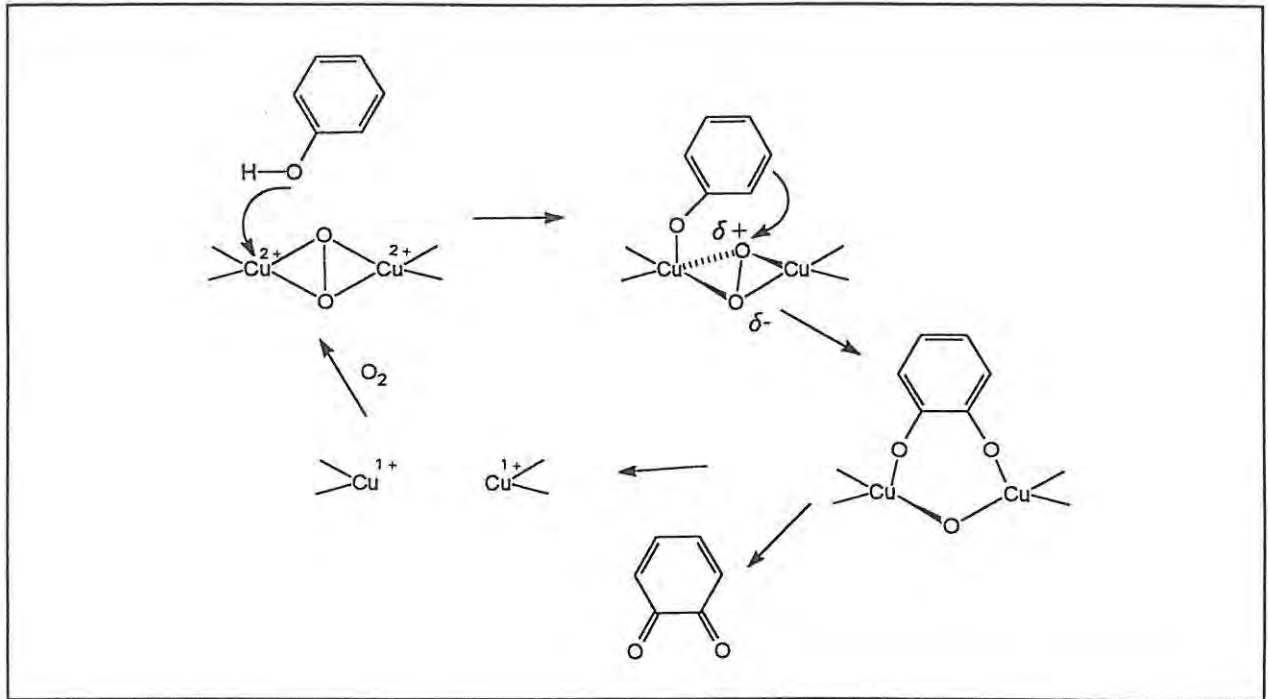


Figure 1.3: Proposed mechanism for tyrosinase phenolase activity (Solomon *et al.*, 1992)

1.3 BIOCATALYSIS WITH POLYPHENOL OXIDASE

1.3.1 Biocatalysis

The term "biocatalysis" refers to the use of enzymes or living cells to catalyse organic reactions *in vitro*, for synthetic purposes. The field of biocatalysis is one of the most exciting recent developments in synthetic organic chemistry, and it has grown rapidly in the past decade. The field has enormous potential, since it can draw on a wide range of enzymes which catalyse many different reactions. In fact, the only known organic reaction for which an enzyme catalyst has not yet been reported is the Diels Alder cycloaddition (Jones, 1993). Established industrial applications include synthesis of products such as amino acids, antibiotics and fine chemicals (Yamada and Shimizu, 1985). The large number of reviews which have appeared in the literature recently is a reflection of the prolific research taking place in the field of biocatalysis (for example, Jones, 1986; Khmelnitsky *et al.*, 1988; Wong, 1989; Zaks *et al.*, 1988; Margolin, 1991; Leuenberger, 1990; Drueckhammer *et al.*, 1991; Faber and Riva, 1992).

Selectivity is one of the key issues in organic catalysis, and one major advantage of using enzymes as catalysts for synthetic reactions is their high substrate specificity, regioselectivity and stereospecificity. Additional advantages include the following:

- enzymes are extremely efficient catalysts
- they function under very mild conditions
- the rates of reaction are high
- there are few side reactions
- the reactions are very predictable
- the enzymes can often be prepared by fermentation processes

(Suckling, 1990; Dordick, 1989).

In their natural environment, enzymes function in an aqueous medium, with closely regulated conditions of temperature, pH and ionic strength. Being proteins, they are susceptible to denaturation by agents such as heat, pH extremes, chemical reagents etc. *In vitro*, they generally require the same controlled conditions, particularly in aqueous solutions, and the low stability of an expensive catalyst can be a major drawback in utilisation of enzymes. The need to supply and regenerate a cofactor may add to the complexity and expense of the system (Good, 1989). In efforts to overcome these problems, various biological technologies have been developed, including immobilisation techniques and electrochemical methods (Linko and Linko, 1985).

1.3.2 Biocatalysis in organic media

Innovative research, pioneered largely by Klibanov and co-workers (Zaks and Klibanov, 1984; Hammond *et al.*, 1985; Klibanov, 1986; Kazandjian and Klibanov, 1986), has shown that many enzymes can function well in non-aqueous organic media, almost anhydrous media, or mixed aqueous-organic media. Interestingly, the researcher who first discovered tyrosinase was also the first to report the functioning of an enzyme in the presence of organic solvents (Bourquelot, 1911). More recent work indicated that biphasic systems, where the substrate and products were dissolved in an organic phase and the enzyme was in an immiscible aqueous phase, could lead to enhanced yields in enzyme-catalysed reactions (Klibanov *et al.*, 1977; Antonini *et al.*, 1981). Theories explaining the functioning and the kinetics of such systems in terms of partitioning processes were proposed (Martinek and Semenov, 1981; Martinek *et al.*, 1981).

Much progress has been made in the last few years in developing theories to explain and predict the behaviour of enzymes in organic media (discussed in Chapter 2). Application of the principles now established for such systems may lead to considerable improvement in the efficiency a biocatalytic process. The ultimate goal of research in non-aqueous biocatalysis is to be able to predict and alter the specificity of enzymes (Zaks and Russell, 1988).

In comparison with aqueous media, organic media have the following possible advantages:

- substrates and products have increased solubility
- substrates, intermediates and products have increased stability
- enzymes have increased stability, especially thermostability
- facile recovery of biocatalyst
- facile separation of products and catalyst.
- chemical equilibria may be shifted to favour a desired product
- microbial contamination is avoided

(Zaks and Russell, 1988; Dordick, 1989; Mattiasson and Adlercreutz, 1991; Blinkovsky *et al.*, 1992).

1.3.3 The manipulation of non-aqueous biocatalytic systems

1.3.3 (1) The effect of the solvent on selectivity

The selectivity of enzymes in organic media is particularly solvent-dependent. For instance, the substrate specificities of porcine pancreatic lipase, and the proteases chymotrypsin and subtilisin are all altered when they function in organic media (Zaks and Klibanov, 1986); the enantioselectivity of proteases can be altered so that *D*-amino acids are utilised (Sakurai *et al.*, 1988); and the regioselectivity and stereoselectivity of lipases can be altered (Rubio *et al.*, 1991; Margolin *et al.*, 1987). Asymmetric transformations catalysed by enzymes are efficient and can be controlled by manipulation of the solvent system (Klibanov, 1990; Fitzpatrick and Klibanov, 1991), and solvent-dependent prochiral selectivity in hydrolytic enzymes has recently been reported (Terradas *et al.*, 1993). In a detailed study, the enantioselectivity of lipase-catalysed reactions was found to be controlled by the solvent hydrophobicity and the substrate structure (Parida and Dordick, 1991).

Certain reactions which do not occur in aqueous systems can be carried out using organic solvents *eg.*, horseradish peroxidase is normally inactive towards lignin, but in 95% dioxane, it vigorously catalyses the polymerisation of lignin (Klibanov, 1986).

1.3.3 (2) The effect of non-aqueous solvents on protein stability

The increased thermostability of enzymes in organic media is valuable in industrial processes, since reaction rates and solubilities may be considerably enhanced by temperature increases. Protein stability depends upon many factors, such as electrostatic and hydrophobic interactions, protein-protein interactions, and compact intramolecular packing (Mozhaev *et al.*, 1988). The reason for the increased thermostability in organic media is that many of the reactions involved in destroying these interactions (*viz.*, denaturation processes) are water-dependent, and in the absence of free water they cannot occur (Gupta, 1991 and 1992). The absence of free water results in conformational rigidity while the enzyme is in the organic environment (see Section 2.1), and hence prevents the denaturation reactions (Volkin *et al.*, 1991).

1.3.3 (3) Immobilisation of enzymes

Since enzymes are not generally soluble in organic solvents, they are frequently immobilised, which can enhance enzyme stability (Khmelnitsky *et al.*, 1988), especially if the immobilisation involves multipoint attachment (Linko and Linko, 1985). Immobilisation of enzymes by cross-linking them

with hydrophobic gels (by UV-activated polymerisation) was found to enhance the activity of lipases (Fukui and Tanaka, 1982). Similarly, horseradish peroxidase was copolymerised with a support to give enhanced reactivity in chloroform and benzene (Naka *et al.*, 1991). Immobilisation has the additional advantage that the biocatalyst can be conveniently recovered and reused, and continuous processing systems can be utilised (Tramper, 1985).

By contrast, lipases may be soluble in some organic solvents, and an interesting variation on these immobilisation systems, *viz.*, solubilisation of the substrates in the organic solvent, was reported to facilitate regioselective acylation of sugars (Ikeda and Klivanov, 1993).

1.3.3 (4) Medium engineering

Medium engineering or reaction engineering are terms used to describe the design of microenvironments for enzymes in biocatalytic systems, taking into account the various parameters which are now known to affect the processes (Laane, 1987; Wandrey, 1993). With the information now available, it is often possible to predict the influence of solvents on equilibrium processes, for instance (Halling, 1990a).

An alternative to heterogenous organic medium systems utilises the developing technology of reverse micelles. Here, the enzyme is contained in one phase which is dispersed in another, giving an optically transparent solution (Khmelnitsky *et al.*, 1988; Andersson and Hahn-Hagerdal, 1990; Bru *et al.*, 1990). Chemical modification of enzymes to solubilise them in organic solvents, for example with detergents or polyethylene glycol, or in detergentless microemulsions (Takahashi *et al.*, 1985; Khmelnitsky *et al.*, 1988) is less common but has the advantage of producing one-phase systems (Mattiasson and Adlercreutz, 1991).

Supercritical fluids provide another alternative to conventional solvents for studying the effects of the environment on enzyme function because their properties (such as viscosity, density and dielectric constant) can be altered by changes in pressure. These changes can in turn alter enzyme specificity and activity, as shown in research by Russell and co-workers, using supercritical fluids such as carbon dioxide, ethane, ethene, sulphur hexafluoride, and fluoroform (Russell and Beckman, 1991; Kamat *et al.*, 1992; Russell, 1993).

The profound effects of the solvent on the structure and functioning of enzymes have become the subject of an important area of research which is discussed more fully in Chapter 2 of this thesis.

1.3.3 (5) Protein engineering

Protein engineering is a newly developing field which complements biocatalysis research (Wong, 1993). Enzymes can now be redesigned and new proteins can be produced by techniques such as site-directed mutagenesis, with altered amino acid sequences making them more compatible with organic solvents. Characteristics such as the number of charged groups on the protein surface (which would require hydration), the number of disulphide bridges (which stabilise internal structure), and hydrophobic interactions (which would contribute little stabilisation of the protein in a non-aqueous environment but may affect the substrate binding), can all be altered (Arnold, 1990). For example, Martinez *et al.* (1992) reported the stabilisation of subtilisin E towards organic solvents by site-directed mutagenesis. Changes in conformational stability, and compatibility with organic solvents resulting from enzyme engineering, can also provide valuable information regarding enzyme mechanisms (Wagner and Benkovic, 1990).

Dordick (1989) concluded: "The field of non-aqueous enzymology is maturing into a discipline of biocatalysis that has the potential to bring together the biotechnology and chemical industries like never before."

1.3.4 Biocatalysis involving polyphenol oxidase

The reaction catalysed by polyphenol oxidase, *viz.*, the regiospecific *ortho*-hydroxylation of phenols, is difficult to perform by conventional synthetic methods (Barton and Ollis, 1979), and thus a biocatalytic method has great potential as an alternative. However, the use of polyphenol oxidase as a biocatalyst has not been widely applied to organic syntheses, largely due to difficulties inherent in dealing with rapid, water-dependent polymerisation of the *o*-quinone products.

In aqueous polyphenol oxidase systems, this can be overcome by the addition of a reducing agent, usually ascorbic acid, to the medium to reduce the quinone product as it is formed, and catechols are then obtained. A variety of catechols have been synthesised using the polyphenol oxidase of alginate-entrapped cells of *Mucuna pruriens* in aqueous medium, in the presence of ascorbic acid (Pras and co-workers, see Section 1.1.8). The catechols were released into the medium by the cells. Other reactions where tyrosinase catalyses the oxidation of various phenolic substrates in aqueous, analytical-scale systems are also mentioned in Section 1.1.8.

An important application of polyphenol oxidase capitalises on the polymerising properties of *o*-quinones: the removal of phenols from polluted waters by tyrosinase-mediated oxidation and the

subsequent non-enzymic polymerisation leads to the formation of melanin-like precipitates. This was first proposed by Atlow *et al.* (1984), and research into developing the system is ongoing (Sun *et al.*, 1992; Goetsch, 1992; Wada *et al.*, 1993; Rose and co-workers, 1993).

1.3.5 Biocatalysis with polyphenol oxidase in organic medium

In one of the first investigations of polyphenol oxidase in organic media, (Tome *et al.*, 1978) the influence of several solvents was reported. Inhibition was observed in the presence of ethanol, methanol, propylene glycol and high proportions of glycerol.

In the course of developing applications of enzymes in organic solvent systems, Kazandjian and Klibanov (1985) investigated the functioning of polyphenol oxidase in various solvents. The enzyme was found to be active in a wide range of solvents, such as dichloromethane, carbon tetrachloride, benzene, toluene, hexane and butyl acetate. In all cases, approximately 0.5% water was required for activity. This work, and developments related to it, are discussed further in Chapter 2.

The activity of tyrosinase has also been investigated in AOT-isooctane reverse micelles, and the 4-methyl-*o*-benzoquinone formed from the conversion of *p*-cresol was found to be stable in the isooctane phase (Bru *et al.*, 1989). A similar system, using Brij 96-cyclohexane reverse micelles was used to show that the system closely resembled the aqueous system in catalytic activity (Sanchez-Ferrer *et al.*, 1988). Polyphenol oxidase in reverse vesicles formed with tetra-(ethylene glycol)-dodecyl ether, *n*-dodecane and water (which have a more complex, multi-layer structure than micelles) showed better activity than it did in reverse micelles (Sanchez-Ferrer and Garcia-Carmona, 1992a). Reverse micellar systems are difficult to apply industrially, and therefore, detergentless microemulsions of tyrosinase were successfully tested (Vulfson *et al.*, 1991).

The activity of polyphenol oxidase in supercritical fluids was examined (Hammond *et al.*, 1985) and found to be similar, in supercritical carbon dioxide and fluoroform, to the activity in water, with significant polymerisation of the quinone product occurring.

An interesting application of the activity of polyphenol oxidase has developed as a result of the importance of detecting phenolic compounds in various circumstances. Biosensors which contain the enzyme have been designed to detect a range of compounds, such as catecholamines (Berenguer *et al.*, 1989) and phenols (Hall *et al.*, 1988; Cosnier and Innocent, 1992). Water detection in organic phases was also demonstrated using a tyrosinase-containing electrode (Wang

and Reviejo, 1992 and 1993). An elegant biosensor for cyanide has been designed using an electrochemical cell to monitor inhibition of tyrosinase by cyanide, and at the same time replacing the substrate of the enzyme with an electrochemical mediator (Smit and Rechnitz, 1993).

Attention has been given to the use of tyrosinase to hydroxylate *L*-tyrosine, because the catechol which could be obtained is *L*-DOPA, the drug used to treat Parkinson's disease. Kazandjian and Klibanov (1985) demonstrated the feasibility of the reaction in chloroform, using commercially available partially purified mushroom tyrosinase, and *N*-acetyltyrosine ethyl ester (ATEE) as the substrate. (Tyrosine itself is not soluble in chloroform). Doddema (1988), using the same enzyme in organic and aqueous systems, showed that while the organic system was preferable in terms of reduced *o*-quinone polymerisation, aqueous systems were also feasible if a reductant such as ascorbic acid was added to reduce the quinones.

1.4 THE BIOMIMETIC APPROACH TO COPPER METALLOPROTEIN MODELS

1.4.1 Introductory remarks

The high efficiency of biological processes in general, and of their catalysts, enzymes, in particular, has prompted extensive research into the development of synthetic processes which approach this efficiency. Such research increases our understanding of the activity of proteins in relation to their structures. A multi-disciplinary bioorganic approach encompassing Biochemistry, Organic chemistry, and in some cases, Inorganic chemistry is required.

The general aims of a bioorganic approach to the study of metalloproteins can be summarised as follows:

- to establish a reasonable model to explain the functioning of the metalloprotein in terms of its structure
- to allow comparison of the observed protein activity with that predicted for the proposed model
- to allow for future utilisation of synthetic systems for analogous catalytic transformations (Tyeklár and Karlin, 1989).

Bioorganic investigations of metalloproteins have, as a basic premise, the idea that the chemistry of the metal and the binding site are strongly related to the nature of the coordinating environment of the metal ion. In metalloproteins this coordination environment is provided by the amino acid side chains, possibly some small molecules such as water or hydroxyl groups, and sometimes by prosthetic groups such as porphyrin rings. (Sorrell, 1989).

Thus ligand systems can be designed to provide specifically selected features in the coordination of a metal ion, with the organic matrix of the complex replacing the metalloprotein peptide chains and serving to position the donor groups appropriately for coordination to the metal.

The total synthesis of an organic ligand system, with subsequent addition of the metal ion, allows incorporation of selected properties such as geometry, steric characteristics, or polarity. Alternatively, a complex may be synthesised by a metal template condensation which allows the complex to adopt an optimal coordination geometry as dictated by the nature of the metal ion.

The synthetic models can be compared with the metalloproteins in respect of spectral and physicochemical properties, catalytic activity, or mechanism of reaction. They may provide

information relating to the intrinsic properties of the active site and/or the effects that environmental variations may have on the active site.

Objectives in the biomimetic modelling of copper-containing metalloproteins have evolved over a number of years, as knowledge has accumulated regarding the structures of the proteins and the chemical properties of the synthetic complexes themselves. These properties include oxygenation reactions, magnetic coupling, spectroscopic properties and basic ligand structure.

1.4.2 The chemistry of copper complexes

1.4.2 (1) Copper-catalysed oxidation reactions

Copper has been used for the catalysis of many oxidation reactions. In particular, oxygenations of phenols catalysed by copper/amine systems, have been known for a long time. For example, a copper/morpholine system was investigated as a tyrosinase model as early as 1955 (Brackman and Havinga, 1955), and a simple CuCl_2 /triethylamine system is known to catalyse the conversion of catechols to *o*-quinones (Karlin and Gultneh, 1987). Various systems have been investigated for catalytic activity with substrates such as *di-tert*-butylphenol and ascorbic acid (Oishi *et al.*, 1980), as well as simple phenols. Table 1.10 shows some systems which have been reported, and the products obtained. These products vary with the structure of the substrates, particularly with respect to *ortho*-substituents which lead to blocking or steric hindrance of the phenolic hydroxyl.

In the case of catechols, the importance of steric matching between electron donor and acceptor groups was demonstrated by Oishi *et al.*, (1980) in the oxidation of catechols with various catalytic copper complexes. The coordination of the catechols with binuclear complexes, as shown below, was suggested to facilitate their oxidation to *o*-quinones at greater rates than in reactions with mononuclear complexes. The isolation of a dicopper (II)-catecholate complex intermediate by Karlin *et al.*, (1985a) lends support to this theory.

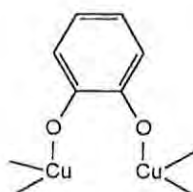
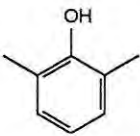
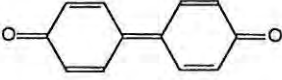
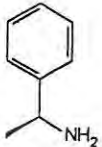
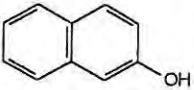
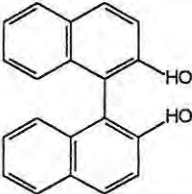
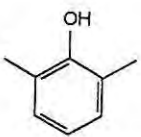
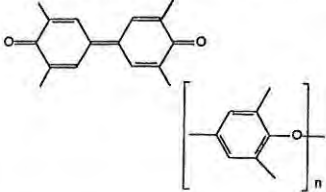
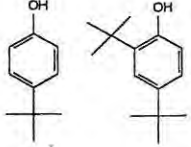
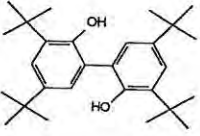
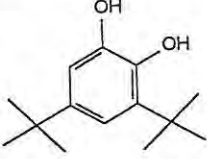
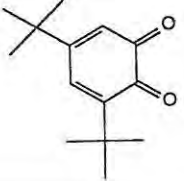
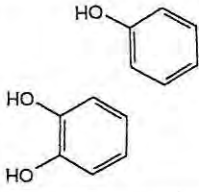
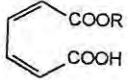
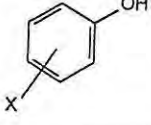
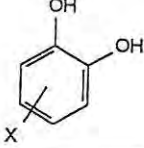
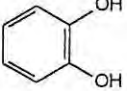
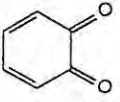
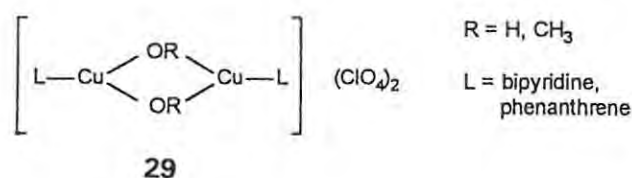


Table 1.10: Copper-catalysed oxidations of phenols

Catalytic system	Substrate	Product	Reference
$\text{Cu}(\text{NO}_3)_2/\text{CH}_3\text{CN}$			Tsuruya <i>et al.</i> , 1977
$\text{Cu}(\text{NO}_3)_2/$ 			Feringa and Wynberg, 1978
$\text{Cu}^{\text{II}}/\text{poly}(\text{amido-amines})$			Flinterman <i>et al.</i> , 1983
$\text{Cu}^{\text{II}}/\text{ethylenediamine}$			Kushioka, 1984
$(\text{CuCl}/\text{py})_n/\text{CH}_2\text{Cl}_2$ or CHCl_3			Speier, 1986
$\text{CuCl}/\text{O}_2/\text{py}$ with ROH			Tsuji and Takayanagi, 1978
$\text{N} \begin{array}{c} \diagup \\ \text{Cu}^{\text{I}} \\ \diagdown \\ \text{N} \end{array} \text{-PPh}_3\text{BH}_4$			Chioccare <i>et al.</i> , 1991
$\text{O}_2/\text{catalytic amount Cu}^{\text{II}}/\text{H}_2\text{O}$			Balla <i>et al.</i> , 1992

1.4.2 (2) Mechanisms of copper-catalysed oxidations of phenols

The mechanisms of copper-catalysed oxidations are not well elucidated. The oxidation of phenols is suggested (Gampp and Zuberbühler, 1981) to involve the formation of radicals within the coordination sphere of the copper (II) ions. Subsequently, further reactions can take place to give, for instance, coupled products. In the cases of complexes such as **29** (Thompson and Calabrese, 1986) at least, the redox reaction was shown to take place in two single-electron transfer steps rather than one two-electron step.



Oxidative coupling reactions only occur with substrates which have labile hydrogen and thus, deprotonation and complexation with the copper are likely to be the initial steps in the reactions. Oxygen serves to reoxidise the copper (I) generated during the reaction. Catalysis of the oxidation of catechols by oxygen, with a CuCl/pyridine catalyst, was proposed (Rogic, cited in Karlin and Gultneh, 1987) to proceed *via* the mechanism shown in Figure 1.4.

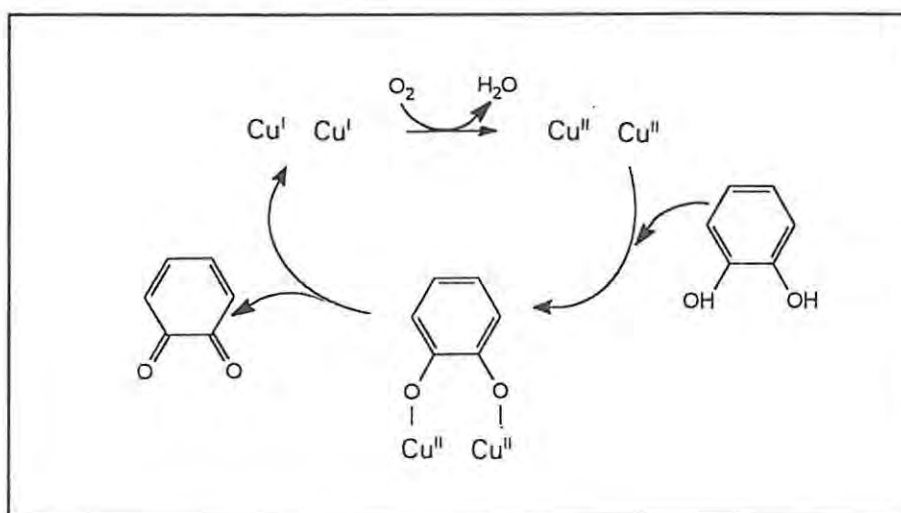
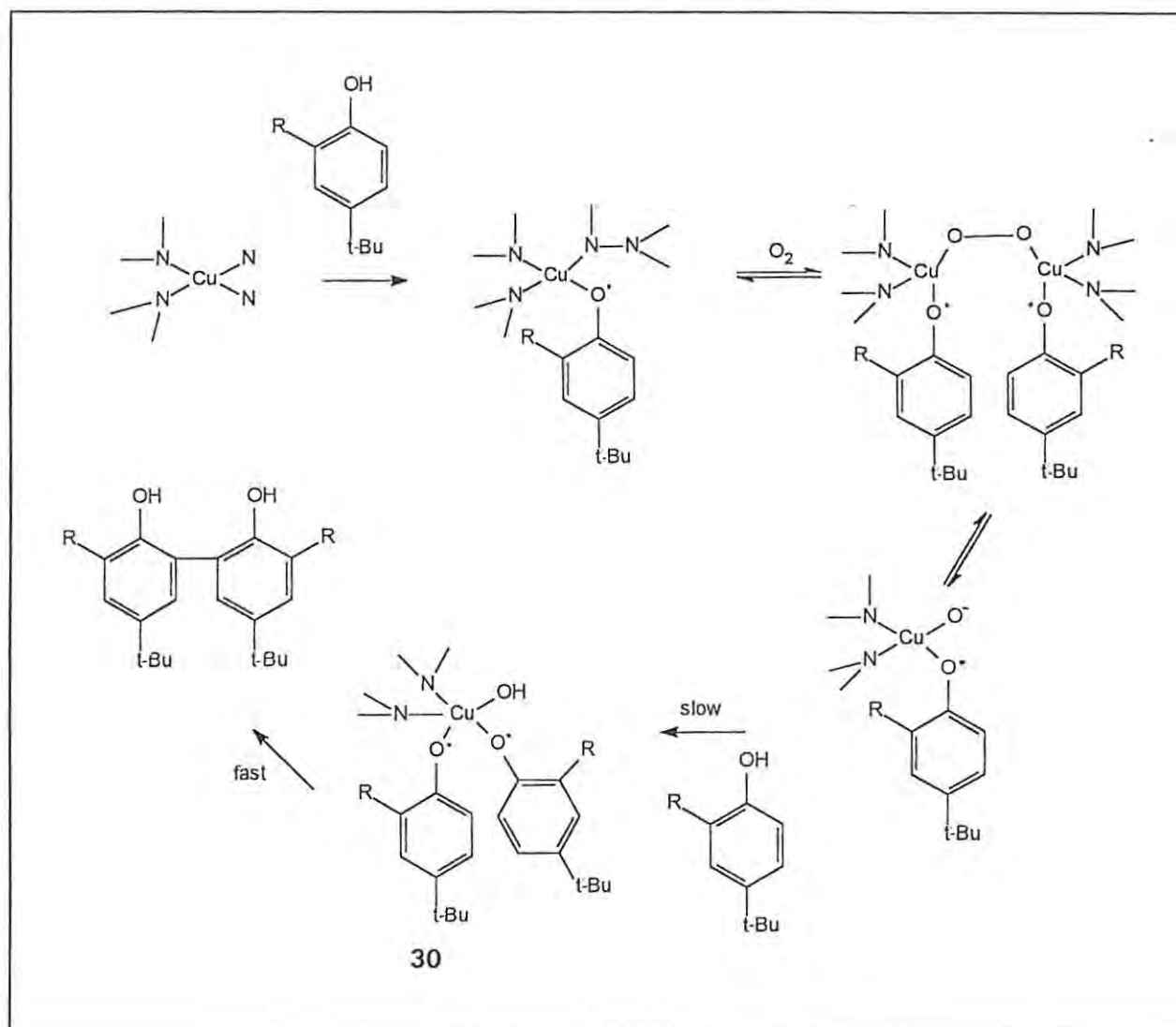


Figure 1.4: Proposed mechanism for the oxidation of catechols, catalysed by CuCl/pyridine (Karlin and Gultneh, 1987)

In a comprehensive study using copper (II)/amine systems to oxidise various phenols, Kushioka (1984) showed that the structure of the ligand in the complex was important. In the proposed

mechanism (see Scheme 1.15 below), steric crowding of the key tetrahedral copper intermediate **30** might facilitate rapid coupling of two phenoxide radicals. It may be speculated that a restricted binding site might not admit two phenol molecules, and thus a single radical might be released to give some other, possibly non-coupled, product.



Scheme 1.15: Proposed mechanism for reaction of copper (II)/amine systems (Kushioka, 1984)

Capdevielle, Maumy, and co-workers developed a catalytic system comprising copper (II) salts and trimethylamine *N*-oxide (TMAO), which was used in the *o*-hydroxylation of various substrates (Reinaud *et al.*, 1990a, b) and (Reinaud *et al.*, 1991). These authors postulated a copper (III) species as an intermediate in a radical mechanism, to explain these reactions and the activity of the CuCl/O₂/acetonitrile system, which they had previously used in the conversion of phenols to

catechols (Capdevielle and Maumy, 1982). They proposed a corresponding mechanism for the action of tyrosinase in the same publication. Interestingly, a similar mechanism involving a copper (III) species has recently been proposed for tyrosinase catalysis (Kitajima, 1992; Kitajima and Morooka, 1993; see section 1.4.5).

1.4.2 (3) Reactions with copper complexes and oxygen: coordination considerations

The reaction of copper complexes with oxygen involves a change in the oxidation state of the metal ions and therefore in the coordination geometry around the ions. The preferred coordination arrangements for copper (I) are linear, trigonal, or tetrahedral, but copper (II) is commonly tetragonal with four equatorial ligands and two less strongly coordinated, axial ligands (see Table 1.11).

Table 1.11: Coordination geometry for Cu (I) and Cu (II)

Ion	Preferred coordination number	Preferred geometry
Cu (I)	2	Linear
	3	Trigonal
	4	Tetrahedral
Cu (II)	4	Square planar
	5	Square pyramidal
	6	Trigonal bipyramidal Octahedral

Thus a redox process will be strongly influenced by the nature of the ligands, their coordination geometry, chelate ring size, and also by solvent effects. For example, if a reduction reaction leads to distortion of a planar coordination arrangement towards tetrahedral geometry, the copper (I) state will be favoured and the reaction may not take place readily. Similarly, a reduction in the size of a chelate ring may favour the reduction of a copper (II) ion to copper (I). Polar solvents are known to favour the higher oxidation state (Karlin and Gultneh, 1987).

When oxygen, O_2 , binds to copper ions, two charge transfer processes can occur, *viz.*, electron donation from oxygen to the metal, and metal- π -to-dioxygen- π^* back donation. The result is at least partial transfer of electrons to the metal, and weakening of the O-O bond. (Karlin and Gultneh, 1987).

1.4.3 Choice of ligands for binuclear copper complexes

In designing model compounds, it is logical to mimic as closely as possible the structure of the metalloprotein (within the limits of existing knowledge). The ligand should contain the appropriate number of donor atoms to coordinate the metal ions, and these should be chemically similar to the protein donor groups i.e. histidyl imidazoles in the case of tyrosinase. The ligands need to be large enough to accommodate both metal ions and any additional coordinating or bridging groups required in the reaction. In some metalloproteins there is evidence for distinct binding sites for separate atoms of the same or different metals, and a ligand would require an asymmetrical structure in order to simulate this feature (Crane and Fenton, 1991).

Since the nitrogen-containing donors in the ligand systems are intended to mimic histidyl imidazoles, they should be aromatic or at least have sp^2 hybridisation. Thus imine-nitrogens are more suitable than amine-nitrogens, and nitrogen-containing heterocycles are an obvious choice. The basicity of potential donor groups (shown in Table 1.12) is also of importance, since the reaction being investigated involves electron transfer (Sorrell, 1989).

Table 1.12: pK_b values for N-donor groups

Donor group	pK_b
Alkyl-NH ₂	3.0
Aryl-NH ₂	9.4
Benzimidazole	8.5
Histidine	8.0
Imidazole	7.0
Pyrazole	11.5
Pyridine	8.7

While imidazole groups are an obvious choice as donors, the chemistry involved in the synthesis of ligands which include them can present difficulties (Casella *et al.*, 1993.) Therefore, benzimidazole groups have often been used as donor groups; they contain the imidazole groups but are more accessible synthetically. However, benzimidazole groups are sterically larger and significantly less basic (see Table 1.12). Their steric bulk may be an advantage in that this may impose geometric constraints on the copper centres of the complexes in a manner similar to the situation pertaining in proteins (Pandiyan *et al.*, 1992).

Pyridine groups have frequently been included, and this may be due, largely, to successful pioneering work using pyridines, by Karlin and co-workers, over a number of years (eg. Karlin *et al.*, 1981 and Sanyal *et al.*, 1992).

Pyrazole groups have also been included in ligands because of their spectroscopic similarity to imidazoles, and the relative facility of syntheses involving them (see, for example, Malachowski and Davidson, 1989 and Malachowski *et al.*, 1992).

An additional requirement is flexibility in the ligand to accommodate changes in coordination geometry around the copper atoms as their oxidation state changes. Copper (I) and copper (II) ions have distinctly different coordination and geometric requirements as shown in Table 1.11 (Sorrell, 1989). Six-membered chelate rings are more flexible than five-membered chelate rings, and thus, the former are better able to accommodate the coordination changes accompanying the redox process (Casella *et al.*, 1993).

Ligands with imine-containing donor groups stabilise complexes with copper in the lower oxidation state better than amine-containing analogs, because the unsaturated ligands have the ability to delocalise electron density from the metal ions by π -back bonding (Bernhardt *et al.*, 1992). However, a combination of both types is common, particularly in binucleating ligands.

1.4.4 Complexes synthesised as biomimetic models for Haemocyanin and Tyrosinase

This field has been reviewed by several authors, and from various viewpoints (for example, Sorrell, 1985; Karlin and Gultneh, 1987; Karlin 1993; Spodine and Manzur, 1992). Therefore, the following is a summary of the information relevant to the present study, and does not aim to cover all copper dinuclear complexes which have been reported.

1.4.4 (1) Early complexes

Early studies on biomimetic copper complexes were stimulated by progress in the characterisation of the proteins long before the structure of haemocyanin was elucidated by X-ray crystallography (Gaykema *et al.* 1985). Therefore they were focussed on oxygen-binding reactions and related physical and spectroscopic properties. Central issues in this research have included:

- the structure of the deoxy-binding site
- the existence and nature of an endogenous protein bridge
- the nature and geometry of the Cu_2O_2 unit
- the reversibility of oxygen binding
- the origin of the magnetic coupling of the copper atoms
- the activation of molecular oxygen by tyrosinase (Sorrell, 1989)

The model upon which early studies were based was proposed by Solomon (1983) (Figure 1.5 below). The two copper atoms were suggested to be coordinated to two or three histidyl-imidazole ligands each, and they were assumed to be in the +2 oxidation state, with tetragonal geometry, when oxygen was bound. The peroxide ion was proposed to bridge the two copper ions in a *cis- μ -1,2*-fashion. An endogenous ligand originating in the protein was suggested to be responsible for the observed anti-ferromagnetic coupling of the binuclear unit. This model was generally accepted until recently, when alternative proposals were made subsequent to characterisation of new complexes [see Section 1.4.4 (6)].

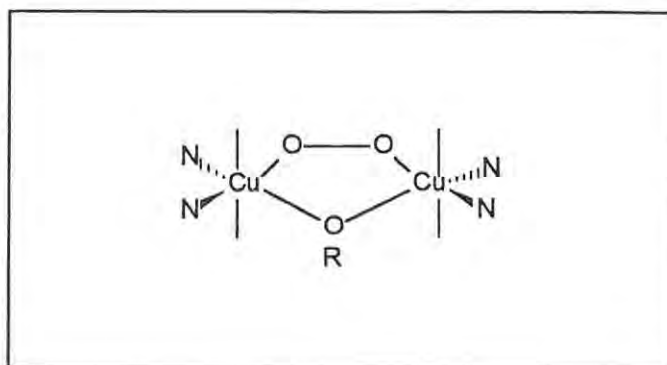
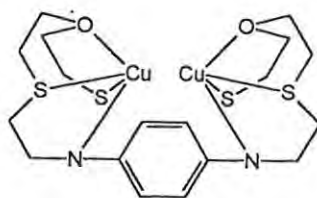


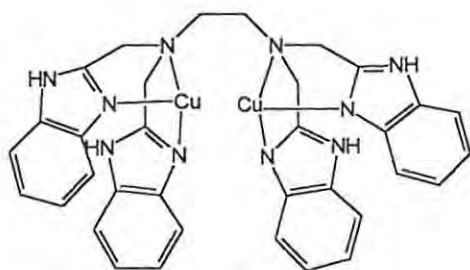
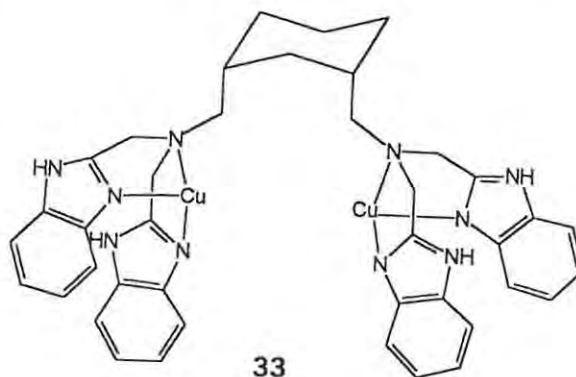
Figure 1.5: Model of the dinuclear copper binding site (Solomon, 1983)

Biomimetic complexes thus required two copper ions to be coordinated by donor groups in a ligand whose structure presented a "reaction space" suitable for binding and activating oxygen and/or organic substrates. The chemical reactivity and physicochemical characteristics of the complex would depend, of course, on the environment of the metal centre and hence on the nature of the

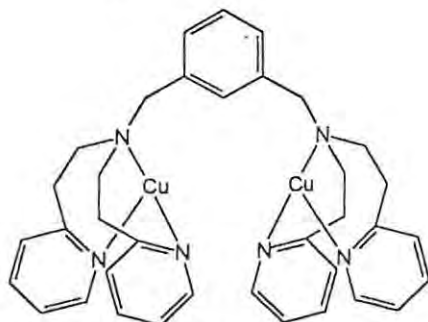
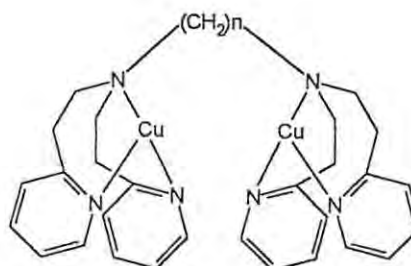
ligand system. Careful design of ligand systems with specifically positioned donor groups is necessary to coordinate two copper ions so that they are sufficiently close together to be able to be bridged by a dioxygen molecule. While complex **31** does contain sulphur and oxygen donor atoms (these had not been ruled out as possible donors at the time of this synthesis), it represents one of the first successful binuclear complexes able to bind dioxygen (Bulkowski *et al.*, 1977).

**31**

The complex **32**, reported in 1982 (Hendricks *et al.*, 1982), reacted with oxygen but not reversibly, and without evidence for a dioxygen bridge being formed. A similar complex, **33**, which differs from **32** only in the nature of the central spacer part of the ligand, also provided three nitrogen donors per copper atom and was found to react "semi-reversibly" with oxygen (Sorrell, 1989).

**32****33**

Major contributions to the field of dinuclear copper complexes have been made by Karlin and co-workers over a number of years (see, for example, Karlin *et al.*, 1981 and Sarwar-Nasir *et al.*, 1993). These authors have reported work on many complexes, and notably complexes **34** (Karlin *et al.*, 1981), and **35** (Karlin *et al.*, 1985b). The properties of these and related complexes are discussed in following sections.

**34****35**

1.4.4 (2) Dinuclear copper complexes synthesised to model the protein endogenous bridge

Since the proteins were observed to be EPR-silent i.e. diamagnetic overall, the existence of some bridging group originating in the protein structure was proposed. This was thought necessary, to account for the strong anti-ferromagnetic coupling of the two paramagnetic copper (II) ions in oxyhaemocyanin and oxytyrosinase. Possible bridging groups included the phenolate, alkoxide, sulphhydryl, and hydroxyl groups of the amino acids, or water, or other separate groups (such as hydroxide). The bridging group concept was partially clarified later when the X-ray crystal structure of haemocyanin was elucidated (Gaykema *et al.*, 1985), but even then the existence of an endogenous bridging group was not ruled out completely (Lerch, 1987).

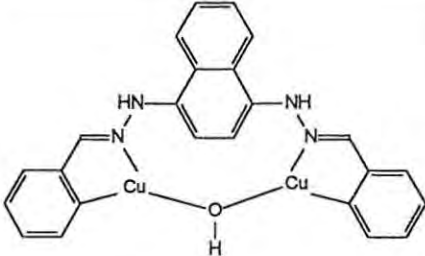
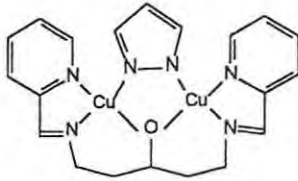
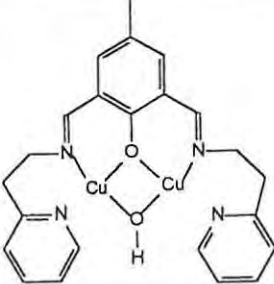
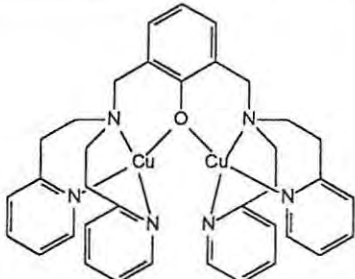
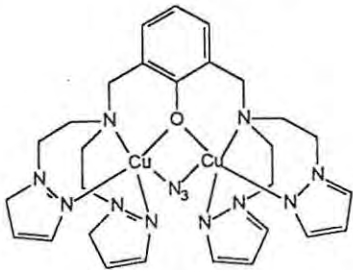
Thus complexes were synthesised in which various groups bridged two copper ions, as part of the ligand system or separately. (See Table 1.13). Many phenolate-bridged complexes were reported because the tyrosine phenolic side chain was considered a likely bridging group in haemocyanin. (eg. Karlin *et al.*, 1987). Since most of these complexes exhibited similarity to the metalloproteins in terms of magnetic properties, it seemed that many different bridging groups could facilitate the magnetic coupling. The crystal structure of haemocyanin has shown that the most likely groups are hydroxyl or water, if a bridging group is present at all. More recently complexes have been synthesised without bridging groups.

Recent spectroscopic studies of the hydroxy-bridged complex 40 (Table 1.13) have unambiguously identified the wavelengths associated with the vibrational modes of Cu-OH-Cu and Cu-OR-Cu chromophores, but comparison with the spectral properties of the oxy-proteins is not sufficiently conclusive, and leaves the presence of an OH bridge in the proteins unconfirmed.

1.4.4 (3) The nature of the peroxide bridge in dioxygen-containing complexes

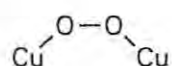
Studies on the coordination of oxygen to haemocyanin, using resonance Raman spectroscopy (Loehr *et al.*, cited in Kitajima *et al.*, 1992) have indicated that the dinuclear copper site is symmetrically bridged by a peroxide ion, and that the copper (I) ions of deoxyhaemocyanin are oxidised to copper (II) upon coordination of the oxygen. Both oxytyrosinase and oxyhaemocyanin exhibit intense absorption bands due to peroxide-to-copper charge-transfer (CT) transitions, at 350 nm ($\epsilon = 20000 \text{ M}^{-1}\text{cm}^{-1}$) and 570 nm ($\epsilon = 1000 \text{ M}^{-1}\text{cm}^{-1}$). The presence of more than two peroxide-to-copper CT transitions, as observed in oxyhaemocyanin, is further evidence for the peroxide bridging of both copper ions, because this would cause the observed splitting of the

Table 1.13: Examples of complexes with different bridging groups

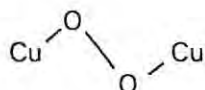
Complex	Bridging group	Structure	Reference
36	Hydroxide		Sorrell, 1989
37	Alkoxide		Nishida <i>et al.</i> , 1986
38	Phenoxide		Karlin <i>et al.</i> , 1987
39	Phenoxide		Karlin <i>et al.</i> , 1984
40	Phenoxide		Sorrell, 1989

absorptions. In a mononuclear copper-peroxide complex (Cu-O-O) only two peroxide-to-copper CT transitions would be expected (Baldwin *et al.*, 1992). The issue of anti-ferromagnetic coupling of the two copper ions is also important here, since there is debate as to whether the peroxide bridge alone is capable of mediating this coupling, or whether an additional bridging group is necessary.

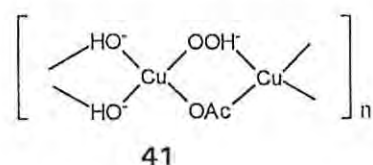
With evidence available from optical spectra, EXAFS studies, and the known geometry for transition metal-peroxide complexes, Eickmann *et al.* (1979) proposed a *cis-μ-1,2*-peroxide bridging mode as shown below:



Many complexes, subsequently prepared in attempts to mimic this type of bridging, were found to have *trans-μ-1,2*-peroxide bridging:

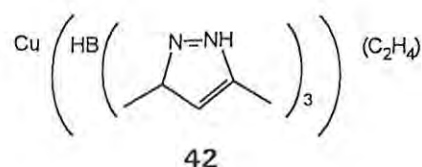


The observed spectral features of these *trans*-bridged complexes differed widely from those of oxyhaemocyanin (Larrabee and Spiro, 1980, and Jacobson *et al.*, 1988). Theoretical calculations have shown that the electronic structure of complexes with either mode of bridging would be similar (Baldwin *et al.*, 1992) and thus their reactivities would be similar. The synthesis of *μ*-peroxo copper complexes which could be isolated and fully characterised has proved difficult (Kitajima, 1992). In an early attempt, Ochiai (1973) synthesised the compound **41** which showed an absorption band at 360-390 nm, due to the peroxo-copper (II) group, and the complex was EPR-silent.

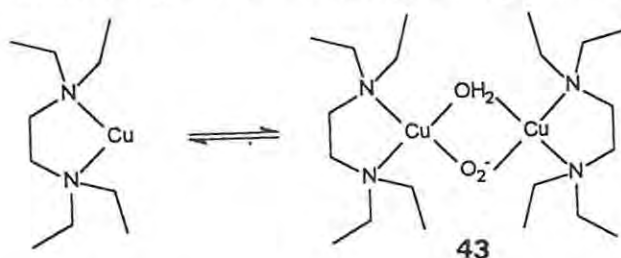


1.4.4 (4) Mononuclear and dimerising complexes

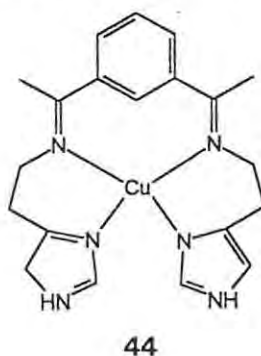
The first reported example of reversible oxygen binding was by Thompson (1984a) with a copper (I) complex **42** involving 3,5-dimethyl-1-pyrazolyl borate ligands, but a superoxide complex was obtained i.e. Cu-O₂.



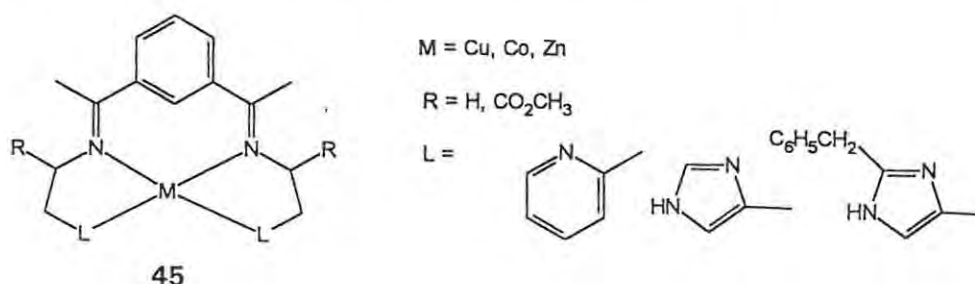
Subsequently the same author (Thompson, 1984b) reported a dicopper (II)-peroxide complex with $[\text{Cu}(\text{N,N,N',N'}\text{-tetraethylethylenediamine})(\text{C}_2\text{H}_4)]\text{ClO}_4$ where the independent mononuclear copper (I) precursors reacted with oxygen to form a dioxygen-bridged dimer, **43**.



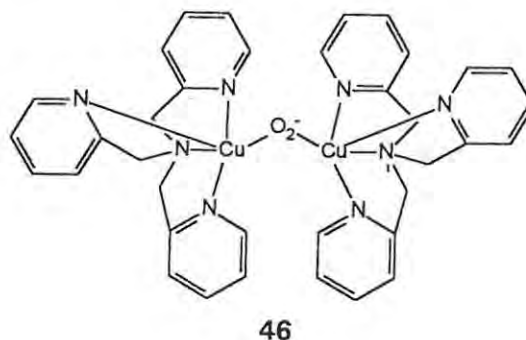
Simmons *et al.* (1978 and 1980) prepared the imidazolyl complex **44** and its pyridyl analog, both of which dimerised upon reaction with oxygen. The reversible reaction with oxygen was accompanied by distinct spectral changes, and EPR measurements showed that the oxygen adduct was diamagnetic, indicating that a $\text{Cu}^{\text{II}}\text{-O}_2\text{-Cu}^{\text{II}}$ species was likely to have been formed.



Casella *et al.*, (1984) prepared similar complexes **45** by using a synthetic method which allowed variation of the donor groups in the ligand system, so that the effect of varying basicity could be examined. In particular, the complex in which R was COOCH_3 and L was imidazole, was reported to bind oxygen reversibly, with corresponding spectral changes. However, the EPR signals increased as the copper was oxidised, showing a lack of coupling. The copper (I) complex was difficult to purify and therefore could not be fully characterised. Dinuclear complexes with the same ligands were later synthesised, and will be discussed later [see Section 1.4.4 (5)].



Jacobson *et al* (1988) reported the first complete characterisation of a complex formed by the bridging two mononuclear units by dioxygen, *viz.*, complex **46**. The analysis revealed differences between the complex and oxyhaemocyanin in respect of spectral features, copper-copper separation, and the geometric arrangement around the copper ions. The peroxide bridge was μ -1,2-*trans* rather than *cis*, the former being the sterically preferred conformation. The diamagnetic nature of the complex lent weight to the theory that no endogenous bridge is necessarily involved in the coupling of the metal ions.



In an extension of this line of study, complexes **47** with substituents R were synthesised and shown to dimerise *via* a peroxide bridge. The reaction with oxygen was temperature-dependent, and copper (I) complexes were not kinetically stable (Sanyal *et al.*, 1992). Simple imidazole donors were used to synthesise complex **48** also *via* the dimerisation of mononuclear copper (I) units. The properties of these products were again found to be different to those of oxyhaemocyanin and the peroxide bridge was again suggested to be in a *trans*- μ -1,2 or μ - η^2 : η^2 mode (Figure 1.6). The ease with which pyridine donors could replace imidazoles was suggested to be due to a self-assembly process being facilitated by the preformed Cu_2O_2 unit (Sanyal *et al.*, 1991).

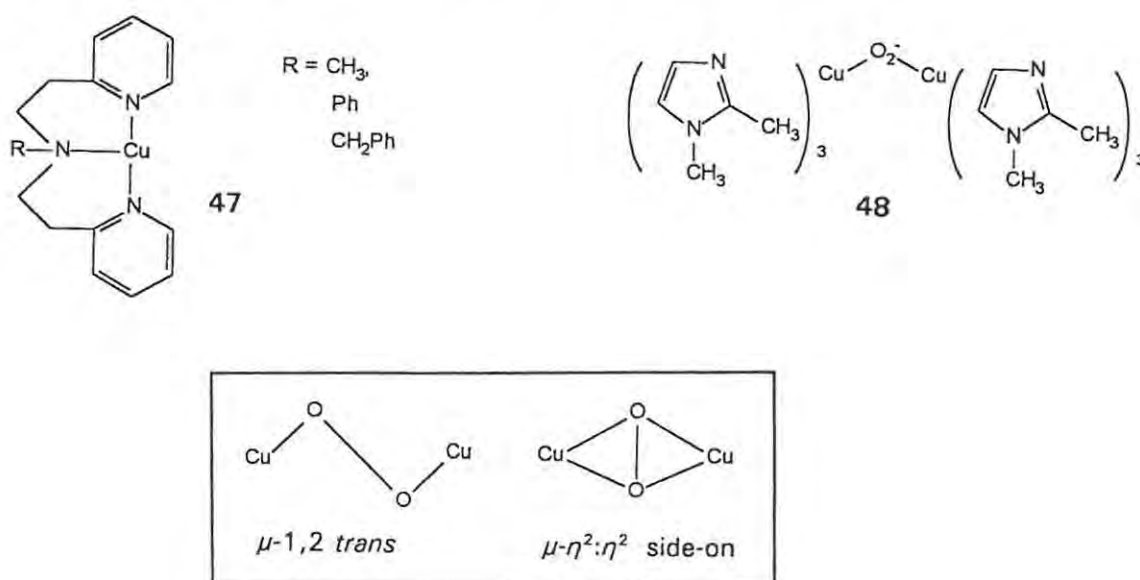
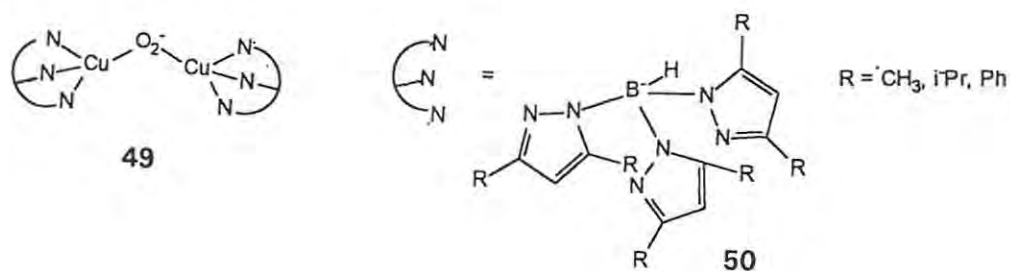


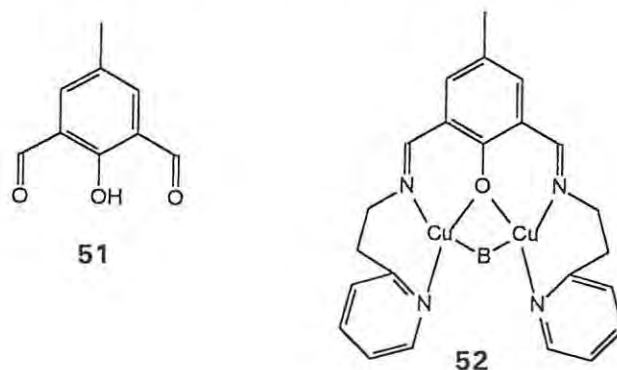
Figure 1.6: Possible modes of binding of oxygen in dinuclear copper binding site

Major progress in this area was made by Kitajima and co-workers, in the synthesis of complex **49**, using *tris*(pyrazolyl) borate ligands, **50** (Kitajima *et al.*, 1988). This complex exhibited features closely resembling those of oxyhaemocyanin, with respect to electronic spectra, magnetic character, copper-copper separation, and μ -peroxo IR stretching frequency. The structure of the complex was determined by X-ray crystallography (Kitajima *et al.*, 1991), and the μ - η^2 : η^2 coordination of the peroxide was confirmed. The detailed analysis of this complex has given a convincing argument for the side-on peroxide bridging proposed for oxyhaemocyanin and oxytyrosinase [see Section 1.4.4 (6)].

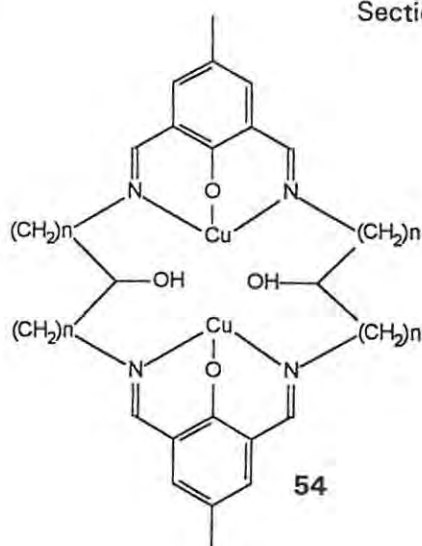
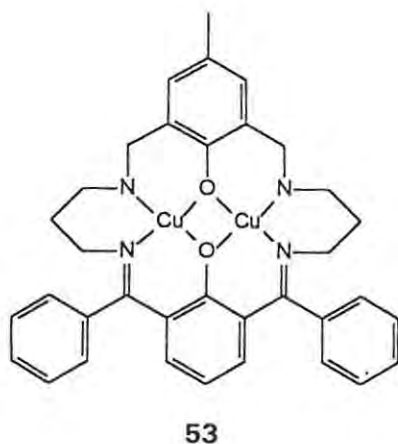


1.4.4 (5) Dinuclear complexes

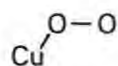
Binucleating ligands allow more control over magnetic and electronic exchange properties than dimeric systems, and thus attention has been focussed on compounds such as **51** for use in building ligand systems capable of coordinating two copper ions (O'Connor, 1986), as for example, in complex **52**.



Antiferromagnetic coupling was observed in the case of complex **52**, and the X-ray crystal structure (Nishida *et al.*, 1985) showed the copper ions to have trigonal bipyramidal geometry, but with the peroxide axially disposed. This implies the involvement of the exogenous ligand B in the exchange. The nature of such exogenous ligands can strongly influence the magnetic coupling (Mallah *et al.*, 1986). Macrocyclic dicopper (II) complexes such as **53** (Mandal *et al.*, 1989) and **54** (Tandon *et al.*, 1992) also exhibit antiferromagnetic coupling of the two copper (II) ions.



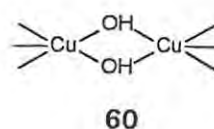
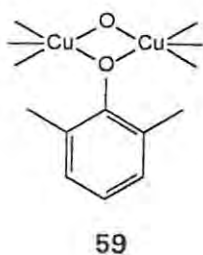
Extensive investigations on the complex **57** have been reported by Karlin and co-workers (Karlin *et al.*, 1987 and subsequent reports). This complex was prepared by the sequence shown in Scheme (1.16), where the reaction of the dicopper (I) complex **55** with oxygen was used to produce complex **56** and hence **57** by reversible reaction with oxygen, at -80°C . The Cu_2O_2 unit was found to be planar, with each copper atom having square planar geometry. Raman spectroscopy was used to demonstrate that the peroxide bridged the copper ions, but the coordination was found to be asymmetrical, and the arrangement was likely to be terminal:

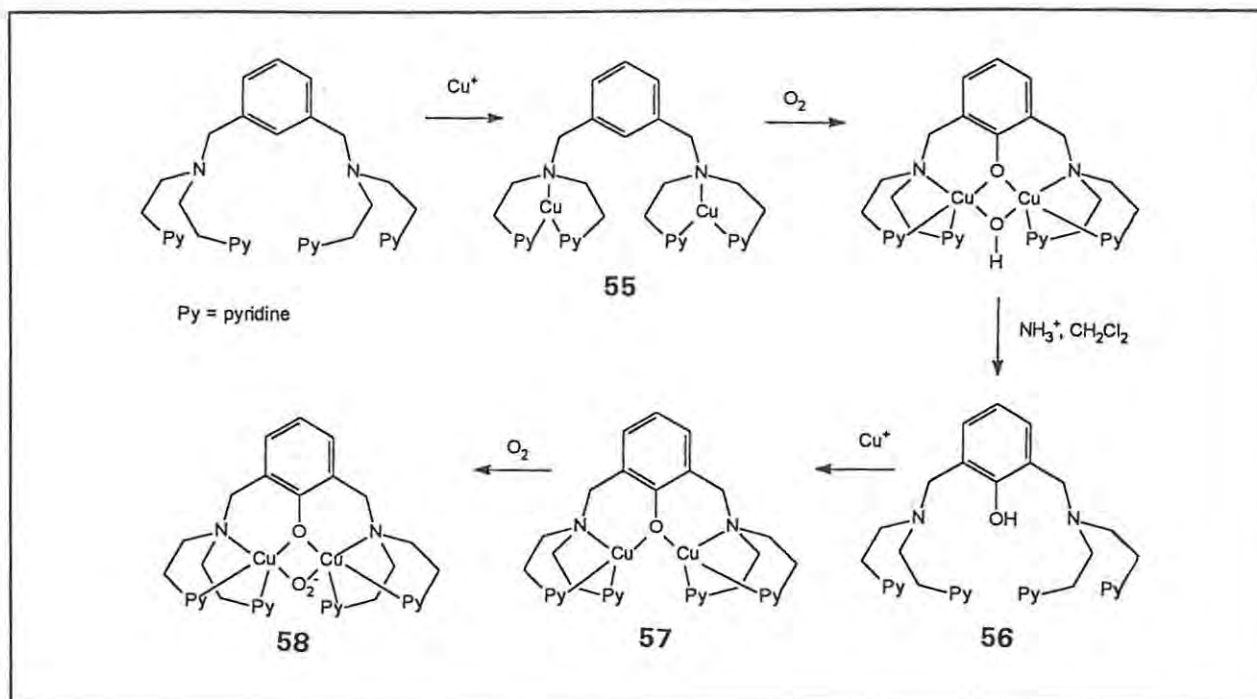


This coordination was supported by the lack of spectral similarity between this complex and oxyhaemocyanin (Pate *et al.*, 1987).

Alkyl substitution on the pyridine ligands has been found to have marked effects on the reactivity of the complexes with oxygen. The presence of a methyl group in the position *ortho* to the heterocyclic nitrogen resulted in no reaction with oxygen, while an ethyl group in the less sterically crowding *meta*-position did not prevent reaction with oxygen (Sarwar-Nasir *et al.*, 1993).

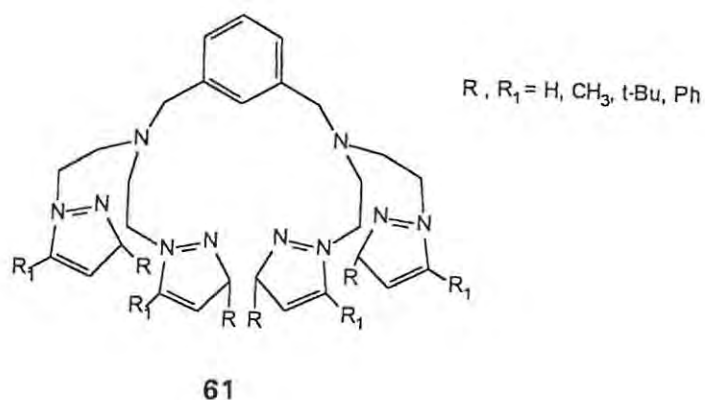
Pyrazole derivatives of these complexes did not bind oxygen in dichloromethane, but reacted with oxygen in methanol, producing intermediates such as **59** and **60**.





Scheme 1.16: Synthesis of complex 57

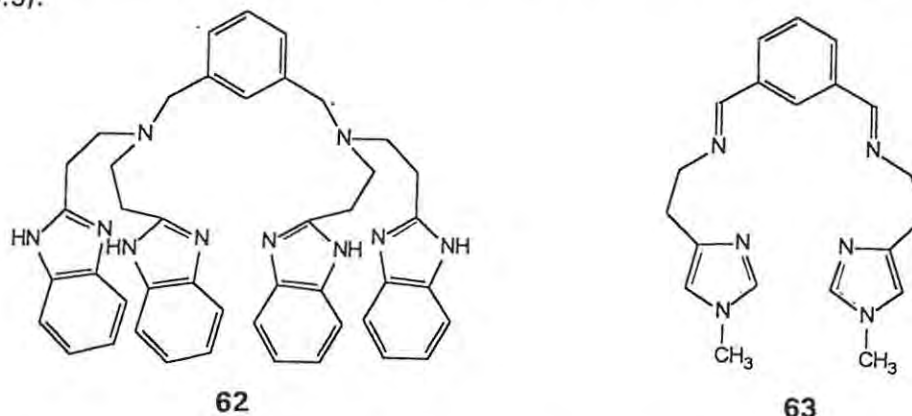
Trends similar to those reported for Karlin's complexes were observed with substituted pyrazole donors in complexes of the ligands 61 (Sorrell, 1989; Sorrell *et al.*, 1991a).



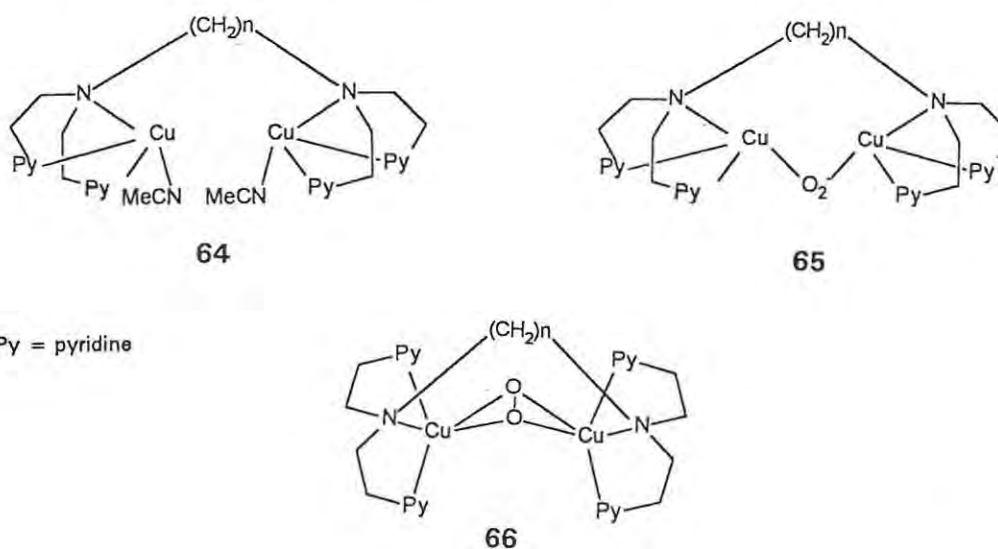
Hybrid ligands containing pyridine and pyrazole donor groups were found to react similarly to pyridine ligands, with peroxo-adducts being formed at low temperatures in dichloromethane (Sorrell and Vankai, 1990).

Thus, while pyrazole is a good structural analog for imidazole in terms of size, pyridine is a better analog with respect to basicity and therefore as a mimic for the electronic features of imidazole (Sorrell and Garrity, 1991). These authors synthesised ligands such as 62 and 63, using imidazole

and benzimidazole donors. Mononuclear complexes of these ligands reacted with oxygen at low temperatures with spectral indications of oxygen binding, and notably, the imidazole-containing complex was found to react as a tyrosinase mimic, with hydroxylation of the arene ring (see Section 1.4.5).



Karlin and co-workers prepared complex **64** which lacked a central aromatic ring but was shown to have coordinated solvent molecules. These complexes reacted reversibly with oxygen, forming diamagnetic peroxide-bridged structures **65**. EXAFS analysis indicated that the coordination was either *cis-μ-1,2* or *μ-η²:η²*, (see below), and that the spectral characteristics were similar to those of oxyhaemocyanin. In the case of the complex **64** when *n* = 4 and the coordinated solvent was acetonitrile, the structure **66** was determined by X-ray crystallography (Karlin *et al.*, 1988). Coordination of the peroxide in a *μ-η²:η²* mode is also indicated by the fact that the O-O IR stretching frequency in the complexes is low, like that in oxyhaemocyanin and oxytyrosinase (Karlin *et al.*, 1992). In addition, the diamagnetism of such structures can be rationalised without invoking an endogenous bridge, and the peroxide would be susceptible to electrophilic attack by an aromatic substrate in the systems exhibiting tyrosinase activity.



1.4.4 (6) A model for the oxygen binding in oxyhaemocyanin and oxytyrosinase

Based on the lack of similarity in spectral and structural properties between complexes such as **57** (Scheme 1.14) and oxyhaemocyanin, and the much greater similarity of complex **49** (section 1.4.4 (4)), Kitajima *et al.*, (1992) have proposed a new model for the dioxygen binding in haemocyanin, involving the side-on coordination illustrated in Figure 1.7.

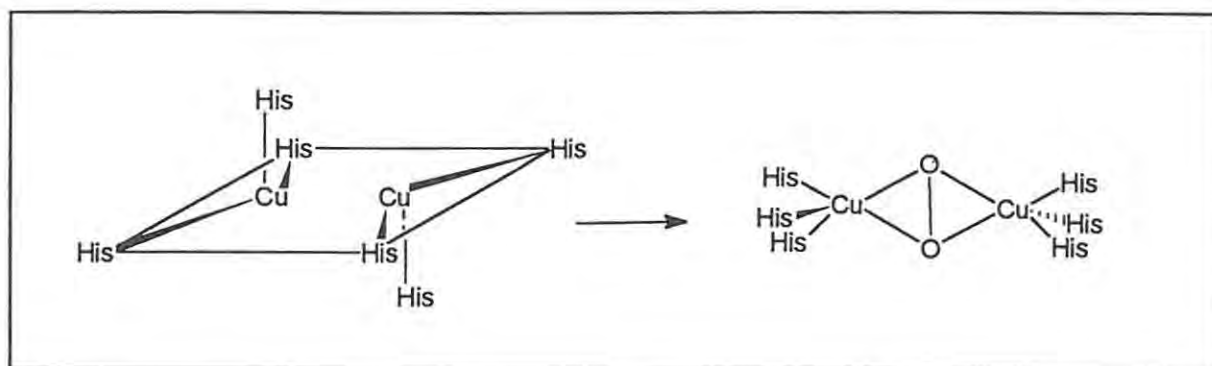


Figure 1.7: Proposed model for binding of oxygen in haemocyanin (Kitajima *et al.*, 1992)

This model takes into account the observed fact that two of the histidine-imidazole ligands in haemocyanin are positioned further away from the copper ions than the other four. Calculations based on the intensities of the peroxide-to-copper CT transitions in the complex **49** and haemocyanin indicate that the peroxide would be expected to occupy four coordination positions of the copper ions, as shown above. The presence of four peroxide-copper interactions explains the observed intensity of absorption bands. The unusually low O-O IR stretching frequency is also rationalised, as being due to back donation into an unoccupied anti-bonding orbital of the peroxide (Baldwin *et al.*, 1992).

Such molecular orbital considerations show the side-on Cu_2O_2 unit to be more stable than an end-on arrangement, and hence the model explains the ability of haemocyanin to act as an oxygen carrier. The functioning of tyrosinase is also explained (Baldwin *et al.*, 1992) because the O-O bond would be weakened due to some anti-bonding character, and is thus activated for cleavage. Theoretical analyses of the peroxide-to-copper (II) LMCT bands indicate that the side-on arrangement is likely for oxyhaemocyanin and oxytyrosinase (Ross and Solomon, 1990 and 1991), and quantum mechanical calculations lend support to the side-on bridging arrangement as the most effective for anti-ferromagnetic coupling between the copper (II) ions (Maddaluno and Geissner-Prettre, 1991).

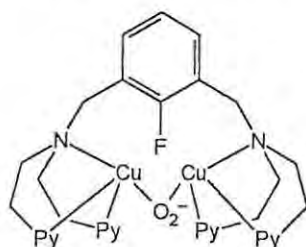
Thus, from theoretical considerations and the synthesis of biomimetic complexes, it is apparent that the peroxide bridge alone is able to provide a pathway for magnetic exchange between the copper ions in oxyhaemocyanin, but the antiferromagnetism of met-haemocyanin is not explained, and it seems likely that some non-peroxide bridge is required in this case (Baldwin *et al.*, 1992). The complex **49** can be bridged by groups such as OH and N_3^- , giving complexes similar to met-haemocyanin in some respects (Kitajima *et al.*, 1992). Similarly, complexes where **47** [Section 1.4.4 (4)] is bridged by ligands such as N_3^- , Cl^- , OAc^- , etc., have been prepared and examined (Karlin *et al.*, 1987), but the question of the endogenous bridge in met-haemocyanin has not been resolved.

1.4.5 Monooxygenase models

Successful models of tyrosinase must catalyse the hydroxylation of an aromatic ring, and models have been reported which fulfil this requirement in one of two possible ways: an aromatic ring in the ligand itself may be hydroxylated, or an exogenous substrate may be hydroxylated.

1.4.5 (1) Hydroxylation of the arene moiety in the ligand

A good example of this reaction is provided by complex **55** in Scheme 1.16, where reaction in dichloromethane gave the hydroxylated product **56** (Karlin *et al.*, 1984). The dinuclear copper (II) analog of complex **55**, synthesised (Blackburn *et al.*, 1984) for comparison of its activity, reacted with hydrogen peroxide to give the same hydroxylated product, but by a different mechanism. The mononuclear analog was found to be unreactive, indicating that the μ -peroxo-dicopper (II) unit was a necessary intermediate. When a fluorine atom was substituted on the xylyl ring, a peroxo intermediate **67** was formed, but no aromatic hydroxylation occurred (Karlin *et al.*, 1986).

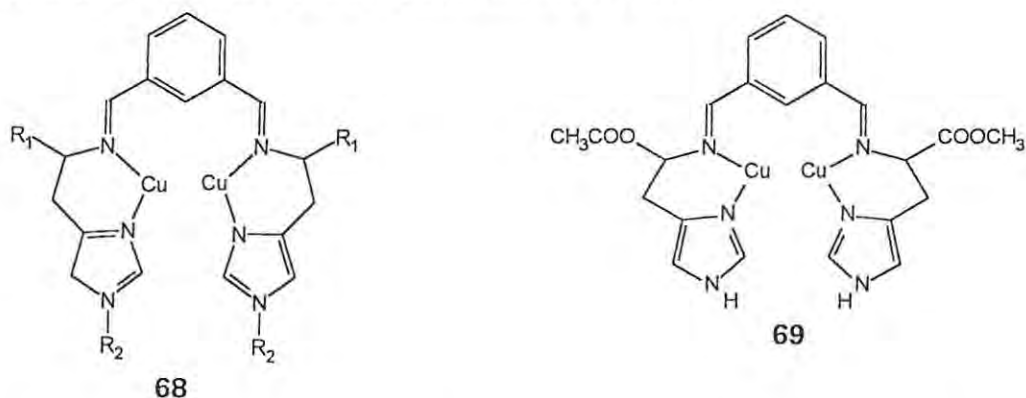


Py = pyridine

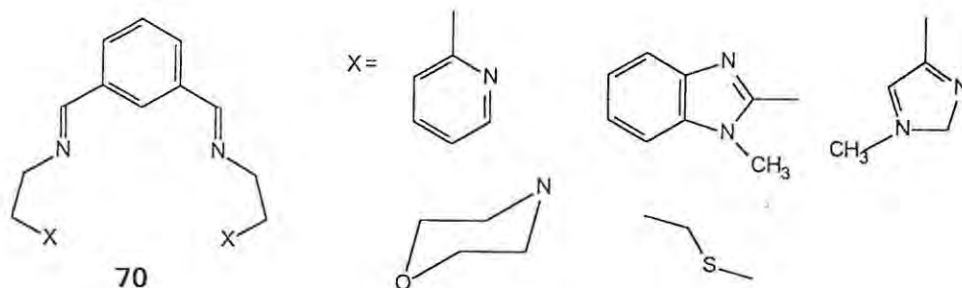
67

Analogs of complex **55**, where other heterocycles replaced the pyridine rings, were prepared by Sorrell *et al.*, (1982) and were found to be less reactive or unreactive, indicating the importance of the electronic nature of the ligand. Sorrell *et al.* (1991) suggested that the differences in

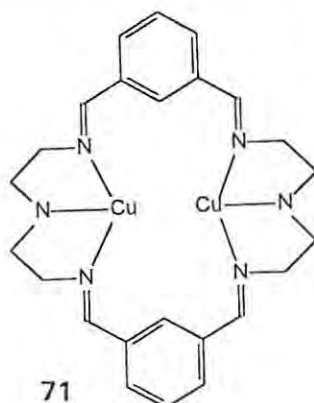
reactivity might also be attributable to geometric features in the oxygenated complexes, since these features could affect the ability of the arene to approach the bound oxygen. Appropriate orientation might also explain the reactivity of complexes such as **68** below:



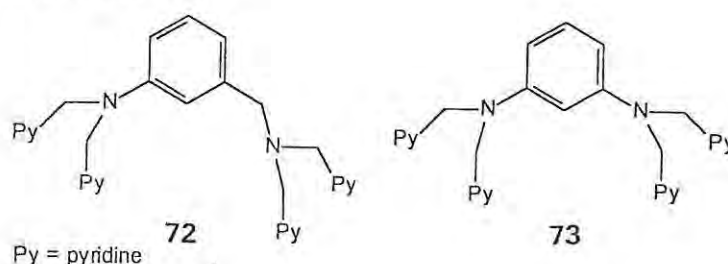
Using ligands which provide only two nitrogen donors per copper ion, Casella and Rigoni (1985) showed that an imine-type ligand system can also be hydroxylated, eg. in the complex **69**, and that the reaction was solvent dependent. In contrast with the amine-type complexes, replacement of the imidazole groups with other heterocycles such as pyridine (Gelling *et al.*, 1988) also gave reactive complexes. A series of such complexes, with ligands as shown below, **70**, were used to demonstrate that the reactivity correlated with the basicity of the nitrogen donor (Casella *et al.*, 1991a).



The first macrocyclic tyrosinase model was reported by Menif and Martell (1989). Complex **71** reacted with oxygen, hydroxylating one of the aromatic rings, and producing a copper (II) complex which was diamagnetic.



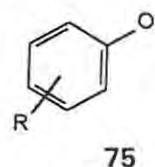
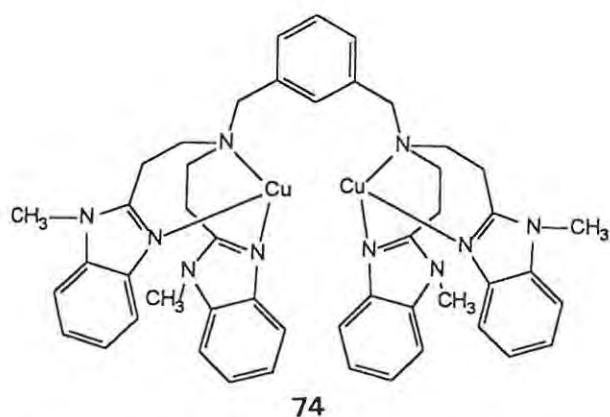
Some indication of asymmetry in the tyrosinase binding site has led to the synthesis of asymmetrical complexes. In many cases where aromatic hydroxylation occurred, the peroxide intermediate was not established, but for the asymmetrical ligand in complex **72**, reaction with oxygen gave a peroxide intermediate which was isolable (Sarwar Nasir *et al.*, 1991). The redox properties of the complex, however, suggest that the oxidation takes place *via* a $\text{Cu}^{\text{I}}\text{Cu}^{\text{II}}$ intermediate producing a superoxide species (Mahroof-Tahir and Karlin, 1992). The more rigid structure of the copper (I) complex of ligand **73** allowed only one acetonitrile ligand to coordinate to one copper, producing asymmetry, but the complex was unreactive with respect to aromatic hydroxylation (Schindler *et al.*, 1992).



Thus it is evident that the nature and number of donor atoms per copper atom are not critical, but the positions of the copper atoms, relative to each other and the coordinating groups, is critical for coordination of oxygen and aromatic hydroxylation.

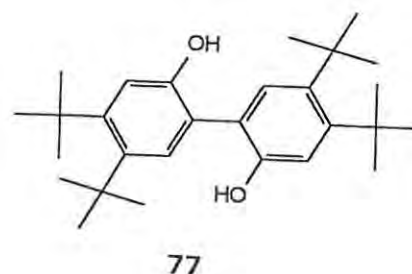
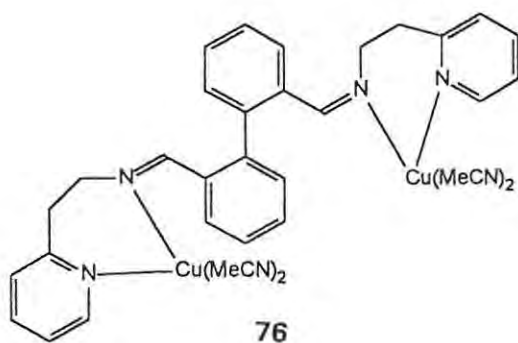
1.4.5 (2) Oxidation of exogenous substrates

Few complexes mentioned thus far successfully catalysed the oxidation of an externally added substrate. The μ -peroxo complex **49** [Section 1.4.4 (4)], which so closely resembles tyrosinase in spectroscopic features, does react with 3,5-di-*tert*-butylphenol (DTBP) in the presence of oxygen, but the reaction is suggested to proceed *via* a radical mechanism, giving coupled products. [This is discussed in Section 1.4.5 (3)]. The complex **65** [Section 1.4.4 (5)] reacted with PhP_3 , CO_2 , SO_2 , etc., in a way that suggested electrophilic character for the peroxide group, but the reaction with DTBP also gave the coupled product *via* a radical mechanism. In contrast, complex **74** did exhibit tyrosinase-like reactivity in the oxidation of DTBP to the quinone, and the phenolic substrates **75** to the dihydroxyphenols. There was also evidence for an initial phenolate adduct being formed (Casella *et al.*, 1991b).

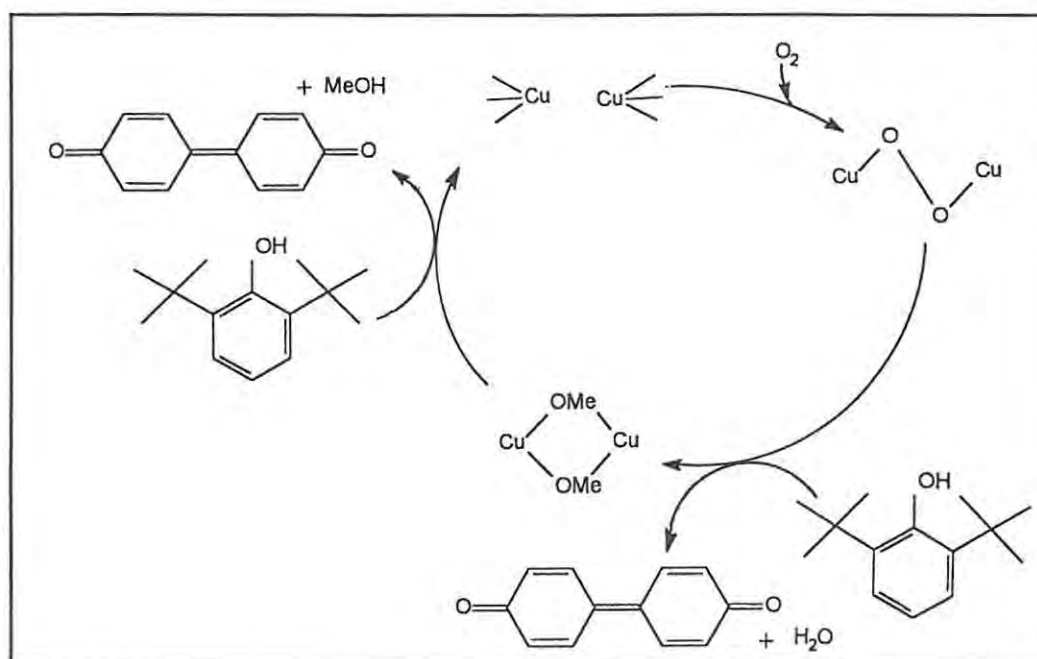
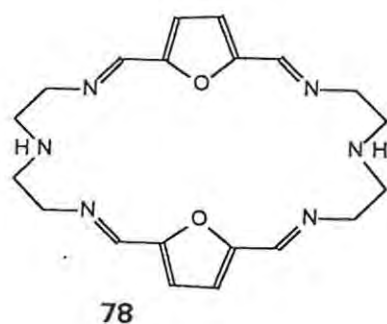


R = *p*-COOCH₃ or
2,4-di-*t*-butyl

Réglier *et al.*, (1990) reported the hydroxylation of DTBP by the complex **76** in the presence of triethylamine, which was suggested to be required to deprotonate the phenolic substrate, thus promoting binding to the catalyst. In the absence of triethylamine, the coupled product **77** was obtained. This complex is of particular interest because the biphenyl spacer in the ligand system provides flexibility and possibly, a conformation which holds the aromatic rings out of the position required for aromatic hydroxylation (see Chapter 6).



Oxidations of several substrates were catalysed by the dinuclear Cu^I/O₂ and Cu^{II}/O₂ complexes of ligand system **78**, with the copper (I) complexes giving faster rates. A cyclic mechanism was proposed (Scheme 1.17) and the interesting point was made that only complexes in which the copper (II) form reacted with the substrate, in the same manner as the copper (I) complex, could be considered to be truly catalytic. This is because the copper (II) form is involved in the catalytic cycle. Conversely, if only the copper (I) complex is reactive, as in the case of the reaction with DTBC, the reaction is stoichiometric rather than catalytic (Rockcliffe and Martell, 1992).

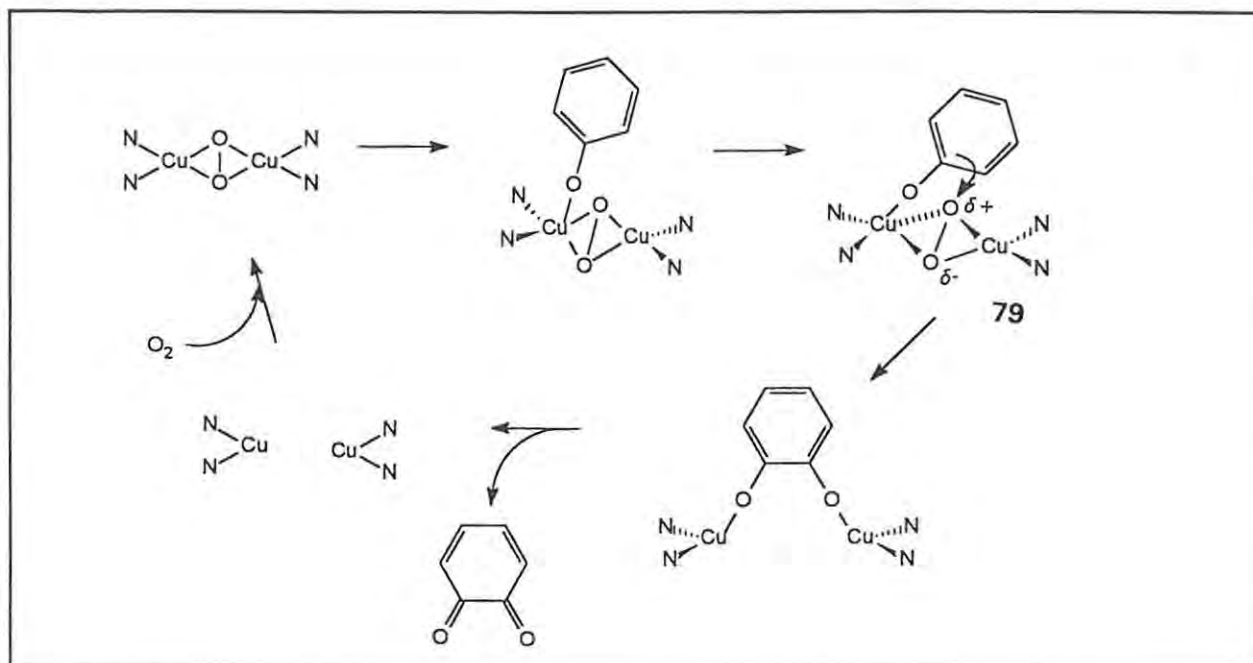


Scheme 1.17: Proposed mechanism for monooxygenase activity of macrocyclic complexes (Rockcliffe and Martell, 1992)

1.4.5 (3) A proposed mechanism for monooxygenase activity

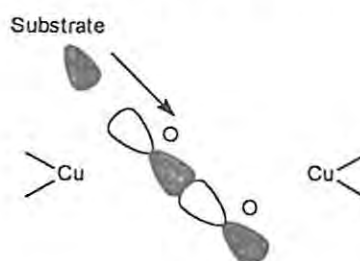
The model proposed by Solomon and co-workers, (Winkler *et al.*, 1981), was based on the suggested *cis*-mode of coordination of oxygen. The phenolic substrate was proposed to coordinate axially to one of the copper atoms, forming a $\text{Cu}_2\text{-O}_2$ -substrate complex in which a rearrangement took place, giving a trigonal bipyramidal intermediate (see Figure 1.2, Section 1.2.6). This allowed *ortho*-hydroxylation of the phenol with loss of water, *via* electrophilic attack by the polarised peroxide, followed by coordination of the catechol. Electron transfer from the bound catechol to the dicopper unit regenerates the deoxy active site, and releases the *o*-quinone (Spodine and Mangur, 1992).

When a side-on peroxide bridge was proposed, which would result in a "butterfly-like" conformation (Karlin *et al.*, 1988), it was suggested (Ross and Solomon, 1991) that the mechanism involved the intermediate **79**, as shown in Scheme 1.18.

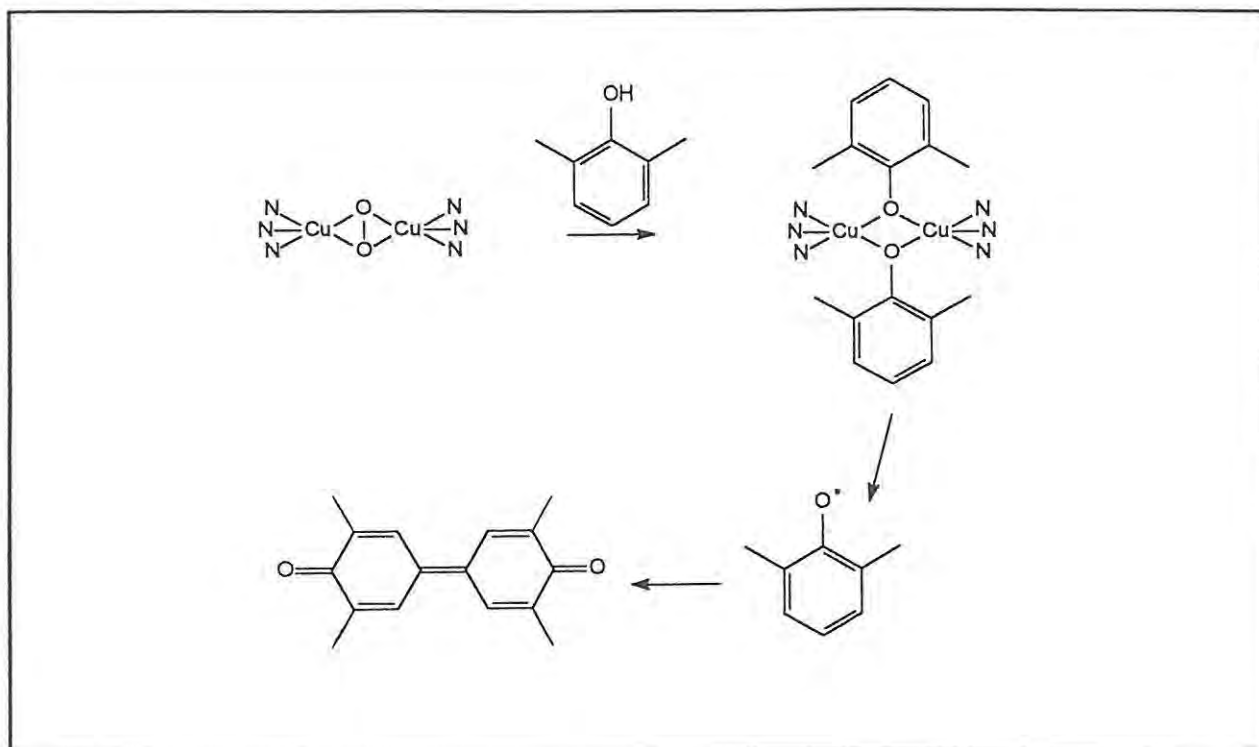


Scheme 1.18: Mechanism proposed for a side-on bridged dicopper site (Ross and Solomon, 1991)

This side-on arrangement would expose an O-O σ^* molecular orbital to a pair of electrons in the approaching substrate, and donation into this anti-bonding energy level would lead to the weakening of the O-O bond (Sorrell, 1989).



A different mechanism has been proposed by Kitajima and co-workers (1992 and 1993) based on the idea that although the peroxide in tyrosinase and in biomimetic complexes has electrophilic character, this is not necessarily enough to allow electron transfer. The possibility of a radical mechanism is suggested, particularly for reactions with sterically hindered substrates. Tyrosinase has been found to give diphenoquinone products, presumably *via* radical-coupling (Pandey *et al.*, 1990), and the spectroscopically successful model complex **49** (Section 1.4.4 (4)) also gave coupled products. Thus the following mechanism is proposed for the activity of the complex:

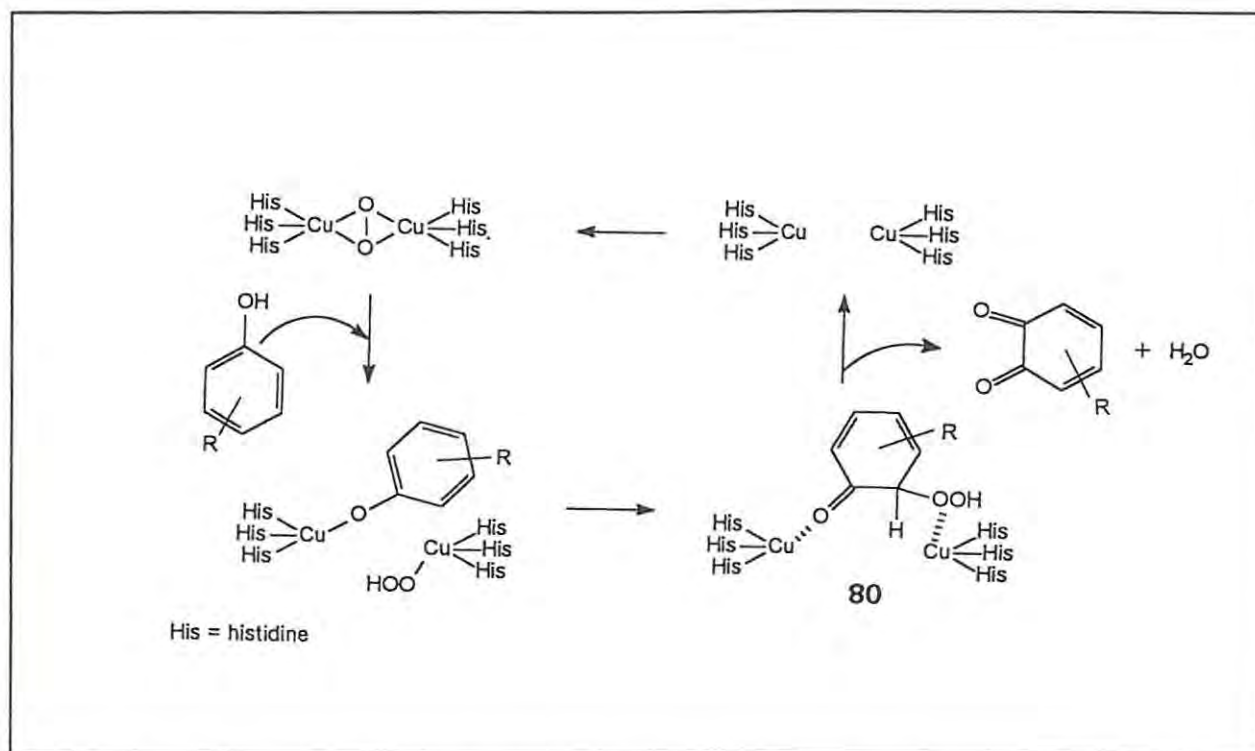


Scheme 1.19: Proposed mechanism for models of tyrosinase (Kitajima, 1992)

The phenol molecules are suggested to bridge the two copper ions, so that electron transfer gives two copper (I) ions and two phenoxy radicals which are close enough to combine. In the reaction of tyrosinase, homolytic cleavage of the peroxide is unlikely because of the fixed positions of the copper ions and, probably, only one phenol molecule can be fitted into the active site at once, so a hydroperoxo-phenoxy-intermediate **80** is proposed (Scheme 1.20).

If the phenol is hindered, the "inner sphere" coupling of phenoxy and hydroperoxo groups may not take place, and then homolysis of the copper (II)-phenoxide complex might result in phenoxy radicals being released; these could couple together subsequently (Kitajima, 1992).

Thus, elucidation of the oxygen binding in haemocyanin and the monooxygenase activity of tyrosinase have presented chemists and biochemists with an interesting problem, and in the course of its solution, much valuable research has been achieved. At the time of conclusion of this review, the problem has apparently been resolved, with the demonstration of side-on binding of oxygen by dinuclear copper centres (Kitajima and Moro-oka, 1993).



Scheme 1.20: Proposed mechanism for tyrosinase monoxygenase activity

1.5 OBJECTIVES

The general aim of this study was to investigate the potential of polyphenol oxidase as a biocatalyst for application in organic syntheses, and to provide a rationalisation for the observed effects of various parameters on the functioning of the enzyme.

Although polyphenol oxidase catalyses a reaction which has considerable synthetic and economic potential, relatively little research has been reported on the exploitation of this potential. The major drawback to the application of polyphenol oxidase is the water-dependent reaction inactivation which precludes its long-term use in aqueous medium. However, with the development of biocatalysis in organic media, this problem has been shown, in certain circumstances, to be reduced. Therefore, the first objective of this study was to design a generally-applicable biocatalytic system in which polyphenol oxidase could be utilised in an organic medium, to synthesise a range of catechols and *o*-quinones. Kinetic studies using a range of substrates would increase present knowledge of the functioning of polyphenol oxidase in organic medium and provide a means of determining the effects of manipulating the conditions within the system.

The steric and electronic requirements for polyphenol oxidase enzyme-substrate interactions in the organic medium (which would not be expected to simulate those in aqueous medium) have not been established previously. Since this information is essential in developing a biocatalyst, correlation of the results obtained from the biocatalytic system with a molecular modelling study of the biomimetic complexes was undertaken, with the aim of identifying characteristics which would enhance biocatalytic efficiency.

A third major objective was the design and synthesis of novel biomimetic organometallic complexes which could be structural and/or functional models of the polyphenol oxidase/organic medium system. Comparison of their catalytic activity with that of the enzyme in organic medium would provide new insights relating to the nature of active site of polyphenol oxidase.

CHAPTER 2

A BIOCATALYTIC SYSTEM USING POLYPHENOL OXIDASE

2.1 INTRODUCTION

2.1.1 Use of polyphenol oxidase in organic medium

At the outset of the present study, it was known that mushroom polyphenol oxidase could function in organic media (as described in Section 1.3.4). Kazandjian and Klibanov (1985) used commercially available, partially purified mushroom polyphenol oxidase to show that the enzyme could be utilised in chloroform to produce catechols. The reaction was followed by gas chromatography (GC), measuring substrate depletion, and the quinone products were subsequently reduced by reaction with ascorbic acid. The reaction inactivation and quinone polymerisation which preclude the application of polyphenol oxidase in aqueous medium were not observed to the same extent in organic solvents. These authors reported the conversion of a range of phenolic substrates, and investigated the use of various solvents (Table 2.1). In all cases, 0.5% aqueous buffer was present in the system. In a subsequent report, polyphenol oxidase was used to investigate the general effects of water on enzyme activity in organic media (Zaks and Klibanov, 1988b). Here, the rate of oxidation of 4-methylcatechol, catalysed by polyphenol oxidase, was monitored in solvents with varying proportions of water (Table 2.1). The conclusion was that hydrophobic solvents were most suitable, and that hydration of the enzyme was essential for activity.

These reports formed the basis for initiating the present study. More recently, two other investigations have been reported, also on the use of the commercially available mushroom enzyme: Estrada *et al.* (1991) examined the characterisation and optimisation of polyphenol oxidase in organic solvents, and Estrada *et al.* (1993) reported the effects of temperature on the system. These results are discussed in the relevant sections below.

Table 2.1: Application of polyphenol oxidase in organic solvents (Kazandjian and Klibanov, 1985; Zaks and Klibanov, 1988)

Solvent systems		Substrates tested ^a
Chloroform	0.5% buffer	R = H CH ₃ CH ₃ O HOOCCH ₂ CH ₂ Cl Br I HOCH ₂ HOCH ₂ CH ₂ C ₆ H ₅ CONHCH ₂
Dichloromethane	-	
Carbon tetrachloride	-	
Dichloroethane	-	
Benzene	-	
Toluene	-	
Hexane	-	
Butyl acetate	-	
Diisopropyl ether	-	
Methyl acetate	1% water	
-	2% water	
-	1% water, + 3% ethylene glycol	
1-Butanol	1% water	Not successful:
	2% water	
	1% water, + 3% ethylene glycol	
<i>n</i> -Octanol	1% water	R = C(CH ₃) ₃ C ₆ H ₅ Naphthols
	2% water	
	1% water, + 3% formamide	

^a Tested in chloroform (Kazandjian and Klibanov, 1985)

2.1.2 The effects of organic solvents on enzymes

Organic solvents can affect the structure of enzymes at the primary, secondary, tertiary and quaternary levels, by disrupting interactions which control the mechanism in the active site, or by altering the thermodynamic nature of the system. Thus the efficiency and selectivity of the enzyme can be affected (Dordick, 1993). Enzymes in organic solvents provide a useful system for investigating protein-water interactions, since the solvent becomes a new variable in the system (Zaks and Klibanov, 1988b).

The solvent affects the electrostatic forces operating within the protein, and to a lesser extent, the hydrophobic interactions (Ryu and Dordick, 1992). Differences in the hydrophobicity and dielectric constant of the medium lead to variations in the free energies of substrate-enzyme and substrate-

solvent binding and hence, the enzyme's ability to make use of the free energy of binding to form the substrate-active site complex may be diminished. In kinetic measurements, this is reflected in altered K_m values. In addition, the ground state of the substrate may be destabilised by the solvent. For instance, very polar compounds may partition into the active site, which might result in stronger binding than normal, and the product may be less amenable to leaving the active site. This would be observed as apparent inactivation. The converse would be true for a non-polar substrate in a hydrophobic solvent (Dordick, 1992). The apparent K_M value is usually increased in organic solvents, due to hydrophobic substrates binding in hydrophobic active sites (Russell *et al.*, 1992).

2.1.3 The role of water in non-aqueous biocatalysis

In any investigation of non-aqueous biocatalysis, the role of water must be regarded as crucial. Even in anhydrous solvents, enzymes have been found to retain some tightly bound water, sometimes referred to as "structural water". Although it may amount to only a few molecules of water per protein molecule, it is essential for the activity of the enzyme and its loss results in deactivation. Redistribution of bound water, *eg.* by sonication, may also reduce activity, while rehydration leads to recovery of activity (Blinkovsky *et al.*, 1992). The water present in the active site is required for maintaining conformational flexibility, and thus it plays an important role in allowing accessibility and favourable orientation of substrates in the active site. The water is bound to polar groups in the protein, screening these groups from each other and facilitating their freedom of movement within the active site. Its loss allows direct interaction between the polar groups, resulting in reduced conformational flexibility (Dordick, 1992). Spin-labelling experiments showed that hydration facilitates changes in conformation from the dehydrated form, as a result of this dielectric screening (Affleck *et al.*, 1992). Molecular dynamics simulations have been used to show that it is most likely the amino acid side chains which acquire additional flexibility upon hydration (Hartsough and Merz, 1992).

A solvent which is capable of hydrogen bonding with the polar groups may allow enhanced flexibility, but polar solvents can strip the bound water from the active site, thus reducing flexibility (Gorman and Dordick, 1992). Recently, it was shown that pressure changes affect enzyme activity in organic solvents because it alters this water stripping (Kim and Dordick, 1993). Narayan and Klibanov (1992) reported that enzymes are more flexible in solvents with high dielectric constants.

Enzymes retain their ionic state when water is removed from the system, so that polar and charged groups remain ionised as if they were in the aqueous solution. This "pH memory" can be most useful in enhancing the activity of an enzyme which is to be immobilised for application in a non-

aqueous medium. The enzyme can be deposited from a buffer of optimal pH by drying, or freeze-dried from solution in the buffer, and it will then retain the optimal ionic state when it is placed in the organic solvent (Klibanov, 1986).

The interesting phenomenon of ligand-induced enzyme "memory" is a result of decreased flexibility in the binding site. If an enzyme is lyophilised in the presence of a particular ligand, *eg.* an inhibitor or substrate analog, and the ligand is then washed out using an organic solvent, the enzyme retains the shape of the ligand which is "imprinted" on the "frozen" binding site. Subsequent addition of the ligand or similar molecules results in binding and activity which may not be possible in the normal (aqueous) situation (Klibanov, 1989; Braco *et al.*, 1990). The addition of lyoprotectants reduces denaturation during freeze-drying by this mechanism (Dabulis and Klibanov, 1993). Subtilisin, for example, exhibits ligand-induced alterations in substrate specificity and stability (Russell and Klibanov, 1988), and a similar effect was observed with chymotrypsin (Stahl *et al.*, 1990).

2.1.4 Practical systems for non-aqueous biocatalysis

It is obvious from the above description that in any practical system for studying an enzyme in a non-aqueous system, water content must be carefully monitored and controlled. Where an enzyme is deposited on a solid support, cognisance must be taken of the tendency of support materials to adsorb water. This may result in removal of essential hydrating water from the protein, or it may create a requirement for additional hydration of the system (Reslow *et al.*, 1988). Similarly, extraneous impurities may cause unpredictable variations in the amount of available water (Mattiasson and Adlercreutz, 1991). Since enzymes frequently have improved activity and stability when deposited on solid supports, it is usually an advantage to immobilise them (Klibanov, 1978; Wehtje *et al.*, 1992).

Hydration of the protein can be effected equally well by equilibration with water present in the vapour phase or in the organic solvent (Halling, 1990b). Control of variations in water content may be necessary, as for instance, in the case of reactions which have water as a product, and this can be problematic. Possible solutions include the addition of water-adsorbent polymers such as ethyl cellulose (Otamiri *et al.*, 1991) and sodium polyacrylate (Nakamura *et al.*, 1993). Alternatively, in analytical scale systems, the addition of salt hydrates can give precise control of water content (Halling, 1992).

Mixing conditions are also important; reaction rates for an enzyme suspended in an organic solvent have been found to be dependent upon the speed of stirring (Lilly and Woodley, 1985). Differences between the actions of shaking and stirring may affect measurements of activity and the stability of the biocatalyst (Kvittingen *et al.*, 1992). Diffusional characteristics are also affected by the morphology of the enzyme, which is in turn dependent on the degree of hydration of the protein (Roziewski and Russell, 1991). These authors showed that the presence of an organic solvent itself does not alter the morphology of the enzyme particles.

2.1.5 The biocatalytic system in the present study

The first objective in the study was to devise a biocatalytic system using polyphenol oxidase obtained from mushrooms (as opposed to using the commercially available enzyme), and to examine its properties with respect to the effects of variation in conditions such as the nature of the solvent or the nature of the substrate, hydration, and degree of purification. This chapter describes the preliminary experimental results obtained in setting up suitable procedures for enzyme isolation and purification, assays, and kinetic measurements. Every effort was made to ensure consistency and to take into account the various influencing factors discussed in the preceding section.

Chloroform was chosen as the organic solvent for the non-aqueous biocatalytic system for a number of reasons. Kazandjian and Klibanov (1985) reported that quinone polymerisation was minimal in chloroform containing 0.5% aqueous buffer, and that since it is a good radical quencher, coupling reactions should not interfere with quantitative measurements. The *o*-quinone products of the reaction are soluble and stable in chloroform. In addition, oxygen is much more soluble in chloroform than in many other solvents, including water (Linke, 1958), and therefore would not be a limiting factor in reaction rate determinations.

2.2 RESULTS AND DISCUSSION

2.2.1 Isolation and purification of polyphenol oxidase from mushrooms

Although they are not a particularly economical source of polyphenol oxidase, mushrooms are convenient to deal with, and have been utilised by various other workers (for instance, Hruskocý and Flurkey, 1986; Menon *et al.*, 1990). The production of polyphenol oxidase by microbial fermentation would seem to be an attractive alternative, but a suitable system for obtaining large quantities of the enzyme has not yet been reported (Goetsch, 1992).

In the application of a biocatalytic system to synthetic-scale reactions, economic factors must be considered, and the fewer purification procedures that are required, the more economical the process will be, in terms of time and money. In order to assess the degree of purification necessary for polyphenol oxidase to be applied as a biocatalyst, a crude extract was first obtained and utilised in kinetic investigations. Later, partially purified isolates were obtained and analysed for comparison.

2.2.1 (1) Extract A: Crude polyphenol oxidase extract from mushrooms

A crude extract was obtained by adapting the procedures of Goetsch (1992), Bouchilloux *et al.* (1963) and Nelson and Mason (1970) (see Section 2.4.1). Fresh mushrooms (*Agaricus bisporus*) were homogenised in acetone to remove lipids and pigments, the homogenate was filtered, and the air-dried residue was frozen with liquid nitrogen. The crude enzyme was obtained from the frozen residue by adding water, and standing the slurry overnight at 0°C, then filtering the mixture. The filtrate was flushed of residual acetone by bubbling with nitrogen. This may also have flushed oxygen from the extract, reducing the likelihood of endogenous oxidation reactions, and possibly preserving the polyphenol oxidase in the deoxy state. The solution was freeze-dried, and the powder, extract A, was stored in the dry, frozen state.

Extract A was found by protein analysis (Folin-Lowry assay method, see Section 2.4.9) to contain 28.1% protein. The amount of active tyrosinase in the extract was 3.0 ± 0.3 % (determined by PAGE analysis, Section 2.2.2). A comparison of extract A with the commercially available enzyme, and with the partially purified extracts obtained as described below, was carried out electrophoretically (Section 2.2.2). The immobilisation of the crude extract is described in Section 2.2.3.

In later stages of the present study, other batches of the crude extract **A** were obtained by the identical procedure to the one described here. For each new batch, PAGE analysis was carried out to ensure that the protein composition was consistent, and the protein concentration and dopachrome activity were measured after immobilisation. Small variations in these properties were taken into account in comparative calculations (see Section 2.2.4).

2.2.1 (2) Extract B: Partial purification of crude polyphenol oxidase

A crude extract, such as extract **A**, is likely to contain a large proportion of extraneous protein, including other enzymes. While the majority of these would be inactive with respect to the substrates of polyphenol oxidase, their presence may dilute the polyphenol oxidase. More specifically, in non-aqueous biocatalytic systems the extraneous protein can interfere by adsorbing water at the expense of the enzyme under consideration, causing reduced reactivity. In addition, any investigations of water requirements in the biocatalytic system would be affected by the presence of the extraneous protein.

Significant purification (126x) was achieved in the preparation of grape polyphenol oxidase by use of an ammonium sulphate precipitation step in the isolation procedure (Sánchez-Ferrer *et al.*, 1988a). Since this is a simple and inexpensive method of purification, it was utilised in the present study, as a means of removing extraneous protein from the crude extract. A fractional precipitation was carried out, initially using 40% saturation with ammonium sulphate and proceeding as shown in Figure 2.1 (Nelson and Mason, 1970; Jolley *et al.*, 1969a). The greatest proportion of polyphenol oxidase activity occurred in the 52% saturated precipitate. After dialysis of this fraction and freeze drying, 0.25g of extract **B** was obtained, from 3.5g crude extract.

Electrophoretic analysis and protein and activity assays were carried out and compared with those of the crude extract (see Table 2.3 below). The specific activity of the 52% precipitate was higher than that measured for the freeze-dried powder and the biocatalyst obtained from it. This may have been due to some denaturation during these procedures, or to the solution of the 52% precipitate being more aerated, so that a greater proportion of the polyphenol oxidase was oxygenated.

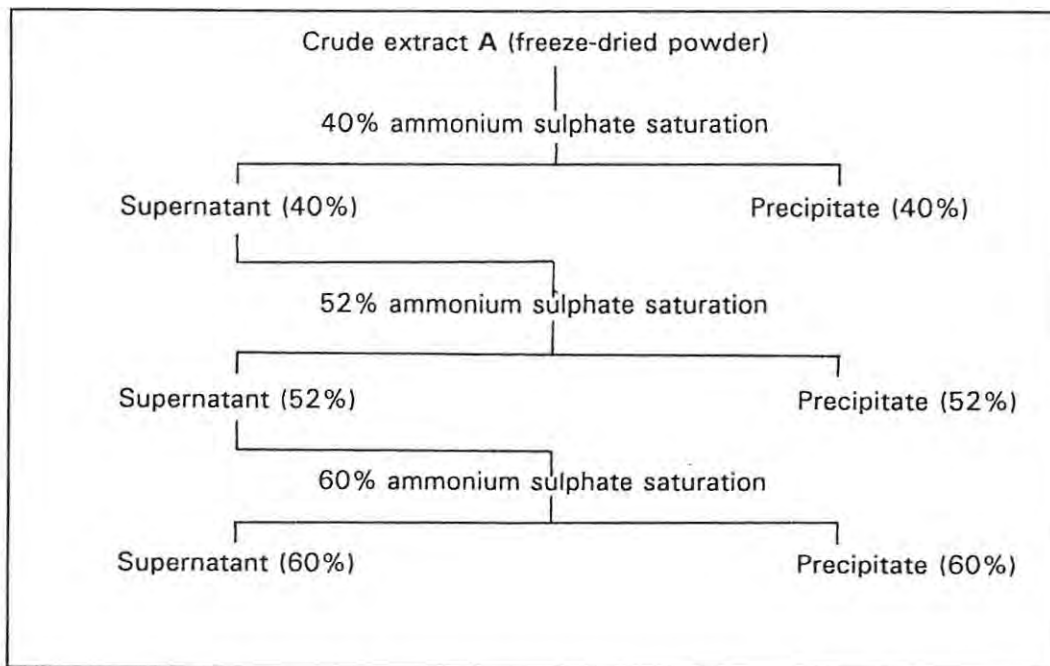


Figure 2.1: Procedure for fractional ammonium sulphate precipitation of crude polyphenol oxidase

Table 2.2: Results of ammonium sulphate fractionation of Extract A

Fraction	Protein (mg.mL ⁻¹)	Dopachrome activity (Units ^c .mL ⁻¹)	Specific activity (Units.mg ⁻¹) ^d	Total activity (Units)
40% ppt ^a	19.81	3.771	0.19	190
40% sup ^b	5.36	10.74	1.88	4300
52% ppt	5.11	71.70	14.03	3580
52% sup	1.19	1.57	1.32	470
60% ppt	2.68	0.36	0.13	134
60% sup	1.55	0.30	0.19	120

^a Precipitate

^b Supernatant

^c 1 Unit = 1 μ mol dopachrome produced per minute (Gardner and Cadman, 1990)

^d Per mg protein

2.2.1 (3) Extract C: Removal of endogenous phenolics from the crude extract

Most plant extracts contain phenolic or polyphenolic compounds (such as flavonoids and tannins) which have various functions, largely in secondary metabolism (Geigenheimer, 1990). These phenolics are potential substrates of polyphenol oxidase, particularly in homogenates where substrates may be exposed to the enzyme by membrane rupture, and where oxygen is available. The result of tyrosinase reactivity with these phenolics is formation of quinoid and melanoid products which can discolour the extract and can polymerise in the presence of water. Polymerised melanins can form insoluble deposits which could physically occlude the enzyme surface. Also, proteins can be included in the melanins, which may remove them from solution. Such contamination is in itself a disadvantage, but in the case of polyphenol oxidase, the presence of quinones or melanins can directly affect the reactivity of the enzyme, for instance by activating cresolase activity (see Section 1.1.5), or by inhibiting the enzyme binding site through itself being tightly bound. This could interfere with the results of kinetic studies and particular note must be taken of this possibility in organic systems, where the only water present might be on the enzyme surface. Complete removal of endogenous phenolic compounds is not easily achieved, but almost complete removal can be achieved using the adsorbent polyvinylpolypyrrolidone (PVPP) or ion exchange resins (Geigenheimer, 1990). In other reports of polyphenol oxidase isolation, similar procedures have reduced melanin formation (Smith and Montgomery, 1985; Sanchez-Ferrer *et al.*, 1988a; Ingebrigtsen *et al.*, 1989).

In the present study, PVPP was utilised as an adsorbent of endogenous polyphenolics in the mushrooms. It was included in the initial aqueous extract of fresh mushrooms, and since the adsorbent is insoluble, it could be filtered off with the solid residue (Section 2.4.3). The filtrate was far paler in colour than that obtained from extract A, which suggests that less melanin formation had occurred. It was freeze-dried to give extract C.

The protein concentration of extract C was 32.1%, and the tyrosinase content was determined, by PAGE analysis, to be 6.8 ± 0.7 % (with respect to mass of extract). The extract was also compared with other extracts using PAGE analysis (see Section 2.2.2).

2.2.1 (4) Comparison of activities of extracts A, B and C

Specific activities were calculated using data from protein and activity assays of the freeze-dried powders and the immobilised biocatalysts obtained from each of the three extracts. The results are shown in Table 2.3. Although the partially purified extract B has the highest specific activity (in

Units per milligram protein), the PVPP-purified extract C gives the highest total activity in terms of units per kilogram of mushrooms. This comparison of activities in the different extracts was extended in a kinetic study as discussed in Chapter 4.

Table 2.3: Extract A, B, and C: Protein concentrations and dopachrome activities

Extract	% protein	Dopachrome activity ^a	Dopachrome activity when immobilised ^b	Units ^c per 1 kg mushrooms ^d
A	28.1	0.29	1.56 ^e	17160
B	60.5	4.51	10.58	7935
C	32.1	1.69	2.60	23400

^a For freeze-dried powder (units per mg protein)

^b As biocatalyst on beads (units per mg protein)

^c 1 unit = 1 μ mol dopachrome produced per minute

^d Refers to freeze-dried extracts

^e Values in the range 1.3 - 1.7 were obtained in subsequent batches; calculations were corrected for this variation (see Section 2.2.4)

2.2.2 Comparison of extracts A, B, and C, using Polyacrylamide Gel Electrophoresis (PAGE)

The protein extracts obtained as described above were analysed by disc-electrophoresis under non-denaturing and denaturing conditions (see Sections 2.4.4 - 2.4.7).

2.2.2 (1) Detection of protein components by SDS-PAGE

Samples of the extracts A, B, and C, and of the commercially available tyrosinase, were dissociated and electrophoresed on denaturing gels. The gels were stained with Coomassie Brilliant Blue protein stain (Weber and Osborn, 1969), and the results are shown in Figure 2.2 and Table 2.4.

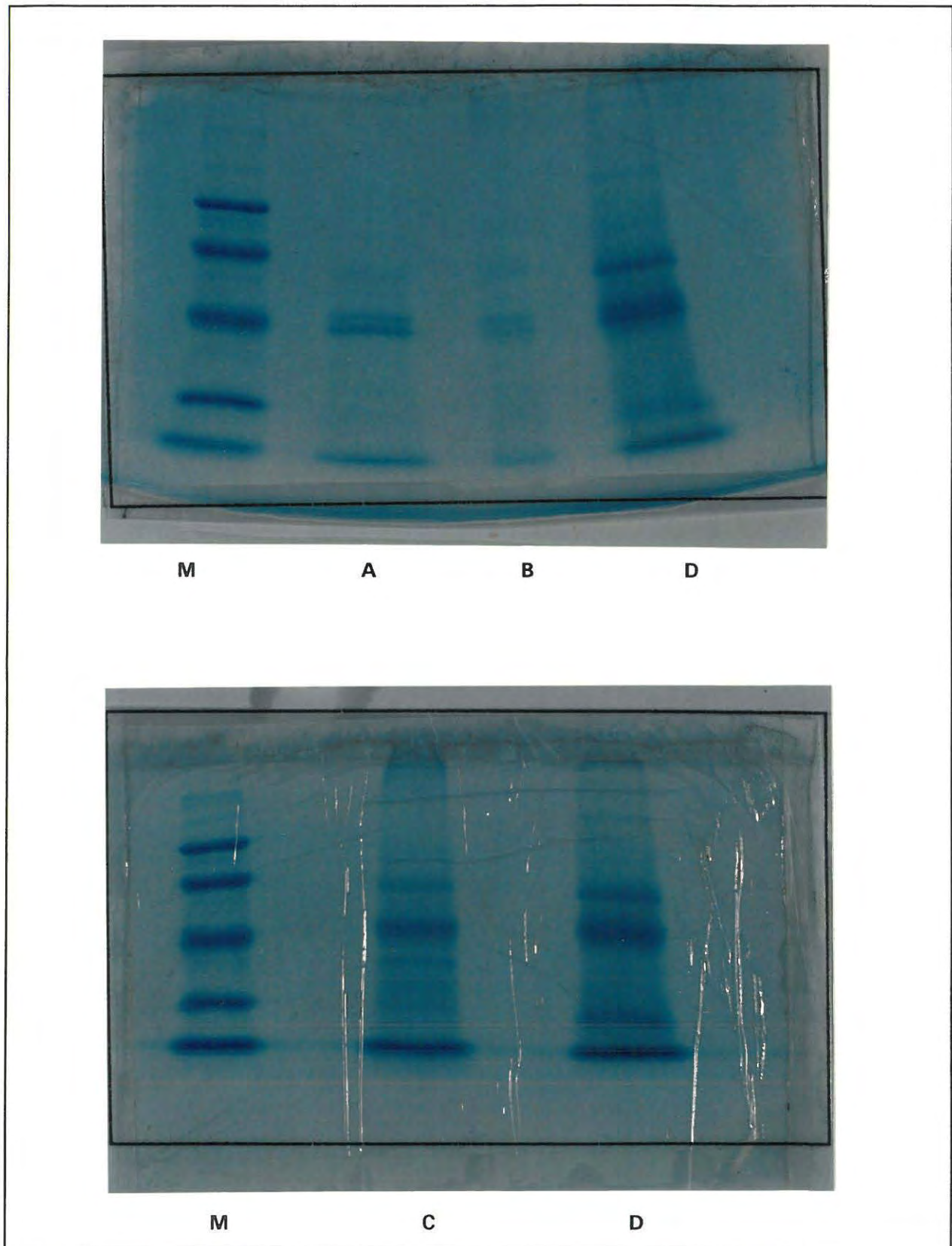


Figure 2.2: SDS-PAGE analysis of polyphenol oxidase extracts; bands contain: marker proteins (M), extract A (A), extract B (B), extract C (C) and commercially available tyrosinase (D)

Table 2.4: Results of SDS-PAGE analysis of polyphenol oxidase extracts

Enzyme	Mass (μg)	Bands observed (relative mobility) ^a	MM ^b
Extract A	100	0.458	56000
		0.542	47000
		0.583	43500
		0.667	35500
Extract B	20	0.429	60000
		0.571	46000
		0.599	42500
		0.714	36000
		0.886	23000
Extract C	100	0.458	56000
		0.542	47000
		0.583	43500
		0.650	35000
Commercial enzyme	50	0.458	56000
		0.563	45000
		0.583	43500
		0.813	25000
Markers	10	0.271	94000
		0.375	67000
		0.563	43000
		0.771	30000
		0.896	20100

^a Calculated from distance moved by band/distance moved by melanins, measuring from the top of the resolving gel

^b Molecular mass calculated from graph in Figure 2.11, Section 2.4.5.

In all of the extracts, only a small number of protein bands were observed. The most mobile band in each case was brown in colour, suggesting that it contained melanins from the extracts. The melanin bands did bind the protein stain, indicating the presence of bound protein, but the bands lacked any tyrosinase activity (determined later), and therefore these proteins are probably denatured or extraneous components.

The extracts A and C were observed to be similar in protein composition, except that extract C contains an additional, lower molecular mass, component. The gel on which extract C was analysed was run at a different time from the others, and it is possible that the small differences are not significant. The partially purified extract B appeared to lack the low molecular mass components present in the other extracts (including the commercial enzyme). In this extract the 43000 D band was a greater proportion of the protein than in the other extracts. The commercially available enzyme was shown to be a mixture of components similar to the crude extract A, but it

contained a lighter component (25000 D). Kumar and Flurkey (1991) reported that the commercially available enzyme varies from batch to batch due to the presence of different proportions of isoenzymes and to variations in the purity.

The molecular masses determined for the observed bands indicates that the tyrosinase was partially dissociated. The enzymes is regarded as having two light (13000 D) and two heavy (43000 D) subunits per tetrameric aggregate, with the active site being in the heavy subunit (Kumar and Flurkey, 1991). Presumably the 56000 D component observed in the present study was a dimer consisting of one of each type of subunit. The band corresponding to a molecular mass of 43500 D is likely to be the large subunit alone, and the 47000 D component could be a subunit of an isoenzyme. Larger protein components were not apparent on the gels. The electrophoresis of tyrosinase is known to be variable (Jolley and Mason, 1965; Flurkey, 1991) but the correlation of the molecular masses observed here with those reported in the literature confirms that the enzyme isolated in this study was comparable in composition to those reported by others (*eg.*, Jolley *et al.*, 1969a).

2.2.2 (2) Determination of activity in extracts by non-denaturing PAGE

Samples of the extracts A, B, and C, and the commercially available enzyme were electrophoresed in duplicate on non-denaturing gels (which do not contain SDS) as shown in Table 2.5 below. One of each pair of gels was stained with protein stain to localise the protein bands. The other gel in each pair was stained by soaking in a buffered solution of DOPA, which, being a substrate for the enzyme, was oxidised to dark-coloured melanin. This allowed detection of the active polyphenol oxidase components in each extract (see Figure 2.3). One major band of activity was observed in all of the extracts (marked Band 1 in Figure 2.3). Some less intense, more mobile bands were also evident in the extracts, particularly in the extract B and the commercial enzyme (Band 2) which were not clearly detected by the protein stain. These must therefore represent very active components in the extracts. These components were observed to have predominantly catecholase activity when tested for activity with other substrates (see Section 3.3.2). The presence of highly mobile bands with strong catecholase activity was also reported by Jolley *et al.* (1969a). The more crude extracts A and C have additional bands (3) near Bands 1 and 2, but it is possible that these are actually present in the extract B and the commercial enzyme, hidden by the intensity of the major components.

The intensities of corresponding bands in pairs of gels, stained for protein and activity respectively, were measured by using a gel documentation system and their concentrations relative to the total

concentration were calculated. The data obtained was used to estimate the amount of polyphenol oxidase in the extracts, as shown in Table 2.5.

Table 2.5: Correlation of activity with protein components in polyphenol oxidase extracts on PAGE gels

Enzyme	Mass ^a	Mass ^b	Band ^c	% of protein	% of activity	% Tyrosinase in extract ^d
Extract A	150	42	Z	9.86	23.9	2.98
Extract B	75	45	X	6.66	23.6	24.5
Extract C	100	32	Y	7.53	34.5	6.82

^a Total mass of extract loaded on gel (μg)

^b Mass protein on gel (μg)

^c See Figure 2.3

^d As % w/w in extract; error: $\pm 10\%$

2.2.2 (3) Detection of laccase activity

Laccases are oxygenase enzymes which can catalyse the oxidation of phenolic substrates. They can be distinguished from tyrosinases by their ability to oxidise *para*-dihydroxybenzenes as well as *ortho*-dihydroxybenzenes. Since their presence in the mushroom extracts used in this study might interfere with determinations of polyphenol oxidase activity, a brief investigation was carried out to ascertain whether their activity was present in the extracts. Non-denaturing PAGE gels were run as described above, but one gel was stained by soaking the gel in a solution of hydroquinone (Bouchilloux *et al.*, 1963). While hydroquinone is an inhibitor of tyrosinase, laccase activity would have been observed as a coloured band resulting from formation of the *para*-quinone product. No such band was observed, and this was taken as adequate evidence that laccase activity was not present. This was of importance in the screening of possible substrates (Section 3.2.1) and in the kinetic investigations (Chapters 3 and 4).

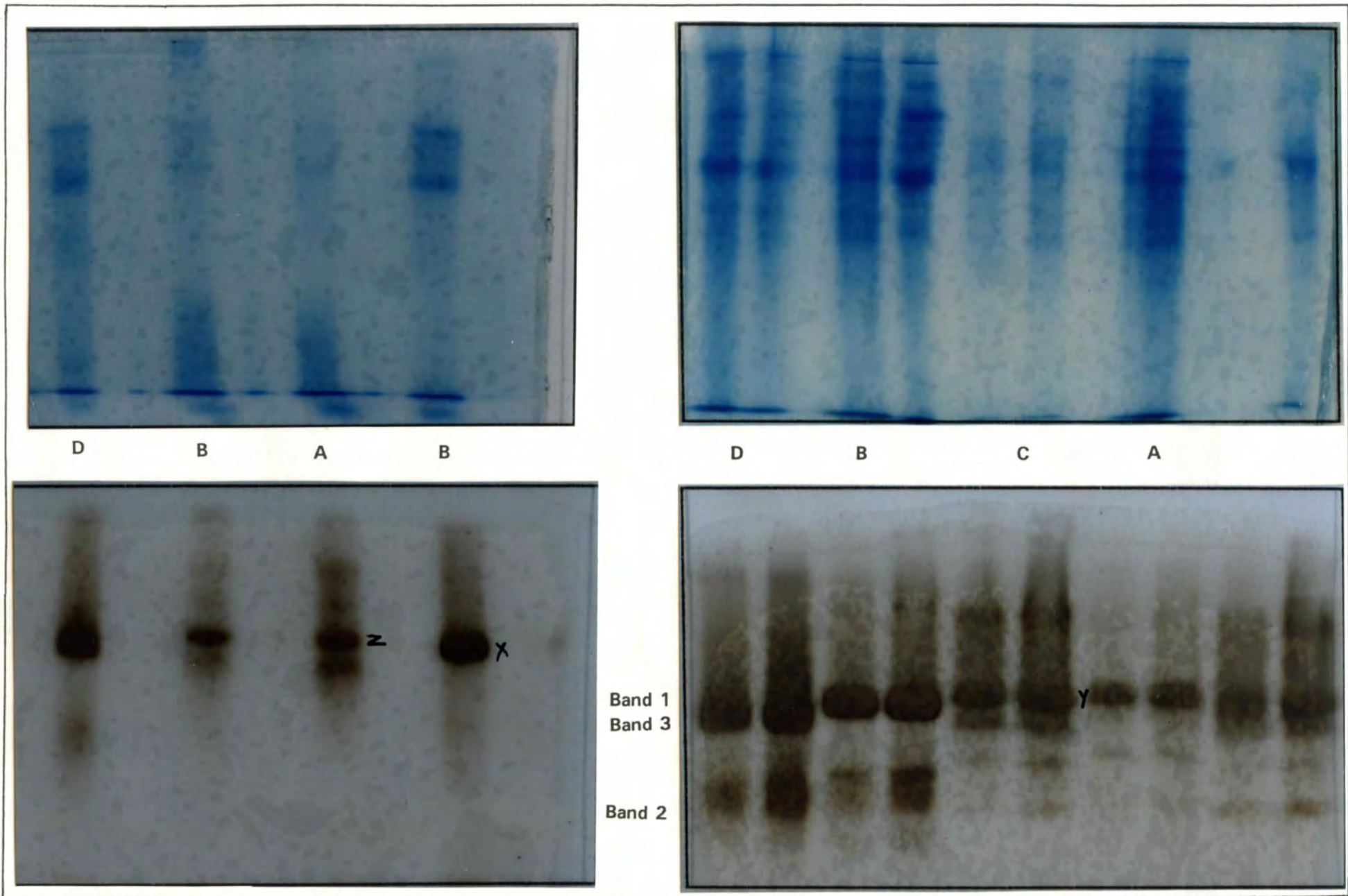


Figure 2.3: Non-denaturing PAGE of polyphenol oxidase extracts: extract A (A), B (B), C (C), and commercially available tyrosinase (D)

2.2.2 (4) Detection of copper-containing proteins by PAGE

It is possible to detect copper-containing proteins on PAGE gels by staining them with biquinoline (Bruyninckx *et al.*, 1978). The copper in the protein is first reduced to the copper (I) state by the ascorbic acid, and biquinoline then reacts with the copper (I) ions. This is achieved by soaking the gels in a solution containing ascorbic acid and biquinoline, and then examining them under UV light. The proteins appear as dark bands due to the copper ions from the polyphenol oxidase quenching the fluorescence of the biquinoline, while the rest of the gel remains fluorescent.

This procedure was used (see Section 2.4.7) to confirm that the bands 1, 2, and 3 (Figure 2.3) were copper-containing proteins, providing additional evidence for the identity of the active proteins as polyphenol oxidase.

2.2.3 Immobilisation of polyphenol oxidase

Various immobilisation procedures have been reported to be suitable for tyrosinase (*eg.*, Iborra and Manjon, 1977; Thompson *et al.*, 1985), most of them involving covalent attachment. However, polyphenol oxidase is insoluble in chloroform (which was the solvent to be utilised in this study), and therefore covalent immobilisation was unnecessary. In the present study, immobilisation was effected using the method of Kazandjian and Klivanov (1985), where protein is deposited on non-porous glass beads. The optimal ionic state of the enzyme was ensured by dissolving it in buffer at its optimal pH, and drying this solution on the beads. This procedure was found to be the most suitable for the application of polyphenol oxidase in organic media, in terms of thermal stability and activity (Estrada *et al.*, 1991).

Thus, the freeze-dried powder was dissolved in buffer of optimum pH, the glass beads were added, and the mixture was then air-dried, leaving the biocatalyst as an almost free-running powder (see Section 2.4.8). In the case of the crude extract A, the beads were more sticky than for the other extracts. The protein loadings in the biocatalysts were measured by Folin-Lowry determinations on small portions of the beads (See Section 2.4.9). The biocatalyst was stored frozen, in small portions, for later use. The specific activities of the immobilised biocatalyst containing extracts A, B, and C were all found to be greater than the freeze-dried powders from which they were made (see Table 2.3, Section 2.2.1). Although this is a typical effect of immobilising enzymes (Khmelnitsky *et al.*, 1988), these large differences may also be partly due to increased oxygenation of the biocatalyst during the drying process.

2.2.4 Assay procedures

2.2.4 (1) Activity assay in aqueous medium: the "Dopachrome assay"

An aqueous system for measuring the activity of polyphenol oxidase samples was desirable, in that it would be independent of several parameters involved in the organic system *viz.*, effects of the solvent on the enzyme, effects of the solvent on the substrate, degree of hydration, heterogeneity and inherent diffusional factors, stirring rates, *etc.* This would provide a means of assessing whether observed trends were dependent on differences in activity of samples rather than experimental conditions.

Various assays for polyphenol oxidase have been published, measuring properties such as the rate of production of benzoquinone from catechol (Ingebrigtsen *et al.*, 1989), the rate of dopaquinone formation (Pifferi and Baldassari, 1973), the rate of dopachrome formation (Behbahami *et al.*, 1993), the rate of oxygen consumption (Naish-Byfield and Riley, 1992), and the change in electrochemical potential (Cvetkovska *et al.*, 1992).

In the present study, an adaptation of the spectrophotometric "dopachrome" method (Gardner and Cadman, 1990) was used to measure the catecholase activity of enzyme samples, with DOPA as the substrate, in phosphate buffer at pH 6 (see Section 2.4.10). The DOPA is converted to dopachrome (see Scheme 1.1, Section 1.1.2) which has a molar extinction coefficient of $3600 \text{ M}^{-1} \text{ cm}^{-1}$ at wavelength 475nm. In addition to being a convenient and consistent assay, this method has the advantage that the lag phase characteristic of cresolase activity is avoided, since only catecholase activity is measured.

Small portions of the biocatalyst were added to the substrate solution in a cuvette, allowing the enzyme to dissolve off the beads, and reaction then took place in a homogenous solution. The rates of absorbance increase were determined from the linear part of the graph (see Figure 2.4). Where variations in this "dopachrome activity" of different samples of biocatalyst were indicated by this assay, they were compensated in comparisons of reactivity in the organic system. For instance, storage of the biocatalyst at -4°C was found to cause small reductions in the dopachrome activity. In such cases, the activity in chloroform was multiplied by a correction factor (equal to the dopachrome activity measured for freshly prepared biocatalyst divided by the dopachrome activity of the present sample).

In a typical experiment, the polyphenol oxidase activity of freshly prepared biocatalyst (containing $31.76 \mu\text{g}$ protein per mg beads, made from the crude extract A), was $1.65 \mu\text{mol}$ dopachrome produced per minute per milligram protein. Figure 2.4 shows the absorbance/time graph for this dopachrome activity assay.

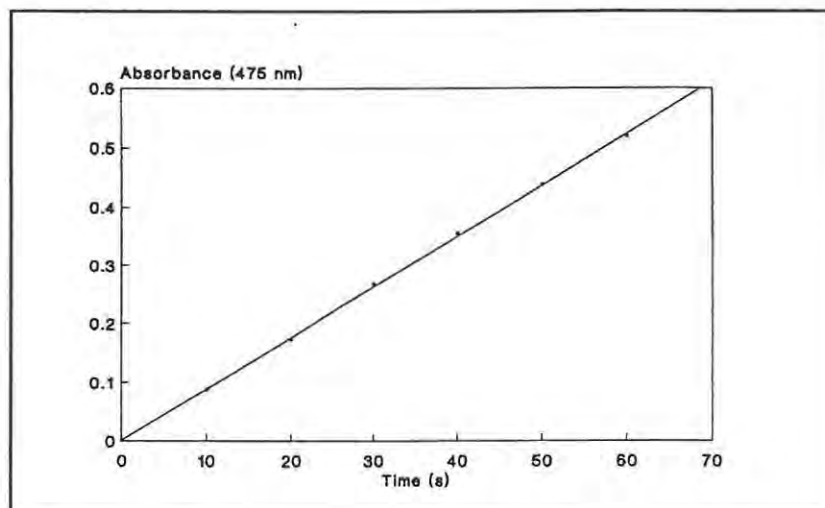


Figure 2.4: Graph of absorbance vs time for a typical dopachrome assay

2.2.4 (2) Activity assay for the biocatalyst in organic medium

A method was required to measure the activity of polyphenol oxidase in an organic system where conditions could be easily controlled, and in which reaction rates could be measured rapidly and reproducibly. It was necessary to ensure adequate hydration of the protein without having excess water present, and to allow control and measurement of water content in the system. The method devised in the present study involved adding a portion of the biocatalyst to a measured volume of chloroform in a closed volumetric flask, and then adding a measured amount of water to hydrate the whole system (see Section 2.4.11). After addition of the buffer, one minute of stirring was allowed for hydration of the protein. The substrate was then added in a small volume of chloroform, and timing was commenced simultaneously with the addition. At two minute intervals, an aliquot of the reaction mixture was removed, its absorbance was measured, and it was returned to the flask as rapidly as possible.

Mixing, to maximise contact between the substrate and the enzyme, was effected by magnetic stirring. This was also a means of ensuring that the oxygen content of the chloroform was not depleted, since stirring would facilitate the dissolving of oxygen from the air in the headspace in the flask. Although magnetic stirring may not be ideal (see Section 2.1.4), it was found to be the

most consistent method of mixing, as long as a constant stirring speed was maintained. A bench shaker was tested as an alternative, but the speed was found to be difficult to control, and solutions tended to become opaque.

In order for this assay to be used to examine the effects of parameters other than the nature of the substrate, *para*-cresol was selected as a "standard" substrate. It was used, at a concentration of 25 mM, in experiments where other conditions, such as water content, were varied. The molar absorption coefficient of the product, 4-methyl-*o*-benzoquinone, was determined (see Section 3.2.2) to be $1460 \text{ mM}^{-1}\text{cm}^{-1}$ in chloroform, at its wavelength of maximum absorbance (395nm). In each assay, the procedure was repeated at least three times, and sometimes several times, for any particular set of conditions, to achieve a standard error in the mean of less than 10%. A typical reaction is illustrated in Figure 2.5.

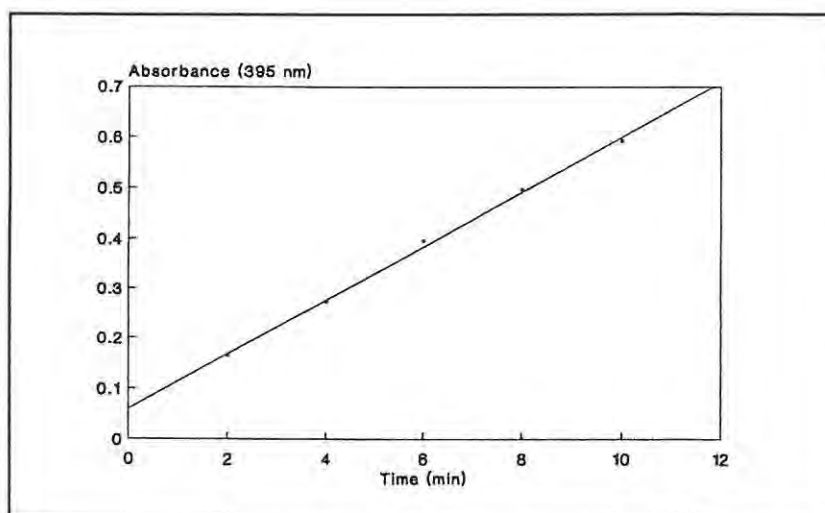


Figure 2.5: Absorbance vs time graph for a typical biocatalytic assay in the organic system, using *p*-cresol as the substrate; rate of absorbance increase = $0.0413 \pm 0.0005 \text{ min}^{-1}$.

2.2.4 (3) Correlation of dopachrome and *p*-cresol assays

For a system in which all factors were known to be equal, the dopachrome and *p*-cresol assays should correlate well, since they would be measuring the activities of the same biocatalyst under consistent conditions; this is the basis for use of the dopachrome assay as an indicator of variations in the activity of biocatalyst samples [see Section 2.2.4 (1)]. This was tested by comparing results from the two assays carried out on samples of the same biocatalyst, but which had been stored under slightly variable conditions, so that their activities were altered. The graph (Figure 2.6) shows a convincing correlation for these samples, and thus the use of the dopachrome assay is justified.

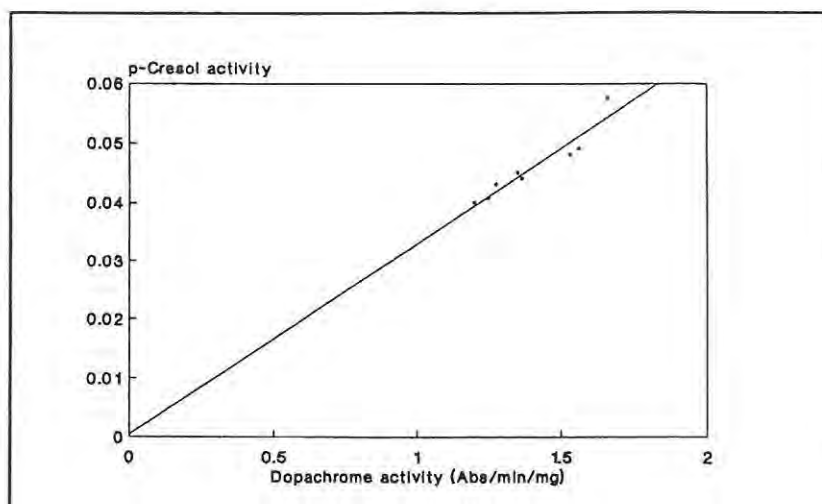


Figure 2.6: Correlation of dopachrome and *p*-cresol assays for biocatalyst prepared from crude extract A

2.2.5 Optimisation of the water requirement in the biocatalytic system

The degree of hydration of the enzyme in a biocatalyst has a critical effect on the activity of the biocatalyst in an organic medium (see Section 2.1.3). In the present study, the activity of the polyphenol oxidase was required to be optimised to obtain maximum conversion of substrates. In addition, the role of water in the functioning of the enzyme could be examined.

Hydration of the enzyme in the present biocatalytic system would be governed by the initial water content of the solvent and that of the protein, as well as the extent to which the solvent "strips" the water from the protein. The optimal amount of water required for addition to the system would depend on these factors. The rate of catalysis would be optimised by maximising the hydration of the enzyme, thereby maximising protein flexibility, but any excess water would lead to phase separation and to *o*-quinone polymerisation.

The presence of extraneous protein which would require hydration additional to that required for tyrosinase itself, and the degree to which the glass beads would adsorb water, were unknown quantities in the present study. Therefore, an empirical determination of the optimal amount of water to be added to the organic system was undertaken.

The water content of the chloroform was measured by Karl-Fischer titration (Laitinen and Harris, 1975) before it was added to the flasks, and again after the biocatalyst was added (see Table 2.6). The small difference indicated that very little water was stripped from the protein by the chloroform in this system; the stripping represents the transfer of 0.2 μL water to the 10 ml of chloroform, which would certainly be compensated in the volume of buffer added to the flask. The water content of the biocatalyst itself was determined by weighing a sample before and after freeze-drying and then heating for 24 hours (see Section 2.4.12).

Table 2.6: Water content of constituents of the biocatalytic system

Component	% water (w/w)
Chloroform before hydration	0.038
Chloroform addition of biocatalyst	0.040
Biocatalyst	2.83

The standard organic assay (Section 2.2.2) was used to determine optimal hydration conditions, by adding varying proportions of buffer to the chloroform, and determining the rates of conversion of *p*-cresol to 4-methyl-*o*-benzoquinone. The assays were repeated several times for each proportion of water, and the mean of each set of readings is reported in Table 2.7.

Table 2.7: Effect of varying hydration on initial rates of reaction in the organic biocatalytic system

Volume of buffer (μL)	% water in 10 ml reaction mixture	Initial rate ^a
20	0.238	0.263 \pm 0.02
25	0.288	0.317 \pm 0.03
30	0.338	0.393 \pm 0.03
35	0.388	0.380 \pm 0.02
40	0.438	0.363 \pm 0.01

^a μmol *o*-quinone produced per minute per mg protein

The highest initial reaction rate corresponded to the system in which the chloroform had an aqueous content of 0.338% (v/v). With lower water concentrations, the rates would be decreased because of limitations on protein flexibility, and with higher water concentrations the polymerisation of the *o*-quinone would lead to inactivation. In the latter case, the precipitation of polymer was visible in the flasks. In addition to the water added to the system, the biocatalyst itself contained 2.83% water, so that the amount of water hydrating the protein was 5.9% (w/w) with respect to the protein, and 0.65% (v/v) with respect to the chloroform.

This optimisation procedure was repeated for each new batch of biocatalyst, since small variations in their water content were observed. The differences in the amount of buffer required in each case were within 8% of the amount determined for the first batch.

2.2.6 Investigation of further purification procedures

Some further purification steps (subsequent to the ammonium sulphate fractionation to produce extract B) were investigated, to ascertain whether the efficiency of the biocatalytic system would be improved, and whether such procedures would be straightforward enough to warrant being included in the preparation of the biocatalyst.

2.2.6 (1) Chromatography using DEAE-Cellulose

A sample of extract B was subjected to liquid chromatography on DEAE-cellulose (Frieden and Ottesen, 1959) (see Section 2.4.13). The chromatography was monitored by protein and dopachrome activity assays (see Figure 2.7).

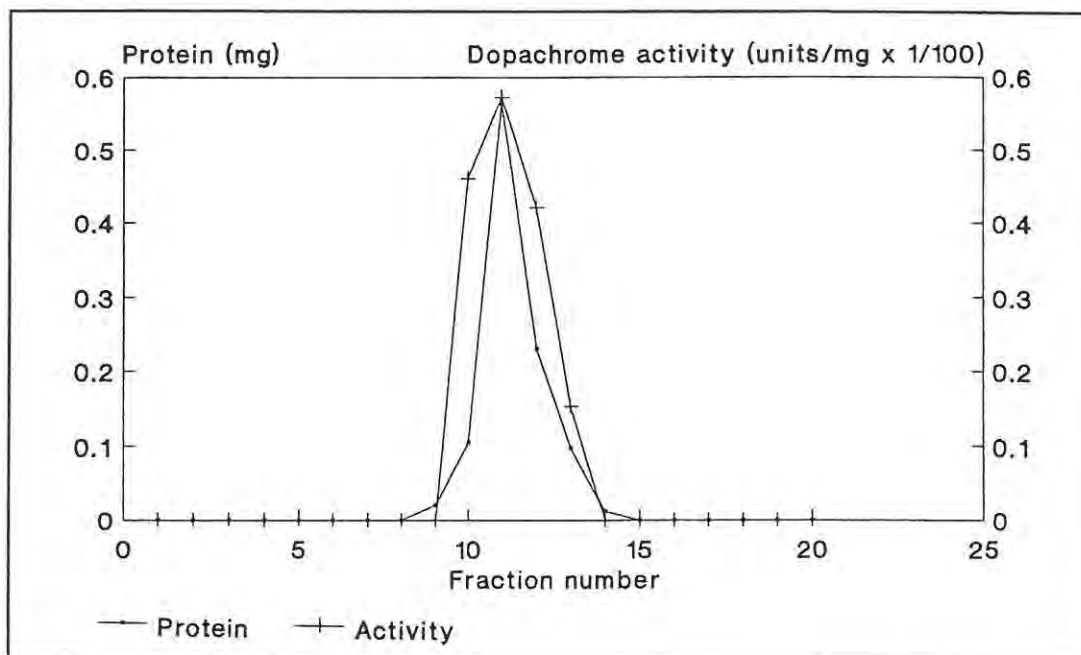


Figure 2.7: Elution profile of protein and polyphe nol oxidase activity for DEAE-cellulose column

A single protein fraction was obtained, which exhibited a relatively high specific activity (see Table 2.8 below), but which comprised only a small proportion of the protein originally loaded on the column was isolated; the remaining protein apparently bound to the column packing. A large increase in the ionic strength of the buffer failed to elute any further fractions. The active fraction from this column was analysed by SDS-PAGE, and was found to contain the same protein components as the extract B, although the 56000 band appeared more concentrated, relative to the other bands, after the chromatography. The active component comprised only 5% by mass of the original sample of extract. This small yield of purified protein indicates that this purification would not be practicable in the production of the biocatalytic system.

2.2.6 (2) Chromatography by size exclusion

Chromatography on a high-flow rate size exclusion chromatography gel, Toyopearl HW-50S, which was expected to provide a convenient and rapid purification, was investigated (Section 2.4.14). Here, three protein fractions were separated, of which one contained inactive protein, one exhibited low specific activity, and the other contained polyphenol oxidase with high specific activity (see Table 2.8 and Figure 2.8). However, the yield of active, purified protein was only 13%, and PAGE analysis again showed that the protein as not homogenous. The purified protein was found to be far less stable than the less pure extracts, in that it lost approximately 40% activity during storage in solution at 4°C for two days. Therefore, it was concluded that although this method of purification was successful to a certain extent, it would not be of advantage to apply it in the production of a biocatalyst.

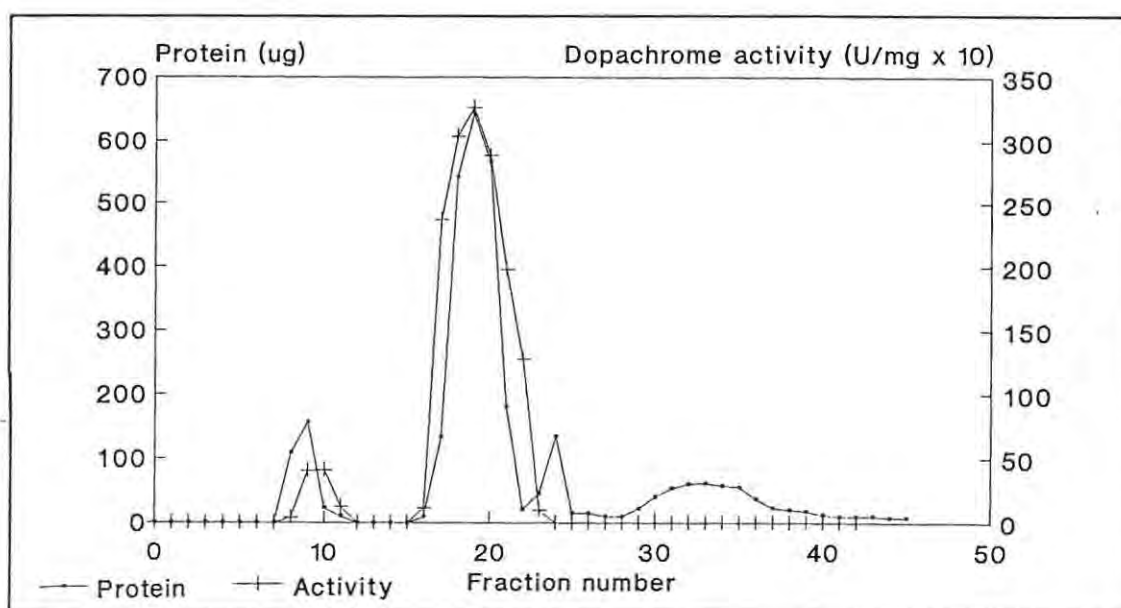


Figure 2.8: Elution profile for protein and polyphenol oxidase activity for size exclusion (Toyopearl HW-50S) column

Table 2.8: Results of protein and activity assays of purified polyphenol oxidase

Enzyme fraction	Mass loaded (mg)	Mass obtained (mg)	Specific activity (Units.mg ⁻¹)	PAGE analysis ^a
Extract B	10 mg		10.58	
DEAE-cellulose - Active fraction	20 mg	0.998	48.48	56000 47000 43500
Toyopearl HW-50S - Active fraction 1	20 mg	0.288	29.03	56000 to 47700
Active fraction 2		1.586	2.71	40000 to 33000

^a Approximate molecular masses determined as in Section 2.5.5

Purification of tyrosinase is known to be difficult, and tends to cause a decrease in the proportion of cresolase activity as compared with catecholase activity (Scott, 1975), and thus the difficulties encountered in this study were not unexpected. The two methods investigated were chosen for their convenience, since a lengthy purification procedure would not be suitable for the production of a biocatalyst. Neither was particularly successful, in that the yields of purified protein were very low, and the products did not differ significantly from the extract B from which they were obtained, except in the separation of some lighter, inactive protein. Improved results might be achieved using hydroxyapatite chromatography (Bouchilloux *et al.*, 1963; Nelson and Mason, 1970) but this is a notoriously slow method. Affinity chromatography has been reported to be more practical (O'Neill *et al.*, 1973; Gutteridge and Robb, 1973) and this would seem the most promising method to pursue. However, in terms of preparation of a biocatalyst, there is no apparent advantage in undertaking purification procedures which deplete the yield and are time-consuming and costly.

2.2.7 Application of the polyphenol oxidase biocatalytic system in chloroform

The polyphenol oxidase biocatalyst prepared from extract A was utilised in two preliminary investigations of its activity in chloroform, *viz.*, the oxidation of *p*-cresol, and the oxidation of *N*-acetyl-*L*-tyrosine ethyl ester (ATEE). In both cases, the primary objective of the investigation was to achieve conversion of the substrates to their corresponding quinone products in reasonably high yields, and thus to demonstrate the successful functioning of the biocatalyst.

2.2.7 (1) Oxidation of *p*-cresol in chloroform, by the polyphenol oxidase biocatalyst

Biocatalyst, prepared from Extract A (as described in Section 2.2.1), was added to a solution of *p*-cresol in chloroform, and the reaction was initiated by the addition of aqueous phosphate buffer to bring the water content of the solvent to 0.5% (Kazandjian and Klibanov, 1985). In this preliminary reaction, the water present in the biocatalyst was not taken into account in determining the amount of water required. The reaction mixture was shaken continuously for several hours, during which time the reaction was monitored by UV-visible spectroscopy and gas chromatography (GC). Periodically, a small aliquot was removed from the flask, and the absorbance of the sample was measured to determine the *o*-quinone concentration in the chloroform. The amount of unreacted substrate in the sample was determined by GC, by measuring the decrease within time of the peak due to *p*-cresol (see Figure 2.9). The concentration of *p*-cresol in the reaction mixture was reduced to 9 % of the starting concentration, after 6 hours.

The levelling off in the rate of increase of UV absorbance demonstrates a reduced reaction rate as the substrate is depleted. The rate of absorbance increase (approximately 2.5 absorbance units per hour) corresponds to a rate of quinone production of 2.9 mmol per hour per milligram protein, and the final concentration of *o*-quinone in the chloroform solution after 6 hours was 11.1 mM, indicating a yield of 74% (see Table 2.9).

After six hours, the chloroform solution was decanted, and extracted with an aqueous solution of ascorbic acid, which reduced the quinone in the organic layer to 4-methylcatechol. The catechol was soluble in the aqueous layer, and could be detected by high performance liquid chromatography (HPLC). Although the extraction was unlikely to be complete, comparison with standard solutions of 4-methylcatechol indicated that the concentration of 4-methylcatechol in the final reaction mixture was 9 mM (see Section 2.4.14), which corresponds to a yield of approximately 60%.

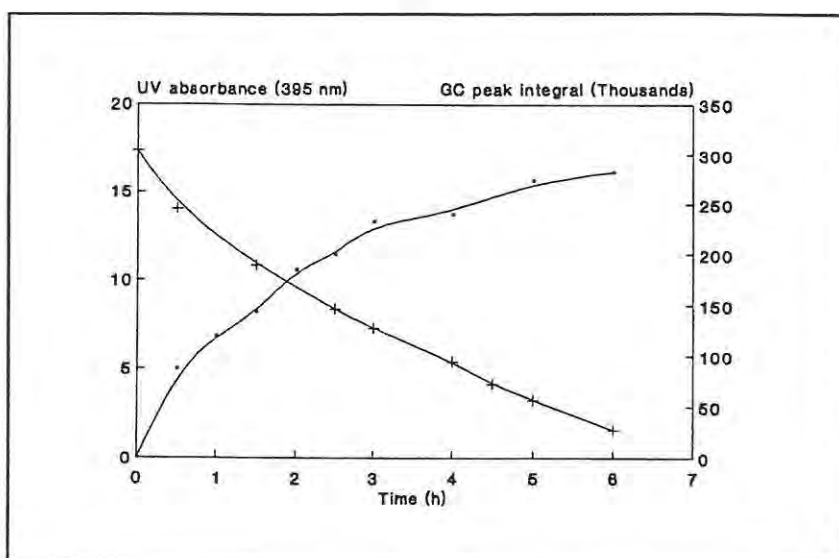


Figure 2.9: Progress of the utilisation of *p*-cresol by polyphenol oxidase in the biocatalytic system

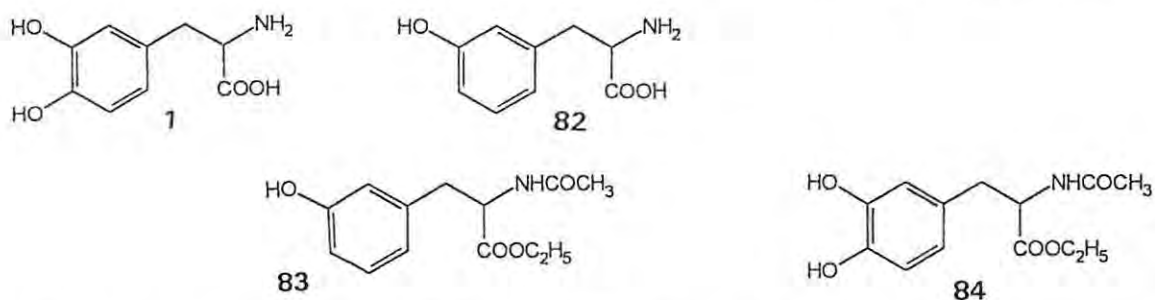
Table 2.9: Results of conversion of *p*-cresol to 4-methylcatechol, catalysed by polyphenol oxidase biocatalyst in chloroform

Method of detection	Results	% yield
GC - reduction of phenol	Initial GC peak integral: 302860 Final GC peak integral: 27257 % substrate remaining = 9%	91
UV - formation of <i>o</i> -quinone	Initial total absorbance: 0.00 Final total absorbance: 16.15 Concentration product: 11.1 mM	74
HPLC - formation of catechol	Initial substrate conc: 15 mM Final concentration: 9 mM	60

This investigation demonstrated that the biocatalyst could successfully be applied in a simple system, and that good conversion rates were achievable. The apparent discrepancy between the yields determined by GC, HPLC and UV spectroscopy was attributable to the formation of polymeric material on the biocatalyst and flask, which is likely to be a melanoid product from the quinone. This would remove some quinone from the solution, resulting in lower UV absorbances being observed. This demonstrates the necessity to control the water content of the system so that the water-dependent polymerisation would be minimised.

2.2.7 (2) Conversion of ATEE to *L*-DOPA

One of the most obvious potential applications of a polyphenol oxidase biocatalyst is the production of *L*-DOPA **1**, the drug used to treat Parkinson's disease, from *L*-tyrosine, **82**. This drug is required in relatively large quantities, in an enantiomerically pure form, and there is a considerable world market for it. Kazandjian and Klibanov (1985) demonstrated that purified polyphenol oxidase could be utilised successfully to oxidise ATEE, **83** in chloroform, and that ascorbic acid reduction by aqueous extraction was suitable as a means of obtaining the catechol *L*-DOPA in its protected form, **84**. The same authors also reported a synthetic method of deprotecting the *L*-DOPA derivative, **84**.



In the present study, the procedure of Kazandjian and Klibanov was repeated, using the crude extract A in place of the commercially available, purified enzyme (Sections 2.4.15 and 2.4.16). The reaction was carried out using a similar method to that described for *p*-cresol above, monitoring the reaction by GC. The rate of utilisation of the substrate is shown in Figure 2.10, and the yields are shown in Table 2.10. Again, the discrepancy between the yields measured by the different methods is attributed to the formation of polymeric melanoid products.

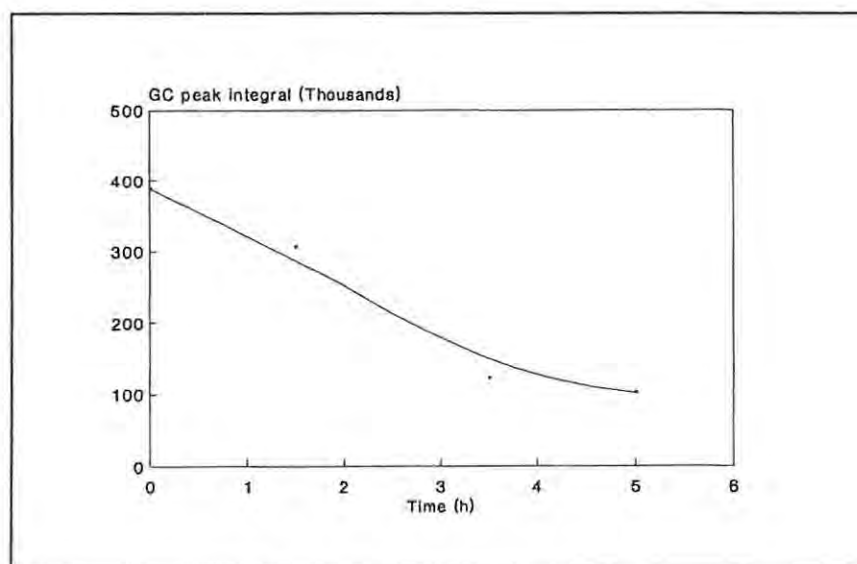


Figure 2.10: Graph of GC count (area of ATEE peak) vs time for the conversion of ATEE, catalysed by polyphenol oxidase

Deprotection of the protected *L*-DOPA, **84**, was carried out by the method of Kazandjian and Klibanov (1985), which involved alkaline hydrolysis, under nitrogen. The product, *L*-DOPA, was identified and quantified by HPLC, by comparison with standard samples of *L*-DOPA. The yield was determined, from comparison of HPLC peaks on the reaction mixture and standard solutions, to be 48% with respect to the starting material (ATEE). Thus the biocatalyst prepared from the crude extract **A** was shown to be a useful source of polyphenol oxidase, and to have activity comparable to that reported for the commercially available enzyme.

Table 2.10: Results from the oxidation of ATEE, catalysed by polyphenol oxidase biocatalyst, in chloroform

Detection method	Results (after 5 hours)	% yield
GC - reduction of substrate	Initial GC peak integral: 388392 Final GC peak integral: 101485 % substrate remaining: 26%	74
HPLC - yield of <i>L</i> -DOPA	Initial substrate conc: 25 mM Final concentration product: 12.1 mM	48

2.3 CONCLUSIONS

A crude, or partially purified, extract from fresh mushrooms was found to be a plentiful source of polyphenol oxidase, which could be immobilised and stored with only minor loss in activity. The biocatalyst prepared in this way was shown to function in an organic medium with sufficiently high rates to make its application feasible.

Assays were devised for use in determining the activity of the biocatalyst in aqueous and organic systems, and comparison of results from the two methods, obtained under standardised conditions, demonstrated that the assays could be correlated. The assay method designed for measurement of rates of reaction in the organic medium is simple, convenient, and adaptable. The dopachrome assay provides a suitable means of monitoring any variations in the activity of the biocatalyst which is independent of the effects of an organic solvent.

An investigation into the optimal hydration of the organic system showed that small changes in the degree of hydration of the protein would significantly alter reaction rates in the organic system, and that the water content of the system should be carefully monitored and controlled.

Chromatographic methods of purifying the enzyme extracts were found to offer little advantage in the preparation of the biocatalyst. The investigation demonstrated that while it would be possible to obtain pure samples for detailed biochemical studies, chromatographic methods are not practical or necessary for the production of a biocatalyst.

The biocatalytic system was successfully applied to the oxidation of *p*-cresol, and the product was converted to the corresponding catechol by a simple aqueous extraction. The utilisation of the system for production of *L*-DOPA was also demonstrated, using a crude enzymes extract rather than the partially purified enzyme which is available commercially, and which is considerably more expensive.

2.4 EXPERIMENTAL

Materials

Mushrooms (*Agaricus bisporus*) were generously donated by Tongaat Mushrooms, Natal, South Africa. Chloroform was purified by distillation over CaH₂ before use. Water content in chloroform was determined by Karl Fischer titrations (Laitinen and Harris, 1975).

Gas chromatography was carried out using a Hewlett Packard 5980A gas chromatograph. UV spectroscopy was carried out using a Shimadzu UV-160A UV-Visible recording spectrophotometer.

2.4.1 Crude extract A

Fresh mushrooms (1kg) were frozen and then homogenised in cold acetone (2.5 L) using a Waring blender. The resulting slurry was filtered rapidly on a Buchner funnel, and the residual pulp was air-dried briefly before being frozen with liquid N₂. It was then stirred into cold water (500 mL), and the mixture was allowed to stand overnight at 4°C. The paste was filtered through cheesecloth, and the filtrate was stood in ice while N₂ was bubbled gently through the solution for 2 - 3 h, to remove residual acetone. This aqueous extract was freeze-dried, giving a pale brown powder (11 g, approximately). The protein content of the powder was determined by the Folin-Lowry method (Section 2.4.9) to be 28.1%, (w/w). This extract was analysed by PAGE (Sections 2.4.5 and 2.4.6) and later immobilised (Section 2.4.8).

2.4.2 Partially purified extract B: Ammonium sulphate fractionation

The freeze-dried crude extract A, prepared as described above, (11 g) was dissolved in H₂O (200 mL) at 4°C, and (NH₄)₂SO₄ (54.2 g) was added to achieve 40% saturation. The solution was allowed to stand overnight at 4°C, and the precipitate was then separated by centrifugation (10000g, 10 min). The supernatant was mixed with (NH₄)₂SO₄ (46.3 g in 100 mL H₂O) to bring it to 52% saturation, the solution was again allowed to stand overnight and centrifuged in the same manner. The supernatant was brought to 60% saturation by the addition of (NH₄)₂SO₄ (52.9 g in 100 mL H₂O), and the mixture was stood and then centrifuged as before. The precipitates in each case were dissolved in H₂O (50 mL), and protein determinations (using the Folin-Lowry method) and dopachrome activity assays were carried out (Table 2.11).

The precipitate from the 52% saturated fraction was dialysed against phosphate buffer (10mM, pH 7, then 50mM, pH 7) for 72 h. The resulting solution was freeze-dried, giving 0.25 g extract containing 60.5% protein. This was analysed by PAGE and later immobilised (see Section 2.4.8).

Table 2.11: Ammonium sulphate fractionation of extract A

Fraction	Protein (mg.mL ⁻¹)	Dopachrome activity (A.min ⁻¹ .mL ⁻¹) ^a x 10 ⁻³	Dopachrome activity (units.mL ⁻¹) ^b	Specific activity (units.mg ⁻¹) ^b
40% ppt	19.81	4.525	3.77	0.19
40% sup	5.36	12.87	10.74	1.88
52% ppt	5.11	86.0	71.70	14.03
52% sup	1.19	1.88	1.57	1.32
60% ppt	2.68	4.395	0.36	0.13
60% sup	1.55	0.365	0.30	0.19

^a Absorbance per min per mL solution of fraction

^b 1 Unit = 1 μmol dopachrome produced per minute

^c Units per mg protein

2.4.3 PVPP-purified extract C

The procedure for obtaining the crude extract was carried out as described in Section 2.4.1, but when the frozen residue was added to the water, PVPP (purchased from Aldrich, 80g) was added and the mixture was stirred well before being left to stand overnight. It was then filtered and

treated as above. The freeze-dried powder which was obtained (9 g) was found to contain 32.1% protein. It was analysed by PAGE (Section 2.4.5) and stored frozen until required for immobilisation.

2.4.4 PAGE analysis of polyphenol oxidase extracts

PAGE separations were carried out using Hoeffer SE 250 "Mighty Small" II electrophoresis apparatus and run according to the accompanying manual. Gels were prepared according to the Laemmli method (Laemmli, 1970; Davis, 1964), with 3% stacking and 7.5% resolving gel concentrations, and gel thickness of 1.5 mm. SDS was only added where specified. Coomassie Brilliant Blue (CBB) was used to stain for protein (Weber and Osborn, 1963), and DOPA solution (100 mg in 100mL phosphate buffer, 50 mM, pH 7) was used for enzyme activity detection (Gabriel and Gersten, 1992).

2.4.5 SDS-PAGE comparison of extracts and commercial enzyme

Solutions of the extracts, and commercial tyrosinase (Sigma, 2000 units per mg) were made up (with 0.1% SDS) as indicated in Table 2.12 below, and heated in boiling water (3 min). They were loaded on to denaturing (SDS-containing) gels and run with a constant current of 25 mA, for approximately 2 h. Marker proteins (Merck, as listed below) were run simultaneously; the graph of mobility vs log of molecular mass is shown in Figure 2.11. The results are illustrated in Figure 2.2, Section 2.2.2.

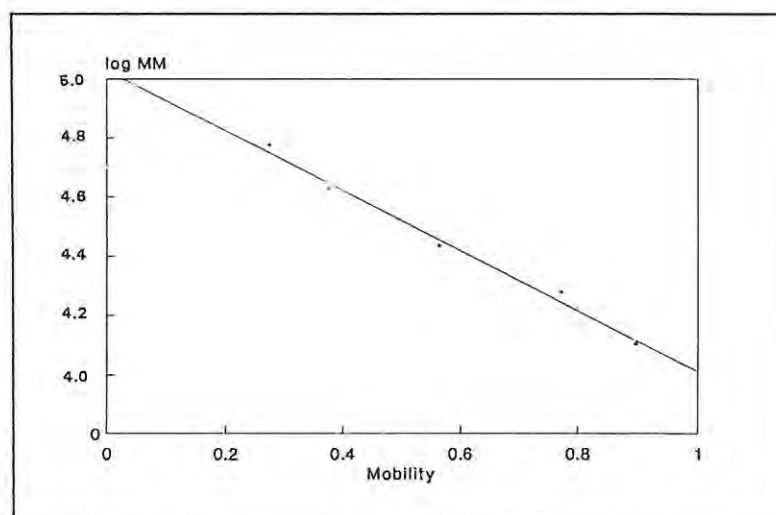


Figure 2.11: Graph of mobility vs log(Molecular mass) from SDS-PAGE results

Table 2.12: SDS-PAGE analysis of polyphenol oxidase extracts

Sample	Amount protein (μg)	Bands (distance, mm) ^a	Distance of front (mm) ^b
Crude	28	22 26 28 32	48
A.S. purif.	12	22 26 28	48
PVPP-purif.	32	16 20 21 25 30	35
Commercial	30	22 27 28 39	48
Markers:	M.W:		48
Phosphorylase b	94000	13	
Bovine serum albumin	67000	18	
Ovalbumin	43000	27	
Carbonic anhydrase	30000	37	
Soybean trypsin inhibitor	20100	43	
α -lactalbumin	14400	48	

^a Distance measured from top of resolving gel to band

2.4.6 Non-denaturing PAGE analysis of polyphenol oxidase extracts

Solutions of polyphenol oxidase extracts were made up as shown in Table 2.13 and run on non-denaturing gels (in the absence of SDS), under the conditions described above. Gels were run in duplicate, and one of the pair was stained with CBB (for protein), while the other was stained for enzyme activity. The activity stain was prepared by dissolving DOPA (100 mg) in potassium phosphate buffer (50 mM; pH 7; 100 mL). In the case of gels stained for activity, the reaction was stopped and the stain was fixed by soaking the gels in trichloroacetic acid solution (15%) for 15 min, and then in glycerol solution (10%) for 30 min. The intensities of the bands were quantified by computational analysis using a UVP gel documentation system, and the relative intensities as shown in Table 2.13 below. This provided data for calculation of the proportion of protein which was tyrosinase, in each case, as shown in the table.

Table 2.13: Determination of tyrosinase in extracts A, B and C by PAGE analysis

Enzyme	Stain	Mass ^a	Total intensity ^b	Peak intensity ^c	% ^d
Extract A	CBB ^e	150 (42)	50421	1270	2.51
	DOPA		58159	15884	23.6
Extract B	CBB	75 (45)	65251	6372	9.76
	DOPA		65138	13153	23.9
Extract	CBB	100 (32)	59754	4499	7.53
	DOPA		47556	16413	34.5

^a Mass (μg) of extract loaded on gel; mass of protein present in brackets

^b Total of intensity counts for all peaks

^c Intensity count for peak of interest

^d % peak intensity / total intensity

^e Coomassie Brilliant Blue

2.4.7 Detection of copper in the polyphenol oxidase extracts by PAGE

Duplicate non-denaturing gels were run with solutions of the polyphenol oxidase extracts as shown in Table 2.13. One gel was stained for protein as before, and the other was stained according to the method of Bruyzninckx *et al.* (1978) to show the presence of copper. The gel was soaked in 16 mM ascorbic acid (2 min), and then in the visualising reagent (3 min) [Biquinoline (0.3 mM, with 15mM ascorbic acid, in glacial acetic acid)]. The gel was transferred to a white card support, and viewed under UV light. The bands 1, 2, and 3 (Figure 2.3) were observed as dark bands against a fluorescent background, indicating that they contained copper.

2.4.8 Immobilisation of polyphenol oxidase extracts

The freeze-dried crude extract was immobilised on glass beads (250 μm , non-porous, obtained from Supelco) by dissolving the powder (1 g) in potassium phosphate buffer (50 mM; pH 7; 2 mL), and then adding the beads (6 g). The mixture was stirred gently but thoroughly, then placed in an air draught to facilitate evaporation of the water. The mixture was stirred periodically, until it was (more-or-less) free-running. The biocatalyst was stored, sealed, in small portions, at -4°C .

2.4.9 Protein assays

The Folin-Lowry method of protein determination (Lowry *et al.*, 1951; Clark and Switzer, 1977) was used to determine protein concentrations in the freeze-dried extracts, and it was adapted for use with the immobilised biocatalyst. In the latter case, small portions (5-15 mg) of biocatalyst beads were added to water (1 mL) and shaken to dissolve the immobilised protein. This solution was used as the sample solution. Bovine serum albumin was used as the standard (Table 2.14), and the standard curve is shown below (Figure 2.12). Absorbances were read at 500 nm, using the automatic concentration determination facility on the spectrophotometer. The protein concentrations determined for the extracts A, B, and C are shown in Table 2.15.

Table 2.14: Data from standard curve for protein determinations

[Protein] ($\mu\text{g}\cdot\text{mL}^{-1}$)	Absorbance
0	0.00
60	0.092
120	0.168
180	0.241
240	0.311
360	0.397

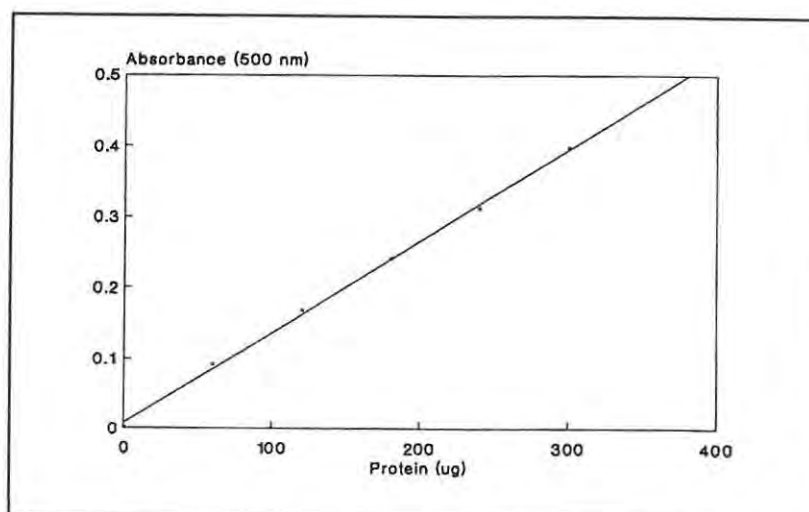


Figure 2.12: Standard curve for protein determinations using Folin-Lowry method

Table 2.15: Protein assays for freeze-dried polyphenol oxidase extracts

Extract	Mass powder (mg)	Mass protein present (mg)	% protein
A	0.602	0.169	28.1
B	0.740	0.448	60.5
C	1.005	0.322	32.1

2.4.10 "Dopachrome" assay for polyphenol oxidase activity (Gardner and Cadman, 1990)

In the case of samples of the immobilised biocatalyst, small portions of the beads were weighed out, and added to the cuvette containing the substrate solution (DOPA, 10 mM; in potassium phosphate buffer, 50mM; pH 6). The cuvette was closed and rapidly shaken for 5s, then placed in the spectrophotometer. Timing was commenced as the spectrophotometer was closed, and absorbance was recorded every 10 s for up to 90 s. The linear portion of the graph of absorbance vs. time was used to measure the rate of absorbance increase (as shown in the example in Figure 2.4, Section 2.2.4). Assays were carried out in triplicate and mean values were used to calculate activities (Table 2.16). The molar extinction coefficient of dopachrome, $\epsilon = 3600 \text{ M}^{-1} \text{ cm}^{-1}$, was used as shown in the following example:

$$\text{Rate (absorbance per min per mg biocatalyst beads)} = 0.0585$$

$$\text{Rate (absorbance per min per mg protein)} = 1.842$$

$$\text{Rate (dopachrome produced per min per mg protein)} = 5.12 \times 10^{-4} \text{ M} \cdot \text{min}^{-1} \cdot \text{mg}^{-1}$$

$$\begin{aligned} \text{Rate (dopachrome produced per min per mg protein)} &= 1.535 \mu\text{mol} \cdot \text{min}^{-1} \cdot \text{mg}^{-1} \\ &= 1.535 \text{ Units} \cdot \text{mg}^{-1} \end{aligned}$$

[1 Unit = Amount of protein which catalyses the production of 1 μmol dopachrome per minute]

Table 2.16: Dopachrome activities of biocatalysts containing extracts A, B, and C

Sample	Protein conc ^a	Dopachrome activity (Absorbance.min ⁻¹ .mg ⁻¹) ^b	Dopachrome activity (Units.mg ⁻¹) ^c
A (immob)	31.76	0.0585	1.54
B (immob)	13.96	0.177	10.56
C (immob)	36.46	0.114	2.61
A (powder)	1.4	0.348	0.30
B (powder)	0.045	8.94	4.51
C (powder)	0.064	2.03	1.69

^a For biocatalyst: μg per mg beads; for freeze dried powder: mg per mL

^b Absorbance per minute per mg protein

^c Per mg protein

2.4.11 Enzyme activity assay in the organic system

The following is the standardised method which was established; other substrates and substrate concentrations were used in kinetics experiments as described elsewhere.

A portion of biocatalyst, containing approximately 1 mg protein, was added to CHCl_3 (9 mL) in a 100 mL volumetric flask fitted with a stopper, in a water bath at 25°C. Buffer (potassium phosphate buffer, 50 mM; pH 7) was added, and the mixture was stirred magnetically (1 min). The volume of buffer was dependent on the state of the biocatalyst and the experiment being performed. The substrate (*p*-cresol, 250 mM; in CHCl_3 , 1 mL) was added, to make its concentration in the flask 25 mM. Timing was commenced upon addition of the substrate. Every 2 min, an aliquot (2 mL) was removed from the flask, its absorbance (at 395 nm) was recorded, and it was returned to the flask as rapidly as possible. The molar absorption coefficient, $\epsilon = 1460 \text{ M}^{-1}\text{cm}^{-1}$ (determined as described in Section 3.2.2) was used to convert rates of absorbance increase to rates of production of 4-methyl-*o*-benzoquinone. Figure 2.5 (Section 2.2.4) shows an example of a typical assay.

2.4.12 Optimisation of water requirement in the biocatalytic system

The standard procedure for the organic system assay was carried out with biocatalyst prepared from extract A (40 mg, containing 1.1 mg protein), and varying amounts of phosphate buffer (50

mM, pH 7) being added to the chloroform. At the end of each assay, the flasks were inspected for the presence of water droplets or precipitated polymeric material. The initial rates of reaction were measured at least in triplicate, ensuring less than 10% standard deviations for the rates and the mean values (determined by linear regression analysis using QuattroPro)(see Table 2.17).

The water content of the biocatalyst was determined by freeze-drying a pre-weighed sample (initial mass 1.068 g), and then placing it in an oven at 100°C for 24 h. The loss in mass was 0.30 g, which shows the loss of 2.83% (w/w) as water.

Table 2.17: Results from organic assays, using *p*-cresol as substrate, to determine optimal hydration requirements in the biocatalytic system

Volume buffer (μL)	Rate ($\Delta\text{A}\cdot\text{min}^{-1}$) ^a	Mean rate ^a	Mean rate ^b
20	0.0362 0.0408 0.0354 0.0362 0.0336	0.0384 ± 0.003	0.263
25	0.0402 0.0428 0.0521 0.0498	0.0463 ± 0.004	0.317
30	0.0511 0.0588 0.0582 0.0573 0.0621	0.0575 ± 0.004	0.393
35	0.0576 0.0565 0.0507 0.0574	0.0555 ± 0.003	0.380
40	0.0503 0.0541 0.0541 0.0532	0.0529 ± 0.002	0.363

^a Absorbance increase per minute

^b $\mu\text{mol } o\text{-quinone}$ produced per minute per mg protein

2.4.13 Chromatography on DEAE-cellulose

A column (1 cm diameter x 10 cm length) was packed with DEAE-cellulose (Sigma, medium mesh) using sodium phosphate buffer (40 mM, pH 8). A sample of Extract B (see Section 2.4.2) (20 mg) was dissolved in the same buffer (1 mL), and loaded on the column. Elution with this buffer was continued until 6 x 5 mL fractions had been collected, with a flow rate of 10 mL per h (using an EYELA Microtube MP-3 pump and an LKB 2112 REDIRAC fraction collector). The ionic strength of the buffer was increased to 80 mM, and elution was continued with the same flow rate. Fractions (5 mL) were collected until the total volume collected was 250 mL. The concentration of the elution buffer was changed to 1.2 mM, and a further 20 fractions were collected. The protein concentrations in the fractions were assayed by reading their absorbance at 280 nm (see standard curve, Table 2.18 and Figure 2.13 below). Dopachrome activity assays were carried out by adding aliquots of each fraction (50 μ L) to the DOPA solution (3 mL) and proceeding as described in Section 2.4.10). The results are shown in Table 2.19. Fractions 10 - 13 were combined to give a solution of tyrosinase with specific activity 48.48 units per mg protein. The solution was analysed by PAGE as in Section 2.4.5. Components with molecular masses 56000, 47000, and 47700 were observed.

Table 2.18: Data for protein standard curve using absorbance at 280 nm

[Protein] (μ g.mL ⁻¹)	Absorbance
0	0.000
60	0.037
120	0.073
180	0.110
240	0.144
300	0.184
360	0.236
480	0.311
600	0.393

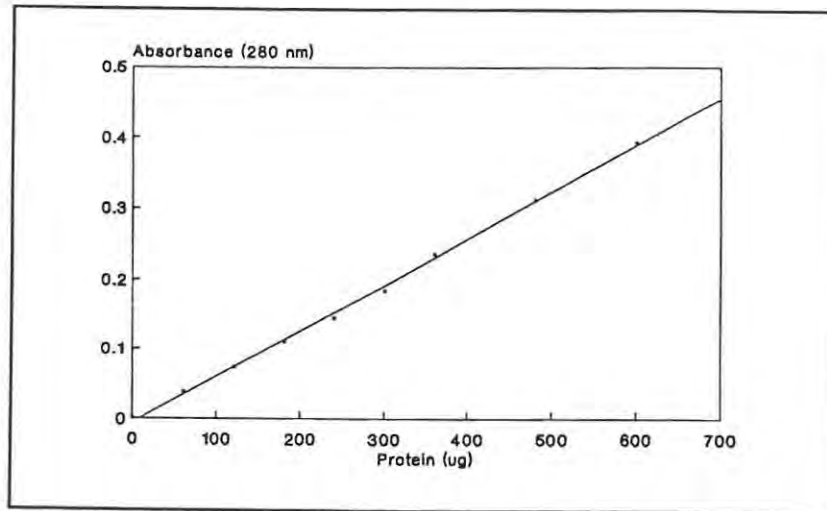


Figure 2.13: Protein standard curve using absorbance at 280 nm

Table 2.19: Results of activity and protein assays of fractions from DEAE-cellulose column

Fraction	Mass protein (mg)	Dopachrome activity ^a
1 - 8	-	-
9	0.021	-
10	0.105	46.03
11	0.564	57.32
12	0.230	42.03
13	0.098	15.31
14	0.012	-
15 - 40	-	-

^a Units per mg protein

2.4.14 Chromatography on Toyopearl HW-50S

Toyopearl HW-50S (30 μ m, Tosohaas) was suspended in sodium phosphate buffer (50 mM, pH 7, containing 50 mM KCl) and packed into a column (2 cm diameter x 20 cm length). A sample of extract B (20 mg) was dissolved in the same buffer and loaded on the column. The flow rate was maintained at 10 mL per h and 5 mL fractions were collected and assayed as described in the

previous section. Three major protein-containing fractions were eluted (see Table 2.20) of which two had tyrosinase activity. A broad tailing fraction was eluted after these, but was found to have no tyrosinase activity.

Table 2.20: Results of protein and activity assays of fractions from Toyopearl column

Fraction	Mass protein (μg)	Dopachrome activity (units per mg)
1 - 7	-	-
8	109	0.405
9	156	4.03
10	23	4.06
11	10	1.25
12 - 15	-	-
16	9	1.15
17	133	23.7
18	542	30.4
19	643	32.6
20	567	28.9
21	181	19.8
22	21	12.7
23	45	1.10
24	134	-
25	15	-
26	15	-
27	10	-
28	10	-
29	22	-
30	40	-
31	53	-
32	60	-
33	61	-
34	57	-
35	55	-
36	37	-
37	23	-

2.4.15 Oxidation of *p*-cresol

Biocatalyst (100mg beads, containing 0.61 mg protein, prepared from extract **A**) was added to a 10 mL conical flask (fitted with ground glass stopper) containing *p*-cresol solution (15 mM in chloroform, 3 mL). Potassium phosphate buffer (50 mM; pH 7; 15 μ L) was added, the flask was closed, and the mixture was shaken on a bench shaker for 6 h. Periodically, 2 x 50 μ L aliquots were removed from the flask, and used (a) for GC analysis and (b) for UV spectroscopic analysis (see Table 2.22 below). The solution was decanted, and extracted with ascorbic acid solution (100 mM, 2 mL). The aqueous layer was analysed by HPLC using a Hewlett Packard 1050 liquid chromatograph (see Table 2.23 below).

Conditions for GC: Capillary column, SE-30 (4%), 4 film μ m thickness

Carrier gas: N₂, 31 mL.min⁻¹

Column head pressure: 65 kPa

Injection port temperature: 250°C

Detector: FID, 250°C

Initial temperature: 140°C for 6 min

Temperature gradient: 7°C per min

Final temperature: 180°C

Injection volume: 0.5 μ L

Retention time for *p*-cresol: 8.8 min

Conditions for HPLC: Column: Reverse phase

Mobile phase: Acetonitrile: water 4:6

Flow rate: 1 mL.min⁻¹

Detection: Absorbance at 280 nm

Injection volume: 5 μ L

Table 2.21: Results of GC and UV analysis of samples from oxidation of *p*-cresol by tyrosinase

Time (h)	UV absorbance	GC (peak integral)	% substrate remaining
0	0	302860	100
0.5	4.95 ^a	244907	81
1.0	6.8		
1.5	8.2	188922	62
2.0	10.55		
2.5	11.4	146664	48
3.0	13.25	127560	42
4.0	13.7	93775	31
5.0	15.65	56331	18
6.0	16.15	27257	9

Table 2.22: Results of HPLC analysis of product from oxidation of *p*-cresol

Sample	Retention time (min)	Peak height (mm)	Concentration (mM) ^a
<i>p</i> -Cresol	3.0	32	5
		65	10
		80	12.5
		150	25
Ascorbic acid	1.7		
4-Methylcatechol	2.3	40	5
		75	10
		108	15
Reaction mixture ^b	1.7 2.3 3.0	250	-
		68	9
		3	0.5

^a Standard solutions for *p*-cresol and 4-methylcatechol; calculated for reaction mixture

^b Reaction mixture after ascorbic acid extraction

2.4.16 Oxidation of ATEE and production of *L*-DOPA

Biocatalyst (210 mg, containing 13 mg protein, prepared from extract **A**) was added to ATEE solution (25 mM; 2 mL; in chloroform), the flask was shaken briefly, and potassium phosphate buffer (50 mM; pH 7; 20 μ L) was added. The mixture was shaken using a bench shaker, for 5 h. Periodically, aliquots were removed for GC analysis (Table 2.23). After 5 h, the chloroform solution was decanted and extracted with ascorbic acid (100 mM, 2 mL), and the aqueous layer was analysed by HPLC (Table 2.24).

GC conditions: As in Section 2.4.14, but temperature program:

Initial temperature: 200°C for 3 min

Temperature gradient: 7° per min

Final temperature: 240°C

Retention time for ATEE: 26.1 min

HPLC conditions: As in Section 2.4.14,

Mobile phase: Acetonitrile-sodium acetate buffer (10 mM, pH 4); 1:4

Retention time for ATEE: 3.74 min

Retention time for ascorbic acid: 0.98 min

Table 2.23: Results of GC analysis of oxidation of ATEE by polyphenol oxidase

Time (h)	GC (counts)	% substrate remaining
0	388392	100
1.5	305531	79
3.5	121736	31
5.0	101485	26

Table 2.24: HPLC analysis of product from oxidation of ATEE

Sample	Retention time (min)	Peak height (mm)	Concentration (mM)
ATEE	3.74	140 55	25 10
Ascorbic acid	0.98	-	-
Reaction mixture	0.98 2.17 3.74	- 90 26	- 4.7

2.4.17 Isolation of DOPA from oxidation of ATEE by polyphenol oxidase

The aqueous solution from the ascorbic acid extraction (Section 2.4.16) was extracted with ethyl acetate and the organic layer was evaporated under N₂. The residue was treated with NaOH (3 M; 3 mL), under N₂ and the reaction mixture was warmed to 65°C for 3h. Ascorbic acid was added to neutralise the solution, which was then analysed by HPLC (Table 2.25). Since the peaks were broad, they were quantified by triangulation of their areas.

Conditions for HPLC: As in Section 2.4.16, except for:

Mobile phase: Acetonitrile : water 4:96, containing
Trifluoroacetic acid (0.1%)

Injection volume: 1 µL

Table 2.25: Formation of DOPA: HPLC analysis of product

Sample	Retention time (min)	Peak area (mm ²)	Concentration (mM)
DOPA	10.4	396 196	20 10
Ascorbic acid	7.0		
Reaction product	7.0 10.4	- 239	- 12.1

CHAPTER 3

A KINETIC STUDY OF THE POLYPHENOL OXIDASE BIOCATALYST

3.1 INTRODUCTION

The potential for exploitation of the polyphenol oxidase biocatalytic system is dependent on the range of applications which are possible. In order to identify this range, investigations of the substrate specificity and kinetic efficiency of the system were undertaken. In addition to their usefulness in assessing the versatility of the biocatalyst, such investigations would contribute to a rationalisation of the effects of the organic medium on the functioning of the enzyme. Reports of quantitative kinetic studies in non-aqueous biocatalysis are relatively scarce in the literature (Ryu and Dordick, 1989) but they are essential in the development of a theoretical basis for the application of enzymes in organic media.

3.1.1 Substrate specificity

In an aqueous environment polyphenol oxidase can utilise a wide range of substrates, varying from phenols with relatively unhindered structures to some with surprisingly large molecular size, such as steroids (see Section 1.1.8). However, the range of substrates was reported to be more limited when the enzyme functions in an organic medium (Kazandjian and Klivanov, 1985), which might be a disadvantage in terms of its application as a general biocatalyst for aromatic hydroxylations. These authors reported the conversion of a number of phenols by partially purified polyphenol oxidase, based on GC analysis of substrate utilisation, but enzyme kinetic parameters were only determined for one *viz.*, *p*-cresol. Thus, an objective of the present investigation was to obtain further quantitative data on the enzyme kinetics of polyphenol oxidase in a chloroform medium as a function of substrate structure. The activity of polyphenol oxidase in transforming a range of selected phenolic substrates was examined under standardised conditions to allow the measurement of initial reaction rates and hence, quantitative kinetic parameters could be calculated. One aim of this study is the application of the biocatalyst in a larger scale process and therefore, a crude enzyme extract was utilised for the investigations described in this chapter.

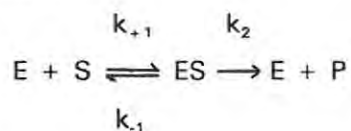
The chloroform medium employed in the present study represents a very different environment from the aqueous one in which polyphenol oxidase normally functions. Consequently, differences between the kinetic characteristics of the immobilised biocatalyst in chloroform, and the free enzyme in water, are to be expected. The organic solvent could affect enzyme-substrate interactions, the partitioning of the substrate and/or product between the solvent and the binding site, the thermodynamics of the reaction, and the stability of the enzyme (Dordick, 1992) (see Section 2.1.2).

The flexibility of the protein in the biocatalyst in the presence of the chloroform is likely to be decreased by the lack of free water (Section 2.1.3), and this was expected to affect sterically-related factors in the catalytic reaction. Therefore, the range of substrates selected for detailed kinetic analysis included *p*-alkylphenols with increasingly hindered side chains, as well as other *p*-substituted phenols, chosen for the variation in their electronic characteristics.

In addition to permitting the determination of kinetic data, the polyphenol oxidase biocatalytic system provides a means of examining the oxidation of substrates which have limited solubility in water, or which are oxidised to water-labile products. In this way, the range of known substrates of polyphenol oxidase could be extended.

3.1.2 Principles involved in enzyme kinetic studies

Enzyme catalysed reactions involve, primarily, the binding of one or more substrates to the active site of the enzyme, the establishment of a transition state which is stabilised by the enzyme, and the subsequent formation and release of the product. The most well-known method of analysis of enzyme kinetics is the Michaelis-Menten theory, which is based on the following reaction mechanism:



Thus, the enzyme E and the substrate S initially combine reversibly, forming an intermediate ES, and this intermediate then releases the product P and the enzyme. The reaction is represented by the Michaelis-Menten equation:

$$v = Vs/(K_m + s)$$

where v is the initial rate of the reaction
 s is the initial substrate concentration
 V is the maximum velocity
 K_m is the Michaelis constant.

The quantities V and K_m are specific to a particular system, and are used as a means of characterising the catalytic activity of enzymes. The parameter K_m is equal to $(k_{-1} - k_2)/k_{+1}$, and is an indication of the ability of the enzyme to bind the substrate. For the simple system represented above, the quantity V has the value $k_2 \cdot e_0$ where e_0 is the concentration of the enzyme. Thus V depends on the enzyme concentration, and it is a measure of the maximum reaction rate achievable for a given system. The more fundamental quantity k_{cat} , equal to V/e_0 , called the catalytic constant or the turnover number, can be used in cases where the enzyme concentration is known. In real situations, this is not always possible. In simple systems, k_{cat} is equal to k_2 , but in more complex systems, this is not necessarily the case. The ratio V/K_m is known as the catalytic efficiency, and can be regarded as a measure of the effectiveness of the enzyme as a catalyst, for a particular set of conditions (Cornish-Bowden, 1979).

An enzyme-catalysed reaction which conforms to the Michaelis-Menten equation would show a rate vs substrate concentration graph like the example shown in Figure 3.1. The rate v tends to V at high substrate concentrations, and at this stage the enzyme is saturated. At the half-maximal reaction rate, the substrate concentration equals K_m .

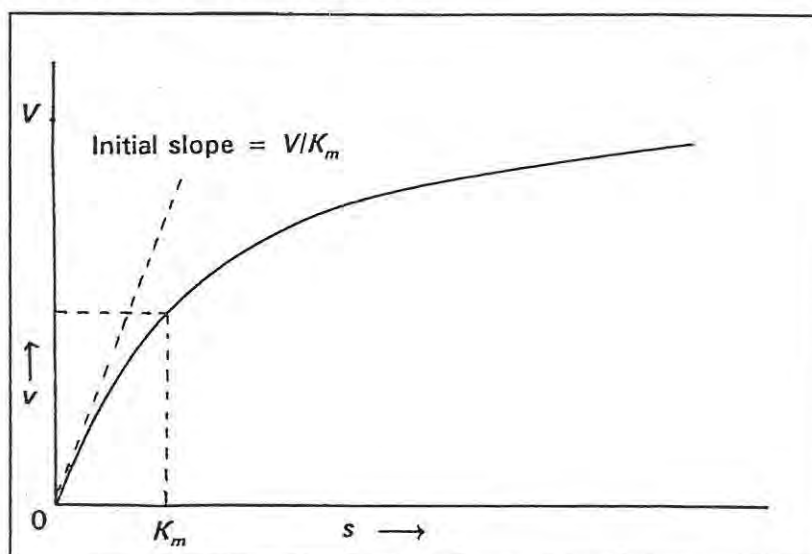


Figure 3.1: Graph of initial rate v against substrate concentration s for an enzyme-catalysed reaction which obeys the Michaelis-Menten equation.

Various graphs can be plotted to determine the parameters V and K_m , of which the most common is the Lineweaver-Burke plot of $1/v$ vs $1/s$. However, this method tends to give undue weighting to measurements taken at low concentrations, which is the least precise region, and therefore in the present study, Hanes plots were used. These graphs are obtained by plotting s/v against s , as shown in Figure 3.2.

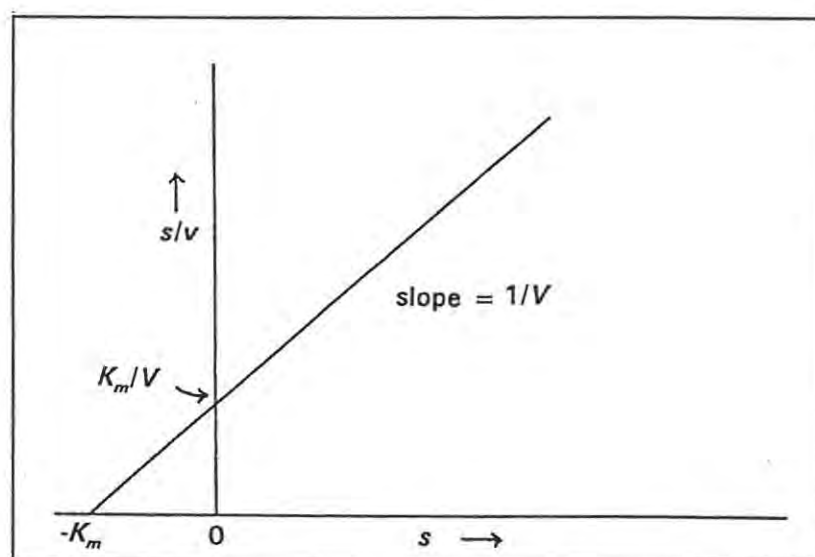


Figure 3.2: Hanes plot of s/v against s , used to determine kinetic parameters.

3.1.3 Investigation of the kinetic properties of biocatalysts in non-aqueous media.

In experiments to investigate enzyme kinetics in non-aqueous media, special attention must be paid to factors which need not be considered in "normal" enzyme kinetics experiments. For instance, the system must be optimised with respect to diffusional limitations, and there should be no changes in the diffusion properties during the experiments (Russell *et al.*, 1992).

For many substrates, the Michaelis constant, K_m , is likely to be increased when the enzyme functions in an organic solvent rather than water. For hydrophobic substrates especially, where binding to the active site often involves hydrophobic bonding, the entropy gain during binding is decreased in the organic system, and this enhances binding. However, this does allow high substrate concentrations to be used without inactivating the enzyme. The need to saturate the enzyme may be problematic in the non-aqueous situation, because this may require so much substrate that its solubility is exceeded, or that it alters the physical properties of the enzyme (Russell *et al.*, 1992).

The influence of immobilisation on the activity of an enzyme in a non-aqueous medium must also be taken into account. The apparent kinetic parameters measured for the immobilised enzyme are likely to differ from the intrinsic parameters (parameters independent of carrier dimension or enzyme loading), and from the parameters measured when the enzyme is suspended in the organic solvent. Diffusional factors, interactions with the carrier, and the altered activity of the enzyme itself, can affect the measurements. Since the intrinsic parameters are difficult to determine, except by complex numerical methods, the parameters determined with the suspended enzyme can be used as an approximation (Hooijmans *et al.*, 1991). For the purposes of the present study, however, apparent parameters are sufficient to give an indication of the effects of the solvent and substrate on the kinetics.

In order to examine the effects of substrate structure on enzyme kinetics, linear free energy relationships (LFER's) can be used to describe the influence of factors such as steric effects and hydrophobicity. Ryu and Dordick (1992) have developed a rational basis for quantifying and predicting the correlation of non-aqueous enzyme kinetics with substrate and solvent properties. The relationship between the catalytic efficiency (V/K_m) and the substrate hydrophobicity, its steric properties, and its electronic properties can be expressed in the equation:

$$\text{Log } (V/K_m) = a\pi + b\sigma + cE_s + C$$

where π is the hydrophobicity, represented by the Hansch parameter
 σ is the electronic character, represented by the Hammett parameter
 E_s is the steric character, represented by the Taft parameter

and a , b and c are the gradients of the graphs of each parameter, individually plotted against $\log (V/K_m)$. The constant C represents the catalytic efficiency of the enzyme when it utilises a standard substrate for which π , σ and E_s are zero, and any substrate-independent effects are included in it. Ryu and Dordick (1992) used this relationship to examine the combined effects of variations in substrate and solvent on the activity of horseradish peroxidase in organic solvents.

The results of the kinetic analysis in the present study were prepared for publication (Burton *et al.*, 1993) before the results of Ryu and Dordick were published. In the former publication, a correlation between the steric size of the phenolic p -substituent and the catalytic efficiency of polyphenol oxidase was suggested to demonstrate the reduced flexibility of the enzyme active site in the chloroform medium. In this thesis, correlations of these results are extended to include hydrophobicity and electronic factors, using the approach of Ryu and Dordick.

3.1.4 Investigation of the polyphenol oxidase biocatalyst in chloroform

The kinetic mechanism of polyphenol oxidase is complex in itself: the enzyme has a multi-subunit structure, with two active sites per molecule in the case of mushroom tyrosinase, and there are two substrates (oxygen and a phenol or catechol) involved in the two-stage reaction (if the substrate is a phenol). However, some simplifications can reasonably be assumed. For instance, if one substrate is in excess, the reaction can be considered to be pseudo-first order, and in the case of polyphenol oxidase, the oxygen concentration can be maintained at a high level because it is readily soluble in chloroform. It is also reasonable to assume that there is no positive or negative cooperativity between the binding sites in the protein, since there is no evidence (to the author's knowledge) of such interdependence. Also, a dimeric enzyme, in which there is cooperativity, can be expected to exhibit a sigmoidal curve for the graph of initial rate vs substrate concentration (Ishikawa *et al.*, 1991). [This was not observed in the present study using immobilised polyphenol oxidase biocatalyst in chloroform (see Section 3.2.3, Figure 3.7)]. Therefore, the two binding sites can be considered to be independent, as they would be if they were in separate molecules.

The cresolase activity of tyrosinase is generally far slower than the catecholase activity and therefore, in the two-stage reaction to hydroxylate and oxidise phenols, the first (hydroxylation) step is rate-limiting. Thus, if a phenol is used as the substrate in rate measurements, the reaction which is monitored is specifically the cresolase activity, and the catecholase activity will follow at the rate of the cresolase activity.

In the light of these simplifications, it becomes possible to apply Michaelis-Menten kinetic principles to the analysis of the biocatalyst. In the kinetic study described in the present chapter, a Michaelis-Menten treatment of the initial reaction rate measurements was used to obtain apparent values of the kinetic parameters of the polyphenolase biocatalytic system, and the results were correlated with substrate properties. While more sophisticated techniques are available for measuring enzyme kinetics, measurements from the present method can provide data with sufficient accuracy for investigations using crude or impure enzymes (Russell, 1993).

3.2 RESULTS AND DISCUSSION

3.2.1 Selection of substrates for a kinetic analysis

A range of potential substrates was first screened to determine whether tyrosinase was able to oxidise them at all, by adapting the non-denaturing PAGE method described in Chapter 2. One of the advantages of this method was that substrates which were not soluble in water (or buffer) could be still screened. The substrates were dissolved in an organic-aqueous solvent mixture (see Section 3.4.1), and the gels were soaked in this solution so that the enzyme reacted with the substrate at the interface between the predominantly organic solvent medium, and the aqueous gel medium. This does not represent non-aqueous biocatalysis but the method provides a sensitive means of detecting tyrosinase activity with substrates which are not water soluble. Although the activity of tyrosinase may be slower in the presence of an organic solvent such as acetonitrile, it was not inhibited. Thus, activity could be detected and correlated with the various protein components in the extract, by comparison of gels stained with protein stain. The results of this substrate screening are illustrated in Figure 3.3 and Table 3.1.

It was clear from these results that a number of substrates could be oxidised, and could be utilised in a kinetic study. The phenols with cyano- and nitro- *p*-substituents are known to be inhibitors of tyrosinase, and the lack of reactivity observed for these compounds confirms that the oxidation of the other substrates would not occur in the absence of enzyme activity. The positive result shown by the oxidation of *o*-cresol in Band 2 is interesting, since this band appears to have only catecholase activity with respect to other substrates, and it can be surmised that the enzyme recognises the substrate because of its *ortho*-substitution pattern. This result requires further investigation at a later stage.

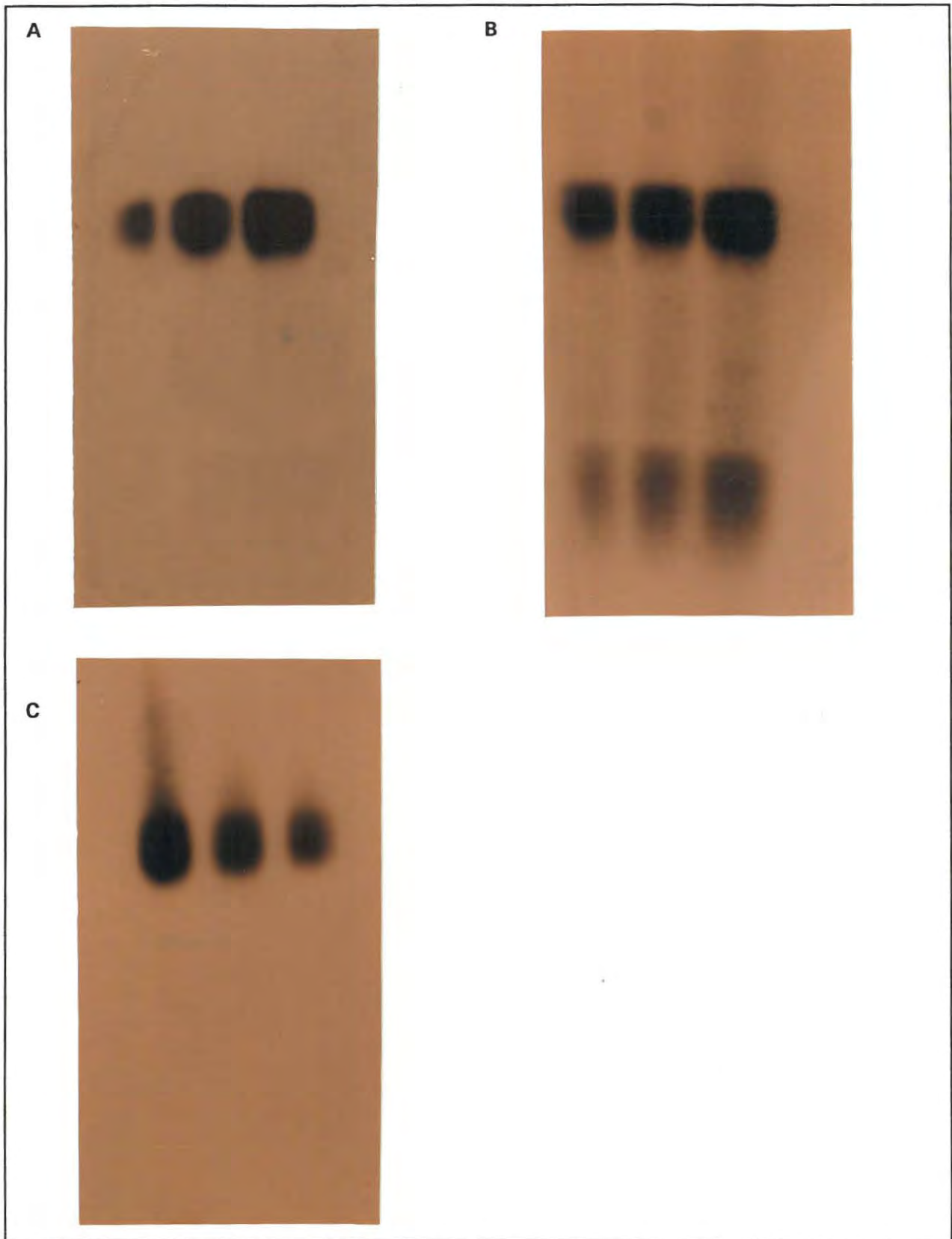


Figure 3.3: Photographs showing PAGE gels stained to detect tyrosinase activity using a range of substrates: tyrosine (A), DOPA (B), and *p*-cresol (C)

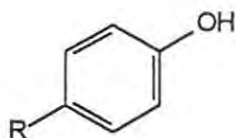
Table 3.1: Results of PAGE screening of substrates

Substrate used to stain	Solvent for stain	Activity in Band 1 ^a	Activity in Band 2 ^a
Coomassie blue	-		
<i>L</i> -DOPA	buffer	+	+
<i>L</i> -tyrosine	buffer	+	-
<i>p</i> -cresol	buffer	+	-
<i>p</i> -ethylphenol	buffer	+	-
<i>p</i> -isopropylphenol	buffer: MeCN 4:1	+	-
<i>p</i> - <i>t</i> -butylphenol	buffer: MeCN 3:2	+	-
<i>p</i> -methoxyphenol	buffer: MeCN 3:2	+	-
<i>p</i> -fluorophenol	buffer: MeCN 4:1	+	-
<i>p</i> -chlorophenol	buffer: MeCN 3:2	+	-
<i>p</i> -bromophenol	buffer: MeCN 3:2	+	-
<i>p</i> -cyanophenol	buffer: MeCN 3:2	+	-
<i>p</i> -nitrophenol	buffer: MeCN 3:2	-	-
<i>p</i> -hydroxy-benzaldehyde	buffer: MeCN 3:2	+	-
<i>m</i> -cresol	buffer	+	-
<i>o</i> -cresol	buffer	+	+
1-naphthol	buffer: MeCN 3:2	-	-
2-naphthol	buffer: MeCN 3:2	-	-
<i>o</i> -methoxyphenol (guaiacol)	buffer: MeCN 3:2	+	-
2,4-di- <i>t</i> -butylphenol (DTBP)	buffer: MeCN 2:3	-	-

^a Bands correspond to those in non-denaturing PAGE gels discussed in Section 2.2.2 (2).

From the substrates listed in Table 3.1, a range were selected (see Table 3.2), including the *p*-alkylphenols (to represent an increasing steric factor), and the *p*-halophenols and *p*-methoxyphenol (to give a variation in electronic nature). The range was limited to phenols, rather than including catechols, so that only the cresolase activity was measured (Vanni *et al.*, 1990). Kinetic measurements were made for each of these substrates, as discussed below.

Table 3.2: Phenols selected as substrates for the kinetic analysis using polyphenol oxidase



Name	<i>p</i> -substituent, R	Abbreviation ^a
<i>p</i> -cresol	CH ₃	Me
<i>p</i> -ethylphenol	C ₂ H ₅	Et
<i>p</i> -isopropylphenol	CH(CH ₃) ₂	i-Pr
<i>p</i> - <i>tert</i> -butylphenol	C(CH ₃) ₃	<i>t</i> -Bu
<i>p</i> -fluorophenol	F	F
<i>p</i> -chlorophenol	Cl	Cl
<i>p</i> -bromophenol	Br	Br
<i>p</i> -methoxyphenol	OCH ₃	OMe

^a Used in the following chapters

3.2.2 Determination of UV-visible absorption characteristics of *o*-quinone products

o-Quinones are not easily characterised, largely because of their lack of stability and as a result, properties such as their UV-visible absorbance spectra and molar absorption coefficients were not generally available from the literature. However, in order to determine the enzyme kinetic parameters of the oxidation of the phenolic substrates by a spectrophotometric method, these quantities were required. The polyphenol oxidase biocatalytic system lends itself to synthesis of *o*-quinones in a chloroform solution, where they are likely to be stable, and their physical properties can then be examined. The solution of the product is easily separated from the biocatalyst by decantation, and the reaction can be conducted in small volumes, which was of particular advantage for experiments involving NMR spectroscopy [see (2) below].

3.2.2 (1) Measurement of wavelengths of maximum absorbance for *o*-quinones

Immobilised crude polyphenol oxidase was utilised to synthesise samples of the *o*-quinones from the respective *p*-substituted phenols, the UV-visible spectra of the product solutions were recorded, and hence the wavelengths of maximum absorbance (λ_{\max}) were determined for the quinones.

These are shown in Table 3.3 below. Figure 3.4 shows the increase in absorbance with time for the oxidation of *p*-cresol.

Table 3.3: Wavelengths of maximum absorbance for *o*-quinones

Substrate ^a	λ_{\max} ^b of quinone product
<i>p</i> -cresol	395
<i>p</i> -ethylphenol	390
<i>p</i> -isopropylphenol	390
<i>p</i> - <i>t</i> -butylphenol	375
<i>p</i> -methoxyphenol	405
<i>p</i> -fluorophenol	400
<i>p</i> -chlorophenol	400
<i>p</i> -bromophenol	400

^a From which the *o*-quinone was formed

^b Wavelength of maximum absorbance of quinone product in nm

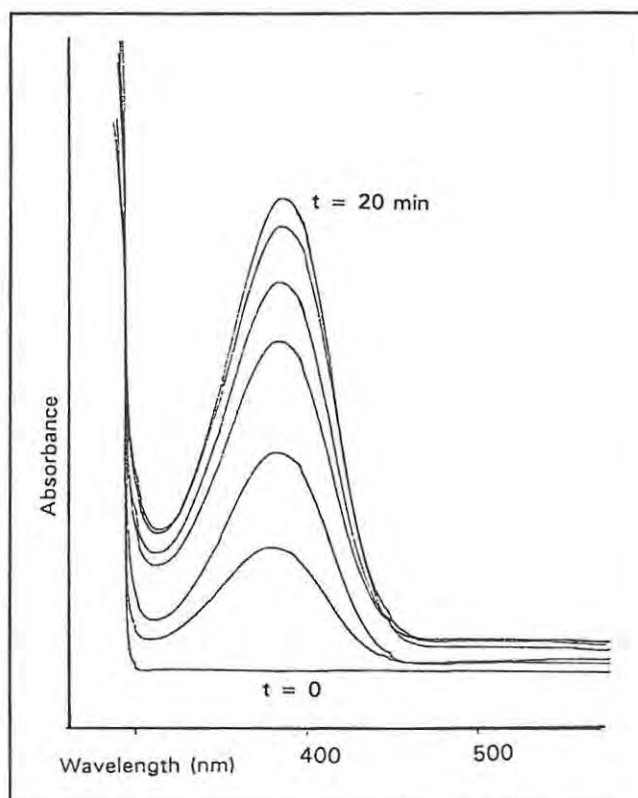


Figure 3.4: UV-visible spectra showing the formation of 4-methyl-*o*-benzoquinone from *p*-cresol, catalysed by polyphenol oxidase in chloroform.

3.2.2 (2) Determination of molar absorption coefficients, ϵ

The oxidation of the phenols by polyphenol oxidase could be investigated using NMR spectroscopy, by substitution of deuterated solvents for the chloroform and the water in the biocatalytic system. This provided a means of determining the molar absorption coefficients of the products as well as confirming the nature of the products of the reaction. The biocatalyst was added to a solution of the respective substrate in deuterated chloroform, and the system was hydrated by the addition of deuterated water. The mixture was shaken during the reaction, which was allowed to proceed for several hours (see Table 3.4). The UV absorbance of a suitably diluted aliquot of the final reaction mixture was measured. The ^1H NMR spectrum of the reaction mixture was also recorded, and the extent of reaction was calculated by comparison of NMR peak integrals associated with protons in the corresponding substrate and product spectra (see Section 3.4.3). Correlation of UV absorbance and concentration of the *o*-quinone product in a solution permitted the calculation of the molar absorption coefficients, ϵ (see Table 3.4). The ϵ values obtained correspond well with literature values where these are available (Waite, 1976). The table also shows the extent of reaction as a percentage yield of *o*-quinone. The ^1H NMR spectra used in these calculations are shown in Figure 3.5, and they also show that the reactions gave the *o*-quinones as the only products.

Table 3.4: Molar absorption coefficients of *o*-quinones produced by polyphenol oxidase from corresponding phenolic substrates

Substrate	ϵ ($\text{M}^{-1}\text{cm}^{-1}$)	Time taken (h)	% reaction ^a
Me	1460 \pm 100	3	26.8
Et	1190 \pm 50	6	51.3
i-Pr	1580 \pm 30	6	27.5
<i>t</i> -Bu	1660 \pm 100	6	10.6
F	3320 \pm 30	6	16.6
Cl	3800 \pm 300	6	21.1
Br	3600 \pm 400	6	23.5
OMe	1800 \pm 100	6	36.6

^a Determined from NMR analysis

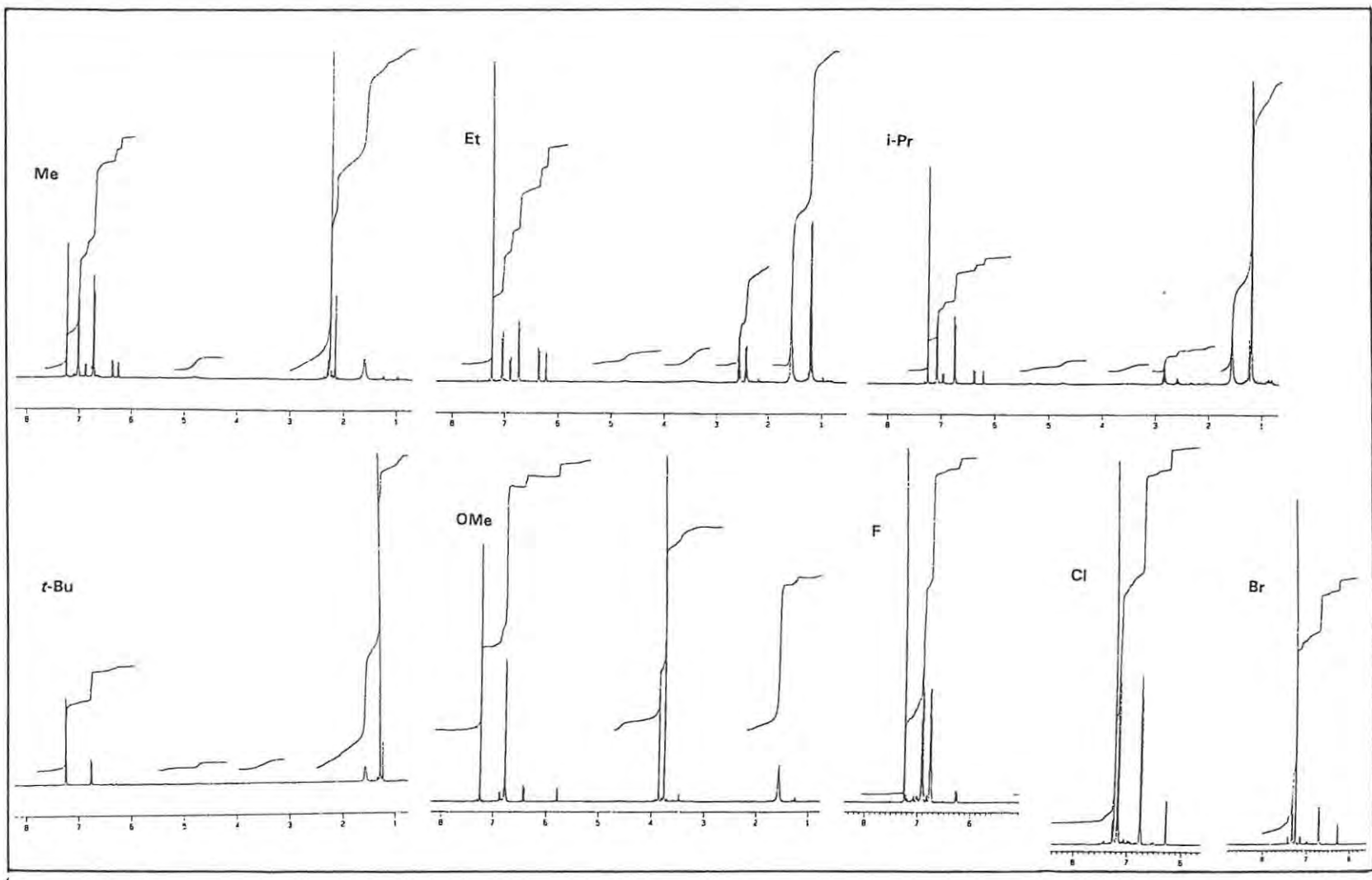


Figure 3.5: ¹H NMR spectra of reaction mixtures used to determine molar absorption coefficients for *o*-quinones; *p*-substituents shown on respective spectra

3.2.3 Determination of kinetic parameters for the biocatalyst in chloroform

The system devised for the measurement of polyphenol oxidase activity in chloroform [described in Section 2.2.5 (3)] was used to measure initial rates of reaction for the range of substrates listed in Table 3.5 below. For each substrate, five different concentrations were chosen, depending on the solubility of the substrate, to give measurable rates, while avoiding substrate inhibition. Assays were repeated several times to obtain mean rates with standard errors of less than 10%; [errors of 5 - 15 % can be regarded as acceptable for simple systems such as the present one (Russell, 1993)]. Linear regression analysis of the data from each assay gave initial rates in terms of UV absorbance per minute, and these results were converted to rates of increase in concentration of product per minute using the molar absorption coefficients measured as described in Section 3.2.2 (Section 3.4.4). The rates, v , were calculated per milligram of protein rather than per milligram of tyrosinase, because the protein concentrations were accurately determined (Section 2.2.5) but the tyrosinase concentrations were only known approximately (Section 2.2.2).

No lag phase was observed in the activity assays carried out for the different substrates, in spite of the fact that they were phenols (as opposed to catechols). This may be attributable to the presence of melanins in the crude extract, which are able to act as activators of the enzyme (see Section 1.1.5). This aspect of the biocatalyst activity is discussed further in the next chapter.

For the reactions using *p*-cresol as substrate, the graph of v vs s was plotted (Figure 3.6) to demonstrate the saturation of the enzyme (by the levelling out of the curve) and to show that the graph was not sigmoidal as would be expected for an enzyme in which the two binding sites functioned cooperatively. The choice of *p*-cresol as a standard substrate [see Section 2.2.4 (2)] is supported by the lack of substrate or product inhibition under these conditions.

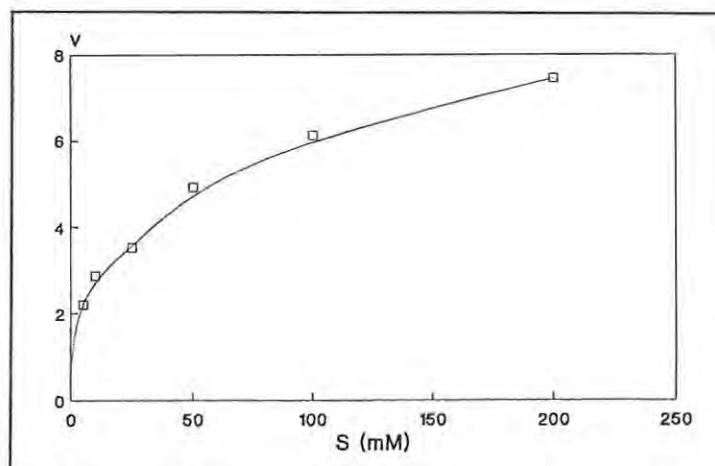


Figure 3.6: Graph of v vs s for the oxidation of *p*-cresol by polyphenol oxidase in chloroform; units of v : $M \cdot \text{min}^{-1} \cdot \text{mg}^{-1} \times 10^{-6}$

Using the data obtained from initial reaction rate measurements for the oxidation of the selected substrates by polyphenol oxidase, the apparent kinetic parameters, V , K_m , and the catalytic efficiency V/K_m , were calculated using Hanes plots (Table 3.5 and Figure 3.7). The results obtained for the activity of crude polyphenol oxidase utilising *p*-cresol as substrate were similar in magnitude to those reported for the partially purified enzyme, *viz.*, $K_m = 1.22$ mM and $V/K_m = 36.8$ (Estrada *et al.*, 1991). The results obtained for *t*-butylphenol, although less precise, are included for the sake of completeness, and can be regarded as reasonable in view of their consistency with the observed trends. The large error margins for this substrate are attributable to the very slow rates of conversion measured, and to some turbidity produced in the reaction mixtures as the product was formed.

Table 3.5: Apparent kinetic parameters measured for the formation of *o*-quinones from a range of *p*-substituted phenols, by polyphenol oxidase in chloroform

<i>p</i> -substituent	V^a $\times 10^2$	K_m (mM)	V/K_m^b
Me	8.12 \pm 0.5	24.81	3.27
Et	4.52 \pm 0.2	38.64	1.17
<i>i</i> -Pr	0.94 \pm 0.02	12.47	0.75
<i>t</i> -Bu	4.4 \pm 1.0	83.29	0.53
OMe	5.1 \pm 0.09	21.76	2.34
F	1.16 \pm 0.02	3.56	3.26
Cl	0.68 \pm 0.01	5.95	1.43
Br	0.99 \pm 0.01	52.3	0.19

^a Units of V are M per min per mg protein

^b Units of V/K_m are (min.mg protein)⁻¹

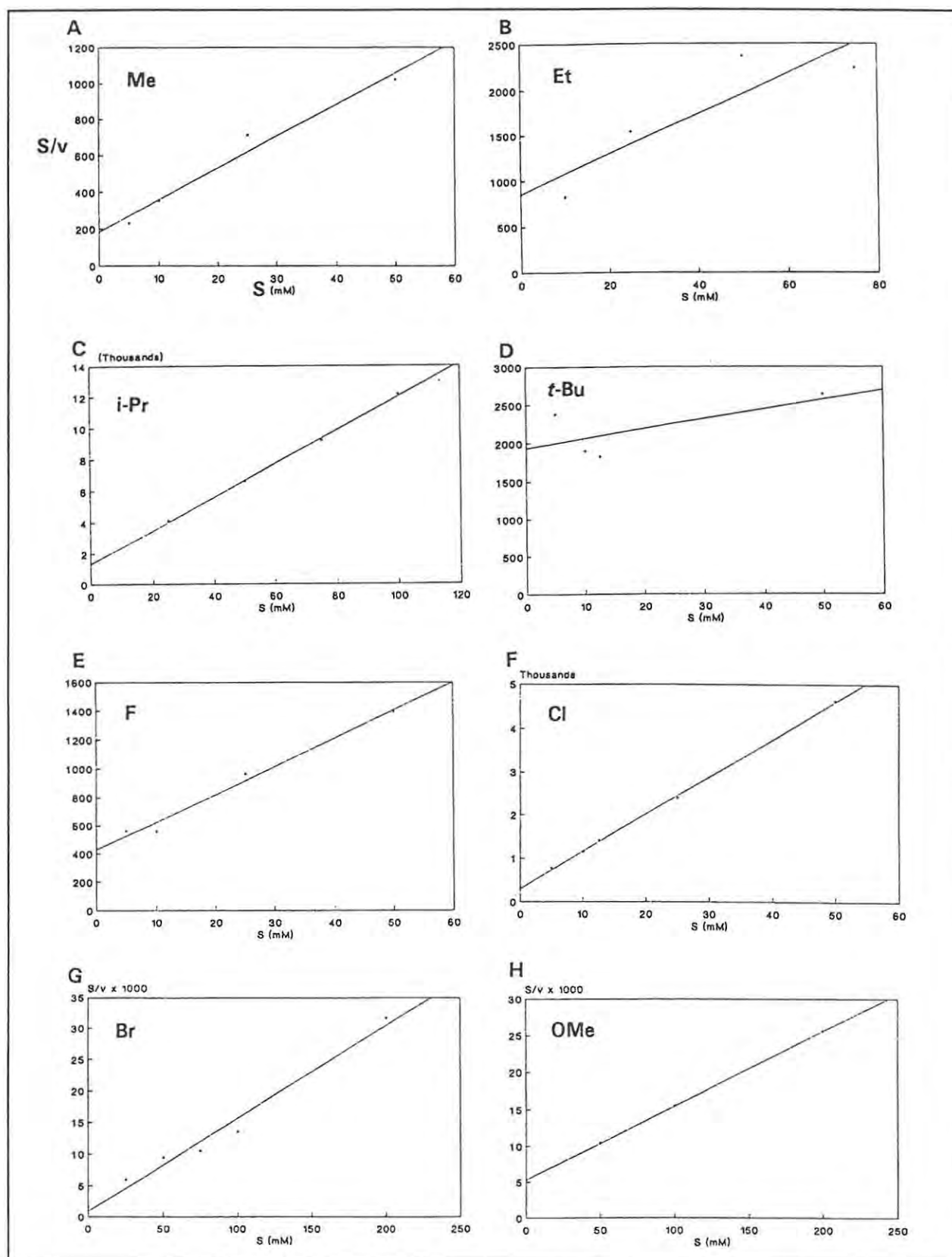


Figure 3.7: Hanes plots obtained from kinetic measurements using polyphenol oxidase to oxidise selected p -substituted phenols; p -substituents shown on respective graphs

3.2.4 Correlation of the calculated kinetic parameters with the properties of the substrates

Initially, the values calculated for V/K_m were compared directly with the steric volume of the p -substituent groups on the substrates (see Figure 3.8), represented by the Taft parameter, E_s which is determined from a scale of steric effects based on relative reaction rates (Gallo, 1983; March, 1985). If the substrates are considered in two groups, *viz.*, the p -alkylphenols (Group 1), and the p -halophenols and p -methoxyphenol (Group 2), a correlation is observed in that as the steric bulk of the p -substituent increases in each group, the value of V/K_m decreases (Figure 3.8A). No clear correlation was observed in the comparison of K_m with E_s (Figure 3.8B).

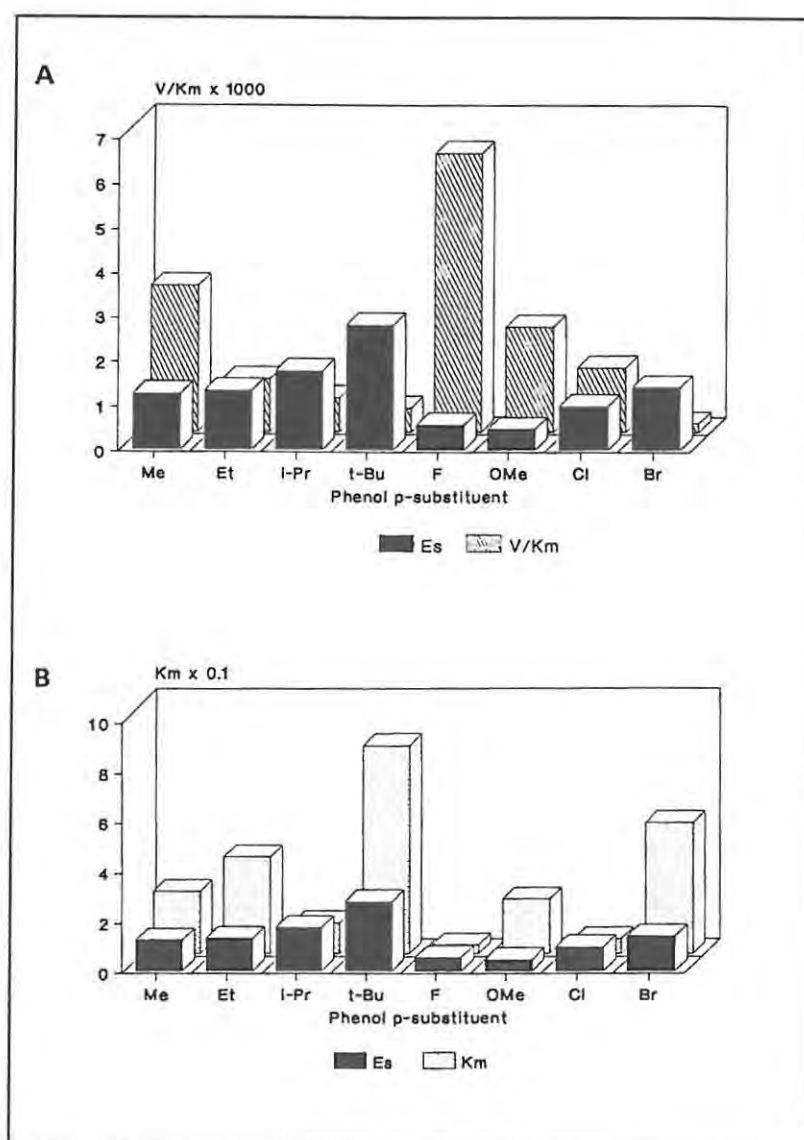


Figure 3.8: Correlation of catalytic efficiency (A) and Michaelis constant (B) of the polyphenol oxidase biocatalyst with the steric nature of p -substituted phenols; units: K_m (mM), V/K_m ($\text{min} \cdot \text{mg}^{-1}$), E_s relative to Hydrogen = 0.

Applying the equation proposed by Ryu and Dordick (1992) (see Section 3.1.3), the kinetic parameters obtained for polyphenol oxidase were correlated with the steric character of the substrates using the Taft parameter, with electronic character using the Hammett parameter (March, 1985), and for the *p*-alkylphenols, the Hansch parameter (Ryu and Dordick, 1992) (see Figure 3.9 and Table 3.6).

Table 3.6: Correlation of kinetic parameters with steric, hydrophobic, and electronic properties of the substrates

<i>p</i> -Substituent	V/K_m^a	E_s^b	σ^b	π^b
Me	3.27	-1.24	-0.17	0.56
Et	1.17	-1.31	-0.15	1.0
<i>i</i> -Pr	0.75	-1.75	-0.13	1.55
<i>t</i> -Bu	0.53	-2.78	-0.20	1.98
OMe	2.34	-0.55	-0.27	-0.02
F	3.26	-0.46	0.15	0.14
Cl	1.43	-0.97	0.23	0.71
Br	0.19	-1.30	0.26	0.86

^a Units: min.mg⁻¹

^b (March, 1985; Ryu and Dordick, 1992; Hansch and Leo, 1979); relative to the standard, H ($E_s, \sigma = 0$)

The correlation of E_s with $\log V/K_m$ for the alkylphenols (Figure 3.9A) does not show a linear relationship, which suggests that the relationship is a more complex one. There is a clear linear relationship between the hydrophobic nature of the alkylphenols and $\log V/K_m$ (shown in Figure 3.9B) which indicates that the catalytic efficiency decreases as the hydrophobicity of the substrate increases. The relationship between the electronic nature of the alkylphenols and the catalytic activity shows a linear trend for the methyl, ethyl and isopropyl substituents (Figure 3.9D), but *tert*-butylphenol does not fit this trend (Figure 3.9C).

For the group 2, the correlation of $\log V/K_m$ with steric volume (E_s) is approximately linear (Figure 3.9E), which confirms the importance of this parameter in evaluating the activity of polyphenol oxidase in chloroform. The relationship between the log of catalytic efficiency and the electronic nature is not completely linear, from the graph (Figure 3.9F), but there does appear to be a general trend in which the catalytic efficiency increases with decreasing σ values. Similarly, the trend for

the hydrophobicity of the group 2 phenols is not linear with respect to the log of the catalytic activity, but there is a general trend indicating a decrease in catalytic activity with increasing hydrophobicity (Figure 3.9G). These trends could be determined more precisely by extending the range of phenolic substrate, at a later stage.

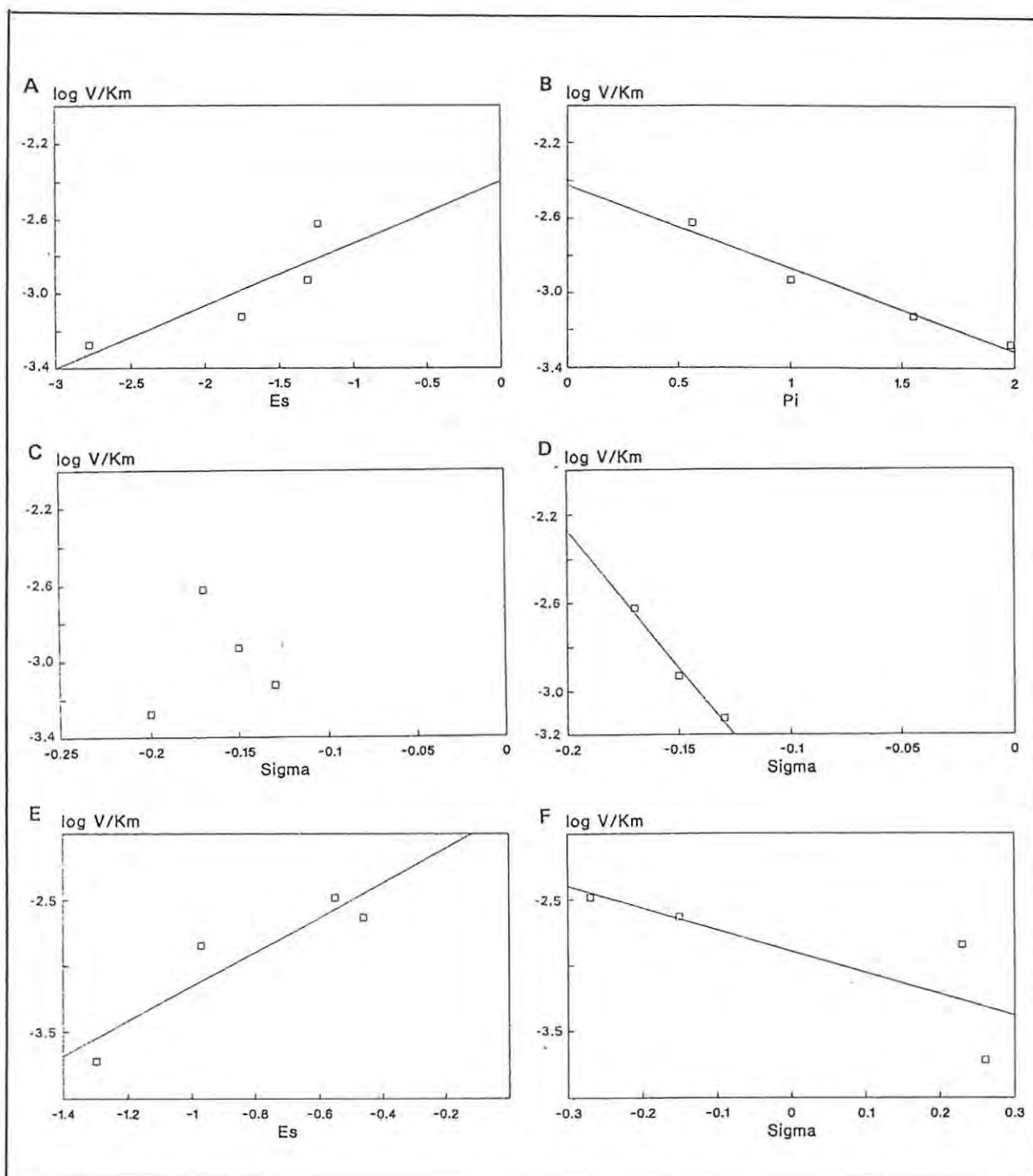


Figure 3.9: Correlation of catalytic efficiencies for the oxidation of phenolic substrates, catalysed by polyphenol oxidase; substrates: *p*-alkylphenols (A, C, D), *p*-halophenols and *p*-methoxyphenol (B, E, F)

3.2.5 Limitations on the size of substrates which can be oxidised by polyphenol oxidase in chloroform

Since the steric volume of the substrates seems to have a marked effect on the catalytic efficiency of polyphenol oxidase activity in chloroform, and this can be related to the reduced flexibility in the active site, the substrates were modelled using the molecular mechanics method discussed in Chapter 6. The objective of this exercise was to establish the maximum dimensions of the active site binding pocket in the enzyme as it exists in the biocatalyst in chloroform, using the "box model" approach (Luytens, *et al.*, 1989). *p*-Butylphenol was found to be the most bulky substrate for which the reaction rate could be measured, and the dimensions of this substrate could be considered to represent the size of the enzyme binding pocket, in that more sterically bulky molecules would be unable to fit into the pocket. Thus, the *p*-substituted phenols which were used in the kinetic study were modelled and their molecular dimensions were measured from the minimised structures of the models (see Table 3.7). These data show that while the length and width of the phenols do not vary significantly, the thickness does, and it can be speculated that substrates with a "thickness" greater than that of *t*-butylphenol would be too bulky to fit into the restricted binding site of polyphenol oxidase when it is in chloroform. Thus a "box" model of the enzyme binding site would have a maximum depth of approximately 6.6 Å (see Figure 3.10).

Table 3.7: Dimensions of substrates from molecular modelling

<i>p</i> -substituent	Length (Å)	Width (Å)	Thickness (Å)
Me	8.82	6.51	2.00
Et	10.16	6.50	3.98
<i>i</i> -Pr	10.16	6.50	5.26
<i>t</i> -Bu	10.15	6.59	6.58
OMe	10.25	6.52	4.05
F	8.34	6.52	1.85
Cl	8.63	6.52	1.99
Br	9.11	6.52	2.28

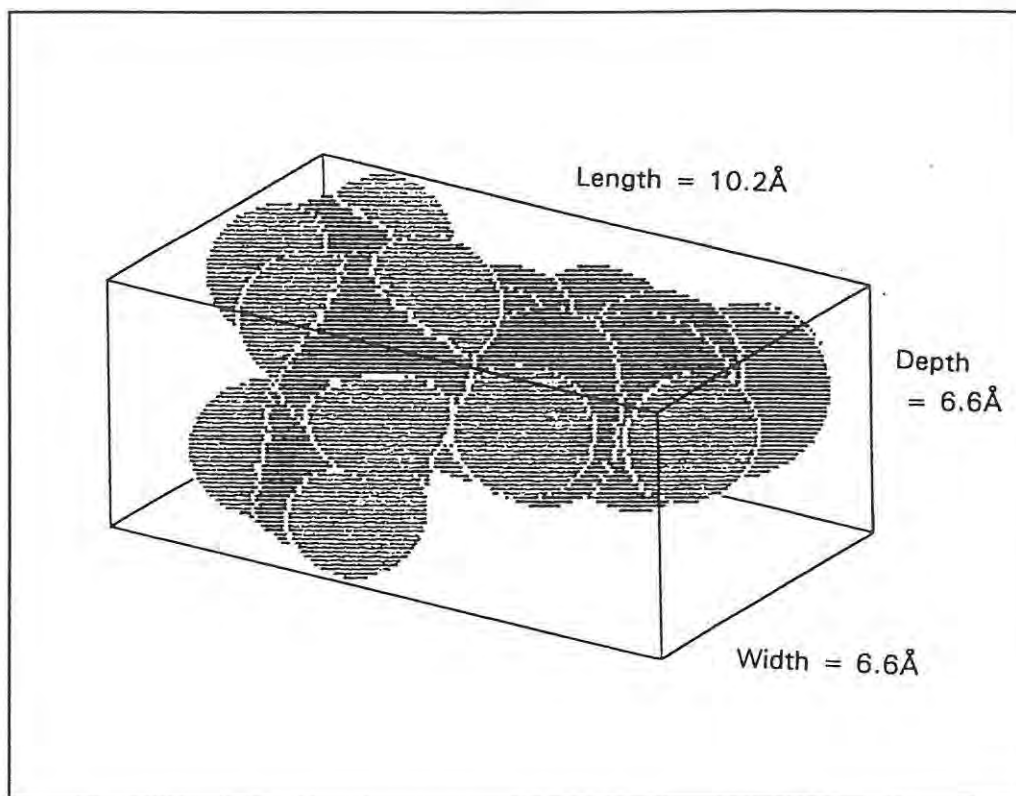


Figure 3.10: Proposed "Box" model of the binding pocket in polyphenol oxidase in chloroform, with *t*-butylphenol molecule "fitted" into available space

3.3 CONCLUSIONS

The crude, immobilised polyphenol oxidase was shown to catalyse the conversion of a range of selected *p*-substituted phenols to their respective *o*-quinones, using an electrophoretic method. The activity in chloroform was successfully quantified using measurement of initial reaction rates. The results of this kinetic study demonstrate that the method used, albeit a simple one, provides consistent data within acceptable error margins.

The kinetic parameters determined for different substrates correlate to some extent with steric and hydrophobicity parameters. Thus it is possible to predict, to some extent, the ability of the biocatalyst to catalyse the conversion of phenolic substrates in chloroform, by considering the molecular dimensions of the substrate and its hydrophobicity. The trends observed are consistent with, and confirm, current general theories on the effects of organic solvents in limiting the conformational flexibility of proteins.

The relationship between substrate utilisation by the biocatalyst and the electronic nature of the *p*-substituent of the phenol is less clear. The mechanism of the enzyme-catalysed reaction has not been fully elucidated, and it is a matter for conjecture as to whether electron-donation facilitates the reaction. If the reaction does take place by nucleophilic attack of the phenolic aromatic ring on the polarised peroxide bridge in the enzyme, as has been proposed (see Section 1.2.6), the electron donation may be important, and further investigations would be useful in establishing this.

In the course of the kinetic study, a novel NMR spectroscopic method was devised, utilising the activity of polyphenol oxidase in chloroform, to determine molar absorption coefficients for *o*-quinones without the necessity for isolation of these very reactive products.

3.4 EXPERIMENTAL

All experiments described in this chapter were carried out using extract **A** as the source of tyrosinase. Unless otherwise stated, the buffer used in these investigations was potassium phosphate buffer (50 mM, pH 7).

UV-visible spectra were recorded using a Shimadzu UV-160A UV-Visible recording spectrophotometer. NMR spectra were obtained using a Bruker 400 MHz AMX NMR spectrometer.

3.4.1 Screening of substrates using PAGE

Crude polyphenol oxidase extract **A** (prepared as described in Section 2.4.1), was dissolved in water and loaded on non-denaturing gels (150 and 300 μg in each of 2 wells, in duplicate on each gel) and run as described in Section 2.4.6. When the band containing melanins reached the bottom of the gel, the electrophoresis was stopped, and the gels were cut to separate the duplicate pairs of wells. One half of the gel was stained for protein using Coomassie Brilliant Blue stain, and the other was stained by soaking for 1 h in a solution of one of the substrates listed in Table 3.8. Where possible, the solutions were made up by dissolving the substrate (100 mg) in potassium phosphate buffer (50 mM; pH 7; 100 mL). In cases where the compound was not soluble in the buffer, acetonitrile was used to dissolve the compound, and buffer was added in proportions as shown in the Table 3.8. The results are summarised in Table 3.8 and are illustrated in Figure 3.3, Section 3.2.1.

3.4.2 Determination of wavelengths of maximum absorbance for *o*-quinones

Biocatalyst prepared from extract **A** (100 mg, containing 2.6 mg protein) was added to a solution of the respective substrates (25 mM, 5 mL, listed in Table 3.3, Section 3.2.2). Phosphate buffer (25 μL) was added and the mixture was shaken on a bench shaker for 3 h. The solution of reaction mixture was decanted, and its UV spectrum was measured, using suitable dilutions with chloroform where necessary. The wavelength of maximum absorbance was recorded (see Table 3.3). The UV spectra of the substrates were also recorded, and none were found to have significant absorbance at the wavelengths determined for the *o*-quinones.

Table 3.8: Results of PAGE screening of substrates

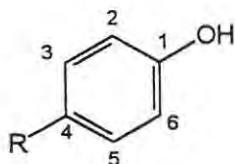
Substrate used for staining	Solvent for stain	Mobility ^a			
Coomassie blue	-	0.26	0.41	0.60	0.75
<i>L</i> -DOPA	buffer		0.41		0.75
<i>L</i> -tyrosine	buffer		0.40		
<i>p</i> -cresol	buffer		0.41		
<i>p</i> -ethylphenol	buffer		0.40		
<i>p</i> -isopropylphenol	buffer: MeCN 4:1		0.40		
<i>p</i> - <i>t</i> -butylphenol	buffer: MeCN 3:2		0.40		
<i>p</i> -methoxyphenol	buffer: MeCN 3:2		0.40		
<i>p</i> -fluorophenol	buffer: MeCN 4:1		0.40		
<i>p</i> -chlorophenol	buffer: MeCN 3:2		0.40		
<i>p</i> -bromophenol	buffer: MeCN 3:2		0.40		
<i>p</i> -cyanophenol	buffer: MeCN 3:2		-		
<i>p</i> -nitrophenol	buffer: MeCN 3:2		-		
<i>p</i> -hydroxy-benzaldehyde	buffer: MeCN 3:2		0.41		
<i>m</i> -cresol	buffer		0.41		
<i>o</i> -cresol	buffer		0.41		0.75
1-naphthol	buffer: MeCN 3:2		-		
2-naphthol	buffer: MeCN 3:2		-		
<i>o</i> -methoxyphenol (guaiacol)	buffer: MeCN 3:2		0.40		
2,4-di- <i>t</i> -butylphenol (DTBP)	buffer: MeCN 2:3		-		

^a Calculated as a fraction of the distance moved in the resolving gel by melanins during the electrophoresis; these melanins moved with the "front" as indicated by the movement of bromothymol blue which was loaded in a separate well.

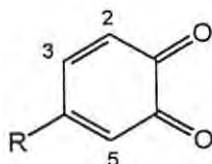
3.4.3 Determination of molar absorption coefficients

Biocatalyst (50 - 200 mg) was added to a solution containing a weighed amount (5 - 20 mg) of the respective substrate in a measured volume (1 - 3 mL) of CDCl_3 . D_2O (20 - 40 μL) was added, and the mixture was shaken continuously for 3 - 6 h in a closed flask. The absorbance of the chloroform solution was measured before and after the reaction, using appropriate dilutions where necessary. The solution was decanted into an NMR tube and the 400MHz ^1H NMR spectrum of the undiluted solution was recorded. The integrals were measured for signals corresponding to substrate and product protons, and the concentration of the product *o*-quinone was calculated as shown below. The results are summarised in Table 3.9. For each substrate, reactions were carried out in duplicate, and two sets of integrals were measured on each spectrum. The mean values of the molar absorption coefficients are shown in Table 3.4, Section 3.2.3. The NMR data from the spectra is summarised in Table 3.10.

Calculation:



Substrate A



Product B

a = integral height for substrate A aromatic protons (4H, H-2, H-3, H-5, H-6)

b = integral height for product B aromatic protons (2H, H-2 and H-3)

c = initial number of moles of substrate

$$c = [\text{A}] + [\text{B}] \text{ after reaction}$$

$$[\text{A}] / [\text{B}] = c \times b / (\frac{1}{2}a + b)$$

The molar absorption coefficient was calculated using Beer's Law.

Table 3.9: Results of NMR determination of molar absorption coefficients

R ^a	Conc ^b (mM)	Integral ^c (substrate)	Integral ^c (product)	Abs ^d	Conc quinone (mM)	ϵ (M ⁻¹ cm ⁻¹)
Me	16.05	Ar (2H) 18.5 Me (3H) 28.2	Ar (1H) 3.2 Me (3H) 9.3	5.544	4.213 3.970	1490.1 1396.5
Me	53.3	Ar (2H) 40.4 Me (3H) 61.5	Ar (1H) 6.5 Me (3H) 22.0	20.94	12.98 14.05	1612.6 1490.1
Et	17.05	Ar (2H) 26.3 CH ₂ (2H) 14.5	Ar (1H) 13.8 CH ₂ (2H) 15.5	10.44	8.731 8.809	1195.5 1184.8
i-Pr	16.7	Ar (2H) 35.6 CH ₂ (2H) 54.0	Ar (1H) 7.0 CH ₂ (2H) 20.0	7.266	4.734 4.532	1535.0 1603.0
<i>t</i> -Bu	10.7	Ar (2H) 38.8	Ar (1H) 1.3	1.029	0.675	1524.5
<i>t</i> -Bu	11.5	Ar (2H) 31.0 CH ₂ (2H) 69.2	Ar (1H) 1.8 CH ₂ (2H) 7.6	2.016	0.119 0.114	1689.3 1776.1
OMe	12.9	Ar (4H) 55.0 OMe (3H) 43.0	Ar (1H) 5.0 OMe (3H) 15.4	6.51	3.440 3.402	1892.4 1913.7
OMe	26.13	Ar (4H) 34.75 OMe (3H) 29.5	Ar (1H) 5.8 OMe (3H) 19.2	17.24	9.84 10.30	1751.6 1673.5
F	20.3	Ar (2H) 40.5	Ar (1H) 5.1	12.83	4.096	3132.3
F	28.2	Ar (2H) 41.2	Ar (1H) 4.1	15.50	4.68	3318.9
F	13.99	Ar (2H) 28.5	Ar (1H) 1.0	3.44	0.917	3739.8
Cl	29.6	Ar (2H) 40.2	Ar (1H) 3.5	17.91	4.39	4079.9
Cl	28.6	Ar (2H) 37.8	Ar (1H) 7.5	28.62	8.13	3520.4
Br	9.48	Ar (2H) 22.2	Ar (1H) 5.6	10.50	3.28	3201.7
Br	13.18	Ar (2H) 28.8	Ar (1H) 3.9	11.24	2.81	4067.1

^a Phenol *p*-substituent^b Initial concentration of phenolic substrate^c Relative heights measured from NMR spectrum^d Absorbance before dilution

Table 3.10: 400 MHz ¹H NMR data for phenolic substrates and *o*-quinone products

Phenol <i>p</i> -substituent	Phenol NMR spectrum	<i>o</i> -quinone spectrum
Me	2.26 (3H,s,Me), 6.70 (2H,d,Ar H) 6.95 (2H,d,Ar H)	2.12 (3H,s,Me) 6.25 (1H,s,Ar H) 6.35 (1H,d,Ar H) 6.71 (1H,d,Ar H)
Et	1.13 (3H,m,Me) 2.53 (2H,m,CH ₂) 6.73 (2H,m,Ar H) 7.06 (2H,m,Ar H)	1.13 (3H,m,Me) 2.40 (2H,m,CH ₂) 6.23 (1H,s,Ar H) 6.35 (1H,d,Ar H) 6.88 (1H,d,Ar H)
<i>i</i> -Pr	1.24 (6H,m,Me) 2.83 (1H,m,CH) 6.74 (2H,d,Ar H) 6.98 (2H,d,Ar H)	1.26 (6H,m,Me) 2.61 (1H,m,CH) 6.22 (1H,s,Ar H) 6.41 (1H,d,Ar H) 6.92 (1H,m,Ar H)
<i>t</i> -Bu	1.28 (9H,s,Me) 6.76 (2H,d,Ar H) 7.23 (2H,d,Ar H)	1.23 (9H,s,Me) 6.27 (1H,s,Ar H) 6.38 (1H,d,Ar H) 7.17 (1H,d,Ar H)
F	6.76 (2H,m,Ar H) 6.81 (2H,m,Ar H)	6.72 (1H,m,Ar H) 6.98 (1H,m,Ar H) 7.06 (1H,m,Ar H)
Cl	6.75 (2H,m,Ar H) 7.15 (2H,m,Ar H)	6.26 (1H,m,Ar H) 7.15 (1H,m,Ar H) 7.28 (1H,m,Ar H)
Br	6.75 (2H,d,Ar H) 7.30 (2H,d,Ar H)	6.27 (1H,s,Ar H) 7.13 (1H,d,Ar H) 7.43 (1H,d,Ar H)
OMe	3.78 (3H,s,OMe) 6.76 (4H,m,Ar H)	3.85 (3H,s,OMe) 5.78 (1H,s,Ar H) 6.44 (1H,d,Ar H) 6.78 (1H,d,Ar H)

3.4.4 Measurement of reaction rates for biocatalysis

The organic assay system devised for measurement of reaction rates in chloroform (described in Section 2.4.11) was used to measure the rates of oxidation of each substrate, at the concentrations shown in Table 3.11. Thus, the biocatalyst (a weighed sample containing 1.14 mg protein) was added to chloroform (9 mL) in a flask which was maintained at 25°C. Buffer (30 μ L) was added, and the solution was stirred for 1 min. The substrate (in 1 mL) was then added and timing was commenced. After each 2 min time interval, an aliquot was removed, its absorbance was measured at the wavelength of maximum absorbance for the respective quinone product, and it was then returned to the flask. Stirring was maintained at a constant speed throughout the reaction time.

The gradient of the absorbance-time graphs were determined using a linear regression analysis (QuattroPro) and this was used as the initial rate of reaction for the kinetics calculations. The mean of several results was obtained for each concentration of each substrate; standard errors (SEM) were found to be approximately 10%. The rate ($\Delta A \cdot \text{min}^{-1}$) was converted to rate v , the increase in the concentration of quinone, using the ϵ values determined as described in Section 3.4.2, and corrected for differences in dopachrome activity (see section 2.2.5). The units of v are $\text{mol} \cdot \text{dm}^{-3}$ per minute per milligram protein.

Table 3.11: Data from measurement of initial rates of oxidation of *p*-alkylphenols

Substrate	Conc, S (mM)	Rate ($\Delta A \cdot \text{min}^{-1}$) (SEM)	Mean rate ($\Delta A \cdot \text{min}^{-1}$) (SEM)	Rate, v ($\text{M} \cdot \text{min}^{-1} \cdot \text{mg}^{-1}$) $\times 10^5$
<i>p</i> -cresol	200	0.0709 0.004	0.0664 0.004	7.44
		0.0698 0.002		
		0.0640 0.002		
		0.0610 0.002		
	100	0.0553 0.002	0.0545 0.003	6.12
		0.0578 0.001		
		0.0503 0.003		
		0.0545 0.001		
	50	0.0441 0.001	0.0484 0.003	4.91
		0.0475 0.003		
		0.0507 0.005		
		0.0468 0.003		
	25	0.0342 0.003	0.0347 0.002	3.52
		0.0331 0.002		
		0.0354 0.0008		
		0.0335 0.004		
		0.0395 0.001		

Substrate	Conc, S (mM)	Rate (SEM) (ΔA min ⁻¹)	Mean rate (SEM) (ΔA min ⁻¹)	Rate, v (M.min ⁻¹ .mg ⁻¹) x 10 ⁵
	10	0.0295 0.003 0.0283 0.004 0.0264 0.002 0.0277 0.001	0.0282 0.002	2.86
	5	0.0181 0.002 0.0212 0.001 0.0255 0.002 0.0216 0.002	0.0216 0.003	2.19
Et	75	0.0251 0.001 0.0281 0.001 0.0262 0.002 0.0236 0.0002	0.0257 0.002	3.35
	50	0.0183 0.0009 0.0147 0.001 0.0172 0.001	0.0163 0.001	2.12
	25	0.0129 0.001 0.0132 0.001 0.0117 0.0009 0.0120 0.0004	0.0124 0.0006	1.62
	10	0.0101 0.0005 0.0095 0.0006 0.0092 0.0005 0.0087 0.0003	0.0094 0.0005	1.22
i-Pr	100	0.0089 0.0008 0.0064 0.0008 0.0012 0.001 0.0019 0.001	0.0087 0.0001	0.822
	75	0.0091 0.0005 0.0076 0.0001 0.0011 0.002 0.0075 0.0007	0.0086 0.0002	0.816
	50	0.0062 0.005 0.0102 0.001 0.0063 0.0006 0.0099 0.0007	0.0080 0.0007	0.755
	25	0.0063 0.001 0.0053 0.0006 0.0079 0.0006 0.0061 0.0003	0.0065 0.0005	0.609
t-Bu	25	0.0071 0.002 0.0106 0.002 0.0134 0.001	0.018 0.001	0.951
	12.5	0.0125 0.002 0.0150 0.001 0.0107 0.003 0.0136 0.002	0.0127 0.002	0.687

Substrate	Conc, S (mM)	Rate (ΔA min^{-1}) (SEM)	Mean rate (ΔA min^{-1}) (SEM)	Rate, v ($\text{M}\cdot\text{min}^{-1}\cdot\text{mg}^{-1}$) $\times 10^5$
	10	0.0099 0.002 0.0080 0.0007 0.0071 0.001 0.0083 0.001	0.0083 0.001	0.528
	5	0.0036 0.003 0.0055 0.001 0.0045 0.001 0.0029 0.001	0.0041 0.0005	0.211
OMe	50	0.0532 0.003 0.0470 0.004 0.0507 0.002 0.0580 0.003 0.0581 0.001	0.0538 0.004	3.95
	25	0.0395 0.002 0.0378 0.003 0.0388 0.003	0.0387 0.001	2.61
	10	0.0301 0.002 0.0259 0.001 0.0255 0.002	0.0272 0.002	1.80
	5	0.0113 0.002 0.0124 0.001 0.0139 0.001 0.0156 0.002	0.0133 0.001	0.896
F	50	0.0213 0.003 0.0198 0.003 0.0185 0.003	0.0205 0.0007	1.08
	25	0.0219 0.001 0.0208 0.002 0.0187 0.0006 0.0201 0.003 0.0182 0.002	0.0199 0.001	1.05
	12.5	0.0144 0.0008 0.0180 0.002 0.0179 0.002 0.0172 0.002	0.0169 0.002	0.891
	10	0.0153 0.002 0.0170 0.002 0.0153 0.001	0.0165 0.002	0.872
	5	0.0122 0.0004 0.0121 0.001 0.0141 0.0009 0.0123 0.001 0.0109 0.0006	0.0123 0.001	0.65

Substrate	Conc, S (mM)	Rate (ΔA /min) (SEM)	Mean rate (ΔA /min) (SEM)	Rate, v ($M \cdot \text{min}^{-1} \cdot \text{mg}^{-1}$) $\times 10^5$
Cl	200	0.0130 0.002	0.0123 0.001	0.632
		0.0107 0.001		
		0.0129 0.0009		
		0.0109 0.0006		
		0.0141 0.0006		
	100	0.0144 0.003	0.0145 0.0008	0.739
		0.0136 0.002		
		0.0158 0.001		
		0.0141 0.0008		
	75	0.0134 0.003	0.0140 0.0008	0.716
		0.0137 0.002		
		0.0145 0.002		
		0.0153 0.002		
		0.0130 0.002		
	50	0.0099 0.002	0.0104 0.00006	0.531
		0.0114 0.002		
		0.0103 0.0001		
		0.0103 0.0009		
	25	0.0071 0.0001	0.00835 0.0009	0.425
		0.0078 0.0008		
		0.0093 0.002		
		0.0093 0.0007		
Br	200	0.0163 0.003	0.0150 0.001	0.782
		0.0130 0.003		
		0.0141 0.002		
		0.0140 0.002		
		0.0166 0.001		
	100	0.0114 0.0008	0.0125 0.001	0.648
		0.0150 0.0008		
		0.0119 0.001		
		0.0117 0.002		
	50	0.0095 0.001	0.0093 0.001	0.482
		0.0087 0.0006		
		0.0052 0.001		
		0.0089 0.002		

Table 3.12: Results of kinetic analysis of rate measurements

R	Conc (mM)	v^a	S/v^b	K_m (mM)	V	V/K_m
Me	5	2.19	228.0	24.81	0.0812	3.27
	10	2.86	349.7			
	25	3.52	711.3			
	50	4.91	1018.5			
	100	6.10	1638.3			
	200	7.44	2686.7			
Et	10	1.22	819.7	38.64	0.0452	1.17
	25	1.62	1543.3			
	50	2.12	2358.5			
	75	3.85	2238.9			
i-Pr	25	0.609	4105.1	12.47	0.0094	0.75
	50	0.755	6622.5			
	75	0.816	9191.2			
	100	0.822	12165.5			
t-Bu	5	0.211	2369.7	83.29	0.044	0.53
	10	0.528	1893.9			
	12.5	0.687	1819.5			
	25	0.951	2628.8			
OMe	5	0.896	558.1	21.76	0.051	2.34
	10	1.80	555.6			
	25	2.60	961.8			
	50	3.59	1392.3			
F	5	0.650	769.4	3.56	0.0116	3.26
	10	0.872	1146.9			
	12.5	0.891	1403.9			
	25	1.05	2381.2			
	50	1.08	4629.6			
Cl	25	0.425	5882.3	5.95	0.0068	1.43
	50	0.531	9426.2			
	75	0.716	10480			
	100	0.739	13531			
	200	0.632	31645			
Br	50	0.487	10373	52.3	0.0099	0.19
	100	0.648	15432			
	200	0.787	25575			

^a Units of v : mol.dm⁻³.min⁻¹.mg⁻¹ (refers to mg protein)

^b Units of S/v : min⁻¹.min⁻¹

^c Units of V : mol.dm⁻³.min⁻¹.mg⁻¹

^d Units of V/K_m : min⁻¹.mg⁻¹

CHAPTER 4

MODIFICATIONS TO THE POLYPHENOL OXIDASE BIOCATALYTIC SYSTEM

4.1 INTRODUCTION

In the course of the research described in the previous chapters, some aspects of the polyphenol oxidase biocatalytic system were identified as areas where modifications might lead to improved enzyme activity and/or substrate specificity. The present chapter describes some alterations to the system which were investigated to determine their possible value in improving the functioning or the applications of the biocatalyst in chloroform.

4.1.1 Purification of polyphenol oxidase

The kinetic analysis described in the previous chapter was carried out using the crude mushroom extract A (see Section 2.2.1) to prepare the biocatalyst. This extract contained a large proportion of extraneous, inactive protein which could affect the functioning of polyphenol oxidase in the biocatalyst in several ways. Its presence might lead to physical occlusion of the enzyme on the immobilisation support and consequently to reduction of the enzyme activity in the biocatalyst. In addition, this protein might compete with the enzyme for available water, causing a decrease in the activity of the enzyme as a result of reduced conformational flexibility. The importance of conformational flexibility in the substrate selectivity of polyphenol oxidase in chloroform was demonstrated in the preceding chapter, where sterically bulky substrates were found to be converted at very slow rates. Any alteration to the flexibility of the binding site could be expected to lead to altered substrate specificity, and the presence of extraneous proteins may thus impose limitations on the range of substrates suitable for oxidation.

The extraneous protein may also compete with the enzyme for the buffer salts present in the freeze-dried extract, which act as protectants of the optimal ionic state of the enzyme. The salts promote enzyme activity by maintaining the local polarities in the binding site in a state equivalent to that pertaining in the enzyme when it is in an aqueous system of optimal pH (see Section 2.1.3). Decreased availability of these salts could result in lowered enzyme activity or stability.

Thus it would seem that purification of a crude enzyme which is to be utilised in a biocatalytic system would be advantageous. However, there is evidence that the presence of inactive protein acts as a protectant itself, in immobilised biocatalysts, by preventing denaturation during and after immobilisation. Reduced denaturation has been reported as a result of addition of a non-active protein such as gelatin or casein to the enzyme solution before immobilisation, in quantities sufficient to provide a monolayer covering of protein on the support (Wehtje *et al.*, 1992). A possible explanation for this stabilisation is that proteins can act as buffers themselves and thus, the non-active protein might replace the lyoprotectant buffer salts in preserving the ionic state of the active enzyme. This suggests that the presence of extraneous protein in the polyphenol oxidase biocatalyst may not necessarily be a disadvantage.

A kinetic study was conducted using the partially purified enzyme, extract **B**, with the objective of comparing the kinetic parameters obtained with those previously obtained using the crude extract **A**, and hence assessing the effect of the extraneous protein.

4.1.2 Removal of melanins from the polyphenol oxidase catalyst

The crude extract from fresh mushrooms (which were used as a source of polyphenol oxidase) contained endogenous substrates for the enzyme, and during the extraction process some of these substrates would be converted to melanins. The melanins were observed as a mobile band during electrophoresis (see Section 2.2.2), and as a dark brown colour in aqueous solutions of the extract. Melanins are known to accelerate the reaction rates of tyrosinase in some aqueous systems and to decrease the lag time for phenolic substrates (Menter *et al.*, 1990) and thus the presence of melanins in the biocatalyst may be an advantage. The activation of tyrosinase is attributed to the melanins acting as an "electron channel," accepting electrons from phenolic substrates and donating them to the enzyme. In contrast to this possible advantage is the fact that melanins are insoluble in chloroform and in water once they are polymerised. Their presence or formation in the chloroform-based polyphenol oxidase biocatalyst is, therefore, a potential cause of deactivation due to physical occlusion of the enzyme.

In the present study, polyphenolic compounds were removed from the crude extract using PVPP in the preparation of extract **C**, which contained far less melanoid material than the crude extract **A** (see Section 2.2.1). The investigation of the kinetic properties of this extract, and a comparison with those of extracts **A** and **B**, are described in this chapter.

4.1.3 Activation of polyphenol oxidase

A number of reports in the literature have described the activation of polyphenol oxidases from different sources, as a result of addition of various protein-modifying agents to aqueous solutions of the enzymes. The polyphenol oxidase of the broad bean, *Vicia faba*, is activated by the addition of detergents such as sodium dodecyl sulphate (SDS) and Aerosol-OT® (AOT) (Robb *et al.*, 1966), by denaturants (Swain *et al.*, 1966) and by the action of non-specific proteases (King and Flurkey, 1987). Activation of grape polyphenol oxidase was also reported as the result of addition of ionic detergents or proteases, but not by the non-ionic detergent Brij-96 (Sanchez-Ferrer and Garcia-Carmona, 1992b). Similarly, frog epidermis tyrosinase (Wittenberg and Triplett, 1985) and mushroom polyphenol oxidase (Yamaguchi *et al.*, 1970; Angleton and Flurkey, 1984) are activated by SDS in aqueous systems.

The reason for this activation has not been fully explained. It has been proposed to result from partial denaturation or from a limited change in conformation, and electrophoresis experiments have indicated that the activation is accompanied by a small decrease in the apparent mass of the protein, from 48 kd to 47 kd in the case of the broad bean enzyme (Moore and Flurkey, 1990). The interaction of SDS with mushroom polyphenol oxidase does not cause changes in the isoenzyme pattern on electrophoresis, indicating that no change in the mass of the protein occurs as a result of dissociation (Angleton and Flurkey, 1984). Mammalian tyrosinase was found to be activated by polyamines such as putrescine and 1,3-diaminopropane, but these amines did not affect the enzymes from frog epidermis or mushroom and this effect was attributed to alterations in the oligmeric nature of the mammalian enzyme (Galindo *et al.*, 1987).

The question arises as to whether similar activation is possible in non-aqueous systems, where the presence of water is limited to the structural water bound to the protein. Denaturation is essentially a water-dependent process, since it involves hydrolysis as one of the major reactions. In fact, many enzymes are more stable in organic systems because of the lack of free water to facilitate denaturation. Activation of some dehydrogenases by the denaturants urea and guanidine hydrochloride, in non-aqueous systems, was recently reported (Garza-Ramos *et al.*, 1992), and these authors attributed the effect to the release of constraints on the conformation of the proteins.

In view of the importance of local polarities and electrostatic interactions within the active site of enzymes in non-aqueous media (as discussed in Section 2.1.2), the addition to the system of a component which alters these properties is very likely to affect the protein conformation. The results obtained in the kinetic study described in Chapter 3 indicate that conformational flexibility

is a critical factor in the substrate selectivity of the polyphenol oxidase biocatalyst. Thus, it is possible that an ionic detergent such as SDS could increase the flexibility of this enzyme by interacting electrostatically with polar groups in the binding site. If the result was an increase in protein flexibility, the accessibility of the binding site for sterically hindered substrates might be increased. Not only would such an effect be advantageous in the application of the polyphenol oxidase biocatalyst in chloroform, but observation of this effect would also serve to confirm modern theories on the importance of electrostatic interactions in non-aqueous biocatalysis. Thus, the effect of addition of SDS on the kinetic parameters of the polyphenol oxidase system was investigated.

4.2 RESULTS AND DISCUSSION

4.2.1 The effects of partial purification on the kinetics of the biocatalyst

The rates of oxidation of three phenolic substrates were measured at varying concentrations, using the biocatalyst prepared by immobilisation of the partially purified polyphenol oxidase extract **B** (see Section 2.2.1). The data (see Section 4.4.1) were treated in the same manner as described in the kinetic analysis in the previous chapter, and the Hanes plots obtained are shown in Figure 4.1. The kinetic parameters determined using the extract **B** are compared with those obtained using the crude extract **A** in Table 4.1 and in Figure 4.2.

Table 4.1: Kinetic parameters determined for the oxidation of selected *p*-substituted phenols by biocatalysts prepared from extracts **A** and **B**

Extract	Substrate <i>p</i> -substituent	K_m (mM)	V (mM.min ⁻¹ .mg ⁻¹)	V/K_m (min ⁻¹ .mg ⁻¹)
A	Me	24.81	81.2	3.27
B	Me	6.5	13.0	2.00
A	F	3.56	11.6	3.26
B	F	3.3	20.0	6.06
A	i-Pr	12.47	9.4	0.75
B	i-Pr	623	16.0	0.025

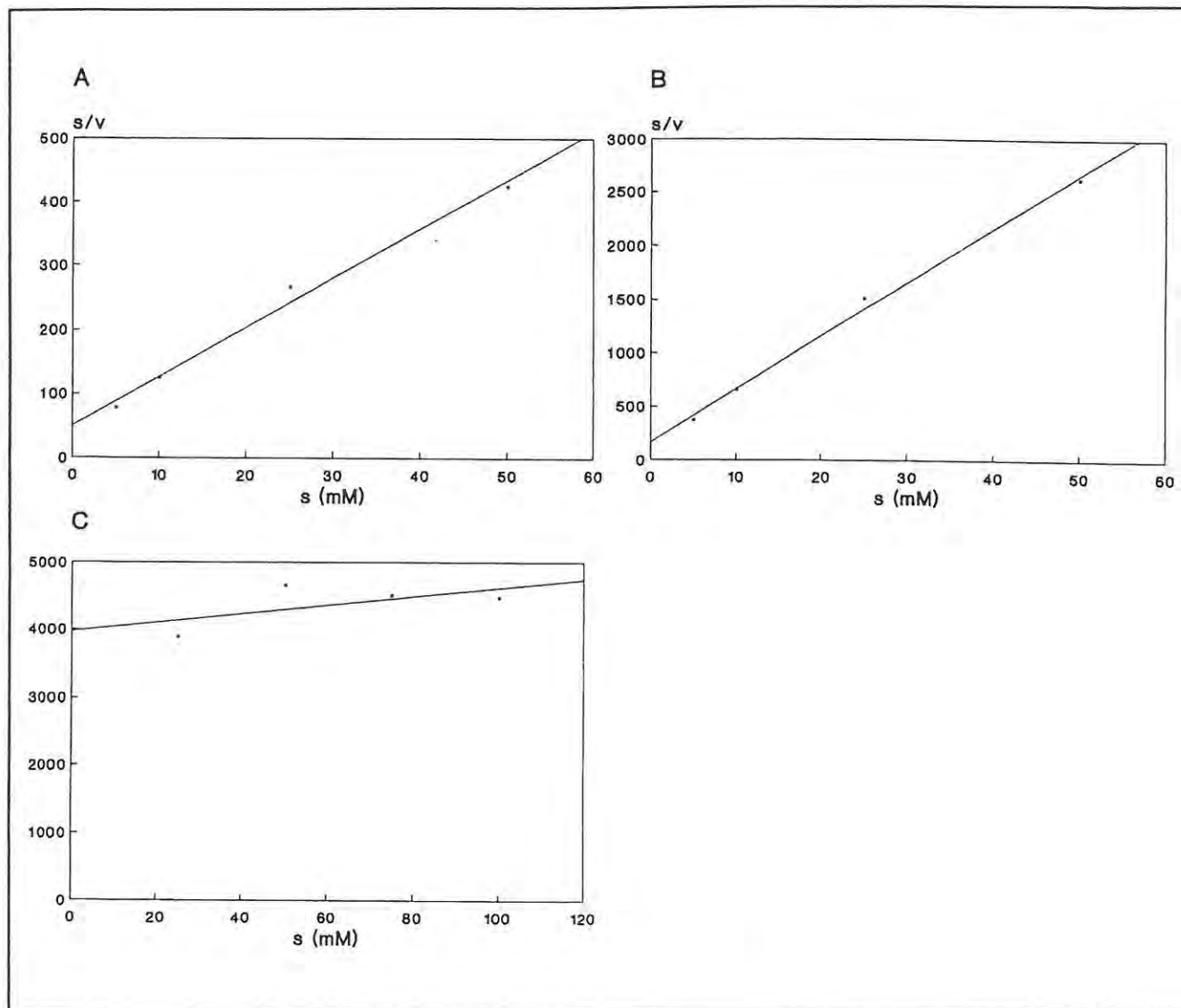


Figure 4.1: Hanes plots for the oxidation of selected p -substituted phenols, catalysed by the biocatalyst prepared from partially purified polyphenol oxidase extract B (units of s/v are min.mg); substrates: (A) p -cresol (B) p -fluorophenol (C) p -isopropylphenol

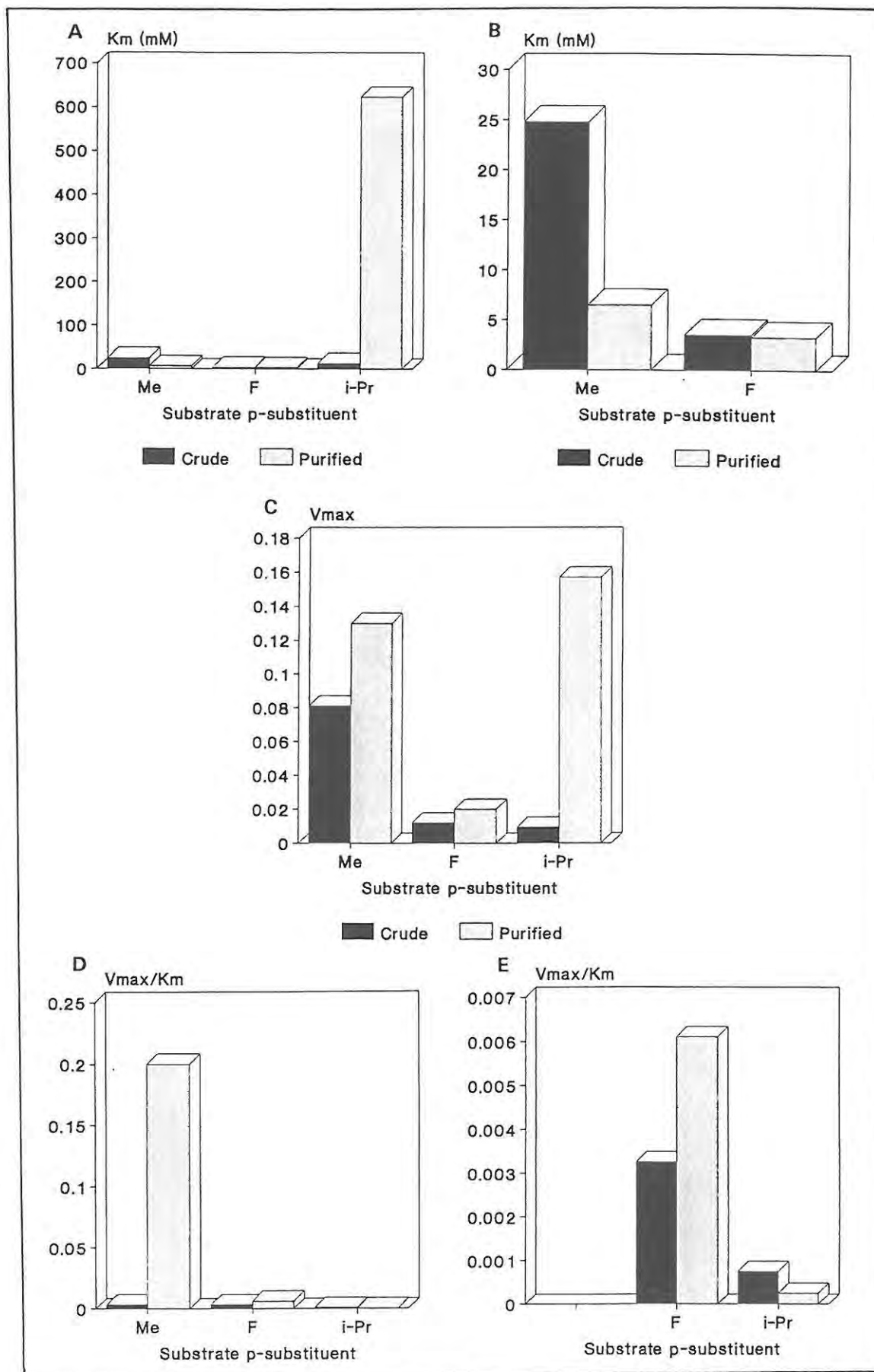


Figure 4.2: Comparisons of the kinetic parameters determined for selected *p*-substituted phenols, catalysed by polyphenol oxidase biocatalyst prepared from extract B

The K_m values obtained using the purified polyphenol oxidase were found to be lower than those obtained using the crude enzyme in the cases of *p*-cresol and *p*-fluorophenol, but much higher in the case of *p*-isopropylphenol. This indicates stronger binding of the less sterically hindered phenols, which may be attributable to the purified polyphenol oxidase being less occluded by extraneous protein. Both of the former substrates were found to be good substrates for polyphenol oxidase in chloroform when compared with a wider range of substrates examined using the crude enzyme (Section 3.2.3), and thus it might be expected that any effect which makes the enzyme more available to these substrates would result in more efficient binding. However, weaker binding of the sterically hindered *p*-isopropylphenol is indicated by the very much higher K_m value obtained using the purified enzyme as opposed to the crude enzyme, and this may be due to the purified enzyme being less accessible to this substrate.

In all three cases, the V values were lower for the purified enzyme, the difference being most marked for the *p*-isopropylphenol. The catalytic efficiencies were greater for the purified enzyme in the cases of *p*-cresol and *p*-fluorophenol, but decreased for *p*-isopropylphenol.

The overall conclusion can be drawn that the absence of extraneous protein in the partially purified polyphenol oxidase biocatalyst leads to greater catalytic efficiency for less sterically hindered substrates, but the flexibility of the protein is possibly reduced so that more sterically bulky substrates are not so readily able to enter the binding pocket. This would be the case if the extraneous proteins in the crude extract were acting to mask polar groups which would interact in their absence. In the purified enzyme, the polar groups might bind together to hold the pocket in a restricted conformation.

An alternative explanation is that the hydrophobicity of the polyphenol oxidase binding site may be decreased by the absence of the extraneous proteins, so that the binding site in the purified enzyme is less hydrophobic than it was in the crude extract. Low catalytic efficiency for a particular substrate was found to correlate with high hydrophobicity in the kinetic study on crude polyphenol oxidase (see Section 3.2.4), and since *p*-isopropylphenol is more hydrophobic than *p*-cresol and *p*-fluorophenol, its ability to interact with the active site of the purified may be lower. In addition to these possibilities, the lack of buffering action by the extraneous proteins may be more significant in the purified protein where lower concentrations of buffer salts were present. In the biocatalyst prepared from the crude extract, greater amounts of the extract (in terms of mass of freeze-dried powder) were required to be immobilised to give sufficient activity for the measurements, and these would have contained more buffer salts. However, the smaller amounts of protein used to prepare biocatalyst from extract B would require less buffering and therefore, this difference between the biocatalysts is likely to have a minor effect.

4.2.2 The effects of removing endogenous melanins from the biocatalytic system

The rates of oxidation of the same three *p*-substituted phenols as examined in the previous section were measured using biocatalyst prepared from the extract C, from which melanins had been removed (see Section 4.4.2). The kinetic parameters determined using this biocatalyst were found to be altered by the absence of melanins, as indicated in Table 4.2 and Figure 4.3 and 4.4.

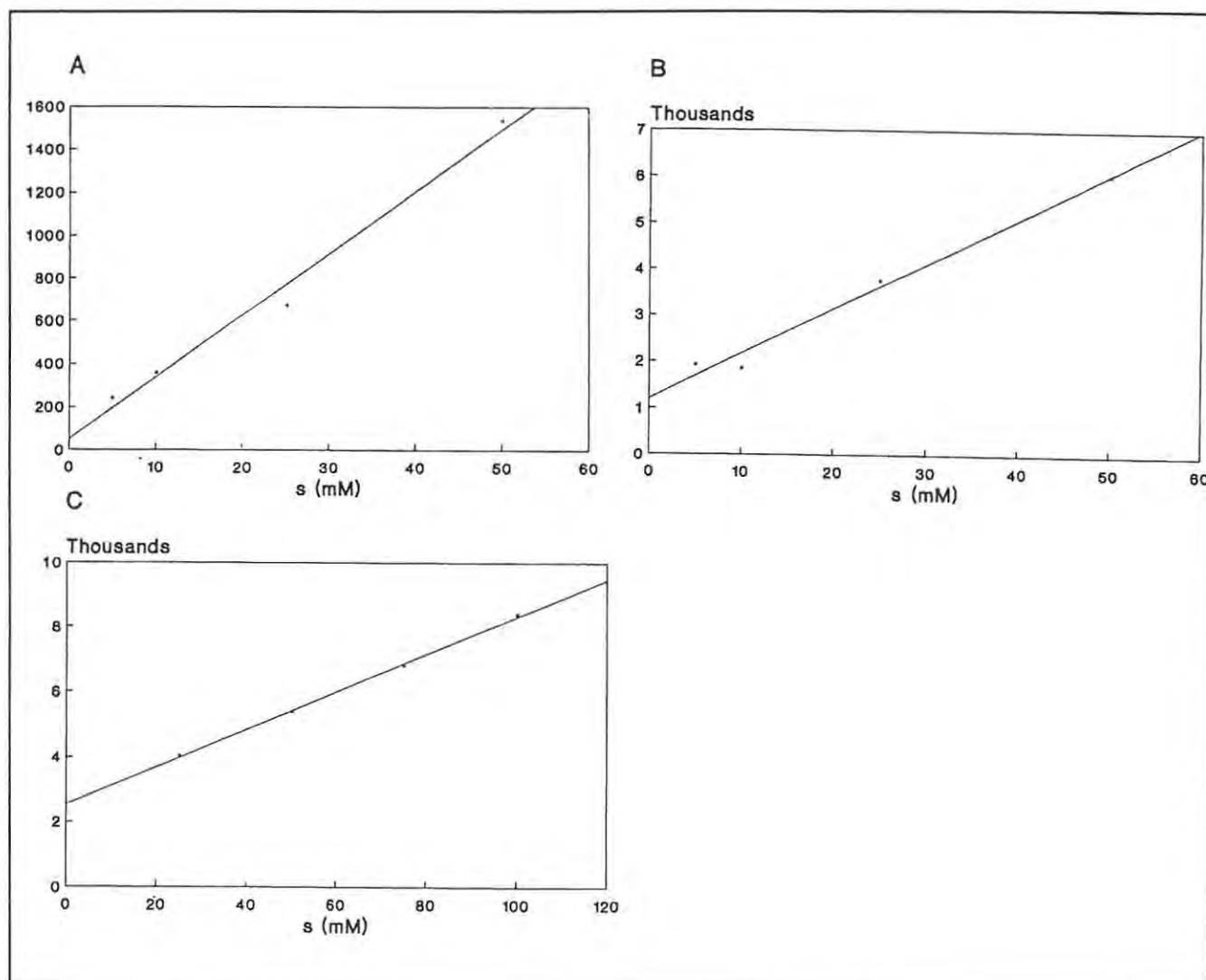


Figure 4.3: Hanes plot for the oxidation of selected *p*-substituted phenols, catalysed by the biocatalyst prepared from extract C; substrates: (A) *p*-cresol (B) *p*-fluorophenol (C) *p*-isopropylphenol

Table 4.2: Comparison of kinetic parameters determined for the oxidation of selected *p*-substituted phenols, using biocatalyst prepared from extracts A and C

Extract	Substrate <i>p</i> -substituent	K_m (mM)	V (mM.min ⁻¹ .mg ⁻¹) ^a	V/K_m (min ⁻¹ .mg ⁻¹)
A	Me	24.81	8.12	3.27
C	Me	1.81	3.5	19.3
A	F	3.56	11.6	3.26
C	F	12.4	10.3	0.83
A	i-Pr	12.47	9.4	0.75
C	i-Pr	43.7	17.3	0.395

The effects of removing melanins from the polyphenol oxidase extracts were found to include a reduction in K_m in the case of *p*-cresol indicating stronger binding to the polyphenol oxidase in extract C than in the crude enzyme. As in the case of extract B, the effect could be attributed to less occlusion of the active protein by impurities (in this case the melanins) and hence greater accessibility for this substrate to the binding site. The reduced concentration of melanins resulted in significantly higher K_m values for *p*-fluorophenol and *p*-isopropylphenol, indicating weaker binding of these substrates than in the crude enzyme.

The catalytic efficiency was significantly increased in the case of *p*-cresol. There was a decrease in catalytic efficiency for *p*-fluorophenol and *p*-isopropylphenol which might be attributable to the absence of enzyme activation by the melanins. This activation could be more important in the case of less favourable substrates, where activity is relatively low, and the activation is proportionately more effective.

The higher hydrophobicity of *p*-isopropylphenol than that of the other two substrates could again be an important factor, because the removal of melanins (which are themselves quite hydrophobic) would reduce the hydrophobic nature of the binding site. This may cause the binding and reaction of *p*-isopropylphenol to be less favoured in the absence of the melanins than in their presence.

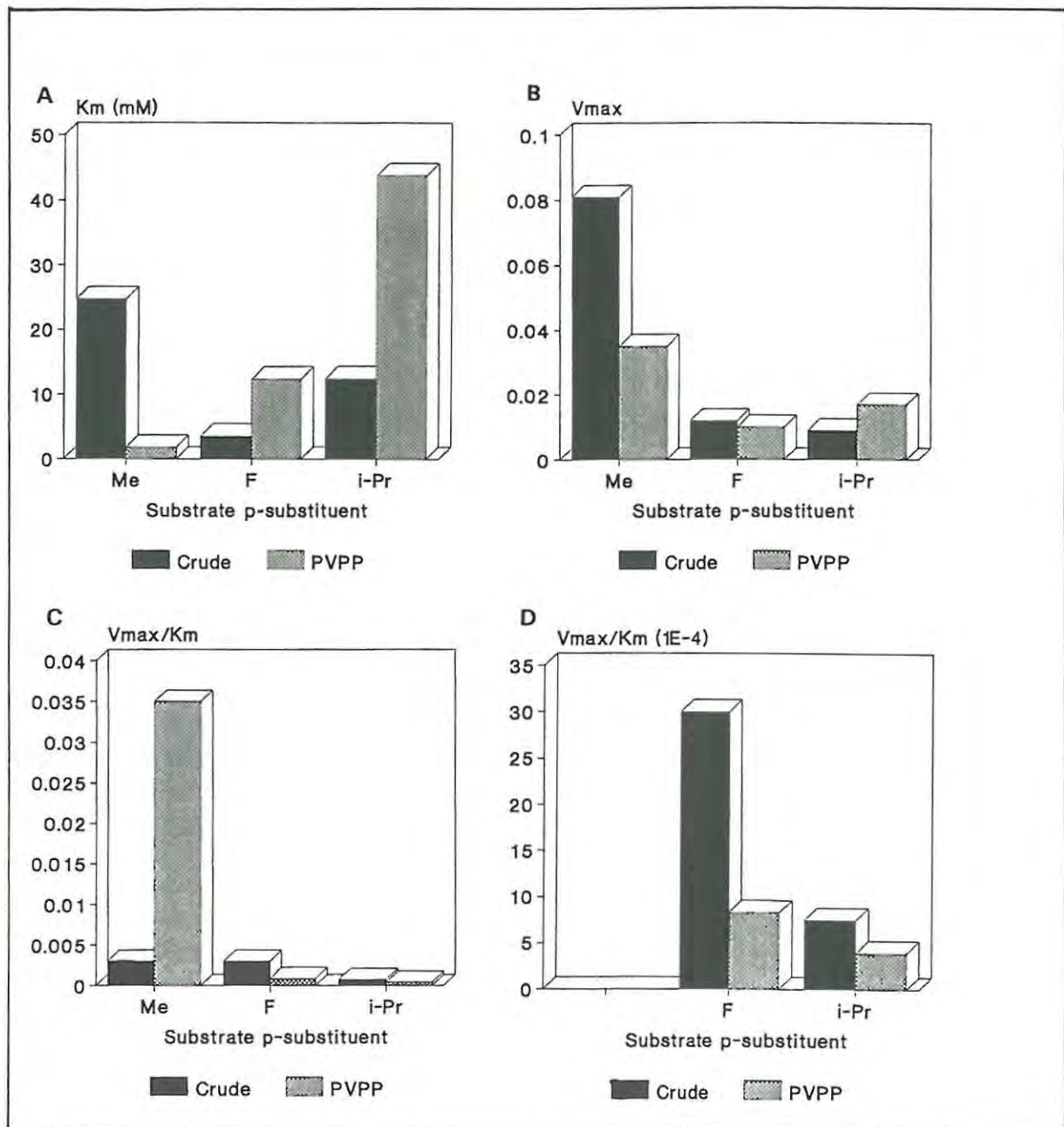


Figure 4.4: Comparison of the kinetic parameters for the oxidation of selected *p*-substituted phenols, catalysed by biocatalysts prepared from the extracts A (Crude) and C (PVPP)

4.2.3 Determination of the effects of varying concentrations of SDS on the rate of oxidation of *p*-cresol

It was observed that addition of a small amount of SDS to the buffer used to hydrate the biocatalyst caused an increase in the rates of oxidation of *p*-cresol and ATEE in preliminary experiments measuring the rates of formation of their respective *o*-quinones using the standardised organic assay method (Section 4.4.3). In the oxidation of *p*-cresol an 18% increase was observed, and for ATEE the increase was approximately 55%. In order to investigate this effect, the optimal concentration of SDS was first determined, and a kinetic study in the presence of SDS was carried out.

Since it was observed that SDS was not soluble in the phosphate buffer that had been utilised for hydration of the protein in other kinetic investigations, water was used to make SDS solutions. The rates of oxidation of phenolic substrates were not expected to be greatly affected by this change, since there were already buffer salts present in the freeze-dried enzyme extracts before immobilisation. This was investigated (Section 4.4.4) and it was found that the rates of oxidation of *p*-cresol were very slightly decreased when water was used. Since the reduction in rate was small (3%) in comparison with the increase caused by the addition of SDS, and it would represent a constant factor in the investigation, it was assumed to be insignificant.

The standardised organic assay (Section 2.2.5) was used to determine the concentration of SDS which would produce the greatest increase in rates of reaction (Section 4.4.5). The concentrations used were kept below the critical micellar concentration of SDS [8.2 mM (Sanchez-Ferrer and Garcia-Carmona, 1992b)] in order to avoid any phase separation effects. The concentration at which the most marked increase in activity (30%) was observed was 2 mM (Table 4.3) and consequently, this concentration of SDS was used in the kinetic study described in the next section.

Table 4.3: Rates of oxidation of *p*-cresol catalysed by the polyphenol oxidase biocatalyst in the presence of varying concentrations of SDS

Concentration SDS (mM)	Rate ($\Delta A \cdot \text{min}^{-1}$)
0.0	0.026 ± 0.001
0.5	0.030 ± 0.006
1.0	0.036 ± 0.006
2.0	0.039 ± 0.003
3.0	0.033 ± 0.006
5.0	0.033 ± 0.006
6.0	0.033 ± 0.004

4.2.4 The effects of addition of SDS on the kinetics of the biocatalytic system

A small range of *p*-substituted phenols, particularly those with sterically bulky side chains, were selected for the investigation of the effects of addition of SDS, since it was expected that rates of oxidation would be most affected for these substrates.

The kinetic data were obtained using the biocatalyst prepared from extract **A** and the same method as in other kinetic investigations, but adding the same volume of 2 mM SDS solution as was determined to be the optimal volume of buffer (see Section 4.4.6). The Hanes plots obtained from the data are shown in Figure 4.5 and the kinetic parameters are compared with those obtained in the absence of SDS, in Table 4.4 and Figure 4.6.

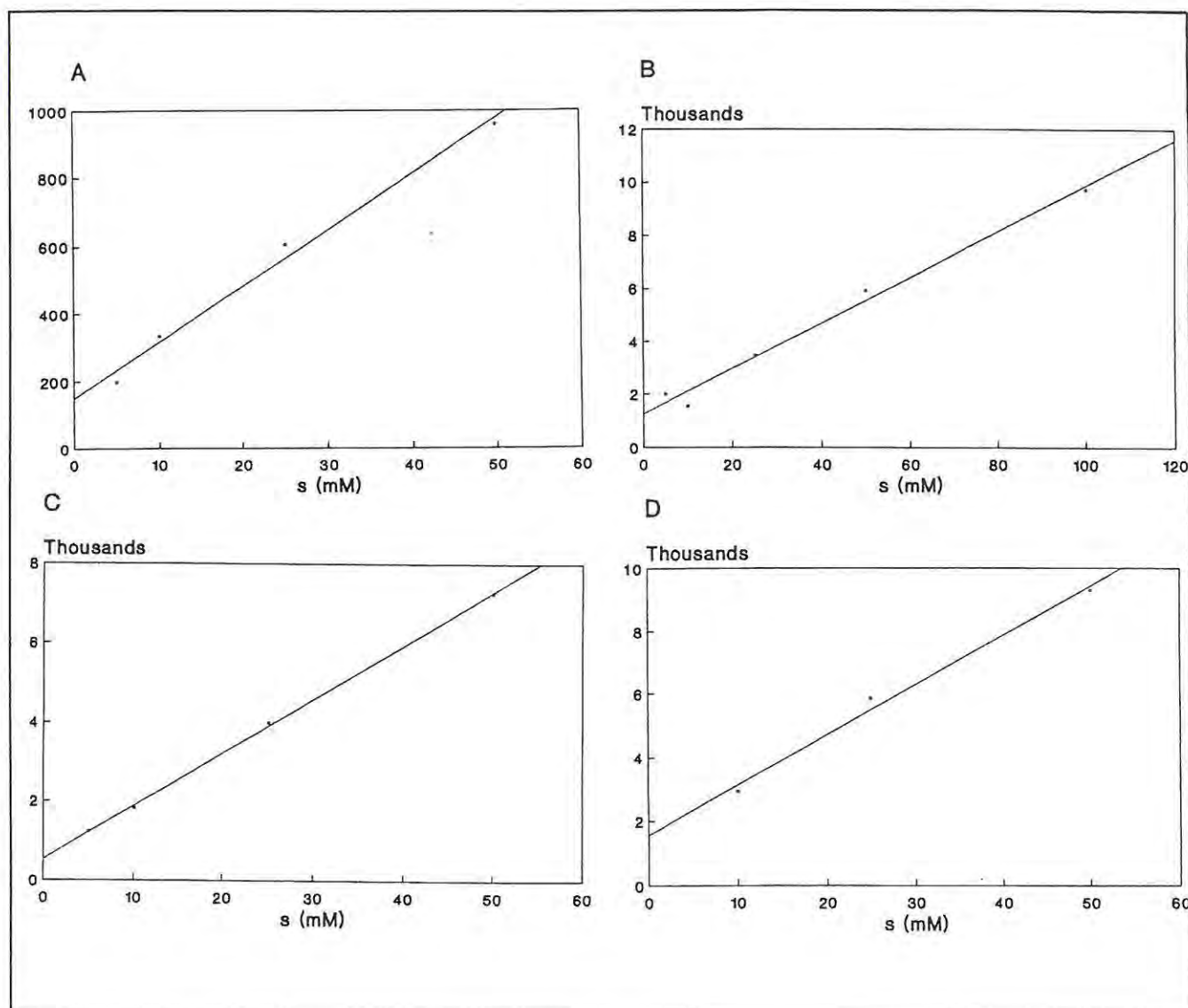


Figure 4.5: Hanes plots for the oxidation of selected *p*-substituted phenols, catalysed by the polyphenol oxidase biocatalyst prepared from extract A, in the presence of 2 mM SDS; substrates: (A) *p*-cresol (B) *p*-isopropylphenol (C) *p*-*tert*-butylphenol (D) 2,4-di-*tert*-butylphenol (DTBP)

Table 4.4: Comparison of kinetic parameters determined for the oxidation of selected *p*-substituted phenols by the polyphenol oxidase biocatalyst in the presence and absence of 2 mM SDS

SDS (mM)	Substrate <i>p</i> -substituent	K_m (mM)	V (mM.min ⁻¹ .mg ⁻¹)	V/K_m (min ⁻¹ .mg ⁻¹)
0	Me	24.81	81.2	3.27
2	Me	9.1	60	6.68
0	<i>i</i> -Pr	12.47	9.4	0.75
2	<i>i</i> -Pr	14.3	22	1.51
0	<i>t</i> -Bu	83.3	4.4	0.53
2	<i>t</i> -Bu	3.87	14.6	3.75
0	2,4-di- <i>t</i> -Bu	-	-	-
2	2,4-di- <i>t</i> -Bu	9.9	0.0063	0.64

Lower K_m values were observed for the reactions with *p*-cresol and *p*-*tert*-butylphenol, indicating that the presence of SDS leads to stronger binding of the substrates. (The small increase in the K_m for *p*-isopropylphenol may not be significant in view of a large error observed in this particular result). The increased strength of binding can be attributed to the ionic nature of SDS, since it may interact with, and bind to, polar groups in the active site, altering the local polarities in the binding pocket. The non-polar ends of the SDS molecules may also contribute increased hydrophobic nature to the binding site, enhancing the binding of non-polar, hydrophobic phenols such as *p*-*tert*-butylphenol.

Increased accessibility and enhanced binding would both contribute to the increased catalytic efficiencies observed for all of the substrates investigated. The results obtained using 2,4-di-*tert*-butylphenol (DTBP) are of particular significance. The rates of utilisation of this compound were not measurable in the biocatalytic system in which buffer was used to hydrate the protein, but in the presence of SDS, the rates were measurable and the kinetic parameters could be calculated for this substrate. It can be speculated that the SDS affects the protein conformation to the extent that it becomes sufficiently flexible to accommodate this bulky substrate. The increase in hydrophobicity proposed to occur in the presence of SDS would also enhance the binding of DTBP.

The effect of SDS, as discussed above, occurs in the presence of a very small proportion of the detergent relative to the protein. If it is assumed that the SDS interacts only with polyphenol oxidase molecules (and not other protein molecules, which would dilute the effect), the ratio of

SDS molecules to polyphenol oxidase molecules is approximately 8 to 1. (This was estimated by calculation of the number of moles of SDS and of polyphenol oxidase present in the system used to measure rates of reaction). Thus the quantity of SDS present was not enough to form a monolayer on the protein or even to line the binding pocket, which suggests that the SDS is not acting as a phase transfer agent but rather, that it has a localised effect on specific areas within the binding pocket.

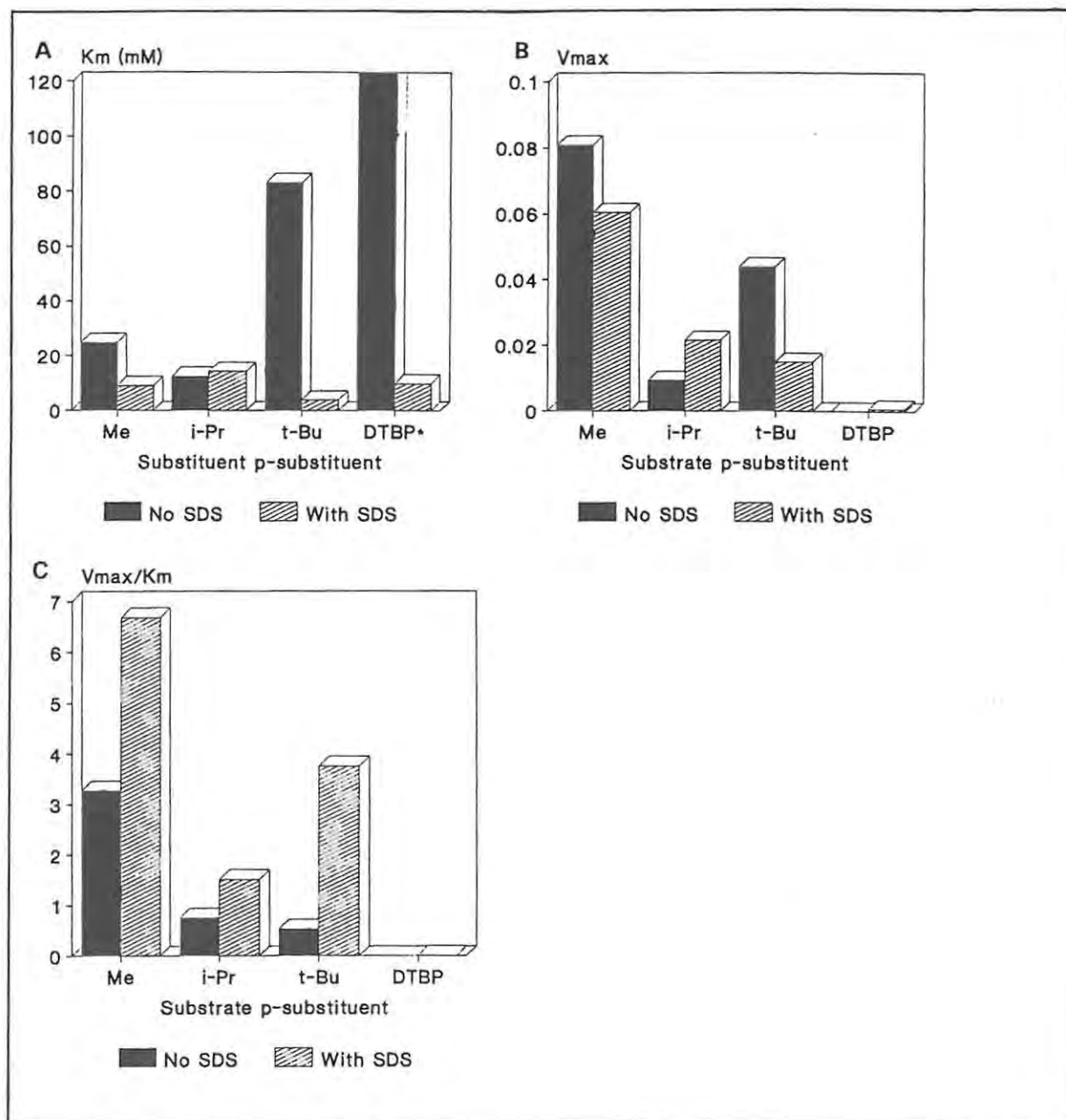


Figure 4.6: Comparison of kinetic parameters for the oxidation of selected *p*-substituted phenols, catalysed by the polyphenol oxidase biocatalyst prepared from extract A, in the presence of 2 mM SDS. * K_m for DTBP would be off scale

4.2.5 Longer-term effects of SDS on the biocatalyst

Since SDS is a denaturant of proteins, it is possible that in time it would cause a loss in polyphenol oxidase activity in the biocatalyst. However, many proteins are more stable with respect to denaturation when they are in non-aqueous environments (see Section 2.1.2). A preliminary investigation into the longer term effects of SDS on the biocatalyst was carried out by allowing the biocatalyst to stand for eighteen hours at room temperature, in chloroform, in the presence of SDS. The activity of the biocatalyst was then assayed using the dopachrome and *p*-cresol assays, and the results were compared with those obtained in control experiments where SDS was omitted for the eighteen hour period, but was added in equivalent concentrations at the time of the assays. Both sets of results were compared with the activities of fresh samples of biocatalyst to allow the detection of any denaturation of the protein in the absence of SDS. These results are summarised in Table 4.5.

Table 4.5: Comparison of the extent of denaturation occurring in the biocatalyst in the presence and absence of SDS

Assay method	Aqueous component	% decrease in activity
Dopachrome	SDS (1 mM)	36
	Buffer	31
	Water	61
<i>p</i> -Cresol in CHCl ₃	SDS (1 mM)	30
	Buffer	34
	Water	49

The results of this experiment, while only approximate, indicate that while some denaturation of all of the samples was observed (as might be expected for hydrated proteins standing at room temperature), the presence of SDS did not cause more loss in activity than was found in its absence. In fact, the use of water (as opposed to buffer) apparently lead to more deactivation than the addition of SDS.

4.3 CONCLUSIONS

The investigations described in this chapter have shown that the state of the enzyme in the biocatalyst has a significant effect on the rates of reaction which can be catalysed, and on the range of substrates which can successfully be utilised. Although the crude extract **A** was shown in the previous chapter to be useful as a source of polyphenol oxidase for application as a biocatalyst for the conversion of a range of phenols to their corresponding *o*-quinones, the range of substrates was limited to those with relatively unhindered structures.

Biocatalyst prepared using partially purified polyphenol oxidase, which contained less extraneous protein than the crude extract, was shown to be a more efficient catalyst for substrates which are readily converted. These substrates have relatively unhindered structures and relatively low hydrophobicity. A more sterically hindered, more hydrophobic substrate was shown to be less readily converted by the purified biocatalyst, and this effect could be attributed to decreased flexibility or decreased hydrophobicity in the enzyme binding site.

Similarly, increased catalytic efficiency was observed for the conversion of the favoured substrate *p*-cresol, by biocatalyst prepared with low melanin content. However, the catalytic efficiency was decreased for a more hydrophobic sterically hindered substrate, and for a more polar substrate. The removal of melanins could result in a loss of activation due to the ability of melanins to act as an electron channel, and possibly also in a change in the hydrophobicity of the binding site of the enzyme.

Significantly enhanced rates of reaction were observed when the protein was hydrated with a solution containing the anionic detergent SDS. In particular, the rates of conversion and the catalytic efficiencies were increased for phenolic substrates with sterically hindered structures, and the conversion of 2,4-di-*tert*-butylphenol (DTBP), which could not be detected in the absence of SDS, was observed at appreciable rates in the presence of SDS. These results indicate that SDS has a marked effect on the flexibility of the binding site, causing it to become more flexible and thus more accessible for bulky substrates. The ionic nature of SDS, and its ability to interact with polar or charged groups, may be the reason for its effect on the biocatalyst because if it screens polar groups in the binding site from each other, the conformation within the binding site may be made more flexible.

In addition to having an effect on protein conformational flexibility, SDS may play a role in altering the hydrophobicity of the binding site in such a way as to enhance the binding of more hydrophobic substrates. With the data available from the present study, these two effects of SDS cannot be

differentiated, and further investigations using a wider range of substrates and conditions would be useful in this regard.

The conclusions which can be drawn from the present study, as discussed above, confirm the current theories on the effects of organic media on biocatalysts, and add to the information presently available concerning the effects of protein modifications on such systems. In addition, these results provide some explanation for the activation of polyphenol oxidase by SDS, at the level of binding site interactions.

4.4 EXPERIMENTAL

In the results shown in this section, rates are given per mg protein (as opposed to per mg polyphenol oxidase). Thus, the units of the rate of formation of quinone product, v ($M, \text{min}^{-1} \cdot \text{mg}^{-1}$), are $\text{mol} \cdot \text{dm}^{-3}$ per minute per milligram protein.

$\Delta A \cdot \text{min}^{-1}$ = Change in absorbance per minute, measured at the wavelength of maximum absorption for the *o*-quinone product, as determined in Section 3.2.2. Rates were converted to units of concentration using the molar absorption coefficients determined as described in Section 3.2.2.

SEM = standard error in the mean

4.4.1 Measurement of kinetic parameters for biocatalyst prepared from the partially purified extract B

Rates of oxidation of *p*-substituted phenols (listed in Table 4.6) by biocatalyst prepared from extract B (see Section 2.2.1; 10mg beads containing 0.14 mg protein) were measured using the optimised organic assay method as described in Section 3.4.3. The results are listed in Table 4.6 below and the kinetic parameters calculated from them are shown in Table 4.7.

Table 4.6: Rates of oxidation of *p*-substituted phenols by polyphenol oxidase biocatalyst prepared from extract B

<i>p</i> -Substituent	Concentration (mM)	Rate		Rate, v (M.min ⁻¹ .mg ⁻¹) $\times 10^4$
		(ΔA .min ⁻¹)	SEM	
Me	50	0.02450	0.002	1.18 \pm 0.02
		0.01860	0.004	
		0.02586	0.0004	
		0.02705	0.0004	
	25	0.0165	0.002	0.94 \pm 0.13
		0.0240	0.003	
		0.0189	0.0009	
		0.0169	0.001	
		0.0195	0.003	
	10	0.0141	0.001	0.80 \pm 0.13
		0.0127	0.0005	
		0.0204	0.002	
		0.0173	0.003	
		0.0166	0.002	
	5	0.0122	0.0007	0.65 \pm 0.05
		0.0127	0.0005	
		0.0144	0.002	
F	50	0.0193	0.003	0.19 \pm 0.02
		0.0148	0.001	
		0.0179	0.0009	
		0.0190	0.001	
	25	0.0160	0.001	0.166 \pm 0.002
		0.0148	0.0006	
		0.0154	0.001	
	10	0.0111	0.001	0.15 \pm 0.02
		0.0152	0.0009	
		0.0153	0.0009	
		0.0151	0.0006	
	5	0.0136	0.0007	0.135 \pm 0.007
		0.0123	0.0005	
		0.0119	0.0008	
		0.0123	0.0005	
i-Pr	100	0.0117	0.002	0.22 \pm 0.03
		0.0132	0.0008	
		0.0098	0.0009	
	75	0.0060	0.0004	0.17 \pm 0.04
		0.0061	0.0002	
		0.0103	0.0009	
		0.0071	0.001	
	50	0.0032	0.0002	0.11 \pm 0.02
		0.0057	0.001	
		0.0042	0.0002	
		0.0037	0.0001	
	25	0.0041	0.0001	0.07 \pm 0.04
		0.0033	0.0006	
		0.0012	0.0003	
		0.0010	0.0002	

Table 4.7: Kinetic parameters for oxidation of *p*-substituted phenols, catalysed by biocatalyst prepared from extract B

<i>p</i> -Substituent	Conc, <i>s</i> (mM)	<i>s/v</i> (min.mg)	<i>V</i> (mM.min ⁻¹ .mg ⁻¹)	<i>K_m</i> (mM)	<i>V/K_m</i> (min ⁻¹ .mg ⁻¹)
Me	50	424.1	0.130 ± 0.009	6.50 ± 0.05	0.02
	25	266.0			
	10	124.4			
	5	77.5			
F	50	2618.4	0.020 ± 0.001	3.3 ± 0.2	6.10 × 10 ⁻³
	25	1506.0			
	10	653.6			
	5	370.4			
i-Pr	100	4464.1	0.16 ± 0.1	623.4 ± 51	2.54 × 10 ⁻⁴
	75	4491.2			
	50	4647.2			
	25	3882.3			

4.4.2 Measurement of kinetic parameters for oxidation of *p*-substituted phenols, catalysed by biocatalyst prepared from extract C

Rates of oxidation of *p*-substituted phenols (listed in Table 4.8 below) by biocatalyst prepared from extract C (see Section 2.4.3; 30 mg beads containing 1.1 mg protein) were measured using the same method as described for biocatalyst prepared extract B (above). The results are listed in Table 4.8 below and the kinetic parameters calculated from them are shown in Table 4.9.

Table 4.8: Rates of oxidation of *p*-substituted phenols by biocatalyst prepared from extract C

<i>p</i> -Substituent	Conc (mM)	Rate		Rate, v (M.min ⁻¹ .mg ⁻¹) $\times 10^5$
		(ΔA .min ⁻¹)	SEM	
Me	50	0.0408	0.003	3.25 \pm 0.54
		0.0529	0.002	
		0.0618	0.004	
	25	0.0043	0.005	3.73 \pm 0.07
		0.0666	0.004	
		0.0712	0.001	
		0.0576	0.002	
	10	0.0445	0.0006	2.52 \pm 0.02
		0.0452	0.001	
		0.0455	0.002	
	5	0.0337	0.002	2.09 \pm 0.16
		0.0360	0.002	
		0.0299	0.0006	
F	50	0.0375	0.005	0.83 \pm 0.14
		0.0310	0.001	
		0.0241	0.001	
		0.0274	0.001	
	25	0.0254	0.004	0.67 \pm 0.06
		0.0251	0.002	
		0.0254	0.002	
		0.0206	0.0008	
	10	0.0181	0.001	0.54 \pm 0.03
		0.0201	0.001	
		0.0201	0.001	
	5	0.0067	0.0003	0.26 \pm 0.07
		0.0132	0.001	
		0.0073	0.0003	
		0.0109	0.0009	
i-Pr	100	0.0135	0.002	1.19 \pm 0.24
		0.0208	0.0006	
		0.0245	0.0007	
		0.0225	0.002	
	75	0.0133	0.0006	1.11 \pm 0.25
		0.0205	0.0005	
		0.0251	0.001	
		0.0177	0.001	
	50	0.0113	0.002	0.93 \pm 0.19
		0.0201	0.002	
		0.0175	0.0009	
		0.0148	0.002	
	25	0.0160	0.001	0.62 \pm 0.09
		0.0101	0.0008	
		0.0132	0.0003	
		0.0132	0.001	

Table 4.9: Kinetic parameters calculated for the biocatalyst prepared from extract C

ρ -Substituent	Conc, s (mM)	s/v (min.mg)	V (mM.min ⁻¹ .mg ⁻¹) $\times 10^2$	K_m (mM)	V/K_m (min ⁻¹ .mg ⁻¹)
Me	50	1536.1	3.5 ± 0.3	1.81 ± 0.05	0.019
	25	669.7			
	10	355.2			
	5	239.7			
F	50	6036.5	1.03 ± 0.08	12.4 ± 0.3	8.30×10^{-3}
	25	3760.5			
	10	1851.9			
	5	1906.2			
i-Pr	100	8382.3	1.73 ± 0.05	43.7 ± 1.6	3.95×10^{-4}
	75	6787.3			
	50	5376.3			
	25	4033.6			

4.4.3 Preliminary experiment to show increased rates of reaction in the presence of SDS

Biocatalyst prepared from extract A (35mg, containing 1,1 mg protein) was added to chloroform (9 mL). An aqueous solution of SDS (1 mM; 25 μ L) was added, and the mixture was stirred for 2 min. In separate experiments, solutions of the substrates (a) p -cresol and (b) ATEE (1 mL; 250 mM) were added and the absorbance of the chloroform solutions were measured at (a) 395 nm and (b) 475 nm respectively. The rates were compared with those measured in control experiments in which water was substituted for the SDS solution. The results are shown in Table 4.10 below.

Table 4.10: Results of preliminary experiment to show the increase in reaction rates for the biocatalyst in the presence of SDS

Aqueous component	Substrate	Rate ($\Delta A \cdot \text{min}^{-1}$) SEM		Mean rate ($\Delta A \cdot \text{min}^{-1}$)
SDS (1 mM)	p -cresol	0.0314	0.0006	0.0308 ± 0.001
		0.0319	0.0009	
		0.0291	0.0003	
Water	p -cresol	0.0261	0.0005	0.0253 ± 0.0007
		0.0245	0.0006	
		0.0260	0.001	
SDS (1 mM)	ATEE	0.0139	0.0002	0.0133 ± 0.0004
		0.0128	0.002	
		0.0132	0.0007	
Water	ATEE	0.0063	0.0004	0.0057 ± 0.0005
		0.0058	0.0002	
		0.0051	0.0003	

4.4.4 Comparison of rates of oxidation of *p*-cresol catalysed by polyphenol oxidase biocatalyst hydrated with buffer or water

The standardised assay of polyphenol oxidase in chloroform (see Section 2.4.11) was used to measure the rates of oxidation of *p*-cresol (25 mM) by biocatalyst prepared from extract A (35 mg, containing 1.1 mg protein), but the system was hydrated with (a) buffer and (b) water, to measure the difference in the rates. The results are shown in Table 4.11 below.

Table 4.11: Comparison of rates of oxidation of *p*-cresol, catalysed by biocatalyst hydrated by buffer and water

Aqueous component	Rate ($\Delta A \cdot \text{min}^{-1}$)	SEM	Mean rate ($\Delta A \cdot \text{min}^{-1}$)	SEM
Buffer	0.0259	0.001	0.0267	0.001
	0.0274	0.0003		
	0.0251	0.002		
	0.0263	0.002		
Water	0.0263	0.0004	0.0259	0.001
	0.0259	0.0004		
	0.0252	0.002		
	0.0260	0.0009		

4.4.5 Measurement of rates of oxidation of *p*-cresol by the polyphenol oxidase biocatalyst in the presence of varying concentrations of SDS

The rates of oxidation of *p*-cresol by the biocatalyst prepared from extract A (35 mg containing 1.1 mg protein) were measured by the method for the standard assay in chloroform (see Section 2.4.11) but the buffer was replaced by an aqueous solution of SDS (25 μL ; concentrations as listed in Table 4.12 below).

Table 4.12: Rates of oxidation of *p*-cresol, catalysed by polyphenol oxidase biocatalyst in the presence of varying concentrations of SDS

Conc SDS (mM)	Rate ($\Delta A \cdot \text{min}^{-1}$)	Mean rate ($\Delta A \cdot \text{min}^{-1}$)*
0.5	0.0271 0.0274 0.0395 0.0389 0.0257 0.0259 0.0256	0.030 \pm 0.006
1.0	0.0356 0.0384 0.0397 0.0335 0.03135 0.02795 0.0257 0.0428	0.036 \pm 0.006
2.0	0.03675 0.0374 0.03755 0.0458 0.0405 0.0374	0.039 \pm 0.003
3.0	0.0377 0.0237 0.0245 0.0355	0.033 \pm 0.006
5.0	0.02215 0.0267 0.0360 0.03395 0.0386	0.033 \pm 0.006
6.0	0.0299 0.0343 0.0334 0.0298 0.2455 0.0330 0.0385	0.033 \pm 0.004

* Corrected for variations in dopachrome activity

4.4.6 Measurement of rates of oxidation of *p*-substituted phenols, catalysed by polyphenol oxidase biocatalyst in the presence of 2 mM SDS

The rates of oxidation of the *p*-substituted phenols (listed in Table 4.12 below) by the biocatalyst prepared from extract A (35 mg containing 1.1 mg protein) were measured by the same method as was used in the kinetic studies described previously (see Section 4.4.1), but substituting SDS solution (25 μ L; 2 mM) for the buffer that was used before. The results are listed in Table 4.13 below, and the kinetic parameters calculated from them are shown in Table 4.14.

Table 4.13: Rates of oxidation of *p*-substituted phenols, catalysed by the polyphenol oxidase biocatalyst in the presence of 2 mM SDS

<i>p</i> -Substituent	Concentration (mM)	Rate		Rate, v (M.min ⁻¹ .mg ⁻¹) $\times 10^5$
		(ΔA .min ⁻¹)	SEM	
Me	50	0.0346	0.0002	5.22 \pm 0.17
		0.0353	0.003	
		0.0325	0.001	
		0.0351	0.002	
	25	0.0260	0.0008	4.14 \pm 0.41
		0.0308	0.002	
		0.0252	0.002	
	10	0.0223	0.001	3.02 \pm 0.026
		0.0194	0.0003	
		0.01805	0.001	
	5	0.0151	0.001	2.55 \pm 0.27
		0.0196	0.0005	
		0.0154	0.0009	
		0.0173	0.002	
i-Pr	100	0.0085	0.002	1.03 \pm 0.07
		0.0077	0.0003	
		0.0090	0.001	
	50	0.0053	0.009	0.85 \pm 0.15
		0.0074	0.0007	
		0.0081	0.0007	
	25	0.0078	0.0005	0.72 \pm 0.3
		0.0030	0.0005	
		0.0072	0.0003	
	10	0.0056	0.0006	0.65 \pm 0.07
		0.0060	0.0002	
		0.0046	0.002	
	5	0.0025	0.0004	0.25 \pm 0.07
		0.0013	0.0003	
		0.0023	0.0003	

<i>p</i> -Substituent	Concentration (mM)	Rate		Rate, v (M.min ⁻¹ .mg ⁻¹) $\times 10^5$
		(ΔA .min ⁻¹)	SEM	
<i>t</i> -Bu	50	0.0060	0.0005	0.69 \pm 0.12
		0.0044	0.001	
		0.0076	0.0004	
	25	0.0055	0.0001	0.63 \pm 0.05
		0.0059	0.0002	
		0.0049	0.001	
	10	0.0049	0.0001	0.55 \pm 0.02
		0.0048	0.0001	
		0.0045	0.0008	
	5	0.0035	0.0005	0.41 \pm 0.01
		0.0036	0.0006	
		0.0034	0.001	
2,4-di- <i>t</i> -Bu	50	0.0013	0.009	0.54 \pm 0.15
		0.0009	0.0001	
		0.0012	0.002	
		0.0019	0.001	
	25	0.0100	0.0008	0.43 \pm 0.08
		0.0120	0.0003	
		0.0007	0.002	
		0.0110	0.001	
	10	0.0070	0.002	0.34 \pm 0.03
		0.0060	0.001	
		0.0074	0.001	

Table 4.14: Kinetic parameters for the oxidation of *p*-substituted phenols catalysed by the polyphenol oxidase biocatalyst in the presence of SDS

<i>p</i> -Substituent	<i>s</i> (mM)	<i>s/v</i>	<i>V</i> (mM.min ⁻¹ .mg ⁻¹)	<i>K_m</i> (mM)	<i>V/K</i> (min ⁻¹ .mg ⁻¹) x 10 ³
Me	50	958.3	0.060 ± 0.004	9.1 ± 0.2	6.68
	25	603.9			
	10	331.1			
	5	196.2			
i-Pr	100	9711.9	0.022 ± 0.002	14.3 ± 5.0	1.509
	50	5900.0			
	25	3454.3			
	10	1528.1			
<i>t</i> -Bu	50	7254.4	0.015 ± 0.002	3.87 ± 0.5	3.75
	25	3981.3			
	10	1528.1			
	5	1209.1			
DTBP	50	9311.0	0.0063 ± 0.005	9.9 ± 2.0	0.64
	25	5841.1			
	10	2915.5			

4.4.7 Determination of longer term effects of SDS on the biocatalyst

SDS solution in water (25 μ L; 2 mM) was added to a volumetric flask containing biocatalyst (32 mg, containing 1 mg protein) in CHCl₃ (9 mL). The flask was stoppered and the mixture was stirred vigorously for 2 min being allowed to stand at room temperature for 18h. Flasks were set up in quadruplicate. In a second and third set of samples, water and buffer respectively were used in place of the SDS solution. After the 18 h standing, the chloroform was decanted from 2 flasks in each set, and the residual biocatalyst was air-dried. Water (1 mL) was added, and aliquots of the resulting protein solution were assayed by the dopachrome method (see Section 2.4.10). Control experiments were carried out by measuring the dopachrome activity of samples of fresh biocatalyst in the presence of equivalent concentrations of SDS.

The other pair of samples from each set were assayed using the standardised organic medium assay (see Section 2.4.11), by adding *p*-cresol (250 mM; 1 mL) and measuring the rate of absorbance increase due to *o*-quinone production as before. Control experiments were carried out by measuring the activities of fresh samples of the biocatalyst by the organic assay method. The results are shown in Tables 4.15 and 4.16.

Table 4.15: Dopachrome assays of activity in samples of biocatalyst exposed to SDS in chloroform for 18 h.

Aqueous component	Rate ($\Delta A \cdot \text{min}^{-1} \cdot \text{mg}^{-1}$)	Mean rate
SDS solution	1.045 0.968	1.007
Buffer	0.996 1.189	1.093
Water	0.621 0.590	0.606
Control	1.647 1.503	1.575

Table 4.16: Rates of oxidation of *p*-cresol by biocatalyst after exposure to SDS for 18 h.

Aqueous component	Rate ($\Delta A \cdot \text{min}^{-1}$)	Mean rate
SDS solution	0.0201 0.0214 0.0234	0.0216
Buffer	0.0215 0.0268 0.0230	0.0238
Water	0.0191 0.0174	0.0183
Control	0.0382 0.0335	0.0359

CHAPTER 5

APPLICATION OF POLYPHENOL OXIDASE IN A CONTINUOUS FLOW SYSTEM

5.1 INTRODUCTION

In order to assess the feasibility of the practical application of immobilised polyphenol oxidase for synthesis of *o*-quinones or catechols from phenolic substrates, a continuous flow system was designed and tested using columns packed with the biocatalyst. The three different enzyme extracts were used: a crude extract, a partially purified enzyme obtained by ammonium sulphate precipitation, and a crude extract prepared in the presence of polyvinylpolypyrrolidone (PVPP) to remove endogenous phenolics. These enzymes were immobilised on glass beads in a manner similar to that used in the kinetics study (see Chapter 3). Since economic factors would be important in a practical situation, and a minimal degree of processing in the preparation of the biocatalyst would be preferable, crude extract was utilised in a number of columns under various conditions. The other two extracts were tested for comparison.

5.2 RESULTS AND DISCUSSION

The system consisted of a glass column containing the biocatalyst, connected to a reservoir and peristaltic pump (see Figure 5.1) and the hydrated solvent, containing the substrate, was pumped continuously for a number of hours. The reaction was followed by removing aliquots of solution from the reservoir at intervals, and measuring the absorbance at the appropriate wavelength for the *o*-quinone product, as determined previously [Section 3.2.2 (1)]. The yields of the respective *o*-quinones in the solutions drained from the columns were determined using the molar extinction coefficients calculated using ¹H-NMR [Section 3.2.2 (2)]. The decrease in the concentration of substrate was also followed, using GC.

The data obtained is summarised in Table 5.1. Since conditions and rates varied widely in different columns, the amount of *o*-quinone produced after six hours, per gram of protein present in the column, was calculated as a means of comparing the results.

Table 5.1: Data from continuous flow system; columns 1 - 9

COLUMN	CONDITIONS		RESULTS			
	Biocatalyst (Dry mass protein,g)	Substrate	UV		GLC	Mass gain (g)
			% yield quinone	Product after 6h (mmol/g protein)	Decrease in substrate peak (%)	(Increase in mass of biocatalyst)
1	Crude extract (0.493g)	<i>p</i> -Cresol 1.0 mmole in 100ml	44.4 (7h)	0.901	79.0	0.03
2	Crude extract (0.312g)	<i>p</i> -Cresol 3.75 mmole in 75ml	4.4 (12h)	0.346		
3	Crude extract (0.318g)	<i>p</i> -Cresol 1.5 mmole in 75ml	1.97 (6h)	0.095		
4	Crude extract (0.483g)	<i>p</i> -Cresol 1.0 mmole in 100ml + 2mM SDS	45.0 (7h)	0.839	94.3	0.05
5	Ammonium sulphate purified enzyme (0.085g)	<i>p</i> -Cresol 1.0 mmole in 100ml	76.9 (6h)	9.047	94.9	
6	PVPP-treated enzyme (0.608g)	<i>p</i> -Cresol 1.0 mmole in 100ml	51.3 (6h)	0.843	97.1	0.018
7	Crude extract (0.573g)	ATEE 1.0 mmole in 100ml	41.5 (9h)	0.552	55.6	0.04
8	Crude extract (0.533g)	<i>p</i> -iso-propylphenol 1.0 mmole in 100ml	8.4 (6h)	0.158	19.7	
9	Crude extract (0.506g)	<i>p</i> -iso-propylphenol 1.0 mmole in 100ml + 2mM SDS	28.9 (8h)	0.507	53.3	0.03

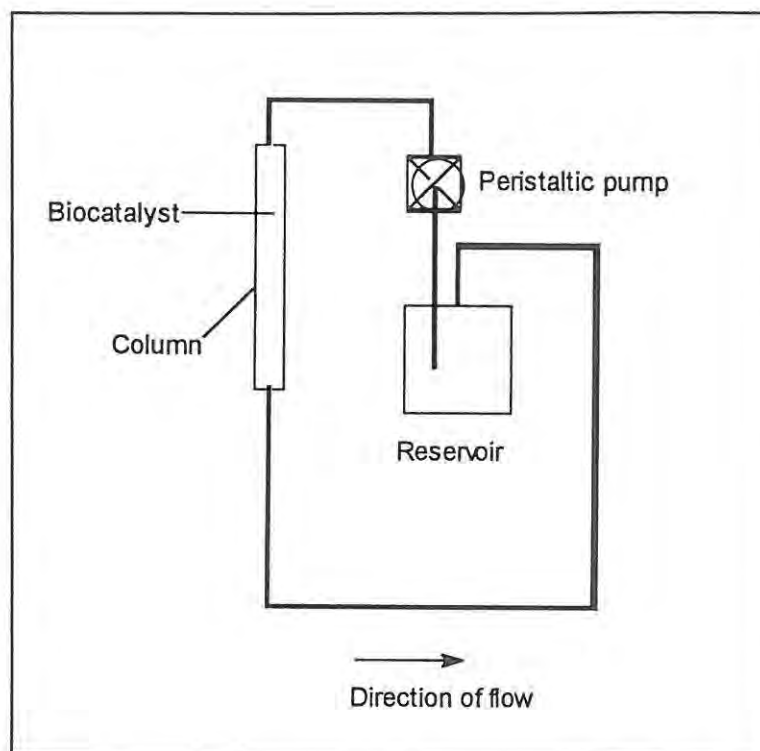


Figure 5.1: Continuous flow system

5.2.1 Columns 1 - 4, using *p*-cresol as substrate and crude enzyme

The conversion of the substrate, *p*-cresol, to 4-methyl-*o*-benzoquinone was successfully demonstrated. In Column 1, for example, the yield of the *o*-quinone measured in the mobile phase after seven hours was 44.4%, which corresponds to the conversion of 0.9 mmol of substrate per gram of impure protein, in six hours. However, the GC analysis indicated that 79% of the substrate had been removed from the solution, and therefore 35% of the product was presumably bound to the column packing, as insoluble polymer. This correlates with the 0.03g found to be the approximate increase in mass of the biocatalyst. The formation of insoluble polymeric material is a recognised problem in the synthesis of quinones, and this is discussed further in Section 5.2.6.

In Columns 2 and 3, the biocatalyst was prepared from crude extract which had been stored for some weeks, and it appears that a significant proportion of the enzyme activity had been lost, since the rates measured in these columns were relatively low. However, it is also possible that the higher concentrations of substrate caused some substrate inhibition, and lower concentrations were

used subsequently. The results from these two columns are included because they show that the rates of conversion were appreciable and remained uniform under these conditions (see Figure 5.2). The irregularity in the graph for Column 2 during the second hour is due to alteration in the water content during this time, and is discussed in Section 5.2.6.

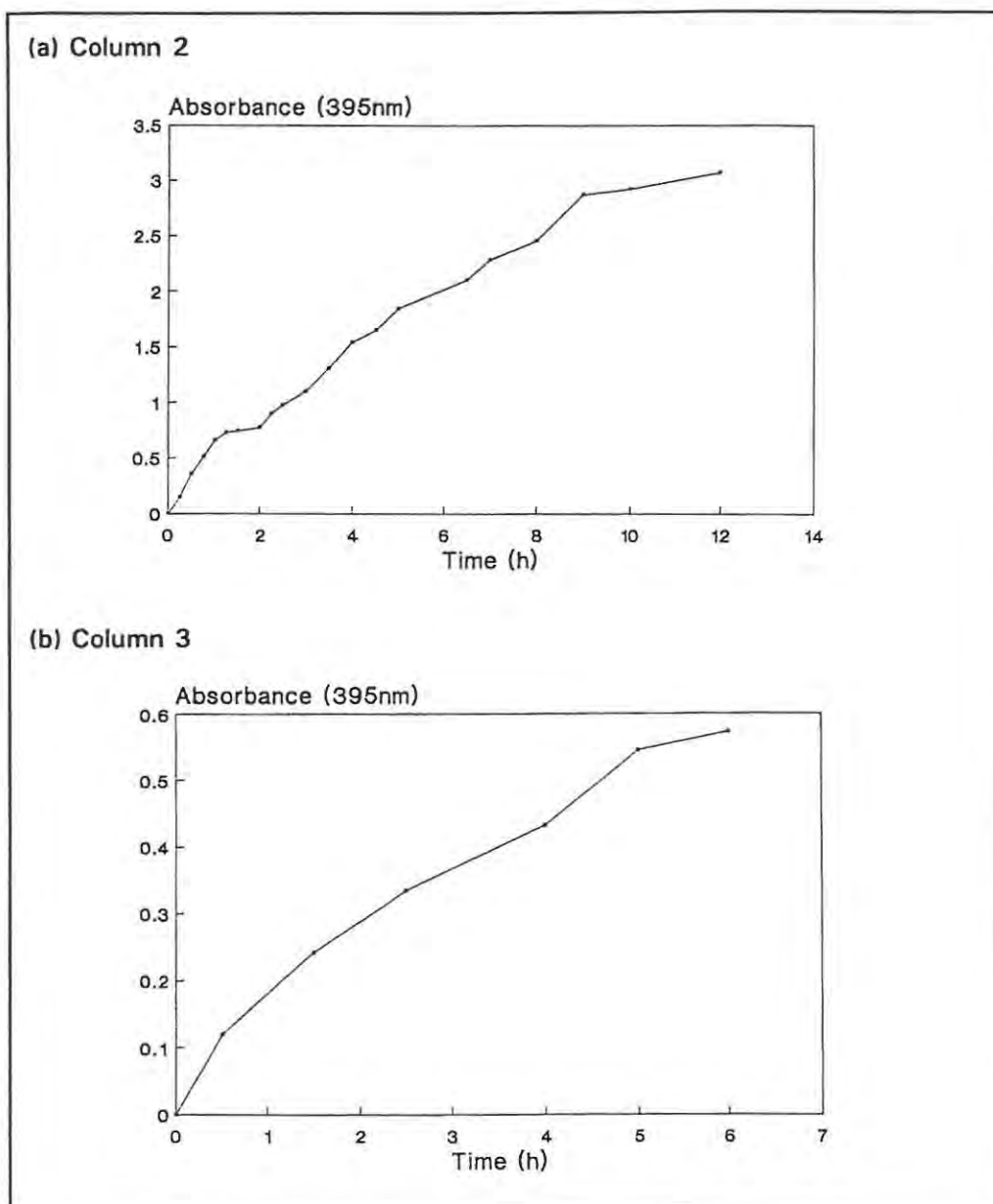


Figure 5.2: Rates of reaction for Columns 2 and 3

The inclusion of 2mM SDS in the mobile phase of Column 4 caused an increase in the rate of utilisation of the substrate, although the overall yield of *o*-quinone (0.84 mmoles per gram of protein in six hours) was not very different from that of Column 1. It might be speculated that the

presence of the SDS caused more polymerised product to bind to the biocatalyst, so that although most of the substrate was removed from the solution, only 45% was detected as *o*-quinone in solution. If the SDS is assumed to promote the relaxation of the enzyme conformation, it is possible that this provides more access for permanent binding of polymeric material.

5.2.2 Column 5, using partially purified enzyme

The biocatalyst in Column 5, having been partially purified, had a much higher specific activity than that prepared from crude extract, and the efficiency of the column is correspondingly greater. This biocatalyst contained far less inactive material, was less sticky and more convenient to use. The discrepancy between the reduction in substrate concentration and the yield of *o*-quinone was smaller in this column than in others, suggesting less binding of polymerised product, and therefore purification of the protein to this extent might be of advantage in a practical situation. In the GC analysis of this reaction mixture, a small quantity of 4-methylcatechol was detected, (see Figure 5.3) and its presence was confirmed by TLC using an authentic sample as a standard. It is possible that this catechol was released from the enzyme active site under saturating conditions, although this is not a feature of the normal mechanism of polyphenol oxidase, or it may have originated from reaction between polyphenols, quinones and/or phenols (Mason, 1959).

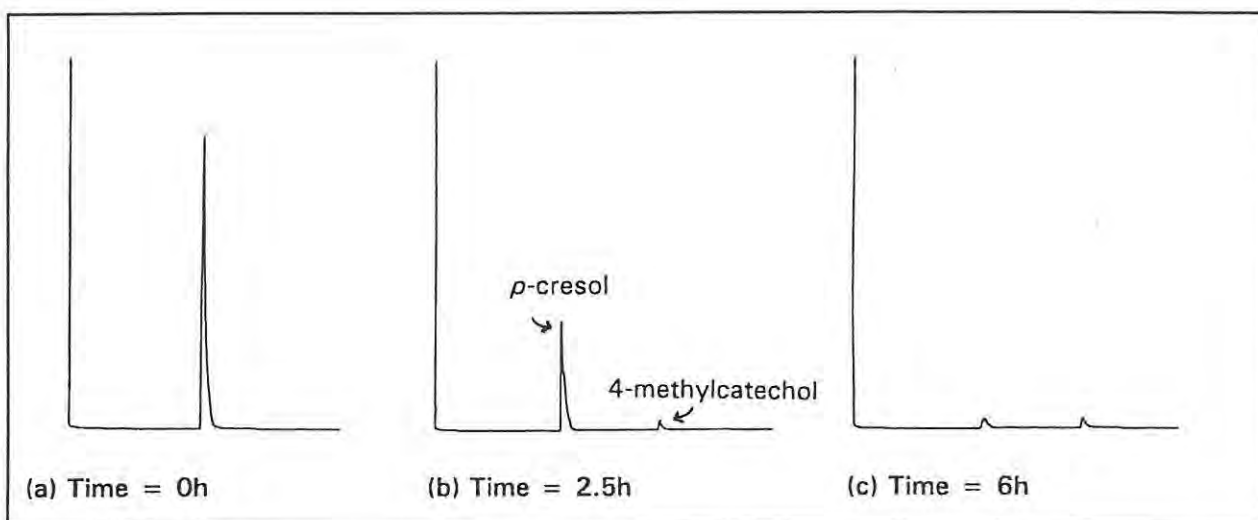


Figure 5.3: Peaks from GC analysis for Column 5

5.2.3 Column 6, using PVPP-treated enzyme

The PVPP-treated enzyme extract used to prepare the biocatalyst for Column 6 would contain less endogenous phenolic or polyphenolic material than the crude extract, and it was observed to be paler on colour. However, the comparison of results from the UV and GC analyses for this column indicate that this treatment had little effect with respect to reducing the binding of polymerised product, as compared with Column 1. The extent of reaction as measured by GC was higher, and thus the removal of endogenous polyphenolics during the extraction procedure does appear to enhance the activity of the enzyme.

5.2.4 Column 7, using ATEE as substrate.

The substrate used in Column 7, *N*-acetyltyrosine ethyl ester (ATEE), is the protected tyrosine which can be used as a starting material to prepare L-DOPA (Kazandjian and Klivanov, 1985 and Section 2.2.7). This experiment was carried out to extend the results obtained in Section 2.2.7, where a sample of L-DOPA was prepared using crude polyphenol oxidase, to a larger scale system. However, the quinone product appeared to be particularly prone to polymerisation, and the spent biocatalyst from the column was highly coloured by bound product. This substrate is likely to be more hydrophilic than the other phenol substrates used in the present study since it contains more polar groups. It is possible that more water would be associated with the bound substrate, leading to the formation of more polymerised product. If this is so, a lower water content in the column might have been preferable for more efficient conversion of the substrate to the *o*-quinone. In view of the success of the smaller scale experiment described in Section 2.2.7, it should be possible to optimise the present system to produce a better yield.

5.2.5 Columns 8 and 9, using *p*-isopropylphenol as substrate.

The sterically bulky substrate, *p*-isopropylphenol, was used as a substrate, in the presence and absence of 2mM SDS respectively. One advantage of the use of polyphenol oxidase in chloroform is the conversion of bulky, hydrophobic substrates such as this, since in this medium the substrates and products are more soluble. The significant effect of the SDS in increasing the rate of conversion of bulky substrates, as illustrated by the kinetic study (Chapter 4, Section 4.4.6), is also demonstrated here. In the presence of the SDS, the amount of *o*-quinone measured in the mobile phase was increased by a factor of three, suggesting again that the SDS plays a role in promoting the flexibility of the protein, facilitating access of the substrate to the active site.

5.2.6 Water content in the continuous flow systems

The amount of water present in the system, and its variation during reaction, are important considerations in the application of polyphenol oxidase. While the protein must be adequately hydrated in order to function (Zaks and Russell, 1988), any excess water might promote the polymerisation of *o*-quinone product. Binding of the polymer to the biocatalyst could lead to decreased accessibility of substrate to the enzyme active site, and hence to decreased efficiency in the system. Polymerised products formed in aqueous systems are reported to inhibit the enzyme (Lerch, 1983), but water-promoted polymerisation should be less significant in a chloroform medium provided there is no excess of free water, and hence this inhibition should be reduced. In a preliminary experiment (Section 2.2.7), the reaction was shown to continue at a uniform rate for several hours and similarly, in the columns being described here, the rates of reaction were approximately uniform for up to ten hours (Figures 5.2 and 5.4), suggesting the absence of inhibition.

Conversely, insufficient water to hydrate the system would cause slow reaction rates. In the case of Column 2, this was demonstrated by the markedly reduced rate of UV absorbance increase following the addition of molecular sieve to the reservoir flask after one hour. This reduction was reversed by re-addition of water to the flask after two hours (Figure 5.2). The water content of the biocatalyst and mobile phase used in the present system are shown in Table 5.2 below.

Table 5.2: Water content in constituents of continuous flow system

Constituent	% water ^a	Method of determination
Biocatalyst before use	1.94	Drying at 100°C
Biocatalyst after 8h use	1.20	
Chloroform saturated with buffer used in mobile phase	0.12	Karl-Fischer titration
Chloroform solution drained from column after reaction ^a	0.16	

^aMean value for Columns 5,9,10, and 11; contains excess water.

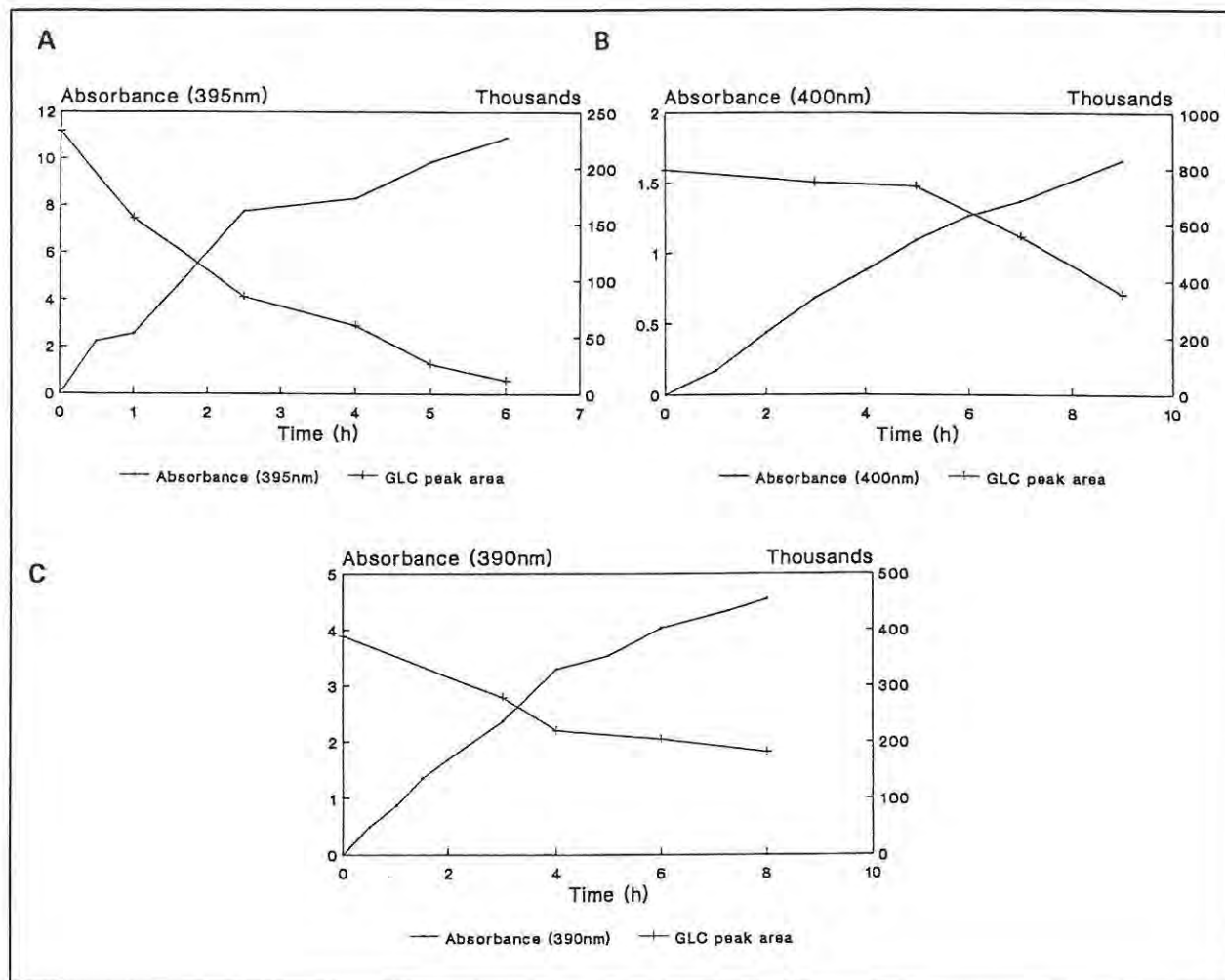


Figure 5.4: Rates of reaction for Columns 5 (A), 7 (B), and 9 (C)

The water content of the chloroform solution removed from the columns was found to be, on average, slightly higher than that of the chloroform used to prepare the solutions, which suggests that water was actually removed from the biocatalyst. It is apparent that the biocatalyst was wetter than was necessary for hydration of the protein, and starting with it drier might have led to less polymerisation on the column, and hence improved yields. This also suggests that the initial step in the procedure, of washing hydrated chloroform through the columns was unnecessary, and could be omitted.

It must be borne in mind that water is a product of the reaction being catalysed by polyphenol oxidase. In the present system, the amount produced would be negligible. One mmole in 100 ml, produced in the complete conversion of 1 mmole of substrate, would contribute an extra 0.018% water in the solution, and would probably not even be released by the protein. However, in alternative systems if there were larger substrate loading, this may be a significant factor.

Some quinone product and/or polymerised material was apparently bound in all of the columns, indicated by changes in the colour of the biocatalyst, and the small mass gains measured after removal of the biocatalyst from some of the columns (see Table 5.1). In some cases, washing clean solvent through the column after draining the product effected removal of some bound quinone, and the quantities were then measured and added to the final mass of product in the calculations of yield. The loss of product due to binding on the biocatalyst would explain the observed discrepancy between the rate and extent of the reduction in concentration of substrate as determined by GC, and the concentration of *o*-quinone in the mobile phase as measured by UV-visible spectroscopy, which is shown in Table 5.1.

5.2.7 Isolation of products and reduction of *o*-quinones to catechols

Isolation of *o*-quinones is often problematic, particularly if any water is present, due to their tendency to polymerise. Since catechols are generally more useful than quinones as starting materials for organic syntheses, it would be practical to convert the quinones produced by polyphenol oxidase to catechols, by a chemical reduction. In this investigation, in common with other work in this area (for instance, Doddema, 1988; Kazandjian and Klibanov, 1985), ascorbic acid was used as the reductant. Although it would seem wise to avoid use of aqueous systems, the ascorbic acid was found to be insufficiently soluble in organic (chloroform or chloroform/methanol) solvents, even in the presence of a phase transfer catalyst, to effect the complete reduction of the quinones. In Column 6, benzyltriethylammonium chloride was added to the chloroform solution drained from the column, to which ascorbic acid had been added, in an attempt to reduce the quinone. The reduction was found to be incomplete, however, with the presence of residual quinone being shown in the ¹H NMR and IR spectra of the reaction mixture.

An aqueous solution of ascorbic acid was therefore used in the successful reduction of the quinones from other columns, with phase separation to extract the catechols which were found to dissolve in the aqueous layer. This procedure was followed in the cases of Columns 4 and 11, where clean samples of the respective catechols were obtained. The catechols were identified by ¹H NMR spectroscopy, comparing the spectra with those of authentic standards, and those of the corresponding phenols and quinones. The reduction of quinones was verified by the absence of quinone-carbonyl signals (1700 - 1660 cm⁻¹) and the presence of broad signals (near 3300cm⁻¹) due to the hydroxyl groups, in the IR spectra of the products.

5.3 CONCLUSIONS

These experiments demonstrate that the application of polyphenol oxidase in a continuous flow system is feasible, although the system was not fully optimised. Nevertheless, the continuous process functioned successfully for a considerable time without significant decrease in the reaction rates. This indicates that in the use of chloroform as a medium, the reaction inactivation which is characteristic of aqueous systems, is avoided. This is attributable to the high solubility of the quinone products in chloroform which would result in their being removed from the binding site immediately after formation, so that they would not be available for the inactivation process. In overcoming the reaction inactivation to an extent where reasonable yields of product were obtained, the major advantage of the use of chloroform as a medium has been demonstrated, and polyphenol oxidase has been shown to be a feasible biocatalyst.

Further work would be necessary to optimise the system for a practical situation. In particular, the water content in the different parts of the system would need careful control, in order to minimise polymerisation and binding of the product, while maintaining sufficient hydration of the protein to give workable conversion rates. Although reaction rates did not decrease a great deal in the experiments conducted here, more complete drying of the biocatalyst, perhaps by freeze-drying, might be advantageous. Hydration of the protein could then be effected (and controlled), for instance, by washing with hydrated chloroform. It may be beneficial to have conditions of less than maximal hydration, and to use relatively low substrate concentrations, because although the resulting rates might be slower, there might be a compensating decrease in the overall loss of product. There might also be some advantage in a simple purification step, such as ammonium sulphate precipitation, in decreasing the amount of extraneous protein present to bind water and thus promote polymerisation of quinones.

Separation of the product from any unreacted phenolic substrate may also be necessary if reaction are not carried to completion, and although no attempt was made in the present study to obtain quantitative separation, the constituents of the reaction mixture from Column 5 were successfully separated on analytical TLC. This seem to indicate that chromatographic separation would be not be difficult.

Since the need to reduce the quinones to catechols may increase economic costs, an inexpensive, or regenerable reducing agent would be desirable. Ideally, the reduction step would be an integral part of a continuous flow system, applied to the effluent from the biocatalyst column after complete reaction.

5.4 EXPERIMENTAL

5.4.1 Protein determinations

Protein determinations were carried out (by Folin-Lowry method, see Section 2.4.9) on the enzyme extracts and on samples of the prepared biocatalysts. Results are shown in Table 5.3

Table 5.3: Protein concentrations in enzyme extracts

Enzyme	% protein
Crude extract	31.0
PVPP-treated extract	32.1
(NH ₄) ₂ SO ₄ precipitated enzyme	60.1
Biocatalyst	Protein (g/g beads)
For Columns 1,4,7,8,9	0.0102
For Columns 2,3	0.0062
For Column 5	0.0018
For Column 6	0.0107

5.4.2 (1) Column 1 - Conversion of *p*-cresol to 4-methyl-*o*-benzoquinone.

The biocatalyst was prepared by immobilisation of the freeze-dried crude extract (see Sections 2.4.1 and 2.4.9) (2g) on glass beads (300 μ m; 60g), using phosphate buffer (pH 7; 50mM; 15mL) to dissolve the powder. The solution was stirred with the beads, and the slurry was dried in an air draught, with occasional stirring, until it was almost dry, although sticky. The water content of the biocatalyst was determined to be 1.94% by measuring the mass loss when a sample was heated at 100°C for 96h.

The biocatalyst (48.15g dry mass, 0.493g total protein) was loosely packed into a glass column (2x15cm) fitted with a glass frit at the lower end. Buffer-saturated CHCl₃ (50mL; 0,12% water) was passed through the column to ensure hydration of the protein. A solution of *p*-cresol in buffer-saturated chloroform (10mM; 100mL) was loaded on the column, and circulated (see Figure 5.1)

by pumping with an EYELA Microtube Pump MP-3, at a rate of 5mL/min. The reservoir flask was covered to minimise evaporation losses. Periodically, aliquots were removed for analysis: (a) UV-visible spectroscopy: absorbance due to the *o*-quinone product was measured at the appropriate wavelength (as determined in Section 3.2.2), diluting the sample with CHCl_3 when necessary, and (b) GC: aliquots (50 μl) were dried (anhydrous MgSO_4) and 1 μl injections were made (in duplicate) on the SE-30 capillary column (conditions as described in Section 2.4.15). The area under the substrate peak was measured by integration. The results are shown in Table 5.4.

After 7h, the CHCl_3 solution was drained from the column, its volume (96mL) was measured, and the water content (0.16%) was determined by Karl-Fischer titration. CHCl_3 (40mL) and acetone (40mL) were used consecutively to wash further coloured product from the column. The UV absorbances of these solutions were measured and their *o*-quinone contents were calculated, to be added to the total yield. The column packing (which was dark brown) was removed, air-dried for 24h at room temperature, and 12h at 100°C, then weighed. The mass gained by the biocatalyst was approximately 0.03g.

Table 5.4: Data from Column 1, converting *p*-cresol using crude enzyme.

Time (h)	UV absorbance (395nm)	GC substrate peak area
0	0.00	529659
1	2.44	
2	3.30	352519
3	3.50	
4	4.20	318509
6	5.37	153638
7	5.86	110056
CHCl ₃ wash (40mL)	1.123	Reduction in area = 79%
Acetone wash (40mL)	0.320	

Total *o*-quinone produced = 0.444 mmoles

% Conversion = 44.4%

o-Quinone produced after 6h = 0.901 mmoles/g protein

5.4.2 (2) Reduction of product from Column 1

A portion (30mL) of the solution of the product solution from the column was treated with ascorbic acid (0.15g) in MeOH (5mL) and stirred for 2h. The mixture was filtered and evaporated to dryness. The major constituent of the residue was found by ^1H NMR spectroscopy to be 4-methylcatechol, $\delta_{\text{H}}(\text{CDCl}_3)$ 2.23(3H,s,CH₃), 5.23(1H,br s,OH), 5.35(1H,br s,OH), 6.58(1H,dd, J 8 and 1.2, H-5), 6.68(1H,d, J 1.2, H-6), and 6.73(1H,d, J 8,H-3).

5.4.3 Column 2, using 50mM *p*-cresol as substrate

The procedure described for Column 1 was followed, but the biocatalyst was prepared from previously prepared crude extract (1g) on glass beads (50g), and 50.3g(dry mass, containing 0.312g protein) was packed into the column. *p*-Cresol solution (50mM; 75mL) in buffer-saturated CHCl_3 was added as before and the reaction was followed for 12h. Molecular sieve (3Å, 5g) was added to the reservoir flask after 1h. The rate of absorbance increase was observed to decrease dramatically during the second hour. The chloroform was then re-hydrated by addition of buffer (90 μl , equivalent to 0.12%) to the flask, with swirling for 2 min. After 12h, the solution was drained as before, and the CHCl_3 (20mL) was used to wash further product from the column. Results of the UV analysis are shown in Table 5.5. GC analysis did not show any significant decrease in the substrate peak.

A portion of the solution from the column was dried (anhydrous MgSO_4) and evaporated to dryness leaving a residue which contained, as the major constituent, *p*-cresol $\delta_{\text{H}}(\text{CDCl}_3)$ 2.29(3H,s,CH₃), 6.75(2H,d, J 8.2,H-3 and H-5), and 7.05(2H,d, J 8.2,H-2 and H-6). Very small peaks corresponding to 4-methyl-*o*-benzoquinone, $\delta_{\text{H}}(\text{CDCl}_3)$ 2.37(3H,s,CH₃), 6.25(1H,s,H-5), 6.35(1h,d, J 10,H-6) and 6.87(1H,d, J 10,H-3), were observed in the ^1H NMR spectrum, but integral ratios could not be measured accurately.

Table 5.5 Data from Column 2, using 50mM *p*-cresol as substrate

Time (h)	Absorbance (395nm)	Time (h)	Absorbance (395nm)
0	0.00	3.5	1.303
0.25	0.145	4.0	1.540
0.50	0.355	4.5	1.650
0.75	0.512	5.0	1.840
1.00	0.661	6.5	2.10
1.25	0.728	7.0	2.28
1.50	0.747	8.0	2.45
2.00	0.774	9.0	2.87
2.25	0.898	10.0	2.92
2.50	0.974	12.0	3.07
3.00	1.100	CHCl ₃ wash (20mL)	0.582

Total *o*-quinone produced = 0.166 mmoles

% conversion = 4.4%

o-Quinone produced after 6h = 0.346 mmoles/g protein

5.4.4 Column 3, using 20mM *p*-cresol as substrate

The procedure described for Column 1 was followed, using the same biocatalyst as used for Column 2 (51.2g, containing 0.318g protein). A solution of *p*-cresol (20mM; 75mL) was added and the reaction was followed for 6h. The data obtained are shown in Table 5.6.

Table 5.6: Results from Column 3, using 20mM *p*-cresol as substrate.

Time (h)	Absorbance (395nm)
0	0.0
0.5	0.120
1.5	0.242
2.5	0.334
4.0	0.432
5.0	0.545
6.0	0.573

Total *o*-quinone produced = 0.0295 mmoles

% conversion = 1.97%

o-Quinone produced after 6h = 0.095 mmole/g protein.

5.4.5 (1) Column 4, using *p*-cresol in the presence of SDS

The procedure described for Column 1 was followed, using the same freshly prepared biocatalyst (47.24g, containing 0.483g protein). The *p*-cresol solution (10mM; 100mL) was prepared using CHCl₃ which had been shaken with 2mM SDS solution then separated. The reaction was followed for 7h, and the data obtained are shown in Table 5.7. The mass gained by the biocatalyst (after drying) was 0.05g.

Table 5.7: Results obtained for Column 4, in the presence of SDS

Time (h)	UV Absorbance (395nm)	GC substrate peak area
0	0.0	505939
0.5	2.26	
1.0	3.33	
2.0	4.27	180027
3.0	4.52	
4.0	4.91	52546
5.0	5.53	
6.0	5.91	52062
7.0	7.27	29204
CHCl ₃ wash (30mL) 1.018		% Reduction = 94%

Total *o*-quinone produced = 0.45 mmoles

% Conversion = 45%

o-Quinone produced after 6h = 0.839 mmoles/g protein.

5.4.5 (2) Reduction of product from Column 4

A portion of the reaction mixture from the column was treated with ascorbic acid (0.25g) in MeOH (5mL) and the mixture was stirred for 1h, then allowed to stand overnight. The colour (due to *o*-quinone) was observed to have decreased but was not removed. An aqueous solution of ascorbic acid (10%; 20mL) was added, and the mixture was shaken for 5 min before allowing the layers to separate. The aqueous layer was extracted with EtOAc (3 x 15mL), and the combined organic fractions were dried (anhydrous MgSO₄). The solvent was removed under reduced pressure, and the product was found to be 4-methylcatechol (9mg, 29%), $\nu_{\max}(\text{CHCl}_3)$ 3250 br(OH); $\delta_{\text{H}}(\text{CDCl}_3)$ 2.23(3h,s,CH₃), 4.82(1h,br s,OH), 4.92(1h,br s,OH), 6.58(1h,dd, J 8 and 1.2,H-5), 6.68(1h,d, J 1.2,H-6) and 6.73(1h,d, J 8,H-3).

5.4.6 (1) Column 5, using partially purified enzyme

The procedure described for Column 1 was followed, but the biocatalyst was prepared by immobilising the partially purified enzyme obtained by ammonium sulphate precipitation (Section 2.4.2). The freeze-dried powder (0.15g) was dissolved in phosphate buffer (50mM, pH 7, 5mL), glass beads (300 μ m, 50g) were added, and the mixture was allowed to air dry. This biocatalyst (47.0g, containing 0.092g protein) was loosely packed into the column, and treated as before, using *p*-cresol (10mM, 100mL) in buffer-saturated chloroform. The reaction was followed for 6h. The spent biocatalyst, after drying, was found to have gained 0.04g, and the water content of the solution after reaction was 0.12%. The results obtained are shown in Table 5.8. In the GC analysis, a small peak was observed to develop at retention time 11.8 min (see Figure 5.3), which was identified as 4-methylcatechol by co-elution with a standard sample. This was also indicated by TLC comparison (silica,, EtOAc:hexane 1:1) of the reaction mixture with standard 4-methylcatechol.

The solvent from a portion (20mL) of the final solution from the column was removed under reduced pressure, and the residue (0.022g, approximate yield 90%) was found to contain mainly 4-methyl-*o*-benzoquinone δ_{H} (CDCl₃) 2.22(3H,s,CH₃), 6.23(1H,s,H-5), 6.33(1H,d,*J* 10.1,H-6), and 6.87(1H,d, *J* 10, H-3). Small peaks correlating with *p*-cresol (approx. 5%) and 4-methylcatechol (less than 1%) were also observed, as well as small impurities which may be polymerised material.

Table 5.8: Data from Column 5, using partially purified enzyme

Time (h)	UV Absorbance (395nm)	GC substrate peak area
0	0.0	232651
0.5	2.225	
1.0	2.547	155439
2.5	7.740	85494
4.0	8.296	60321
5.0	9.860	26498
6.0	10.900	11979
CHCl ₃ wash (30mL)	1.089	% Reduction = 94.9%

Total *o*-quinone = 0.769 mmoles

% Conversion = 76.9%

o-Quinone produced after 6h = 9.047 mmoles/g protein

5.4.6 (2) Reduction of product from Column 5

A further portion (30mL) of the solution from the column was treated with ascorbic acid (0.07g, 2 equivalents) in MeOH (20mL), and the mixture was stirred for 2h, then filtered, and the solvent was removed under reduced pressure. The residue was extracted with EtOAc (3 x 10mL), giving 4-methylcatechol (12mg, 33%), identified by ¹H NMR spectroscopy.

5.4.7 (1) Column 6, using PVPP-treated enzyme extract

The procedure described for Column 1 was followed, but the biocatalyst was prepared by immobilising the PVPP-treated enzyme extract (see Section 2.4.3). The freeze-dried powder (2g) was dissolved in phosphate buffer (50mM; pH 7; 15mL) and glass beads (300 μ m; 60g) were added. The mixture was stirred and allowed to dry under a stream of air. The column was loosely packed with the biocatalyst (56.95g, dry mass, containing 0.608g protein) and treated as before. The substrate solution, *p*-cresol (10mM; 100mL) in buffer-saturated chloroform, was added, and the reaction was followed for 6h. The spent biocatalyst, after drying, was found to have gained 0.018g. The data obtained is shown in Table 5.9.

Table 5.9: Data from Column 6, using PVPP-treated enzyme

Time (h)	UV Absorbance (395nm)	GC substrate peak area
0.0	0.00	836209
0.83	2.814	
2.0	4.876	
3.0	6.58	260004
4.0	6.84	167900
6.0	7.43	24700
CHCl ₃ wash (52mL) 0.108		% Reduction = 97.1%

Total *o*-quinone produced = 0.513 mmoles

% Conversion = 51.3%

o-Quinone produced after 6h = 0.843 mmoles/g protein.

5.4.7 (2) Reduction of product from Column 6

A portion (25mL) of the product solution from the column was stirred with ascorbic acid (0.15g) in MeOH (5mL) for 1h, and allowed to stand overnight. The solution was observed to have retained some colour (due to *o*-quinone). The phase transfer catalyst, benzyltriethylammonium chloride (0.01g), was added and the mixture was stirred for 1h. The solvent was removed under reduced pressure, and the residue was extracted with CHCl₃ (3 x 10mL). The combined CHCl₃ fractions were evaporated under reduced pressure, giving mainly 4-methylcatechol, contaminated with *p*-cresol (approximately 20%) and 4-methyl-*o*-benzoquinone (1%), identified by ¹H NMR spectra as before and IR: ν_{\max} (CHCl₃) 3250 br s(OH) and 1710(C=O) cm⁻¹.

5.4.8 (1) Column 7, using ATEE as substrate

The procedure described for Column 1 was followed, using the same biocatalyst (56.20g, containing 0.573g protein). The substrate solution (100mL) contained *N*-acetyltyrosine ethyl ester (10mM), and the reaction was followed for 9h. The results obtained are shown in Table 5.10. The spent biocatalyst, after drying, was found to have gained 0.04g.

Table 5.10: Data from Column 7, using ATEE as substrate

Time (h)	UV Absorbance (395nm)	GC substrate peak area
0.0	0.0	795329
1.0	0.167	
2.0	0.437	
3.0	0.680	750582
4.0	0.874	
5.0	1.093	738267
6.0	1.264	
7.0	1.370	557821
8.0		
9.0	1.658	353483
CHCl ₃ wash (50mL)	0.061	% Reduction = 55.6%

Total *o*-quinone produced = 0.109 mmoles

% Conversion = 10.9%

o-Quinone produced after 6h = 0.140 mmoles/g protein

A portion (25mL) of the solution from the column was dried (anhydrous MgSO_4) and evaporated to dryness under reduced pressure, giving a residue which appeared polymerised, and ^1H NMR spectroscopy showed the presence of *N*-acetyltyrosine ethyl ester δ_{H} (CDCl_3) 1.23(3H,t, J 3.8, CH_3), 1.95(3H,s, CH_3), 2.96(2H,ddd, J 6.3,5.4 and 8.3, CH_2), 4.16(2H,dd, J 4.0 and 3.0, ethyl- CH_2), 4.80(1H,dd, J 4.0 and 2.0,CH), 6.23(1H,d, J 8.0, arom-H), 6.6.72(2H,d, J 8.5,arom-H), and 6.92(2H,d, J 8.5,arom-H): the σ -quinone product had presumably polymerised, and was not soluble in CDCl_3 .

5.4.8 (2) Reduction of product from Column 7

A further portion (25mL) of the solution from the column was treated with ascorbic acid (0.15g) in MeOH(5mL) and then as an aqueous solution, in the same way as Column 4. The resulting extract was found to contain mainly ATEE, with a small proportion of the σ -quinone, identified by comparison of ^1H NMR spectra.

5.4.9 Column 8, using *p*-isopropylphenol as substrate

The procedure described for Column 1 was followed, using the same biocatalyst (52.24g, containing 0.533g protein). The substrate solution (100mL) contained *p*-isopropylphenol (10mM), and the reaction was followed for 6h. The data obtained is shown in Table 5.11.

Table 5.11: Data from Column 8, using *p*-isopropylphenol as substrate

Time (h)	UV Absorbance (390nm)	GC substrate peak area
0.0	0.0	563501
0.0	0.213	
2.0	0.433	530921
3.0	0.691	
4.0	0.936	488232
5.0	1.157	
6.0	1.320	452703
CHCl ₃ wash (40mL) 0.021		% Reduction = 19.7%

Total σ -quinone produced = 0.084 mmoles

% Conversion = 8.41%

σ -Quinone produced after 6h = 0.158 mmoles/g protein

5.4.10 Column 9, using *p*-isopropylphenol as substrate, and SDS

The procedure described for Column 1 was followed, using the same biocatalyst (49.55g, containing 0.506g protein). The substrate solution (100mL) contained *p*-isopropylphenol (10mM), dissolved in CHCl_3 which had been shaken with 2mM SDS solution. The reaction was followed for 8h. The spent biocatalyst, after drying, was found to have gained 0.03g, and the solution from the column contained 0.202% water after reaction. The data obtained is shown in Table 5.12.

Table 5.12: Data from Column 9, using *p*-isopropylphenol as substrate, in the presence of SDS

Time (h)	UV Absorbance (390nm)	GC substrate peak area
0.0	0.0	389286
0.5	0.484	
1.0	0.871	
1.5	1.351	
3.0	2.364	278942
4.0	3.292	220780
5.0	3.540	
6.0	4.024	204817
7.25	4.336	
8.0	4.540	181629
		% Reduction = 53.3%

Total *o*-quinone produced = 0.289 mmoles

% Conversion = 28.9%

o-Quinone produced after 6h = 0.507 mmoles/g protein

The solvent from a portion (20mL) of the solution from the column was removed under reduced pressure, leaving 0.018g residue, containing polymerised material, some 4-isopropyl-*o*-benzoquinone, and some starting material, identified by ^1H NMR spectroscopy.

5.4.10 (2) Reduction of product from Column 9

A further portion (25mL) of the solution from the column was treated with ascorbic acid in the same manner as for Column 4, giving 4-isopropylcatechol (11mg, 56%, correcting for starting material), $\nu_{\text{max}}(\text{CCl}_3)$ 3250 br s(OH), and $\delta_{\text{H}}(\text{CDCl}_3)$ 1.19(3H, s, CH₃), 1.20(3H, s, CH₃), 2.85(1H, m, CH), 6.66(1H, dd, J 8 and 2.1, H-5), 6.75(1H, d, J 2.0, H-3) and 6.88(1H, d, J 8, H-6). The sample contained some contaminating starting material (16%, calculated from integral ratios in the ¹H NMR spectrum).

CHAPTER 6

BIOMIMETIC STUDIES OF TYROSINASE: MOLECULAR MODELLING

6.1 INTRODUCTION

6.1.1 Biomimetic chemistry

The efficiency of biological reactions is at least partly attributable to specific molecular interactions, such as those which occur between an enzyme and its substrate. The nature of these interactions and the mechanisms of biological reactions have been elucidated to some extent, in recent years. The term "biomimetic chemistry" was first used by Breslow (1972), in referring to a newly developing field in which the principal aim was to imitate biological processes by classical techniques of organic chemistry (Katchalski-Katzir, 1983). A reciprocal relationship has evolved in which modelling of biological systems, using information derived from biochemical investigations and theoretical data, contributes to our understanding of the biological processes. "The biological model provides the organic chemist with inspiration, challenge, and identification of interesting problems" (Cram, 1983).

6.1.2 Molecular recognition considerations

Biomimetic chemistry must take into account the characteristic process by which biological molecules recognise and selectively interact with each other within a complex chemical environment - a process which has become known as "molecular recognition" (Hamilton, 1991). Ideally, a biomimetic model should simulate the interactions which occur in the biological system. The recognition of a substrate by a protein is characterised by several features:

- (i) Complementarity between the substrate and the binding site, which may involve pairing of oppositely charged or polarised groups, hydrophobic groups, and hydrogen bond donors and acceptors.
- (ii) Specificity, which is related to the steric match and an optimisation of attractive interactions between the protein and the ligand.
- (iii) Dynamic factors such as conformational changes and flexibility.

(Katchalski-Katzir, 1983).

Hydrogen bonds and $\pi - \pi$ stacking interactions have been identified as the major binding forces in molecular recognition. Generally, the recognition process involves multiple interactions, which increase the strength of the binding as well as improving selectivity (Hamilton, 1991). Many enzymes have a concave "pocket" containing the receptor site in a hydrophobic environment; in these cases, catalysis apparently requires non-polar conditions. Thus information about nature's strategy for optimising a biological system provides direction for the design of biomimetic models which simulate that system.

6.1.3 Molecular mechanics

Molecular mechanics was developed as a theoretical method for estimating steric effects. As modern computational techniques have improved, molecular mechanics has become increasingly useful as a tool for the prediction not only of molecular shapes and steric interactions, but also of molecular dynamics and charge distributions. In a biomimetic context, molecular mechanics can be used to predict and/or explain these aspects of structure-function relationships in biological and biomimetic systems (Hancock, 1989).

Molecular mechanics involves the construction of a molecular model and the calculation of the potential energy of a particular conformation. The total potential energy in the molecule is then minimised by a sequence of iterative calculations of the potential energies for consecutively varied conformations until a structural model is obtained which represents the optimal (most stable) conformation. The final model generally represents an idealised gas phase structure of the molecule, which would be independent of lattice interactions in the solid state, or of solvent effects in solution.

Data required for such calculations include:- the atomic size of each of the component atoms, ideal (strain-free) bond lengths, and force constants for the various bond types. The former two parameters are generally derived from experimental data such as X-ray crystallographic measurements of closely similar structures, correlated with theoretical values. The force constant (interaction constant) of an atom depends on the type of bonds involving the atom, and determines the limits of the allowed bond distortions. For any molecular species, the force field (empirical potential) is determined; this takes into account bond deformations, angle deformations, torsional strains, and non-bonded interactions, as well as the strain-free bond lengths. The force field of a molecule is a description of that molecule as a collection of the component atoms interacting with each other, and this is the data set which is incorporated into the programme used to perform the calculations (Brubaker and Johnson, 1984). The minimisation of strain energy is achieved *via*

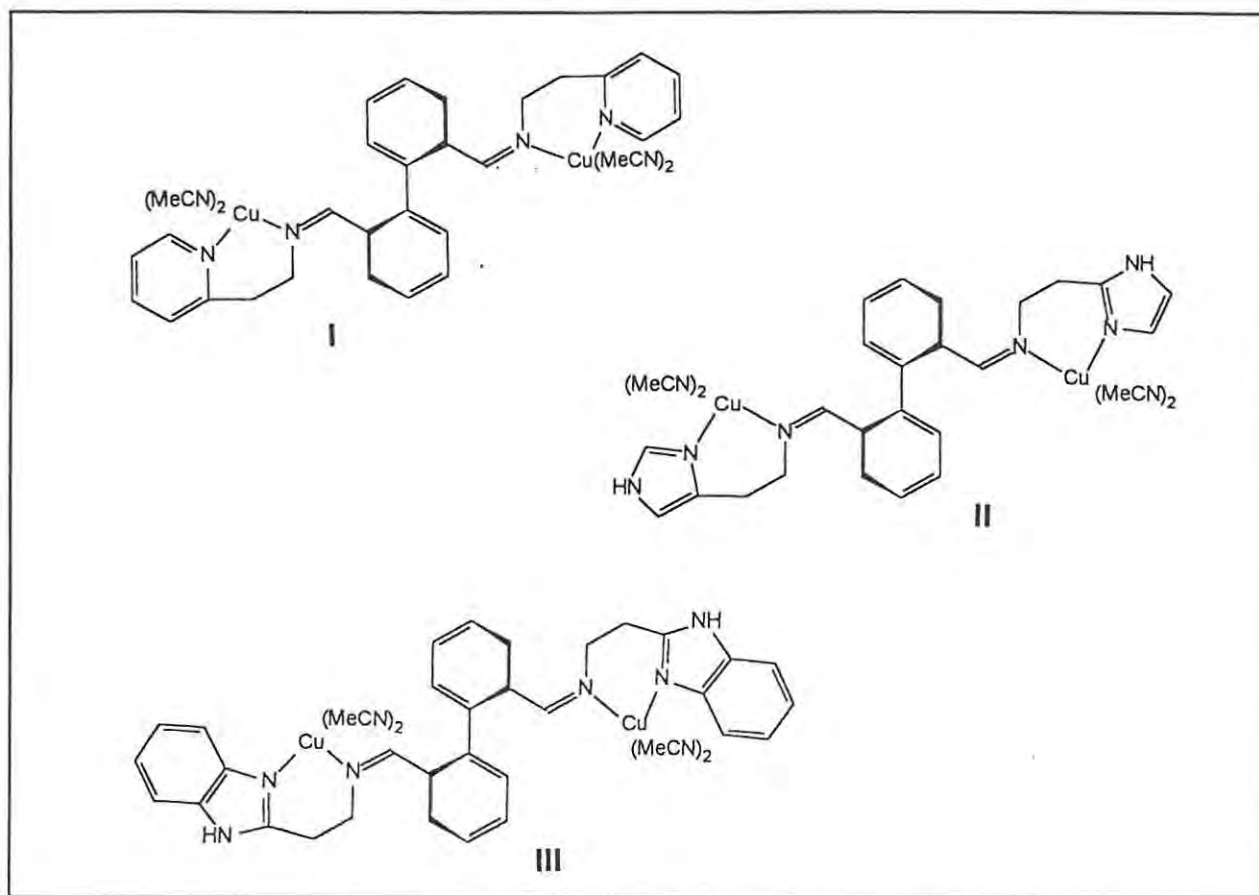
potential energy calculations at points on an internally mapped potential surface, for a gradually varied set of intramolecular dimensions. The starting point for the calculations is an initial guess at the atomic positions; this must be based on an energetically reasonable conformation, but modern programmes may include methods for differentiating between local and global minima on the potential surface. As would be expected in a new and rapidly developing field such as this, refinements to the techniques of molecular mechanics are reported regularly in the current literature (for example, Halgren, 1992 and Rappé *et al.*, 1992).

In the molecular mechanical treatment of coordination chemistry, the selection of force field parameters is especially important because the lengths of metal-to-ligand bonds are dependent on the structure of a complex, as well as on the nature of the ligand donor groups. For example, steric crowding can cause coordinate bonds to be elongated, particularly when small metal ions are involved. Where ideal bond lengths have not been determined for metal/donor sets, it is reasonable to use an average force constant for all metal ions of the same size (Hancock, 1989).

6.1.4 Molecular mechanics calculations for dinuclear copper complexes

Copper (II) complexes require special consideration, in that octahedral geometry cannot be assumed for the copper ions, due to a strong Jahn-Teller effect. Thus, the coordination number and arrangement of the copper ions should be predicted and specified in the calculation parameters (Bernhardt and Comba, 1992). These authors have published a force field for copper (II) in organometallic complexes, determined by modelling a series of amine and imine complexes, and correlated the results with X-ray crystal structures (Bernhardt and Comba, 1992; Bernhardt *et al.*, 1992). The close similarity reported for these correlations provides support for the validity of molecular mechanics calculations on copper complexes.

In the present study, a molecular mechanics approach was used to predict the conformational characteristics of the proposed biomimetic dinuclear copper complexes I,II and III (Scheme 6.1). Since these complexes are models of tyrosinase, the molecular mechanics investigation was extended to assess (a) the feasibility of a dioxygen peroxide bridge between the two copper ions, and (b) the accessibility of the Cu-O₂-Cu unit for binding phenolic substrates. Réglier *et al.* (1990) proposed that the presence of the biphenyl spacer in complex I would facilitate a conformation in which the copper ions could reasonably be bridged by dioxygen.



Scheme 6.1: Complexes to be modelled by molecular mechanics, prior to their proposed synthesis

6.1.5 Factors to be considered in modelling polyphenol oxidase

The structure and functioning of the dinuclear binding site in polyphenol oxidase are discussed in detail in Section 1.2, but aspects relevant to the design and modelling of biomimetic complexes are mentioned here.

The distance of separation between the oxygen-bridged copper atoms is important in the complexes, because the initial stage of the enzyme-catalysed reaction involves the binding of dioxygen across the dinuclear site. A good steric match for this requires that the copper ions be separated by a distance of 5\AA for rigid planar complexes, but less for more flexible systems (Oishi *et al.*, 1980). The copper-copper separation in the enzyme active site is believed to be approximately 3.5\AA , and many of the successful complexes reported in the literature have similar copper-copper separation. Models can be judged to be reasonable if they exhibit a copper-copper distance approximating that in the enzyme.

The coordination arrangement of the copper ions in the complexes is also an important consideration. In tyrosinase, the phenolic substrate initially binds axially, while the peroxide is thought to bind in the equatorial plane, in what is now considered to be a $\mu:\eta^2-\eta^2$ bridging mode (Kitajima and Moro-oka, 1993; see Section 1.4.4). Previously, the most likely bridging mode was thought to be *cis* $\mu-1,2$ (Solomon, 1988b). A change of coordination from tetragonal copper (II) to trigonal bipyramidal copper (II) is thought to result from binding of the phenolic substrate (see Figure 6.1 and Section 1.2.6) (Solomon *et al.*, 1992).

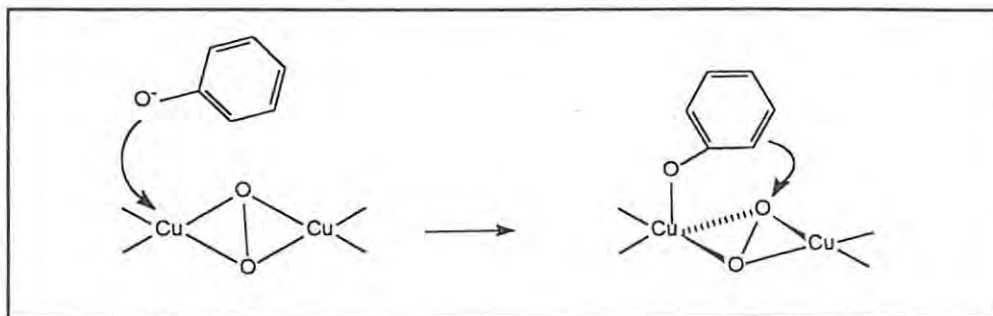


Figure 6.1: Rearrangement of the copper coordination upon binding of phenol

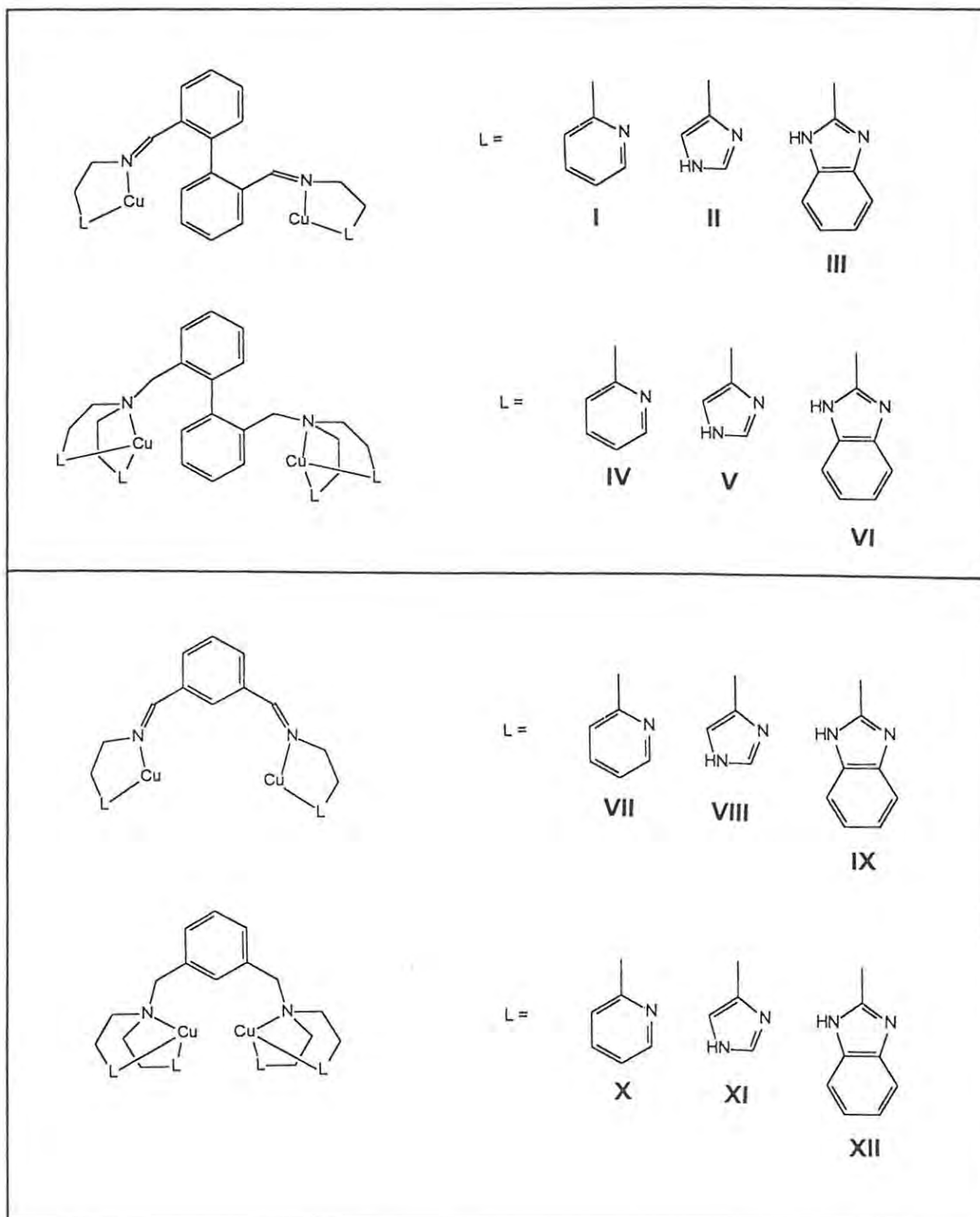
The electron transfer involved in the catalytic activity of tyrosinase would occur most readily when the phenolic substrate is coordinated equatorially to the copper (II) ions, since this would maximise the overlap of the substrate donor groups with the half empty $d_{x^2-y^2}$ orbitals of the copper (II) ions (Kida *et al.*, 1983). The oxidation of catechols is less geometrically and sterically demanding, because rearrangement from axial to equatorial binding is not required. In the binding of either type of substrate, the protein pocket is thought to contribute to stabilisation of the binding, possibly through π -stacking interactions (Wilcox *et al.*, 1985).

6.2 RESULTS AND DISCUSSION

6.2.1 Molecular Modelling using ALCHEMY II®

In the earlier stages of the present investigation, the molecular modelling program ALCHEMY II® was utilised to model the complexes I, II and III, and related structures, as shown in Scheme 6.2. This package is relatively unsophisticated, and the results obtained must be considered in the light of its limitations. Later, the more advanced package HyperChem® became available, and was used

to model various derivatives of complex III and to establish more refined conformational relationships.



Scheme 6.2: Complexes modelled using ALCHEMY II®

The structures VII - XII include a xylene spacer in place of the biphenyl spacer in complexes I - VI (Scheme 6.2). These xylene-linked complexes have been synthesised and shown to model the activity of tyrosinase, in that they catalysed the hydroxylation of the xylene spacer [see Section 1.4.5 (1)]. The xylene spacer imposes a rather rigid, planar conformation on the complexes. In the present molecular mechanics study, the biphenyl-linked complexes I - VI were modelled because they were expected to have fewer constraints imposed on their copper coordination geometry, to be more flexible, and to have more space for a substrate to approach the binding site. The complexes I - III were subsequently synthesised (see Chapter 7) but syntheses of the complexes IV - VI have not been reported to date.

Solvent molecules can also be coordinated to the copper atoms in organometallic complexes, particularly in imine-linked complexes such as I - III and VI - IX, which provide only two nitrogen-donor atoms per copper atom. In the more crowded amine models IV - VI and X - XII, each copper atom is coordinated to three nitrogen donors from the ligand and, possibly, also to solvent molecules.

Like their imine analogs, the complexes X - XII have been reported (by various workers; see Sections 1.4.4 and 1.4.5) to catalyse the hydroxylation of the arene ring in the ligand. In the hydroxylation of exogenous phenolic substrates, however, the considerably increased steric bulk of the amine complexes might restrict access of the substrates (particularly those with hindered structures) to the binding site more than in the case of the imine-linked analogs.

In this study, the conformation of the phenyl rings in the biphenyl complexes was expected to be such that their relative rotation and out-of-plane distortion (Figure 6.2,A) might draw them away from the plane containing the copper atoms. This might preclude the possibility of arene ring hydroxylation and consequently facilitate the binding and hydroxylation of exogenous phenolic substrates. In Figure 6.2, B shows the conformation proposed for the xylene complexes, which leads to hydroxylation of the arene ring because of its proximity to the peroxide bridge (Karin *et al.*, 1992).

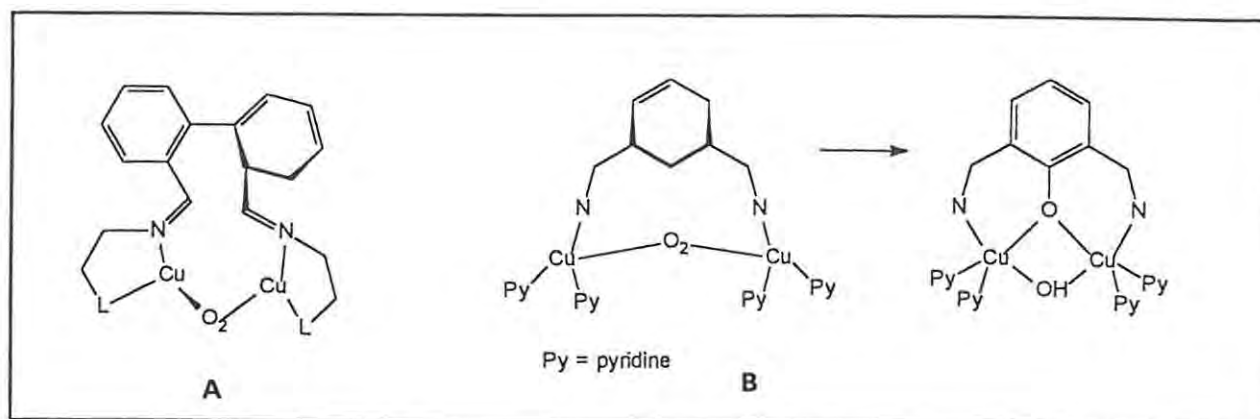


Figure 6.2: Conformations of spacers in copper complexes

Using ALCHEMY II, the organic ligands were constructed before trigonal bipyramidal copper atoms were added to the structures. This copper geometry represents that pertaining in the oxygenated binding site of tyrosinase, during binding of the substrate. Minimisation of these models resulted in open conformations as shown in Figure 6.3 and clearly, steric interactions would be small in conformations such as these. The relative rotation of the phenyl rings in the biphenyl spacer was observed to be retained, which indicates that the copper atoms would be out of the plane of the aromatic rings as discussed above.

For each of the energy-minimised models, a dioxygen bridge was then added across the copper atoms, and the minimisation calculations were repeated. This bridging resulted in the conformations shown in Figure 6.4, where the binding site is concave, the biphenyl spacer is more distorted, and the arene rings are held out of the plane of the copper atoms. The dioxygen bridges were observed to adopt *trans* configurations, as would be expected for the most stable arrangement in dinuclear copper complexes (Kitajima and Moro-oka, 1993). The copper-copper distances were measured for the energy-minimised models with peroxide bridges (Table 6.1). These distances were observed to be consistent with those required in tyrosinase models and with those reported in the literature from crystal structures of similar complexes (see Section 1.4.4).

Table 6.1: Copper-copper separations in modelled complexes

Complex	Copper-copper separation (Å)
I	3.077
II	3.175
III	3.149
IV	3.468
V	3.113
VI*	4.105
VII	3.248
VIII	3.211
IX	3.195
X	3.374
XI	3.431
XII*	4.253

* Modelled using HyperChem®

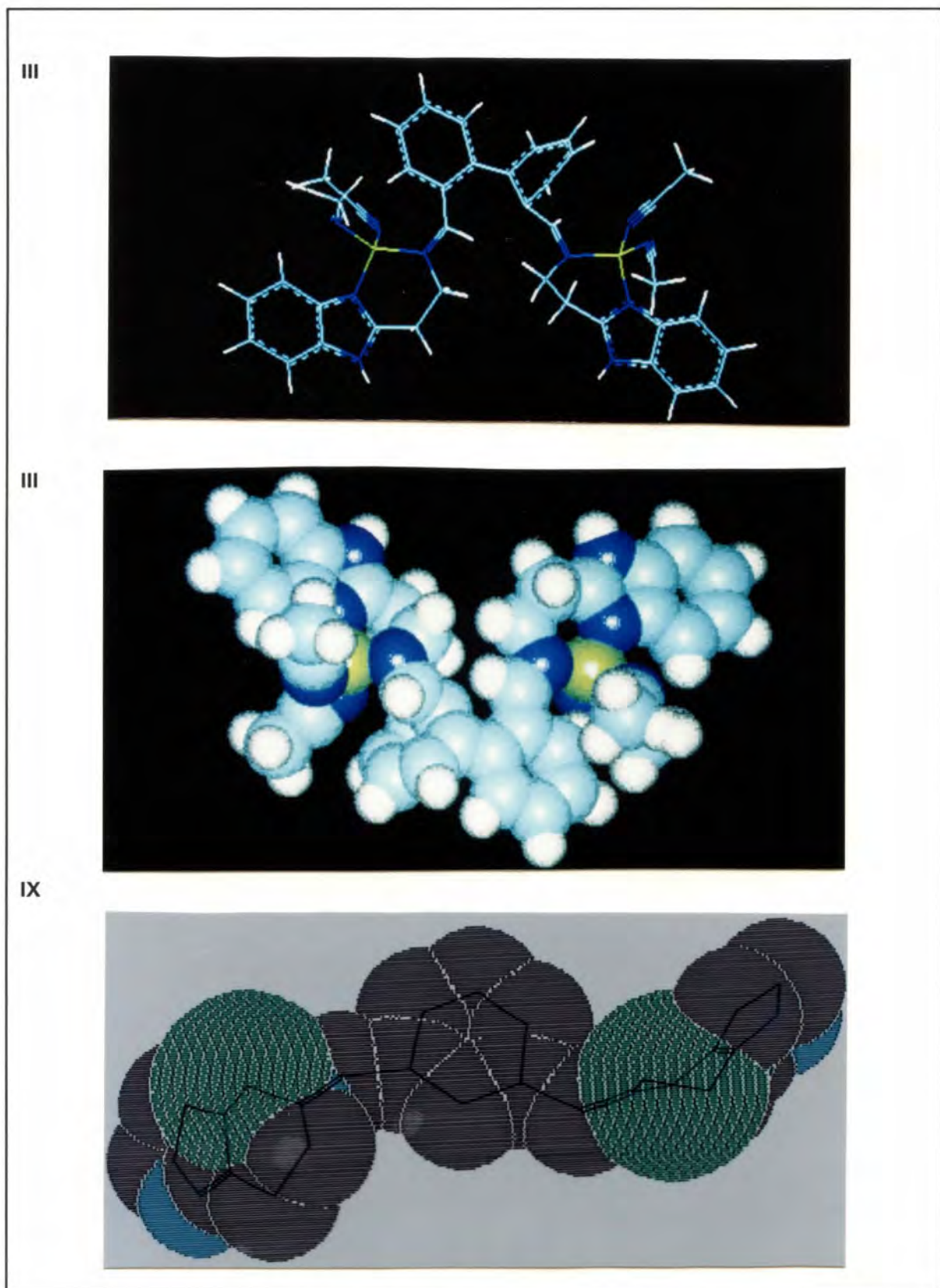


Figure 6.3: Photographs showing the open conformations of biomimetic models of complexes III and IX, prior to addition of the dioxygen bridge

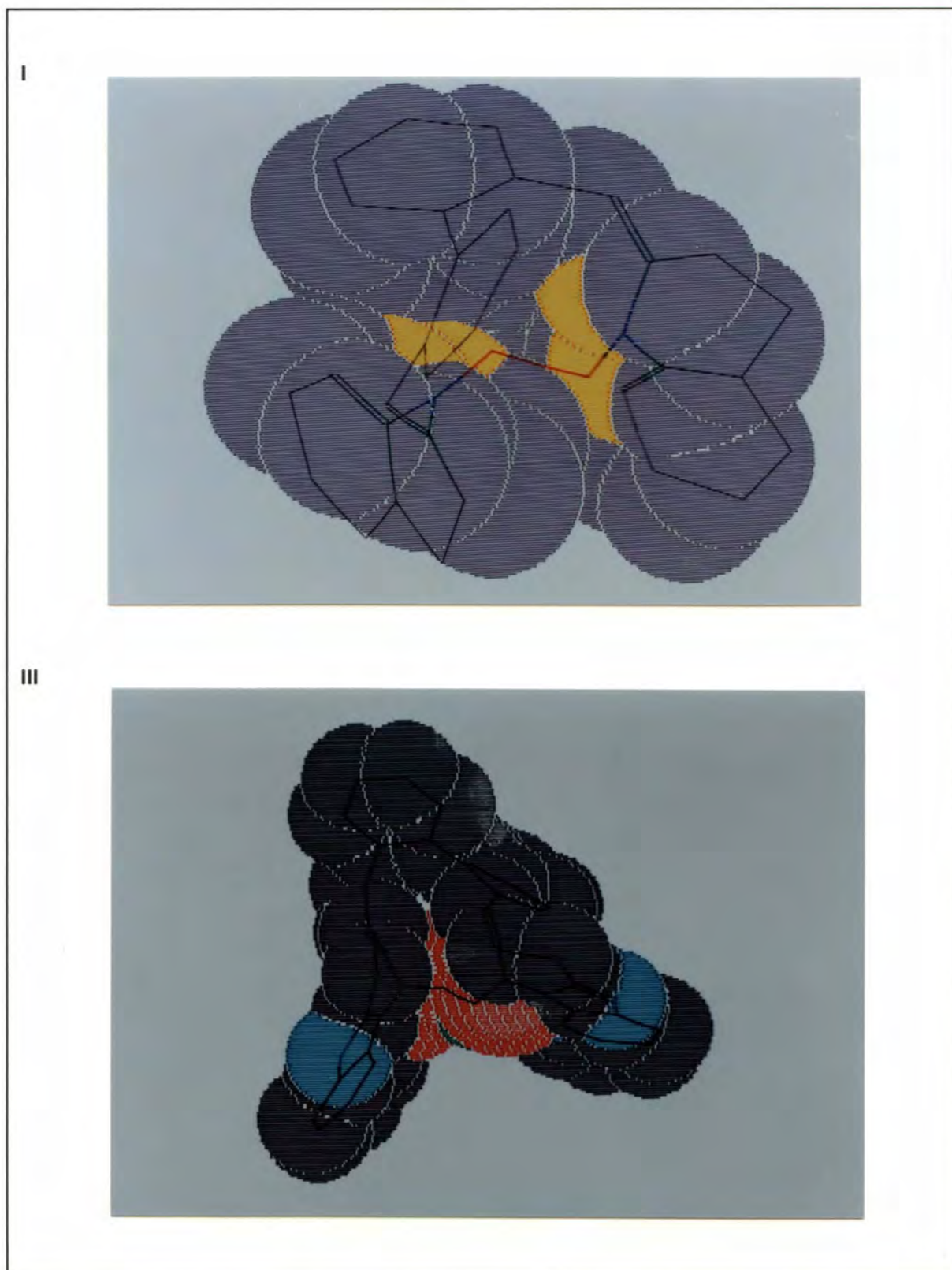


Figure 6.4: Photographs showing the conformations of biomimetic models with dioxygen bridges, modelled using Alchemy II[®]. Coloured atoms: nitrogen; grey atoms: carbon; numbers correspond with Scheme 6.2

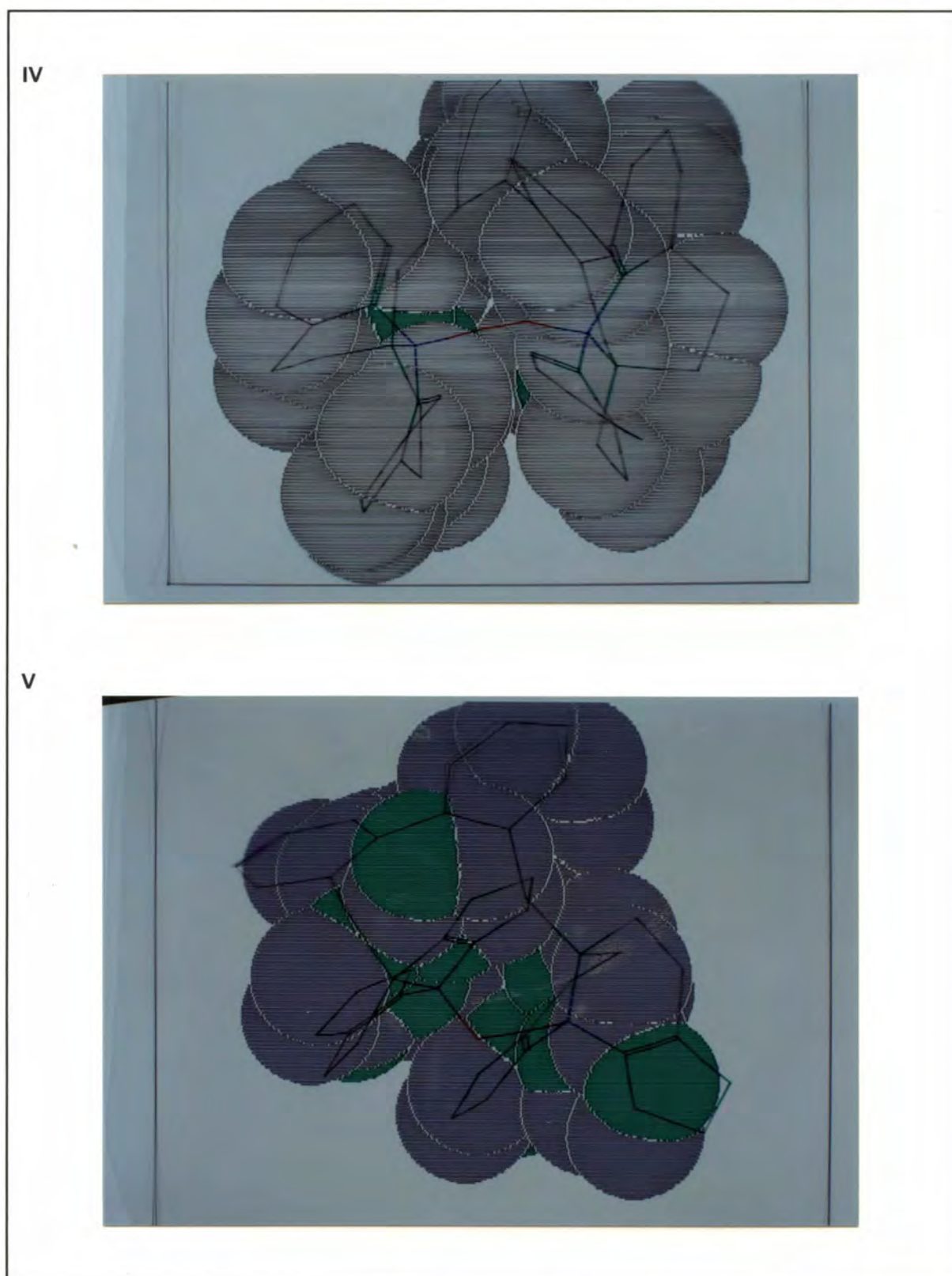


Figure 6.4: Photographs showing the conformations of biomimetic models with dioxigen bridges, modelled using Alchemy II[®]. Coloured atoms: nitrogen; grey atoms: carbon; numbers correspond with Scheme 6.2

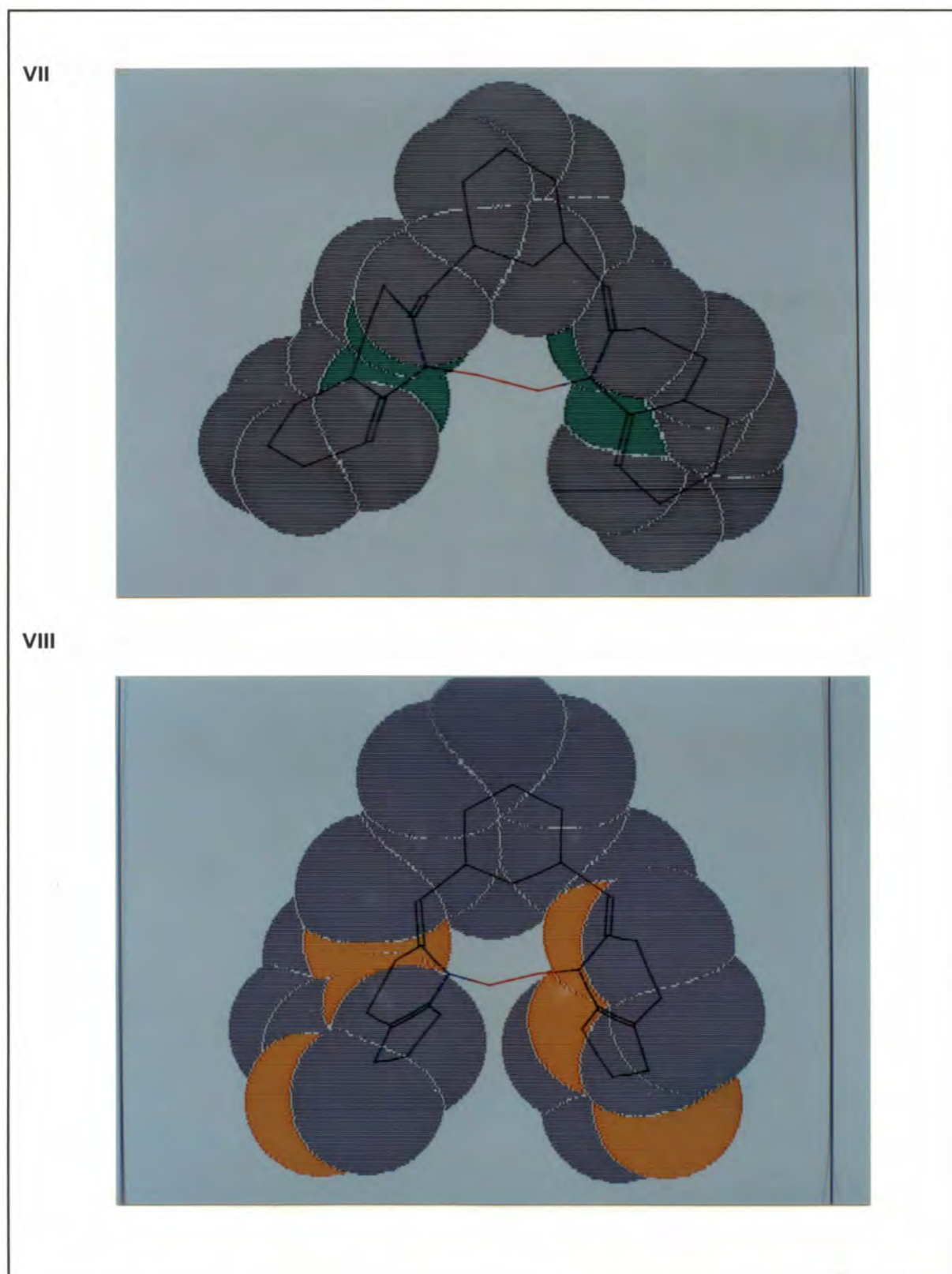


Figure 6.4: Photographs showing the conformations of biomimetic models with dioxo bridges, modelled using Alchemy II[®]. Coloured atoms: nitrogen; grey atoms: carbon; numbers correspond with Scheme 6.2

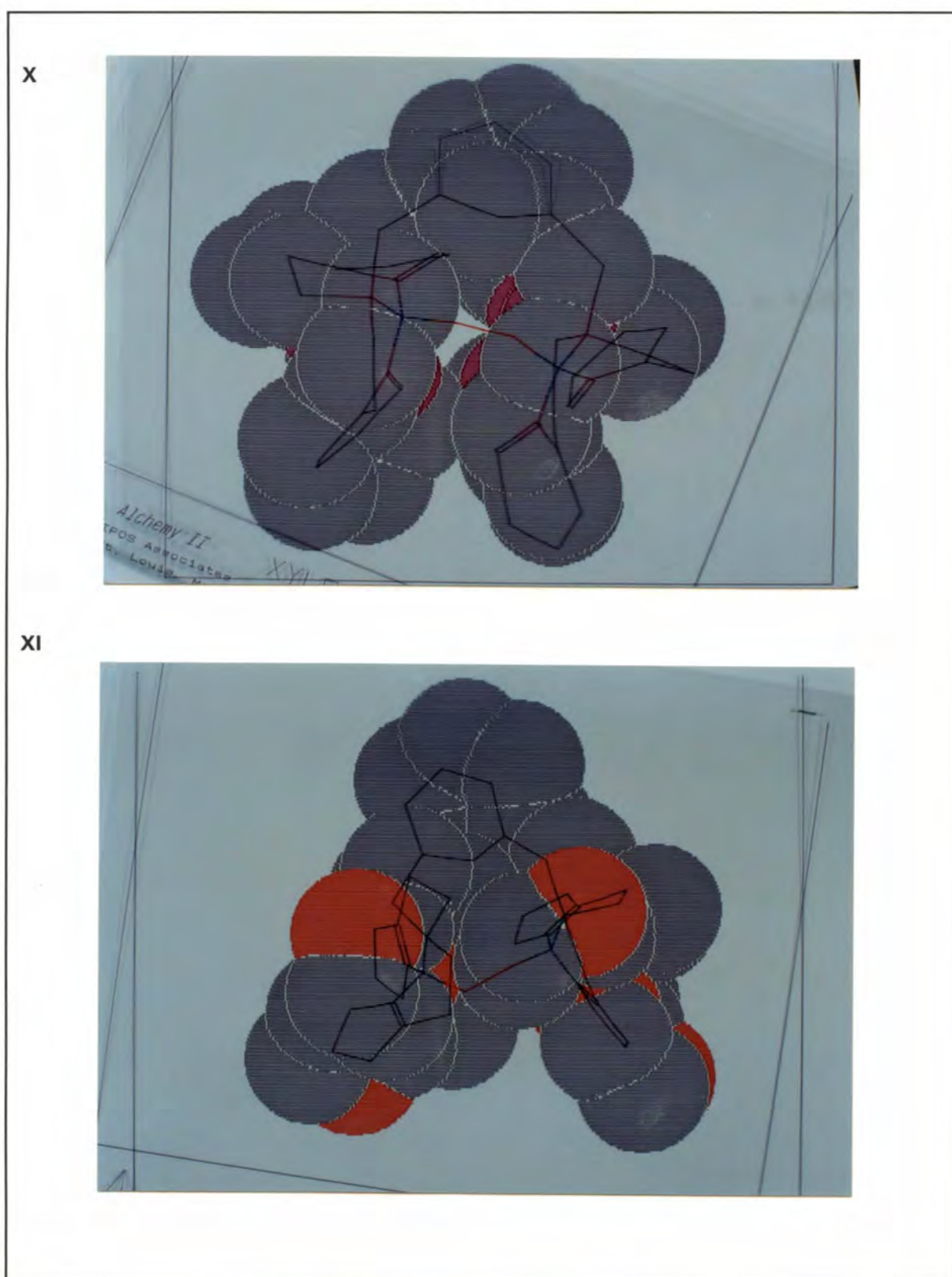


Figure 6.4: Photographs showing the conformations of biomimetic models with dioxygen bridges, modelled using Alchemy II®. Coloured atoms: nitrogen; grey atoms: carbon; numbers correspond with Scheme 6.2

The energy contributions and total potential energies for the modelled complexes in their energy-minimised "met", "oxy", and "deoxy" states are shown in Table 6.2. The "met" form represents the dinuclear copper (II) form, minimised without oxygen present; the "oxy" state represents the oxygenated form which has a dioxygen bridge; and the "deoxy" form represents the complex when oxygen is removed from the minimised "oxy" form. The energies (E_m) of the met forms were determined from the minimised met structures, and these represent the least strained conformations of the complexes in the absence of oxygen. The relative energies required for oxygen binding were determined by the following procedure: The energies (E_o) were recorded after minimisation with the dioxygen bridge in place, the model structure was then modified by removing the oxygen atoms, and one iteration of the energy minimisation was carried out, to give the energies (E_d). The differences ($E_o - E_m$) give an indication of the energy of binding oxygen, and the differences ($E_d - E_m$) give an estimate of the strain imposed on the conformation when the ligand is bent to enable bridging by oxygen. From the energies ($E_d - E_m$), it is clear that the sterically crowded amine models IV - VI and X - XII have greater conformational strain imposed by the bridging oxygen than occurs in the imine-linked models. Comparison of the ($E_d - E_m$) energies of the xylene-linked models with those of the biphenyl-linked models shows that in general, more strain occurs in the more rigid xylene-linked analogs.

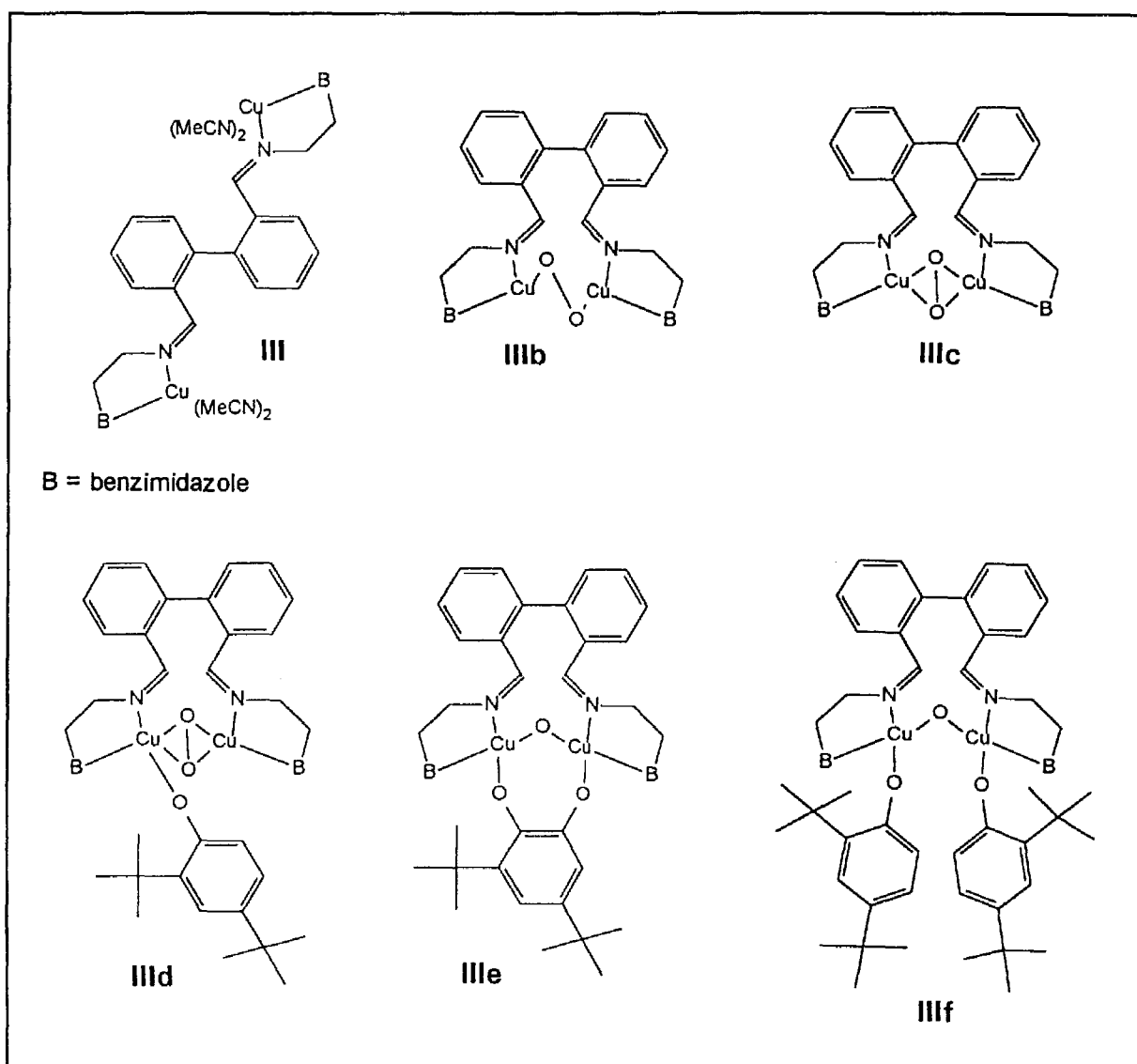
Table 6.2: Conformational energy measurements for complexes I - XII

Complex	Total conformational energy ^a			$E_o - E_m$	$E_d - E_m$
	Met, E_m	Oxy, E_o	Deoxy, E_d		
I	11.3	21.9	18.8	10.6	7.5
II	36.6	47.2	44.0	10.6	7.4
III	112	170	140	58	28
IV	30.4	155	110	124.6	79.6
V	120	220	190	100	70
VI	163	322	312	159	149
VII	13.1	26.6	33.3	13.5	20.2
VIII	27.8	40.3	35.8	12.5	8.0
IX	147	300	180	153	33
X	29.1	110	82.2	80.9	53.1
XI	58.9	180	130	61.1	71.1
XII	62	247	235	185	163

^a Units of energy measurements are kcal.mol⁻¹

6.2.2 Modelling using HyperChem®

The molecules shown in Scheme 6.3 were modelled and their conformational energies minimised using the programme HyperChem, to show that the simultaneous binding of oxygen and a bulky substrate was feasible. Obviously, the actual energy values obtained in the minimisation calculations are not directly comparable, since the models have non-equivalent structures, but the large differences observed do indicate increasing strain in the series (Table 6.3). It is also apparent from visual assessment that the structures are increasingly crowded (Figure 6.5). The copper-copper separations were measured (Table 6.3) and found to be similar to those determined previously (Section 6.2.1).



Scheme 6.3: Derivatives of complex III, including binding of dioxygen and DTBP, modelled using HyperChem®

The model IIIf, in which two molecules of the sterically bulky substrate DTBP are coordinated, one to each copper, is particularly crowded, but is nevertheless feasible (Figure 6.5). This justifies, to some extent, the suggestion made in Section 9.3.3 that the coupling of DTBP could involve two DTBP radicals in association with the complex.

The flexibility of the biphenyl spacer and its non-planarity are shown in the models, and it seems reasonable to assume that these characteristics would be found in the actual molecules. The xylene spacer imposes more rigidity on the complexes, as reflected in the greater energy differences ($E_o - E_d$) involved in binding oxygen. The removal of the phenyl rings from the proximity of the dioxygen-copper plane is also apparent (*e.g.*, in complex IIIc, Figure 6.5).

Table 6.3: Data obtained from modelling derivatives of complex III using HyperChem®

Derivative	Copper-copper separation (Å)	Total conformational energy
III	8.589	24.70
IIIb	4.105	42.78
IIIc	3.062	198.12
IIId	3.236	180.05
IIIe	3.322	207.50
IIIf	3.287	850.75

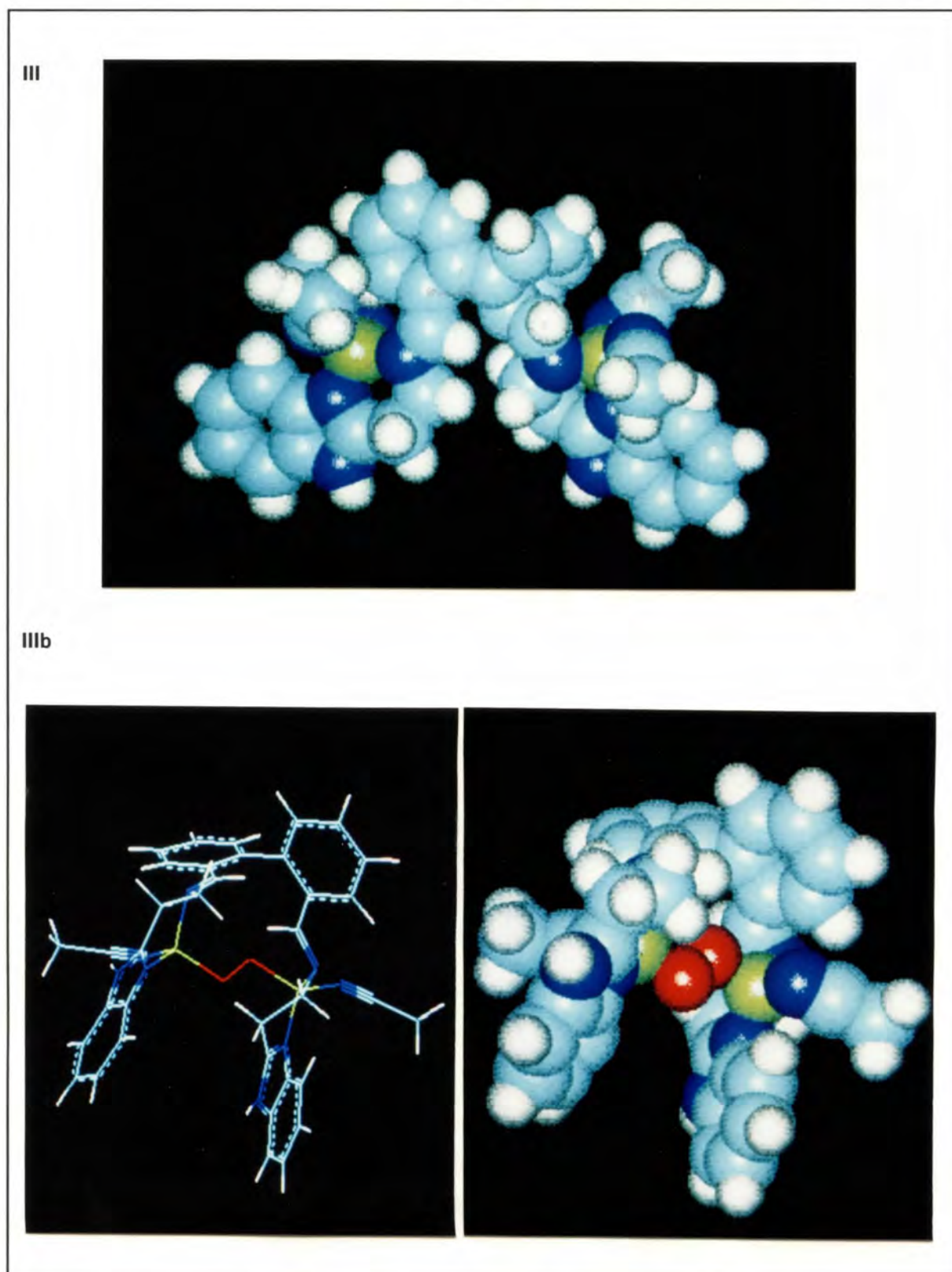
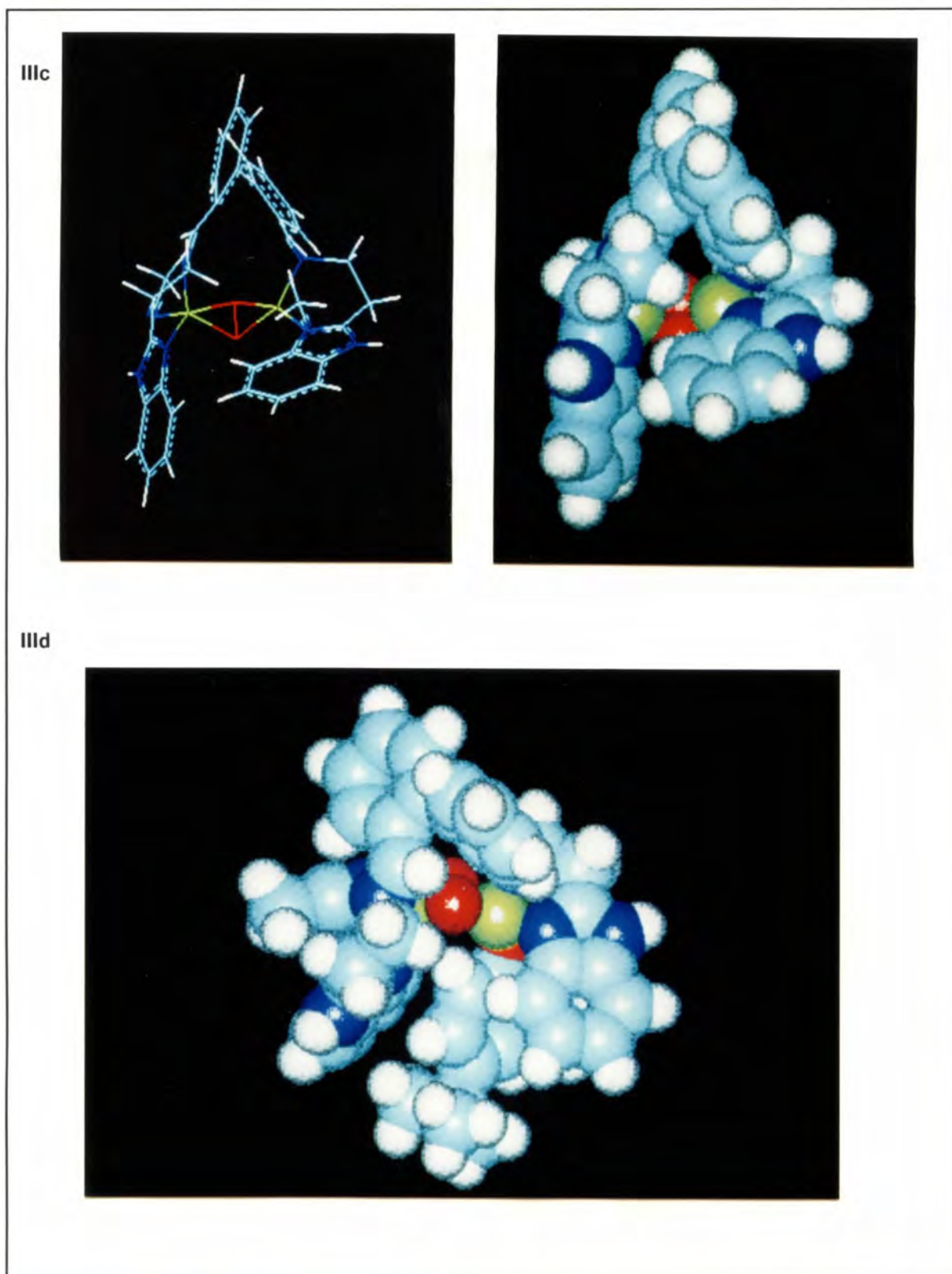


Figure 6.5: Photographs showing models of derivatives of complex III; numbers correspond to Scheme 6.3; blue atoms: carbon; white: hydrogen; red: oxygen; dark blue: nitrogen; yellow: copper.



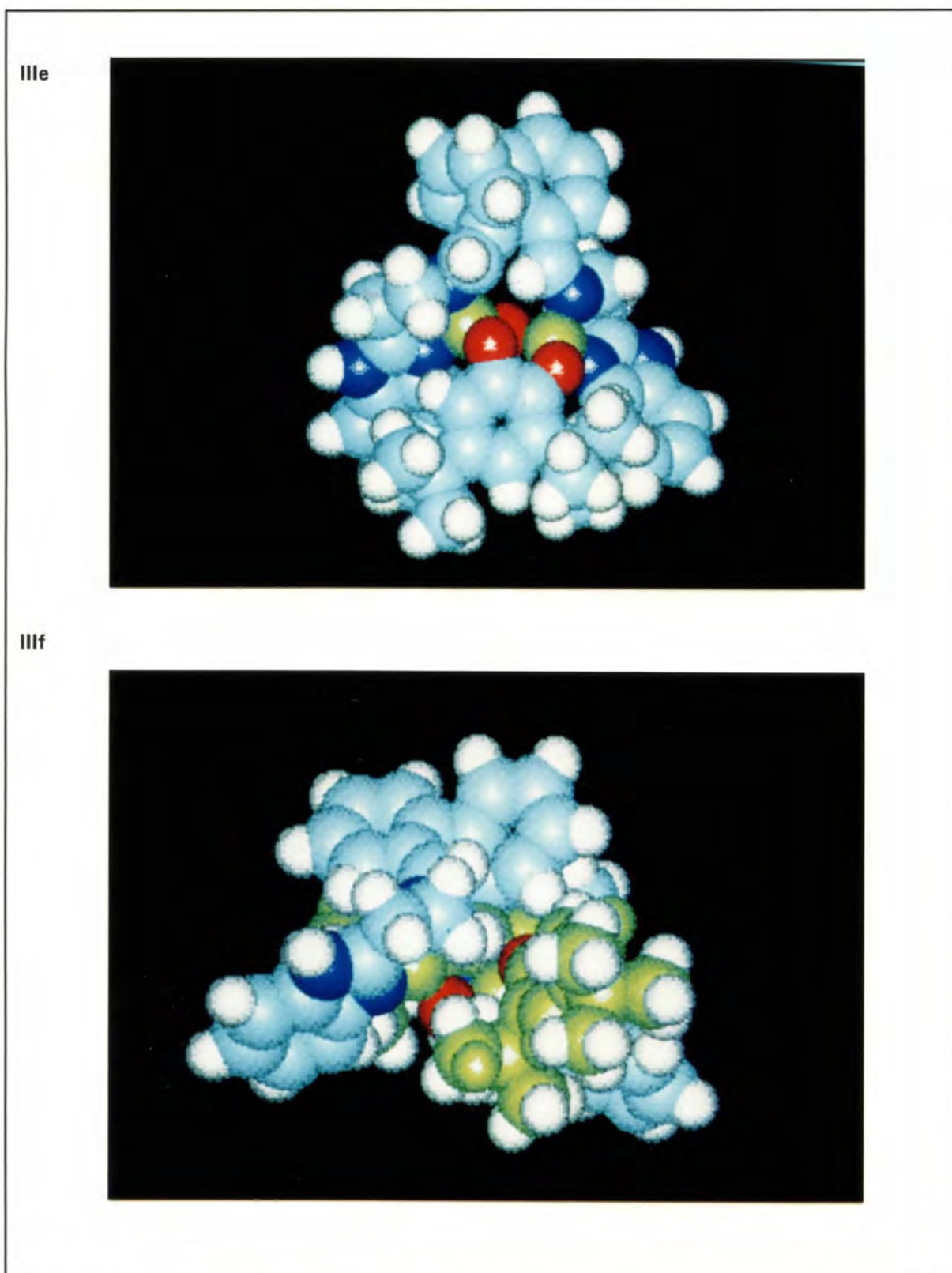


Figure 6.5: Photographs showing models of derivatives of complex III; numbers correspond to Scheme 6.3; blue atoms: carbon; white: hydrogen; red: oxygen; dark blue: nitrogen; yellow: copper. In III f, DTBP is shown in yellow

6.3 CONCLUSION

This theoretical molecular mechanics approach to modelling is, by its very nature, approximate, and can only give an indication of steric and conformational characteristics in molecules. (Only in cases where crystal structure coordinates are available can the structure be truly representative). Nevertheless, it can be deduced that the complexes I, II and III are reasonable structural models of the dinuclear copper site, and that their preparation is justified.

It can also be observed that in the models of the complexes which have a biphenyl spacer, the phenyl rings of the spacer are out of the plane of the oxygen bridging atoms, in contrast to the almost planar situation in models where the spacer is xylene. The biphenyl spacer does appear to be flexible, in that it is bent in the models. Thus, the results of this modelling study support the predictions made in Section 6.1.4.

6.4 EXPERIMENTAL

6.4.1 Modelling with ALCHEMY®

The strain minimisation calculations were performed using a conjugate gradient minimisation method, with the total potential energies E comprising the contributions indicated in equation:

$$E = E_{\text{str}} + E_{\text{ang}} + E_{\text{tor}} + E_{\text{vdW}} + E_{\text{oop}}$$

where E_{str} represents energy strain due to bond stretching

E_{ang} . . . angle bending

E_{tor} . . . torsional deformation

E_{vdW} . . . van der Waals interactions

E_{oop} . . . out of plane bending

For copper (I) and copper (II), the ideal bond length was 1.9Å (Bernhardt *et al.*, 1992), and van der Waals radii of 2.2 and 2.3Å respectively were incorporated into the atomic definition file of the package. Non-bonded interactions involving the metal ions were neglected, following the example of others (Bernhardt and Comba, 1992).

6.4.2 Modelling using HyperChem®

Minimisation calculations were performed with the MM+ program (Allinger, 1977), using a steepest gradient optimisation followed by conjugate gradient (Polak-Ribiere) optimisation. Non-bonded cut-offs with a switched smoothing function were included: inner radius 10Å and outer radius 14Å. A distance-dependent dielectric medium was used, and the calculations were done "*in vacuo*". The program uses bond dipoles as a source of partial atomic charges.

The geometry of the copper (II) ions was specified as tetragonal in the non-oxygenated forms, and trigonal bipyramidal in the derivatives where oxygen and substrate molecules were included. Ideal bond lengths and force constants were included as follows:

Cu(II)-imine Cu-N	1.94Å, 0.6 mdyn.Å ⁻¹
Cu(II)-amine Cu-N	1.97Å, 0.6 mdyn.Å ⁻¹
Cu(II)-heterocyclic Cu-N	1.94Å, 0.6 mdyn.Å ⁻¹ (Bernhardt <i>et al.</i> , 1992)
Peroxide O-O, <i>trans</i>	3.1 mdyn.Å ⁻¹
Peroxide O-O, <i>side-on</i>	2.5 mdyn.Å ⁻¹ (Solomon <i>et al.</i> , 1992).

CHAPTER 7

SYNTHESIS OF BIOMIMETIC COPPER COMPLEXES

7.1 INTRODUCTION

7.1.1 Synthesis of biomimetic dinuclear copper complexes

The design and synthesis of some dinuclear copper complexes was initiated with the aim of producing biomimetic catalysts whose structure, activity, and substrate specificity could be compared with those of tyrosinase itself. From this it might be possible to gain new insights into the structure and function of the enzyme, particularly in relation to its activity in organic medium.

An innovative structural feature reported by Régliez *et al.* (1990), *viz.*, a flexible biphenyl spacer (see Table 7.1), was included in the structure of the organic ligands, thus expanding the range of complexes incorporating this potentially significant unit. The important characteristic of this spacer is that it provides flexibility in the organic ligand, permitting the complex to adopt a conformation in which the two copper ions can be sufficiently close to allow bridging by a dioxygen molecule, without imposing rigid planar geometry. The nature of the hydrocarbon groups linking the coordinating units in dinuclear copper complexes can markedly affect the reactivity of the various complexes (Karlin *et al.*, 1992). Hendricks *et al.* (1982) showed, however, that the linker could be too flexible to allow the binding of a substrate; in complexes which contain the biphenyl spacer, this effect is avoided by having the donor groups relatively closely linked.

The molecular modelling studies on these complexes (see Chapter 6) confirm that non-planar conformations are feasible in terms of steric interactions and bond distortions. Such conformations were also found to allow access for exogenous substrates to the binding site. Since the complexes were likely to adopt non-planar conformations with the arene rings lying outside the coordination plane, the likelihood of hydroxylation of the spacer itself would be small (Sorrell *et al.*, 1991a), and the oxidation of an external substrate might be favoured. This would contrast with the aromatic hydroxylation observed in the case of planar complexes **69** and **70** (see Section 1.4.5), in which the spacer is a xylene ring rather than a biphenyl group (Casella and Rigoni, 1985; Casella *et al.*, 1991a).

The relative rotation of the phenyl rings (Figure 7.1) may contribute some asymmetry to the molecule as a whole, which may influence the preferential binding of the substrate to one copper ion rather than the other. Some asymmetry is suspected in the binding site of tyrosinase, and the phenolic substrate must bind initially to one copper only (Nasir *et al*, 1991, and Pate *et al*, 1989). While it is not known what factors govern the initial binding of substrates to tyrosinase, the complexes reported here may be good structural models for the enzyme in this respect.

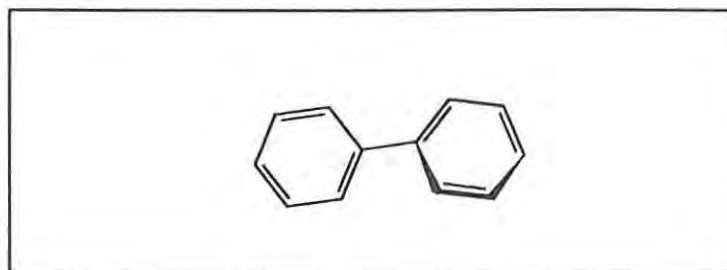


Figure 7.1: Relative rotation of the phenyl rings in the biphenyl spacer

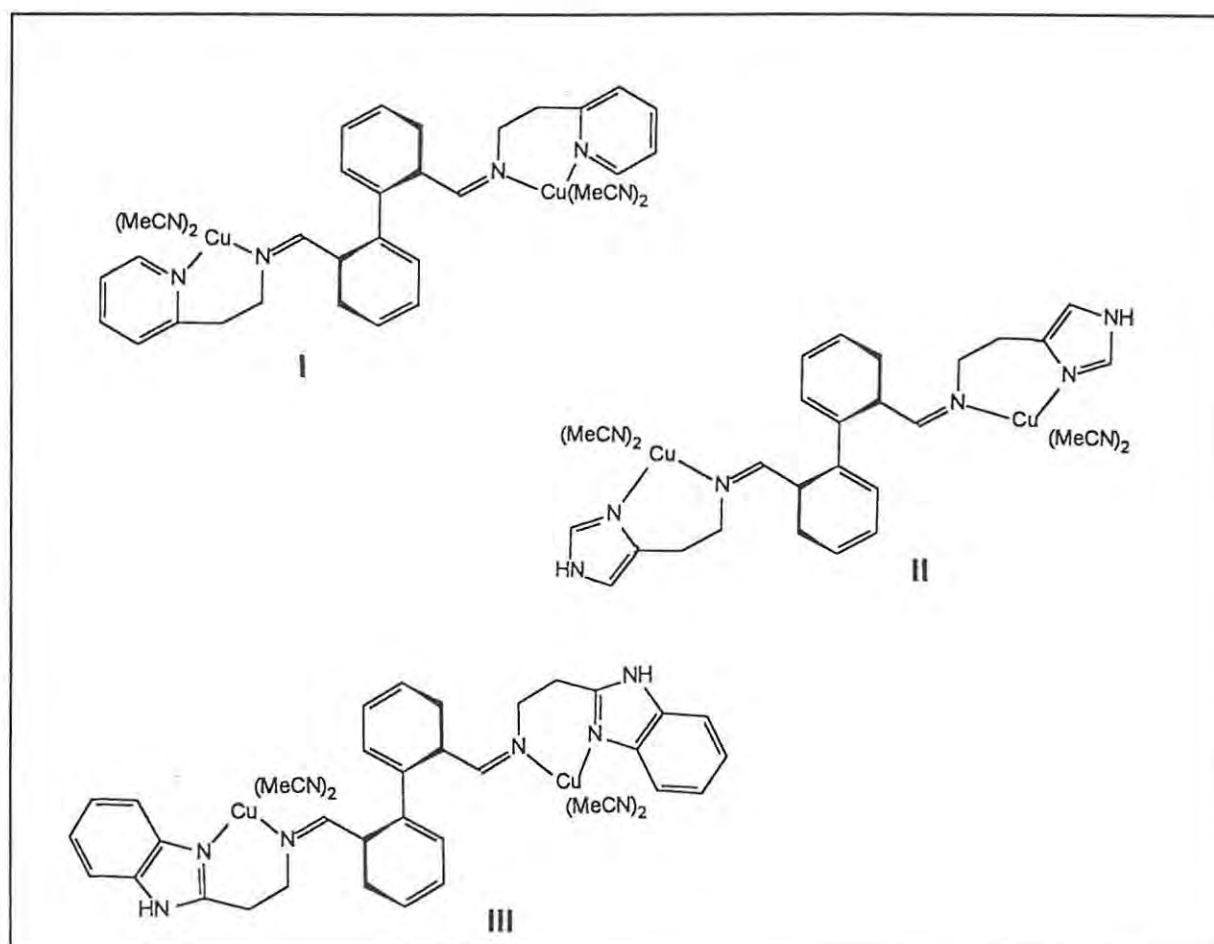


Table 7.1: Structures of complexes I - III, proposed for synthesis

The structures of the complexes chosen to be synthesised are shown in Table 7.1. The complex I was first reported by Réglie *et al.*, (1990), and its synthesis was undertaken partly as an introductory step in establishing the techniques required in the preparation of copper (I) complexes. Also, the new complexes to be synthesised could be compared with this known complex. Since the complexes were intended to mimic tyrosinase, which contains copper (I) ions before it binds oxygen, they were designed to incorporate copper (I) ions. Two different nitrogen donor atoms per copper ion were provided by the ligand: one from the imine group, and one from pyridine, imidazole, or benzimidazole respectively. The electronic characteristics of the nitrogen donors in the different heterocycles provide variation in the electron-availability for donation to the copper ions in the different complexes. The other coordination positions of the copper ions would be occupied by acetonitrile molecules, since this was the solvent used in the synthesis. Acetonitrile is a convenient solvent to use in these syntheses, because it coordinates easily with copper, producing complexes which are generally soluble, but it is also easily replaced by other ligands (Karlin *et al.*, 1988). In haemocyanin, one histidyl imidazole nitrogen is known to be situated further from the copper than the other two imidazole nitrogens (Gaykema *et al.*, 1984), and this is likely to be the case in tyrosinase (Lerch, 1987). Thus, the use of ligands with only two fixed donor atoms is justified (Casella *et al.*, 1991a), and this is further supported by the activity shown by other complexes which have similar configurations (for example, Casella and Rigoni, 1985 and Casella *et al.*, 1988). The complexes each have two copper atoms coordinated in 6-membered rings, which is a stable arrangement for dinuclear copper complexes, and in which the copper readily undergoes changes in oxidation state (Casella *et al.*, 1993).

In the synthesis of metal complexes, a choice must be made between two possible methods: the organic ligand can be synthesised first and the metal ions added later, or a template condensation synthesis can be used. The former method has the advantage that the ligand can be isolated and characterised independently of the metal. This is particularly relevant in cases where the presence of the metal interferes with the analysis eg., a paramagnetic metal, in NMR analyses (see below). In the latter method, the constituents of the ligand are mixed in the presence of the metal ions, and the ligand formation is centred on, and sterically controlled by, the coordination requirements of the metal ion. The template method is not only convenient but, more importantly, the complex will assume a conformation and coordination geometry which is optimal for that metal/ligand combination. Template syntheses lend themselves to the formation of complexes of transition metals such as copper, because the use of d-orbitals in the bonding contributes rigidity to the coordination sphere, and thus allows the metal to govern the geometry of the complex as it forms (Jameson, 1981). Both of these synthetic methods were explored in the present study.

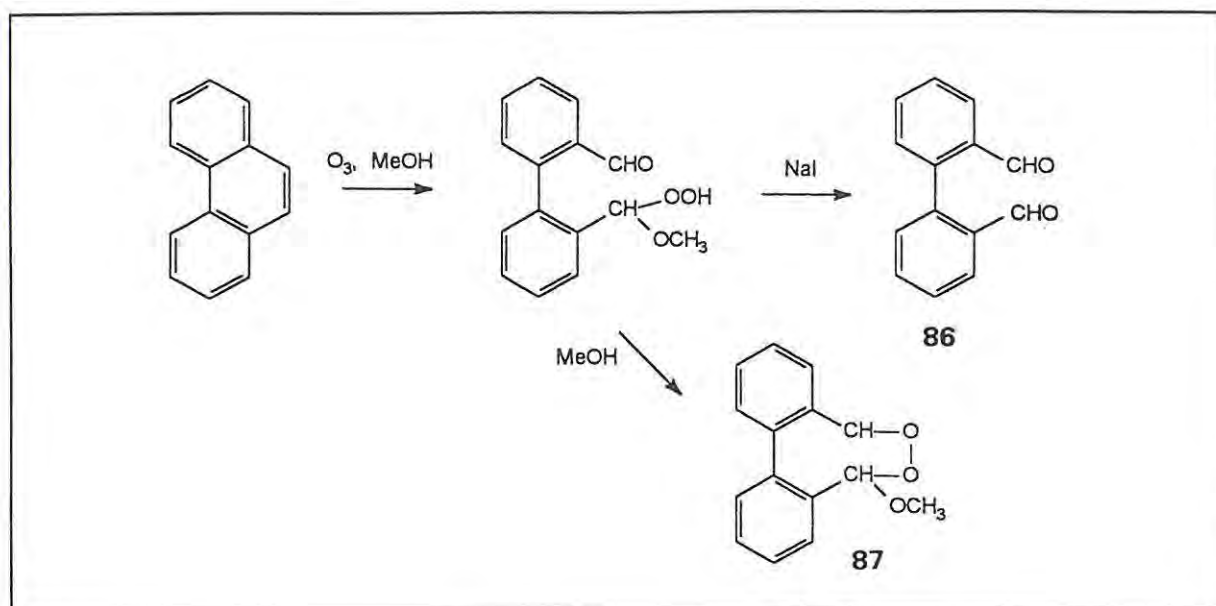
When copper coordinates with donor atoms in an organic ligand system, the chemical shifts in the NMR spectrum of the complex are shifted downfield relative to their positions in the ligand itself, and this serves as a useful indication that coordination is present. The magnitude of the shift is also indicative, to some extent, of the proximity of a particular nucleus to the coordinated copper atom (Karlin *et al.*, 1988). Analysis of copper complexes by NMR is complicated by the fact that copper (II) is paramagnetic and consequently, the signals of the nuclei close to the copper are broadened. This is due to dipolar coupling between the nuclei and the unpaired electron of the copper ion, which leads to increased nuclear relaxation rates. This is obviously not the case for copper (I) compounds, and therefore copper (I) complexes can be analysed by NMR spectroscopy, provided they are not contaminated by oxidation products. The shape of the peaks in an NMR spectrum can also be used as an indication of the state of the complex. In the NMR analysis, it is necessary to use carefully degassed solvents and to exclude air from samples of copper (I) complexes, but deliberate admission of air and re-analysis can be useful in showing changes due to oxidation.

7.2 RESULTS AND DISCUSSION

7.2.1 Syntheses of the copper complexes

7.2.1 (1) Synthesis of biphenyl-2,2'-dicarbaldehyde **86**

The biphenyl dialdehyde **86** was synthesised according to the method of Bailey and Erickson (1961) as shown in Scheme 7.1. The ozonolysis of phenanthrene, in methanol at low temperature gave a peroxide intermediate, which was then reduced with sodium iodide (Section 7.4.1) and the dialdehyde product was isolated by crystallisation. Figure 7.2 shows the ^1H NMR spectrum of the product. The maintenance of a low temperature is necessary to prevent the reaction of the intermediate with methanol to give the peroxide **87**, which is stable.



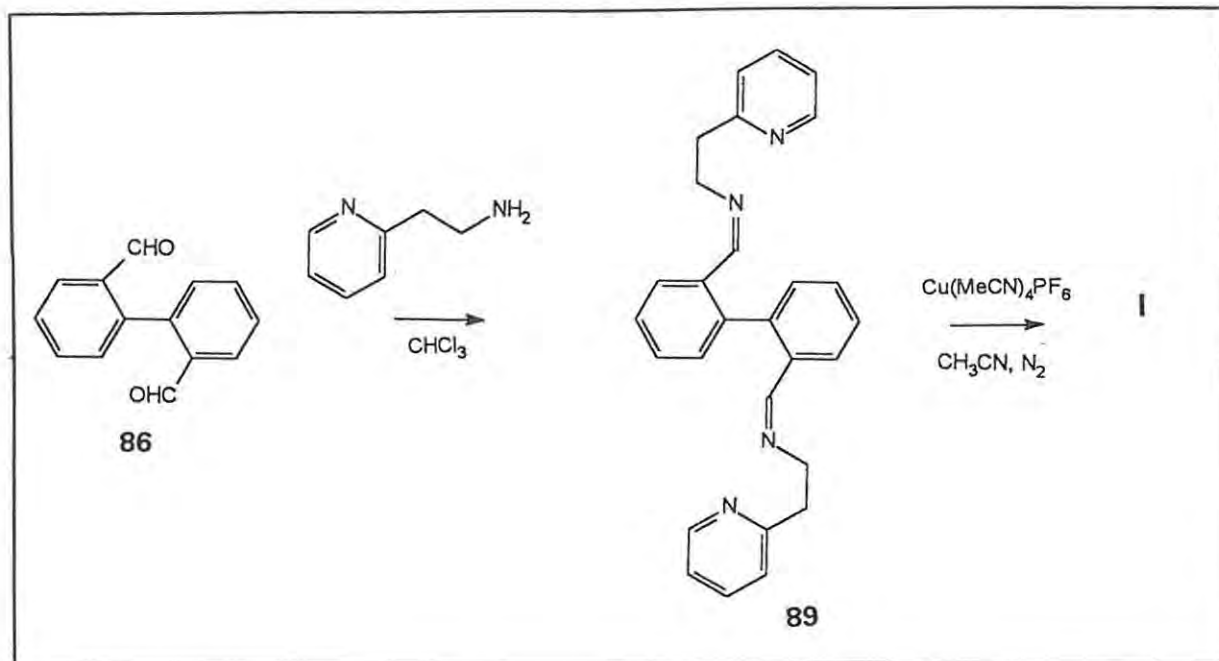
Scheme 7.1: Preparation of biphenyl-2,2'-dicarbaldehyde 86

7.2.1 (2) Synthesis of tetrakis(acetonitrile)copper (I) hexafluorophosphate 88

The salt $[Cu(MeCN)_4][PF_6]$, **88**, in which the complex cation $Cu(MeCN)_4^+$ is stabilised by the large anion PF_6^- , was used as a source of copper (I) for the proposed complexes. This salt is particularly suitable because it is soluble in acetonitrile, and is relatively stable to oxidation in solution. Complex salt **88** was prepared by adding copper (I) oxide to hexafluorophosphoric acid, under an inert atmosphere, using the method of Kubas (1979) (Section 7.4.2). The product was obtained in good yield as a white solid, and was successfully stored at $4^\circ C$ for considerable time.

7.2.1 (3) Synthesis of complex I

The complex I was synthesised using the method reported by Réglie *et al.* (1990) (Scheme 7.2), in which the imine-linked ligand system was synthesised and isolated prior to coordination of the copper (I) ions. The imine-linked ligand system **89** was synthesised by condensation of the dialdehyde **86** with 2-(2-pyridyl)ethylamine (Section 7.4.3). Completion of the reaction was demonstrated by disappearance of the IR $C=O$ absorption band, and the appearance of the $C=N$ band (Figure 7.3). Similarly, the 1H NMR spectrum of the product showed a peak at δ_H 7.9 for the imino-proton and no peak at *ca.* δ_H 10 for residual aldehyde (Figure 7.4).



Scheme 7.2: Preparation of complex I

The complex I was obtained as a dark green solid (Section 7.4.4). The ^1H and ^{13}C NMR spectra of this complex (Figure 7.5) showed a small amount of the dialdehyde starting material (peaks at δ_{H} 7.45, 7.65, 8.05, and 9.85; δ_{C} 127.6, 132.7, 134.2, and 142.1). This seems to indicate some decomposition of the organic ligand during the formation of the complex. A later experiment (Sections 7.4.17 and 9.2.3) showed that the dialdehyde, in the presence of $[\text{Cu}(\text{CH}_3\text{CN})_4][\text{PF}_6]$, did not interfere with the catalytic activity of the complex. In common with the original authors, numerous and varied attempts to recrystallise the complex (see Section 7.4.4) met with little success and, therefore, the solid-state structure of the complex could not be elucidated by X-ray crystallography.

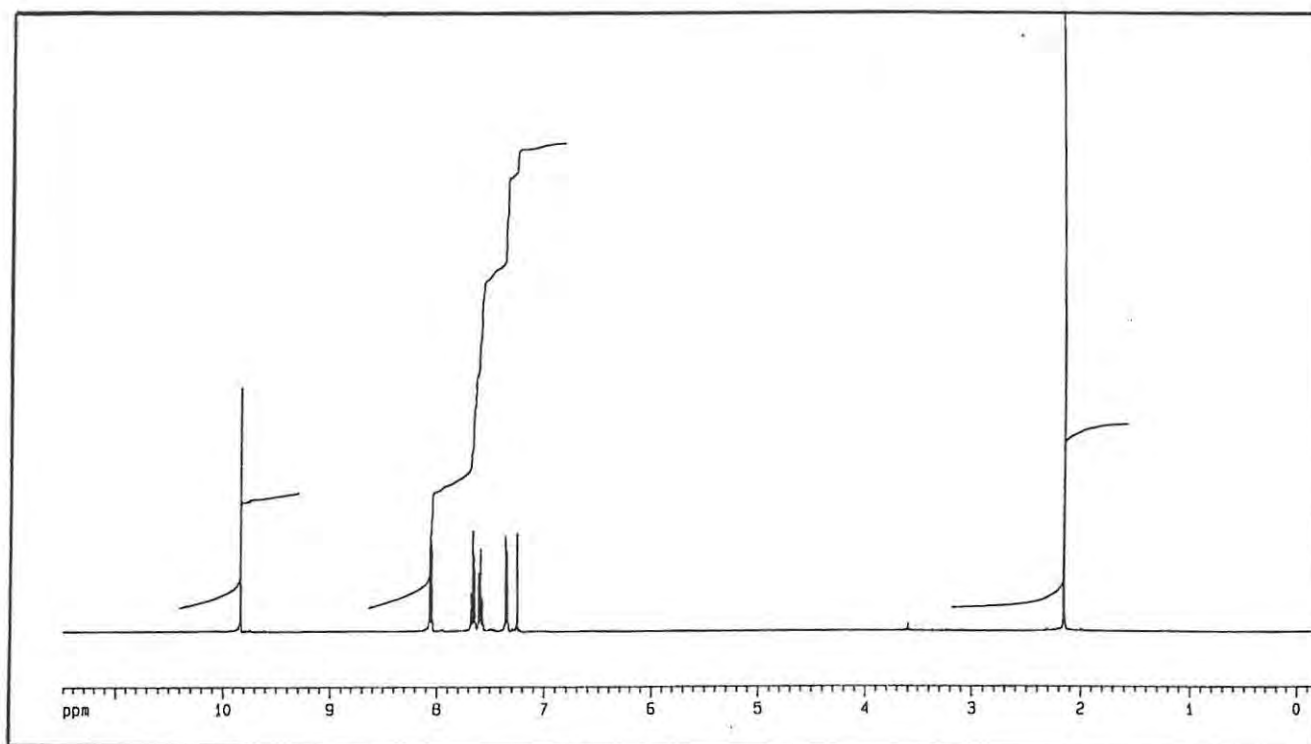


Figure 7.2: ^1H NMR spectrum of biphenyl-2,2'-dicarbaldehyde 86

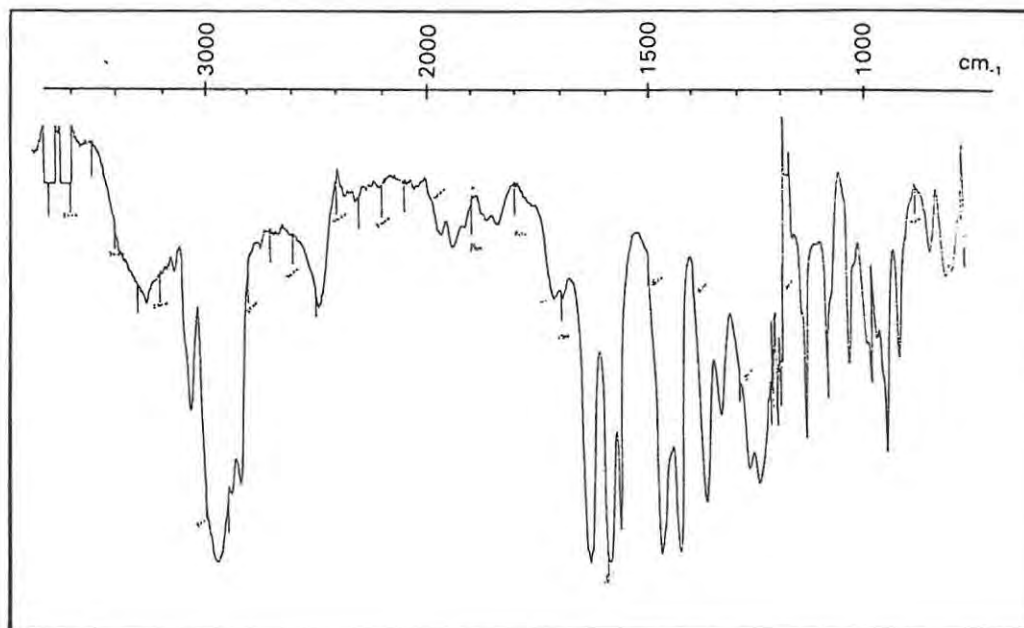


Figure 7.3: IR spectrum of ligand 89, used to prepare complex I

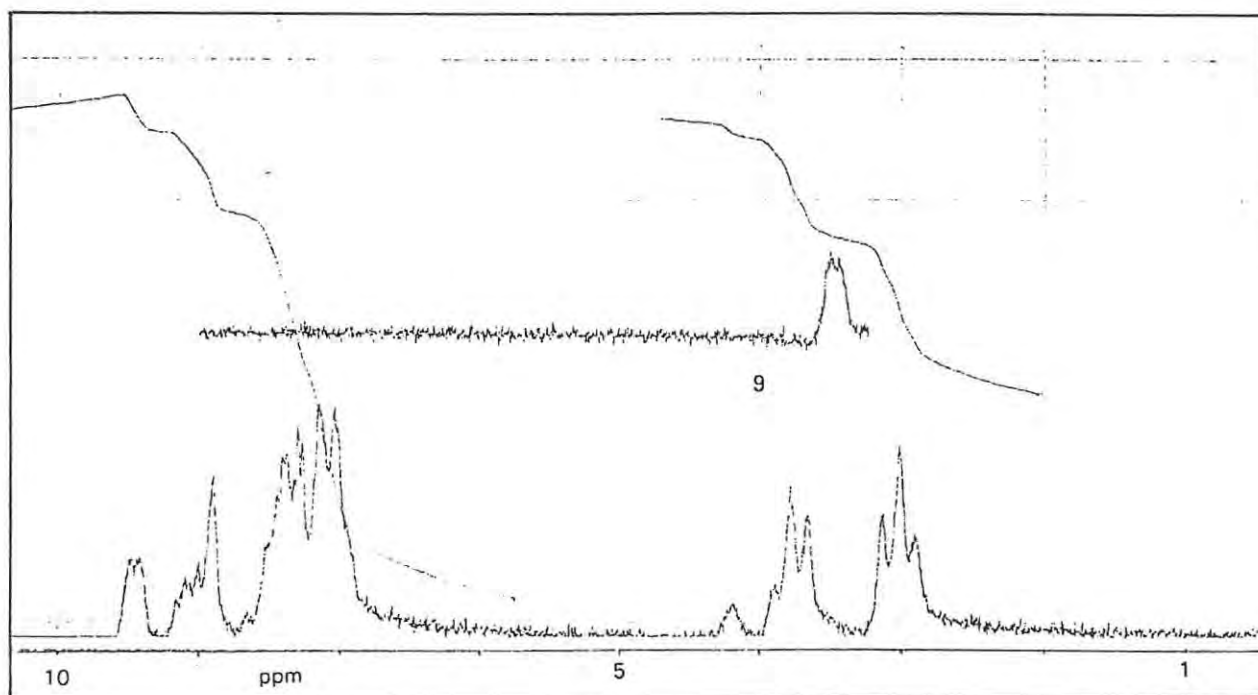


Figure 7.4: 60 MHz ^1H NMR spectrum of ligand 89

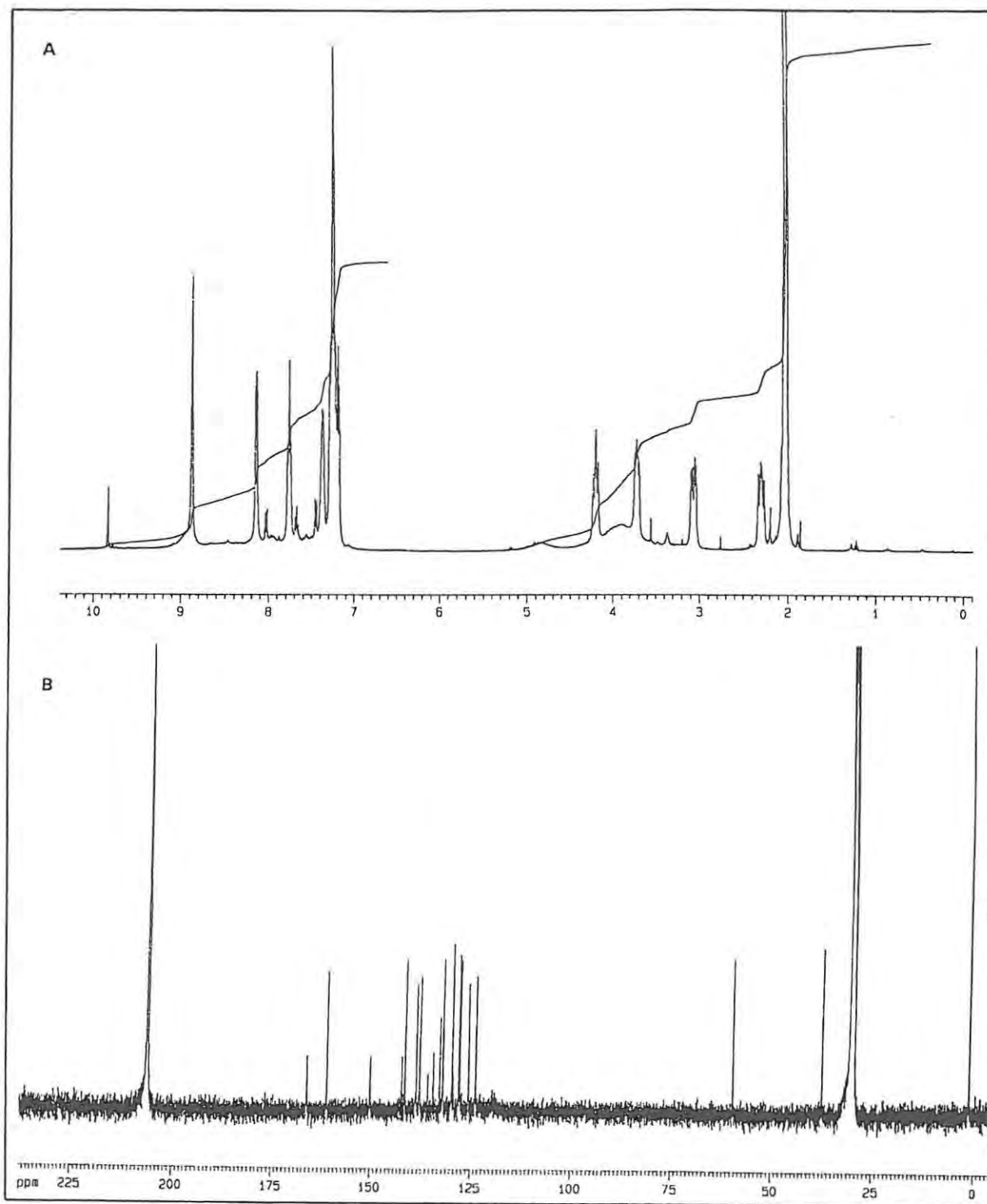
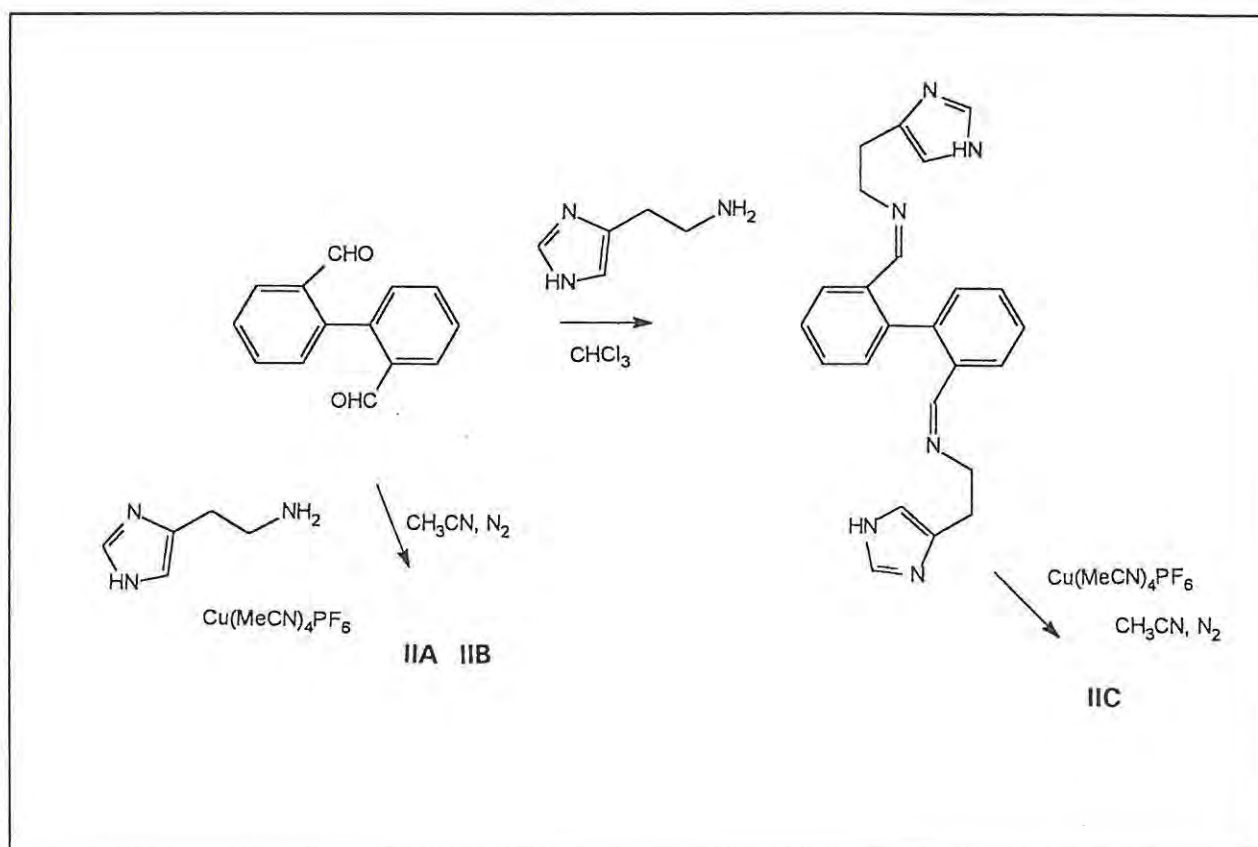
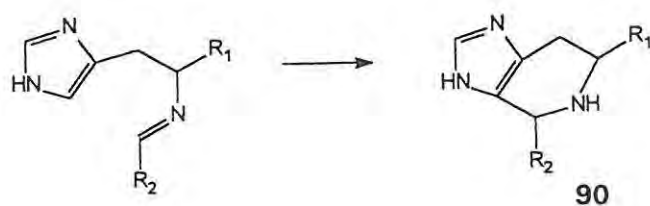


Figure 7.5: ^1H NMR spectrum (A) and ^{13}C NMR spectrum (B) of complex I

7.2.2 Synthesis of complex II

7.2.2 (1) Synthesis of Complexes IIA and IIB by template condensation

Since histidyl-imidazole residues are implicated in the coordination of copper in haemocyanin and tyrosinase, it was logical to attempt to synthesise the complex II, which has imidazole donor groups (see Table 7.1, Section 7.1.1). Imidazole systems are known to present certain synthetic difficulties, however, since they commonly cyclise to form products such as **90**, described by Casella *et al.*, (1988). One method of avoiding this complication is to use a metal template condensation synthesis (as discussed in Section 7.1), and complexes IIA and IIB was synthesised by this method (Scheme 7.3).



Scheme 7.3: Preparation of complexes IIA - IIC

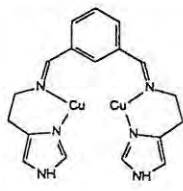
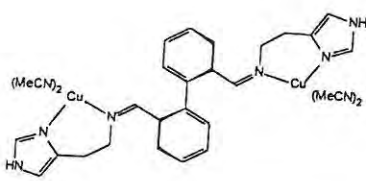
The method described above [Section 7.2.1 (3)] was adapted, for the syntheses of complexes containing imidazole donor groups, by using histamine as the amine in the condensation reaction which formed the ligand (Scheme 7.3). In an initial attempt, histamine (liberated from its hydrochloride salt, see Section 7.4.5) was combined with diphenyl-2,2'-dicarbaldehyde and $[\text{Cu}(\text{CH}_3\text{CN})_4][\text{PF}_6]$ in dry degassed acetonitrile, and the mixture was stirred for three hours (Section 7.4.6). During this time, however, the colour of the solution changed from yellow, at the beginning, to blue, indicating that the copper had been oxidised, probably due to incomplete exclusion of oxygen from the system. After storage for 24 hours at 4°C, a blue precipitate, complex **IIA**, was filtered off and dried. Attempts to recrystallise the product were unsuccessful; colourless crystals were obtained from hexane/acetonitrile, but these were found to be non-organic (from the lack of ^1H NMR signals) and were possibly a $\text{Cu}(\text{PF}_6)_2/\text{acetonitrile}$ complex, as suggested for a similar reaction (Sorrell, 1991b).

The second procedure used to synthesise complex **IIB** *via* a template synthesis involved only fifteen minutes' stirring, and gave a pale yellow/green precipitate which was separated by decantation of the solvent (Section 7.4.7). Attempts at recrystallisation were again unsuccessful.

The IR spectra of the two products were very similar (Figure 7.6), but the ^1H NMR spectra showed distinct differences (Figures 7.7 and 7.8). Complex **IIA** was blue, indicating a copper (II) species, and as such, would be expected to show the broad NMR peaks observed at δ_{H} 7.19 and 8.42 in Figure 7.7. The sharper peaks in the spectrum were attributed to the presence of the corresponding copper (I) complex in the crude product. While the signal at δ_{H} 9.75 is attributable to the imidazole NH, the sharp peak at δ_{H} 9.83 is probably due to aldehydic protons, indicating the presence of some residual starting material.

From its NMR spectrum (Figure 7.8), the complex **IIB** was shown to be the desired product. Its low solubility and stability make it difficult to obtain good spectra and some small baseline peaks suggest the presence of impurities, but the major peaks correlate well with the spectrum reported for the analogous complex **91** (Casella *et al*, 1988), as shown in Table 7.2.

Table 7.2: ^1H NMR spectral data for Complexes IIB and 91

Complex	^1H NMR peak	Assignment
 <p style="text-align: center;">91</p>	2.95 3.97 6.95 7.3-7.85 8.30 8.45 10.4	CH ₂ CH ₂ Imidazole 5-H Aromatic Imidazole 2-H H-C=N Imidazole NH
 <p style="text-align: center;">IIB</p>	3.50 3.92 6.91 7.13-7.65 8.53 10.15	CH ₂ CH ₂ Imidazole 5-H Aromatic Imidazole 2-H H-C=N Imidazole NH

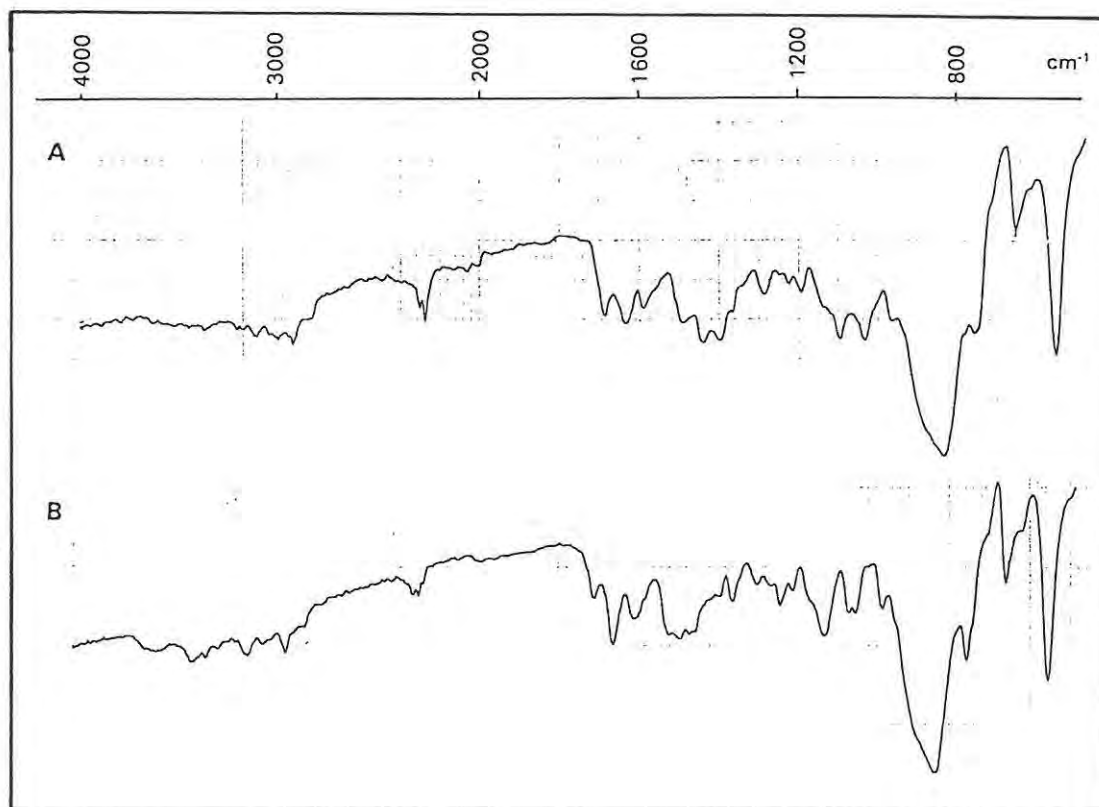


Figure 7.6: IR spectra of complex IIA (A) and complex IIB (B)

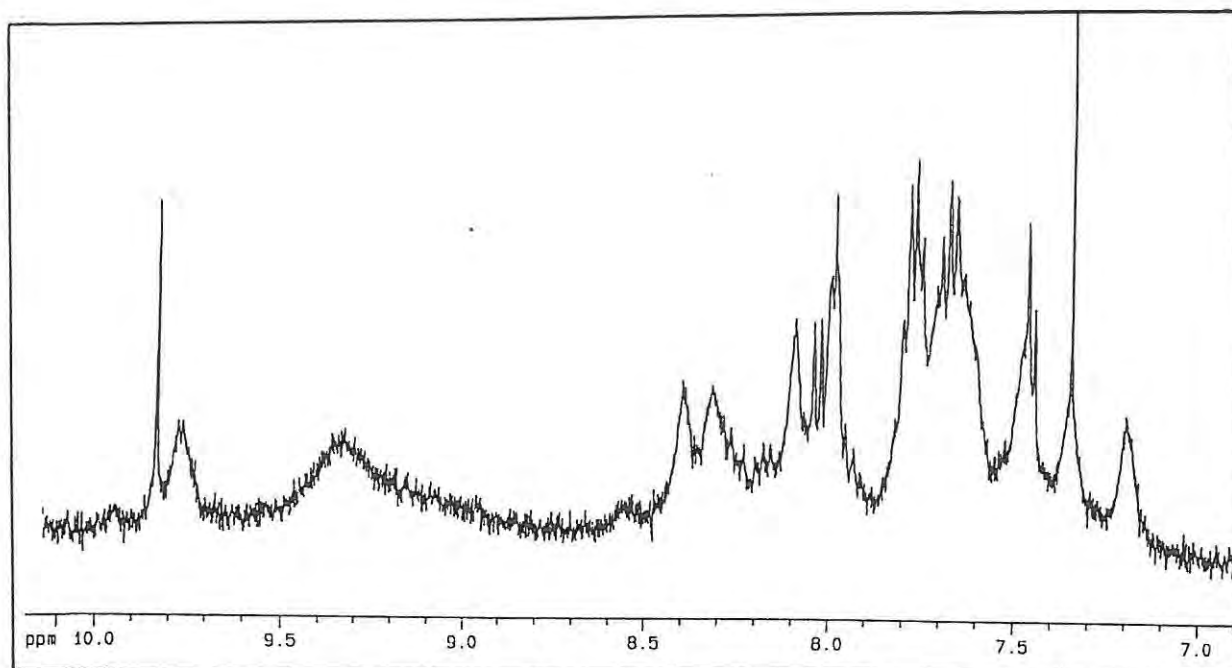


Figure 7.7: ^1H NMR spectrum of complex IIA

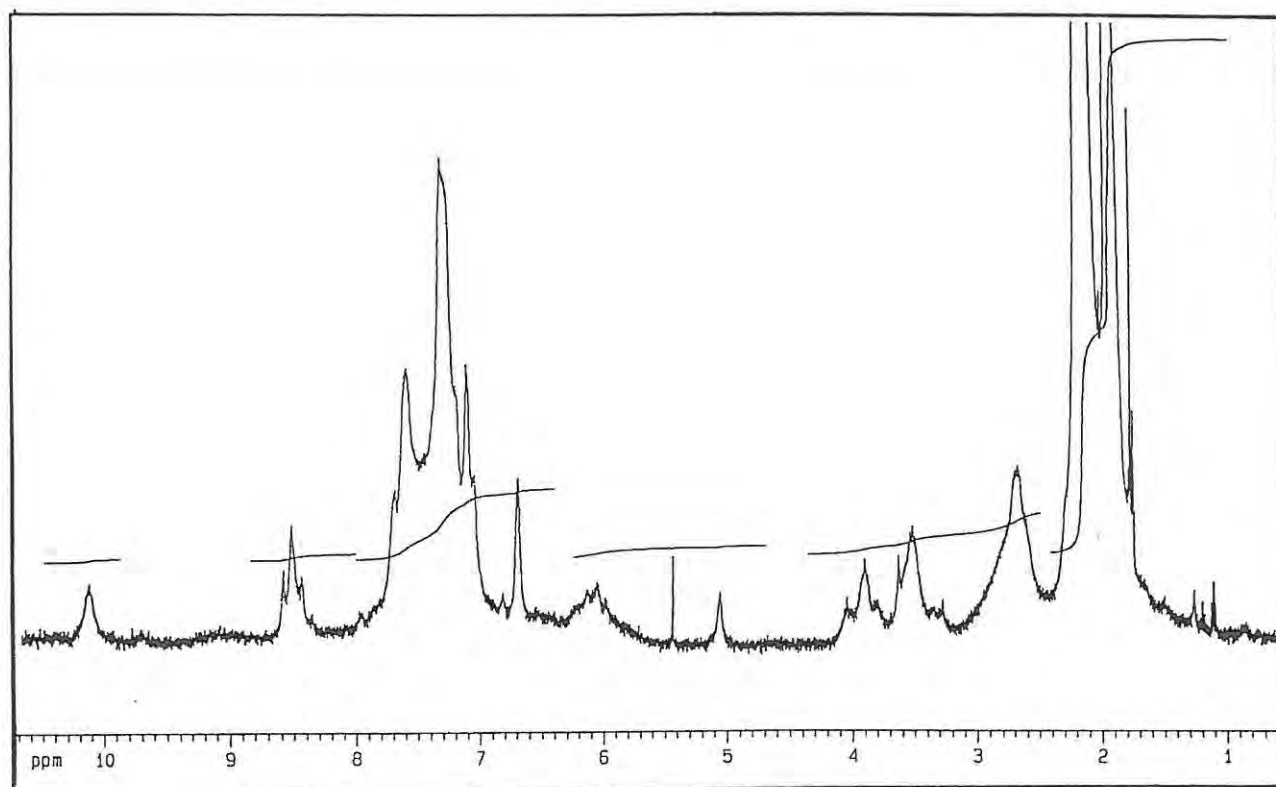
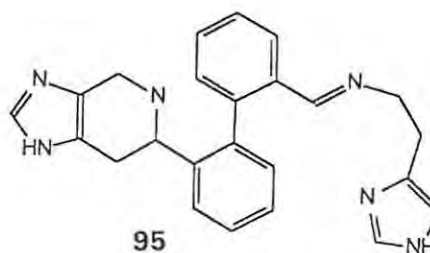
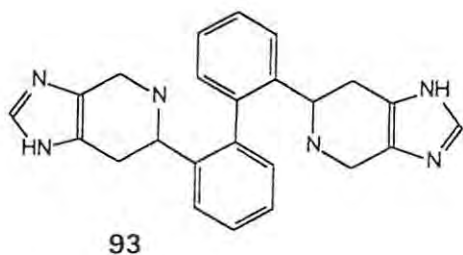


Figure 7.8: ^1H NMR spectrum of complex IIB

7.2.2 (2) Synthesis of the ligand 92

The synthesis of ligand **92** was attempted in order to compare the complex **IIB**, prepared by template synthesis, with the corresponding complex **IIC** obtained *via* the intermediate ligand (Scheme 7.3). Histamine was liberated from its hydrochloride salt, and reacted with biphenyl-2,2'-dicarbaldehyde **86** (Section 7.4.8), with the expectation that an imine would form by a condensation reaction. The crude product obtained was purified by flash chromatography and preparative TLC, but comparison of the crude and purified products by ^1H NMR spectroscopy (Figures 7.9 and 7.10) showed that some decomposition occurred during the purification, resulting in the presence of some of the dialdehyde starting material (as indicated by the aldehydic signal at δ_{H} 9.9). More significantly, the appearance of a peak at δ_{H} 5.96 indicates the presence of the ArCH-N group in the cyclised product **93** (Casella *et al*, 1988). However, the histamine-imidazole 5-H signal is present at δ_{H} 6.86, and the signal at δ_{H} 8.1 is probably the imine-proton peak (both indicating the presence of the non-cyclised product **92**), so the cyclisation appears to have occurred only partially.

The crystalline product **94**, obtained by recrystallisation of a second preparation of the ligand, was analysed using 1-D and 2-D NMR spectroscopy (Figure 7.11). The ^1H NMR spectrum of this product showed some differences from that of the ligand **92**. These were, notably, the absence of the peak at δ_{H} 5.9 and the presence of a peak at δ_{H} 6.11, correlating with a carbon nucleus at δ_{C} 69.37 (correlation by HETCOR). This latter ^1H NMR peak was also present in the spectrum of the crude material (Figure 7.9), but was much smaller in the spectrum of the chromatographically-purified product. These differences could indicate that two different cyclisations occur, to give the two products, **93** and **95** (shown below) both of which contain a ArCH-N group which would give a signal at *ca.* δ_{H} 6. The compound **94** could be one of these, since if only one of the imidazole rings in the ligand molecule was involved in a cyclisation, there would be a sufficient number of different carbon nuclei to account for the number of signals in the ^{13}C NMR spectrum of this product.



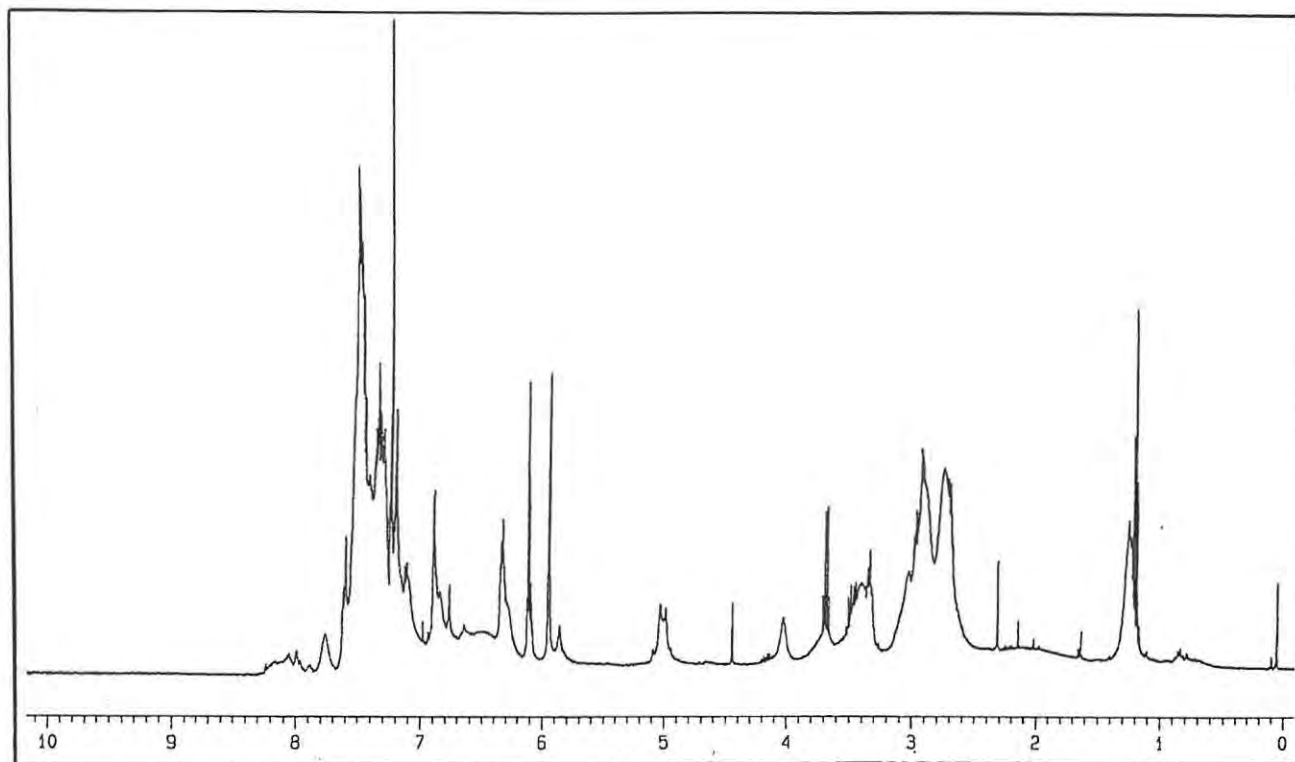


Figure 7.9: ^1H NMR spectrum of crude ligand 92

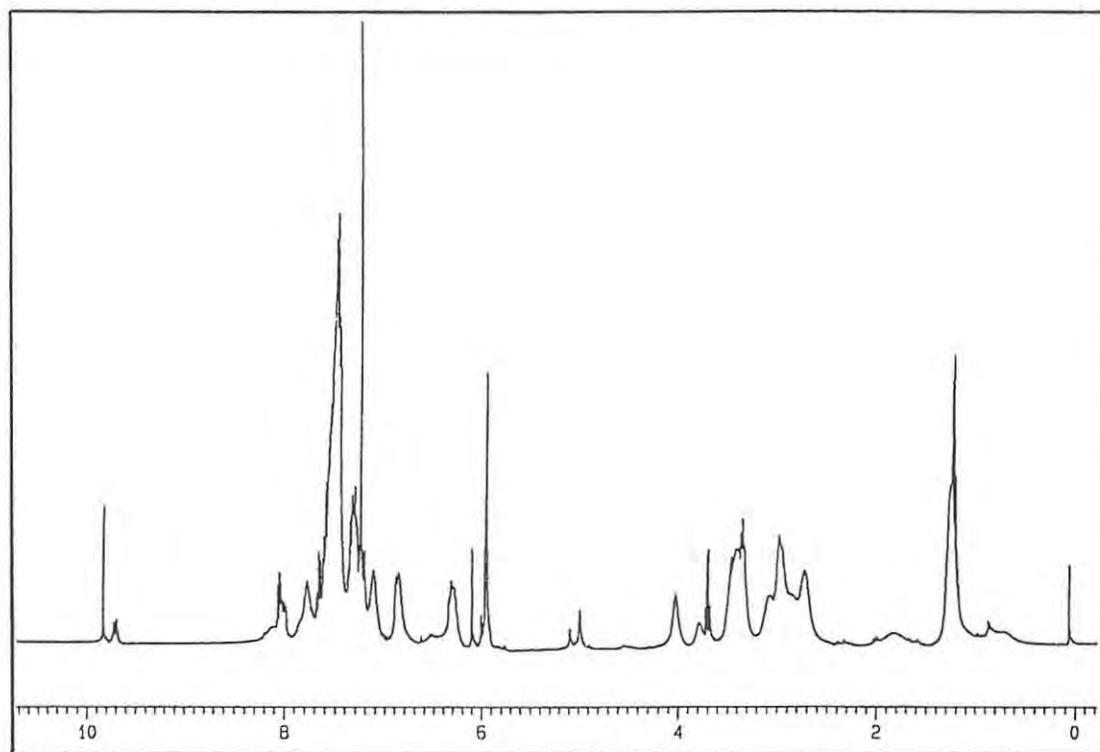


Figure 7.10: ^1H NMR spectrum of ligand 92 after purification by flash chromatography

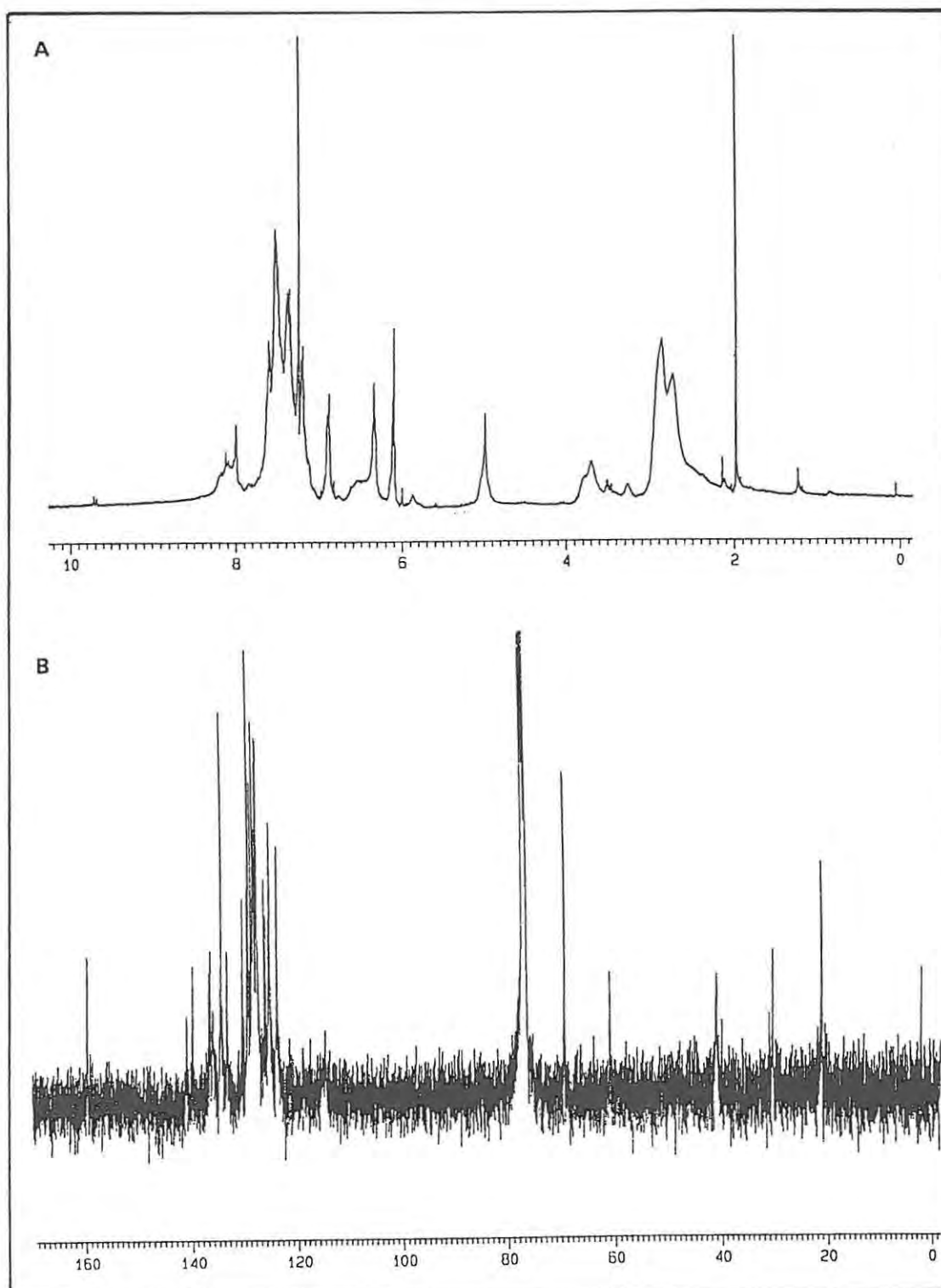


Figure 7.11: ^1H NMR spectrum (A) and ^{13}C NMR spectrum of ligand 94

7.2.2 (3) Synthesis of complex IIC from ligand 92

The ligand **92**, produced as described above, was reacted with $[\text{Cu}(\text{CH}_3\text{CN})_4][\text{PF}_6]$ (before its partially cyclised nature was elucidated) to form a complex, **IIC**, which precipitated from acetonitrile. The ^1H NMR spectrum of this complex suggests partial oxidation of the copper since some broad peaks were observed (Figure 7.12), while the sharper peaks can be assigned to the copper (I) form. The downfield shift of the peaks of the complex, in comparison to those of the ligand, indicate coordination of the copper ions. The broad peak at δ_{H} 9.95 may be attributed to an NH proton (see Table 7.2 above). Unfortunately, contaminants in the deuterated acetone precluded the identification of methylene signals in this spectrum, because the solution was so dilute. However, the spectrum of the complex in deuterated acetonitrile did show methylene signals at δ_{H} 2.43, 3.55 and 3.65; in this case, the aromatic region was less well resolved (Figure 7.13).

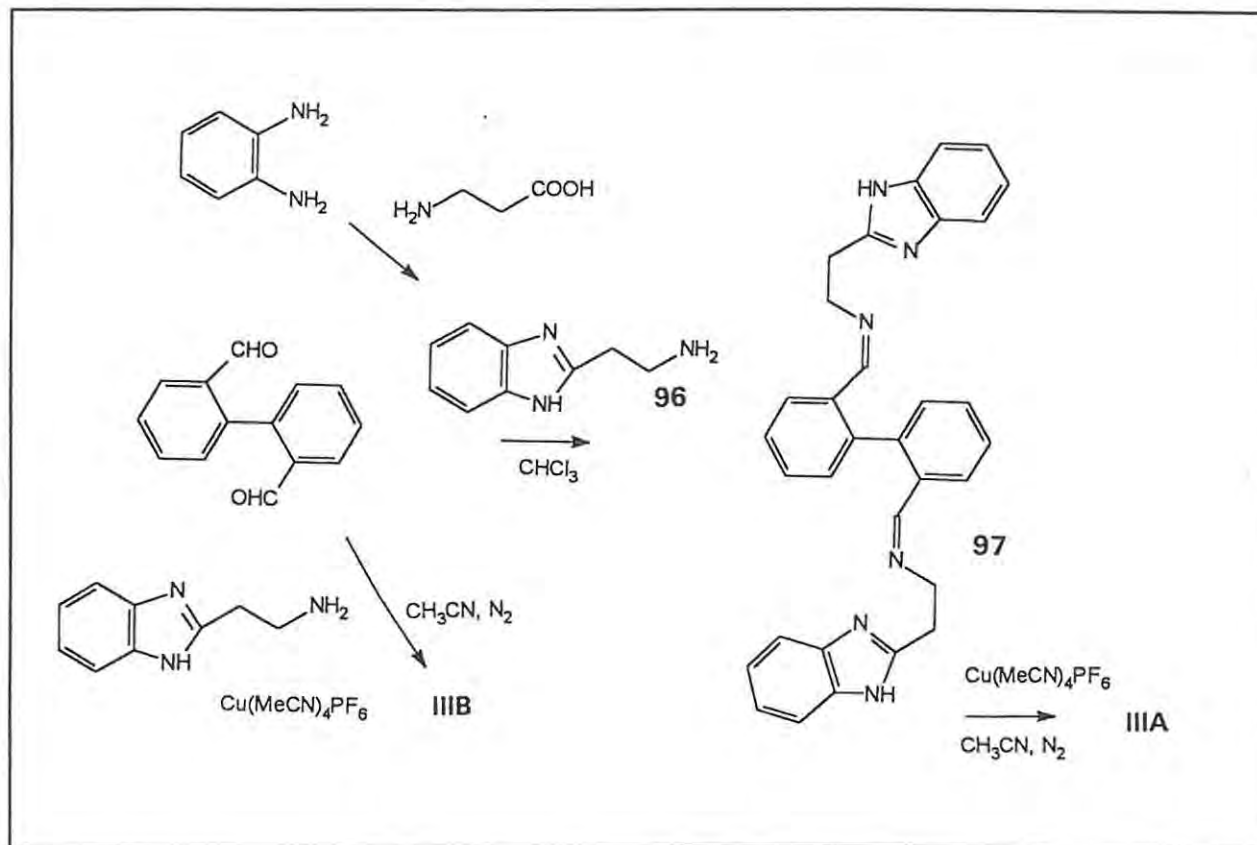
7.2.3 Synthesis of complex III

Ligand systems with benzimidazole donor groups are synthetically more accessible than those with imidazole groups, since the possibility of cyclisation is lessened. The synthesis of complex **III**, in which the imidazole groups of complex **II** are replaced by benzimidazole groups, was therefore undertaken. This strategy offers additional advantages in that the greater steric bulk of the benzimidazole groups might increase the stability of the complex and facilitate crystallisation. Also, the steric bulk could offer a protective envelope to help stabilise the binding of small molecules by the complex, in much the same manner as the protein pocket of the enzyme does, making it a more effective catalyst (Berends and Stephan, 1987 and Pandiyan *et al*, 1992). The energy advantage of π -stacking between the benzimidazole rings and a phenolic substrate would also be greater than in the case of pyridine or imidazole donor groups, which might further enhance the catalytic ability of complex **III** (Masuda *et al*, 1989).

7.2.3 (1) Synthesis of the ligand 97

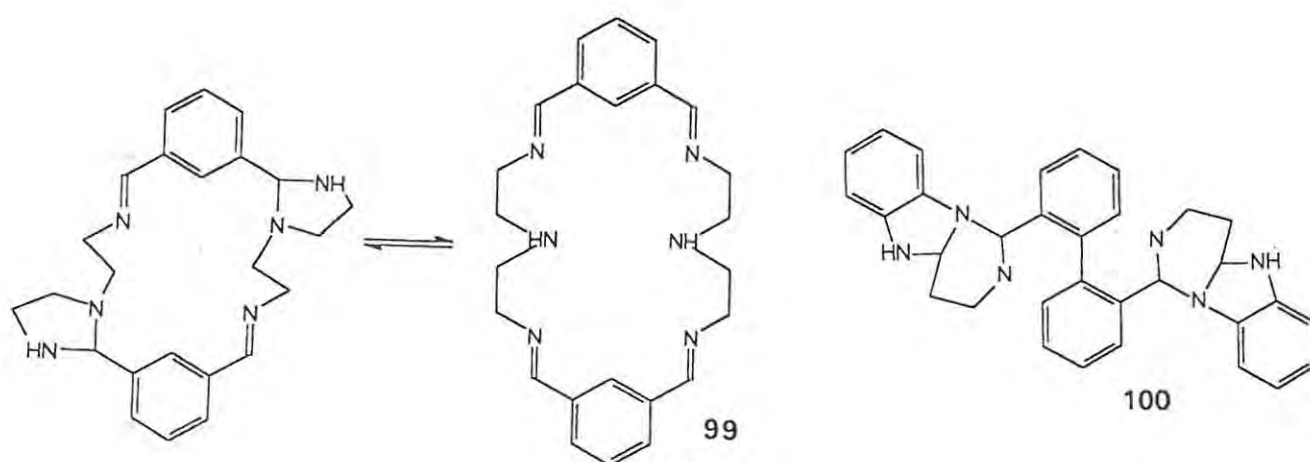
The organic ligand **97** was synthesised according to Scheme 7.4, using 2-(2-aminoethyl)benzimidazole **96**, which was prepared by adapting the method of Casella *et al*, (1991a). Here, β -alanine was condensed with 1,2-diaminobenzene, in hydrochloric acid solution, and the amine **96** was obtained as the hydrochloride salt (Section 7.4.11). It was liberated from the salt using sodium methoxide in dry ethanol, because it is soluble in water and, therefore, could not be precipitated by basification. (The ^1H NMR spectrum of the product is shown in Figure 7.14).

This amine was then condensed with biphenyl-2,2'-dicarbaldehyde, to form the ligand **97** (Section 7.4.12). The ^1H NMR spectrum of the product **97** is shown in Figure 7.15; the lack of an aldehyde proton signal near δ_{H} 10 and the presence of the imine-proton signal at δ_{H} 7.82 indicated successful reaction.



Scheme 7.4: Preparation of complexes **IIIA** and **IIIB**

When this synthesis was repeated, however, the crude product was recrystallised (Section 7.4.13) and the NMR spectra showed that the structure of the crystallised product **98** was not the same as that of **97** (Figure 7.16). Peaks in the ^1H NMR spectrum at δ_{H} 6.07, 6.30 and 6.49 suggest the presence of CH-N groups in the structure. Menif *et al.*, (1990) described the isomerisation of a macrocyclic ligand **99**, as shown below, and an analogous isomerisation in the ligand system **97** would produce the derivative **100**. This gives a feasible explanation for the structure of the recrystallised ligand obtained here.



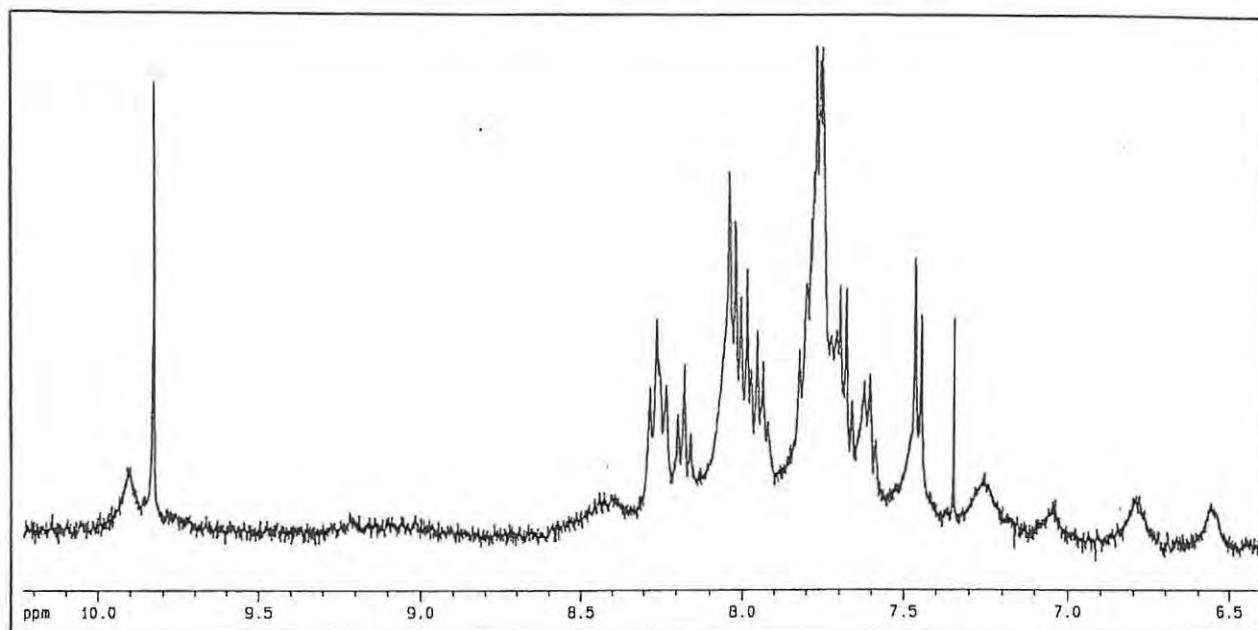


Figure 7.12: ¹H NMR spectrum of complex IIC in CD₃COCD₃

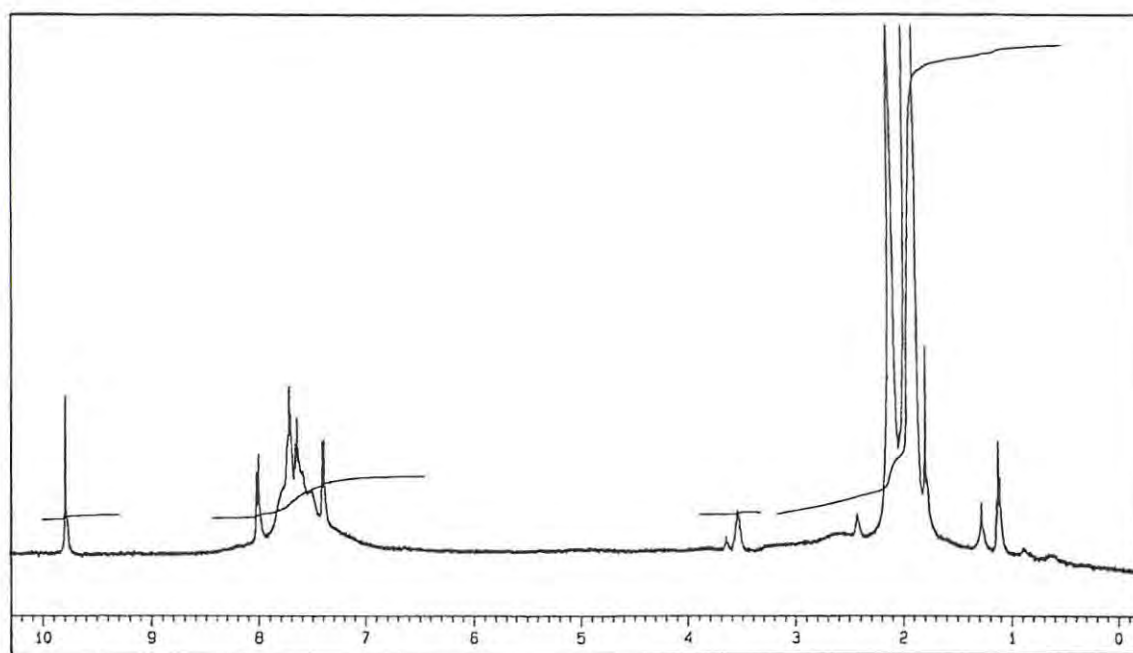


Figure 7.13: ¹H NMR spectrum of complex IIC in CD₃CN

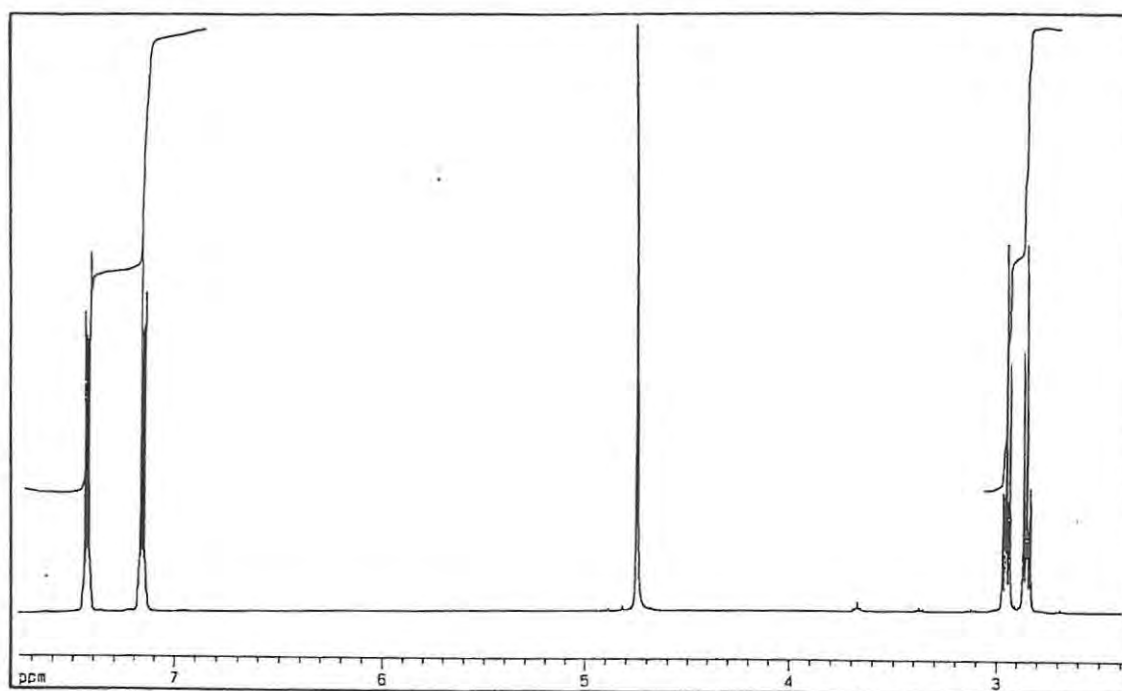


Figure 7.14: ^1H NMR spectrum of 2-(2-aminoethyl)benzimidazole 96

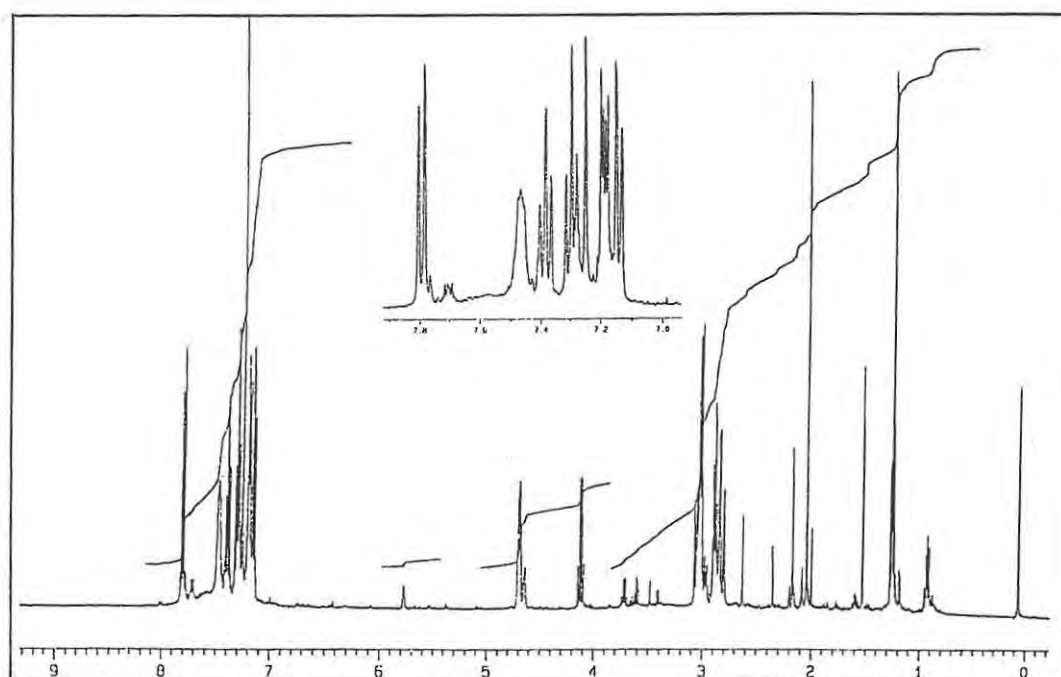


Figure 7.15: ^1H NMR spectrum of ligand 97

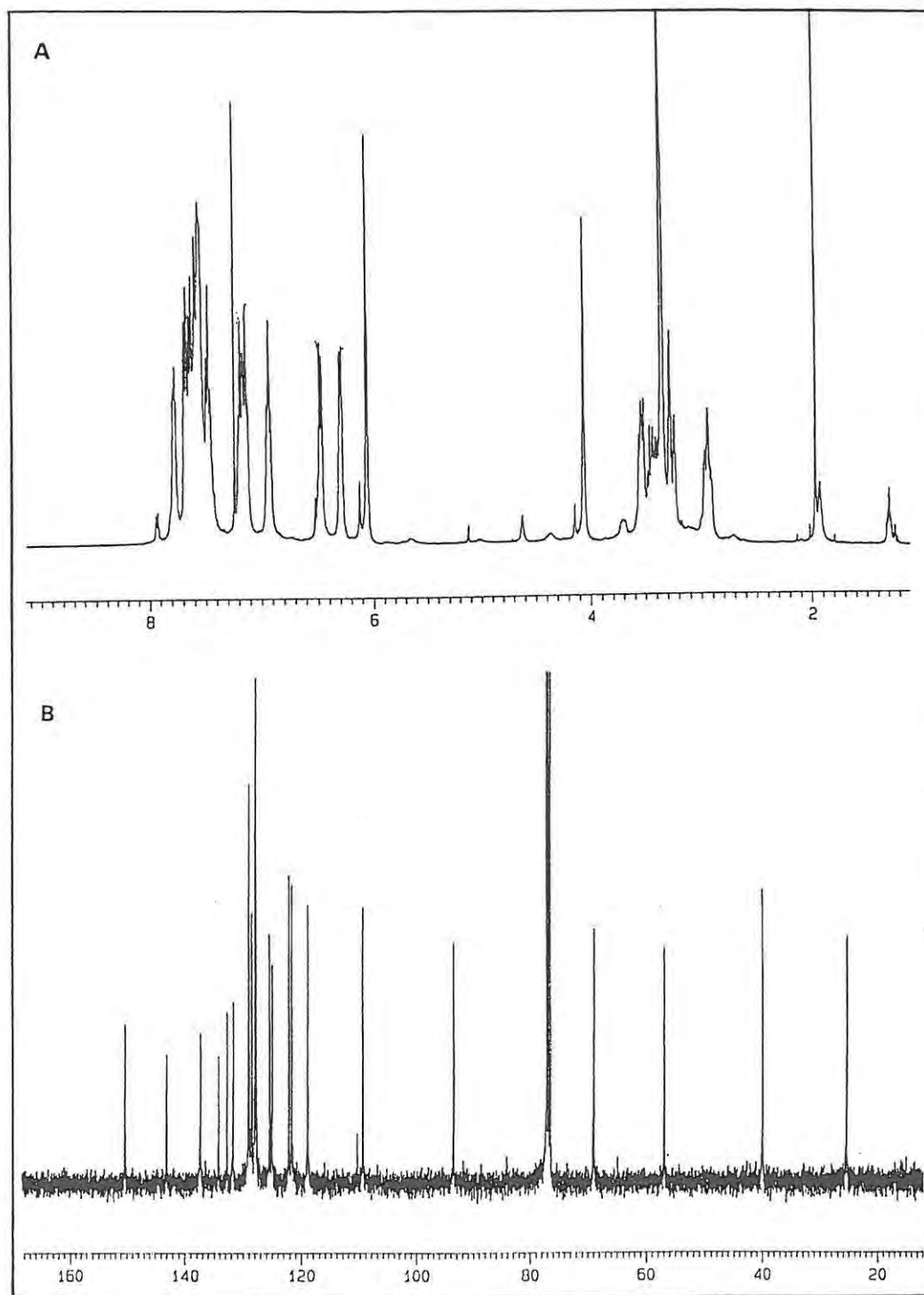


Figure 7.16: ^1H NMR spectrum (A) and ^{13}C NMR spectrum (B) of ligand 98

7.2.3 (2) Synthesis of complex IIIA

The ligand system **97** was used to prepare a copper (I) complex, **IIIA**, by the same method as before (Section 7.4.14 and Scheme 7.4). The complex **IIIA** was obtained as a pale yellow-green powder which again could not be crystallised satisfactorily for X-ray diffraction analysis. However, the NMR analysis correlated well with the proposed structure except for the absence of an imine-proton signal at *ca.* δ_{H} 8.5 (Figure 7.17). The signals due to the methylene and aromatic protons were all shifted downfield by coordination with copper, and the relative sharpness of the peaks confirms the +1 oxidation state of the metal. The structure of this complex was tentatively assigned as the copper (I) complex of ligand **98**; the peaks at δ_{H} 4.6 and δ_{C} 62.8 were assumed to be due to an impurity.

Thus, it would seem that compound **97** was the desired organic ligand, but that it decomposed, at least to some extent, in the preparation of the complex **IIIA**. The structure of **98** appears to be similar to that of the complex **IIIA**, which could be a cyclised derivative of the desired material. The ^1H NMR spectra of this complex were also obtained in deuterated methanol and dichloromethane (Figures 7.18 and 7.19), and the marked differences show the effects of different solvents on the appearance of the spectra. When oxygen was admitted to the methanolic solution, the resolution of the peaks was lost (Figure 7.18B) due to formation of the paramagnetic copper (II). This oxidation occurs most readily in protic solvents such as methanol. Also notable was the change in the spectrum in dichloromethane when oxygen was added and the mixture allowed to react for two hours (Figure 7.19B). Several new peaks developed, including one attributable to an aldehydic proton at δ_{H} 9.0, which suggests that the complex decomposed partially in this solvent.

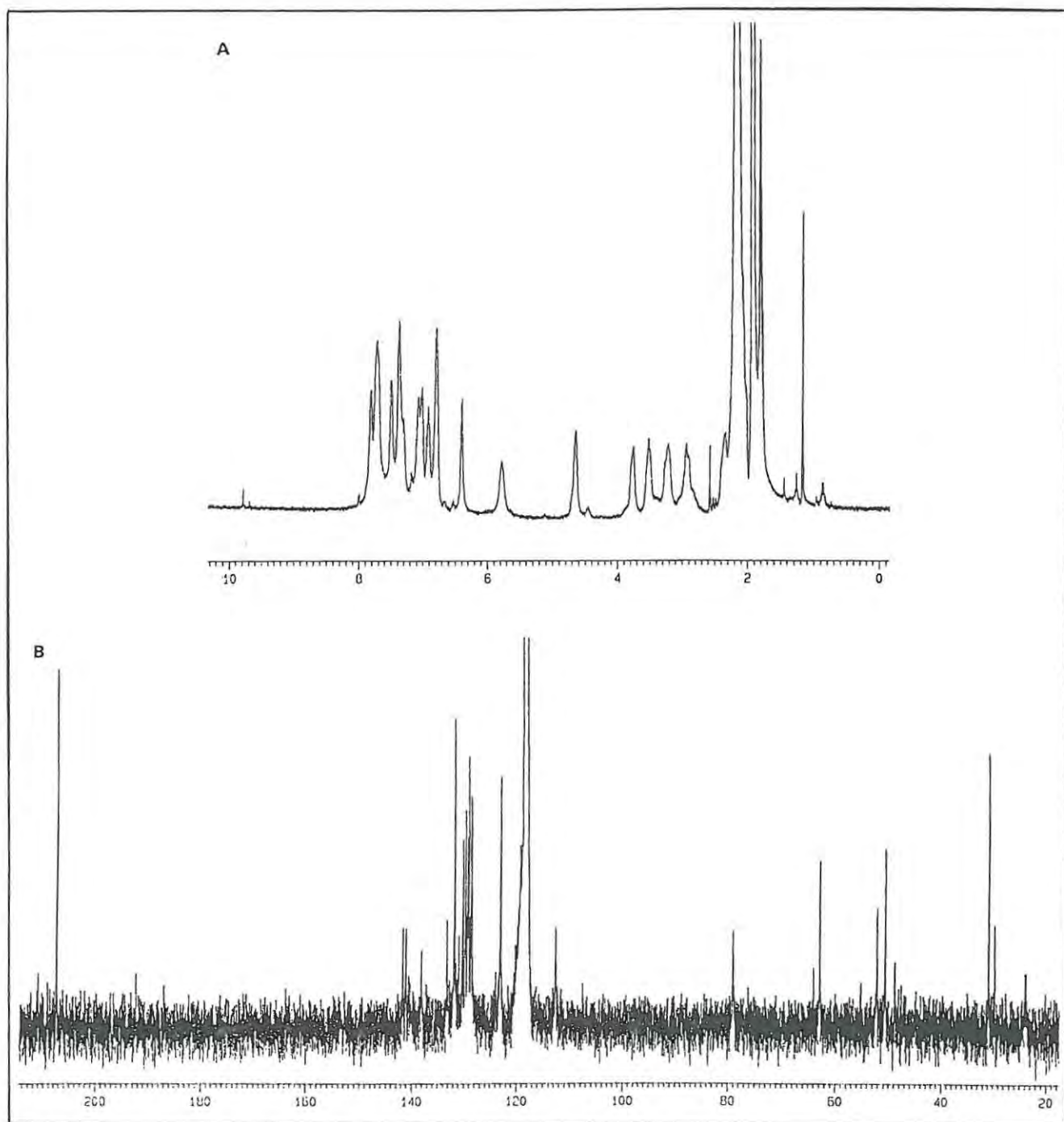


Figure 7.17: ¹H NMR spectrum (A) and ¹³C NMR spectrum of complex IIIA in CD₃CN

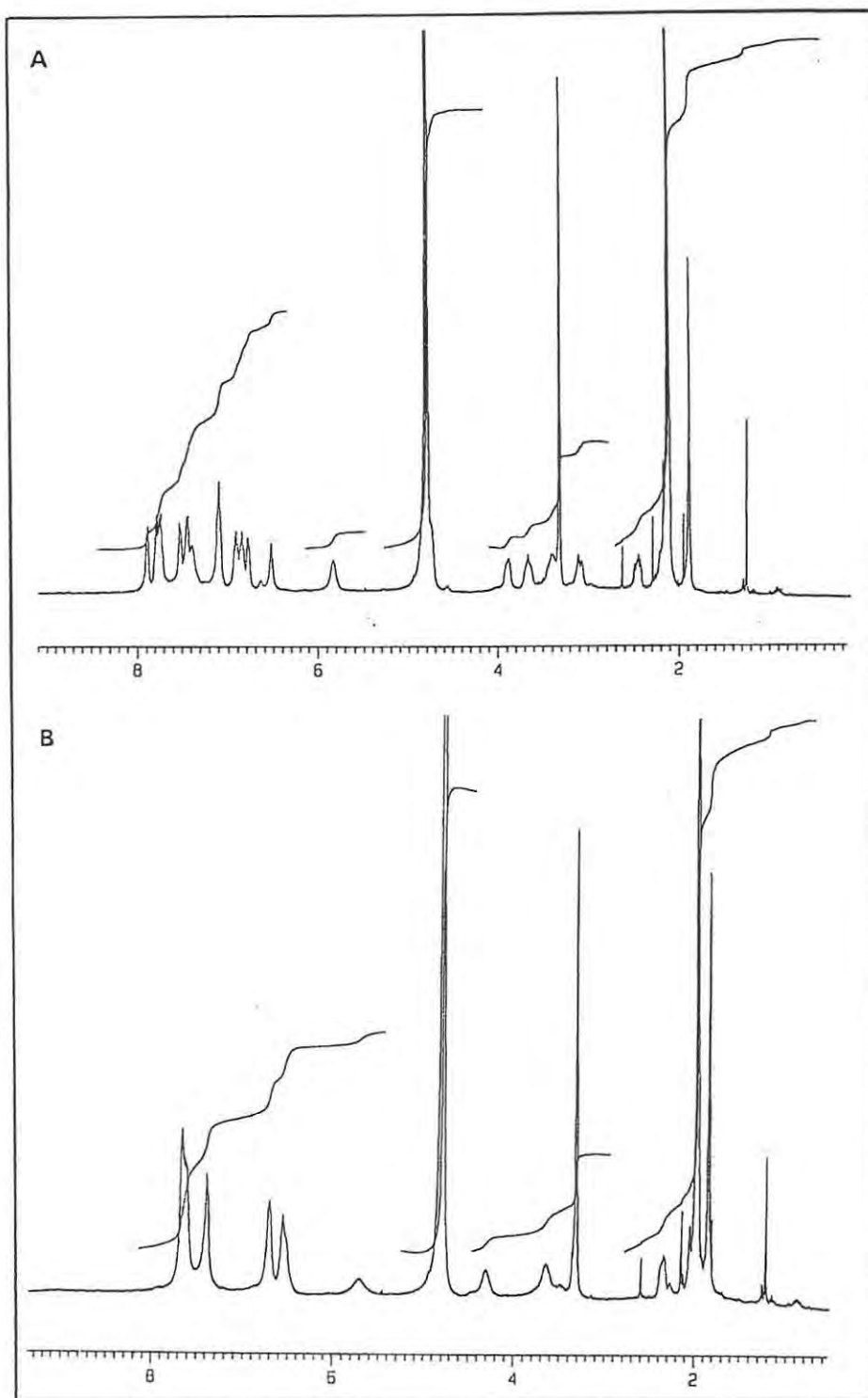


Figure 7.18: ^1H NMR spectrum of complex IIIA in CD_3OD in the absence (A) and the presence (B) of air

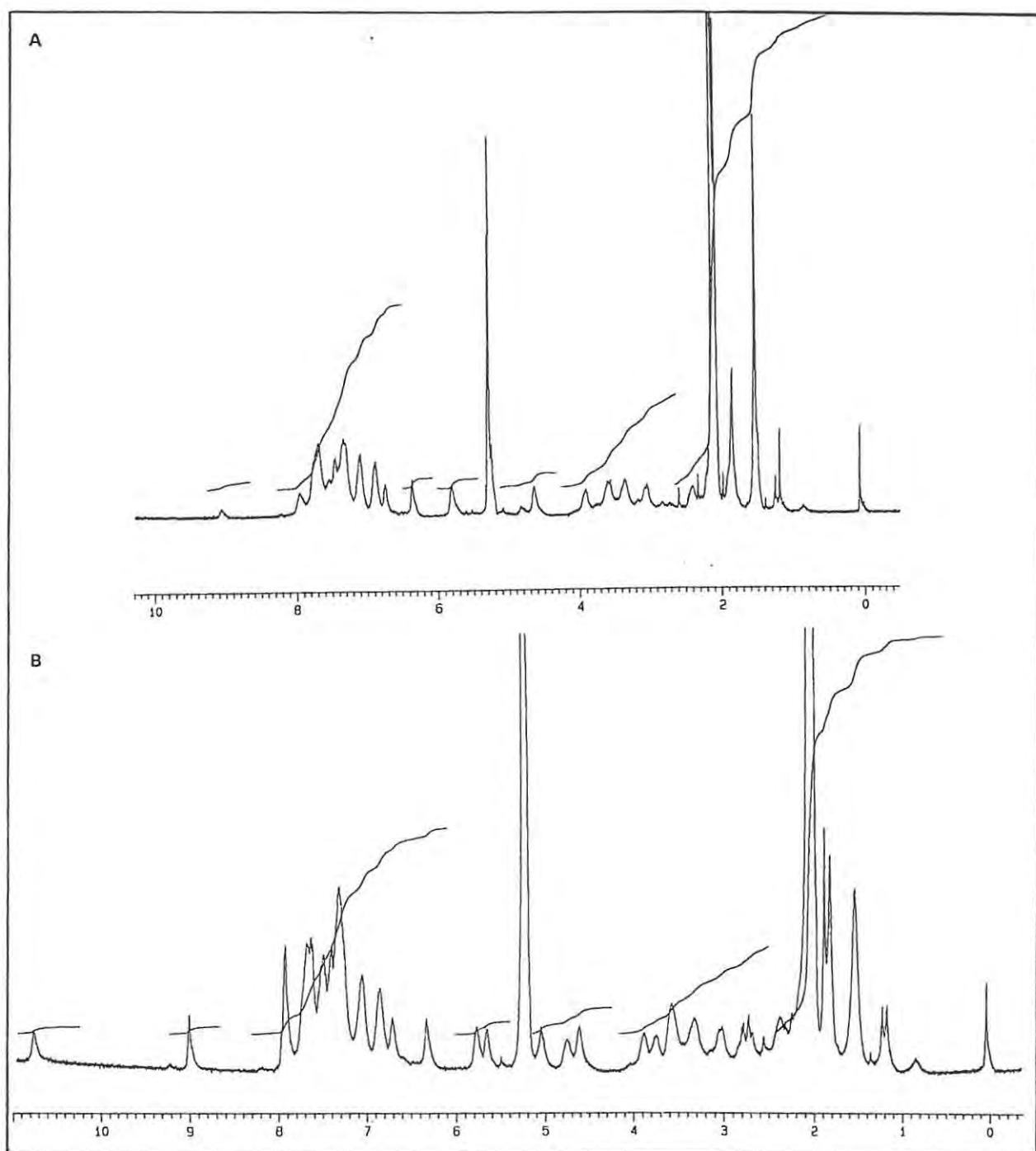


Figure 7.19: ^1H NMR spectra of complex IIIA in CD_2Cl_2 in the absence (A) and the presence (B) of air

7.2.3 (3) Synthesis of complex **IIIB** by template condensation

For the sake of comparison, a template condensation synthesis of complex **III** was undertaken (Section 7.4.15 and Scheme 7.4), but a rather different product, **IIIB**, was obtained, as indicated by comparison of **IIIA** and **IIIB** by TLC and NMR spectroscopy (Figures 7.17 and 7.20). Moreover, the formation of complex **IIIB** was apparently not complete, as indicated by the small starting material peaks slightly upfield from the major peaks in the ^1H NMR spectrum of the crude product (δ_{H} 2.8, 3.6, 6.2 - 6.6). The multiplet at δ_{H} 8.5 is similar in shape and chemical shift to that observed in the spectrum of complex **IIB**, and also to those observed in the spectra of the organic ligands **80MC** and **90M**. This signal is attributable to an imine-proton, which shows that complex **IIIB** does contain an imine linkage. Although impure, the complex **IIIB** is considered to have the desired structure **III**, as formulated in Table 7.1 (Section 7.1.1).

7.2.3 (4) Reactions of the starting materials **86** and **96** with $[\text{Cu}(\text{MeCN})_4][\text{PF}_6]$

In view of the suspected presence of some starting materials in complexes **IIIA** and **IIIB**, the possibility of these contaminants forming copper complexes was investigated. This was of particular relevance to the investigation of the catalytic activity of the complexes, since contamination by active impurities would obviously affect the results. The dialdehyde **86** and the amine, 2-(2-aminoethyl)benzimidazole, **96** were treated separately with $[\text{Cu}(\text{CH}_3\text{CN})_4][\text{PF}_6]$ (Sections 7.4.16 and 7.4.17), and the ^1H NMR spectra of the resulting solutions were obtained, to determine whether either of these mixtures produced a complex. In the case of the mixture containing the dialdehyde **86**, the ^1H NMR spectrum showed peaks due to this starting material and acetonitrile from the copper salt (Figure 7.21), indicating that no complex was formed. The amine **96**, however, reacted with the copper complex, producing a blue solid, the ^1H NMR spectrum of which showed very broad peaks due to the presence of copper (II) ions (Figure 7.22). This products was not analysed further, but was investigated for catalytic activity (Section 9.2.3) and found to be inactive.

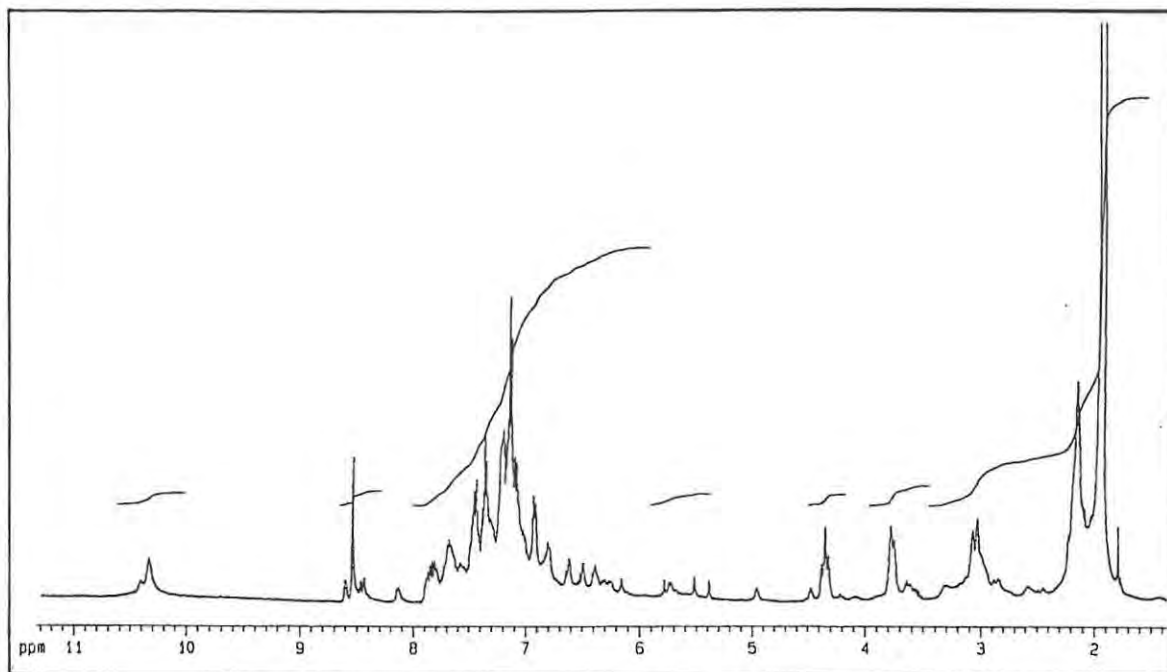


Figure 7.20: ^1H NMR spectrum of complex IIIB in CD_3CN

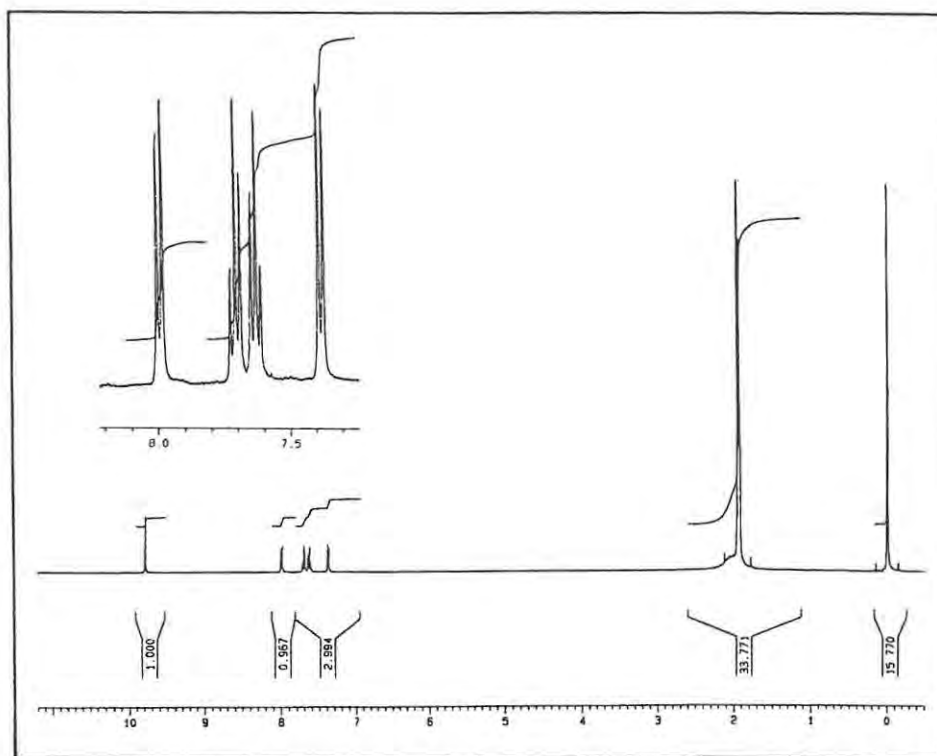


Figure 7.21: ^1H NMR spectrum of the reaction mixture containing biphenyl-2,2'-dicarbaldehyde **86** and $[\text{Cu}(\text{MeCN})_4][\text{PF}_6]$

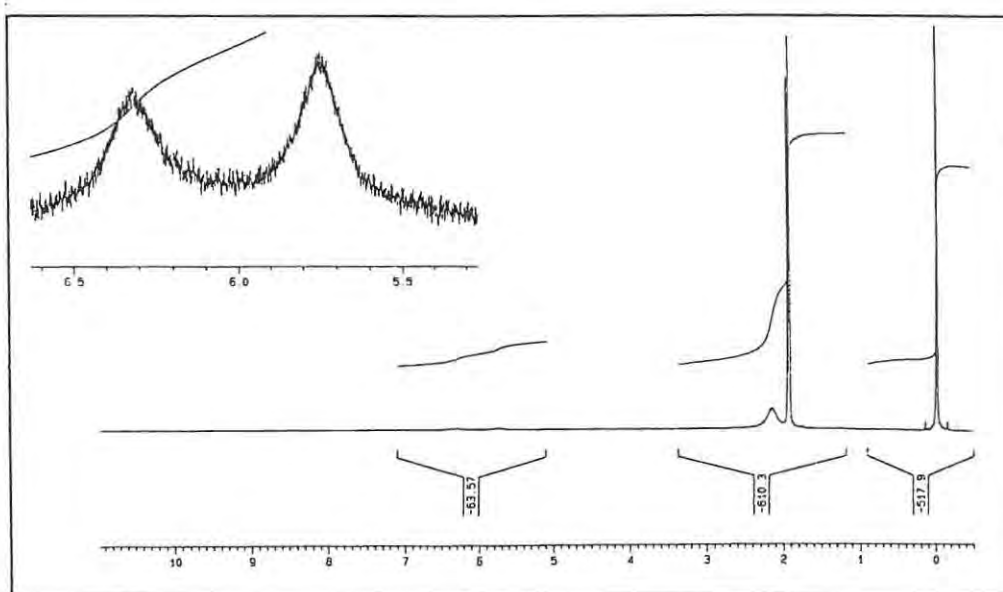


Figure 7.22: ^1H NMR spectrum of the reaction mixture containing 2-(2-aminoethyl)benzimidazole **96** and $[\text{Cu}(\text{MeCN})_4][\text{PF}_6]$

7.2.4 Decomposition of complex I

Réglier *et al.* (1990) reported that complex I decomposed to give the oxo-dinuclear complex 101 and, therefore, in the present study, this decomposition was investigated to assess its possible effect on the catalytic activity of the complex. The decomposition of dinuclear copper complexes in dichloromethane has also been reported by other workers (Sorrell, 1991b, and Jacobson *et al.*, 1988).

The decomposition was investigated using degassed dichloromethane solutions of the complex I, which were rapidly aerated to initiate reaction. The formation of the complex 101 was followed by measuring the UV-visible absorbance at 650 nm [$\epsilon = 180 \text{ M}^{-1}\text{cm}^{-1}$; due to the copper (II)-containing product 101 (Réglier *et al.*, 1990)] in both the presence and absence of triethylamine (see Section 7.4.18). Although these authors suggested that the role of the triethylamine was to promote the formation of a dicopper-phenolate complex, we considered it possible that the triethylamine could also interact with the copper complex I itself. The decomposition to 101 was found to occur to an appreciable extent in the absence of triethylamine, as illustrated in Table 7.3.

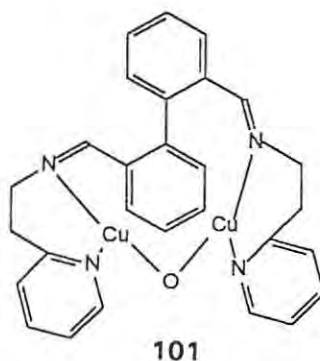


Table 7.3: Decomposition of complex I

Conc _{0a} (mM)	Abs _{0b} (650nm)	Abs _{1^c} (650nm)	Absorbance difference	Conc _{1^d} (mM)	% decomp. ^e
0.3	0.034	0.085	0.052	0.28	94
0.7	0.068	0.190	0.122	0.68	97
1.0	0.101	0.260	0.159	0.88	88

^a : Initial concentration of complex

^b : Initial absorbance of solution

^c : Final absorbance of solution after 3 hours

^d : Concentration of product after 3 hours

^e : % decomposition of complex

The presence of triethylamine was, in fact, found to reduce the rate of decomposition of the complex very significantly. Changes in absorbance at 650 nm were barely measurable, even after a period of one hour. This suggests that the triethylamine is important in maintaining the stability of the complex in its Cu (II)-O₂-Cu (II) form, presumably by replacing the coordinating solvent acetonitrile molecules. It may be speculated that the more bulky triethylamine ligands prevent the two copper ions from approaching each other closely enough to be bridged by a single oxygen atom, while the more linear acetonitrile ligands are less effective.

7.3 CONCLUSIONS

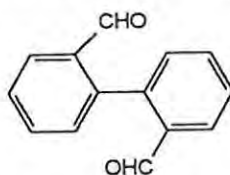
Several dinuclear copper complexes were prepared, which gave satisfactory AA and IR analyses, and which exhibited biomimetic activity (see Chapter 9). However, complete structure elucidation of the products by NMR spectroscopy was prevented by their sensitivity with respect to both decomposition and intramolecular cyclisation. The tendency of the ligands to hydrolyse resulted in the presence, in some products, of starting materials. In addition, it was found that the copper (I) complexes were readily oxidised if left in solution, even under nitrogen. Thus, complexes **IIA** and **IIC** were found to contain some copper (II) contaminants (see Section 8.2.2).

The complex **I** was successfully prepared, and its NMR spectral characteristics were found to correlate well with those reported by Réglie *et al.*, (1990). Intramolecular cyclisation reactions were encountered in the syntheses of ligands bearing imidazole and benzimidazole donor groups, which lead to the presence of isomeric contaminants and precluded their complete structural characterisation. The preparation of the complex **II**, bearing imidazole donor groups, was complicated by cyclisation and oxidation, but the successful synthesis of **IIB** demonstrates the greater suitability of the template method for preparing such organometallic complexes. However, in the cases where the template method was utilised (*viz.*, complexes **IIA**, **B** and **IIIB**) the products were impure, which is a disadvantage in reactions where purification procedures may lead to further decomposition. Although the benzimidazole-containing complexes were designed with the intention of avoiding the cyclisation reactions encountered with imidazole, isomerisations again lead to the formation of two different ligand structures in complexes **IIIA** and **IIIB**.

The complexes **I**, **IIB** and **IIIB** were assigned the structures formulated in Table 7.1, and further analyses of these, and the other complexes described in this chapter, were subsequently undertaken (see Chapter 8 and 9).

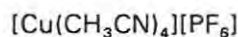
7.4 EXPERIMENTAL

7.4.1 Synthesis of biphenyl-2,2'-dicarbaldehyde (86) (Bailey and Erickson, 1961)

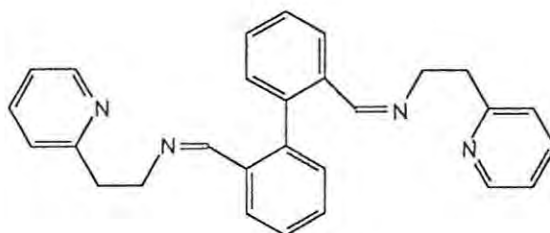


A suspension of phenanthrene (2.5g, 14mmol) in dry MeOH (50mL) in an ozonolysis vessel, was cooled to -30°C . O_3 was bubbled gently through the mixture until all of the starting material had dissolved (2h). The reaction mixture was kept cold (0°C) while KI (8.5g) and glacial CH_3COOH (7.5mL) were added, and it was then allowed to stand at room temperature for 1h. A solution of $\text{Na}_2\text{S}_2\text{O}_3$ (10%,) was added to reduce the released iodine, and the mixture was placed under a stream of air for 2h. Cold H_2O (0°C ; 50mL) was added, and the solid product was filtered off, and recrystallised from Et_2O /hexane, giving pale yellow crystalline biphenyl-2,2'-dicarbaldehyde (2.8g, 95.0%), m.p. $61\text{-}63^{\circ}\text{C}$ [lit. Bailey and Erickson, 1961) $62\text{-}63^{\circ}\text{C}$]; ν_{max} (KBr) 1700 cm^{-1} br s (CO); δ_{H} (60MHz, CDCl_3) 7.60(8H,m,Ar-H) and 9.85(2H,s,CHO).

7.4.2 Synthesis of tetrakis(acetonitrile)copper (I) hexafluorophosphate (88) (Kubas, 1979)

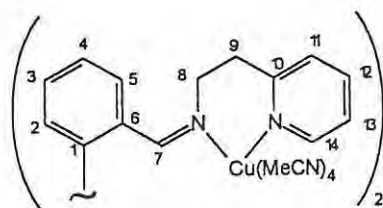


Copper(I) oxide (4.0g, 28mmol) was stirred with CH_3CN (80mL) in a closed flask fitted with a pressure-compensating dropping funnel, under nitrogen. HPF_6 (60-65%, 10mL, 113mmol) was added from the funnel, and the mixture was stirred slowly for 5min. The solution was filtered, and cooled to -20°C , when the product precipitated. The solid product was recrystallised by redissolving in CH_3CN (100mL), adding Et_2O (100mL), and then cooling for 6h. The white crystalline product (9.3g, 45%) was filtered off and dried under reduced pressure and stored in a desiccator at 4°C .

7.4.3 Preparation of ligand system 89 (Réglier *et al*, 1990)

A solution of biphenyl-2,2'-dicarbaldehyde **86** (1.0g, 4.76mmol) in CHCl_3 (50mL) was placed in a round-bottomed flask fitted with a modified Dean-Starke apparatus. 2-(2-Pyridyl)ethylamine (1.1g, 9.0mmol) was added, and the solution was boiled under reflux for 12h, after which the reaction was shown to be complete by the absence of the CO band in the IR spectrum. The solvent was removed under reduced pressure, giving the product, **89**, as a brown oil (1.9g, 98%), ν_{max} (CHCl_3) 2950 (CH_2), 1650 cm^{-1} (conjugated $\text{C}=\text{N}$); δ_{H} (CDCl_3) 3.01(4H,t, CH_2), 3.8(4H,t, CH_2), 7.25(16H,m,ArH) and 7.9(2H,m, $\text{CH}=\text{N}$)

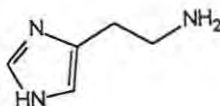
7.4.4 Preparation of complex I (Réglier *et al*, 1990)



The imine **89** was dissolved in dry, degassed CH_3CN (100mL) under N_2 . $[\text{Cu}(\text{CH}_3\text{CN})_4][\text{PF}_6]$ **88** (2.56g, 4.8mmol) was added and the reaction mixture was stirred under N_2 at room temperature for 3h, during which time the mixture turned dark green. The mixture was stored overnight under N_2 at 4°C . Approx half of the solvent was removed by evaporation under a stream of N_2 , and the yellow/green solid which precipitated was filtered off and dried in a vacuum desiccator, giving the complex I (3.9g, 84.6%); ν_{max} (CHCl_3) 1640 ($\text{C}=\text{N}$), 1600 (pyridine CN) and 840 and 780 cm^{-1} (PF_6); δ_{H} (CD_3COCD_3) 2.13(s,coordinated CH_3CN), 2.31(2H,dd, J 10 and 5.4,2H-9), 3.07(2H,m,2H-9), 3.73(2H,dd, J 7.1 and 5.4,2H-8), 4.21(2H,t, J 11.3,2H-8), 7.25(14H,m,Ar-H), 7.77(2H,t, J 7.3,2H-12), 8.15(2H,d, J 3.8,2H-14), and 8.88(2H,s,2H-7); δ_{C} (CD_3COCD_3) 37.35(C-9), 59.38(C-8), 123.62(C-13), 125.48(C-11), 127.94, 129.53, 129.59, 131.89(C-2, C-3, C-4, C-5), 137.55(C-1), 141.23(C-6), 150.00(C-14), 160.94(C-10), 165.91(C-7) and 206.3(co-ord. CH_3CN); correlations established by COSY and HETCOR experiments.

Recrystallisation of the product was attempted, by placing a solution of the product (in dry, degassed CH_2Cl_2 or CH_3CN) under N_2 in a closed desiccator, and allowing vapour diffusion of hexane, C_6H_6 , ether, or CH_3OH to take place over several days, but no crystals were obtained.

7.4.5 Preparation of histamine



NaOMe (1.2g, 22mmol) was added to a solution of histamine hydrochloride (2g, 11mmol) in dry EtOH (100mL); the mixture was stirred at room temperature for 1h, then filtered. The solvent was removed from the filtrate under reduced pressure, and CHCl_3 was added to the residue. The flask was warmed to aid dissolution of the liberated amine, and evaporation of the solvent from the resulting solution gave histamine (1.1g, 90%), $\nu_{\text{max}}(\text{KBr})$ 3480 (imidazole NH), 3250 (NH_2) and 1580 cm^{-1} (NH_2); $\delta_{\text{H}}(\text{CDCl}_3)$ 2.70(2H,t, CH_2), 2.96(2H,s, CH_2), 6.78(1H,s,imidazole H-2), and 6.51(1H,s,imidazole H-4).

7.4.6 Preparation of complex IIA

Biphenyl-2,2'-dicarbaldehyde **86** (1.05g, 4.91mmol) and $[\text{Cu}(\text{MeCN})_4][\text{PF}_6]$ **88** (3.72g, 9.8mmol) were added to a solution of histamine (1.1g, 9.8mmol) in dry, degassed CH_3CN (100mL), in a closed flask, under N_2 . The mixture was stirred for 3h, then stored overnight at 4°C, during which time it changed colour from yellow to torquoise. The solvent was decanted from the precipitated solid which was dried under reduced pressure, giving complex **IIA** (4.4g); $\nu_{\text{max}}(\text{KBr})$ 1640 (imine C=N), 1590 (imidazole), and 860 cm^{-1} (PF_6^-); $\delta_{\text{H}}(\text{CD}_3\text{COCD}_3)$ 3.25(br s, CH_2), 4.0(br s, CH_2), 7.20(2H,s,imidazole 5-H), 7.35 - 8.38(m, ArH), 8.48(br s,H-C=N), 9.76(br s,imidazole NH), and 9.84(s,HCO contaminant).

7.4.7 Preparation of complex IIB

A mixture containing biphenyl-2,2'-dicarbaldehyde **86** (0.095g, 0.45mmol), histamine (0.1g, 0.9mmol), and $[\text{Cu}(\text{CH}_3\text{CN})_4][\text{PF}_6]$ **88** (0.34g, 0.9mmol) in dry degassed CH_3CN (50mL) was stirred under N_2 , for 15 min, during which time a yellow solid precipitated. Most of the solvent was decanted, and the rest was removed under reduced pressure, giving Complex **IIB** (0.4g,90%), $\nu_{\text{max}}(\text{KBr})$ 3400 br (NH), 1640 (imine C=N), 1580 (imidazole) and 850 cm^{-1} (PF_6^-); $\delta_{\text{H}}(\text{CD}_3\text{CN})$ 3.50(4H,m, CH_2), 3.92(4H,m, CH_2), 6.70 - 7.65(m,ArH), 8.53 (4H,m,HC=N and imidazole 2-H), and 10.15(2H,br s, NH).

7.4.8 Preparation of ligand system **92**

Biphenyl-2,2'-dicarbaldehyde **86** (0.72g, 3.4mmol) was added to a solution of histamine (0.75g, 6.8mmol) in CHCl_3 (150mL). The mixture was boiled under reflux for 6h, using a modified Dean-Stärke apparatus to remove water. The solvent was removed under reduced pressure, leaving a glassy yellow solid (1.6g) found to be an imine, $\nu_{\text{max}}(\text{KBr})$ 1650 cm^{-1} (conjugated C=N), but shown by ^1H NMR to be impure. The product was subjected to repeated flash chromatography [silica; elution with $\text{Et}_2\text{O}-\text{CHCl}_3-\text{EtOH}$ (5:1:5)]. Further purification of the product by PLC [silica; elution with $\text{Et}_2\text{O}-\text{CHCl}_3-\text{EtOH}$ (5:1:1)] gave the product **92** (0.25g); $\delta_{\text{H}}(\text{CDCl}_3)$ 2.52 - 3.15(4H,m, CH_2), 3.25 - 3.42(4H,m, CH_2), 5.96(2H,s,CH), 6.86(2H,s,imidazole 5-H), 7.06(10H,m ArH) and 8.10(2H,m,HC=N). The product was shown, by ^1H NMR spectroscopy, to contain some aldehyde, $\delta_{\text{H}}(\text{CDCl}_3)$ 9.81(m,HC=O).

7.4.9 Preparation of ligand system **94**

The procedure described for the synthesis of ligand **92** was repeated, using histamine (0.55g, 4.96mmol) and biphenyl-2,2'-dicarbaldehyde **86** (0.52g, 2.48mmol), and refluxing for 8h. A sample of the product obtained after work-up was recrystallised (EtOAc/hexane), to give **94**, $\nu_{\text{max}}(\text{KBr})$ 3200 br (NH), 1640 (conjugated imine); $\delta_{\text{H}}(\text{CDCl}_3)$ 2.42 and 3.68(8H,m, CH_2), 4.99(1H,s,NH), 6.11 - 6.42(m,CH-N), 6.89 - 7.75(m,Ar-H), and 8.15(m,HC=N); $\delta_{\text{C}}(\text{CDCl}_3)$ 21.03, 30.25, 40.90, 60.93, 69.38, 124.12, 125.49, 126.59, 127.93, 128.12, 128.29, 128.48, 128.76, 128.82, 129.15, 129.58, 129.85, 130.69, 133.99, 134.77, 136.70, 136.99, 140.06, and 159.77 (24 signals expected). HETCOR shown in Figure 7.23 (at end of section).

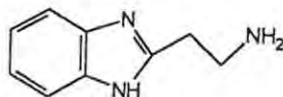
7.4.10 Preparation of complex **IIC**

$[\text{Cu}(\text{MeCN})_4][\text{PF}_6]$ **88** (0.395g, 1.1mmol) was added to a solution of the imine **92** (0.21g, 0.5mmol) in dry degassed CH_3CN (20mL) under N_2 . The mixture was stirred, under N_2 , at room temperature, for 1h, then allowed to stand, under N_2 at 4°C for 4h. Most of the solvent was decanted from the solid product, and the rest was removed under reduced pressure, giving the pale green product **IIC**, $\nu_{\text{max}}(\text{KBr})$ 3100 br (NH), 1630 (imine C=N), and 860 cm^{-1} (PF_6^-); $\delta_{\text{H}}(\text{CD}_3\text{COCD}_3)$ 7.45 - 8.15(m,ArH), 8.18 and 8.26(m,imidazole 2-H and H-CN), 9.83(s,HCO) as well as broad signals at 6.55, 6.79, 7.05, 7.25, 8.40, and 9.90 ppm; $\delta_{\text{H}}(\text{CD}_3\text{CN})$ 2.45, 3.55, and 3.65 (3 x br s, CH_2).

Recrystallisation was attempted by allowing dry hexane to diffuse into a concentrated solution of

the complex in dry CH_3CN . White crystals were obtained, but these were found to show no aromatic signals in the ^1H NMR spectrum and to contain a high proportion of copper (36%) by AA (method as described in Section 8.4.1), indicating their mainly inorganic nature.

7.4.11 Preparation of 2-(2-aminoethyl)benzimidazole 96



A stirred solution of 1,2-diaminobenzene (8.31g, 77mmol) and β -alanine (10.2g, 115mmol) in HCl (6M, 90mL) was refluxed for 48h, then allowed to stand for 48h. Completion of reaction was confirmed by TLC (silica, elution with EtOAc). The solvent was removed under reduced pressure at 90°C , and the residual solid was dissolved in water (50mL). EtOH (100mL) was added, and on cooling, the hydrochloride salt crystallised as blue needles. Recrystallisation from EtOH containing approx. 5% water gave the dihydrochloride of **96** (4.1g, 33%). This salt (2g, 8.55mmol) was stirred with NaOMe (0.93g, 17.1mmol) in dry EtOH (80mL) for 1h. The resulting mixture was filtered and the solvent was removed from the filtrate under reduced pressure. Dry CHCl_3 (50mL) was added to dissolve the amine, and residual solids were removed by filtration. Removal of the CHCl_3 under reduced pressure gave a pale pink product which was recrystallised from THF, producing 2-(2-aminoethyl)benzimidazole (**96**) (1.3g, 94%), m.p. $134\text{--}136^\circ\text{C}$; ν_{max} (KBr) 3350 (NH), 1605 (NH_2), and 1540 cm^{-1} (CN); δ_{H} (D_2O) 2.83(2H,t, J 6.8, CH_2), 2.94(2H,t, J 6.8, CH_2), 7.16(2H,m,Ar-H) and 7.42(2H,m,Ar-H).

7.4.12 Preparation of ligand system 97

A solution of 2-(2-aminoethyl)benzimidazole **96** (0.74g, 4.6mmol) and biphenyl-2,2'-dicarbaldehyde **86** (0.49g, 2.3mmol) in CHCl_3 (100mL) was refluxed using a modified Dean-Starke apparatus for 48h, after which time the reaction was found to be complete by TLC [silica; elution with $\text{CHCl}_3\text{--CH}_3\text{OH}$ (1:1)]. The solvent was removed under reduced pressure, yielding a sticky product which was purified by flash chromatography [silica, elution with EtOAc: CH_3OH (16:1)] to give compound **97** (0.11g, 10%), ν_{max} (KBr) 3100 (NH), 1610 (conjugated C=N), 1510 cm^{-1} (NH); δ_{H} (CDCl_3) 2.84(4H,m, CH_2), 3.00(4H,m, CH_2), 4.60(2H,br,NH), 7.13 - 7.52(16H,m,Ar-H), and 7.79(2H,m,HC=N).

7.4.13 Preparation of ligand system **98**

The procedure described for the synthesis of ligand **97** was repeated using 2-(2-aminoethyl)benzimidazole **96** (0.74g, 4.5mmol) and biphenyl-2,2'-dicarbaldehyde **86** (0.49g, 2.3mmol), and refluxing for 48h. The product was not purified by flash chromatography, but was recrystallised from CH₃CN to give yellow crystals of **98** (0.7g). m.p. 198 - 200°C; ν_{\max} 3300 (NH), 2950 (CH₂), 1620 cm⁻¹ (C=N); δ_{H} (CDCl₃) 2.95(2H, m, CH₂), 3.42 - 3.55(6H, m, CH₂), 4.07(2H, s, NH), 6.07, 6.30, 6.49, (4 x m, H-C=N), 6.80 - 7.60(m, ArH) and 7.79(m, HC=N); δ_{C} (CDCl₃) 25.47, 40.15, 57.06, 69.10, 93.64, 109.66, 119.08, 121.18, 122.29, 125.10, 125.37, 125.61, 127.89, 128.63, 129.14, 131.83, 132.87, 134.27, 143.07, 150.40. COSY and HETCOR spectra shown in Figure 7.24 (at end of section).

7.4.14 Preparation of complex IIIA

The imine ligand system **97** (0.108g, 0.22mmol) was dissolved in dry degassed CH₃CN (10mL) in a closed flask, under N₂. A solution of [Cu(CH₃CN)₄][PF₆] (0.17g, 0.46mmol) in dry, degassed CH₃CN (10mL) was added *via* a canula. The mixture was stirred, under N₂, for 0.25h, during which time a pale yellow precipitate formed. The supernatant was decanted, and the solid was dried in a vacuum desiccator, giving, as a single compound [TLC; silica; elution with CHCl₃-CH₃OH (4:1)], the complex IIIA (0.25g, 50%), ν_{\max} (KBr) 1710 (C=N), 750 and 560 cm⁻¹ (PF₆⁻); δ_{H} (CD₃CN) 2.94(2H, s, CH₂), 3.22(2H, s, CH₂), 3.53(2H, s, CH₂), 3.76(2H, s, CH₂), 5.78(2H, br s, NH), 6.79 - 7.81(m, ArH); δ_{C} (CD₃CN) 23.74, 52.09, 62.80, 78.79, 112.55, 122.89, 128.53, 129.08, 129.65, 130.13, 130.83, 131.15, 137.95, 140.99, and 141.58.

7.4.15 Preparation of complex IIIB

2-(2-Aminoethyl)benzimidazole **96** (0.076g, 0.47mmol), biphenyl-2,2'-dicarbaldehyde (0.049g, 0.23mmol) and [Cu(CH₃CN)₄][PF₆] (0.174g, 0.47mmol) were placed in a closed flask under N₂. Dry, degassed CH₃CN (20mL) was added *via* a canula, and the mixture was stirred for 0.25h at room temperature, during which time, a pale yellow solid precipitated. Some of the solvent was decanted and the rest was removed under reduced pressure, and the product was dried in a vacuum desiccator, giving complex IIIB (0.27g, 90%), shown to be pure by TLC [silica; elution with CHCl₃-CH₃OH (4:1) and CH₃CN:Et₂O (4:1)], ν_{\max} (KBr) 1630 (conjugated imine), 840 cm⁻¹ (PF₆⁻); δ_{H} (CD₃CN) 3.05(4H, s, CH₂), 3.77(2H, m, CH₂), 4.35(2H, m, CH₂), 6.60 - 7.9(16H, m, ArH), 8.51(2H, m, H-C=N), and 10.33(br s, NH); δ_{C} (CD₃CN) 28.1, 58.97, 112.12, 122.96, 123.83, 127.28, 127.77, 129.58,

130.14, 131.64, 134.50, and 165.61; correlations established by HETCOR experiment, shown in Figure 7.25 (at end of section).

7.4.16 Reaction of biphenyl-2,2'-dialdehyde **86** with $[\text{Cu}(\text{MeCN})_4][\text{PF}_6]$ **88**

The dialdehyde **86** (0.05g) was added to a solution of $[\text{Cu}(\text{MeCN})_4][\text{PF}_6]$ **88** (0.18g) in dry degassed MeCN (10mL) under N_2 . The mixture was stirred under N_2 for 2h. The solvent was removed under reduced pressure, leaving a white solid product, δ_{H} (CD_3CN) 2.00(s, CH_3CN), 7.40(2H,d,ArH), 7.69(4H,m,ArH), 8.01(2H,d,ArH), and 9.78(2H,s,CHO), indicating the presence of the starting materials.

7.4.17 Reaction of 2-(2-aminoethyl)benzimidazole **96** with $[\text{Cu}(\text{MeCN})_4][\text{PF}_6]$

The procedure described in section 7.4.16 was repeated, using the amine **96** (0.075g) in place of the aldehyde. The product was a blue residue indicated, by ^1H NMR spectroscopy, to be a copper (II) complex, δ_{H} (CD_3CN) 5.75(br s) and 6.80(br s).

7.4.18 Decomposition of complex I

The complex I (0.003g, 0.003 mmol) was placed in a 3-necked, round-bottomed flask, fitted with a burette, a gas inlet tap, and a septum. The system was flushed with N_2 . Dry, degassed CH_2Cl_2 (10mL) was added from the burette, under N_2 , dissolving the complex (final concentration 3mM). To start the reaction, air was admitted to the flask, and the solution was stirred rapidly. The changes in absorbance at 650nm and 400nm were measured over a period of 1h, using a Beckman DU-68 UV spectrophotometer. A final (t_{∞}) reading was taken after 3h. This procedure was carried out in triplicate, and repeated using solutions of concentration 0.7 mM and 1 mM. The results are shown in Table 7.4. The experiment was repeated with the addition of Et_3N (to give a final concentration = 2 x concentration of complex), and the absorbance was observed for 1h. In the presence of the Et_3N , absorbance changes with time were too small to be measured.

Kinetic analysis of the data obtained by following the changes in absorbance at 650 nm (reported in Table 7.4) indicated that the decomposition was first order at least for the initial part

(approximately 10 minutes) of the reaction (see Figure 7.26). The gradients of the graphs of $\ln(A_{\infty} - A_0/A_t - A_0)$ vs time indicate that the rate constant for the decomposition is 0.056 min^{-1} .

Table 7.4: Data for decomposition of Complex I

Time (min)	Concentration	Absorbance (650 nm)		
0	0.3mM	0.035	0.033	0.034
1		0.043	0.038	0.040
2		0.046	0.043	0.046
3		0.052	0.047	0.053
4		0.058	0.057	0.059
5		0.062	0.056	0.065
7		0.067	0.062	0.073
10		0.069	0.068	0.083
15		0.071	0.073	0.085
20		0.073	0.075	0.086
25				0.090
30		0.076	0.081	0.090
50		0.078	0.083	0.093
60				0.094
		$A_{\infty} = 0.085$		
0	0.7 mM	0.069	0.066	0.068
1		0.084	0.082	0.077
2		0.095	0.091	0.091
3		0.106	0.098	0.099
4		0.118	0.105	0.111
5		0.126	0.112	0.119
7		0.140	0.133	0.131
9		0.147	0.150	0.142
11		0.152	0.157	0.145
15		0.156	0.158	0.152
20		0.161	0.161	0.154
30		0.166	0.166	0.159
40		0.171	0.166	0.162
50		0.179	0.173	0.182
		$A_{\infty} = 0.178$		
0	1.0 mM	0.101	0.101	0.102
1		0.109	0.112	0.119
2		0.122	0.133	0.133
3		0.136	0.150	0.145
4		0.150	0.167	0.159
5		0.166	0.181	0.172
7		0.188	0.204	0.195
9		0.214	0.220	0.213
15		0.234	0.237	0.221
20		0.241	0.241	0.242
25		0.245	0.243	
30		0.252	0.248	0.252
40		0.254	0.256	0.258
50		0.257	0.257	0.260
		$A_{\infty} = 0.259$		

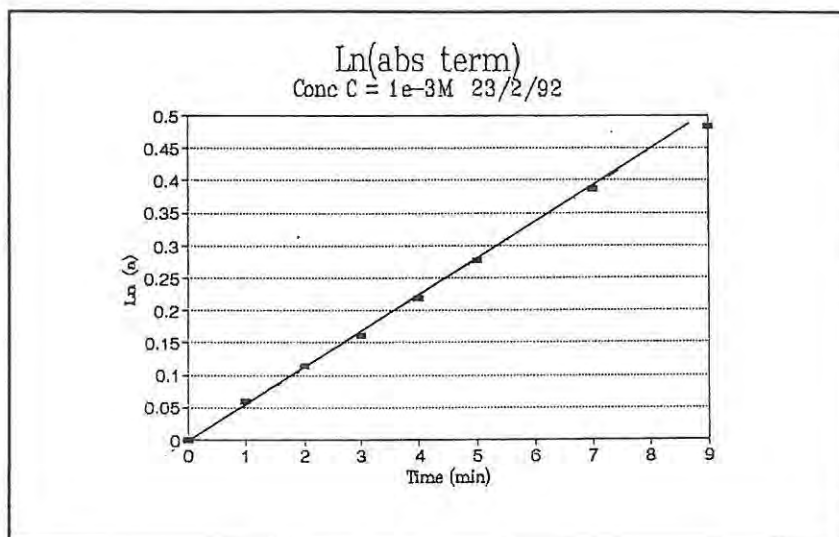


Figure 7.26: Graph of $\ln(A_{\infty} - A_0/A_t - A_0)$ vs time for the decomposition of complex I

7.4.19 Isolation of oxygenated product from complex IIIA

Dry oxygen was bubbled gently into a stirred solution of complex IIIA (15mg) in dry CH_2Cl_2 (5mL) for 10min. Dry ether (10mL) was added, causing a slight precipitate to form, and the solution turned green. The solvent was removed under reduced pressure, leaving a green solid, IIIA', which was analysed by IR spectroscopy, giving a spectrum identical to that of IIIA. This procedure was repeated using methanol as the solvent, with the same result.

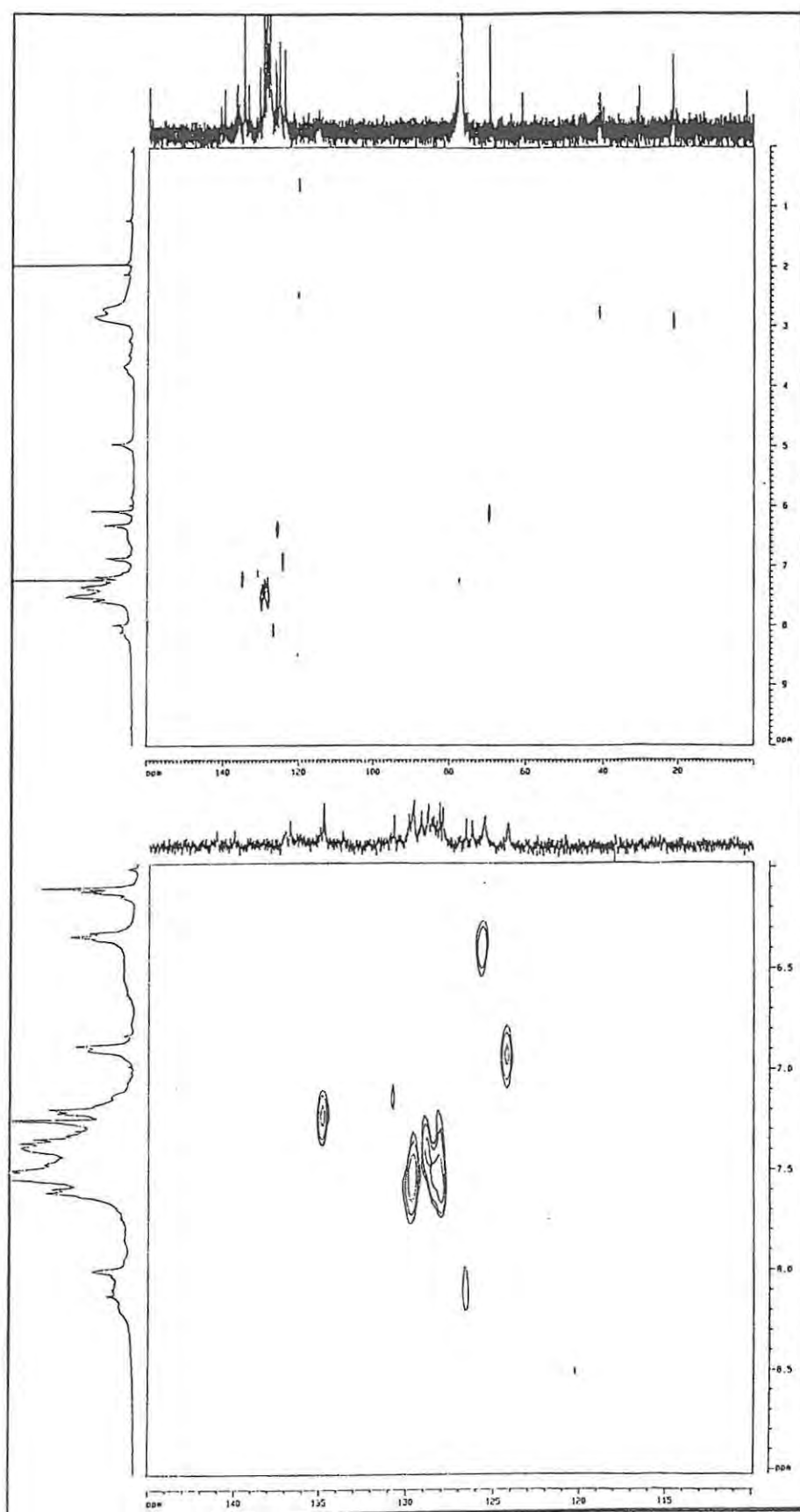


Figure 7.23: 2-D NMR (HETCOR) spectra of ligand 94

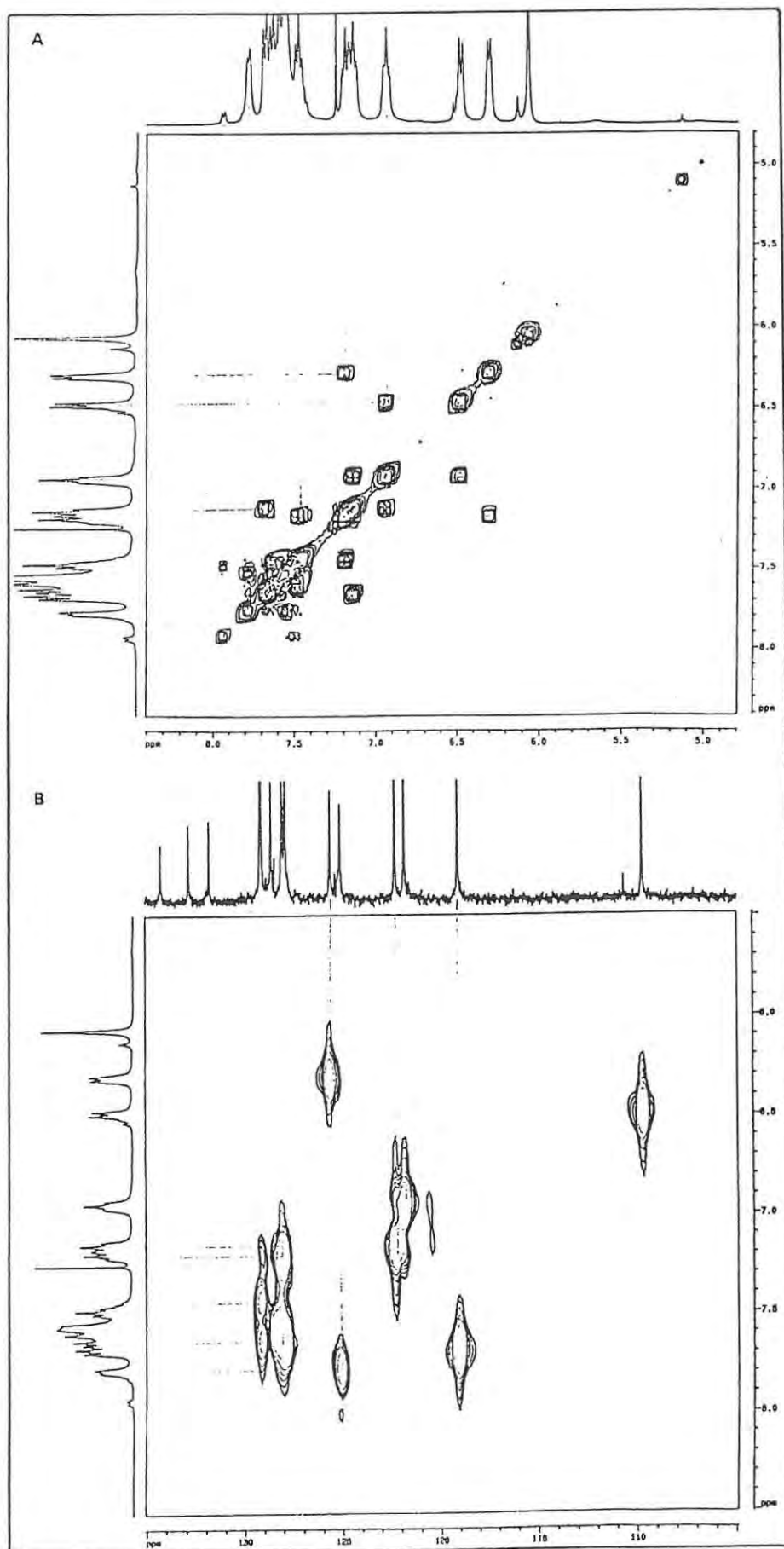


Figure 7.24: 2-D NMR [COSY (A) and HETCOR (B)] spectra of ligand 98

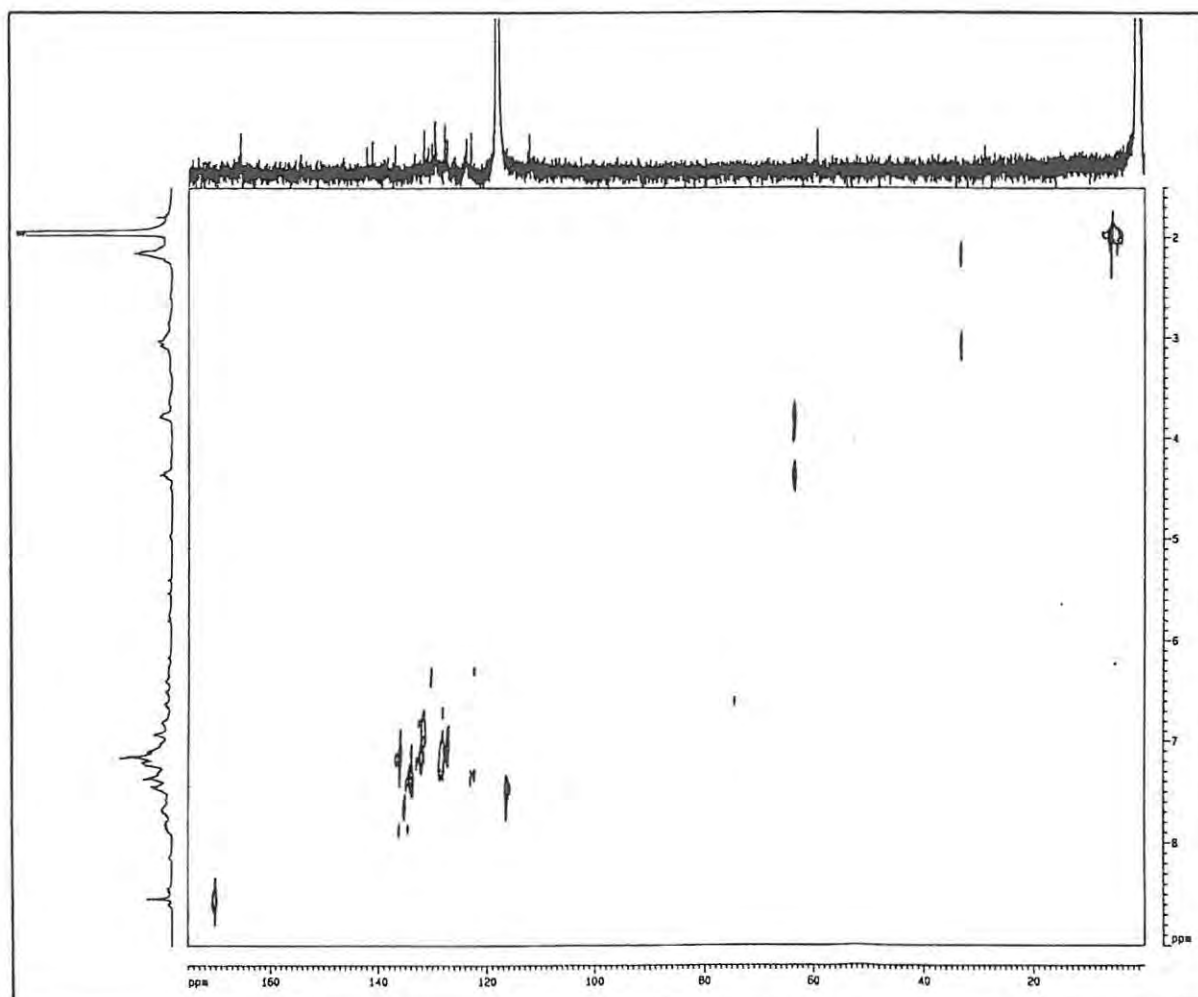


Figure 7.25: 2-D NMR (HETCOR) spectrum of complex IIIB

CHAPTER 8

ANALYSES OF THE COPPER COMPLEXES

8.1 INTRODUCTION

Important information, which can be derived from the analyses of biomimetic copper complexes, is directly relevant to the evaluation of the complexes as successful structural models of copper proteins. In this chapter, analyses of the copper complexes synthesised in the present study, utilising atomic absorption spectrophotometry, UV-visible spectrophotometry and cyclic voltammetry, are discussed.

8.1.1 Atomic Absorption Spectrophotometry

The dinuclear character of the copper complexes which had been synthesised (Chapter 7) was confirmed by determination of their proportion of copper. Atomic absorption spectrophotometry measures the energy absorbed by free atoms at wavelengths which are specific to a particular element, since the energy of the absorption depends on the electronic structure of the atoms. Thus, the copper atoms present in the copper complexes would absorb energy at a specific wavelength (324.8nm), which is different from the absorption wavelengths for atoms of other elements present in a solution of the complex. (The complex must be hydrolysed to liberate the copper ions.) The parameter which is measured in this technique is the absorbance A , given by the equation:

$$A = 0.43k_{\nu}b$$

where k_{ν} is the absorption coefficient of the solution, and b is the path length of the radiation in the sample; k_{ν} is proportional to the concentration of the element being measured, in the solution (Bauer *et al.*, 1978).

The usefulness of atomic absorption as a means of measuring concentration lies in its high sensitivity; in the case of copper ions, the detection limit for flame atomic absorption is 0.1ppm (1.7 μ M) (Wilson and Goulding, 1986).

8.1.2 UV-visible Spectrophotometry

Analysing the electronic spectra of structurally defined copper complexes has been of considerable importance in understanding the electronic structures of the binding sites in copper proteins. The copper proteins themselves often exhibit unusual spectral properties [see Section 1.4.4 (3)], and the synthesis of copper complexes which have similar spectral characteristics has been a major goal in the biomimetic study of these proteins. The correlation of results from spectral studies with those from molecular orbital studies, X-ray crystallography of the complexes, and protein crystallography have enabled workers to develop a detailed understanding of the electronic structures of the protein active sites. Notable in this area is the elegant work of Solomon and co-workers (summarised by Solomon *et al.*, 1992), who have recently proposed detailed models for the electronic structure of the active sites in haemocyanin and tyrosinase (see Section 1.2.7). Techniques used to determine the electronic structures include Raman, EXAFS (extended X-ray absorption fine structure), EPR (electroparamagnetic resonance) and UV-visible spectroscopy, as well as quantum mechanical SCF-X α -SW (self-consistent field-X α -scattered wave) calculations. UV-visible spectroscopy was utilised in the present study.

In transition metal compounds, the absorption of light (and hence the colour of the compounds) is associated with d-d (crystal field) transitions, and with charge transfer processes. Ligand-to-metal charge transfer (LMCT) transitions result from electron donation from a ligand atom orbital to a metal orbital, *e.g.* nitrogen to copper (II). Metal-to-ligand charge transfer (MLCT) transitions occur where a ligand has low energy empty orbitals, *e.g.* the empty π anti-bonding orbitals in pyridine. Easily oxidisable metal ions, such as copper (I), can transfer electrons to these orbitals.

Copper (II) complexes generally show d-d transitions composed of broad bands at wavelengths 500 - 1600 nm (ϵ 100 - 1000 M⁻¹cm⁻¹); the wavelength is dependent on the coordination arrangement. Table 8.1 illustrates the effect of coordination on the d-d transitions of copper (II) (Lever, 1984, Chapter 6).

Table 8.1: Examples of UV-visible d-d absorptions of copper (II) complexes (Lever, 1984)

Coordination	Geometry	Absorption λ_{\max} (nm)
6-coordinate	Tetragonal octahedral	550-650
	Rhombic octahedral	590-720
	Trigonal octahedral	760-1100
5-coordinate	Square-based pyramidal	580-770
	Trigonal bipyramidal	680-950
4-coordinate	Square planar	470-580
	Tetrahedral	600-850

While the d-d transitions are not greatly affected by the nature of the solvent, the energies of CT transitions are affected by the solvent. CT transitions are also influenced by the coordination number and stereochemistry, and by the nature of the ligands. For example, primary amine (NH₂)-to-copper (II) LMCT absorptions occur around 250nm, while secondary amine/copper (II) complexes, where Cu-N bonds are longer and weaker, show absorption bands at lower energies (Lever, 1984, Chapter 8). If different types of Cu-N bonds exist in one complex, different absorptions will occur for each.

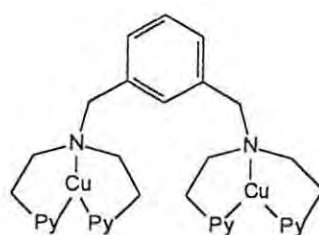
While copper (I) complexes do not exhibit d-d transitions because the copper (I) ion has full d orbitals, they do show CT transitions. These may be ligand(π) \rightarrow 4s or ligand(σ) \rightarrow 4s LMCT transitions. MLCT transitions also occur, as illustrated by the examples shown in Table 8.2 (Sorrell and Borovik, 1986).

Table 8.2: MLCT absorptions of copper (I) complexes (Sorrell and Borovik, 1986)

Coordination	Transition	Absorption (λ_{max} /nm)
4-coordinate	$d\pi \rightarrow \pi^*$, $d\sigma \rightarrow \pi^*$	215 - 225, 260sh ^a
3-coordinate		220-230, 254, 302(sh)
2-coordinate		210-230, 240(br sh)

^a Occurs as a shoulder on the higher energy absorption band

Copper complexes which can coordinate dioxygen are of particular interest because oxygen binding is a biological function of haemocyanin and tyrosinase. Oxygen can be bound to copper as superoxide (O₂⁻) or peroxide (O₂²⁻), with variable coordination geometry. Specific spectral changes are observed when copper (I) complexes bind oxygen to form copper (II)-peroxide complexes. These absorption bands can be distinguished from those attributable to the formation copper (II) d-d transitions by their wavelength and intensity (see Table 8.3 below). Another aspect of the reactivity of complexes with oxygen which can be demonstrated by UV-visible spectroscopy is the hydroxylation of aromatic rings in the ligands. The formation of a phenoxy-bridged dinuclear copper (II) group is accompanied by the development of an intense absorption band around 360nm which is not reversible. Karlin and co-workers have devised a sophisticated system to examine the low temperature spectra of oxygen-bridged complexes which are not stable at normal temperatures. For instance, close spectroscopic similarity to haemocyanin was achieved in the case of complex 103, which also binds oxygen reversibly, giving absorption bands at 365 ($\epsilon = 15000 \text{ M}^{-1}\text{cm}^{-1}$), 490 ($\epsilon = 5250 \text{ M}^{-1}\text{cm}^{-1}$), 600(shoulder) and 850nm ($\epsilon = 100 \text{ M}^{-1}\text{cm}^{-1}$) (Karlin *et al.*, 1992).



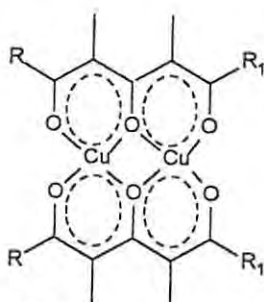
103

Table 8.3 UV-visible spectral features of products from reactions of copper complexes with oxygen

Transition	Wavelength λ_{\max} /nm, (ϵ /M ⁻¹ cm ⁻¹)	Indication
Peroxo-to-copper (II)	350-365 (20000), 500 (1000)	Reversible binding of oxygen
Phenoxy-to-copper(II)	360 (15000)	Aromatic hydroxylation
Copper (II) d-d	500-1200 (1000)	Simple oxidation of copper (I)

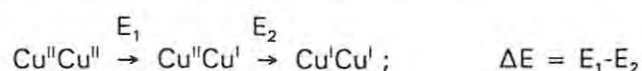
8.1.3 Electrochemical characteristics of copper dinuclear complexes

"Type 3" copper sites in proteins exhibit single two-electron reductions at redox potentials which are higher than would be expected for their proposed coordination arrangements. However, with the exception of the triketonate complex 104 (Fenton *et al.*, 1978) which does undergo a single, two-electron reduction, synthetic dinuclear copper complexes have generally been found to be reduced in two single-electron steps, with an intermediate Cu(I)Cu(II) species being formed. Thus the study of the electrochemical characteristics of biomimetic dinuclear copper complexes is of considerable relevance.

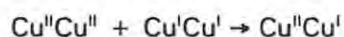


104

The redox processes can be quantified by measuring standard redox potentials and the separation ΔE between the two consecutive reduction potentials i.e.



where ΔE is a measure of K_{com} , the comproportionation constant, which is the equilibrium constant for the reaction:

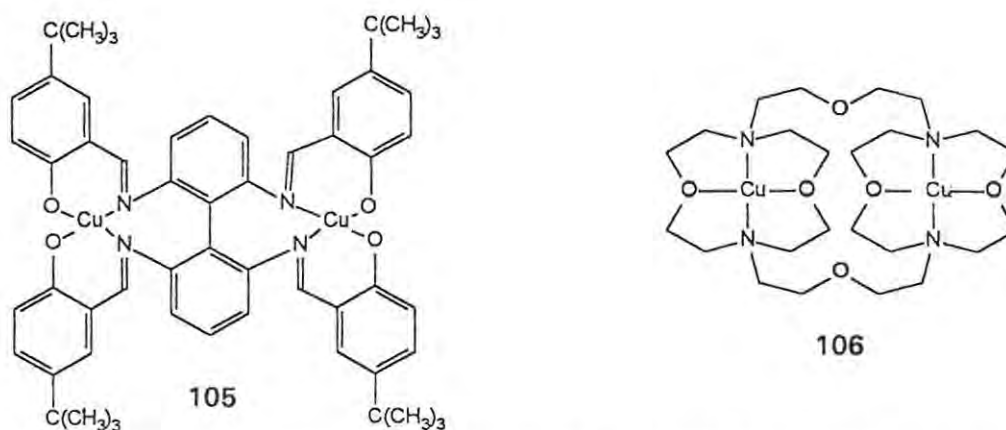


and K_{com} is related to ΔE by the equation: $E_1 - E_2 = 0.0591 \log K_{\text{com}}$ (Gagné *et al.*, 1979).

The standard redox potentials, and therefore ΔE , are dependent on various factors such as:

- solvent effects
- the electronic nature of the donor ligands and their substituents
- the steric demands of the ligand
- the flexibility of the ligand and the size of the chelate rings in the complex (Zanello *et al.*, 1987).

The electronic nature of the donor ligands in complexes is of particular importance: the presence of electron donating groups coordinated to a metal ion would be expected to favour electron removal from a metal, and thus facilitate oxidation. Conversely, pyridine (an electron withdrawing system) is able to stabilise a metal in a low oxidation state, such as Cu(I), because it can delocalise electron density from the metal by π -back-bonding ligand (Simmons *et al.*, 1980). Steric effects may, in some cases, overshadow the electronic effects. For instance, the ligand structure in a copper complex may be such that the binding of a fourth donor to a newly generated Cu(II) centre requiring square planar geometry, is sterically hindered; the Cu(I) state could then be more stable. The effect of the flexibility of bridging systems in ligands is also important, as illustrated by the example of complexes 105 and 106 below. The complex 106 is more easily reduced because it is more flexible (Zanello *et al.*, 1987).



The protein ligand system in tyrosinase is assumed to be fairly rigid in comparison to synthetic ligands. Such rigidity, however, is not necessary for a high redox potential, since Haanstra *et al.* (1992) have reported relatively flexible complexes with high redox potentials.

Electrochemical techniques can thus be used for the investigation of the redox properties of organometallic complexes. In this study, cyclic voltammetry was utilised, primarily to determine the oxidation state of the copper in the complexes which had been synthesised. This technique measures the redox potential of a redox couple, and also demonstrates the reversibility (or irreversibility) of a redox process.

An electrochemical cell is set up, and the cell current is measured as a function of the varying electrode potential. Commonly, a three-electrode system is used: the redox reaction under investigation occurs at the working electrode; the auxiliary electrode completes the circuit; and the reference electrode is used to standardise the potential of the working electrode. The process is illustrated in Figure 8.1. The shape of the cyclic voltammogram depends to some extent on the conditions.

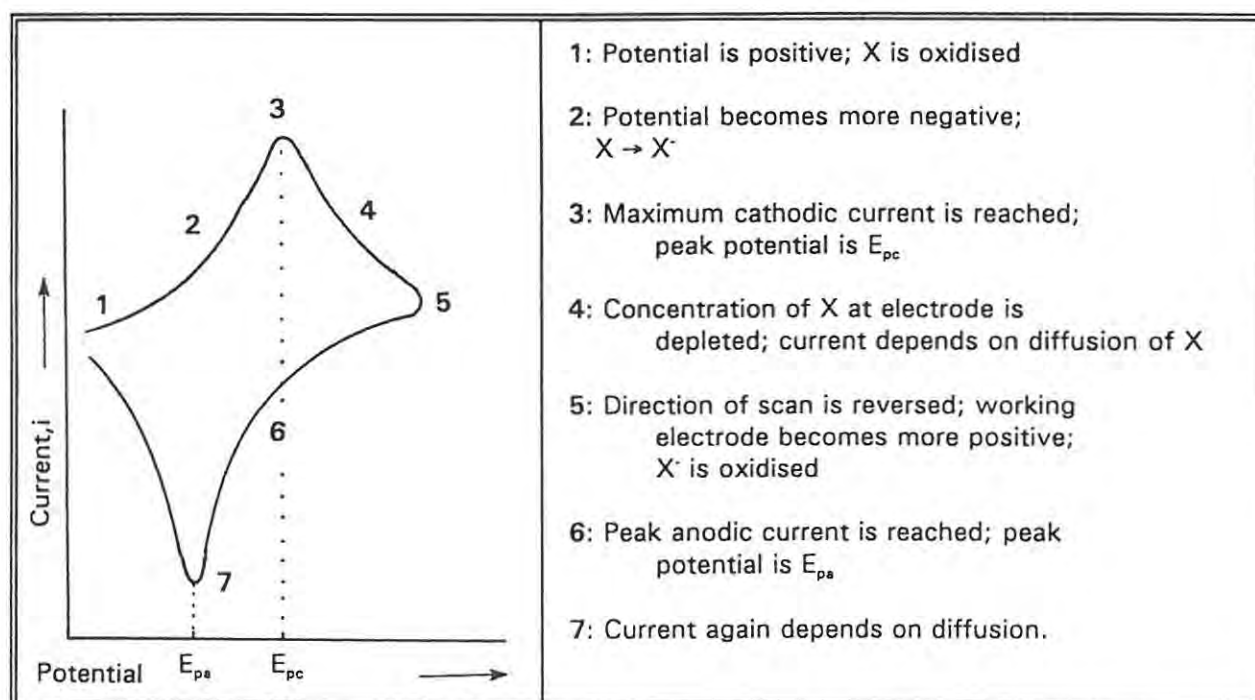


Figure 8.1: A typical cyclic voltammogram, for the redox process $X \rightarrow X^+$

Various properties can be determined from a cyclic voltammogram: The separation of the peak potentials, $E_{pa} - E_{pc}$, in millivolts, equals $59/n$, where n is the number of electrons required in the redox process, for a reversible process. Reversibility is indicated by the existence of an anodic feature corresponding to a cathodic feature; if this is lacking, the process is irreversible. Reactions such as disproportionation cause irregularities in the shapes of the curves (Rossiter and Hamilton, 1986).

8.2 RESULTS AND DISCUSSION

8.2.1 Atomic Absorption Spectrophotometric Analysis

The number of copper atoms per molecule of each complex was established by determining the percentage copper by mass in the complexes, using atomic absorption spectrometry. Samples of the complexes were treated with hydrochloric acid to liberate the copper by hydrolysing the organic ligand, and then diluted to make solutions of suitable concentrations. Concentrations of copper in the solutions were found using of a calibration curve determined using standard solutions of copper (II) chloride (see Section 8.4.1). The results are shown in Table 8.4.

Table 8.4: Analysis of the copper content in the copper complexes by atomic absorption spectrometry.

Complex	Molecular formula ^a	MM ^b	% Cu (calc) ^c	% Cu (found) ^d
I	[Cu ₂ (C ₂₈ H ₄₂ N ₄)(CH ₃ CN) ₄](PF ₆) ₂	997	12.74	11.13
IIA	[Cu ₂ (C ₂₄ H ₄₂ N ₆)(CH ₃ CN) ₄](PF ₆) ₂	977	13.00	13.07
IIB				11.59
IIC				13.05
IIIA	[Cu ₂ (C ₃₂ H ₄₆ N ₆)(CH ₃ CN) ₄](PF ₆) ₂	1077	11.79	11.20
IIIB				10.54

^a As for structures shown in Table 7.1 (Section 7.1.1) and including 2 CH₃CN ligands per copper atom

^b MM = molecular mass

^c Calculated from the formulae shown in this table

^d Mean of duplicate measurements

The theoretical values of relative molecular masses and hence percentages of copper, as shown in the table, were calculated assuming the presence of four solvating acetonitrile molecules per molecule of complex (two per copper atom) as was proposed for complex I (Réglier *et al.*, 1990). The presence of coordinated acetonitrile was apparent in the NMR spectra of the complexes (Section 7.2). In this analysis, the margin of error was approximately 5%, due to the limited precision of scale readings. Duplicate analyses were carried out for each complex, and mean values for the duplicate measurements are quoted in the table.

8.2.2 UV-Visible Spectrophotometric Analysis

The UV-visible spectra of the copper complexes synthesised in the present study were investigated for two reasons. Firstly, the spectral characteristics of the complexes could be correlated with those of similar complexes reported in the literature, permitting confirmation of their proposed structures. UV-visible characteristics can also be correlated with properties such as oxidation state, coordination number, and coordination geometry (see Section 8.1.2), as well as with ligand structure.

Secondly, the interaction of the complexes with oxygen could be investigated. Successful tyrosinase models should bind oxygen reversibly as peroxide, or show aromatic hydroxylation by exhibiting the characteristic absorptions described in Section 8.1.2. Alternatively, complexed copper might react with oxygen by a straightforward oxidation to give copper (II) complexes, and this would be demonstrated by the development of absorption bands due to copper (II) d-d transitions and LMCT transitions, replacing the MLCT transitions.

The UV-visible spectra of the complexes synthesised in this study are summarised in Table 8.5. and shown in Figures 8.2 to 8.15 (at end of Section 8.2.2). The spectra were measured in the absence and then in the presence of oxygen, at room temperature, and in some cases, at approximately -70°C . The low temperature spectra can be compared with those obtained at room temperature, but in the absence of advanced apparatus such as that of Karlin and coworkers, cycling of the addition and removal of oxygen is not possible. Three different solvents, *viz.*, acetonitrile, methanol, and dichloromethane were used, in order to detect any solvent effects. Solvent dependence of the spectra would indicate that the solvent molecules can coordinate with the metal ions of a complex, or that they interact with the ligands in a way which alters the geometry of the complex (Casella *et al.*, 1993). Acetonitrile is able to coordinate with the copper ions (coordinated acetonitrile was found to be present in the solid complexes; see Section 7.2) and therefore the complexes were thought likely to be most stable in this solvent. Methanol could replace the coordinated acetonitrile, and in addition, protic solvents such as methanol can promote the reaction of oxygen with some dinuclear copper complexes (Sorrell *et al.*, 1991a and b). However, dichloromethane is a better solvent for oxygen and thus, oxidation should be more clearly demonstrated in this solvent. In this section, the results obtained for complexes synthesised from prepared ligands are discussed before the corresponding products of template syntheses, for the sake of consistency.

Table 8.5: Results of UV-visible spectral analysis of copper complexes

Complex	Solvent	Conc ^a (mM)	Conditions ^b	Absorption bands λ_{\max} nm (ϵ M ⁻¹ cm ⁻¹)	Figure ^d	
I	MeCN	0.1	25°C, N ₂	213 (22000), 360sh ^c	8.2A	
		0.1	25°C, O ₂	241 (6000), 365sh 710 (100)	B	
		0.05	-70°C, N ₂	224 (26000), 280sh, 350sh	C	
		0.05	-70°C, O ₂	224 (26000), 280sh, 350sh, 730 (2700)	D	
	MeOH	0.1	25°C, N ₂	223(17000), 260sh, 350sh	8.3A	
		0.1	25°C, O ₂	246 (6400), 360sh 536 (500)	B	
	CH ₂ Cl ₂	0.2	25°C, N ₂	260, 340sh	8.4A	
		0.2	25°C, O ₂	260(8800), 340sh	B	
		0.56	25°C, O ₂	250, 755 (50)	C	
		0.1	25°C, O ₂	257, 345sh	D	
		0.1	-70°C, N ₂	257 (14000), 355sh, 635 (6400), 680(6400)	D	
	0.1	-70°C, O ₂	257, 345sh	E		
	IIC	MeCN	0.1	25°C, N ₂	220 (25000)	8.5A
			0.1	25°C, O ₂	236 (6200), 673(1300)	B
0.1			-70°C, N ₂	214 (25000)	C	
0.1			-70°C, O ₂	226 (7000), 660(100)	D	
MeOH		0.1	25°C, N ₂	217 (24000), 360sh	8.6A	
		0.1	25°C, O ₂	246 (9000), 361sh 535 (700)	B	
		0.2	-70°C, N ₂	228 (10000), 255sh	C	
		0.2	-70°C, O ₂	228 (7000), 255sh	D	
CH ₂ Cl ₂		0.36	25°C, N ₂	220, 750	8.7A	
			25°C, O ₂	220, 755 (100)	B	

^a Concentration

^b N₂ denotes spectrum measured in absence of oxygen

^c O₂ denotes spectrum measured after oxygenation of solution

^d Figures show spectra with comparable vertical scales, and therefore maximum absorbances at lower wavelengths are not always visible. Insets show the shapes of these peaks, obtained using more dilute solutions

Complex	Solvent	Conc ^a (mM)	Conditions ^b	Absorption bands λ_{\max} nm (ϵ M ⁻¹ cm ⁻¹)	Figure ^d
IIA	MeCN	0.1	25°C, N ₂	220 (24000)	8.8A
		0.1	25°C, O ₂	238 (7400), 615(1000)	B
		0.1	-70°C, N ₂	227 (19000), 400sh	C
		0.1	-70°C, O ₂	227 (21000), 400sh, 700 (1000)	D
	MeOH	0.1	25°C, N ₂	222 (25000), 370sh	8.9A
		0.1	25°C, O ₂	247 (4000), 360sh, 536 (500)	B
		0.1	-70°C, N ₂	224 (12000), 270 (11000)	C
		0.1	-70°C, O ₂	227 (16000), 270sh, 660 (1000)	D
	CH ₂ Cl ₂	0.04	25°C, N ₂	220 (50000), 280sh	8.10A
		0.36	25°C, O ₂	220, 260sh, 612 (190)	B
IIB	CH ₂ Cl ₂	0.16	25°C, N ₂	224 (50000)	8.11A
		0.16	25°C, O ₂	220 (13000), 584(300), 785 (200)	B
IIIA	MeCN	0.05	25°C, N ₂	221 (50000)	8.12A
		0.05	25°C, O ₂	220(5000), 750(3000)	B
	MeOH	0.02	25°C, N ₂	230 (70000), 264 (70000), 340sh	8.13A
		0.02	25°C, O ₂	257 (40000), 763 (2000)	B
		0.10	25°C, O ₂	250 (40000), 390 (20000)	C
	CH ₂ Cl ₂	0.04	25°C, N ₂	248 (51500), 301sh, 360sh	8.14A
		0.04	25°C, O ₂	248(40000), 624 (200)	B
		0.04	-70°C, N ₂	240(52500), 300sh, 360sh	C
		0.04	-70°C, O ₂	240(17500), 360sh	D
		0.04	25°C, O ₂	251 (20000), 300sh, 360sh	E

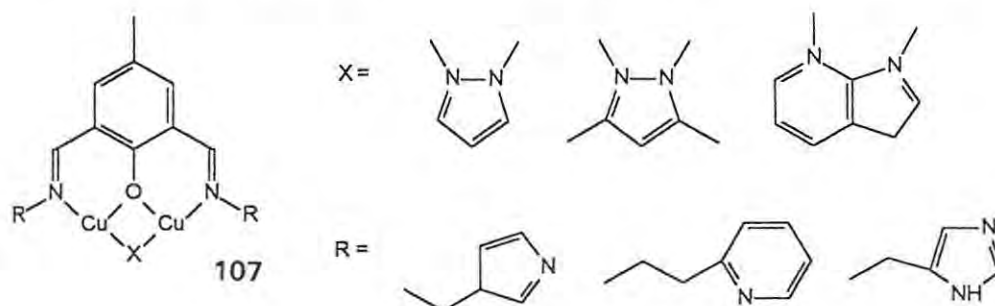
The effect of chelate ring size is attributable to the different coordination requirements of Cu(I) and Cu(II) ions (see Section 1.1.3). For example, while six-membered chelate rings stabilise Cu(II), a decrease in chelate ring size may favour the reduction of copper (II) to copper (I) (Pandiyani *et al.*, 1992).

Many detailed studies on the electrochemical characteristics of both amine and imine copper complexes have been reported. For example, standard redox potentials for complexes **107** were found to be in the ranges shown below (Gagné *et al.*, 1979):

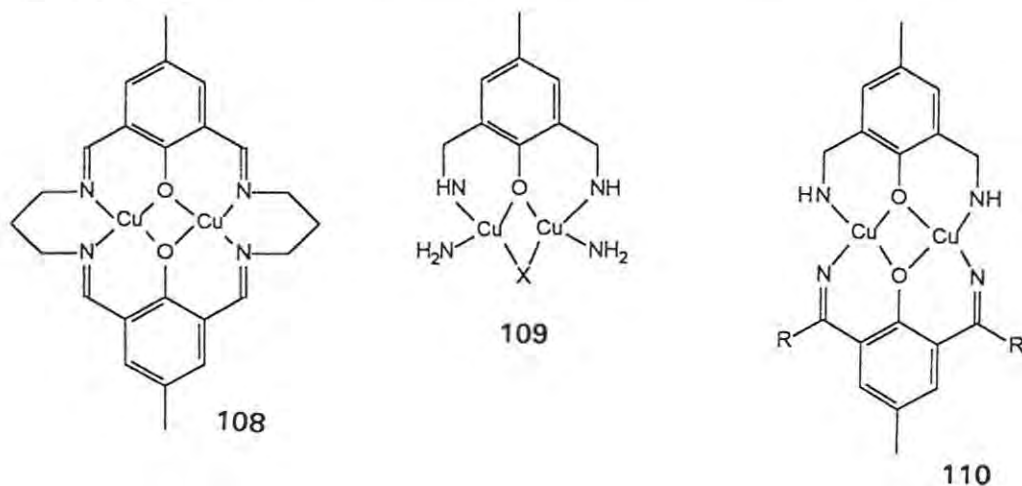
$$E_0 \text{ Cu}^{\text{II}}\text{Cu}^{\text{II}}/\text{Cu}^{\text{II}}\text{Cu}^{\text{I}} \quad -0.52 - +0.15 \text{ V}$$

$$\text{Cu}^{\text{II}}\text{Cu}^{\text{I}}/\text{Cu}^{\text{I}}\text{Cu}^{\text{I}} \quad -0.91 - +0.08 \text{ V}$$

These authors reported the following trends: (a) high redox potentials were obtained when copper ions were surrounded by hydrophobic and/or bulky ligands, and (b) more flexible ligands with softer (more polarisable) coordinating groups gave complexes with more positive redox potentials.



Mandal and Nag (1984) extended this type of research to include macrocyclic and other complexes **108 - 110**, and reported stabilisation of the Cu(I)/Cu(II) species in the case of the macrocyclic system **110**.



Complex	Solvent	Conc ^a (mM)	Conditions ^b	Absorption bands λ_{\max} nm (ϵ M ⁻¹ cm ⁻¹)	Figure ^d
IIIB	CH ₂ Cl ₂	0.01	25°C, N ₂	245 (65000), 280sh	8.15A
		0.04	25°C, O ₂	215 (55000), 280sh, 350sh	B
		0.36	25°C, O ₂	220, 702 (80)	C

^a Concentration

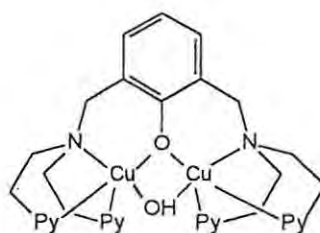
^b N₂ denotes spectrum measured in absence of oxygen

^c O₂ denotes spectrum measured after oxygenation of solution

^d Figures show spectra with comparable vertical scales, and therefore maximum absorbances at lower wavelengths are not always visible. Insets show the shapes of these peaks, obtained using more dilute solutions

8.2.2 (1) Complex I

The spectrum obtained for complex I in degassed acetonitrile (Figure 8.2A) showed a broad absorption band at 213nm (ϵ 22000 M⁻¹cm⁻¹) with shoulders at 300 and 360nm. The absorption bands at 213 and 300 nm can be attributed to $d\pi \rightarrow \pi^*$ and $d\sigma^* \rightarrow \pi^*$ MLCT transitions in a copper (I) complex (Sorrell and Borovik, 1986). The origin of the small shoulder at 360nm is less clear. A similar shoulder is shown in the spectrum of complex 111, reported without explanation by Sarwar Nasir *et al.* (1991), although they do report that a much smaller shoulder at 410nm is an artifact.



111

Py = pyridine

Intense bands in the region 300 - 360nm can be attributed to phenoxy-to-copper (II) LMCT transitions (Casella *et al.*, 1991a) or peroxo-to-copper (II) LMCT transitions (Casella *et al.*, 1991b), but the shoulder observed for complex I is not intense and no evidence of aromatic hydroxylation was found in the present study. This seems to rule out either of these LMCT transitions being responsible for the shoulder. However, complexes of copper and pyridine donor ligands can exhibit absorption bands near 350nm due to $\pi \rightarrow \pi^*$ transitions in the pyridine rings (Sorrell *et al.*, 1991a and Karlin *et al.*, 1992).

Oxygenation of the solution caused a marked decrease in the band intensity and a slight red shift of the high energy peak to 241nm (ϵ 6000 M⁻¹cm⁻¹; Figure 8.2B). This can be explained in terms of the oxidation of copper (I) to copper (II), since this would result in loss of the MLCT transitions due to the copper (I) ions and leave ligand $\pi \rightarrow \pi^*$ absorption bands below 300nm. The development of a weak d-d band at 710nm also indicates the presence of copper (II), and suggests tetrahedral geometry around each copper ion; absorption bands at 550 - 800nm are characteristic of tetrahedral (four-coordinated) copper (II) complexes (Lever, 1984, Chapter 6). At -70°C, the spectra were similar (Figure 8.2C and D), and the absence of intense absorption bands near 360nm, shows that a peroxo-complex was not formed (Karlin *et al.*, 1992 and Tyeklár *et al.*, 1993).

In methanol, I gave similar spectra (Figure 8.3A and B) and oxygenation again caused the development of a d-d band (536nm); the wavelength of this latter absorption band seems to indicate square planar geometry (see Table 8.1). In dichloromethane, the MLCT transitions were at lower energy than in the other solvents used, presumably as a result of a change in solvation (Figure 8.4A and B). A d-d transition was not detected in dilute solution, but was observed at 755nm in a more concentrated solution (Figure 8.4C) and at -70°C (Figure 8.4E).

8.2.2 (2) Complex IIC

The spectrum of complex IIC, in acetonitrile, showed a broad band at 220nm (Figure 8.5A), and when the acetonitrile solution was oxygenated (Figure 8.5B), a weak d-d band developed at 673nm due to oxidation of the copper ions. The decrease in intensity of the high energy absorption band upon oxygenation suggests that the product contained the corresponding copper (I) complex (as a mixture with the copper (II) analog) which was able to give rise to MLCT transitions, and which was subsequently oxidised to copper (II). Spectra measured at -70°C (Figure 8.5D and E) were similar to those measured at ambient temperature.

In methanol, complex IIC showed an absorption band at 217nm with a small shoulder at 260nm (Figure 8.6A). This is in keeping with the proposed structure, since the coordination in imidazole-copper (II) complexes can give rise to three LMCT transitions near 220nm, 260nm, and 330nm, with the latter two appearing as poorly defined shoulders on the high energy absorption band (Lever, 1984, Chapter 5 and Bernarducci *et al.*, 1983). Oxygenation again resulted in a decrease in the intensity of the highest energy peak (Figure 8.6B). A shoulder was observed at 360nm which seemed to increase with oxygenation and, in this case, the absorption band may be due to imidazole-to-copper (II) LMCT transitions (Sanyal *et al.*, 1991). When this complex was dissolved in methanol which had not been previously degassed and was therefore probably well oxygenated,

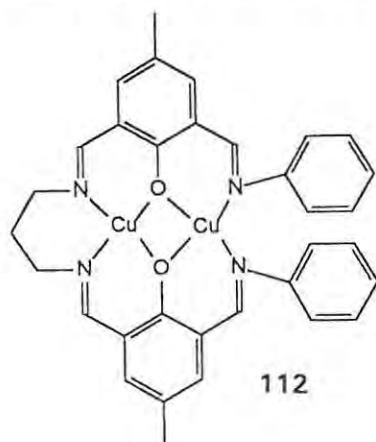
the band at 360nm was particularly strong (Figure 8.6C). A d-d transition was observed at 535nm for the oxidised complex. At -70°C, the spectrum of IIC in methanol showed an absorption band at 228nm, which was accompanied by a marked shoulder at 255nm. Four-coordinate copper (II) complexes typically give absorption bands of this form (Sorrell and Borovik, 1986, see Section 8.1.2), and this confirms the coordination of solvent molecules. When complex IIC was dissolved in dichloromethane, the absorption band at 220nm was accompanied by a shoulder at 260nm, and a d-d band developed at 755 after oxygenation (Figure 8.7A and B).

8.2.2 (3) Complex IIA

The spectra obtained for complex IIA were similar to those for complex IIC. Absorption bands near 220nm were observed in acetonitrile and in methanol solutions, and the shoulder at 360nm was more marked in the methanol solution (Figures 8.8A and 8.9A). Oxygenation of these solutions lead to a decrease in the intensities of the high energy bands, suggesting the presence of the corresponding copper (I) complex in the sample (Figure 8.8B and 8.9B). The absorption bands which developed at 615nm and 634nm respectively, are attributable to copper (II) d-d transitions and again suggest four-coordination of the copper (II) ions. The spectra measured in acetonitrile at -70°C (Figure 8.8C and D) were similar to those measured at ambient temperature but, in the methanol solution, the high energy absorption band showed two peaks, at 224 and 270nm (Figure 8.9C and D). This type of spectrum was reported to be characteristic of four-coordinated copper (II) complexes (Sorrell and Borovik, 1986). In dichloromethane, the high energy absorption band at 220nm again showed a shoulder at 280nm (Figure 8.10A). The d-d transition in this case was observed at 612nm (Figure 8.10B).

8.2.2 (4) Complex IIB

Complex IIB was analysed in dichloromethane (Figure 8.11). The oxygenated complex showed absorption bands at 584nm and 785nm (Figure 8.11B), which are at similar wavelengths to those reported for the square planar copper (II) complex 112 (Srinivas and Zaccharias, 1992).

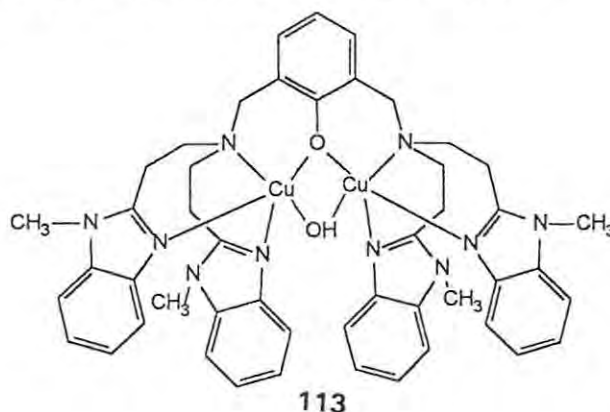


8.2.2 (5) Complex IIIA

The acetonitrile solution of complex IIIA showed a broad absorption band at 221nm, which decreased in intensity with oxygenation, due to loss of MLCT transitions as discussed above (Figure 8.12A and B). Oxidation also gave rise to a d-d absorption band at 750nm. In methanol, however, the spectrum showed two intense high energy absorption bands, at 230 and 275nm respectively (Figure 8.13A), indicating four-coordination of the copper (I). This pattern was lost with oxygenation, and a d-d absorption band developed at 763nm due to the formation of copper (II) ions (Figure 8.13B). When complex IIIA was dissolved in methanol which had not been degassed, the spectrum obtained showed a marked absorption band at 390nm (Figure 8.13C).

In dichloromethane, the complex IIIA showed an intense absorption band at 249nm, with shoulders at 301 and 360nm (Figure 8.14A). This type of spectrum is characteristic of three-coordinated copper (I) complexes (Sorrell and Borovik, 1986), which suggests that the dichloromethane caused the removal of one of the acetonitrile ligands.

Oxygenation of the dichloromethane solution of complex IIIA exhibited decreased intensity of the high energy peak, and a weak d-d transition at 624nm. An oxidation product IIIA' was isolated by precipitation with ether, from oxygenated solutions of the complex in dichloromethane and methanol (Section 8.4.3), and this product also showed absorption bands at 251, 300 (shoulder) and 360nm (shoulder) (Figure 8.14E). In the case of complex 113, an absorption band near 300nm was attributed to σ (amino)-to-copper (II) LMCT transitions and one at 350 - 400nm to π (benzimidazole)-to-copper (II) LMCT transitions (Casella *et al.*, 1993).



8.2.2 (6) Complex IIIB

The analysis of complex IIIB was carried out in dichloromethane (Figure 8.15A). The spectrum showed a high energy absorption band at 245nm with a shoulder at 280nm, which suggests the presence of three-coordinated copper (I) ions (Sorrell and Borovik, 1986). Oxygenation caused

oxidation of the copper (II) to copper (III), as indicated by the appearance of an absorption band due to a d-d transition, at 766nm (Figure 8.15B).

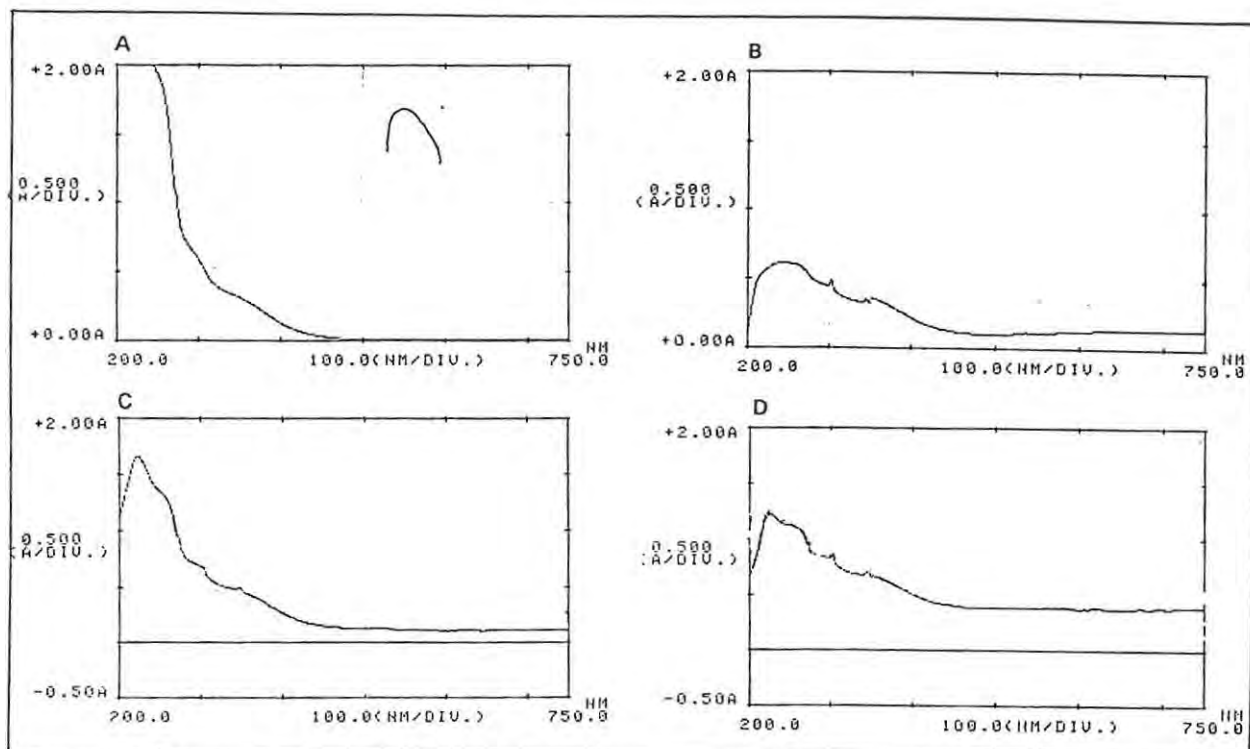


Figure 8.2: UV spectrum for complex I in MeCN (A) in the absence of air at 25°C; (B) in the presence of air at 25°C; (C) in the absence of air at -70°C; (D) in the presence of air at -70°C

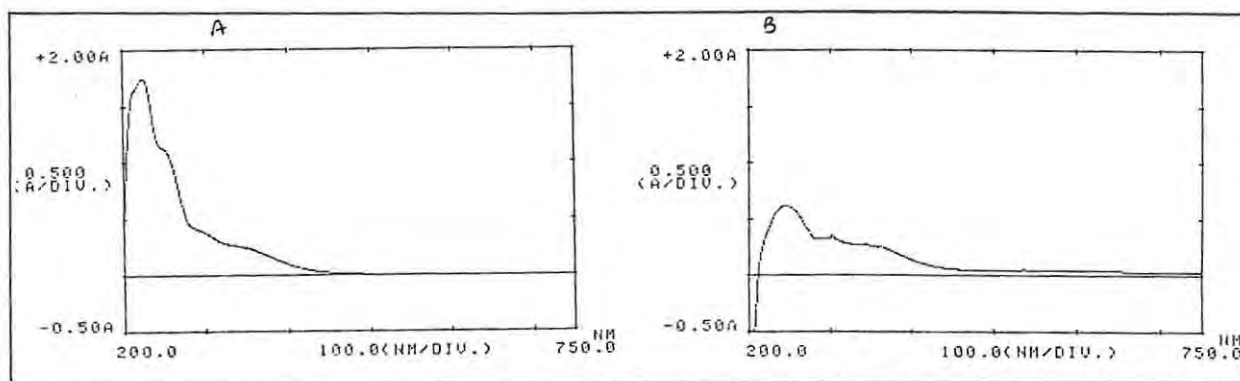


Figure 8.3: UV spectrum for complex I in MeOH (A) in the absence of air at 25°C; (B) in the presence of air at 25°C

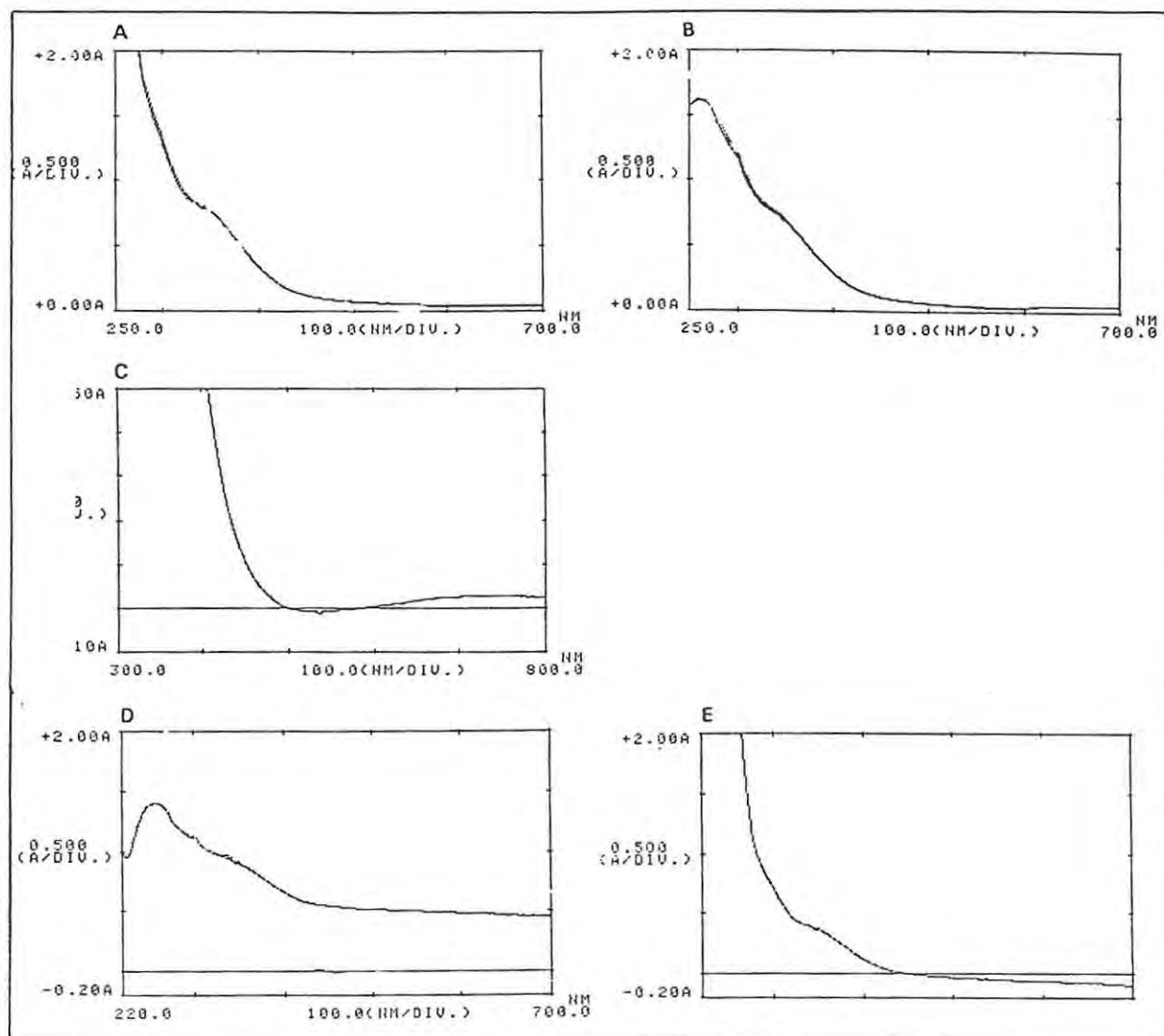


Figure 8.4: UV spectrum for complex I in CH_2Cl_2 (A) in the absence of air at 25°C; (B,C) in the presence of air at 25°C; (D) in the absence of air at -70°C; (E) in the presence of air at -70°C

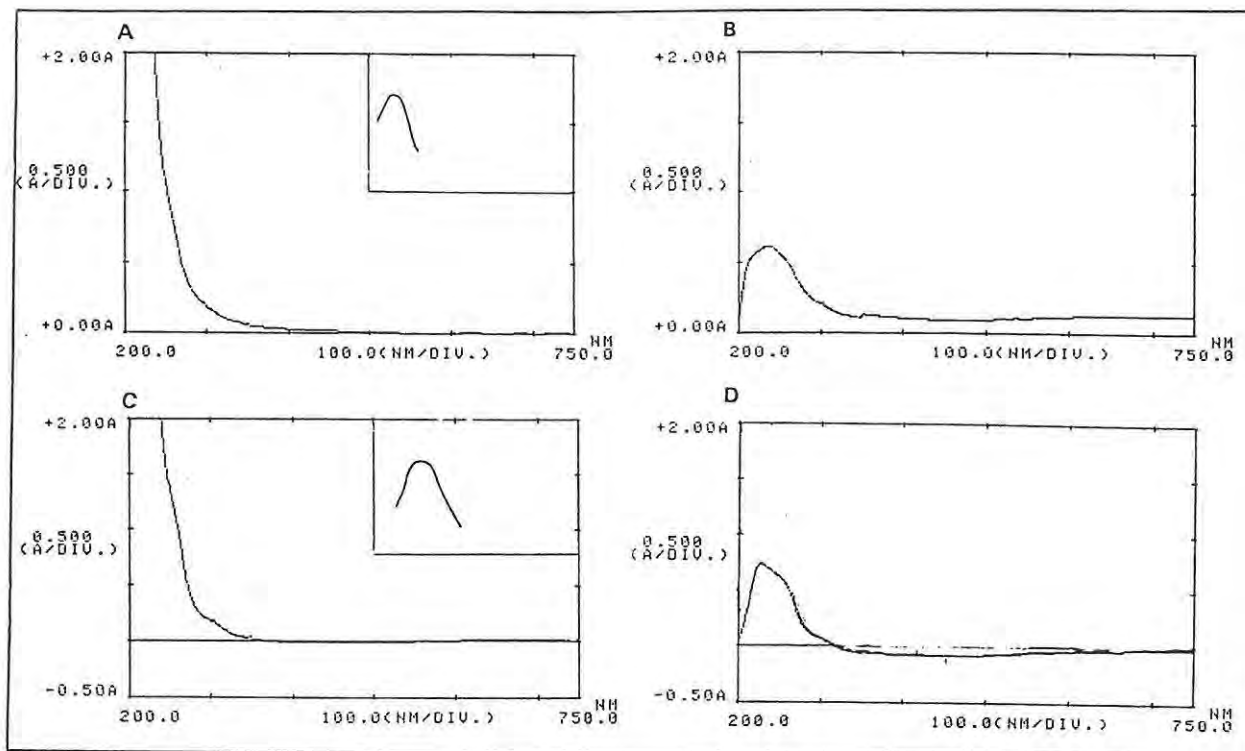


Figure 8.5: UV spectrum for complex IIC in MeCN (A) in the absence of air at 25°C; (B) in the presence of air at 25°C; (C) in the absence of air at -70°C; (D) in the presence of air at -70°C

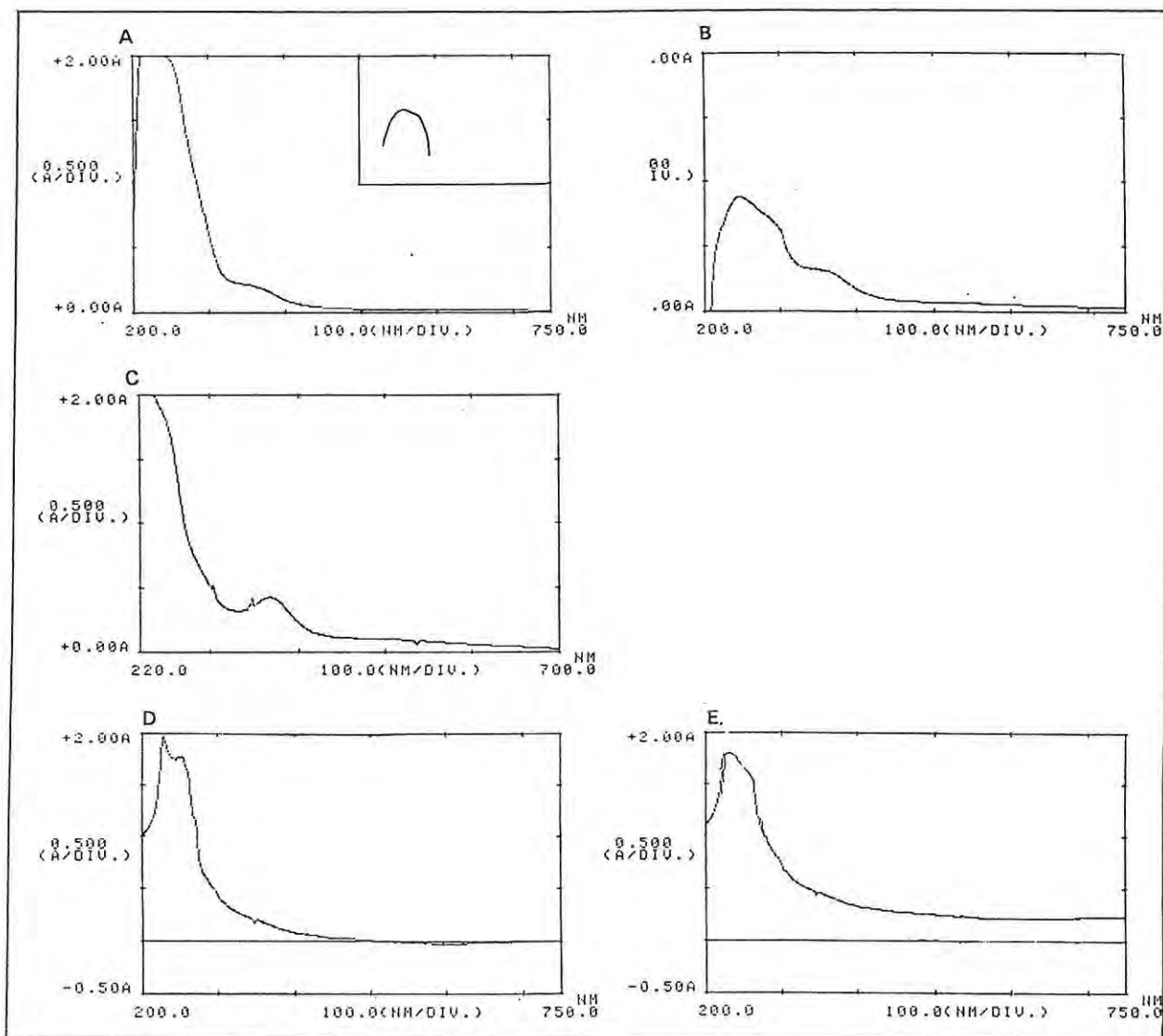


Figure 8.6: UV spectrum for complex IIC in MeOH (A) in the absence of air at 25°C; (B,C) in the absence of air at -70°C; (D) in the absence of air at -70°C; (E) in the presence of air at -70°C

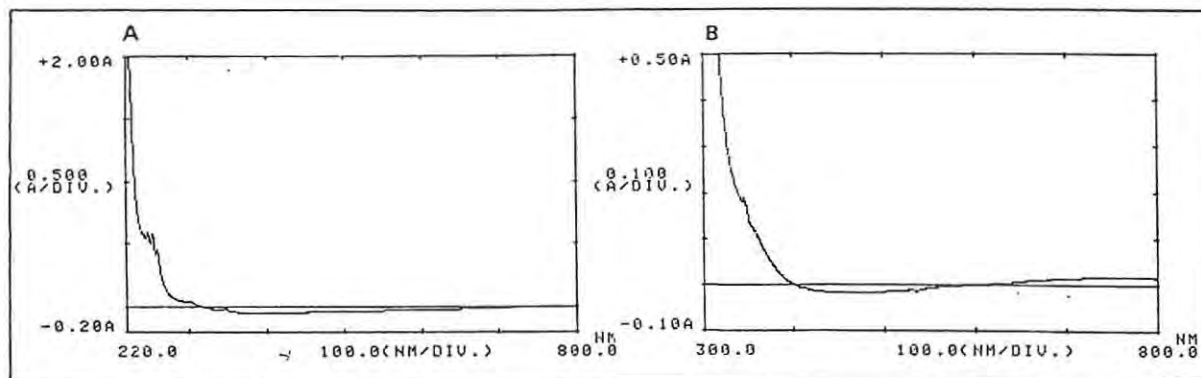


Figure 8.7: UV spectrum for complex IIC in CH_2Cl_2 (A) in the absence of air at 25°C ; (B) in the presence of air at 25°C

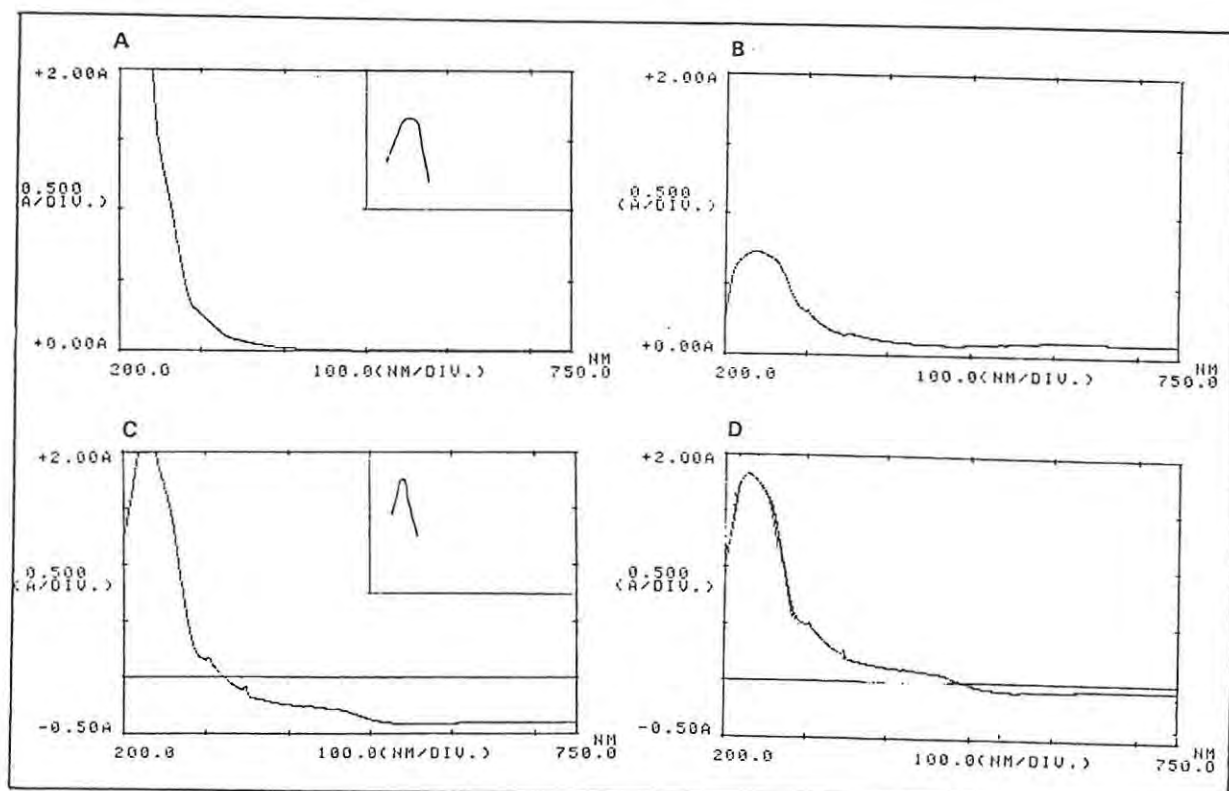


Figure 8.8: UV spectrum for complex IIA in MeCN (A) in the absence of air at 25°C ; (B) in the presence of air at 25°C ; (C) in the absence of air at -70°C ; (D) in the presence of air at -70°C

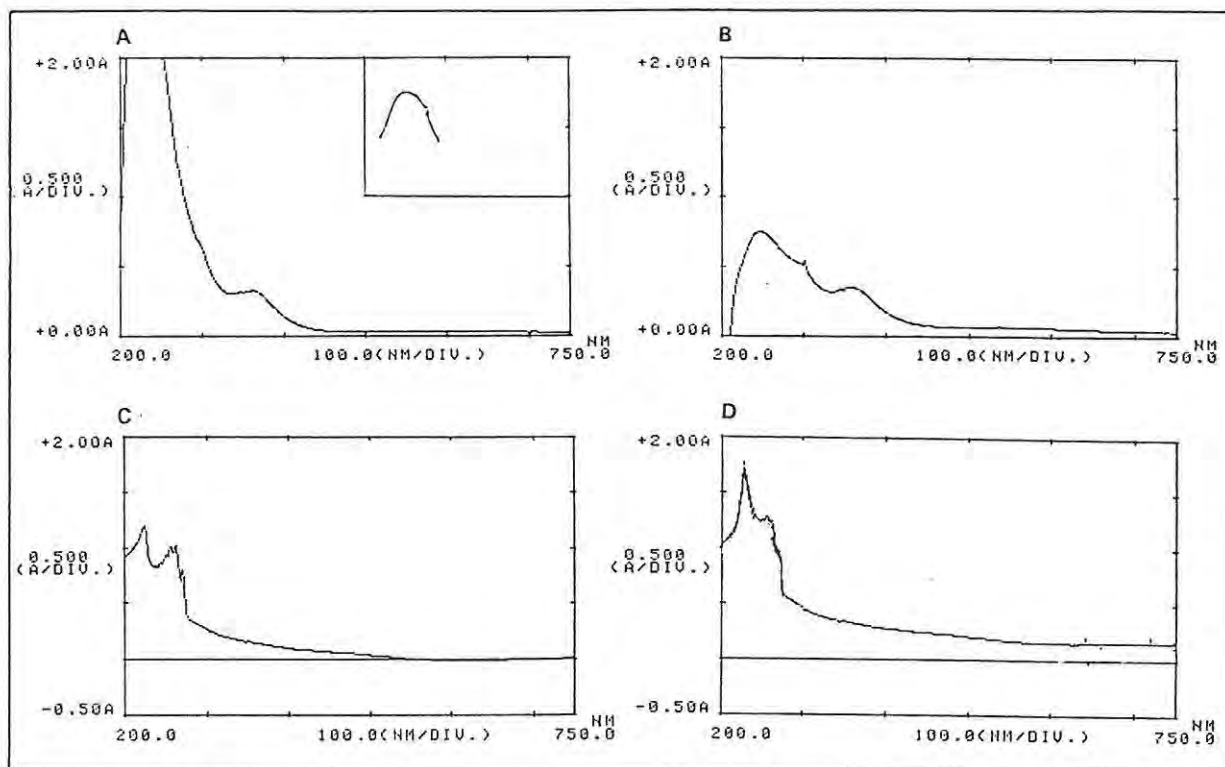


Figure 8.9: UV spectrum for complex IIA in MeOH (A) in the absence of air at 25°C; (B) in the presence of air at 25°C; (C) in the absence of air at -70°C; (D) in the presence of air at -70°C

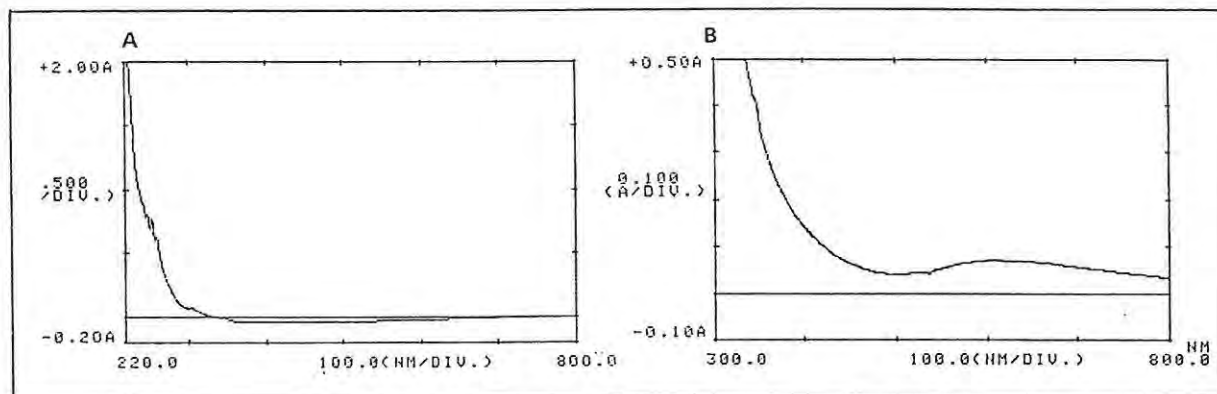


Figure 8.10: UV spectrum for complex IIA in CH_2Cl_2 (A) in the absence of air at 25°C; (B) in the presence of air at 25°C

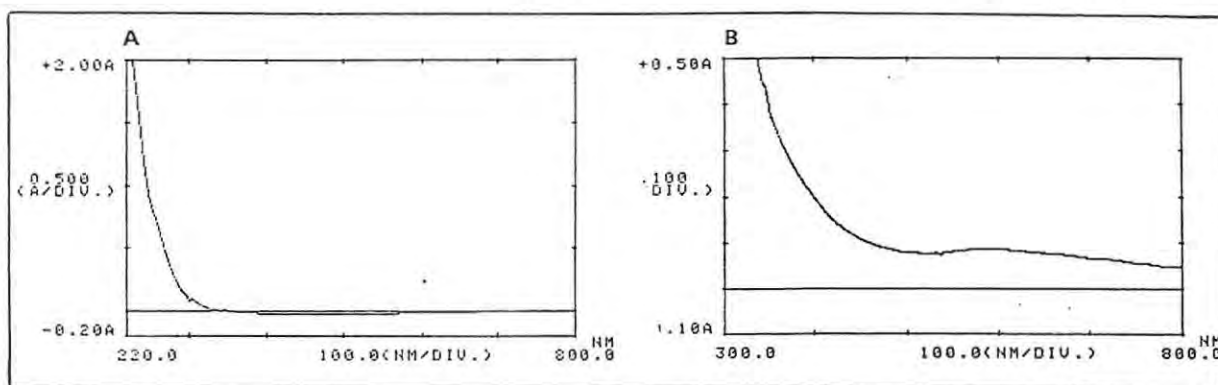


Figure 8.11: UV spectrum for complex IIB in CH_2Cl_2 (A) in the absence of air at 25°C ; (B) in the presence of air at 25°C

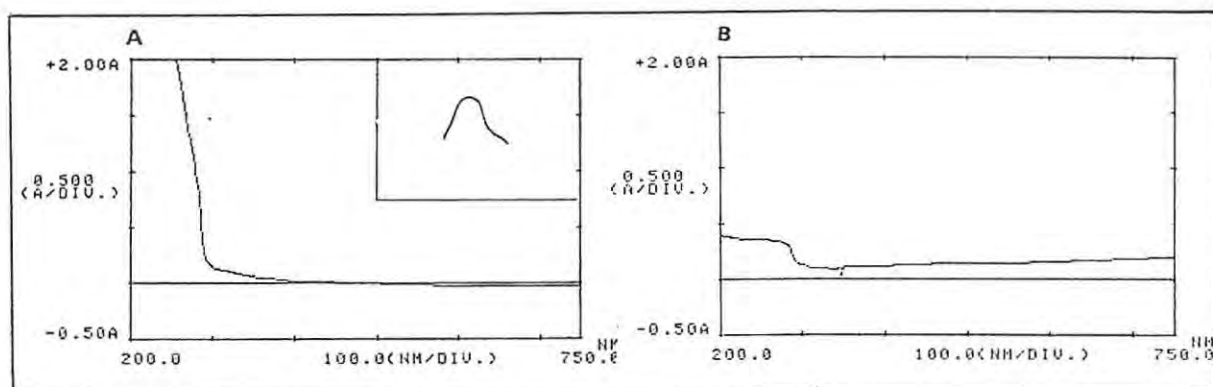


Figure 8.12: UV spectrum for complex IIIA in MeCN (A) in the absence of air at 25°C ; (B) in the presence of air at 25°C

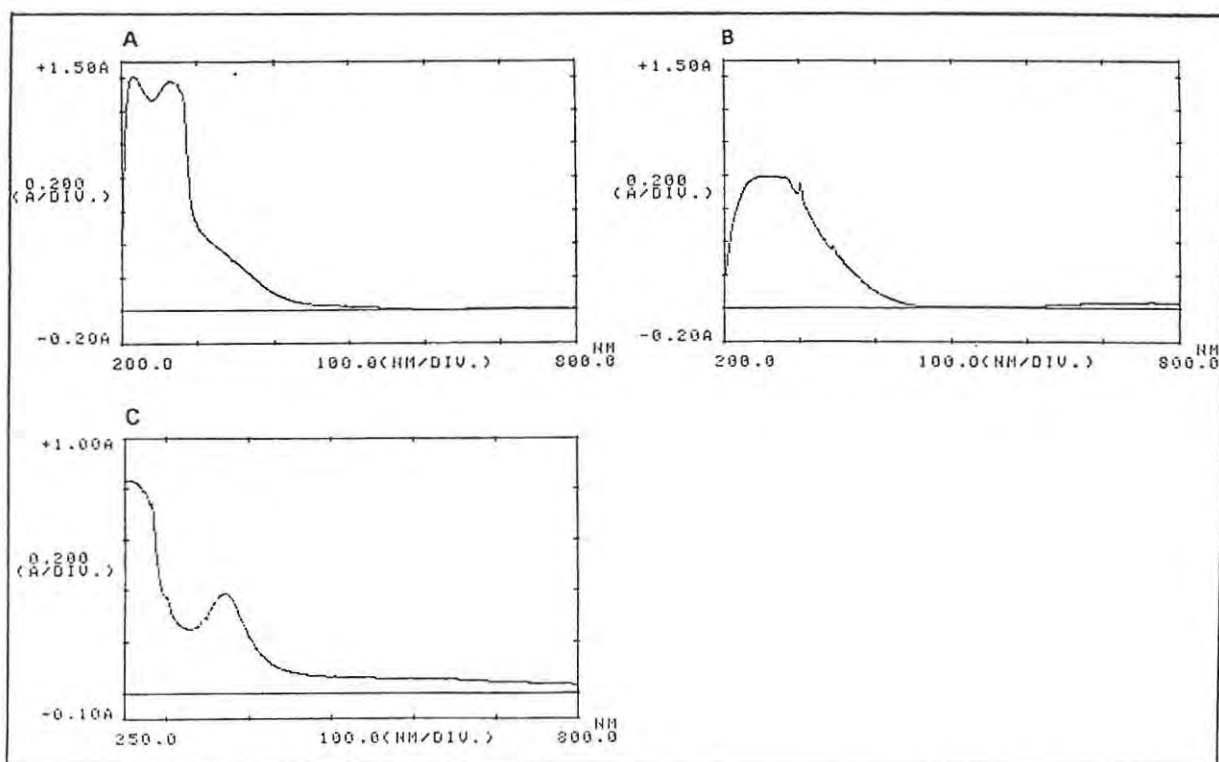


Figure 8.13: UV spectrum for complex IIIA in MeOH (A) in the absence of air at 25°C ; (B,C) in the presence of air at 25°C

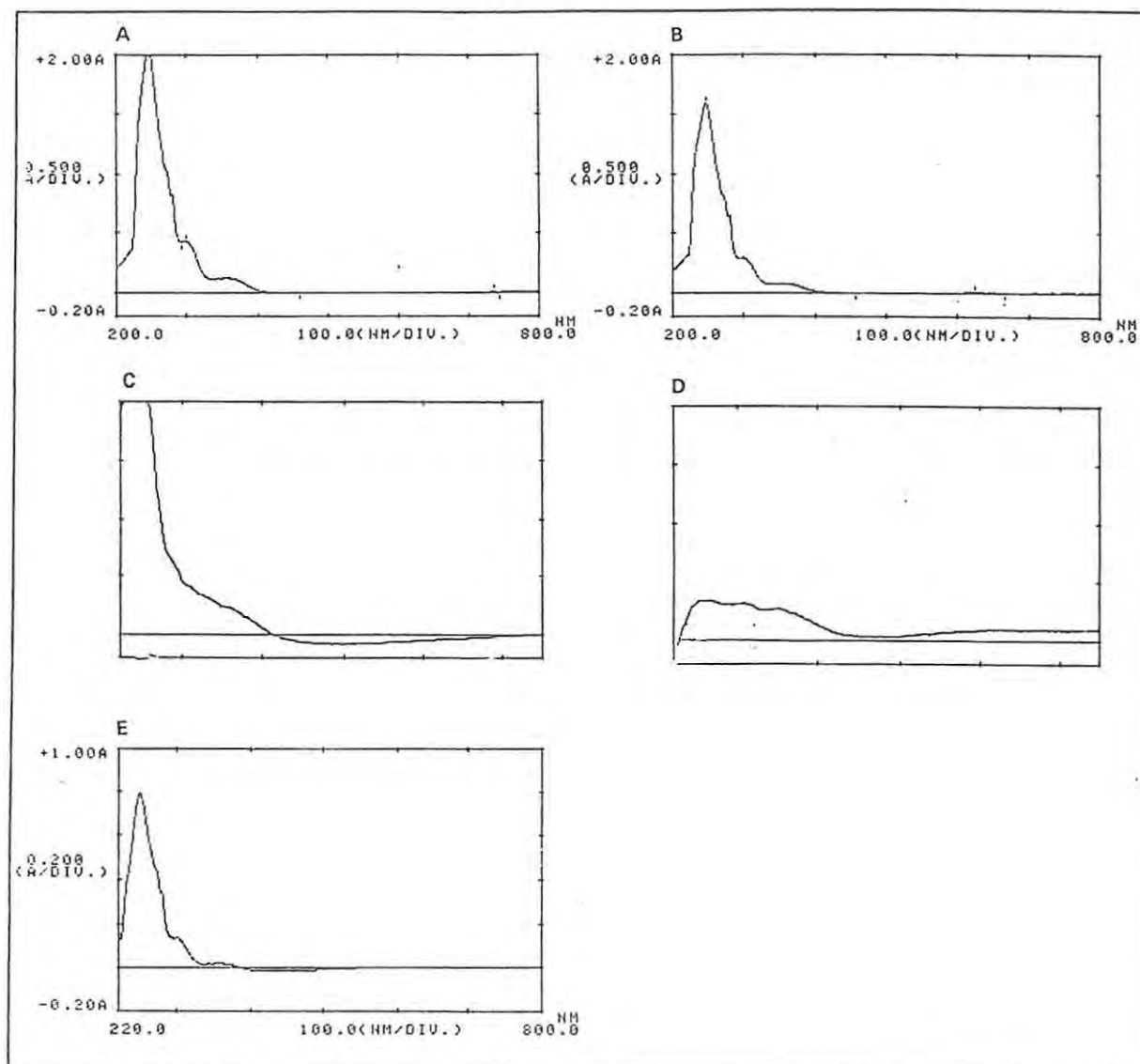


Figure 8.14: UV spectrum for complex IIIA in CH_2Cl_2 (A) in the absence of air at 25°C ; (B) in the presence of air at 25°C ; (C) in the absence of air at -70°C ; (D) in the presence of air at -70°C (E) oxidation product IIIA'

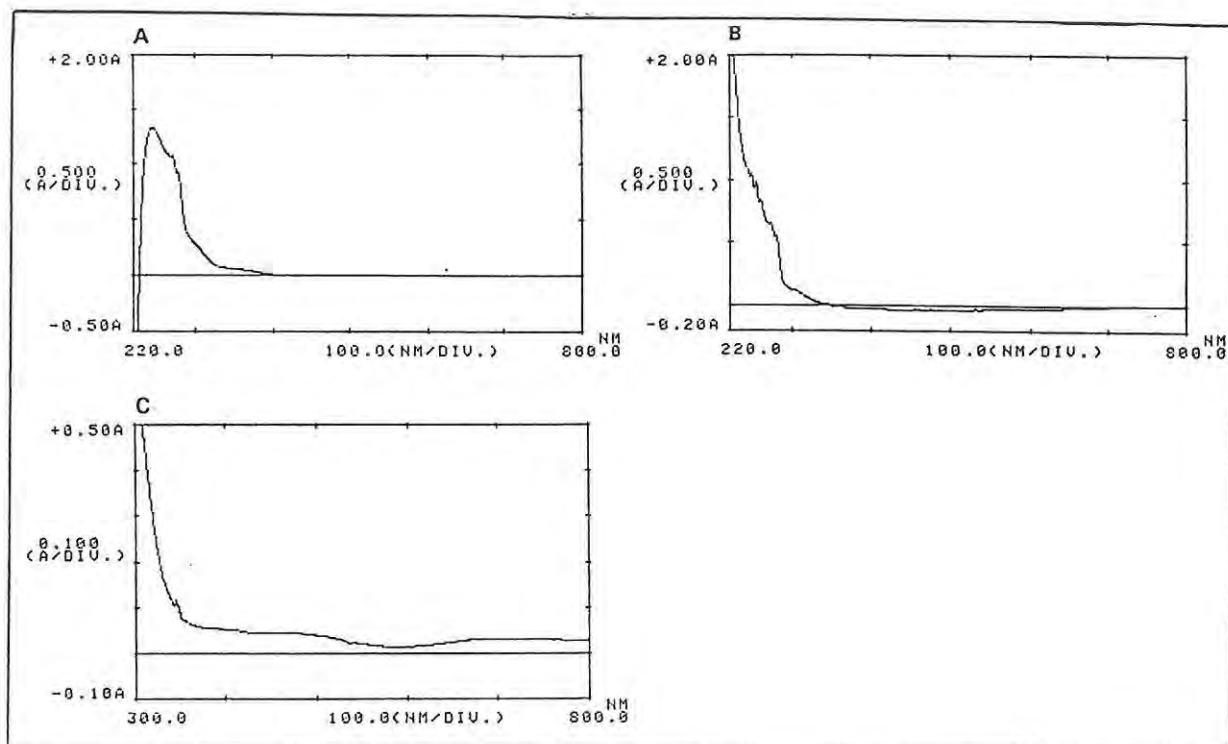


Figure 8.15: UV spectrum for complex IIIB in CH_2Cl_2 (A) in the absence of air at 25°C; (B,C) in the presence of air at 25°C

8.2.3 Electrochemical analysis

Cyclic voltammograms were measured for all the complexes, as illustrated in Figure 8.16, and the potentials and $E_{1/2}$ values (half wave potentials) are summarised in Table 8.6. The complexes **I**, **IIB**, **IIIA** and **IIIB** were all found to contain copper (I) ions, since each exhibited one reduction [to copper (0)] and one oxidation step [to copper (II)]. In complexes **IIA** and **IIC**, where only reductions were observed, the copper was predominantly in the +2 oxidation state. The deposition of metallic copper was observed during cyclic voltammetry with complexes **IIC** and **IIIB**, indicating that these complexes were unstable under the conditions used for the analysis. The benzimidazole-copper complexes (**IIIA** and **IIIB**) exhibited higher (more negative) potentials than the pyridine- and imidazole-copper complexes, indicating their greater tendency towards oxidation.

Table 8.6: Results of cyclic voltammetric analysis of complexes

Complex	Potentials measured in cyclic voltammogram (V)	$E_{1/2}$ (vs Fc/Fc ⁺) ^a (V)	Oxidation state of copper
I	-0.38 (cathodic) -0.20 (anodic) 0.00 (cathodic) 0.17 (anodic)	-0.29(red) 0.09(ox)	I
IIA	-1.06 (cathodic; irreversible reduction) 0.38 (anodic; irreversible oxidation)		II
IIB	-0.39 (cathodic) -0.26 (anodic) -1.05 (cathodic) -0.55 (anodic)	-0.33(red) -0.80 (ox)	I
IIC	-0.51 (cathodic) -0.09 (anodic) -0.91 (cathodic; copper deposited)	-0.30(red)	II
IIIA	-0.91 (cathodic) -0.51 (anodic) 0.24 (cathodic) 0.83 (anodic)	-0.71(red) 0.63(ox)	I
IIIB	-0.93 (cathodic) -0.54 (anodic; metal deposited) 0.32 (cathodic) 0.12 (anodic)	-0.74(red) 0.22(ox)	I

^a Half wave potentials, measured with reference to the ferrocene-ferrocinium couple

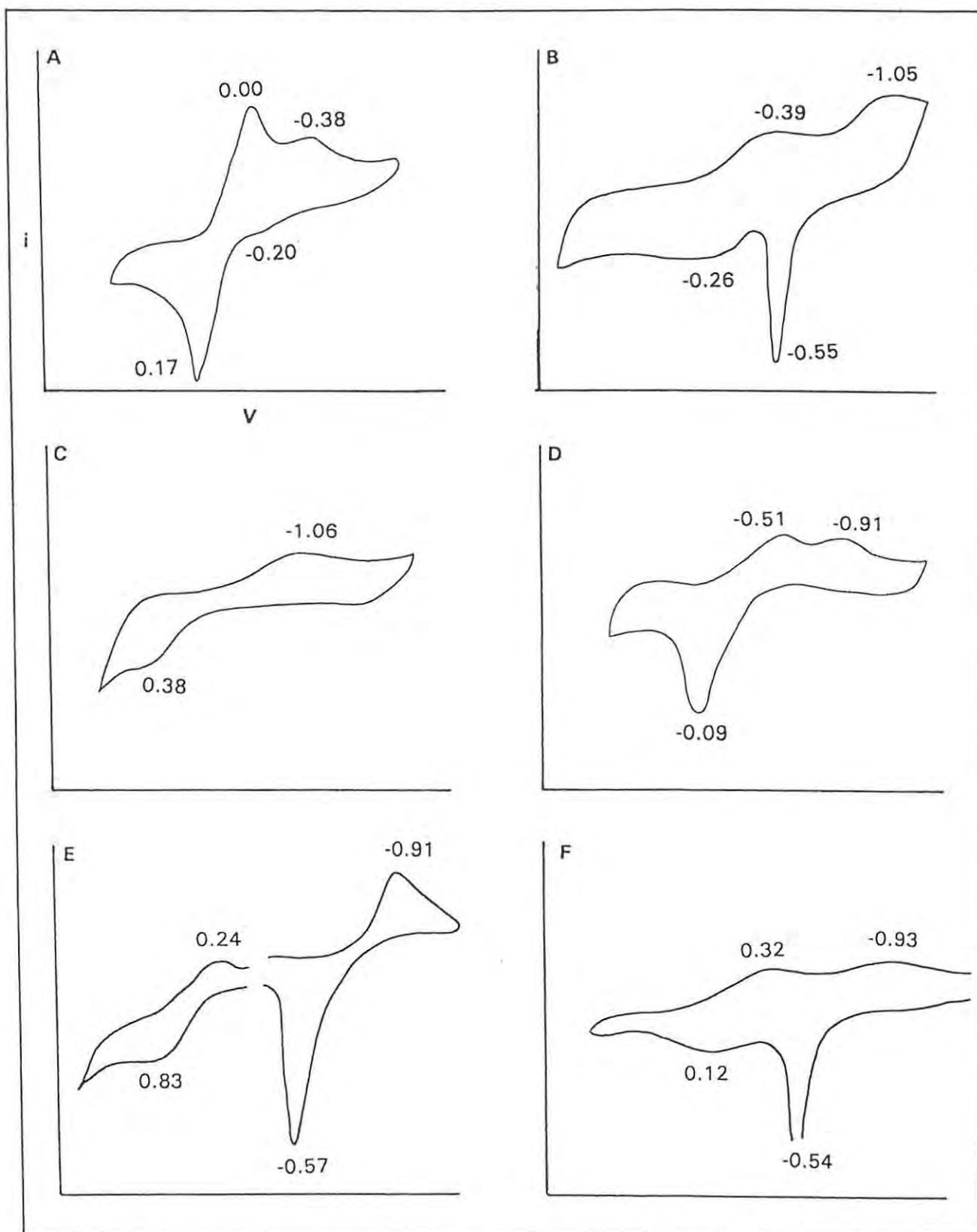


Figure 8.16: Cyclic voltammograms obtained for dinuclear copper complexes: (A) complex I (B) complex IIA (C) complex IIB (D) complex IIC (E) complex IIIA (F) complex IIIB; numbers show potentials of redox reactions in volts, vs Fc/Fc⁺.

8.3 CONCLUSIONS

8.3.1 Atomic absorption analysis

The percentages of copper measured by this method approximate the theoretical values, confirming the dinuclear nature of the complexes. The percentage of copper found in complex I was somewhat lower than the theoretical value, and this may indicate the presence of some mononuclear complex 101 (see Section 7.2.4) in the sample. This mononuclear complex was reported by Réglie *et al.*, (1990) to be inactive as a catalyst.

The complexes which were synthesised by the template method (*viz.*, IIB, IIC, and IIIB) gave lower copper contents than the theoretical values. This indicates that the products were not pure, and possibly contained mononuclear contaminants.

8.3.2 UV-Visible spectroscopy

This analysis has shown that UV-visible spectra of the complexes correlate with the proposed structures. Absorption bands were observed at the expected wavelengths for the respective copper and ligand-copper transitions, as shown in Table 8.7.

Table 8.7: Transitions observed in UV-visible spectra of copper complexes

Donor group	Transition	Complex
Pyridine	MLCT copper(I)-to-pyridine LMCT pyridine-to-copper(II)	I I ^a
Imidazole	LMCT imidazole-to-copper(II)	IIA, IIB
Benzimidazole	MLCT copper(I)-to-benzimidazole LMCT (benzimidazole)-to-copper(II)	IIIA, IIIB IIIA, IIIA'

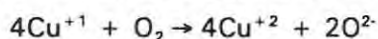
^a After reaction with oxygen

The oxidation of the copper (I) ions to copper (II) was observed to occur readily in all cases, and the d-d absorption bands in the oxygenated complexes were generally in the wavelength region 650 - 760nm (see Table 8.8). This is characteristic of tetrahedral geometry around the copper (II) ions (Section 8.1.2), and substantiates the predictions made by molecular mechanical modelling (Chapter 6); the presence of the biphenyl spacer, in which there can be relative rotation of the two phenyl rings, is likely to distort the dinuclear copper site so that it does not have planar geometry.

Table 8.8: Copper (II) d-d transitions observed for oxygenated copper complexes

Complex	Solvent	Wavelength of d-d absorption band (nm)
I	Acetonitrile	710
	Methanol	536
	Dichloromethane	755
IIC	Acetonitrile	673
	Methanol	660
	Dichloromethane	755
IIA	Acetonitrile	615/700
	Methanol	536
	Dichloromethane	612
IIB	Dichloromethane	584/785
IIIA	Acetonitrile	750
	Methanol	763
	Dichloromethane	624
IIIB	Dichloromethane	702

In the UV spectrophotometric analysis, no clear evidence was found for the formation of peroxo-bridged products resulting from the reaction of the complexes with oxygen. This suggests that, rather than binding dioxygen as a peroxide bridge across a dinuclear binding site, the copper in the complexes I - III may have been oxidised by the simple four-electron process:



Similarly, no direct evidence was found for aromatic hydroxylation of the organic ligand itself. The marked absorption bands observed in the cases of IIC and IIIA, when they were dissolved in methanol which had not been degassed (Figures 8.6 and 8.13) might seem to indicate the presence of phenoxy-to-copper transitions, resulting from aromatic hydroxylation. However, in both cases, an oxidation product was precipitated from the solution using ether, and the IR spectra of these products were identical to the starting materials. If aromatic hydroxylation had taken place, broad bands would have been observed around 3400cm^{-1} in the IR spectra.

8.3.3 Electrochemical analysis

The primary objective of this analysis was to ascertain the oxidation states of the copper in the complexes, as shown in Table 8.6 (Section 8.2.3). The complexes IIA and IIC were found to be predominantly copper (II) complexes, as expected from their appearance. The variations in the shapes of the cyclic voltammograms obtained show that their redox properties vary significantly with differences in the structures of the complexes.

8.4 EXPERIMENTAL

8.4.1 Atomic Absorption Spectrophotometric analysis of copper complexes

The following procedure was carried out in duplicate for each of the complexes: I, IIA, IIB, IIC, IIIA, and IIIB. An accurately weighed sample (1 - 3mg) of the complex was heated in a closed tube with HCl (5M, 1mL) for 1h at 100°C. The resulting solution was diluted with deionised water to 25 or 50mL and this solution was used for the AA analysis. Standard solutions were prepared using Analar $\text{CuCl}_2 \cdot 2\text{H}_2\text{O}$ (0 - 0.3 $\mu\text{mol}/\text{mL}$) in deionised water containing amounts of HCl equivalent to those in the sample solutions. The standard curve obtained is shown in Figure 8.17. Results of the analysis of the complexes are shown in Table 8.9.

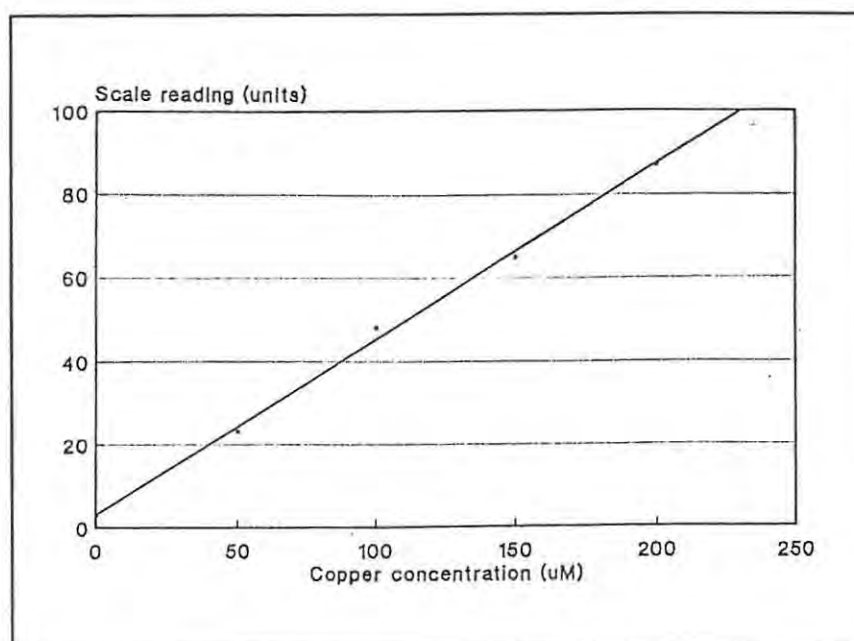


Figure 8.17: Standard curve for AA analysis of copper

Table 8.9: Results of atomic absorption analysis

Complex	Concentration (mg/mL)	Concentration copper found ($\mu\text{g/mL}$)	% copper (w/w)
I	0.080	8.51	10.64
	0.072	8.37	11.62
IIA	0.080	10.29	12.86
	0.066	8.76	13.28
IIB	0.036	4.00	11.11
	0.074	9.34	12.70
IIC	0.084	10.89	12.96
	0.088	11.55	13.13
IIIA	0.032	3.56	11.13
	0.068	7.66	11.26
IIIB	0.030	3.04	10.12
	0.064	6.99	10.92

8.4.2 Measurement of UV-Visible spectra

The UV-visible spectra of the copper complexes I, IIA, IIB, IIC, IIIA, and IIIB were measured in solution in acetonitrile, methanol, or dichloromethane, at concentrations of 0.02 to 0.5 mM (see Table 8.10), using a Shimadzu UV-160 spectrophotometer. The wavelength range was 200 to 800nm. Where spectra were measured in the absence of air, the solvents were first degassed by repeated freezing and evacuation. The solvent was then transferred under nitrogen, *via* a burette, to a flask containing the complex, also under nitrogen. The solution was transferred to the cuvette using a canula, under a blanket of nitrogen, and the cuvette was stoppered. Subsequent oxygenation was achieved by bubbling dry oxygen into the solution for 1 minute, and allowing the solution to stand for 5 minutes. The volume of the solution was adjusted with oxygenated solvent where necessary. The spectra of complexes I and IIIA were also measured in solvents (methanol and dichloromethane respectively) which had not been degassed. To obtain spectra at -70°C , acetone was cooled using liquid nitrogen, and this was circulated through the constant temperature unit of the spectrophotometer. The outer surfaces of the cuvettes were wiped with glycerol to minimise frosting. The spectra obtained are shown in Figures 8.2 - 8.15, Section 8.2.2, and the results are summarised in Table 8.10. The molar extinction coefficients, ϵ , were calculated using the Beers law equation $A = \epsilon cl$, where A is absorbance, c is concentration and l is optical path-length in the solution.

Table 8.10: Results of UV-Visible analysis of Copper complexes

Complex	Solvent	Conc ^a	T (°C)	Atm ^b	Wavelength (nm),(A ^c)	
I	MeCN	0.1	25	N ₂	213(2.2), 300sh, 360sh	
				O ₂	241(0.616), 3160sh, 710(0.01)	
		0.05	-70	N ₂	224(1.70), 280sh, 350sh	
						224(1.33), 280sh, 350sh, 730(0.13)
	MeOH	0.1	25	N ₂	223(1.744), 260sh, 350sh	
				O ₂	246(0.614), 360sh, 536(0.053)	
	CH ₂ Cl ₂	0.2	25	N ₂	260(2.5), 340sh	
				O ₂	260(1.76), 340sh, 755(0.025)	
			-70	N ₂	260(2.5), 340sh	
				O ₂	257(1.39), 635(0.64), 680(0.65)	
IIC	MeCN	0.1	25	N ₂	220(2.5)	
				O ₂	236(0.62), 673(0.13)	
				-70	N ₂	214(2.5)
					O ₂	227(0.74), 660(0.01)
	MeOH	0.1	25	N ₂	217(2.35), 360sh	
				O ₂	246(0.88), 360sh, 535(0.073)	
		0.2	-70	N ₂	228(1.97), 255sh	
				O ₂	228(1.8), 255sh	
IIA	CH ₂ Cl ₂	0.04	25	O ₂	210(2.3), 755(0.017)	
	MeCN	0.1	25	N ₂	220(2.4)	
				O ₂	238(0.74), 615(0.10)	
				-70	N ₂	227(2.15), 400sh
					O ₂	227(1.89), 400sh, 700(0.01)
	MeOH	0.1	25	N ₂	222(2.5), 370sh	
				O ₂	247(0.76), 370sh, 536(0.08)	
MeOH	0.1	-70	N ₂	224(1.22), 270sh		
			O ₂	227(1.65), 270sh, 660(0.01)		
IIA	CH ₂ Cl ₂	0.04	25	N ₂	220(2.15)	
				O ₂	220, 260sh, 612(0.07)	
		0.36		N ₂	224(2.06)	
				O ₂	220(0.52), 584(0.05), 785(0.03)	
IIIA	MeCN	0.05	25	N ₂	221(2.5)	
				O ₂	220(0.20), 750(0.15)	
	MeOH	0.02	25	N ₂	215(1.42), 264(1.38), 340sh	

^a Concentration (mM)

^b N₂: under nitrogen, in degassed solvent; O₂: after aeration

^c A = Absorbance

Complex	Solvent	Conc ^a	T (°C)	Atm ^b	Wavelength (nm),(A ^c)
III A'	CH ₂ Cl ₂	0.04	25	O ₂	257(0.79), 763(0.04)
				Air	250(0.84), 390(0.39)
				N ₂	248(2.06), 301(0.43), 360sh
			-70	O ₂	248(1.59), 624(0.01)
				N ₂	240(2.1), 300sh, 360sh
				O ₂	240(0.7), 350sh
III A	CH ₂ Cl ₂	0.01	25	Air	251(0.79), 300sh, 360sh
III A	CH ₂ Cl ₂	0.01	25	N ₂	245(0.65), 280sh
		0.04		O ₂	215(2.2), 280sh, 350sh
		0.36		O ₂	220, 702(0.03)

^a Concentration (mM)

^b N₂: under nitrogen, in degassed solvent; O₂: after aeration

^c A = Absorbance

8.4.3 Isolation of oxygenated product III A' from complex III A

Dry oxygen was bubbled gently into a stirred solution of complex III A (15mg) in dry CH₂Cl₂ (5mL) for 10min. Dry ether (10mL) was added, causing a slight precipitate to form, and the solution turned green. The solvent was removed under reduced pressure, leaving a green solid, III A', which was analysed by IR spectroscopy, giving a spectrum identical to that of III A (see Section 7.4.14). This procedure was repeated using methanol as the solvent, with the same result.

8.4.4 Electrochemical analysis

Electrochemical data were collected with a BAS CV-27 voltammograph connected to an HP 7047A X-Y recorder. All measurements were carried out under an atmosphere of nitrogen, using dried, degassed solvents. A platinum disc (1.6mm diameter) was used as the working electrode and a platinum wire as the auxiliary electrode. A silver wire coated with silver chloride was used as a quasi-reference electrode. Potentials were referenced internally to the ferrocenium/ferrocene (Fc⁺/Fc) couple. The conditions used are summarised in Table 8.11. The cyclic voltammograms are shown in Section 8.2.3.

Table 8.11: Conditions used to measure cyclic voltammograms of copper complexes

Complex	Solvent	Supporting electrolyte	Scanning range (V)	Scanning speed (mV.s ⁻¹)
I	DMF	Et ₄ NClO ₄	1.2 to -1.0	500
IIC	DMF	.	1.2 to -1.2	500
IIA	MeCN	.	1.0 to -1.0	500 and 200
IIB	DMF	.	1.0 to -1.0	500
IIIA	MeCN	.	1.0 to -1.0	800
IIIB	MeCN	Bu ₄ NClO ₄	0.9 to -0.9	500 and 200

CHAPTER 9

THE CATALYTIC ACTIVITY OF THE COPPER COMPLEXES

9.1 INTRODUCTION

The purpose of preparing dinuclear copper complexes in this study was to produce models of tyrosinase and therefore, the assessment of their ability to catalyse the oxidation of phenols and catechols was of primary importance. Successful functional models of tyrosinase would exhibit cresolase and catecholase activity, producing *o*-quinones, using molecular oxygen. To fully mimic the enzyme, the mechanism should involve the binding of both oxygen and the substrate to the dinuclear copper site. The complexes should also be stable and active under conditions comparable to those under which tyrosinase functions. Since this study has shown that tyrosinase can function in an organic solvent medium, it is not necessary for the complexes to be applied in aqueous systems in order for them to be models of the enzyme. Thus the objectives for this section of the present study were to determine:

- (a) whether the complexes catalyse the oxidation of appropriate substrates
- (b) the nature of the products of these reactions
- (c) the kinetic parameters for the catalytic reactions
- (d) a possible mechanism for the reaction.

An enzyme kinetic approach is often used when investigating the kinetic properties of biomimetic complexes (for example, Prati *et al.*, 1992; Paul *et al.*, 1991; Rockcliffe and Martell, 1992), since this gives a useful means of comparing the catalytic activity of the complexes with that of the enzyme they are intended to mimic. The most frequently encountered method of analysing reaction rate data uses the Michaelis-Menten equation:

$$v = Vs/(K_m + s)$$

where v is the initial rate of the reaction

s is the initial substrate concentration

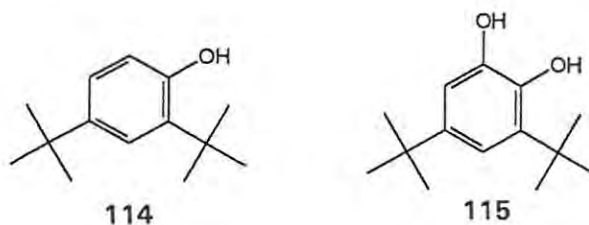
V is the maximum velocity

K_m is the Michaelis constant.

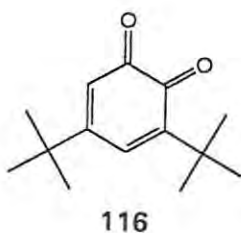
[The theory of this method is explained in detail in Chapter 3 (Section 3.1.2)].

The measurement of reaction rates in this investigation was carried out using dichloromethane as the solvent. The ability of this solvent to dissolve oxygen efficiently makes it especially suitable because oxygen acts as the electron acceptor in the catalytic oxidation reaction, and is required to be present at a non-rate limiting concentration.

While tyrosinase is able to catalyse the oxidation of a wide range of substrates in aqueous medium (Yasunobu, 1959; Passi and Nazarro-Porro, 1981), the work presented in previous chapters of this study has shown that this range is considerably reduced in organic medium. It would be most appropriate to use relatively unhindered phenolic substrates from the selection used in the kinetic analysis (Chapter 3), but it was found that these compounds were not oxidised by the complexes, and thus more bulky substrates were used. The cresolase activity of the complexes was studied using the substrate 2,4-di-*tert*-butylphenol (DTBP), **114**, and the corresponding catechol, 3,5-di-*tert*-butylcatechol (DTBC), **115**, was used to investigate catecholase activity. These compounds are frequently used for this purpose (Vigato *et al.*, 1990; Chyn and Urbach, 1991), because they are activated for electron donation, by the alkyl substituents (Oishi *et al.*, 1980). Also, the oxidation products from these substrates are less prone to polymerisation than those from less sterically hindered phenols.



The *o*-quinone product of the oxidation of DTBP and DTBC is 3,5-di-*tert*-butyl-*o*-benzoquinone (DTBQ) **116**, which exhibits a characteristic UV absorption band at wavelength 400nm ($\epsilon = 1830 \text{ M}^{-1}\text{cm}^{-1}$). Thus the reaction can conveniently be followed spectrophotometrically.



9.2 RESULTS AND DISCUSSION

9.2.1 Uncatalysed reaction of DTBP and DTBC with oxygen

The possibility of DTBP and DTBC reacting with oxygen in the absence of a catalyst was investigated. The UV-visible spectra of solutions of the substrates before and after oxygenation were compared, and small increases in the absorbances near 400nm were observed (Figure 9.1). To compensate for this, reaction rates in the presence of the copper complexes were measured with substrate solution in the reference cell of the spectrophotometer, and this solution was oxygenated at the same rate as the sample solution.

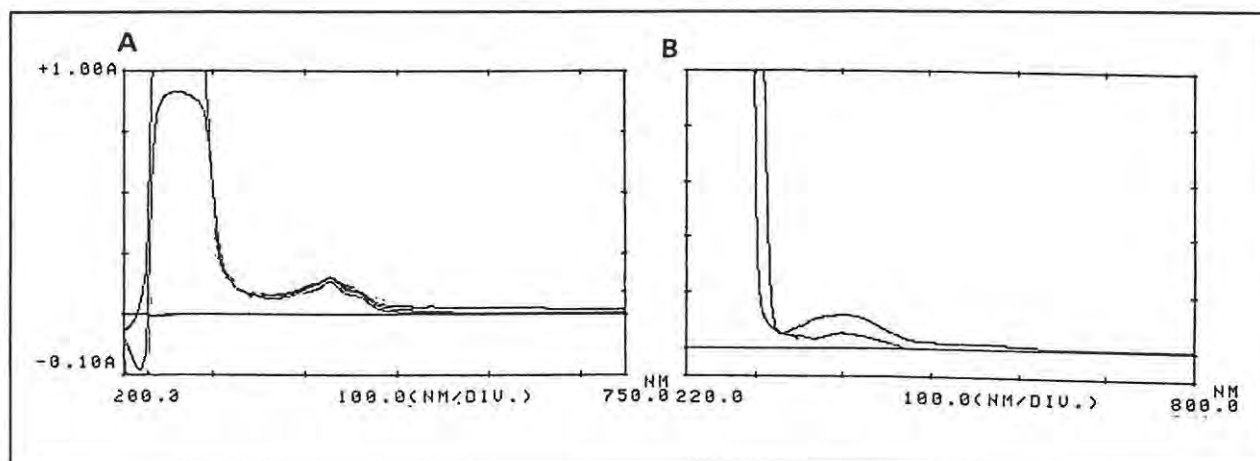


Figure 9.1: UV-visible spectra of DTBP (A) and DTBC (B), before and after oxygenation. The spectrum showing higher absorbance is the oxygenated sample, in each case.

9.2.2 Oxidation of DTBP catalysed by complex I

Initially, the reaction of complex I with DTBP was investigated: the reaction was followed spectrophotometrically, reading the absorbance at 400nm (due to the *o*-quinone product) and at 650nm (to detect the decomposition product of the complex, as discussed in Section 7.2.4). Since triethylamine was found to prevent the decomposition of the complex, it was added to the reaction mixtures, and in the presence of triethylamine, the absorbance at 650nm was found to remain negligible during the reactions. (A reaction in which the triethylamine was omitted did show an increase in absorbance at 650nm). Reaction of DTBC with the complex I was also shown to occur, by addition of I to a solution of DTBC and measuring the spectrum after a colour change had been observed. The UV-visible spectra of the products are shown in Figure 9.2, and the rates of absorbance change for DTBP are shown in Figure 9.3. The results are tabulated in Section 9.4.1.

Although these spectra show absorbances in the region where they might be attributed to ligand-to-copper CT transitions (see Section 8.1.2), it must be borne in mind that the complex was only present in a 1:100 ratio, relative to the substrate. Therefore peaks due to such transitions are likely to be very much smaller than the large absorbances of the more concentrated products.

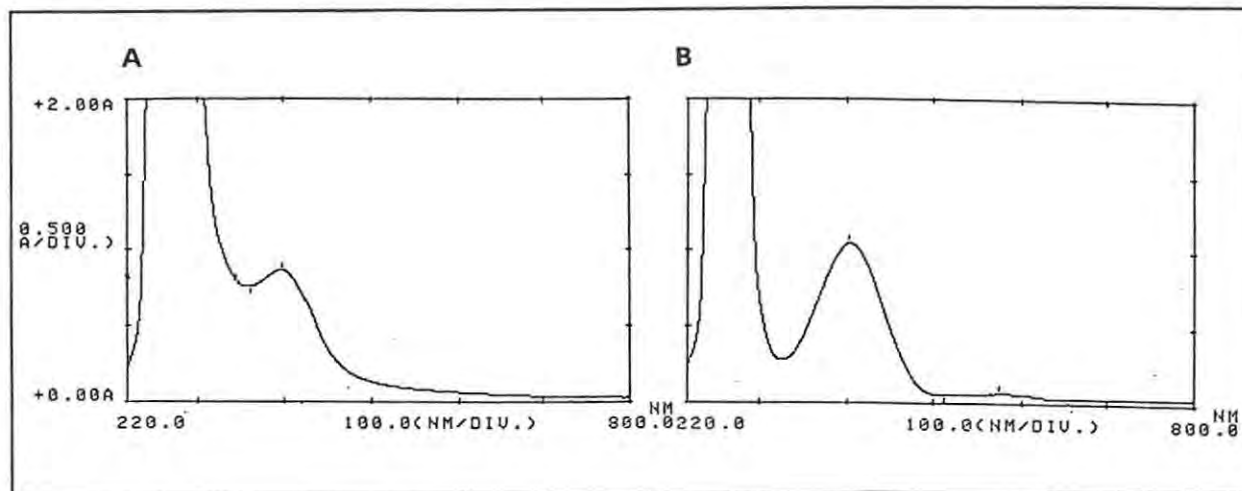


Figure 9.2: UV-visible spectra of the products of oxidation of DTBP (A) and DTBC (B), catalysed by complex I

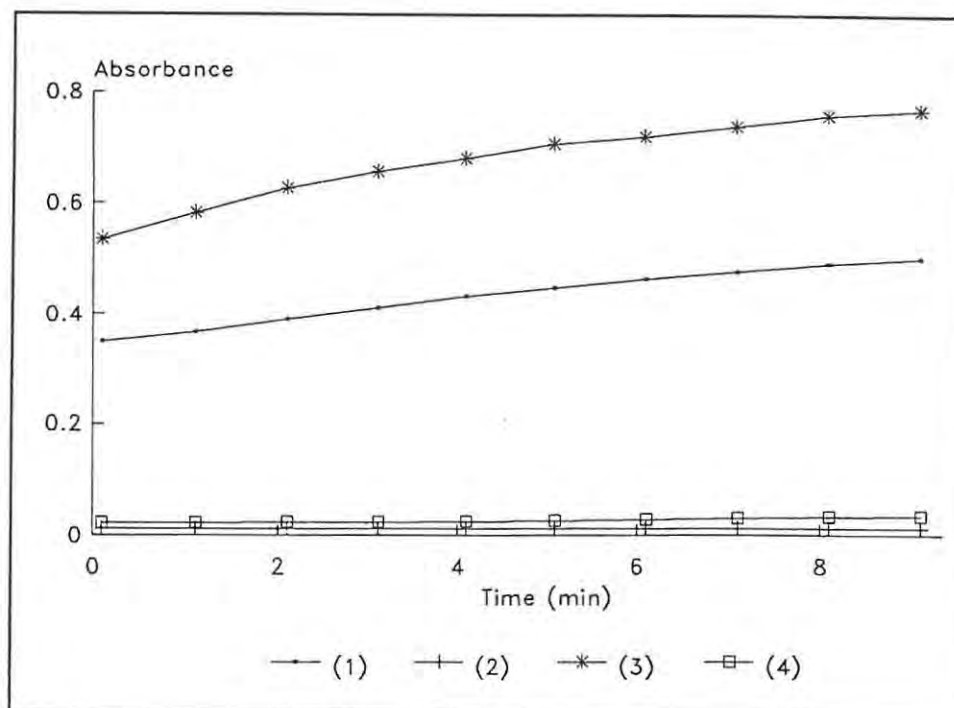


Figure 9.3: Rates of oxidation of DTBP, catalysed by complex I, in the presence (1) and (2), and the absence (3) and (4), of triethylamine. Absorbance rates in (1) and (3) were measured at 400nm for the reaction product, and in (2) and (4), at 650nm, for the decomposition product of the complex.

9.2.3 Oxidation of DTBP and DTBC, catalysed by other copper complexes

Having established that complex I was catalytically active, a survey involving the complexes I, IIA - C, and IIIA,B was undertaken, to determine the extent of reaction which could be achieved [see Section (9.4.2)]. The two substrates, DTBP and DTBC, were added to separate solutions of the complexes in dry, degassed dichloromethane, in molar ratios of 100:1 substrate to complex. The solutions were aerated by vigorous stirring under air, to provide oxygen for the reaction, and were then allowed to stand for twenty four hours. The resulting reaction mixtures were analysed by ^1H NMR and TLC. The experiments were repeated using *p*-cresol and *p*-*tert*-butylphenol as the substrates, but no colour changes were detected, and the NMR spectra showed only the peaks attributable to the substrates. The complexes IIA and IIC were found to react with DTBC, but not with DTBP.

Reaction mixtures in which the triethylamine was omitted gave the same products as those obtained in its presence (as illustrated in Table 9.1) but the colours were far less intense, indicating lower conversions. In addition, these solutions were observed to be cloudy after standing overnight, suggesting the likely presence of decomposition products. Consequently, triethylamine was included in the reaction mixtures used for measurement of reaction rates.

The products prepared directly from the reaction of $[\text{Cu}(\text{MeCN})_4][\text{PF}_6]$ with the ligand precursors [see Section 7.2.3 (4)] were also tested for catalytic activity. Their presence was suspected, at least in complexes IIB and IIIB, obtained by template condensation. If these impurities were to have catalytic activity, they would interfere with the measurements for the the complexes in which they occurred. These products were added to solutions of DTBP and DTBC, in the same way as described above. Fortunately, none of these solutions show indications of catalytic activity; the solutions showed no colour changes, and TLC analysis showed that they did not contain the oxidation products.

9.2.4 Identification of the products of the catalytic oxidations of DTBP and DTBC

It was initially expected that the products of the oxidations of DTBP and DTBC would be identical, *viz.*, the *o*-quinone DTBQ. However, the reaction mixtures described above were observed to differ in colour, with DTBP solutions becoming orange in colour, while DTBC solutions became dark green. TLC analysis of the reaction mixtures showed that the same oxidation products were obtained for all the complexes tested (see Table 9.1). However, the product of the reactions with DTBP was obviously not DTBQ, since it had different colour and chromatographic properties. The

identification of this product is described below. The product of oxidation of DTBC was identified chromatographically as the *o*-quinone, DTBQ, by comparison with a sample of the quinone prepared by *o*-chloranil oxidation of DTBC (see Table 9.1 and Section 9.4.3).

Table 9.1: Results of TLC analysis of reaction mixtures resulting from the oxidation of DTBP and DTBC, catalysed by copper complexes.

Substrate	Complex	Et ₃ N ^a	R _f in solvent 1 ^b	R _f in solvent 2 ^c
DTBP	-	-	0.84	0.93
	I	+ -	0.84, 0.95	0.73, 0.93
	IIB	+ -	0.84, 0.95	0.73, 0.93
	IIIA	+ -	0.84, 0.94	0.73, 0.93
	IIIB	+ -	0.84, 0.95	0.73, 0.93
DTBC	-	-	0.70	0.72
	I	+ -	0.70, 0.78	0.72, 0.81 (0.90) ^d
	IIA	+ -	0.70, 0.78	0.72, 0.81
	IIB	+ -	0.70, 0.78	0.72, 0.81 (0.90)
	IIC	+ -	0.70, 0.78	0.72, 0.81
	IIIA	+ -	0.70, 0.78	0.72, 0.81
	IIIB	+ -	0.70, 0.78	0.72, 0.81 (0.90)
DTBQ	-	-	0.78	0.81

^a: indicates presence or absence of triethylamine

^b: ethyl acetate:hexane 1:2

^c: chloroform:ether 2:3

^d: trace of presumed impurity

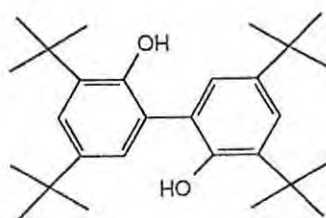
The reaction mixtures were evaporated to dryness and the residues redissolved in deuterated chloroform for analysis by NMR spectroscopy. The ¹H NMR spectrum of the solutions were obtained, and then selected samples were separated by preparative TLC to give clean samples of the reaction products (see Section 9.3.2). Figure 9.4 shows the ¹H NMR spectra of DTBP, DTBC, and DTBQ. The conversion of DTBC to DTBQ was shown by ¹H NMR spectroscopy to be complete, (see Figure 9.5 and Table 9.2), while the spectrum of a clean sample of DTBQ, obtained from the reaction of DTBC with complex IIB, is shown in Figure 9.6.

Table 9.2: ^1H NMR and IR spectral data for DTBC, DTBQ, and the product of the catalytic oxidation of DTBC

Compound	^1H NMR data (δ_{H} , ppm)	IR data (cm^{-1})
DTBC	1.27, s, 9H, Bu ^t 1.42, s, 9H, Bu ^t 6.76, d, J 2.2Hz, 1H, H-4 6.89, d, J 2.2Hz, 1H, H-6	3400 br (OH) 2940 (alkyl)
DTBQ - synthetic sample	1.22, s, 9H, Bu ^t 1.26, s, 9H, Bu ^t 6.21, d, J 2.3Hz, 1H, H-4 6.90, d, J 2.3Hz, 1H, H-6	
DTBQ - catalytically produced ^a	1.21, s, 9H, Bu ^t 1.25, s, 9H, Bu ^t 6.20, s, 1H, H-4 6.68, s, 1H, H-6	2940 (alkyl) 1640 (C=O)

^a Obtained from reaction of complex IIB with DTBC

The ^1H NMR spectra of the reaction mixtures from oxidation of DTBP, however, showed the presence of residual DTBP and a product which was clearly different from DTBQ (Figure 9.7). This product was identified spectroscopically, after isolation by preparative TLC, as the biphenyl 117, arising from coupling of DTBP substrate molecules (see Table 9.3 and Figures 9.8 and 9.9). It was also apparent that when triethylamine was omitted, very little oxidation was observed.



117

Table 9.3: Spectral data for the coupled product 117

Spectroscopy	Data
^1H NMR	δ_{H} 1.31, s, 18H, <i>t</i> -Bu 1.41, s, 18H, <i>t</i> -Bu 7.10, d, <i>J</i> 2.3Hz, 2H, H-4 and H-4' 7.38, d, <i>J</i> 2.3Hz, 2H, H-6 and H-6' δ_{C} 29.68, 31.64, 34.46, 35.20, 122.37, 124.82, 125.28, 136.26, 143.01, 149.78
IR	3200 br (OH); no C=O (See Figure 9.9)
MS	M^+ 410.3215 ($\text{C}_{28}\text{H}_{42}\text{O}_2$ requires 410.3185)

The ^1H NMR spectra of the DTBP reaction mixtures were used to estimate the extent of reaction, by comparison of the heights of the peak integrals. The results are shown in Table 9.4, where the percentage conversion represents the proportion by which the phenolic substrate was depleted. Two moles of substrate couple to give one mole of product.

Table 9.4: Extent of oxidative coupling of DTBP, catalysed by copper complexes

Complex	Integral ratio	% conversion ^a
I	3.8 : 1	20.8
IIB	3.5 : 1	22.2
IIIA	1 : 1	50.0
IIIB	1 : 4.7	82.5

^a After 24h

9.2.5 Determination of the molar extinction coefficient for the coupled oxidation product 117

It was necessary to determine the UV-visible spectral characteristics of the coupled product 117, in order to quantify the reaction rates. This was achieved by determining the concentrations of substrate and product in the reaction mixture of DTBP with complex I (starting with a known concentration of DTBP), from the measurement of the integrals of the respective ^1H NMR peaks. The UV-visible spectrum of the solution was found to correspond to that shown in Figure 9.2A. The UV-absorbance of a known dilution (1 in 10) of the solution was measured, and the Beer's law equation was used to calculate the molar extinction coefficient at 400nm, which was found to be $89 \text{ M}^{-1} \text{ cm}^{-1}$ (see Section 9.4.4).

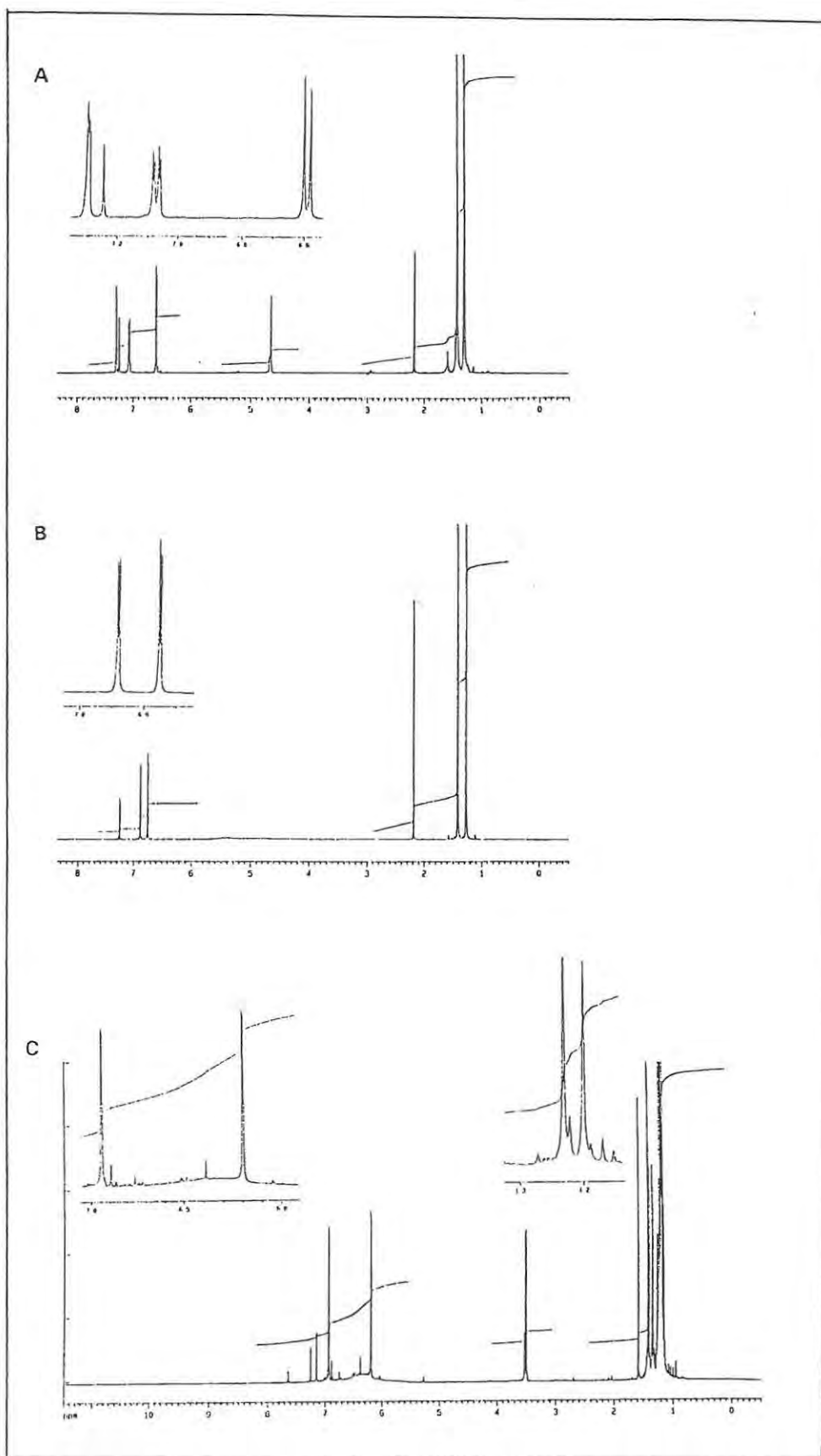


Figure 9.4: ^1H NMR spectra of DTBP (A), DTBC (B) and DTBQ (C)

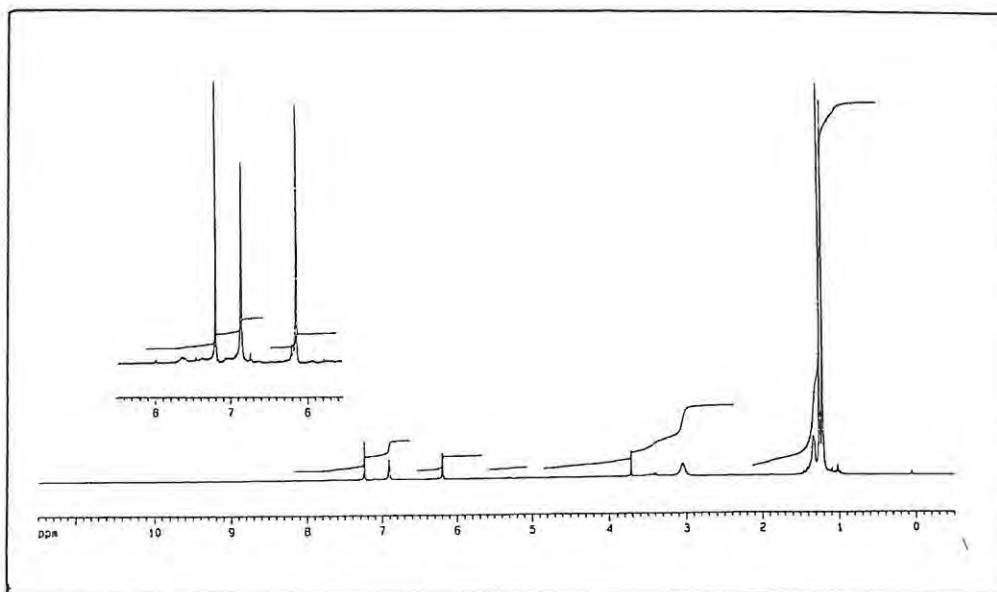


Figure 9.5: ¹H NMR spectra of the reaction mixture obtained in the oxidation of DTBC, catalysed by the complex IIIA

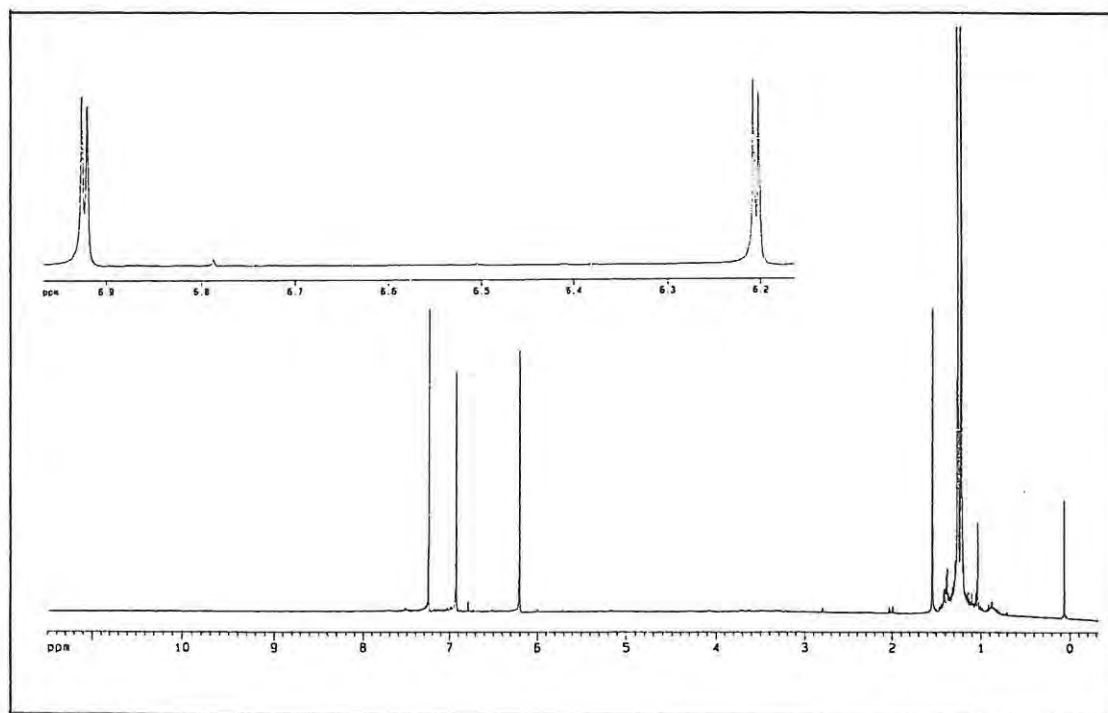


Figure 9.6: ¹H NMR spectra of DTBQ obtained by TLC after oxidation of DTBC, catalysed by complex IIB

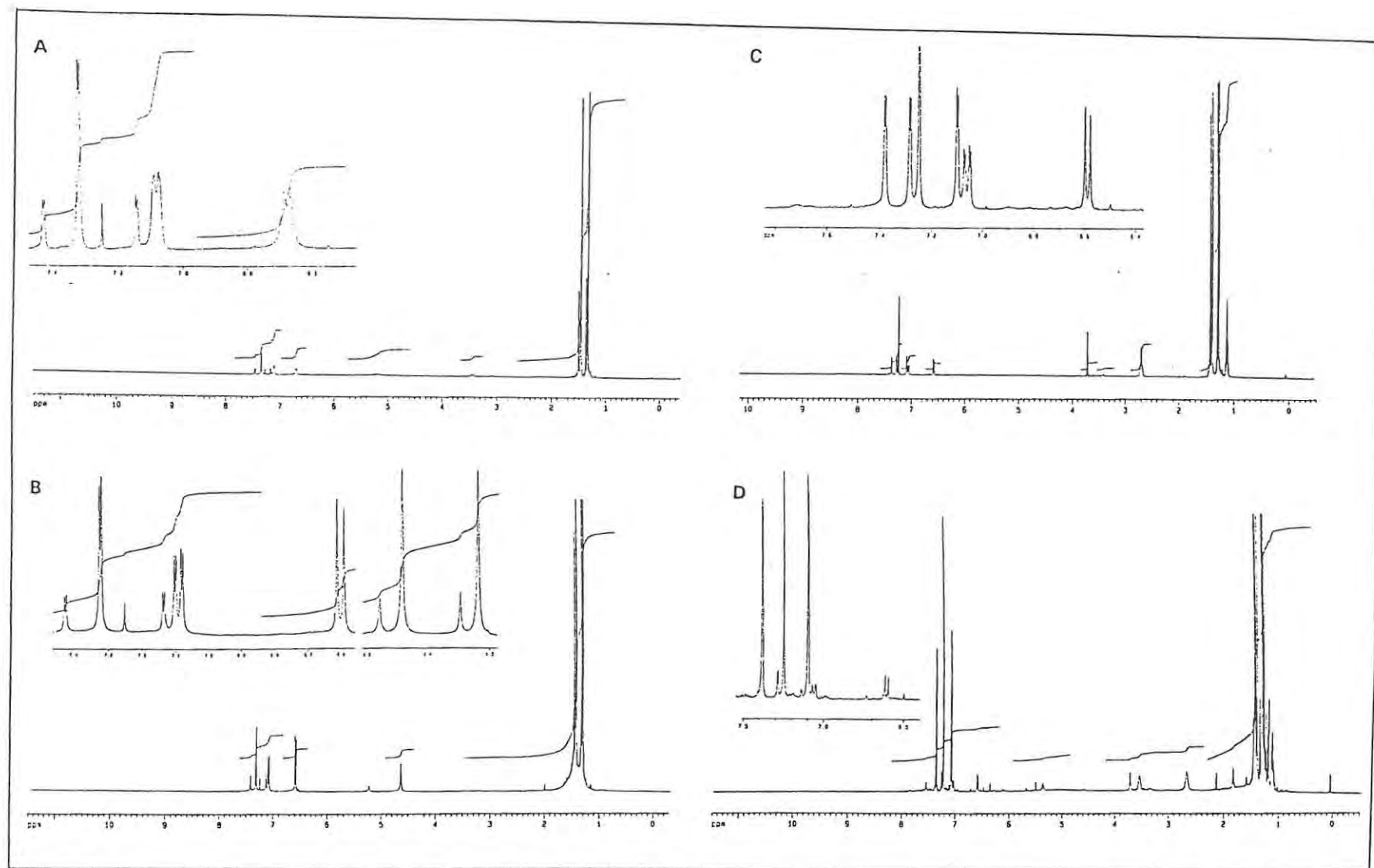


Figure 9.7: ¹H NMR spectra of the reaction mixtures obtained in the oxidation of DTBP, catalysed by the complexes I (A), IIB (B), IIIA (C) and IIIB (D)

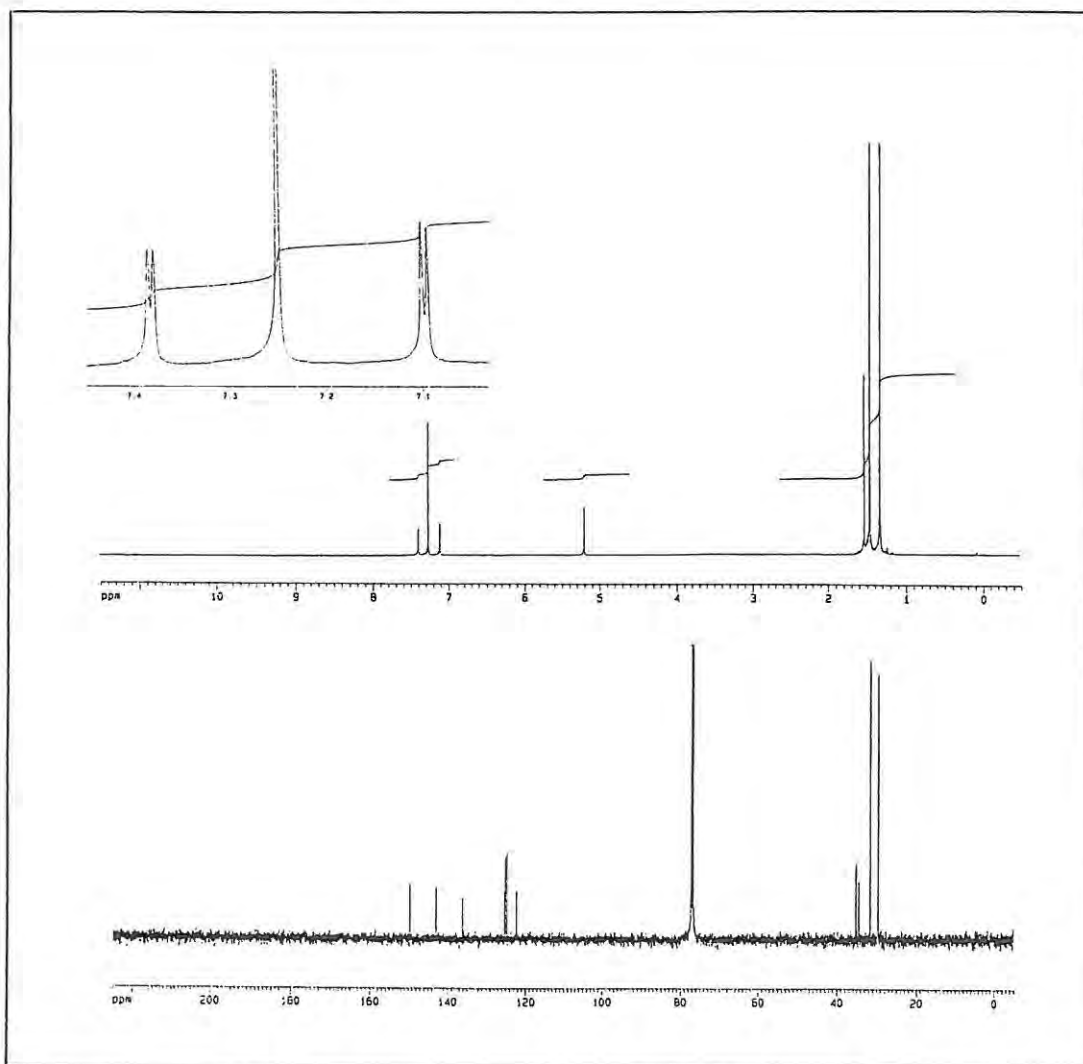


Figure 9.8: ^1H and ^{13}C NMR spectra of the product of oxidation of DTBP, catalysed by the complex IIIB

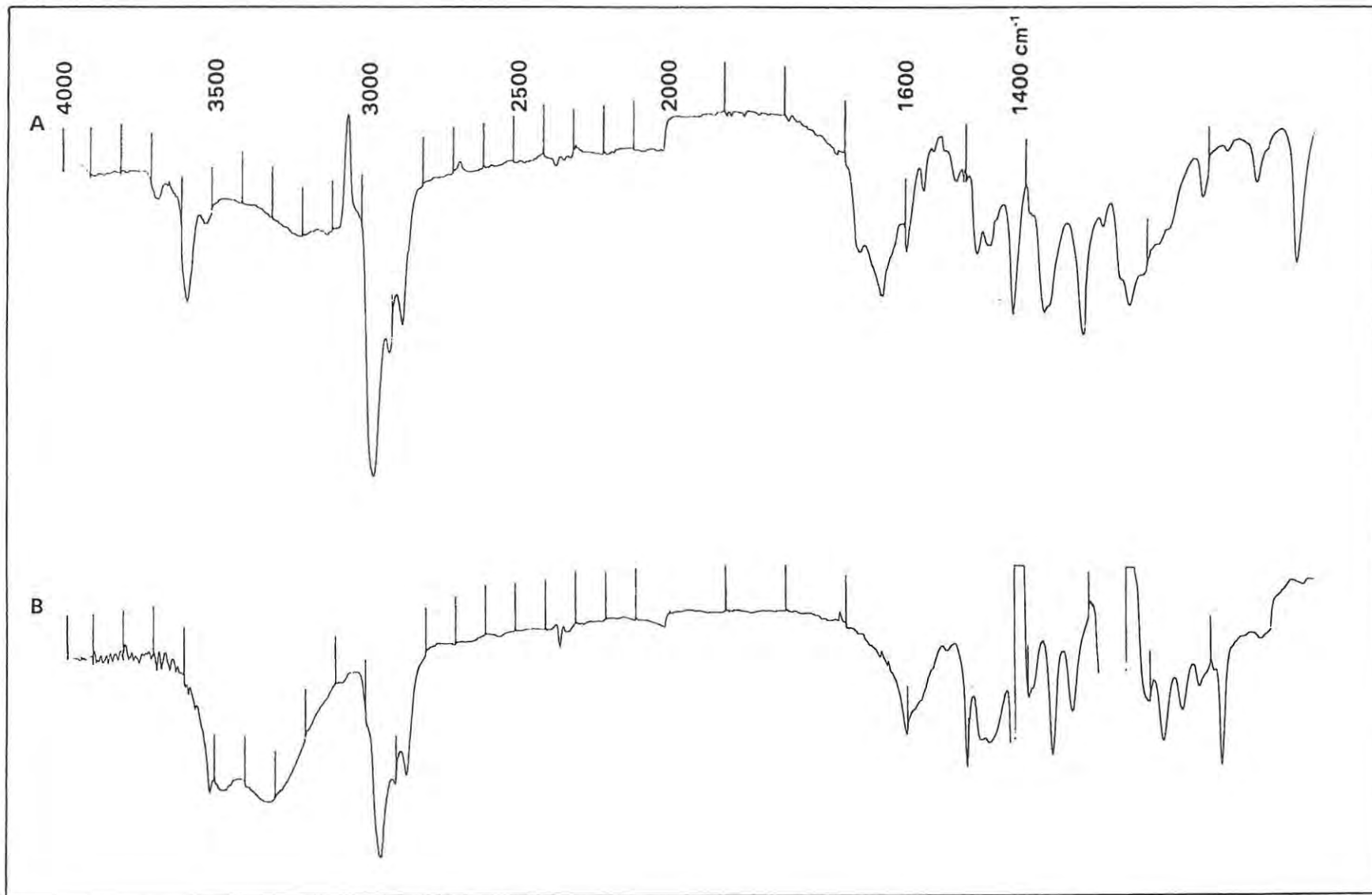


Figure 9.9: IR spectra of the oxidation products obtained in the oxidation of DTBC (A) and DTBP (B), catalysed by complex III B

9.2.6 Measurement of the enzyme kinetic parameters for the oxidation of DTBP and DTBC, catalysed by the copper complexes

In order to determine the enzyme kinetic parameters K_m and V for each of the complexes, initial rates of reaction were measured spectrophotometrically, using a fixed amount of the catalyst in each run, with substrate solutions having a range of concentrations. These concentrations were chosen to give conveniently measurable rates within the range of accuracy of the spectrophotometer. For each complex investigated, the runs were duplicated (Tables 9.10 and 9.11 in Section 9.4.5) and the mean rates are reported in Tables 9.12 and 9.13 (Section 9.4.5). These rates were converted to rates of formation of the products using the appropriate molar extinction coefficients, and then used in the Hanes plots shown in Figures 9.10 and 9.11. The enzyme kinetic parameters are summarised in Tables 9.5, 9.6, and 9.7.

Table 9.5: Analysis of enzyme kinetic data obtained with DTBC as substrate

Complex	Data from Hanes plot		V = 1/gradient (M.min ⁻¹)	K_m = $V \times$ intercept (mM)	k_{cat} = $V/[c]^a$ (h ⁻¹)
	Gradient	Intercept			
I	15411	120.75	6.49×10^{-5}	7.84	39
IIB	20726	-5.67	4.82×10^{-5}	14.00	28.9
IIC	62921	492.65	1.5×10^{-5}	7.83	10
IIIA	102997	641.37	9.71×10^{-6}	6.23	6
IIIB	10139	26.41	9.86×10^{-5}	2.61	59.2

^a: c = concentration of complex

Table 9.6: Analysis of enzyme kinetic data obtained using DTBP as substrate

Complex	Data from Hanes plot		V = 1/gradient (M.min ⁻¹)	K_m = $V \times$ intercept (mM)	k_{cat} = $V/[c]^a$ (h ⁻¹)
	Gradient (M ⁻¹ .min)	Intercept (min)			
I	1864.0	42.59	5.37×10^{-4}	2.29	314
IIB	1543.5	12.59	6.48×10^{-4}	8.16	389
IIIA	4550.3	14.43	2.20×10^{-4}	3.20	132
IIIB	834.1	31.77	1.20×10^{-3}	3.80	720

Table 9.7: Catalytic efficiencies of the copper complexes

Substrate	Complex	V/K_m (min ⁻¹)
DTBC	I	8.3×10^{-3}
	IIA	2.0×10^{-3}
	IIB	3.4×10^{-3}
	IIIA	1.6×10^{-3}
	IIIB	3.2×10^{-1}
DTBP	I	2.3×10^{-2}
	IIB	7.9×10^{-3}
	IIIA	6.9×10^{-1}
	IIIB	3.2×10^{-2}

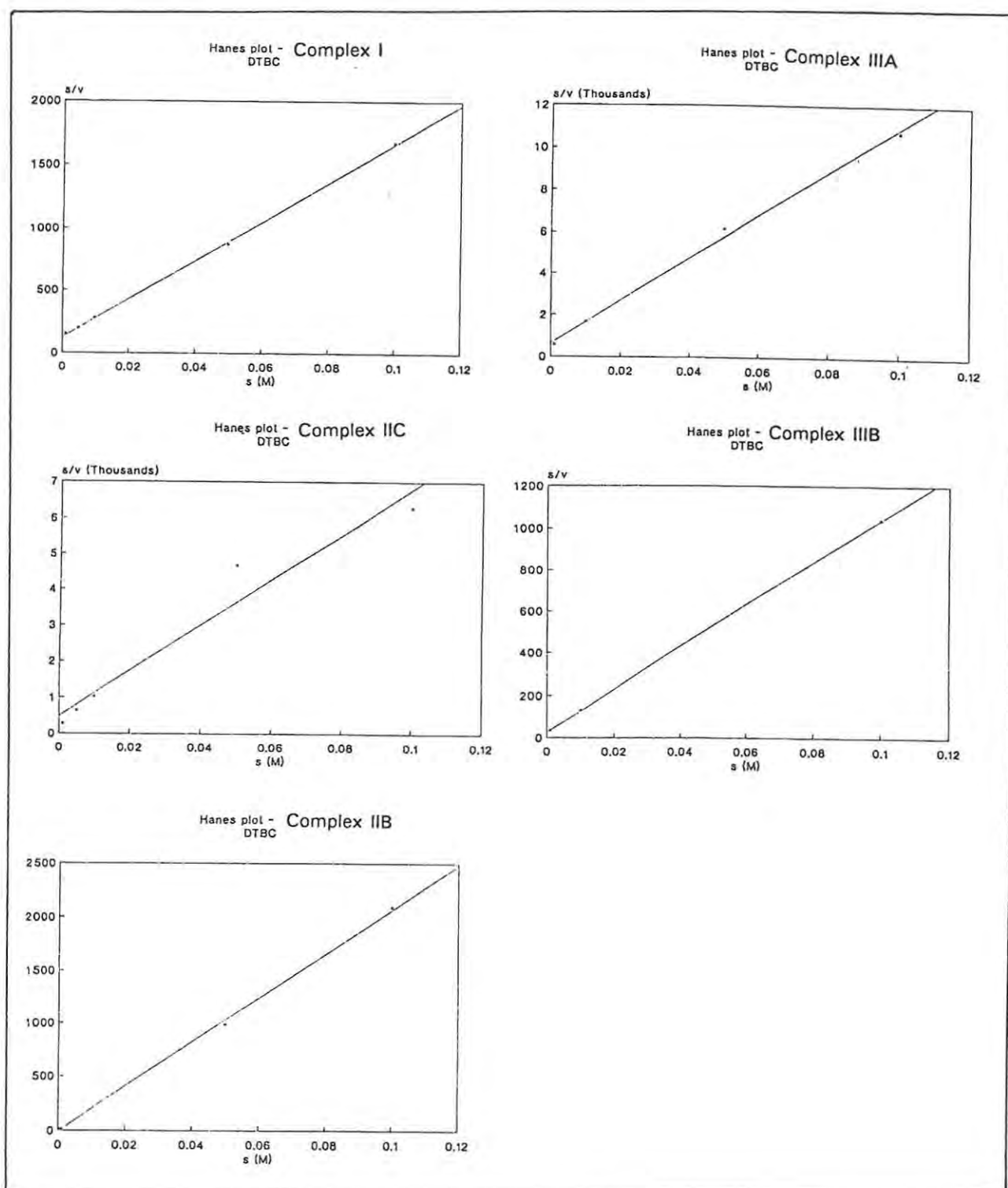


Figure 9.10: Hanes plots for the oxidation of DTBC, catalysed by the copper complexes

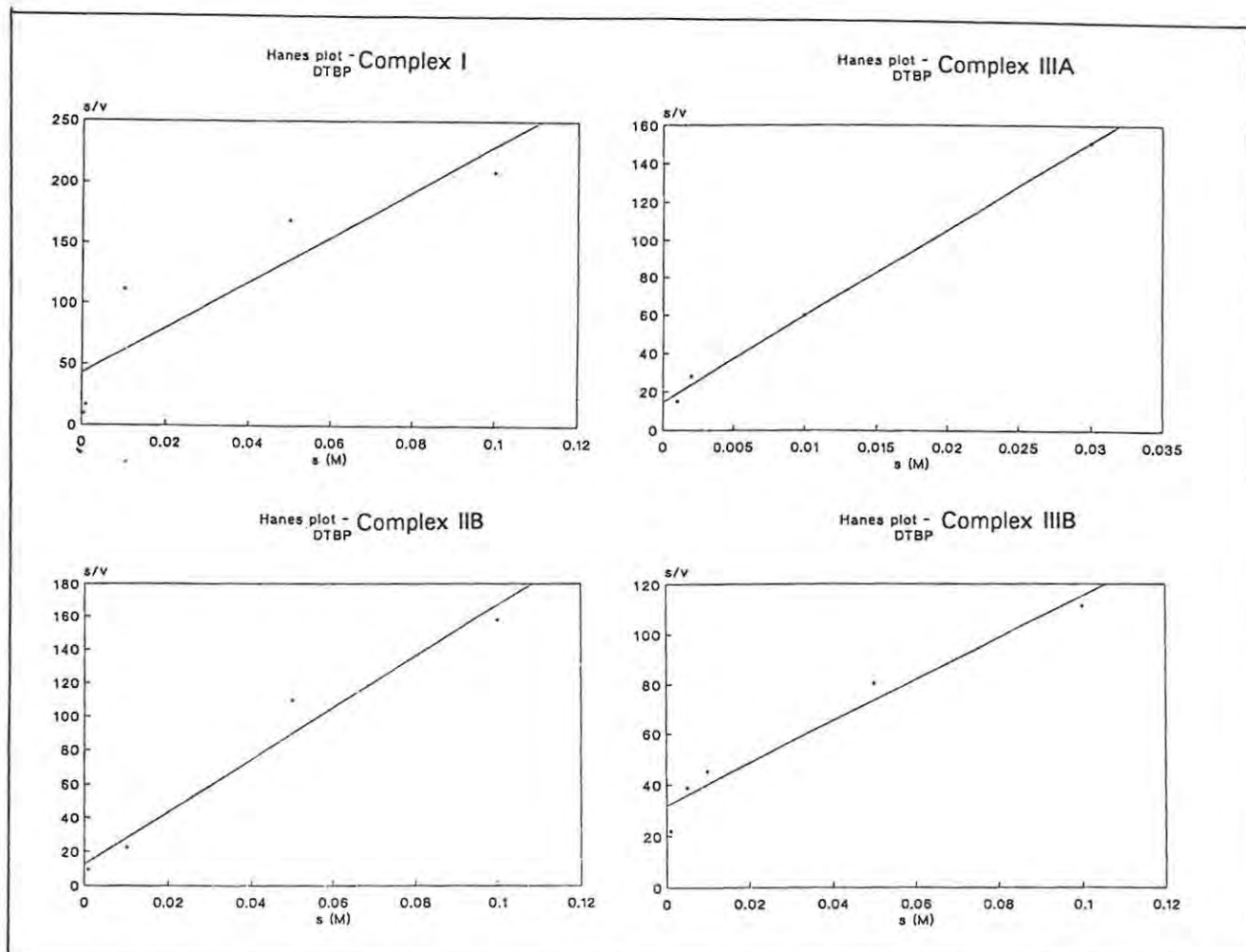


Figure 9.11: Hanes plots for the oxidations of DTBP, catalysed by the copper complexes

9.3 CONCLUSION

9.3.1 The catalytic activity of the copper complexes

The first objective of this section of the project was to determine whether the biomimetic complexes prepared in this study exhibited catalytic activity which modelled that of tyrosinase. All of the complexes investigated were, in fact, found to have some catalytic activity, as demonstrated by their reactivity with DTBC and DTBP.

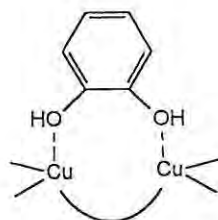
The molecular modelling discussed in Chapter 6 indicated the likelihood of π -interactions between a phenolic substrate molecule and the aromatic groups in the complexes, which would enhance substrate binding. In addition to this, the presence of the bulky *t*-butyl groups on DTBP and DTBC should also enhance binding *via* van der Waals and/or hydrophobic interactions with the organic ligand.

The inability of the complexes to catalyse the oxidation of smaller phenolic substrates such as *p*-cresol and *p*-*tert*-butylphenol may be due to two possible factors: Firstly, these phenols are less strongly activated for electron donation, and secondly, they have smaller steric volumes and fewer groups capable of van der Waals or hydrophobic interactions. The former factor is certainly likely to affect their reactivity, although these phenols can be oxidised by tyrosinase. The molecular modelling study showed that, in the absence of bridging groups such as hydroxide or peroxide the complexes would have a high degree of flexibility. If no such bridging group is present to hold the molecule in a pocket-like conformation, a phenolic substrate molecule might coordinate to only one of the copper ions, making *ortho*-hydroxylation unlikely. Thus the complexes may be too flexible to effectively bind small phenolic substrate molecules. Clearly, a catechol molecule would have greater potential for binding to both copper ions and thereby bridging them.

9.3.2 The nature of the reaction products

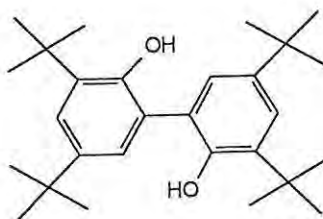
All of the complexes were shown to catalyse the oxidation of DTBC to DTBQ with high conversion rates. The isolated product was identified by NMR spectroscopy and TLC. Such catecholase activity is typical of dinuclear copper complexes (Karlin *et al.*, 1985a; Chyn and Urbach, 1991; Kitajima *et al.*, 1990) and also of copper/amine complexes generally (Speier, 1986; Prati *et al.*, 1992). The catalytic efficiency depends on a good steric match between the complex and the substrate, to form an intermediate **118** which favours electron transfer from the copper (II) ions to the substrate (Oishi *et al.*, 1980) and demonstrates the reason for dinuclear complexes being generally more

efficient catalysts than their mononuclear analogs. The success of the complexes prepared in the present study as catecholase models suggests that the copper-copper distances are suitable for the coordination of a catechol molecule.

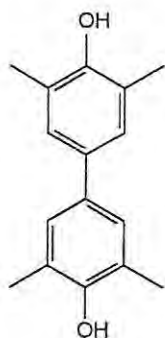


118

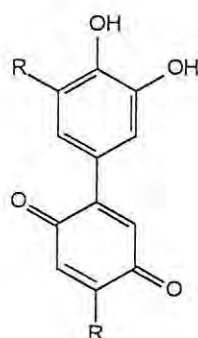
For all of the complexes, the product of the reactions with DTBP was found to be the coupled product 117:



Thus, no cresolase activity, (*i.e.* hydroxylation of a phenol to form a catechol) was observed. Réglie *et al.*, (1990) reported that formation of DTBQ from DTBP was catalysed by complex I, in the presence of triethylamine. Their product was identified by NMR spectroscopy and TLC (Réglie, 1992). In the present study, however, the coupled product was obtained using this complex, even in the presence of triethylamine. This result does not preclude the complexes from being tyrosinase models, because tyrosinase itself has been shown to catalyse the oxidative coupling of substrates such as substituted phenols, giving products such as 119 (Andersen *et al.*, 1992) and 120 (Pandey *et al.*, 1990).

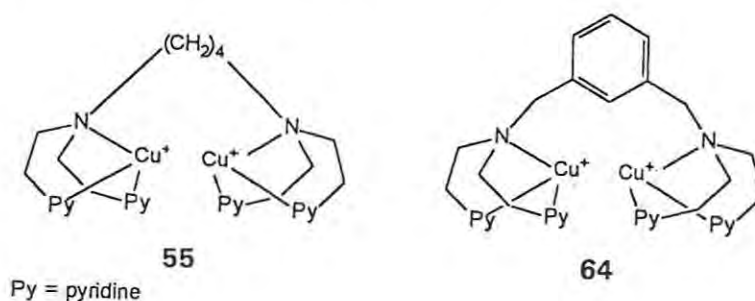


119



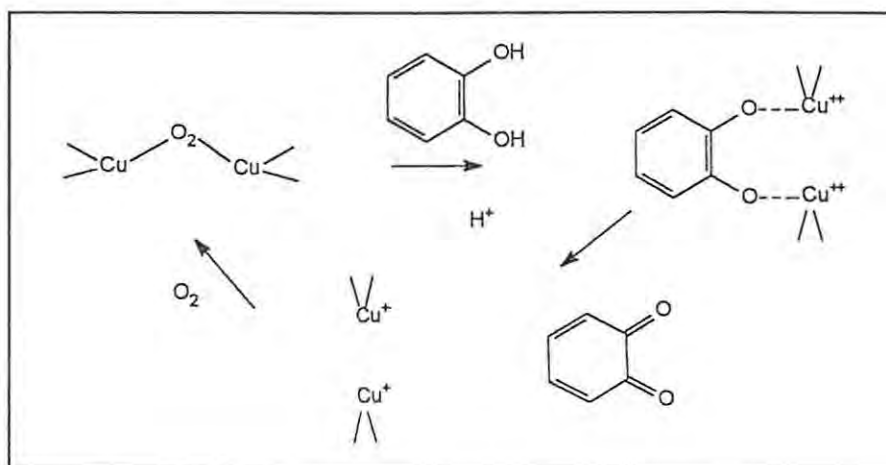
120

The formation of coupled biphenyl products from the reactions of phenols with biomimetic copper complexes has been widely reported (Kushioka, 1984; Flinterman and Challa, 1983; Tsuruya *et al.*, 1977; Feringa and Wynberg, 1978) and the particular product, 117, was reported by Karlin and co-workers (Paul *et al.*, 1991) in their study of the complexes 55 and 64. In addition to coupled hydroxybiphenyl products, coupled diphenoquinones have also been reported (Kitajima., 1990). The mechanism of these reactions is discussed in the next section.



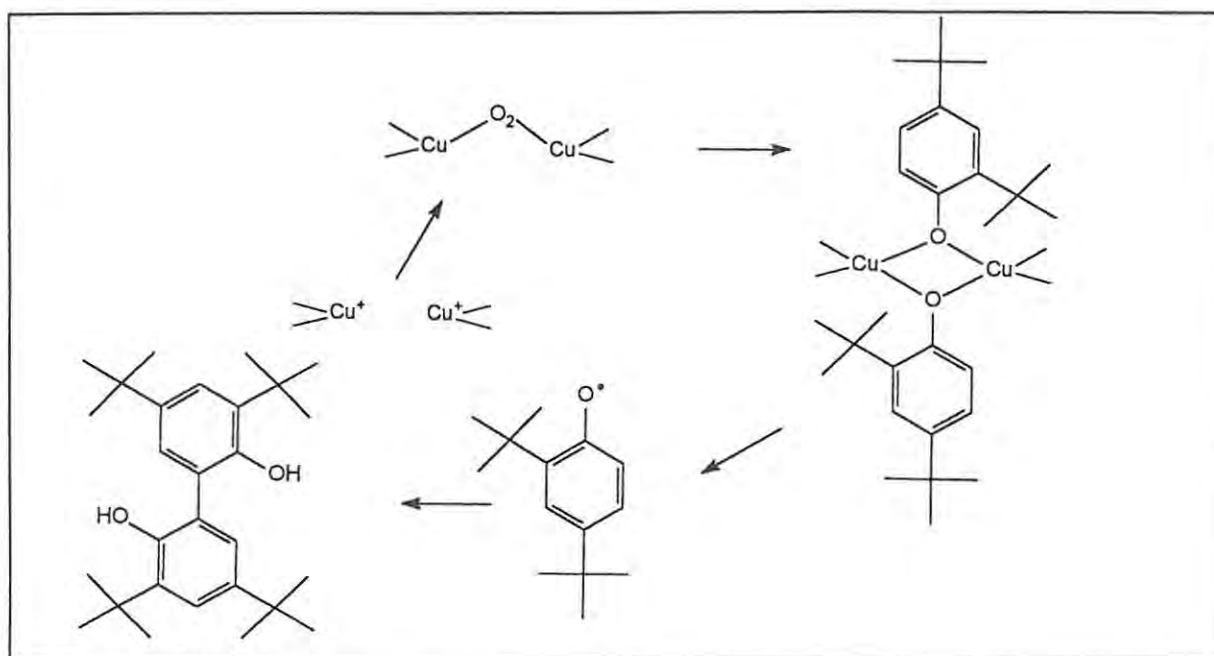
9.3.3 The mechanism of the oxidation reactions

Mechanisms for the oxidation of DTBC and DTBP catalysed by copper complexes have not been conclusively elucidated. The oxidation of DTBC to DTBQ involves the loss of two protons from the substrate and the formation of a dinuclear copper (II) catecholate intermediate, followed by the transfer of two electrons from the substrate aromatic ring to the two copper (II) ions (Balla *et al.*, 1992). Oxygen serves to reoxidise the copper (I) ions and the overall reaction may be represented as shown in Scheme 9.1 (Speier, 1986). The complexes investigated in the present study presumably react *via* the same type of mechanism.



Scheme 9.1: Mechanism of oxidation of catechols by dinuclear copper complexes (Speier, 1986)

The mechanism for the oxidative coupling of DTBP molecules is generally considered to involve radical intermediates (Kitajima, 1992; Kushioka, 1984; Paul *et al.*, 1991) and it is reasonable to presume that the product 117, observed in the present study, results from the dimerisation of such radicals. The flexibility of the complexes may also facilitate the reaction in that it permits the coordination of two substrate molecules at one time, in close enough proximity to enable them to couple, as proposed by Kitajima (1992) for a similar reaction (Scheme 9.2). This author has proposed a corresponding mechanism for the activity of tyrosinase (see Section 1.4.5) and, thus, the complexes can be regarded as models for tyrosinase.



Scheme 9.2: Mechanism of oxidative phenolic coupling (Kitajima, 1992)

9.3.4 The kinetic analysis of the reactions catalysed by the copper complexes

An enzyme kinetic approach to the measurement of the catalytic activity of the complexes was used to determine how closely they mimic the activity of tyrosinase. It should be noted that this method, which formally applies to enzyme-catalysed reactions, is an approximate one and the results only give an indication of the apparent activity of the complexes. The measurement of initial rates of reaction has the advantage that gradual decomposition of the complexes does not interfere with the results, but no allowance is made for the possibility that reactions may stop before they are complete. In fact, the reactions with DTBP were observed to stop before all the substrate was used up, indicating that the complexes were not reacting in a straightforward catalytic manner.

The K_m values determined for catecholase activity of the complexes are comparable with the values reported for tyrosinase itself, using 4-methylcatechol as the substrate [5mM in a reverse micelle system and 9mM in an aqueous system (Sánchez-Ferrer *et al.*, 1988b)]. These values indicate that the complexes do bind the substrate successfully, and the turnover numbers, k_{cat} , indicate appreciable activity. An alternative way of assessing the catalytic activity of the complexes is to compare their catalytic efficiencies, V/K_m (see Table 9.7, Section 9.2.6). In this context, the most effective catecholase activity was demonstrated by complex IIIB. Réglier *et al.*, 1990 reported that complex I gave a turnover number of 11 h^{-1} , and a K_m of $5.4 \times 10^{-2} \text{ mM}$, while in the present study this complex was found to have more effective activity, with a k_{cat} of 39 h^{-1} , and $K_m = 7.8 \text{ mM}$.

Interestingly, the complex IIA, which contains copper (II) ions, was also found to be an effective catalyst for the oxidation of DTBC. This shows that the reaction can be catalytic, rather than stoichiometric, since the copper (II) complex would be reduced to the copper (I) form by the substrate, and reoxidised by oxygen (Rockcliffe and Martell, 1992).

The kinetic parameters obtained for the oxidation of DTBC catalysed by complex IIB could not be determined reliably, since the intercept of the Hanes plot was found to be negative. While this indicates that the complex does not conform to Michaelis-Menten kinetics, the observed rates and extent of reaction show that it is, nevertheless, a very effective catalyst. Similarly, the complex IIIB was found to exhibit a high turnover number, *viz.*, 59.2 h^{-1} . Thus the two complexes prepared by the template condensation method proved to be the most effective catecholase models.

The kinetics of the reactions involving DTBP must be viewed rather differently from those determined using DTBC, since the reactions apparently proceed *via* a completely different mechanism. The turnover numbers shown in Table 9.6 (Section 9.2.6) are comparable with those reported by Karlin and co-workers (Paul *et al.*, 1991) for the formation of the same product (*viz.*, 31 and 55 h^{-1}) (see Section 9.3.3), which indicates that the complexes synthesised in this study were effective as catalysts for this reaction. Since no enzyme kinetic parameters have been reported for the activity of tyrosinase in catalysing coupling reactions, it is not possible to assess the present results in terms of successful biomimetic activity. Further research in this area is warranted, and this could provide useful information relating to the mechanism of tyrosinase.

9.4 EXPERIMENTAL

9.4.1 Oxidation of DTBP and DTBC , catalysed by complex I

A solution of DTBP (50mM; 0.5ml) in CH_2Cl_2 was placed in a 1ml cuvette of path length 1 cm. The reaction was started by the addition of a solution (0.5ml) of the complex I (0.1mM) and Et_3N (0.2mM) in dry, degassed CH_2Cl_2 . The cuvette was rapidly inverted to mix the solutions, and the absorbances at 400 and 650nm were measured every minute for 9 minutes. The temperature was maintained at 25°C using a constant temperature unit fitted to the spectrophotometer, and the instrument was zeroed against the solvent. The reference cell contained the substrate in CH_2Cl_2 (25mM; 1.0 ml). The readings are shown in Table 9.8 below. The UV-visible spectrum of the reaction mixture was measured after 10 min.

The complex I (1mg) was also added to a solution of DTBC (0.1M; 5 ml) in CH_2Cl_2 , with Et_3N , and the UV-visible spectrum of a diluted (1 in 4) sample of this reaction mixture was also recorded (see Figure 9.2).

Table 9.8: Photometric data for the oxidation of DTBP by complex I

Substrate	Time(min)	A_{400}	A_{650}	A_{400}	A_{650}	A_{400}^*	A_{650}^*
DTBP	0.1	0.350	0.011	0.343	0.011	0.535	0.022
	1.1	0.367	"	0.363	"	0.582	0.022
	2.1	0.390	"	0.386	"	0.625	0.023
	3.1	0.411	"	0.404	"	0.654	0.023
	4.1	0.431	"	0.419	"	0.678	0.024
	5.1	0.447	"	0.434	"	0.703	0.025
	6.1	0.463	"	0.446	"	0.715	0.028
	7.1	0.475	"	0.454	"	0.733	0.030
	8.1	0.489	"	0.460	"	0.752	0.032
	9.1	0.499	"	0.470	"	0.762	0.033

*: No Et_3N present, $[\text{I}] = 0.2\text{mM}$, $[\text{DTBP}] = 50\text{mM}$

9.4.2 Investigation of the products from oxidation of DTBP and DTBC, catalysed by copper complexes

The following procedure was carried out using the complexes **I**, **IIB**, **IIC**, **IIIA**, and **IIIB**. The complex (1mg, 0.001mmol) was dissolved in dry, degassed CH₃CN (0.2ml) and this solution was added to a solution of the substrate [DTBP or DTBC (0.1M; 5 ml) containing Et₃N (0.002mmol), in dichloromethane. The mixture was stirred vigorously to facilitate aeration (5min) and then allowed to stand (24h). A similar set of solutions were prepared without including Et₃N. The solutions were analysed by TLC [silica; EtOAc-hexane (1:2) and chloroform-ether (2:3)], using DTBP, DTBC, and DTBQ standards. (The results are summarised in Table 9.1, Section 9.2.4). The solvent was then removed under reduced pressure, and replaced with CDCl₃ for analysis by ¹H NMR. The heights of the integrals were used to determine the relative concentrations of substrate and product in the reaction mixtures.

The reaction mixture from the oxidation of DTBP with **IIIB** was separated by preparative TLC [silica; EtOAc-hexane (4:1)]. The major product (*R_f* = 0.6) of the oxidation of DTBP was found to be 3,3',5,5'-tetra-*tert*-butyl-2,2'-dihydroxybiphenyl, *v*_{max} (CH₂Cl₂) 3300br (OH), 2950 (alkyl); δ_H(CDCl₃) 1.31(18H, s, *t*-Bu), 1.44(18H, s, *t*-Bu), 7.10(2H, d, *J* 2.3Hz, H-4 and H-4'), and 7.38(2H, d, *J* 2.3Hz, H-6 and H-6'); δ_C(CDCl₃) 29.68, 31.64, 34.46, 35.20, 122.37, 124.37, 125.28, 136.26, 143.01, 149.78; *m/z* M⁺ 410.3215. C₂₈H₄₂O₂ requires 410.3185.

The reaction mixture from the oxidation of DTBC with complex **IIB** was separated using the same solvent system. The major product (*R_f* = 0.8) from the oxidation of DTBC was found to be 3,5-di-*tert*-butyl-*o*-benzoquinone, *v*_{max} (CH₂Cl₂) 2950 (alkyl), 1650 (C=O); δ_H(CDCl₃) 1.21(9H, s, *t*-Bu), 1.25(9H, s, *t*-Bu), 6.20(1H, s, H-4) and 6.78(1H, s, H-6).

The complexes were each also added to solutions of *p*-cresol and *p*-*tert*-butylphenol, using the procedure described above. The resulting reaction mixtures were analysed by TLC, and the products from the reactions of complex **I** and **IIIA**, with DTBP and DTBC respectively, were analysed by NMR as above. The reaction mixtures were observed to contain only starting materials. Similarly, the products from [Cu(MeCN)₄][PF₆], obtained as described in Section 7.4.16, were tested for activity by the procedure described above, and the reaction mixtures were analysed by TLC. No products were observed to have been formed.

9.4.3 Preparation of 3,5-di-*tert*-butyl-*o*-benzoquinone (DTBQ) 117

o-Chloranil (0.4g, 1.6mmol) was added to a solution of 3,5-di-*tert*-butylcatechol (0.3g, 1.4mmol) in dry Et₂O (50ml), and the mixture was stirred at room temperature for 0.5h, and then filtered. The solvent was removed from the filtrate under reduced pressure, leaving a red solid residue shown by analytical TLC [silica; CHCl₃-hexane (3:1) and EtOAc-hexane (2:1)] to be almost pure DTBQ: δ_{H} (CDCl₃) 1.20(2H,s,Bu^t), 1.23(9H,s,Bu^t), 6.19(1H,d,*J* 2.2, Ar-H), and 6.94(1H,d,*J* 2.2, Ar-H).

9.4.4 Determination of the UV molar absorption coefficient of 3,3',5,5'-tetra-*tert*-butyl-2,2'-dihydroxybiphenyl, 117

The reaction mixture from the oxidation of DTBP catalysed by complex I (see experiment 9.3.2 above) was evaporated to dryness. CDCl₃ (0.5ml) was added to dissolve the residue, and the ¹H NMR spectrum of the solution was measured (Figure 9.6). The product:substrate ratio was calculated from the ratio of the integrals of the *tert*-butyl and aromatic proton signals, as shown in Table 9.9 below.

Table 9.9: Ratio of product:substrate from integrals in ¹H NMR spectrum of DTBP reaction mixture

Compound	Protons	δ_{H} (ppm)	Integral	Ratio	S:P ratio
DTBP	Bu ^t	1.32, 1.44	38	3.45	3.48:1 indicates
Biphenyl 117	Bu ^t	1.35, 1.48	11		
DTBP	Aromatic	7.32	35	3.50	28.74% conversion
Biphenyl 117	Aromatic	7.43	10		

The solution was diluted tenfold to measure the absorbance at 400nm. This was found to be 1.273. The molar absorption coefficient ϵ was calculated to be 88.6 M⁻¹ cm⁻¹.

9.4.5 Kinetic analysis of catalytic oxidation reactions

Solutions of the substrate (DTBP or DTBC) of concentration 0.1 - 0.001M were prepared using dry, but not degassed, CH_2Cl_2 . For each reaction, substrate solution (3ml) was placed in the sample and reference cuvettes. Solutions of the complex (10mg/ml, making a final concentration of 0.1mM; 30 μl) and Et_3N (1% in CH_2Cl_2 to make the concentration 0.2mM; 20 μl) were added to the sample cell. The cell was rapidly inverted to mix the solutions, and replaced in the spectrophotometer. The absorbance at 400nm was followed for 9 minutes, and the rates of absorbance increase (ΔA) per minute were determined from the gradient of a plot of Absorbance vs time graphs, the best straight line fit being obtained by linear regression analysis using QuatroPro. The experiments were carried out in duplicate for each concentration (Tables 9.10 and 9.11; mean rates shown in Tables 9.12 and 9.13). Rates of absorbance increase were converted to rates of formation of product using the molar extinction coefficients: for DTBP oxidations, 3,3',5,5'-tetra-*tert*-butyl-2,2'-dihydroxybiphenyl has $\epsilon = 90 \text{ M}^{-1}\text{cm}^{-1}$; for DTBC oxidations, 3,5-di-*tert*-butyl-*o*-benzoquinone has $\epsilon = 1830 \text{ M}^{-1}\text{cm}^{-1}$. Hanes plots of the data are shown in Figures 9.11 and 9.12, and the kinetic parameters K_m and V obtained from these graphs are shown Tables 9.5 - 9.7, Section 9.2.6.

Table 9.10: Rates of absorbance increase recorded for oxidations of DTBC, catalysed by copper complexes

Complex	s (M)	Rate (SEM) ($\Delta A \cdot \text{min}^{-1}$)	Complex	s (M)	Rate (SEM) ($\Delta A \cdot \text{min}^{-1}$)
I	0.1	0.1089(0.004) 0.1096(0.0009)	IIIA	0.1	0.015(0.0002) 0.0192(0.0003)
	0.05	0.1038(0.002) 0.1062(0.002)		0.05	0.0149(0.0005) 0.0150(0.0003)
	0.01	0.0663(0.002) 0.0663(0.001)		0.01	0.0091(0.0001) 0.0124(0.0003)
	0.005	0.0480(0.0008) 0.0465(0.0005)		0.001	0.0033(0.0001) 0.0032(0.0001)
	0.001	0.0124(0.0004) 0.0119(0.0004)			
IIB	0.1	0.0907(0.001) 0.0842(0.001)	IIIB	0.1	0.1763(0.005) 0.1748(0.007)
	0.05	0.0907(0.002) 0.0958(0.001)		0.05	0.1747(0.006)
	0.01	0.1274(0.003) 0.1308(0.003)		0.01	0.1384(0.005) 0.1417(0.006)
	0.001	0.09942(0.001) 0.1001(0.0005)		0.005	0.1008(0.003)
	0.0005	0.0587(0.0005) 0.0637(0.0006)		0.001	0.0519(0.0004) 0.0557(0.0004)
	0.0002	0.0281(0.003) 0.0236(0.002)	IIC	0.1	0.0256(0.0004) 0.0315(0.0013)
				0.05	0.0195(0.0006)
				0.01	0.0180(0.0004) 0.0182(0.0005)
				0.005	0.0141(0.0005)
				0.001	0.0064(0.0001) 0.0068(0.0001)

Table 9.11: Rates of absorbance increase recorded for oxidations of DTBP catalysed by copper complexes

Complex	<i>s</i> (M)	Rate (SEM) ($\Delta A \cdot \text{min}^{-1}$) ^a	Complex	<i>s</i> (M)	Rate(SEM) ($A \cdot \text{min}^{-1}$)
I	0.1	0.0407(0.01) 0.0459(0.004)	IIIA	0.03	0.0180(0.0006) 0.0160(0.0005)
	0.05	0.0298(0.008) 0.0233(0.008)		0.01	0.0157(0.0005) 0.0154(0.0007)
	0.01	0.0071(0.0007) 0.009(0.001)		0.002	0.0050(0.0003) 0.0080(0.0003)
	0.005	0.0049(0.0005) 0.0046(0.0009)		0.001	0.0065(0.0005) 0.0058(0.001)
	0.001	0.0054(0.002) 0.0054(0.0016)	IIIB	0.1	0.0803(0.007) 0.0815(0.007)
IIB	0.1	0.0562(0.002) 0.0579(0.002)		0.05	0.0576(0.010) 0.0545(0.011)
	0.05	0.0416(0.004) 0.0405(0.005)		0.01	0.0162(0.002) 0.0237(0.019)
	0.01	0.0411(0.0004) 0.0392(0.0007)		0.005	0.0117(0.002) 0.0114(0.002)
	0.001	0.0096(0.001) 0.0095(0.002)	0.001	0.0032(0.0004) 0.0049(0.0008)	

Table 9.12: Initial reaction rates measured for the oxidation of DTBC, catalysed by copper complexes

Complex	Substrate concentration, s (M)	Rate ($\Delta\text{Abs. min}^{-1}$)	Rate v (M. min^{-1}) $\times 10^5$	s/v (min^{-1})
I	0.1	0.1093 (0.0004)	5.98	1672
	0.05	0.105 (0.001)	5.74	871.1
	0.01	0.0663 (0.0001)	3.63	275.0
	0.005	0.0047 (0.0003)	2.57	194.6
	0.001	0.0122 (0.0002)	0.67	149.3
IIB	0.1	0.0875(0.003)	4.78	2092
	0.05	0.0933(0.003)	5.10	980.4
	0.001	0.129(0.002)	7.05	14.2
	0.0005	0.0612(0.002)	3.34	15.0
	0.0002	0.0259(0.002)	1.42	14.1
IIC	0.1	0.029 (0.003)	1.59	6289
	0.05	0.0195 (0.0003)	1.07	4672
	0.01	0.0180 (0.0001)	0.98	1020
	0.005	0.0141 (0.0005)	0.77	649.4
	0.001	0.0066 (0.0002)	0.36	277.8
IIIA	0.1	0.0171 (0.002)	0.93	10753
	0.05	0.0149 (0.0005)	0.81	6172
	0.01	0.011 (0.003)	0.60	1667
	0.001	0.0033 (0.0001)	0.18	556
IIIB	0.1	0.176 (0.002)	9.62	1040
	0.01	0.140 (0.002)	7.65	130.7
	0.001	0.054 (0.002)	2.95	33.9

Table 9.13: Initial reaction rates measured for oxidation of DTBP catalysed by copper complexes

Complex	Substrate concentration (M)	Rate (Abs.min ⁻¹)	Rate v (M.min ⁻¹) x 10 ⁴	s/v (min ⁻¹)
I	0.1	0.0433 (0.003)	4.81	207.9
	0.05	0.0266 (0.003)	2.96	168.9
	0.01	0.0081 (0.0009)	0.90	111.1
	0.001	0.0054 (0.000)	0.60	16.67
	0.0005	0.0048 (0.0001)	0.53	9.43
IIB	0.1	0.0571 (0.0008)	6.34	157.7
	0.05	0.0411 (0.0005)	4.57	109.4
	0.01	0.0402 (0.0002)	4.47	22.37
	0.001	0.0096 (0.0001)	1.07	9.35
IIIA	0.03	0.017 (0.001)	1.99	150.8
	0.01	0.015 (0.002)	1.67	59.9
	0.002	0.0065 (0.002)	0.72	27.78
	0.001	0.0061 (0.0004)	0.67	14.9
IIIB	0.1	0.0809 (0.0006)	8.99	111.2
	0.05	0.056 (0.002)	6.22	80.39
	0.01	0.020 (0.004)	2.22	45.05
	0.005	0.0116 (0.0002)	1.29	38.76
	0.001	0.0041 (0.0008)	0.456	21.93

CHAPTER 10

CONCLUSION

The research described in this thesis has required an interdisciplinary approach, encompassing a wide range of techniques and theories, with the aim of developing a rationale for the functioning of polyphenol oxidase in an organic medium, and exploring its application in biocatalysis.

Polyphenol oxidase was shown to be suitable for use as a biocatalyst, in chloroform, for the hydroxylation of phenols and their subsequent oxidation to *o*-quinones, which are potentially useful as synthetic intermediates. Practical aspects of the application of the polyphenol oxidase in chloroform have also been investigated and, to some extent, optimised. In the continuous process which was developed as a means of increasing the scale of the biocatalysis yields, a major obstacle to the use of polyphenol oxidase, *viz.*, reaction inactivation and enzyme occlusion by polymerised melanins, has been overcome. This was achieved by efficient removal of quinone products from the locality of the enzyme binding site (due to their high solubility in chloroform) and by control of free water. This improvement significantly enhances the practical and economic feasibility of biocatalysis using polyphenol oxidase.

The activity of the biocatalyst was found to be modified by purification procedures, and it is proposed that the removal of extraneous protein and/or melanoid material reduces the flexibility and alters the hydrophobic nature of the binding site, restricting access for sterically demanding substrates. The role of hydrophobicity in defining the substrate specificity of the biocatalyst could not be separated from steric considerations, but the results indicate that it is also an important controlling factor. In fact, the restriction on the flexibility of the polyphenol oxidase binding pocket, imposed by the chloroform medium, appears to be crucial in defining the steric size of substrates which could have access to the active site. This restricted flexibility, together with hydrophobicity, is apparently responsible for limitations on the range of substrates for which the biocatalytic system is suitable. Addition of an anionic detergent (SDS) to the biocatalyst medium increased both the range of sterically demanding substrates which could be transformed, and the catalytic efficiency of the enzyme. These observations have been attributed to modification of electrostatic interactions within the protein binding pocket, which results in enhanced flexibility.

In a biocatalytic system, where a number of inter-dependent components are involved (*viz.*, the enzyme, the solvent, the support, the system, *etc.*), any modification cannot be regarded as having an isolated effect on one component; it is the whole system which is modified. Optimisation also applies to the whole system, and a number of factors must be considered to be operating together to enhance characteristics such as substrate specificity and reaction rates. Thus, it is reasonable to suggest that the optimal functioning of the polyphenol oxidase biocatalyst is dependent on many factors which could affect, among other properties, both the conformational flexibility and the hydrophobic character of the system.

The observations made and the conclusions drawn, in this study, confirm current theories relating to the effects of organic media on enzyme activity in biocatalytic systems.

Conformational flexibility is a key issue in rationalising and interrelating various aspects of the present study. Molecular mechanical modelling of biomimetic copper complexes also indicated the significance of conformational flexibility in determining substrate specificity. The structure of the organic ligand to which the copper ions were coordinated was shown to affect steric crowding and hence, the availability of space in the binding sites of the complexes.

The dinuclear copper complexes synthesised as polyphenol oxidase models were consequently designed to include a flexible spacer in the ligand to facilitate their reaction with sterically hindered substrates. Their successful reaction with such substrates, and their lack of reactivity with less hindered substrates, suggests that they do possess considerable flexibility. The complexes are considered to be successful models of polyphenol oxidase in that they catalyse the oxidation of catechols and the oxidative coupling of phenols, but there is clearly a difference in their substrate specificity, as compared with that of the enzyme, which can be attributed to differences in conformational flexibility. The highest catalytic efficiency was observed for the complex where benzimidazole donors contributed considerable steric bulk and hydrophobicity to the ligand, possibly simulating the situation within the enzyme binding pocket. These characteristics can also be correlated with increased affinity for hydrophobic or non-polar substrates. A similar trend was observed in the case of polyphenol oxidase, as discussed above, demonstrating the success of the complex as a biomimetic model.

Detailed molecular modelling of this benzimidazole complex showed that it was sufficiently flexible to accommodate two molecules of the sterically demanding substrate 2,4-di-*tert*-butylphenol (DTBP) simultaneously. This justifies the proposed mechanism for the oxidative coupling observed in the reaction of the complexes with this substrate. Since the complexes were biomimetic models, it also suggests that with increased flexibility the polyphenol oxidase molecule would be capable

of binding more sterically hindered substrates, and demonstrates the way in which coupling reactions can be catalysed by the enzyme.

Comparison of the catalytic activities measured in the present study, for the complexes and for the biocatalyst, are particularly meaningful in that both types of catalyst were investigated in hydrophobic, organic solvent media, providing very similar environments for substrates and products, and possibly also within the binding sites of both enzyme and complexes. Although the dinuclear copper complexes were shown to be reasonable models of polyphenol oxidase, their catalytic efficiencies were far lower than those determined for the enzyme. This fact, together with the difficulties inherent in dealing with copper (I) compounds generally, and these imine-linked complexes in particular, has illustrated the advantages of using the enzyme as a catalyst in organic syntheses. The value of the biomimetic investigation, however, lies in the possibility of drawing parallels between the properties of the complexes and those of polyphenol oxidase.

The present investigation of dinuclear copper complexes indicates that much further research is required to produce stable biomimetic complexes. Such complexes could be designed (a) with more stable ligand structures, particularly with respect to intramolecular cyclisation; (b) with more specifically controlled flexibility; (c) to include more asymmetric character. Synthesis of copper (II) analogs of the copper (I) complexes reported in this study may give products which are more stable with respect to oxidation, and which would be more readily characterised.

There is much scope for further development of the biocatalytic system, and even more possibilities will emerge as the field of biocatalysis continues to expand. The substrate specificity of the system may well be broadened by the application of techniques such as molecular imprinting, and also by the addition of other solvating components such as polyols, which could interact with polar groups within the binding pocket to enhance flexibility. The stability and durability of the biocatalyst might be enhanced by alternative immobilisation techniques, by the addition of alternative lyoprotectants, or by application in different solvents.

In view of the successful biocatalytic activity demonstrated, and the value of the reaction products as synthetic intermediates, all of these possibilities warrant investigation. The system developed in the present study lends itself to examination of these alternatives, and could usefully be applied in further development of the polyphenol oxidase biocatalyst.

REFERENCES

- Aasa, R., Deinum, J., Lerch, K., Reinhammar, B. 1978. The reaction of mercaptans with tyrosinases and hemocyanins. *Biochim. Biophys. Acta.* **535**: 287-298.
- Adman, E. T. 1991. Copper protein structures. p. 145-197. In: Anfinsen, C. B., Edsell, J. T., Richards, F. M., Eisenberg, D. S. (eds.). *Metalloproteins: structural aspects, advances in protein chemistry*, Vol. 42. Academic Press, San Diego.
- Affleck, R., Xu, Z.-F., Suzawa, V., Focht, K., Clark, D. S., Dordick, J. S. 1992. Enzymatic catalysis and dynamics in low-water environments. *Proc. Natl. Acad. Sci. USA.* **89**: 1100-1104.
- Al-Kazwini, A. T., O'Neill, P., Cundall, R. B., Adams, G. E., Junio, A., Maignan, J. 1992. Direct observation of the reaction of the quinone-methide from 5,6-dihydroxyindole with the nucleophilic azide ion. *Tetrahedron Lett.* **33(21)**: 3045-3048.
- Allinger, N. L. 1977. Conformational analysis. 130. MM2. A hydrocarbon force field utilizing V_1 and V_2 torsional terms. *J. Am. Chem. Soc.* **99**: 8127-8134.
- Andersen, S. O., Jacobsen, P. J., Bojesen, G., Roepstorff, P. 1992. Phenoloxidase catalyzed coupling of catechols. Identification of novel coupling products. *Biochim. Biophys. Acta.* **1118**: 134-138.
- Andersson, E., Hahn-Hägerdal, B. 1990. Bioconversions in aqueous two-phase systems. *Enzyme Microb. Technol.* **12**: 242-254.
- Andrawis, A., Kahn, V. 1986. Effect of methimazole on the activity of mushroom tyrosinase. *Biochem J.* **235**: 91-96.
- Angleton, E. L., Flurkey, W. H. 1984. Activation and alteration of plant and fungal polyphenoloxidase isoenzymes in sodium dodecylsulfate electrophoresis. *Phytochem.* **23(12)**: 2723-2725.
- Antonini, E., Carrea, G., Cremonesi, P. 1981. Enzyme catalysed reactions in water-organic solvent two-phase systems. *Enzyme Microb. Technol.* **3**: 291-296.
- Arnold, F. 1990. Engineering enzymes for non-aqueous solvents. *TIBTECH.* **8**: 244-249.
- Asimov, I., Dawson, C. R. 1950. On the reaction inactivation of tyrosinase during the aerobic oxidation of catechol. *J. Am. Chem. Soc.* **72**: 820-828.
- Atlow, S. C., Bonadonna-Apro, L., Klibanov, A. M. 1984. Dephenolisation of industrial wastewaters catalyzed by polyphenol oxidase. *Biotechnol. Bioeng.* **XXVI**:599-603.
- Bailey, P. S., Erickson, R. E. 1961. Diphenaldehyde (Biphenyl, 2,2'-diformyl-). *Org. Synthesis.* **41**: 41-45.
- Baldwin, M. J., Ross, P. K., Pate, J. E., Tyeklár, Z., Karlin, K. D., Solomon, E. I. 1991. Spectroscopic and theoretical studies of an end-on peroxide-bridged coupled binuclear copper(II) model complex of relevance to the active sites in hemocyanin and tyrosinase. *J. Am. Chem. Soc.* **113**: 8671-8679.

Baldwin, M. J., Root, D. E., Pate, J. E., Fujisawa, K., Kitajima, N., Solomon, E. I. 1992. Spectroscopic studies of side-on peroxide-bridged binuclear copper(II) model complexes of relevance to oxyhemocyanin and oxytyrosinase. *J. Am. Chem. Soc.* **114**: 10421-10431.

Balla, J., Kiss, T., Jameson, R. F. 1992. Copper(III)-catalyzed oxidation of catechol by molecular oxygen in aqueous solution. *Inorg. Chem.* **31**: 58-62.

Barton, D., Ollis, W. D. 1979. p.739-742. In: *Comprehensive organic chemistry*, Vol. 1. Pergamon Press, Oxford.

Bauer, H. H. et al. 1978. Atomic absorption spectrophotometry. p. 262. In: Bauer, H. H., Christian, G. D., O'Reilly, J. E. (eds), *Instrumental analysis*. Man & Bacon Inc., Boston.

Behbahani, I., Miller, S. A., O'Keefe, D. H. 1993. A comparison of mushroom tyrosinase dopaquinone and dopachrome assays using diode-array spectrophotometry: dopachrome formation vs ascorbate-linked dopaquinone reduction. *Microchem. J.* **47**: 251-260.

Beltramini, M., Ricchelli, F., Salvato, B. 1984a. The kinetics of the reaction of *Octopus vulgaris* with cyanide. Its significance for the structure of the 11 S subunit of molluscan hemocyanin. *Inorg. Chim. Acta.* **92**: 209-217.

Beltramini, M., Ricchelli, F., Tallandini, L., Salvato, B. 1984b. The reaction between cyanide and the hemocyanin of *Carcinus maenas*. A kinetic study. *Inorg. Chim. Acta.* **92**: 219-227.

Beltramini, M., Salvato, B., Santamaria, M., Lerch, K. 1990a. The reaction of CN^- with the binuclear copper site of *Neurospora* tyrosinase: its relevance for a comparison between tyrosinase and hemocyanin active sites. *Biochim. Biophys. Acta.* **1040**: 365-372.

Beltramini, M., Santamaria, M., Salvato, B., Lerch, K. 1990b. Folding of the polypeptide chain(s), conformational flexibility and reactivity of the metal active site of hemocyanin and tyrosinase. *Biol. Metals.* **3**: 93-97.

Beltraminin, M., Bubacco, L., Salvato, B., Casella, L., Gulotti, M, Garofani, S. 1992. The aromatic circular dichroism as a probe for conformational changes in the active site environment of hemocyanins. *Biochim. Biophys. Acta.* **1120**: 24-31.

Berends, H. P., Stephan, D. W. 1987. Toward copper(III) hemocyanin models. 2. Synthesis and characterization of binuclear copper(III) complexes of a heptadentate ligand. *Inorg. Chem.* **26**(5): 749-754.

Berenguer, J. J., Manjon, A., Iborra, J. L. 1989. A pH-tyrosinase biosensor for amino acids, catecholamines and adrenergic drugs determination. *Biotechnol. Techniques.* **3**(3): 211-216.

Bernaducci, E., Bharadwaj, P. K., Krogh-Jespersen, K., Potenza, J. A., Schugar, H. J. 1983. Electronic structure of alkylated imidazoles and electronic spectra of tetrakis(imidazole)copper(II) complexes. Molecular structure of tetrakis(1,4,5-trimethylimidazole)copper(II) diperchlorate. *J. Am. Chem. Soc.* **105**: 3860-3866.

Bernhardt, P. V., Comba, P. 1992. Molecular mechanics calculations of transition metal complexes. *Inorg. Chem.* **31**: 2638-2644.

Bernhardt, P. V., Comba, P., Hambley, T. W., Massoud, S. S., Stebler, S. 1992. Determination of solution structures of binuclear copper(III) complexes. *Inorg. Chem.* **31**: 2644-2651.

Bertrand, G. 1896. *Chimie physiologique*. - Sur une nouvelle oxydase, ou ferment soluble oxydant, d'origine vegetale. *Compt. Rend. Acad. Sci. Paris.* **122**: 1215-1217.

- Bhagvat, K., Richter, D. 1938. Animal phenolases and adrenaline. *Biochem.* **XXXII**: 1397-1406.
- Bhalerao, U. T., Muralikrishna, C., Pandey, G. 1989. An efficient synthesis of coumestans: a probable biogenetic approach. *Synth. Commun.* **19(7,8)**:1303-1307.
- Blackburn, N. J., Karlin, K. D., Concannon, M., Hayes, J. C., Gultneh, Y., Zubieta, J. 1984. Studies on a model copper monooxygenase system: peroxo-copper(II) binuclear intermediates in the hydroxylation of an aromatic ring. *J. Chem. Soc. Chem. Commun.*: 939-942.
- Blinkovsky, A. M., Martin, B. D., Dordick, J. S. 1992. Enzymology in monophasic organic media. *Curr. Opin. Biotechnol.* **3**: 124-129.
- Boekelheide, K., Graham, D. G., Mize, P. D., Jeffs, P. W. 1980. The metabolic pathway catalyzed by the tyrosinase of *Agaricus bisporus*. *J. Biol. Chem.* **255(10)**: 4766-4771.
- Bouchilloux, S., McMahon, P., Mason, H. S. 1963. The multiple forms of mushroom tyrosinase. Purification and molecular properties of the enzymes. *J. Biol. Chem.* **238(5)**: 1699-1707.
- Bouheroum, M., Bruce, J. M., Land, E. J. 1989. The mechanism of the oxidative decarboxylation of 3,4-dihydroxymandelic acid: identification of 3,4-mandeloquinone as a key intermediate. *Biochim. Biophys. Acta.* **998**: 57-62.
- Bourquelot, E., Bertrand, G. 1895. *Compt. Rend. Soc. Biol.* **47**: 582.
- Bourquelot, E., Aubry, A. 1911. Influence of alcohol concentration on the biochemical synthesis of α -ethylglucoside and of α -propylglycoside. *Comp.Rend. Soc. Biol.* **63**: 141.
- Brackman, W., Havinga, E. 1955. The oxidation of phenols copper-amine catalysts and its relation to the mode of action of tyrosinase. *Recueil.* **74**: 1107-1118.
- Braco, L., Dabulis, K., Klibanov, A. M. 1990. Production of abiotic receptors by molecular imprinting of proteins. *Proc. Natl. Acad. Sci. USA.* **87**: 274-277.
- Breslow, R. 1972. Biomimetic chemistry. *Chem. Soc. Rev.* **1**: 553-580.
- Brooks, D. W., Dawson, C. R. 1966. Aspects of tyrosinase chemistry. p. 343-359. In: J. Peisach, P. Aisen, W. E. Blumberg. (eds.), *The biochemistry of copper*. Academic Press, New York.
- Bru, R., Sánchez-Ferrer, A., García-Carmona, F. 1989. Characteristics of tyrosinase in AOT-isoctane reverse micelles. *Biotechnol. Bioeng.* **34**: 304-308.
- Bru, R., Sánchez-Ferrer, A., García-Carmona, F. 1990. The effect of substrate partitioning on the kinetics of enzymes acting in reverse micelles. *Biochem. J.* **268**: 679-684.
- Brubaker, G. R., Johnson, D. W. 1984. Molecular mechanics calculations in coordination chemistry. *Coord. Chem. Rev.* **53**: 1-36.
- Bruyninckx, W. J., Gutteridge, S., Mason, H. S. 1978. Detection of copper on polyacrylamide gels. *Anal. Biochem.* **89**: 174-177.
- Bulkowski, J. E., Burk, P. L., Ludmann, M. -F., Osborn, J. 1977. Two-metal-substrate interactions: the reversible reaction of a $Cu^I \dots \dots Cu^I$ complex with CO and O_2 . *J.Chem. Soc. Chem. Comm.:* 498-499.
- Burton, S. G., Duncan, J. R., Kaye, P. T., Rose, P. D. 1993. Activity of mushroom polyphenol oxidase in organic medium. *Biotechnol. Bioeng.* **42**: 938-944.

- Cabanes, J., García-Cánovas, F., Lozano, J. A., García-Carmona, F. 1987. A kinetic study of the melanization pathway between *L*-tyrosine and dopachrome. *Biochim. Biophys. Acta.* **923**: 187-195.
- Cabanes, J., Sánchez-Ferrer, A., Bru, R., García-Carmona, F. 1988. Chemical and enzymic oxidation by tyrosinase of 3,4-dihydroxymandelate. *Biochem. J.* **256**: 681-684.
- Capdevielle, P., Maumy, M. 1982. Ortho-hydroxylation selective des phenols: 1. Vers un modele chimique des tyrosinases. *Tetrahedron Lett.* **23(15)**: 1573-1576.
- Casella, L., Carugo, O., Gullotti, M., Garfani, S., Zanello, P. 1993. Hemocyanin and tyrosinase models. Synthesis, azide binding and electrochemistry of dinuclear copper(II) complexes with poly(benzimidazole) ligands modelling the met forms of the proteins. *Inorg. Chem.* **32**: 2056-2067.
- Casella, L., Gullotti, M. 1981. Coordination modes of histidine. 2. Stereochemistry of the reaction between histidine derivatives and pyridoxal analogues. Conformational properties of zinc(II) complexes of histidine Schiff bases. *J. Am. Chem. Soc.* **103**: 6338-6347.
- Casella, L., Gullotti, M., Bartosek, M., Pallanza, G., Laurenti, E. 1991(a). Model monooxygenase reactivity by binuclear two-coordinate copper(II) complexes extends to new ligand systems containing nitrogen and sulphur donors. *J. Chem. Soc. Commun.* : 1235-1237.
- Casella, L., Gullotti, M., Pallanza, G., Rigoni, L. 1988 Synthesis and reactivity of a family of copper monooxygenase model systems. *J. Am. Chem. Soc.* **110**: 4221-4227.
- Casella, L., Gullotti, M., Radaelli, R., Di Gennaro, P. 1991(b). A tyrosinase model system. Phenol *ortho*-hydroxylation by a binuclear three-coordinate copper(II) complex and dioxygen. *J. Chem. Soc. Commun.* : 1611- 1612.
- Casella, L., Rigoni, L. 1985. Type 3 copper model chemistry. Dioxygen activation by binuclear two-coordinate copper(II) complexes derived from *L*-histidine and *L-N*⁷-methylhistidine. *J. Chem. Soc. Commun.*: 1668-1669.
- Casella, L., Silver, M. E., Ibers, J. A. 1984. Synthesis and characterization of copper(I), copper(II), zinc(II), cobalt(II) and iron(II) complexes of a chelating ligand derived from 2,6-diacetylpyridine and *L*-histidine. Oxygenation of the copper(I), cobalt(II) and iron(II) complexes. Crystal structure of the zinc(II) complex. *Inorg. Chem.* **23**: 1409-1418.
- Chen, Y. M., Chavin, W. 1972. p. 593-605. In: V. Riley (ed), *Pigmentation: its genesis and biologic control*. Appleton Century Crofts, New York.
- Cheynier, V., Rigaud, J., Moutounet, M. 1990. Oxidation kinetics of *trans*-caffeoyltartrate and its glutathione derivatives in grape musts. *Phytochem.* **29(6)**: 1751-1753.
- Chioccare, F., Di Gennaro, P., La Monica, G., Sebastiano, R., Rindone, R. 1991. Selective *ortho*-hydroxylation of phenols in copper(II) complexes. *Tetrahedron.* **47(25)**: 4429-4434.
- Chyn, J. -P., Urbach, F. L. 1991. Autooxidation of 3,5-di-*t*-butylcatechol catalyzed by two pyrazolate-bridged dicopper complexes with different structural features. *Inorg. Chim. Acta.* **189**: 157-163.
- Clark, J. M., Switzer, R. L. 1977. p. 12. *Experimental biology*, 2nd edition. W. H. Freeman, USA.
- Cornish-Bowden, A. 1979. *Fundamentals of enzyme kinetics*. Butterworths, London.
- Cosnier, S., Innocent, C. 1992. A novel biosensor elaboration by electropolymerization of an adsorbed amphiphilic pyrrole-tyrosinase enzyme layer. *J. Electroanal. Chem.* **328**: 361-366.

Costantini, C., Crescenzi, O., Prota, G. 1991. Mechanism of the rearrangement of dopachrome to 5,6-dihydroxyindole. *Tetrahedron Lett.* **32(31)**: 3849-3850.

Cram, D. J. 1983. Designed host-guest relationships. p. 153-171. In: G. van Binst (ed.), *Design and synthesis of organic molecules based on molecular recognition*. Springer-Verlag, New York.

Crane, J. D., Fenton, D. E. 1991. Iron(III) and copper(II) complexes of polydentate ligands incorporating benzimidazole and phenolic residues. *Polyhedron* **10(15)**: 1809-1815.

Cushing, M. L. 1948. The oxidation of catechol-type substrates by tyrosinase. *J. Am. Chem. Soc.* **70**: 1184-1187.

Cvetkovska, M., Grchev, T., Bogdanovskaya, V., Tarasevich, M. R. 1992. Electrochemical methods for estimation of the ferment activity of a concentrate mixture of polyphenol oxidase. *Bioelectrochem. Bioenergetics.* **27**: 509-512.

Dabulis, K., Klibanov, A. 1993. Dramatic enhancement of enzymatic activity in organic solvents by lyoprotectants. *Biotechnol. Bioeng.* **41**: 566- 571.

Davis, B. 1964. Disc electrophoresis. II. Method and application to human serum proteins. *Ann. N. Y. Acad. Sci.* : 404-427.

Deinum, J., Lerch, K., Reinhammar, B. 1976. An EPR study of *Neurospora* tyrosinase. *FEBS Lett.* **69(1)**: 161-164.

Dietler, C., Lerch, K. 1979. Reaction inactivation of tyrosinase. p. 305-315. In: T. E. King (ed), *Int. Symposium on oxidases and related redox systems, 3rd Proc.*

Doddema, H. J. 1988. Site-specific hydroxylation of aromatic compounds by polyphenol oxidase in organic solvents and in water. *Biotechnol. Bioeng.* **32**: 716-718.

Dordick, J. S. 1989. Enzymatic catalysis in monophasic organic solvents. *Enzyme Microb. Technol.* **11**: 194-211.

Dordick, J. S. 1992. Designing enzymes for use in organic solvents. *Biotechnol. Prog.* **8**: 259-267.

Dordick, J. S. 1993. The chemistry of non-aqueous biocatalysis. *European Symposium on Biocatalysis, Graz, Austria.*

Doucet, J.-P., Murphy, B. J., Tuana, B. S. 1990. Modification of a discontinuous and highly porous sodium dodecyl sulfate-polyacrylamide gel system for minigel electrophoresis. *Anal. Chem.* **190**: 209-211.

Drueckhammer, D. G., Hennen, W. J., Pederson, R. L., Barbas, 111, C. F., Gautheron, C. M. Krach, T., Wong, C-H. 1991. Enzyme catalysis in synthetic carbohydrate chemistry. *Synthesis*: 499-525.

Duckworth, H. W., Coleman, J. E. 1970. Physicochemical and kinetic properties of mushroom tyrosinase. *J. Biol. Chem.* **245(7)**: 1613-1625.

Eickman, N. C., Himmelwright, R. S., Solomon, E. I. 1979. Geometric and electronic structure of oxyhemocyanin: spectral and chemical correlations to met apo, half met, met, and dimer active sites. *Proc. Natl. Acad. Sci. USA* **76(5)**: 2094-2098.

Escribano, J., García, M., Cánovas, F. G., Carmona, F. G., Varón, R., Tudela, J., Lozano, J. A. 1987. Kinetic study of the transient phase of a chemical reaction system coupled to an enzymatically catalyzed step. *Biophys. Chem.* **27**: 15-25.

Estrada, P., Baroto, W., Castillon, M. P., Acebal, C., Arche, R. 1993. Temperature effects on polyphenol oxidase activity in organic solvents with low water content. *J. Chem. Tech. Biotechnol.* **56**: 59-65.

Estrada, P., Sanchez-Muñiz, R., Acebal, C., Arche, R., Castellón, M. P. 1991. Characterization and optimization of immobilized polyphenol oxidase in low-water organic solvents. *Biotechnol. Appl. Biochem.* **14**: 12-20.

Faber, K., Riva, S. 1992. Enzyme-catalyzed irreversible acyl transfer. *Synthesis*: 895-910.

Feringa, B., Wynberg, H. 1978. Biomimetic asymmetric oxidative coupling of phenols. *Bioorg. Chem.* **7**: 397-408.

Fenton, D. E., Schroeder, R. R., Lintvedt, R. L. 1978. A unique two-electron, reversible reduction of a binuclear copper(II) complex. Observation of the electrochemical behaviour predicted by Polycn and Shain for the sequential transfer of two electrons at the same potential. *J. Am. Chem. Soc.* **100(6)**:1931- 1932.

Fitzpatrick, P. A., Klivanov, A. M. 1991. How can the solvent affect enzyme enantioselectivity? *J. Am. Chem. Soc.* **113**: 3166-3171.

Fling, M., Horowitz, N. H., Heinemann, S. F. 1963. The isolation and properties of crystalline tyrosinase from *Neurospora*. *J. Biol. Chem.* **238(6)**: 2045-2053.

Flinterman, M., Challa, G. 1983. Oxidative coupling catalyzed by copper complexes of poly(amidoamines). *J. Mol. Catal.* **18**: 149-157.

Flurkey, W. H. 1991. Identification of tyrosinase in mushrooms by isoelectric focusing. *J. Food Sci.* **56(1)**: 93-95.

Fox, A. S., Burnett, J. B. 1981. The genetics and biochemistry of tyrosinase in *Neurospora crassa*. p. 249-277. In: H. Sigel, A. Sigel. (eds.), *Metal ions in biological systems*, Vol. 13. Marcel Dekker, New York.

Frieden, E., Ottesen, M. 1959. A simplified method for the purification of mushroom polyphenol oxidase. *Biochim. Biophys. Acta.* **34**: 248-251.

Fukui, S., Tanaka, A. 1982. Bioconversion of lipophilic or water insoluble compounds by immobilised biocatalysts in organic solvent systems. *Enzyme Eng.* **6**: 191- 200.

Gabriel, O., Gersten, D. M. 1992. Staining for enzymatic activity after gel electrophoresis, 1. *Anal. Biochem.* **203**: 1-21.

Gagné, R. R., Kreh, R. P., Dodge, J. A. 1979. Unusual structural and reactivity types for copper(I) synthesis and structural and redox properties of binuclear copper(I) complexes which are probably three coordinate in solution and experience intermolecular metal-metal interactions in the solid state. *J. Am. Chem. Soc.* **101(23)**: 6917-6927.

Galindo, J. D., Martinez, J. H., Lopez-Ballester, J. A., Peñafiel, R., Solano, F., Lozano, J. A. 1987. The effect of polyamines on tyrosinase activity. *Biochem. Int.* **15(6)**: 1151-1158.

Gallo, R. 1983. Treatment of steric effects. *Prog. Phys. Org. Chem.* **14**: 115-163.

Gampp, H., Zuberbühler, A. D., 1981. Copper-catalysed oxidation and oxygenation. p. 133-189. In: H. Sigel (ed.), *Metal ions in biological systems*, Vol. 12. Marcel Dekker, New York.

- García-Cánovas, F. G., García-Carmona, F., Sánchez, J. V. Pastor, J. L. I., Teruel, J. A. L. 1982a. The role of pH in the melanin biosynthesis pathway. *J. Biol. Chem.* **257**(15):8738-8744.
- García-Carmona, F., García-Cánovas, F., Iborra, J. L., Lozano, J. A. 1982b. Kinetic study of the pathway of melanization between *L*-DOPA and dopachrome. *Biochim. Biophys. Acta.* **717**: 124-131.
- García-Carmona, F., Cabanes, J., García-Cánovas, F. 1987. Enzymatic oxidation by frog epidermis tyrosinase of 4-methylcatechol and *p*-cresol. Influence of *L*-serine. *Biochim. Biophys. Acta.* **914**: 198-204.
- Gardner, A. R., Cadman, T. W. 1990. Product deactivation in recombinant *Streptomyces*. *Biotechnol. Bioeng.* **36**: 243-251.
- Garza-Ramos, G., Fernández-Velasco, A., Ramírez, L., Shoshani, L., Darszon, A., Tuena de Gómez-Puyou, M., Gómez-Puyou, A. 1992. Enzyme activation by denaturants in organic solvent systems. *Eur. J. Biochem.* **205**: 509-517.
- Gaykema, W. P. J., Hol, W. G. J., Vereijken, J. M., Soeter, N. M., Bak, H. J., Beintema, J. J. 1984. 3.2 Å structure of the copper-containing, oxygen-carrying protein *Panulirus interruptus* haemocyanin. *Nature* **309**: 23-29.
- Gaykema, W. P. J., Volbeda, A., Hol, W. G. J. 1985. Structure determination of *Panulirus interruptus* haemocyanin at 3.2 Å resolution. *J. Mol. Biol.* **187**: 255-275.
- Geigenheimer, P. 1990. Preparation of extracts from plants. *Meth. Enzymol.* **182**: 174-193.
- Gelling, O. J., van Bolhuis, F., Meetsma, A., Feringa, B. L. 1988. Bimetallic oxidation catalysts. Oxygen insertion into an aryl-hydrogen bond of a binuclear copper(I) complex. *J. Chem. Soc. Commun.*: 552-554.
- Goetsch, P. A. 1992. The microbial production of polyphenol oxidase enzyme systems and their application in the treatment of phenolic waters. Ph.D. thesis, Rhodes University, Grahamstown, South Africa.
- Golan-Goldhirsh, A., Whitaker, J. R. 1985. k_{CAT} inactivation of mushroom polyphenol oxidase. *J. Mol. Catal.* **32**: 141-147.
- Good, M. L. 1989. Biotechnology: Chemistry is at the heart of it. p. xi-xiii. In: J. D. Burrington, D. S. Clark. (eds.), *Biocatalysis and biomimetics*. Am. Chem. Soc., Washington D. C.
- Gorman, L. A. S., Dordick, J. S. 1992. Organic solvents strip water off enzymes. *Biotechnol. Bioeng.* **39**: 392-397.
- Gray, H. B., Solomon, E. I. 1981. Electronic structures of blue copper centers in proteins. p. 1-37. In: Spiro, T. G. (ed.), *Metal ions in biology*, Vol 3. Wiley Inter-Science, New York.
- Gupta M. N. 1991. Thermostabilization of proteins. *Biotechnol. Appl. Biochem.* **14**:1-11.
- Gupta, M. N. 1992. Enzyme function in organic solvents. *Eur. J. Biochem.* **203**: 25-32.
- Gutteridge, S., Robb, D. A. 1973. Purification of mushroom tyrosinase by affinity chromatography. *Biochem. Soc. Trans.* **1**: 519-520.
- Gutteridge, S., Robb, D. 1975. The catecholase activity of *Neurospora* tyrosinase. *Eur. J. Biochem.* **54**: 107-116.

- Haanstra, W. G., Cabral, M. F., Cabral, J. de O., Driessen, W. L., Reedijk, J. 1992. Unusually high redox potentials of two copper(II) compounds of 1,8-bis(3,5-dimethyl-1-pyrazolyl)-3,6-dithiaoctane. *Inorg. Chem.* **31**: 3150-3151.
- Halgren, T. A. 1992. Representation of van der Waals (vdW) interactions in molecular mechanics force fields: potential form, combination rules and vdW parameters. *J. Am. Chem. Soc.* **114**: 7827-7843.
- Hall, G. F., Best, D. J., Turner, A. P. F. 1988. The determination of *p*-cresol in chloroform with an enzyme electrode used in the organic phase. *Anal. Chim. Acta.* **213**: 113-119.
- Halling, P. J. 1990a. Solvent selection for biocatalysis in mainly organic systems: predictions of effects on equilibrium position. *Biotechnol. Bioeng.* **35**: 691-701.
- Halling, P. J. 1990b. High-affinity binding of water by proteins is similar in air and in organic solvents. *Biochim. Biophys. Acta.* **1040**: 225-228.
- Halling, P. J. 1992. Salt hydrates for water activity control with biocatalysts in organic media. *Biotechnol. Tech.* **6(3)**:271-276.
- Hamilton, A. D. 1991. Synthetic studies on molecular recognition. *Bioorg. Chem. Front.* **2**: 115-174.
- Hammond, D. A., Karel, M., Klibanov, A. M., Krukonis, V. J. 1985. Enzymatic reactions in supercritical gases. *Appl. Biochem. Biotechnol.* **11**: 393-400.
- Hancock, R. D. 1989. Molecular mechanics calculations as a tool in coordination chemistry. *Prog. Inorg. Chem.* **37**: 187-291.
- Hanlon, D. P., Shuman, S. 1975. Copper ion binding and enzyme inhibitory properties of the antithyroid drug methimazole. *Experientia* **31**: 1005-1006.
- Hansch, C., Leo, A. 1979. Substituent constants for correlation analysis in chemistry and biology. John Wiley, New York.
- Hansen, D. E., Raines, R. T. 1990. Binding energy and enzymatic catalysis. *J. Chem. Ed.* **67(6)**: 483-489.
- Hartsough, D. S., Merz, Jr., K. M. 1992. Protein flexibility in aqueous and nonaqueous solutions. *J. Am. Chem. Soc.* **114**: 10113-10116.
- Healey, D. F., Strothkamp, K. G. 1981. Inhibition of the catecholase and cresolase activity of mushroom tyrosinase by azide. *Arch. Biochem. Biophys.* **211(1)**: 86-91.
- Hearing, Jr., V. J., Ekel, T. M., Montague, P. M., Nicholson, J. M. 1980. Mammalian tyrosinase stoichiometry and measurement of reaction products. *Biochim. Biophys. Acta.* **611**: 251-268.
- Hearing, V. J., Jiménez, M. 1987. Mammalian tyrosinase- the critical regulatory control point in melanocyte pigmentation. *Int. J. Biochem.* **19(12)**: 1141-1147.
- Hendriks, H. M. J., Birker, P. J. M. W. L., van Rijn, J., Verschoor, G. C., Reedijk, J. 1982. Synthesis and characterization of coordination compounds of chelating ligands containing imidazole groups. The crystal and molecular structures of the dinuclear Cu^I and Cu^{II} compounds [N,N,N',N'-tetrakis-(2-benzimidazolymethyl)-1,2-ethanediamine]dicopper(I) bis(perchlorate) and of μ -(nitrate-O, O')-bis(nitrate-O)-{N,N,N',N'-tetrakis[(1-methyl-2-benzimidazolyl)methyl]-1,2-ethanediamine}dicopper(II) nitrate tetrahydrate. *J. Am. Chem. Soc.* **104**: 3607-3617.

- Hider, R. C., Lerch, K. 1989. The inhibition of tyrosinase by pyridones. *Biochem. J.* **257**: 289-290.
- Himmelwright, R. S., Eickman, N. C., LuBien, C. D., Solomon, E. I. 1980(a). Chemical and spectroscopic comparison of the binuclear copper active site of mollusc and arthropod hemocyanins. *J. Am. Chem. Soc.* **102**: 5378-5388.
- Himmelwright, R. S., Eickman, N. C., LuBien, C. D., Lerch, K., Solomon, E. I. 1980(b). Chemical and spectroscopic studies of the binuclear copper active site of *Neurospora* tyrosinase: comparison to hemocyanins. *J. Am. Soc.* **102**: 7339-7344.
- Hooijmans, C. M., Stoop, M. L., Boon, M., Luyben, K. C. A. M. 1991. Comparison of two experimental methods for the determination of Michaelis-Menten kinetics of an immobilized enzyme. *Biotechnol. Bioeng.* **40**: 16-24.
- Horowitz, N. H., Fling, M., Horn, G. 1970. Tyrosinase (*Neurospora crassa*) *Meth. Enzymol.* **17A**:615-620.
- Hruskocy, M., Flurkey, W. H. 1986. Detection of polyphenoloxidase isoenzymes by electroblotting and photography. *Phytochem.* **25(2)**: 329-332.
- Huber, M., Hintermann, G., Lerch, K. 1985. Primary structure of tyrosinase from *Streptomyces glaucescens*. *Biochemistry* **24**:6038-6044.
- Huber, M., Lerch, K. 1987. The influence of copper on the induction of tyrosinase and laccase in *Neurospora crassa*. *FEBS Lett.* **219(2)**: 335-338.
- Huber, M., Lerch, K. 1988. Identification of two histidines as copper ligands in *Streptomyces glaucescens* tyrosinase. *Biochemistry* **27(15)**: 5610-5615.
- Iborra, J. L., Manjon, A. 1977. Stability of immobilised frog epidermis tyrosinase. *J. Solid-Phase Biochem.* **2**: 85-96.
- Ikedo, I., Klivanov, A. M. 1993. Lipase-catalyzed acylation of sugars solubilized in hydrophobic solvents by complexation. *Biotechnol. Bioeng.* **42**: 788-791.
- Ingebrigtsen, J., Kang, B., Flurkey, W. H. 1989. Tyrosinase activity and isoenzymes in developing mushrooms. *J. Food Sci.* **54(1)**: 128-131.
- Ingraham, L. L. 1957. Variation of the Michaelis constant in polyphenol oxidase catalyzed oxidations: substrate structure and concentration. *J. Am. Chem. Soc.* **79**: 666-669.
- Ishikawa, H., Ogino, H., Oshida, H. 1991. Rates of reactions catalysed by a dimeric enzyme. Effects of the reaction scheme and the kinetic parameters on co-operativity. *Biochem. J.* **280**: 131-137.
- Jacobsohn, M. K., Dobre, V. C., Branam, C., Jacobsohn, G. M. 1988. Oxidation of 2-hydroxyestradiol and its incorporation into melanin by mushroom tyrosinase. *J. Steroid Biochem.* **31(4A)**: 377-385.
- Jacobsohn, G. M., Jacobsohn, M. K. 1984. The catalytic effect of tyrosinase upon oxidation of 2-hydroxyestradiol in presence of catechol. *Arch. Biochem. Biophys.* **232(1)**: 189-196.
- Jacobsohn, G. M., Jacobsohn, M. K. 1992. Incorporation and binding of estrogens into melanin: comparison of mushroom and mammalian tyrosinases. *Biochim. Biophys. Acta.* **1116** : 173-182.

Jacobson, R. R., Tyeklar, Z., Farooq, A., Karlin, K. D., Liu, S., Zubieta, J. 1988. A $\text{Cu}_2\text{-O}_2$ complex. Crystal structure and characterisation of a reversible dioxygen binding system. *J. Am. Chem. Soc.* **110**: 3690-3692.

Jameson, R. F. 1981. Coordination chemistry of copper with regard to biological systems. p. 1-29. In: H. Sigel (ed.), *Metal ions biological systems*, Vol. 12. Marcel Dekker, New York.

Janovitz-Klapp, A. H., Richard, F. C., Goupy, P. M., Nicholas, J. J. 1990. Inhibition studies on apple polyphenol oxidase. *J. Agric. Food Chem.* **38**: 926-931.

Jimenez, M., Garcia-Carmona F., Garcia-Canovas, F., Iborra, J. L., Lozano, J. A., Martinez, F. 1984. Chemical intermediates in dopamine oxidation by tyrosinase and kinetic studies of the process. *Arch. Biochem. Biophys.* **235(2)**: 438-448.

Jimenez, M., Garcia-Carmona, F., Garcia-Canovas, F., Iborra, J. L., Lozano, J. A. 1985. Chemical intermediates in α -methylnoradrenaline oxidation by tyrosinase. II. Kinetic study of process. *Int. J. Biochem.* **17(8)**: 891-894.

Jolley, Jr, R. J., Evans, L. H., Makino, N., Mason, H. S. 1974. Oxytyrosinase. *J. Biol. Chem.* **249(2)**: 335-345.

Jolley, Jr., R. L., Mason, H. S. 1965. The multiple forms of mushroom tyrosinase. Interconversion. *J. Biol. Chem.* **240(3)**: 1489-1491.

Jolley, Jr., R. L., Nelson, R. M., Robb, D. A. 1969a. The multiple forms of mushroom tyrosinase. Structural studies on the isozymes. *J Biol. Chem.* **244(12)**: 3251-3257.

Jolley, Jr, R. L., Robb, D. A., Mason, H. S. 1969b. The multiple forms of mushroom tyrosinase: association-dissociation phenomena. *J. Biol. Chem.* **244(6)**: 1593-1599.

Jones, J. B. 1986. Enzymes in organic synthesis. *Tetrahedron.* **42(13)**: 3351-3403.

Jones, J. B. 1993. Probing the specificity of synthetically useful enzymes. European symposium on biocatalysis, Graz, Austria.

Kahn, V., Andrawis, A. 1985. Inhibition of mushroom tyrosinase by tropolone. *Phytochem.* **24(5)**: 905-908.

Kamat, S., Barrera, J., Beckman, E. J., Russel, A. J. 1992. Biocatalytic synthesis of acrylates in organic solvents and supercritical fluids: 1. Optimization of enzyme environment. *Biotechnol. Bioeng.* **40**: 158-166.

Karlin, K. D. 1993. Metalloenzymes, structural motifs and inorganic models. *Science.* **261**: 701-708.

Karlin, K. D., Cruse, R. W., Haka, M. S., Gultneh, Y., Cohen, B. I. 1986. Dioxygen-copper reactivity: intermediacy of a peroxo-dicopper(II) (dioxygen-copper) complex in the hydroxylation reaction of a model monooxygenase system. *Inorg. Chim. Acta.* **125**: L43-L44.

Karlin, K. D., Cruse, R. W., Gultneh, Y., Farooq, A., Hayes, J. C., Zubieta, J. 1987. Dioxygen-copper reactivity. Reversible binding of O_2 and CO to a phenoxo-bridged dicopper(I) complex. *J. Am. Chem. Soc.* **109**: 2668- 2679.

Karlin, K. D., Dahlstrom, P. L., Cozette, S. N., Scensny, P. M., Zubieta, J. 1981. Activation of O_2 by a binuclear copper(I) compound. Hydroxylation of a new xylyl-binucleating ligand to produce a phenoxy-bridged binuclear copper(II) complex; X-ray crystal structure of

$[\text{Cu}_2\{\text{OC}_6\text{H}_3[\text{CH}_2\text{N}(\text{CH}_2\text{CH}_2\text{py})_2]_2-2,6\}(\text{OMe})]$ (py = 2-pyridyl). J. Chem. Soc. Chem. Comm.: 881-882.

Karlin, K. D., Gultneh, Y. 1985. Bioinorganic chemical modelling of dioxygen-activating copper proteins. J. Chem. Ed. **62**(11): 983-989.

Karlin, K. D., Gultneh, Y., Nicholson, T., Zubieta, J. 1985(a). Catecholate coordination to copper: structural characterization of a tetrachloro-*o*-catecholate-bridged dicopper(II) complex as a model for intermediates in copper-catalyzed oxidation of catechols. Inorg. Chem. **24**: 3725-3727.

Karlin, K. D., Gultneh, Y. 1987. Binding and activation of molecular oxygen by copper complexes. Prog. Inorg. Chem. **35**: 219-327.

Karlin, K.D., Haka, M. S., Cruse, R. W., Gultneh, Y. 1985(b). Dioxygen-copper reactivity. Reversible O_2 and CO binding by a new series of binuclear copper(I) complexes. J. Am. Chem. Soc. **107**: 5828-5829.

Karlin, K. D., Haka, M. S., Cruse, R. W., Meyer, G. J., Farooq, A., Gultneh, Y., Hayes, J. C., Zubieta, J. 1988. Dioxygen-copper reactivity. Models for hemocyanin: reversible O_2 and CO binding to structurally characterized dicopper(II) complexes containing hydrocarbon-linked bis[2-(2-pyridyl)ethyl]amine units. J. Am. Chem. Soc. **110**: 1196-1207.

Karlin, K. D., Hayes, J. C., Gultneh, Y., Cruse, R. W., McKown, J. W., Hutchinson, J. P., Zubieta, J. 1984. Copper-mediated hydroxylation of an arene. Model system for the action of copper monooxygenases. Structures of a binuclear Cu(II) complex and its oxygenated product. J. Am. Chem. Soc. **106**: 2121-2128.

Karlin, K. D., Tyeklár, Z., Farooq, A., Haka, M. S., Ghosh, P., Cruse, R. W., Gultneh, Y., Hayes, J. C., Toscano, P. J., Zubieta, J. 1992. Dioxygen-copper reactivity and functional modelling of hemocyanins. Reversible binding of O_2 and CO to dicopper(I) complexes $[\text{Cu}_2^1(\text{L})]^{2+}$ (L = dinucleating ligand) and the structure of a bis(carbonyl) adduct, $[\text{Cu}_2^1(\text{L})(\text{CO})_2]^{2+}$. Inorg. Chem. **31**: 1436-1451.

Katchalski-Katzir, E. 1983. Design and synthesis of organic molecules based on molecular recognition. p. 1-24. In: G. van Binst (ed.), Design and synthesis of organic molecules based on molecular recognition. Springer-Verlag, New York.

Kazandjian, R. Z., Dordick, J. S., Klibanov, A. M. 1986. Enzymatic analyses in organic solvents. Biotech. Bioeng. **XXVII**: 417-421.

Kazandjian, R. Z., Klibanov, A. M. 1985. Regioselective oxidation of phenols catalyzed by polyphenol oxidase in chloroform. J. Am. Chem. Soc. **107**: 5448-5450.

Kean, E. A. 1964. A procedure which demonstrates substrate inhibition of tyrosinase. Biochim. Biophys. Acta. **92**: 602-604.

Kertesz, D. 1965. Mushroom polyphenol oxidase: 1. Purification and general properties. Biochim. Biophys. Acta. **96**: 447.

Kertesz, D., Zito, R. 1965. Mushroom polyphenoloxidase. 1. Purification and general properties. Biochim. Biophys. Acta. **96**: 447-462.

Khan, I. A., Ali, R. 1986. Antigenicity, catalytic activity and conformation of *Agaricus bisporus tyrosinase*: interaction of conformation-directed antibodies with the native and irradiated enzyme. J. Biochem. **99**: 445-452.

- Khmelnitsky, Y. L., Levashov, A. V., Klyachko, N. L., Martinek, K. 1988. Engineering biocatalytic systems in organic media with low water content. *Enzyme Microb. Technol.* **10**: 710-724.
- Kida, S., Okawa, H., Nishida, Y. 1983. K. D. Karlin, J. Zubieta. (eds.), *Copper coordination chemistry: Biochemical and Inorganic perspectives*, Adenine, Guilderland, New York.
- King, R. S., Flurkey, W. H. 1987. Effects of limited proteolysis on broad bean polyphenoloxidase. *J. Sci. Food Agric.* **41**: 231-240.
- Kim, J., Dordick, J. S. 1993. Pressure affects enzyme function in organic media. *Biotechnol. Bioeng.* **42**: 772-776.
- Kitajima, N. 1992. Synthetic approach to the structure of functions of copper proteins. *Adv. Inorg. Chem.* **39**: 1-77.
- Kitajima, N., Fujisawa, K., Fujimoto, C., Moro-oka, Y., Hashimoto, S., Kitagawa, T., Toriumi, K., Tatsumi, K., Nakamura, A. 1992. A new model for oxygen binding in hemocyanin. Synthesis, characterization and molecular structure of the μ - η^2 : η^2 peroxy dinuclear copper(II) complexes, $[\text{Cu}(\text{HB}(3,5\text{-R}_2\text{pz})_3)_2(\text{O}_2)]$ (R = i-Pr and Ph). *J. Am. Chem. Soc.* **114**: 1277-1291.
- Kitajima, N., Koda, T., Iwata, Y., Moro-oka, Y. 1990. Reaction aspects of a μ -peroxy binuclear copper(II) complex.
- Kitajima, N., Koda, T., Hashimoto, S., Kitagawa, T., Moro-oka, Y. 1988. An accurate synthetic model of oxyhaemocyanin. *J. Chem. Soc. Commun.*: 151-152.
- Kitajima, N., Koda, T., Hashimoto, S., Kitagawa, T., Moro-oka, Y. 1991. Synthesis and characterisation of the dinuclear copper(II) complexes $[\text{Cu}(\text{HB}(3,5\text{-Me}_2\text{pz})_3)_2\text{X}]$ (X = O^{2-} , $(\text{OH})_2^{2-}$, CO_3^{2-} , O_2^{2-}). *J. Am. Chem. Soc.* **113**: 5664-5671.
- Kitajima, N., Moro-oka, Y. 1993. μ - η^2 : η^2 -peroxide in biological systems. *J. Chem. Soc. Dalton Trans.*: 2665-2671.
- Klibanov, A. M. 1978. Enzyme stabilization by immobilization. *Anal. Biochem.* **93**: 1-25.
- Klibanov, A. M. 1986. Enzymes that work in organic solvents. *CHEMTECH*: 354-359.
- Klibanov, A. M. 1989. Enzymatic catalysis in anhydrous organic solvents. *TIBS* **14**: 141-144.
- Klibanov, A. M. 1990. Asymmetric transformations catalyzed by enzymes in organic solvents. *Acc. Chem. Res.* **23**: 114-120.
- Klibanov, A. M., Samokhin, G. P., Martinek, K., Berezin, I. V. 1977. A new approach to preparative enzymatic synthesis. *Biotechnol. Bioeng.* **XIX**: 1351-1361.
- Klibanov, A. M., Zaks, A. 1984. Enzymatic catalysis in organic media at 100°C. *Science* **224**: 1249-1251.
- Kubas, G. J., 1979. Tetrakis(acetonitrile) copper(I) hexafluorophosphate. *Inorg. Synth.* **XIX**: 90-92.
- Kubowitz, I. 1938. Resynthesis of phenoloxidase from protein and copper. *Biochem. Z.* **296**: 443.
- Kuiper, H. A., Lerch, K., Brunori, M., Finazzi Agrò A. 1980. Luminescence of the copper-carbon monoxide complex of *Neurospora* tyrosinase. *FEBS Lett.* **111**(1): 232-234.

- Kumar, M., Flurkey, W. H. 1991. Activity, isoenzymes and purity of mushroom tyrosinase in commercial preparations. *Phytochem.***30(12)**: 3899-3902.
- Kushioka, K. 1984. Autooxidation of phenols catalyzed by copper(II)-ethylenediamine complexes: the reaction mechanism. *J. Org. Chem.* **49**: 4456-4459.
- Kvittingen, L., Sjursens, B., Halling, P., Anthonsen, T. 1992. Mixing conditions for enzyme catalysis in organic solvents. *Tetrahedron.* **48(25)**:5259-5264.
- Laane, C. 1987. Medium-engineering for bio-organic synthesis. *Biocatalysis.* **1**: 17-22.
- Laemmli, U. K. 1970. Cleavage of structural proteins during the assembly of the head of bacteriophage T4. *Nature.* **227**: 680-685.
- Laitinen, H. A., Harris, W. E. (eds).1975. Water: Karl Fischer method. p. 361-363. In: *Chemical Analysis*, 2nd edition. McGraw Hill, New York.
- Lang, W. H, van Holde, K. E. 1991. Cloning and sequencing of *Octopus dofleini* hemocyanin cDNA: derived sequences of functional units Ode and Odf. *Proc. Natl. Acad. Sci. USA* **88**: 244-248.
- Larrabee, J. A., Spiro, T. G. 1980. Structural studies of the hemocyanin active site. 2. Resonance Raman spectroscopy. *J. Am. Chem. Soc.* **102(12)**: 4217-4223.
- Lee, C. Y., Kagan, V., Jaworski, A. W., Brown, S. K. 1990. Enzymatic browning in relation to phenolic compounds and polyphenoloxidase activity among various peach cultivars. *J. Agric. Chem.* **38**: 99-101.
- Lerch, K. 1976. *Neurospora* tyrosinase: molecular weight, copper content and spectral properties. *FEBS Lett.* **69(1)**: 157-160.
- Lerch, K. 1981. Copper monooxygenases: Tyrosinase and dopamine β -monooxygenase. p. 143-186. In: H. Sigel. (ed.), *Metal ions in biological systems*, Vol. 13. Marcel Dekker, New York.
- Lerch, K. 1982. Primary structure of tyrosinase from *Neurospora crassa*. *J. Biol. Chem.* **257(11)**: 6414-6419.
- Lerch, K. 1983. *Neurospora* tyrosinase: structural, spectroscopic and catalytic properties. *Mol. Cell. Biochem.* **52**: 125-138.
- Lerch, K. 1987. Molecular and active site structure of tyrosinase. *Life Chem. Reports.* **5**: 221-234.
- Lerch, K. 1988. Protein and active-site structure of tyrosinase. *Adv. Pigment Cell Res.* : 85-98.
- Lerch, K., Ettlinger, L. 1972. Purification and characterisation of a tyrosinase from *Streptomyces glaucescens*. *Eur. J. Biochem.* **31**: 427-437.
- Lerch, K. Germann, U. A. 1988. Evolutionary relationships among copper proteins containing coupled binuclear copper sites. p. 331-348. In: *Oxidases and related redox systems*. Alan R. Liss, Inc.
- Lerch, K. Huber, M., Schneider, H., Drexel, R., Linzen, B. 1986. Different origins of metal binding sites in binuclear copper proteins, tyrosinase and hemocyanin. *J. Inorg. Biochem.* **26**: 213-217.
- Lerch, J. D., Reinhammar, B. 1976. An EPR study of *Neurospora* tyrosinase. *FEBS Lett.* **69(1)**: 161-164.

- Lerner, A. B., Fitzpatrick, T. B. 1950. Biochemistry of melanin formation. *Physiol. Rev.* **30**: 91-126.
- Lerner, H. R., Mayer, A. M. 1976. Reaction mechanism of grape catechol oxidase - a kinetic study. *Phytochem.* **15**: 57-60.
- Leuenberger, H. G. W. 1990. Biotransformation - a useful tool in organic chemistry. *Pure Appl. Chem.* **62(4)**: 753-768.
- Lever, A. B. P. 1984. *Inorganic electronic spectroscopy*. 2nd edition. Elsevier, New York.
- Li, J., Christensen, B. M., Tracy, J. W. 1990. Electrochemical determination of diphenol oxidase activity using high-pressure liquid chromatography. *Anal. Biochem.* **190**: 354-359.
- Lilly, M. D., Woodley, J.M. 1985. Biocatalytic reactions involving water-insoluble organic compounds. p 179-192. In: Tramper, J., van den Plas, H.C., Linko, P. (eds). *Biocatalysis in organic syntheses*. Proceedings of international symposium. Elsevier, Amsterdam.
- Linke, W. F. 1958. Solubilities: Inorganic and metal-organic compounds, p. 1235. In: Vol. 2, 4th edition. *Am. Chem. Soc.*, Washington D. C.
- Linko, Y. Y., Linko, P. 1985. Immobilised biocatalysts in organic synthesis and chemical production. p. 15-17. In: J. Tramper, H. C. van der Plas, P. Linko. (eds.), *Biocatalysis in organic synthesis*. Elsevier, Amsterdam.
- Lowry, O. H., Rosebrough, N. J., Farr, A. L., Randall, R. J. 1951. Protein measurement with the Folin phenol reagent. *J. Biol. Chem.* **193**: 265-271.
- Luytens, M. A., Bur, D., Wynn, H., Parriss, W., Gold, M., Friesen, J. D., Jones, J. B. 1989. An evaluation of the substrate specificity, and of its modification by site-directed mutagenesis, of the cloned *L*-lactatae dehydrogenase from *Bacillus stearothermophilus*. *J. Am. Chem. Soc.* **111**: 6800-6804.
- Maddaluno, J. F., Faull, K. F. 1988. Inhibition of mushroom tyrosinase by 3-amino-*L*-tyrosine: molecular probing of the active site of the enzyme. *Experientia* **44**: 885-887.
- Maddaluno, J. F., Faull, K. F. 1990. Fast enzymatic preparation of *L*-DOPA from tyrosine and molecular oxygen: a potential method for preparing [¹⁶O] *L*-DOPA. *Appl. Radiat. Isot.* **41(9)**: 873-878.
- Maddaluno, J., Giessner-Prettre, C. 1991. Nonempirical calculations on (Cu⁺)₂-O₂: a possible model for oxyhemocyanin and oxytyrosinase active sites. *Inorg. Chem.* **30**: 3439-3445.
- Mahroof-Tahir, M., Karlin, K. D. 1992. A dinuclear mixed-valence Cu(I)/Cu(II) complex and its reversible reaction with dioxygen: generation of a superoxodicopper(II) species. *J. Am. Chem. Soc.* **114**: 7599-7601.
- Mahroof-Tahir, M., Murthy, N. N., Karlin, K. D., Blackburn, N. J., Shaikh, S. N., Zubieta, J. 1992. New thermally stable hydroperoxo- and peroxo-copper complexes. *Inorg. Chem.* **31**: 3001-3003.
- Makino, N., Mason, H. S. 1973. Reactivity of oxytyrosinase toward substrates. *J. Biol. Chem.* **248**: 5731-5735.

- Makino, M., McMahill, P., Mason, H. S., Moss, T. H. 1974. The oxidation state of copper in resting tyrosinase. *J. Biol. Chem.* **249(19)**: 6062-6066.
- Makino, N., Ohnaka, H. 1993. Role of oligomeric interactions in the cooperativity of crayfish hemocyanin. *Biochim. Biophys. Acta.* **1162**: 237-245.
- Malachowski, M. R., Davidson, M. G. 1989. Novel mono- and binuclear Cu(II) complexes: synthesis, characterization and catecholase activity. *Inorg. Chim. Acta.* **162**: 199-204.
- Malchowski, M. R., Tomlinson, L. J., Davidson, M. G., Hall, M. J. 1992. Impact of geometric changes on the oxidation of catechol by copper(II) complexes. *J. Coord. Chem.* **25**: 171-174.
- Mallah, T., Boillot, M. -L., Kahn, O., Gouteron, J., Jeannin, S., Jeannin, Y. 1986. Crystal structures and magnetic properties of μ -phenolato copper(II) binuclear complexes with hydroxo, azido and cyanato-*O* exogenous bridges. *Inorg. Chem.* **25**: 3058-3065.
- Mandal, S. K., Nag, K. 1984. Dinuclear metal complexes. Part 3. Preparation and properties of hydroxo-bridged dicopper(II) complexes. *J. Chem. Soc. Dalton Trans.*: 2141-2149.
- Mandal, S. K., Thompson, L. K., Newlands, M. J., Biswas, A. K., Adhikary, B., Nag, K., Gabe, E. J., Lee, F. L. 1989. Synthesis, structural and magnetic properties of macrocyclic aza-amido binuclear copper(II) complexes. *Can. J. Chem.* **67**: 662-670.
- Margerum, L. D., Liao, K. I., Valentine, J. S. 1988. Oxygen atom transfer reactions at binuclear copper sites. p. 105-115. In: L. Que, Jr. (ed.), *Metal clusters in proteins*. Am. Chem. Soc., Washington D. C.
- Margolin, A. 1991. Enzymes: use them. *CHEMTECH*: 160-167.
- Margolin, A. L., Crenne, J-Y., Klibanov, A. M. 1987. Stereoselective oligomerizations catalyzed by lipases in organic solvents. *Tetrahedron Lett.* **28(15)**: 1607-1610.
- March, J. 1985. *Advanced organic chemistry. Reactions, mechanisms, and structure*. 3rd edition. Wiley-Interscience, New York.
- Martinek, K., Semenov, A. N., Berezin, I. V. 1981. Enzymatic synthesis in biphasic aqueous-organic systems. 1. Chemical equilibrium shift. *Biochim. Biophys. Acta.* **658**: 76-89.
- Martinek, K., Semenov, A. 1981. Enzymatic synthesis in biphasic aqueous-organic systems II. Shift of ionic equilibria. *Biochim. Biophys. Acta.* **658**: 90-101.
- Martinez, P., Van Dam, M. E., Robinson, A. C., Chen, K., Arnold, F. H. 1992. Stabilization of subtilisin E in organic solvents by site-directed mutagenesis. *Biotechnol. Bioeng.* **39**: 141-147.
- Mason, H. S. 1947. The chemistry of melanin. III. Mechanism of oxidation of dihydroxyphenylalanine by tyrosinase. *J. Biol. Chem.* **172**: 83-99.
- Mason, H. S. 1957. Mechanisms of oxygen metabolism. *Adv. Enzymol. Rel. Subjects Biochem.*: 79-233.
- Mason, H. S. 1959. Structure of melanins. p. 563-582. In: M. Gordon (ed.), *Pigment cell biology*. Academic Press, New York.
- Masuda, H., Odani, A., Yamauchi, O. 1989. Structure of an *L*-tyrosyl-*L*-histidyl-copper complex involving an axial copper (II)-phenol OH bonding. Implication for substrate binding at the active site of tyrosinase. *Inorg. Chem.* **28**: 624-625.

- Matheis, G., Belitz, H-D. 1977. Studies on enzymic browning of potatoes (*Solanum tuberosum*).III. Kinetics of potato phenoloxidase. Z. Lebensm. Unters.-Forsch. **163**: 191-195.
- Mattiasson, B., Aldercreutz, P. 1991. Tailoring the microenvironment of enzymes in water-poor systems. TIBTECH **9**: 394-398.
- Mayer, A., Harel, E., Ben-Shaul, R. 1966. Assay of catechol oxidase - a critical comparison of methods. Phytochem. **5**: 783-789.
- Mayer, A. M., Harel, E. 1979. Polyphenol oxidases in plants. Phytochem. **18**: 193-215.
- Medina, M. A., De Veas, R. C., García-Hermoso, A., De Castro, I. N. 1991. An experiment in membrane enzyme purification with Triton X-114: avocado pear polyphenoloxidase. Biochem. Ed. **19(4)**: 210-211.
- Menif, R., Martell, A. E. 1989. Oxygen insertion by a new tyrosinase model binuclear Cu¹ macrocyclic complex. J. Chem. Soc. Commun.: 1521-1523.
- Menif, R., Martell, A. E., Squattrito, P. J., Clearfield, A. 1990. New hexaaza macrocyclic binucleating ligands. Oxygen insertion with a dicopper(I) Schiff base macrocyclic complex. Inorg. Chem. **29**: 4723-4729.
- Menon, S., Fleck, R. W., Yong, G., Strothkamp, K. G. 1990. Benzoic acid inhibition of the α,β and γ isozymes of *Agaricus bisporus* tyrosinase. Arch. Biochem. Biophys. **280(1)**: 27-32.
- Menter, J. M., Townsel, M. E., Moore, C. L., Williamson, G. D., Soteres, B. J., Fisher, M. S., Willis. 1990. Melanin accelerates the tyrosinase-catalyzed oxygenation of p-hydroxyanisole (MMEH). Pigment Cell Res. **3**: 90-97.
- Miller, A. R., Kelley, T. J., Mujer, C. V. 1990. Anodic peroxidase isoenzymes and polyphenol oxidase activity from cucumber fruit: tissue and substrate specificity. Phytochem. **29(3)**: 705-709.
- Moore, B. M., Flurkey, W. H. 1990. Sodium dodecyl sulfate activation of a plant polyphenoloxidase. J. Biol. Chem. **265(9)**: 4982-4988.
- Mozhaev, V. V., Berezin, I. V., Martinek, K. 1988. Structure-stability relationship in proteins: fundamental tasks and strategy for the development of stabilized enzyme catalysts for biotechnology. CRC Crit. Rev. Biochem. **23(3)**: 235-281.
- Murao, S., Oyama, H., Nomura, Y., Tono, T., Shin, T. 1993. Purification and characterization of *Arctium lappa* L.(Edible Burdock) polyphenol oxidase. Biosci. Biotech. Biochem. **57(2)**: 177-180.
- Murata, M., Kurokami, C., Homma, S. 1992. Purification and some properties of chlorogenic acid oxidase from apple (*Malus pumila*). Biosci. Biotech. Biochem. **56(11)**: 1705-1710.
- Naish-Byfield, S., Riley, P. A. 1992. Oxidation of monohydric phenol substrates by tyrosinase. Biochem.J. **288**: 63-67.
- Naka, K., Ohki A., Maeda, S. 1991. Amphiphilic block copolymer-horseradish peroxidase aggregate as a new polymer-enzyme hybrid in organic solvents. Chem. Lett.: 1303-1306.
- Nakamura, N., Takano, S., Ohno, A. 1993. Asymmetric reduction of ketones by immobilised enzymes in an organic solvent. European Symposium on Biocatalysis. Graz, Austria.
- Narayan, V. S., Klivanov, A. M. 1992. Are water-immiscibility and apolarity of the solvent relevant to enzyme efficiency? Biotechnol. Bioeng. **41**: 390-393.

Nasir. See Sarwar-Nasir.

Nelson, R. M., Mason, H. S. 1970. Tyrosinase (mushroom). *Meth. Enzymol.* **17A**: 626-632.

Ngwenya, M. P., Chen, D., Martell, A. E., Reibenspies, J. 1991. Oxygenation of a copper(II) complex of a binucleating macrocyclic Schiff base ligand derived from 1,4,7-triazaheptane and furan-2,5-dicarboxaldehyde. *Inorg. Chem.* **30**: 2732-2736.

Nishida, Y., Shimo, H., Maehara, H., Kida, S. 1985. Crystal structures and magnetic properties of binuclear five-co-ordinate copper(II) complexes with a phenolate bridge and their catalytic functions in multielectron redox reactions. *J. Chem. Soc. Dalton Trans.*: 1945-1951.

Nishida, Y., Kida, S. 1986. Crystal structures and magnetism of binuclear copper(II) complexes with alkoxide bridges. Importance of orbital complementarity in spin coupling through two different bridging groups. *J. Chem. Soc. Dalton Trans.*: 2633-2640.

Ochiai, E. 1973. A μ -peroxo copper(II) compound. *Inorg. Nucl. Chem. Lett.* **9**: 987-990.

O'Connor, C. J., Firmin, D., Pant, A. K., Babu, B. R., Stevens, E. D. 1986. Binuclear molecules incorporating small molecules as bridging ligands. Magnetic properties and molecular structure of $[\text{Cu}_2\text{L}(\mu\text{-B})]^{2+}$. Where B = OH⁻ or Br⁻ and HL = 2,6-bis(*N*-(2-pyridylmethyl)formidoyl)-4-methylphenol. *Inorg. Chem.* **25**: 2300-2307.

Oishi, N., Nishida, Y., Ida, K., Kida, S. 1980. Reaction between various copper(II) complexes and ascorbic acid or 3,5-di-*t*-butylcatechol. *Bull. Chem. Soc. Jpn.* **53**: 2847-2850.

O'Neill, S. P., Graves, D. J., Ferguson, Jr., J. J. 1973. Affinity chromatography of mushroom tyrosinase. *J. Macromol. Sci.-Chem.* **A7(5)**: 1159-1166.

Osaki, S., 1963. The mechanism of tyrosine oxidation by mushroom tyrosinase. *Arch. Biochem. Biophys.* **100**: 374-384.

Otamiri, M., Adlercreutz, P., Mattiasson, B. 1991. Effects on ester synthesis in toluene by immobilised chymotrypsin by addition of polymers to reaction medium. *Biotechnol. Appl. Biochem.* **13**: 54-64.

Palumbo, A., d'Ischia, M., Misuraca, G., Prota, G. 1987. Effect of metal ions on the rearrangement of dopachrome. *Biochim. Biophys. Acta.* **925**: 203-209.

Palumbo, A., d'Ischia, M., Misuraca, G., Prota, G., Schultz, T. M. 1988. Structural modifications in biosynthetic melanins induced by metal ions. *Biochim. Biophys. Acta.* **964**: 193-199.

Palumbo, A., d'Ischia, M., Misuraca, G., Carrutú, L., Prota, G. 1990. Activation of mammalian tyrosinase by ferrous ions. *Biochim. Biophys. Acta.* **1013**: 256-260.

Pandey, G., Muralikrishna, C., Bhalerao, U. T. 1989. Mushroom tyrosinase catalysed synthesis of coumestans, benzofuran derivatives and related heterocyclic compounds. *Tetrahedron.* **45**: 6867-6073.

Pandey, G., Muralikrishna, C., Bhalerao, U. T. 1990. Mushroom tyrosinase catalysed coupling of hindered phenols: a novel approach for the synthesis of Diphenoquinones and bisphenols. *Tetrahedron Lett.* **31(26)**: 3771-3774.

Pandiyan, T., Palandiandavar, M., Lakshminarayanan, M., Manohar, H. 1992. Structure, spectra and redox behaviour of copper(II) complexes of bis(benzimidazolyl)diamine ligands. *J. Chem. Soc. Dalton Trans.*: 3377-3384.

- Parida, S., Dordick, J. S. 1991. Substrate structure and solvent hydrophobicity control, lipase catalysis and enantioselectivity in organic media. *J. Am. Chem. Soc.* **113**: 2253-2259.
- Parkin, K. L., Lowum, S. E. 1990. Active oxygen species involved in the dye-sensitized photoinactivation of mushroom tyrosinase. *J. Agric. Food Chem.* **38(6)**:1297-1302.
- Passi, S., Nazzaro-Porto, M. 1981. Molecular basis of substrate and inhibitory specificity of tyrosinase: phenolic compounds. *Brit. J. Dermatol.* **104**: 659-665.
- Pate, J. E., Cruse, R. W., Karlin, K. D., Solomon, E. I. 1987. Vibrational, electronic and resonance Raman spectral studies of $[\text{Cu}_2(\text{XYL-O})\text{O}_2]^+$, a copper(II) peroxide model complex of oxyhemocyanin. *J. Am. Chem. Soc.* **109**: 2624-2630.
- Pate, J. E., Ross, P. K., Thamann, T. J., Reed, C. A., Karlin, K. D., Sorrell, T. N., Solomon, E. I. 1989. Spectroscopic studies of the charge transfer and vibrational features of binuclear copper(II) azide complexes: Comparison to the coupled binuclear copper active site in met azide hemocyanin and tyrosinase. *J. Am. Chem. Soc.* **111**: 5198-5209.
- Paul, P. P., Tyeklár, Z., Jacobson, R., Karlin, K. D. 1991. Reactivity patterns and comparisons in three classes of synthetic copper-dioxygen $\{\text{Cu}_2\text{-O}_2\}$ complexes: implication for structure and biological relevance. *J. Am. Chem. Soc.* **113**: 5322-5332.
- Pfiffner, E., Lerch, K. 1981. Histidine at the active site of *Neurospora* tyrosinase. *Biochem.* **20**: 6029-6035.
- Phillips, R. S., Fletcher, J. G., Von Tersch, R. L., Kirk, K. L. 1990. Oxygenation of fluorinated tyrosines by mushroom tyrosinase releases fluoride ion. *Arch. Biochem. Biophys.* **276**: 65-69.
- Picardo, M., Passi, S., Nazzaro-Porto, M., Breathnach, A., Zompetta, C., Faggioni, A., Riley, P. 1987. Mechanism of antitumoral activity of catechols in culture. *Biochem. Pharmacol.* **36(4)**: 417-425.
- Pifferi, P. G., Baldassari, L. 1973. A spectrophotometric method for the determination of the catecholase activity of tyrosinase by Besthorn's hydrazone. *Anal. Biochem.* **52**: 325-335.
- Pomerantz, S. H., Warner, M. C. 1967. 3,4-Dihydroxy-L-phenylalanine as the tyrosinase cofactor. *J. Biol. Chem.* **242(22)**: 5308-5314.
- Pras, N. 1988. Biotechnological production of catechols: bioconversion spectrum and related kinetic aspects of entrapped cells of *Mucuna pruriens* L. *Pharm. Weekbl. Sci. Edit.* **11**: 30-31.
- Pras, N., Booi, G. E., Dijkstra, D., Horn, A. S., Malingé, T. M. 1990. Bioconversion of bi- and tri-cyclic monophenols by alginate-entrapped cells of *Mucuna pruriens* L. and by the partially purified *Mucuna*-phenoloxidase. *Plant Cell, Tissue and Organ Cult.* **21**: 9-15.
- Pras, N., Wichers, H. J., Bruins, A. P., Malingré, T. M. 1988. Bioconversion of para-substituted monophenolic compounds into corresponding catechols by alginate entrapped cells of *Mucuna pruriens*. *Plant Cell, Tissue and Organ Cult.* **13**: 15-26.
- Prati, L., Rossi, M., Ravasio, N. 1992. Interaction of molecular oxygen with aminophenols mediated by copper metal and copper compounds. *J. Mol. Catal.* **75**: 347-355.
- Prezioso, J. A., Fitzgerald, G. B., Wick, M. M. 1990. Effects of tyrosinase activity on the cytotoxicity of 3,4-dihydroxybenzylamine and buthionine sulfoximine in human melanoma cells. *Pigment Cell Res.* **3**: 49-54.

- Prota, G. 1972. Structure and biogenesis of phaeomelanins. p. 615-630. In: V. Riley (ed.), *Pigmentation: Its genesis and biologic control*. Appleton Century Croft, New York.
- Raper, H. S. 1928. The anaerobic oxidases. *Physiol. Rev.* **8**: 245-282.
- Rappé, A. K., Casewit, C. J., Colwell, K. S., Goddard III, W. A., Skiff, W. M. 1992. UFF, a full periodic table force field for molecular mechanics and molecular dynamics simulations. *J. Am. Chem. Soc.* **114**: 10024-10035.
- Réglier, M., Jorand, K., Waegell, B. 1990. Binuclear copper complex model of tyrosinase. *J. Chem. Soc. Commun.*: 1752-1755.
- Reglier, M. 1992. Personal communication.
- Reinaud, O., Capdevielle, P., Maumy, M. 1990. Copper(II) mediated aromatic hydroxylation by trimethylamine *N*-oxide. *J. Chem. Soc. Commun.*: 566-568.
- Reinaud, O., Capdevielle, P., Maumy, M. 1991a. *Ortho*-arloxylated of *N*-substituted benzamides: a new oxidizing process induced by the copper(II)/trimethylamine *N*-oxide system. *J. Chem. Soc. Perkin Trans.*: 2129-2134.
- Reinaud, O., Capdevielle, P., Maumy, M. 1991b. 2-(*N*-amido)-4-nitrophenol: a new ligand for the copper-mediated hydroxylation of aromatics by trimethylamine *N*-oxide. *J. Mol. Catal.* **68**: L13-L15.
- Reslow, M., Adlercreutz, P., Mattiasson, B. 1988. On the importance of the support material for bioorganic synthesis. Influence of water partition between solvent, enzyme and solid support in water-poor reaction media. *Eur. J. Biochem.* **172**: 573-578.
- Rice, M E., Moghaddam, B., Creveling, C. R., Kirk, K. L. 1987. Effect of fluorine on the anodic oxidation of catecholamines and amino acids. *Anal. Chem.* **59(11)**: 1534-1538.
- Robb, D. A. 1984. Tyrosinase. p. 208-240. In: R. Lontie (ed.), *Copper proteins and copper enzymes*, vol II. CRC Press, Boca Raton.
- Robb, D. A., Swain, T., Mapson, L. W. 1966. Substrates and inhibitors of the activated tyrosinase of broad bean (*Vicia faba* L). *Phytochem.* **5**: 665-675.
- Rockliffe, D. A., Martell, A. E. 1992. The stoichiometric and catalytic oxidation of various substrates with a novel macrocyclic binuclear copper(I) dioxygen complex as an intermediate. *J. Chem. Soc. Commun.*: 1758-1760.
- Rose, P. D. Personal communication.
- Ros, J. R., Rodríguez-López, J. N., García-Cánovas, F.. 1993. Effect of ferrous ions on the monophenolase activity of tyrosinase. *Biochim. Biophys. Acta.* **1163**: 303-308.
- Ross, P. K., Solomon, E. I. 1990. Electronic structure of peroxide-bridged copper dimers of relevance to oxyhemocyanin. *J. Am. Chem. Soc.* **112**: 5871-5872.
- Ross, P. K., Solomon, E. I. 1991. An electronic structural comparison of copper-peroxide complexes of relevance to hemocyanin and tyrosinase active sites. *J. Am. Chem. Soc.* **113**: 3246-3259.
- Rossiter, B. W., Hamilton, J. F. 1986. *Physical methods of chemistry*, 2nd edition. Vol II, *Electrochemical methods*, Wiley, New York.
- Roziewski, K., Russell, A. J. 1991. Effect of hydration on the morphology of enzyme powder. *Biotechnol. Bioeng.* **39**: 1171-1175.

- Rubio, E., Fernandez-Mayorales, A., Klibanov, A. M. 1991. Effect of the solvent on enzyme regioselectivity. *J. Am. Chem. Soc.* **113**: 695-696.
- Rüegg, C., Ammer, D., Lerch, K. 1982. Comparison of amino acid sequence and thermostability of tyrosinase from wild type strains of *Neurospora crassa*. *J. Biol. Chem.* **257**(11): 6420-6426.
- Rüegg, C., Lerch, K. 1981. Cobalt tyrosinase: replacement of the binuclear copper of *Neurospora* tyrosinase by cobalt. *Biochem.* **20**: 1256-1262.
- Russell, A. J. 1993. Tuning enzyme function in supercritical fluids. European Symposium on Biocatalysis, Graz.
- Russell, A. J., Klibanov, A. M. 1988. Inhibitor-induced enzyme activation in organic solvents. *J. Biol. Chem.* **263**(24): 11624-11626.
- Russell, A. J., Beckman, E. J. 1991. Enzyme activity in supercritical fluids. *Appl. Biochem. Biotechnol.* **31**: 197-211.
- Russell, A. J., Chatterjee, S., Bambot, S. 1992. Mechanistic enzymology in non-aqueous media. *Pure Appl. Chem.* **64**(8): 1157-1163.
- Ryu, K., Dordick, J. S. 1989. Free energy relationships of substrate and solvent hydrophobicities with enzymatic catalysis in organic media. *J. Am. Chem. Soc.* **111**: 8026-8027.
- Ryu, K., Dordick, J. S. 1992. Quantitative and predictive correlations for peroxidase catalysis in organic media. *Biotechnol. Tech.* **6**(3): 277-282.
- Sakurai, T., Margolin, A. L., Russell, A. J., Klibanov, A. M. 1988. Control of enzyme enantioselectivity by the reaction medium. *J. Am. Chem. Soc.* **110**: 7236-7237.
- Sánchez-Ferrer, A., Bru, R., Cabanes, J., García-Carmona, F. 1988(a). Characterization of catecholase and creosolase activities of Monastrell grape polyphenol oxidase. *Phytochem.* **27**(2): 319-321.
- Sánchez-Ferrer, A., Bru, R., García-Carmona, F. 1988(b). Kinetic properties of polyphenoloxidase in organic solvents. A study in Brij 96-cyclohexane reverse micelles. *FEBS Lett.* **233**(2): 363-366.
- Sánchez-Ferrer, A., Bru, R., García-Carmona, F. 1992(a). Reverse vesicles as a new system for studying enzymes in organic solvents. *Biochem. J.* **285**: 373-376.
- Sánchez-Ferrer, A., García-Carmona, F. 1992(b). Activation and inhibition of grape polyphenoloxidase. *Biochem. Ed.* **20**(4): 235-237.
- Sánchez-Ferrer, A., García-Carmona, F. 1992(c). A simple procedure for purifying polyphenol oxidase for a practical biochemistry course. *Biochem. Ed.* **20**(3): 178-179.
- Sanyal, I., Strange, R. W., Blackburn, N. J., Karlin, K. D. 1991. Formation of a copper-dioxygen complex ($\text{Cu}_2\text{-O}_2$) using simple imidazole ligands. *J. Am. Chem. Soc.* **113**: 4692-4693.
- Sanyal, I., Mahroof-Tahir, M., Nasir, M. S., Ghosh, P., Cohen, B. I., Gultneh, Y., Cruse, R. W., Farooq, A., Karlin, K. D., Liu, S., Zubieta, H. J. 1992. Reactions of dioxygen (O_2) with mononuclear copper(II) complexes: temperature-dependent formation of peroxo- or oxo- (and dihydroxo-) bridged dicopper(II) complexes. *Inorg. Chem.* **31**: 4322-4332.

Sarwar-Nasir, M., Jacobson, R. R., Zubieta, J., Karlin, K. D. 1993. Pyridine ligand effects upon structure, redox properties and oxygen reactivity of xylyl dinuclear copper(I) complexes. *Inorg. Chim. Acta.* **203**: 5-7.

Sarwar-Nasir, M., Karlin, K. D., McGowty, D., Zubieta, J. 1991. Unsymmetrical dicopper complexes. Direct observation of reversible O₂ binding in a copper monooxygenase model system. *J. Am. Chem. Soc.* **113**: 698-700.

Schindler, S., Szalda, D. J., Creutz, C. 1992. Syntheses, structures, and properties of copper(II) and copper(I) complexes of the new binucleating ligand 1,3-bis[bis(2-pyridylmethyl)amino]benzene. *Inorg. Chem.* **31**: 2255-2264.

Schoot Uiterkamp, A. J. M., Evans, L. H., Jolley, R. L., Mason, H. S. 1976. Absorption and circular dichroism spectra of different forms of mushroom tyrosinase. *Biochim. Biophys. Acta.* **453**: 200-204.

Schoot Uiterkamp, A. J. M., Mason H. S. 1973. Magnetic dipole-dipole coupled Cu(II) pairs in nitric oxide-treated tyrosinase: a structural relationship between the active sites of tyrosinase and hemocyanin. *Proc. Nat. Acad. Sci. USA.* **70(4)**: 993-996.

Schved, F., Kahn, V. 1992. Synergism exerted by 4-methyl catechol, catechol, and their respective quinones on the rate of *DL*-DOPA oxidation by mushroom tyrosinase. *Pigment Cell Res.* **5**: 41-48.

Scott, D. 1975. Catecholase. p. 236-243. In: A. Reed (ed.), *Enzymes in food processing*. Academic Press, New York.

Shah, M. A., Khan, I. A., Ali, R. 1987. Active site and conformation-directed photoinactivation of copper-dependent oxidoreductases: studies of pig kidney diamine oxidase. *J. Radiat. Res.:* 233-242.

Simmons, M. G., Wilson, L. J. 1978. A haemocyanin model: a synthetic copper(II) complex having imidazole ligands and reversible dioxygen activity. *J. Chem. Soc. Chem. Comm.:* 634-636.

Simmons, M. G., Merrill, C. L., Wilson, L. J. 1980. The {bis-2,6-[1-(2-imidazol-4-ylethylimino)ethyl]pyridine}copper(II) cation. A synthetic Cu^I oxygen carrier as a potential model for oxyhemocyanin. *J. Chem. Soc. Dalton Trans.:* 1827- 1837.

Sizer, I, W. 1953. Oxidation of proteins by tyrosinase and peroxidase. *Adv. Enzymol.* **14**: 129-161.

Smit, M.H., Rechnitz, G. A. 1993. Toxin detection using tyrosinase-coupled oxygen electrode. *Anal. Chem.* **65**: 380-385.

Smith, D. M., Montgomery, M. W. 1985. Improved methods for the extraction of polyphenol oxidase from d'Anjou pears. *Phytochem.* **24(5)**: 901-904.

Solomon, E. I. 1983. Electronic and geometric structure-function of the coupled binuclear copper active site. *Pure Appl. Chem.* **55(7)**:1069-1088.

Solomon, E. I., 1988(a). Coupled binuclear copper active sites. p. 116-150. In: L. Que, Jr. (ed.), *Metal clusters in proteins*. Am. Chem. Soc, Washington D. C.

Solomon, E. I. 1988(b). Coupled binuclear copper proteins: catalytic mechanisms and structure-reactivity correlations. p. 309-329. In: T. E. King (ed), *International symposium on oxidases and related redox systems*.

Solomon, E. I., Allendorf, M. D., Kau, L-S., Pate, J. E., Spira-Solomon, D., Wilcox, D. E., Porras, A. G. 1987. Chemical and spectroscopic studies of copper clusters in proteins. *Life Chem. Rep.* **5**: 37-89.

Solomon, E. I., Baldwin, M. J., Lowery, M. D. 1992. Electronic structures of active sites in copper proteins: contributions to reactivity. *Chem. Rev.* **92**: 521-542.

Solomon, E. I., Lowery, M. D. 1993. Electronic structure contributions to function in bioorganic chemistry. *Science.* **259**: 1575-1581.

Sorrell, T. N. 1989. Synthetic models for binuclear copper proteins. *Tetrahedron.* **45**(1): 3-68.

Sorrell, T. N., Beltramini, M., Lerch, K. 1988. Luminescence of deoxyhemocyanin and deoxytyrosinase. *J. Biol. Chem.* **263**(20): 9576-9577.

Sorrell, T. N., Borovik, A. S. 1986. Ultraviolet absorption and resonance Raman spectra of copper(II) complexes. *J. Am. Chem. Soc.* **108**: 5636-5637.

Sorrell, T. N., Garrity, M. L. 1991. Synthesis and reactivity of imidazolyl- and benzimidazolyl-containing copper complexes. *Inorg. Chem.* **30**: 210-215.

Sorrell, T. N., Malchowski, M. R., Jameson, D. L. 1982. Synthesis, structure and reactivity of a binuclear three-coordinate copper(I) complex. *Inorg. Chem.* **21**: 3250-3252.

Sorrell, T. N., Vankai, V. A. 1990. Synthesis and dioxygen reactivity of dinuclear copper-phenolate and copper-phenol complexes with pyrazole and pyradine donors. *Inorg. Chem.* **29**: 1687-1692.

Sorrell, T. N., Vankai, V. A., Garrity, M. L. 1991. Synthesis and reactivity of dinuclear copper complexes having a *m*-xylyl spacer between coordination units. *Inorg. Chem.* **30**: 207-210.

Speier, G. 1986. Copper-catalysed oxidation of catechols by dioxygen. *J. Mol. Catal.* **37**: 259-267.

Spodine, E., Manzur, J. 1992. Oxygen insertion in organic substrates catalyzed by copper compounds. *Coord. Chem. Rev.* **119**: 171-198.

Srivas, B., Zacharias, P. S. 1992. Dinuclear copper(II), nickel(II) and mixed valence Cu^{II}-Cu^I complexes-influence of donor groups on redox behaviour of dicopper complexes. *Polyhedron.* **11**(5): 1949-1958.

Ståhl, M., Månsson, M-O., Mosbach, K. 1990. The synthesis of a D-amino acid ester in organic media with α -chymotrypsin modified by a bio-imprinting procedure. *Biotechnol. Lett.* **12**(3): 161-166.

Strothkamp, K. G., Jolley, R. L., Mason, H. S. 1976. Quaternary structure of mushroom tyrosinase. *Biochem. Biophys. Res. Commun.* **70**(2): 519-524.

Suckling, C. J. 1990. Infant enzyme chemistry. p. 1-7. In: C. J. Suckling (ed.), *Enzyme chemistry. Impact and applications*, 2nd edition. Chapman and Hall, London.

Suguraman, M. 1986. Tyrosinase catalyzes an unusual oxidative decarboxylation of 3,4-dihydroxymandelate. *Biochem.* **25**: 4489-4492.

Suguraman, M. 1987. Quinone methide sclerotization: a revised mechanism for β -sclerotization of insect cuticle. *Bioorg. Chem.* **15**: 194-211.

Suguraman, M., Dali, H., Semensi, V., Hennigan, B. 1987. Tyrosinase-catalyzed unusual oxidative dimerization of 1,2-dehydro-*N*-acetyldopamine. *J. Biol. Chem.* **262**(22): 10546-10549.

Suguraman, M., Dali, H., Semensi, V. 1990. Formation of a stable quinone methide during tyrosinase-catalyzed oxidation of α -methyl DOPA methyl ester and its implication in melanin biosynthesis. *Bioorg. Chem.* **18**: 144-153.

Suguraman, M., Semensi, V., Dali, H., Mitchell, W. 1989. Novel transformations of enzymatically generated carboxymethyl-*o*-benzoquinone to 2,5,6-trihydroxybenzofuran and 3,4-dihydroxymandelic acid. *Bioorg. Chem.* **17**: 86-95.

Sun, W-Q., Payne, G. F., Moas, M. S. G. L., Chu, J. H., Wallace, K. K. 1992. Tyrosinase reaction / chitosan adsorption for removing phenols from wastewater. *Biotechnol. Prog.* **8**: 179-186.

Swain, T., Mapson, L. W., Robb, D. A. 1966. Activation of *Vicia faba* (L) tyrosinase as effected by denaturing agents. *Phytochem.* **5**: 469-482.

Symons, M. C. R., Petersen, R. L. 1978. Electron addition to the active site of *Cancer magister* haemocyanins. *Biochim. Biophys. Acta.* **535**: 247-252.

Takahashi, K., Ajima, A., Yoshimoto, T., Okada, M., Matsushima, A., Tamaura, Y., Inada, Y. 1985. Chemical reactions by polyethelene glycol modified enzymes in chlorinated hydrocarbons. *J. Org. Chem.* **50**: 3414-3415.

Tandon, S. S., Thompson, L. K., Bridson, J. N., McKee, V., Downard, A. J. 1992. Dinuclear copper(II) and polymeric tetranuclear copper(II) and copper(II)-copper(I) complexes of macrocyclic ligands capable of forming endogenous alkoxide and phenoxide bridges. Structural, magnetic, and electrochemical studies. *Inorg. Chem.* **31**: 4635-4642.

Terradas, F., Teston-Henry, M., Fitzpatrick, P., Klivanov, A. M. 1993. Marked dependence of enzyme prochiral selectivity on the solvent. *J. Am. Chem. Soc.* **115**: 390-396.

Thompson, J. S. 1984(a). Copper-dioxygen chemistry. Synthesis, spectroscopy and properties of a copper(II) superoxide complex. *J. Am. Chem. Soc.* **106**: 4057-4059.

Thompson, J. S. 1984(b). Copper-dioxygen chemistry. Synthesis and properties of a dicopper(II)-peroxide complex. *J. Am. Chem. Soc.* **106**: 8308-8309.

Thompson, J. S., Calabrese, J. C. 1986. Copper-catechol chemistry. Synthesis, spectroscopy and structure of bis(3,5-di-*tert*-butyl-*o*-semiquinato)copper(II). *J. Am. Chem. Soc.* **108**: 1903-1907.

Thompson, R. Q., Mandoke, C. S., Womack, J. P. 1985. A procedure for immobilizing enzymes on nylon. *Anal. Lett.* **18**(B1): 93-107.

Tome, D., Nicolas, J., Drapron, R. 1978. Influence of water activity on the reaction catalyzed by polyphenoloxidase (E.C.1.14.18.1.) from mushrooms in organic liquid media. *Lebensm.-Wiss.u. - Technol.* **11**: 38-41.

Toussaint, O., Lerch, K. 1987. Catalytic oxidation of 2-aminophenols and *ortho* hydroxylation of aromatic amines by tyrosinase. *Biochem.* **26**: 8567-8571.

Tramper, J. 1985. Immobilizing biocatalysts for use in synthesis. *Trends Biotechnol.* **3**(2): 45-50.

Tramper, J., Vermuë, M. H. 1993. Tailoring the medium and bioreactor for biocatalysis. *Chimia.* **47**: 110-115.

- Tsuji, J., Takayanagi, H. 1978. Oxidative cleavage reactions of catechol and phenol to monoester of *cis,cis*-muconic acid with the oxidizing systems of O₂/CuCl, KOH/CuCl₂ and KO₂/CuCl₂ in a mixture of pyridine and alcohol. *Tetrahedron*. **34**:641-644.
- Tsuruya, S., Kishikawa, Y., Tanaka, R., Kuse, T. 1977. Copper(II)-catalyzed oxidative coupling of 2,6-dimethylphenol. *J. Catal.* **49**: 254-264.
- Tyeklár, Z., Ghosh, P., Karlin, K. D., Farooq, A., Cohen, B. I., Cruse, R. W., Gulteh, Y., Haka, M. S., Jacobson, R. R., Zubieta, J. 1988. Models for copper proteins. p. 85-104. In: L. Que, Jr. (ed.), *Metal clusters in proteins*, Am. Chem. Soc, Washington D. C.
- Tyeklár, Z., Karlin, K. D. 1989. Copper-dioxygen chemistry: a bioinorganic challenge. *Acc. Chem. Res.* **22**: 241-248.
- Tyeklár, Z., Jacobson, R. R., Wei, N., Murthy, N. N., Zubieta, J., Karlin, K. D. 1993. Reversible reaction of O₂ (and CO) with a copper(I) complex. X-ray structures of relevant mononuclear Cu(I) precursor adducts and the *trans*-(μ -1,2-peroxo)dicopper(II) product. *J. Am. Chem. Soc.* **115**: 2677-2689.
- Urbach, F. L. 1981. The properties of binuclear copper centres in model and natural compounds. p. 73-108. In: H. Sigel. (ed.), *Metal ions in biological systems*, Vol. 13. Marcel Dekker, New York.
- Valero, E., Varón, R., García-Carmona, F. 1992. Kinetic study of the effect of metabisulfite on polyphenol oxidase. *J. Agric. Food Chem.* **40**: 904-908.
- Vanni, A., Gastaldi, D., Giunta, G. 1990. Kinetic investigations on the double enzymatic activity of the tyrosinase mushroom. *Ann. Chim.* **80**: 35-60.
- Varoquaux, P., Sarris, J. 1979. Influence de l'acide ascorbique sur la cinétique de l'*o*-diphénoloxydase (E. C. 1.14.18.1) du champignon de Paris (*Agaricus bisporus*). *Lebensm. -Wiss. u. -Technol.* **12**: 318-320.
- Vigato, P. A., Tamburini, S., Fenton, D. E. 1990. The activation of small molecules by dinuclear complexes of copper and other metals. *Coord. Chem. Rev.* **106**: 25-170.
- Volbeda, A., Feiters, M. C., Vincent, M. G., Bouwman, E., Dobson, B., Kalk, K. H., Reedijk, J., Hol, W. G. J. 1989. Spectroscopic investigations of *Panulirus interruptus* hemocyanin in the crystalline state. *Eur. J. Biochem.* **181**: 669-673.
- Volbeda, A., Hol, W. G. J. 1989a. Pseudo 2-fold symmetry in the copper-binding domain of arthropodan haemocyanins. Possible implications for the evolution of oxygen transport proteins. *J. Mol. Biol.* **206**: 531-546.
- Volbeda, A., Hol, W. G. J. 1989b. Crystal structure of hexameric haemocyanin from *Panulirus interruptus* refined at 3.2 Å resolution, *J. Mol. Biol.* **209**: 249-279.
- Volkin, D. B., Staubli, A., Langer, R., Klibanov, A. M. 1991. Enzyme thermoinactivation in anhydrous organic solvents. *Biotech. Bioeng.* **37**: 843-853.
- Vulfson, E. M., Ahmed, G., Gill, I., Kozlov, I. A., Goodenough, P. W., Law, B. A. 1991. Alterations to the catalytic properties of polyphenoloxidase in detergentless microemulsions and ternary water-organic solvent mixtures. *Biotech. Lett.* **13**(2): 91-96.
- Wada, S., Ichikawa, H., Tatsumi, K. 1993. Removal of phenols from wastewater by soluble and immobilized tyrosinase. *Biotechnol. Bioeng.* **42**: 854-858.

- Wagner, C. R., Benkovik, S. J. 1990. Site directed mutagenesis: a tool for enzyme mechanism dissection. *TIBTECH* **8**: 263-271.
- Waite, J. H. 1976. Calculating extinction coefficients for enzymatically produced *o*-quinones. *Anal. Biochem.* **V**: 211-218.
- Waite, J. H., Tanzer, M. L. 1981. Specific colorimetric detection of *o*-diphenols and 3,4-dihydroxyphenylalanine-containing peptides. *Anal. Biochem.* **111**: 131-136.
- Wandrey, C. 1993. Enzyme reaction engineering. *Chimia* **47**: 96-99.
- Wang, J., Reviejo, A. J. 1992. Organic-phase enzyme electrode for the determination of phenols in olive oils. *Anal. Lett.* **25(8)**: 1399-1409.
- Wang, J., Reviejo, A. J. 1993. Organic-phase enzyme electrode for the determination of trace water in nonaqueous media. *Anal. Chem.* **65**: 845-847.
- Watanabe, M., Hiraoka, A., Masada, M., Sato, M. 1991. Involvement of oxalate in the reduction of spinach chloroplast phenolase activity in winter and reactivating agents including irradiation. *Phytochem.* **30**: 89-93.
- Weber, K., Osborn, M. 1969. The reliability of molecular weight determinations by dodecyl sulfate-polacrylamide gel electrophoresis. *J. Biol. Chem.* **244(16)**: 4406-4412.
- Wehtje, E., Adlercreutz, P., Mattiason, B. 1992. Improved activity retention of enzymes deposited on solid supports. *Biotechnol. Bioeng.* **41**: 171-178.
- Wilcox, D. E., Long, J. R., Solomon, E. I. 1984. EPR Studies of the "EPR nondetectable" derivative of hemocyanin: perturbations and displacement of the endogenous bridge in the coupled binuclear copper active site. *J. Am. Chem. Soc.* **106**: 2186-2194.
- Wilcox, D. E., Porras, A. G., Hwang, Y. T., Lerch, K., Winkler, M. E., Solomon, E. I. 1985. Substrate analogue binding to the coupled binuclear copper active site in tyrosinase. *J. Am. Chem. Soc.* **107**: 4015-4027.
- Wilson, K., Goulding, K. H. 1986. Atomic/flame spectrophotometry. p296. In: *Principals and techniques of practical biochemistry*, Edward Arnold, London.
- Winkler, M. E., Lerch, K., Solomon, E. I. 1981. Competitive inhibitor binding to the binuclear copper active site in tyrosinase. *J. Am. Chem. Soc.* **103**: 7001-7003.
- Wissermann, K. W., Lee, C. Y. 1980. Polyphenoloxidase activity during grape maturation and wine production. *Am. J. Enol. Vitic.* **31(3)**: 206-211.
- Wittenberg, C., Triplett, E. L. 1985. A detergent-activated tyrosinase from *Xenopus laevis*. *J. Biol. Chem.* **260(23)**: 12535-12541.
- Woerdenberg, H. J., Pras, N., Frijlink, H. W., Lerk, C. F., Malingré, T, M. 1990. *Phytochem.* **29(5)**: 1551-1554.
- Wood, B. J. B., Ingraham, L. L. 1965. Labelled tyrosinase from labelled substrate. *Nature.* **205**: 291-292.
- Woolery, G. L., Powers, L., Winkler, M., Solomon, E. I., Lerch, K., Spiro, T. G. 1984. Extended X-ray absorption fine structure of the coupled binuclear copper active site of tyrosinase from *Neurospora crassa*. *Biochim. Biophys. Acta.* **788**: 155-161.
- Wong, C. -H. 1989. Enzymatic catalysis in organic synthesis. *Science.* **244**: 1145-1152.

- Wong, C. -H. 1993. Development of enzymes for chemoenzymatic synthesis. *Chimia*. **47**: 127-132.
- Yamada, H., Shimizu, S. 1985. Microbial enzymes as catalysts for synthesis of biologically useful compounds. p. 19-41 in Tramper, J., van der Plas, H. C., Linko, P., (eds.). *Biocatalysts in organic syntheses. Studies in organic chemistry*, vol. 22.
- Yamaguchi, M., Hwang, P. M., Campbell, J. D. 1970. Latent *o*-diphenol oxidase in mushrooms (*Agaricus bisporus*). *Can. J. Biochem.* **48**: 198-202.
- Yamamoto, H., Kuno, S., Nagai, A., Nishida, A., Yamauchi, S., Ikeda, K. 1990. Insolubilizing and adhesive studies of water-soluble synthetic model proteins. *Int. J. Biol. Macromol.* **12**: 305-310.
- Yamamoto, H., Tanisho, H., Ohara, S., Nishida, A. 1992. Cross-linking and gel formation of water-soluble lysine polypeptides. An insolubilization model reaction for adhesive proteins. *Int. J. Biol. Macromol.* **14**: 66-72.
- Yasunobu, K. T. 1959. Mode of action of tyrosinase. p.583-608. In: M. Gordon (ed.), *Pigment cell biology*. Academic Press, New York.
- Yasunobu, K. T., Peterson, E. W., Mason, H. S. 1959. The oxidation of tyrosine-containing peptides by tyrosinase. *J. Biol. Chem.* **234**(12): 3291-3295.
- Zaks, A., Empie, M., Gross, A. 1988. Potentially commercial enzymatic processes for the fine and specialty chemical industries. *TIBTECH* **6**: 272-275.
- Zaks, A., Klibanov, A. M. 1984. Enzymic catalysis in organic media at 100°C. *Science*. **224**: 533-540.
- Zaks, A., Klibanov, A. M. 1986. Substrate specificity of enzymes in organic solvents vs. water is reversed. *J. Am. Chem. Soc.* **108**: 2767-2768.
- Zaks, A., Klibanov, A. M. 1988a. Enzymatic catalysis in nonaqueous solvents. *J. Biol. Chem.* **263**(7): 3194-3201.
- Zaks, A., Klibanov, A. M. 1988b. The effect of water on enzyme action in organic media. *J. Biol. Chem.* **263**(17): 8017-8021.
- Zaks, A., Russell, A. 1988. Enzymes in organic solvents: properties and applications. *J. Biotechnol.* **8**: 259-270.
- Zanello, P., Tamburini, S., Vigato, A., Mazzocchin, G. A. 1987. Synthesis, structure and electrochemical characterization of homo- and heterodinuclear copper complexes with compartmental ligands. *Coord. Chem. Rev.* **77**: 165-273.